Saskatchewan
Energy and Mines

Saskatchewan
Geological Survey

Miscellaneous Report 90-4

Summary of Investigations 1990, Saskatchewan Geological Survey

Printed under the authority of the
Minister of Energy and Mines

Although the Department of Energy and Mines has exercised all reasonable care in the compilation, interpretation and production of this report, it is not possible to ensure total accuracy, and all persons who rely on the information contained herein do so at their own risk. The Department of Energy and Mines and the Government of Saskatchewan do not accept liability for any errors, omissions or inaccuracies that may be included in, or derived from, this report.

91-03141/

Editors

R. Macdonald
T.I.I. Sibbald
C.T. Harper
D.F. Paterson
P. Guliov

Production Editors:

C.T. Harper
N. Richmond-Johnson

Production Assistants:

J. Bilkhu
V. Zeigler
R.P. Kydd
K.G. Jones

ISSN 0228 5657
Printed by Printco Graphics Inc.

Foreword

Preliminary results of the 1990 geoscience program of the Saskatchewan Geological Survey are presented in this publication. Funds for the program were provided from the core budget of Saskatchewan Energy and Mines, from the Public Service Commission's Summer Student Employment Program (SSEP) and from the Saskatchewan Mineral Industry Diversification Program (MIDP), now in its second year. Collectively these funds provided for a level of geoscientific activity equivalent to that of the previous year.

The reports in this volume were produced by staff of the Saskatchewan Geological Survey, or under contract mainly with the Saskatchewan Research Council and the Universities of Saskatchewan and Regina, as well as other institutions. The Survey also acknowledges additional contributions to this volume by these agencies and the Geological Survey of Canada using funds outside of the MIDP.

The main thrust of the geoscience program continued to be focussed on geological mapping and related studies in selected parts of northern Saskatchewan judged to have the highest potential for development of precious and base-metal deposits. Diversification into other commodities also received priority and studies related to rare-earths, diamonds, high salinity brines and dimension stone were carried out.

Formal negotiations commenced recently regarding a new five-year Canada-Saskatchewan Mineral Development Agreement (MDA-2) effective April 1, 1990. This will place the current year's provincial MIDP under the first year of the agreement and increase federal commitments in years two to five of the program.

I wish to thank all of the authors who contributed reports to this volume and gratefully acknowledge the efforts of the editorial, cartographic and stenographic staff in maintaining the high standard of publication.

L.S. Beck
Executive Director
Geology and Mines

November 1990

Contents

		Page
	Foreword	iii
	Contents	v
	Review	ix
	Northern Geoscience and Mineral Deposit Studies	
	Location of Projects	2
*	Geology of the Snake Rapids Area, Flin Flon Domain (Parts of NTS 63L-9 and -10) — *K.E. Ashton*	4
*	New Perspectives on the Amisk Group and Regional Metallogeny, Douglas-Phantom Lakes Area, Northern Saskatchewan — *D.J. Thomas*	13
	North Lake Gold Deposit: A Model for Arenite-hosted Gold — *D.J. Thomas*	21
*	Bedrock Geological Mapping, Mystic Lake - West Arm, Schist Lake Area (Part of NTS 63K-12) — *B.A. Reilly*	25
*	Bedrock Geology, Tulabi-Church Lakes Area: Derivation and Significance of Porphyroclastic Gneisses in the Pelican Window — *J.F. Lewry*	36
	Lithogeochemical Studies in the Flin Flon-Amisk Lake Area — *B.R. Watters*	44
	The Wollaston Group and underlying Archean Basement in Saskatchewan: Subsurface and Bedrock Geological Mapping in 1990 — *Irvine R. Annesley and Catherine Madore*	48
	U-Pb Sphene/Zircon Geochronological Investigations — *G.D. Delaney, L.M. Heaman, S. Kamo, R.R. Parrish, W.L. Slimmon and B.A. Reilly*	54
	Structural Controls on Gold Deposits in the Star Lake and Island Lake Plutons — *R.G. Roberts*	58
*	Field Observations on the Corner Lake and Tower East Gold Showings, Byers Fault Area — *P.L. Schwann*	60
	Oxygen, U-Pb and Pb-Pb Isotope Systematics in Uraninite from Complex U-Au-PGE Vein-type and Unconformity-type Uranium Deposits in Northern Saskatchewan — *T.K. Kyser, T. Kotzer and T.I.I. Sibbald*	64
	Reconnaissance Geological Study of the Seabee Gold Deposit, Glennie Domain — *D.J. Schultz*	70
*	Bedrock Geology and Gold Metallogenesis, Nielsen Lake Area, Tabbernor Fault Zone — *K.H.Wilcox*	74
	Petrogenetic Aspects of the Goldfields Granites, Beaverlodge Area, Saskatchewan — *Edward C. Appleyard*	84
	Reconnaissance P-T-t Isotope Studies of Hydrothermal Fluids in the Tabbernor Fault Zone, Saskatchewan — *M.P. Fields and R. Kerrich*	94
*	Metallogenic Environments, Deception Lake Area — *Charlie Harper*	96
*	Rare Earth Element Mineralization in the Athabasca Group - Maw Zone — *D.G. MacDougall*	103
*	Pyett Lake Pegmatites and Fluoritic Granites, Peter Lake Domain (NTS Area 64E-5) — *D.G. MacDougall*	106

Geochemistry of Miscellaneous Pegmatites in the Wollaston, Peter Lake and Glennie Domains ..... *D.G. MacDougall* 113

Aeromagnetic Anomaly Ground Check for Kimberlite in the Precambian Shield Area ..... *W.L. Slimmon* 116

Mineralized Core Collection ..... *A.J. Gracie* 118

Contributed Northern Geoscience Reports

Location of Projects 122

The Snowbird Tectonic Zone, Stony Rapids Area, Northern Saskatchewan ..... *Simon Hanmer, Shao Chengji, Mark Darrach and Chris Kopf* 123

Lithogeochemistry and XRD Mineralogy of the Martin Group and Related Rocks, Greater Beaverlodge Area, Saskatchewan ..... *David H. Quirt* 129

Age of Granitoids from the Flin Flon Domain: An Application of the Single-zircon Pb-evaporation Technique ..... *Kevin M. Ansdell and T.K. Kyser* 136

Rb-Sr Geochronology of the Lodge Bay Granite, a ca. 3.0 Ga Basement in the Beaverlodge Area, Saskatchewan ..... *Michael Bikerman, Keith Bell and John Blenkinsop* 143

Metasomatic Host-rock Alteration at the Frontier Gold Prospect, Goldfields Area, Saskatchewan ..... *David H. Quirt* 146

Fluid History of the Athabasca Basin and its Relation to Uranium Deposits ..... *T. Kotzer and T.K. Kyser* 153

Site Investigation of a Biogeochemical Gold Anomaly near Wadin Bay, Lac La Ronge ..... *C.E. Dunn and P.L. Schwann* 158

Fluid Inclusion, Stable Isotope and Microprobe Data from the Jasper Zone Lode Gold Deposit, La Ronge Domain ..... *F. Hrdy, T.K. Kyser and R.T. Kusmirski* 163

Petrology of Some Mafic Gneisses, Black Birch Lake, Saskatchewan ..... *S. Orrell and J. Tangeman* 166

Petroleum Geology

Location of Projects 174

Ordovician Hydrocarbon Reservoirs, Herald and Yoeman Formations (Red River), Southeastern Saskatchewan ..... *F.M. Haidl* 176

Seismic Mapping of the Northern Williston Basin ..... *Chengnan Zhu and Zoltan Hajnal* 187

Progress of the Pore Geometry Reservoir Model Study for the Devonian Winnepegosis Member in Southeast Saskatchewan ..... *Melinda Yurkowski* 190

Lithogeochemical Study of the Cretaceous in Central Saskatchewan: Preliminary Report ..... *C.E. Dunn* 193

A Paleo-flow Model for a Devonian Winnipegosis Reef, Southeastern Saskatchewan ..... *Ning Quiang and D.M. Kent* 198

Industrial Minerals

Review of Industrial Mineral Investigations ..... *Paul Guliov and Malcolm Gent* 206

Fluid Flow Events in the Elk Point Basin of Western Canada as Recorded in Evaporite Minerals ..... *D. Chipley, T.K. Kyser and T. Danyluk* 211

Stable Isotope Evidence for the Petrogenesis of Carnallite in the Middle Devonian Prairie Evaporite Formation, Saskatchewan ..... *G.D. Koehler, T.K. Kyser and T. Danyluk* 218

Computer Modelling Saskatchewan's Coalfields
Using an Expert System ..... *J.D. Hughes and W.J. McDougall* 223

Appendices

Titles and Abstracts 239

Acknowledgments 245

Organization Chart 246

Staff List ..... Inside back cover

*Asterisked reports are accompanied by maps or sections, as listed on the inside cover of the map package.

Review

During the past year, exploration for metallic minerals in the province, as elsewhere in Canada, has waned significantly. Uranium and gold exploration levels have been much reduced, although production and test mine developments and advanced exploration continue on a number of properties. Base metals have seen some renewed interest and provide a real opportunity for northern exploration, highlighted by the discovery at McIlvenna Bay, and the promise of further finds particularly under the feather-edge of Phanerozoic sediments along the eastern Shield margin. Oil and gas exploration has yet to respond significantly to the higher prices engendered by the Middle East crisis. Industrial minerals are a reserve yet to reach their full potential; while potash remains the core industrial mineral, such commodities as clays, dimension stone, high-salinity brines and silica sands have development potential. Meanwhile the diamond exploration play in the province, which commenced in 1988, continues unabated.

Although the Saskatchewan Geological Survey mandate has in the past been seen primarily as relevant to the development of the mineral industry, there is a rapidly growing need for the use of regional geoscientific data in matters of environmental concern. These concerns include not only the particular environment of mining operations, but a growing range of fields including such things as water supply, epidemiology, land use management, and waste disposal in general. Apart from the basic value of geological mapping and other framework projects, regional geochemical surveys and studies are particularly applicable, and there is expected to be a stronger emphasis on these areas in future years.

The northern geoscience program this year has focussed on projects related to gold and particularly base metal exploration. The main emphasis of this program is to improve the basic geological map of the southeastern part of the Precambrian Shield area, which is currently perceived as having the highest mineral exploration potential (projects 1.03, 1.04A, 1.05, 1.06 and 2.05). Understanding of the geological framework of the north is being supported by other studies including lithogeochemistry, geochronology, isotope geology etc. (1.07, 1.08, 1.09 and 2.09; see also A to D and J on pages ix). A diversity of mineral deposit studies are also in progress in the Precambrian Shield region; on gold (1.04B, 2.01A and B, 2.02, 2.04, 2.06, 2.07; E and H), base metals (2.08 and 2.10), uranium (F), polymetallic uranium + gold + PGE (2.03) and rare metals (2.11).

In 1989 a program aimed at stimulating and assisting the diamond exploration play in the province was commenced, and was continued this year (1.11, 3.02A and 4.04). There are indications that many new kimberlite pipes have been found in the Phanerozoic region of the province, although at this time no diamonds of economic dimension have been reported.

The Saskatchewan Geological Survey embarked this year on a pilot study in the Glennie Domain which will permit us to process and enhance regional geophysical and other regional numeric data using RTI/CAD software (1.10). During the past year substantial funds were also dedicated to upgrading microcomputer systems. Several database files have been published and are being made available in microcomputer formats. These include the Assessment Work Catalogues, Mineralized Core Collection Inventory (2.12), Mineral Deposits Inventory, Saskatchewan Precambrian Bibliography, and the Geochronology File. Internal map production methods are also being computerized through the acquisition of new software, and preliminary planning is in hand towards establishing Geographical Information Systems (GIS).

This year a number of ongoing projects are not reported in the Summary, generally because full final reports are in preparation or press, e.g. Malcolm Gent's report on Phanerozoic Anomalies of Saskatchewan, and Gary Delaney's report on Glennie Gold Deposit Environments. Also during this year several final reports are due to be published on projects emanating from the 1984-88 Mineral Development Agreement. These will include reports by Dave Thomas and Charlie Harper which summarize the the Geology of the Central Metavolcanic Belt, with coloured maps at 1:50,000 scale. A similar report by Gary Delaney will be published with a coloured geological map at 1:50,000 scale for the Laonil-Uskik Lakes area.

Northern Geoscience and Mineral Deposit Studies

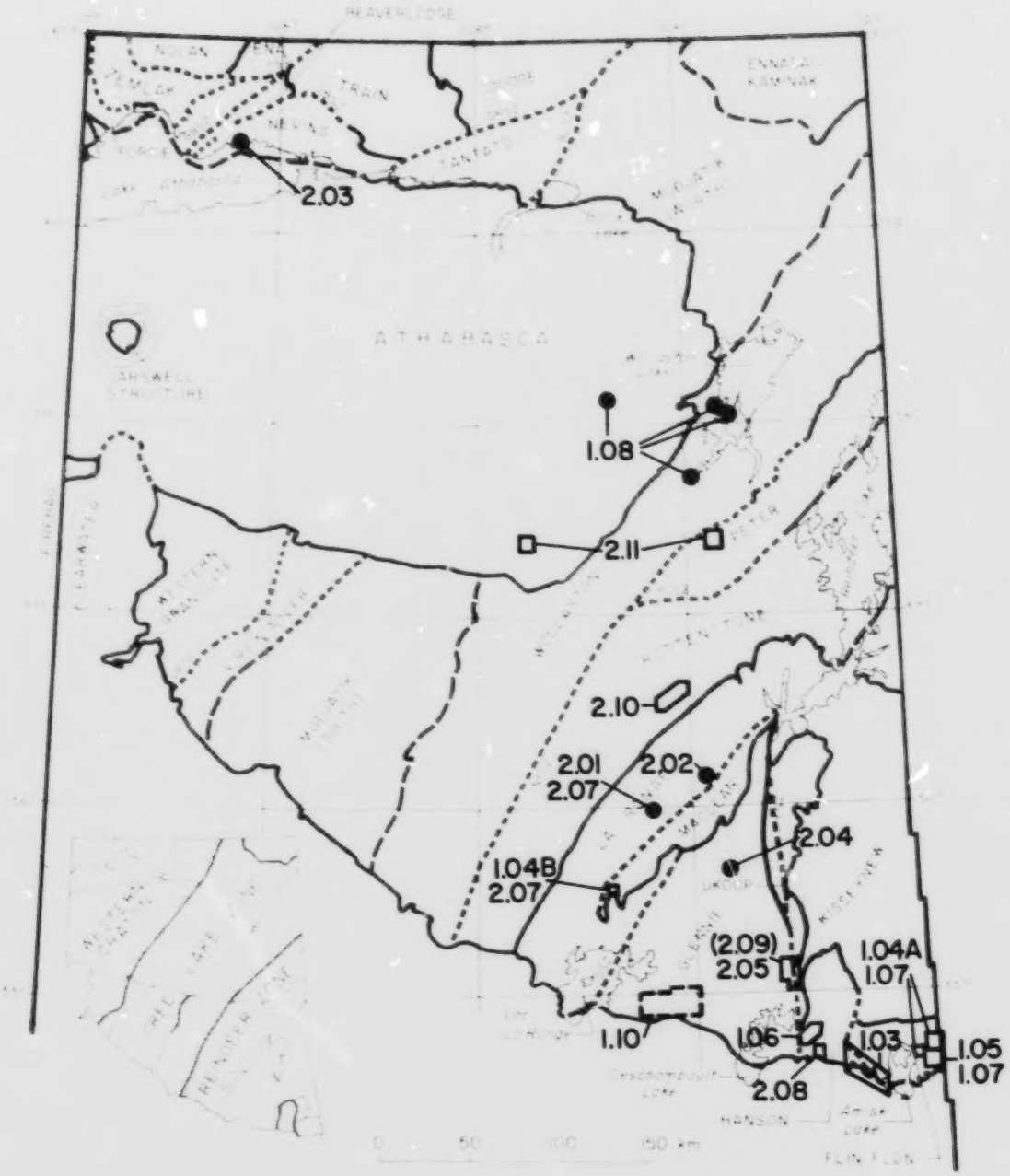

Location of Northern Geoscience and Mineral Deposit Studies projects or reports in hand 1990-91 (excluding compilation maps). Numbers on map refer to the Mineral Industry Diversification Program (MIDP) project number listed opposite. The base map shows in abbreviated form the location of the main lithostructural domains in northern Saskatchewan.

Proj. No.	Data No.*	Title of Paper or Project
1.03	9047	Bedrock Geological Mapping, Snake Rapids Area, Flin Flon Domain (Parts of NTS 63L-9 and -10) *K.E. Ashton* (F,M)
1.04A	9012	New Perspectives of the Amisk Group and Regional Metallogeny, Douglas-Phantom Lakes Area *David J. Thomas* (F,M)
1.04B	9012	North Lake Gold Deposit: A Model for Arenite-hosted Gold *D.J. Thomas* (F)
1.05	9023	Bedrock Geological Mapping, Mystic Lake-West Arm, Schist Lakes Area (Part of NTS 63K-12) *B.A. Reilly* (F,M)
1.06	9017	Bedrock Geology, Tulabi-Church Lakes Area: Derivation and Significance of Porphyroclastic Gneisses in the Pelican Window *J.F. Lewry* (F,M,C)
1.07	9037	Lithogeochemical Studies in the Flin Flon-Amisk Lake Area *B.R. Watters* (F,C)
1.08	9007	The Wollaston Group and Underlying Archean Basement in Saskatchewan: Subsurface and Bedrock Geological Mapping in 1990 *I. Annesley and C. Madore* (W,F,C)
1.09	9028	U-Pb Sphene/Zircon Geochronological Investigations in 1990-91 *G.D. Delaney, L.M. Heaman, S. Kamo, R.R. Parrish, W.L. Slimmon and B.A. Reilly* (J,W)
1.10		Enhanced Geomagnetics, Glennie Domain *G.D. Delaney and B. Czornobay* (O)
1.11	9026	Sub-Phanerozoic Basement Studies *K.D. Collerson and J.F. Lewry* (C,O)
2.01	9029	Structural Controls on Gold Deposits in the Star Lake and Island Lake Plutons *R.G. Roberts* (F,C)
2.02	9035	Field Observations on the Corner Lake and Tower Lake East Gold Showings, Byers Fault Area *P.L. Schwann* (F,M)
2.03	9034	Oxygen, U-Pb and Pb-Pb Isotope Systematics in Uraninite from Complex U-Au-PGE Vein-type and Unconformity-type Uranium Deposits in N.Saskatchewan *T.K. Kyser, T. Kotzer and T.I.I. Sibbald* (F,C)
2.04	9049	Reconnaissance Geological Study of the Seabee Gold Deposit, Glennie Domain *D.J. Schultz* (F,C)
2.05	9040	Bedrock Geology and Gold Metallogenesis, Nielsen Lake Area, Tabbernor Fault Zone *K.H. Wilcox* (F,M)
2.06	9022	Glennie Gold Deposit Environments *G.D. Delaney* (F,O)
2.07	9038	Petrogenetic Aspects of the Goldfields Granites, Beaverlodge Area *Edward C. Appleyard* (C)
2.08	9006	Metallogenic Environments, Hanson Lake Area *T.I.I. Sibbald* (F,O)
2.09	9048	Reconnaissance Isotopic Study of Hydrothermal Fluid History in the Tabbernor Fault Zone *M. Fields and R. Kerrich* (C,F)
2.10	9011	Metallogenic Environments, Deception Lake Area *Charlie Harper* (F,M)
2.11A	9033	Rare Earth Element Mineralization in the Athabasca Group, Maw Zone *D.G. MacDougall* (F,M)
2.11B	9033	Pyett Lake Pegmatites and Fluoritic Granites, Peter Lake Domain (NTS Area 64E-5) *D.G. MacDougall* (F,M)
2.11C	9033	Geochemistry of Miscellaneous Pegmatites in the Wollaston, Peter Lake and Glennie Domains *D.G. MacDougall* (F)
2.12	9005	Mineralized Core Collection *A.J. Gracie* (F,W)
3.02A	9002	Aeromagnetic Anomaly Ground Check for Kimberlite Occurrences in the Precambrian Shield Area *W.L. Slimmon* (F)

* Database Number (used for samples etc.)
O Report not included in this publication
F Field component in 1990
W Project covered wide area (not shown on map)
C Contract project in 1990
J Joint venture with SEM in 1990
M Geological or geochemical map(s) in accompanying package

Geology of the Snake Rapids Area, Flin Flon Domain (parts of NTS 63L-9 and -10)

K.E. Ashton

Ashton, K.E. (1990): Geology of the Snake Rapids area, Flin Flon Domain (parts of NTS 63L-9 and -10); *in* Summary of Investigations 1990, Saskatchewan Geological Survey; Saskatchewan Energy and Mines, Miscellaneous Report 90-4.

A 1:20,000 scale mapping project has been initiated along the southern margin of the exposed Precambrian Shield. The purpose is to provide a basis for the extrapolation of major geological units into the sub-Paleozoic portion of the Shield as a first step in assessing the mineral potential of that area. Work during the summer of 1990 was centred about 45 km southwest of Flin Flon, Manitoba and covered an approximately 10 km wide strip between Amisk and Attree Lakes. The area can be reached from the Sturgeon-Weir River which is accessible from the Hanson Lake Road (Highway 106) at Maligne Lake. Four well-maintained portages must be crossed between the road and Amisk Lake which is also readily accessible by boat from Denare Beach. Several long straight sections of the river allow further access by float-equipped aircraft.

Topographic relief is variable, ranging from 30-35 m in the Amisk and Attree Lakes areas to 15-20 m in the central, southern and southeastern lowlands. This is reflected in the degree of surface exposure which is excellent in the low-grade volcanic rocks of the Amisk Lake area and in the progressively higher-grade rocks approaching Attree Lake, but poor throughout the intervening stretch of the Sturgeon-Weir River.

Field work was carried out by a two-person mapping crew from early June until the end of August and consisted of pace or hip chain and compass traverses supplemented with shoreline work.

Early reconnaissance geological mapping in the area was carried out by McInnes (1914), Bruce (1918), Mawdsley (1934) and Wright and Stockwell (1934). More recent government surveys include 1"=1/2 mile mapping (Byers and Dahlstrom, 1954) of the Amisk Lake area (63L/9) and 1"=1 mile mapping (Eastwood, 1949; Johnson, 1967) of the Snake Rapids area (63L/10). In addition, a detailed volcanological study was carried out along the western side of Amisk Lake (Fox, 1976a). Previous work was compiled and used to help establish contacts in areas of low station density.

1. General Geology

The area studied represents the southwestern edge of the Flin Flon Domain. The boundary between the northwestern Flin Flon Domain and Hanson Lake Block to the west was placed along the north-south section of the Sturgeon-Weir River and interpreted as either a structural discontinuity or an unconformity by MacQuarrie (1979). Subsequent work showed that the inferred boundary was marked by an oblique dextral-reverse high-strain zone termed the Sturgeon-Weir Shear Zone (Ashton *et al.*, 1987; Ashton and Wilcox, 1988). Mapping in 1990 showed that the domainal boundary defined by the Sturgeon-Weir Shear Zone extends through Attree Lake in the northwestern part of the study area (Figure 1). On a 1:250,000 scale compilation of the region, Macdonald (1981) also included the area south of the northwest-striking section of the Sturgeon-Weir River as part of the Hanson Lake Block. In that area, the boundary was interpreted as the Sturgeon-Weir Fault, (Byers and Dahlstrom, 1954), here renamed the Spruce Rapids Shear Zone to focus attention on its ductile nature and to distinguish it from the north-striking Sturgeon-Weir Shear Zone.

Supracrustal rocks in the area include: Amisk Group volcanic and volcaniclastic rocks in the east, a sedimentary sequence in the northwest tentatively thought to be derived from the volcanic suite, and a poorly exposed mixture of volcanic and sedimentary rocks of uncertain origin south of the Spruce Rapids Shear Zone.

Stratigraphic top indicators are generally not preserved, but the oldest supracrustal rocks are tentatively thought to be mafic volcanic rocks, which are best exposed in an early refolded structure in the Muskeg Bay area named the Wolf Lake Fold (Figure 2). Felsic to intermediate volcanic and volcaniclastic rocks are in sheared contact with the mafic suite. Sulphide mineralization occurs along and adjacent to this early structural discontinuity, named the Wolf Lake Shear Zone, which also appears folded by the later Muskeg Bay Synform (Byers and Dahlstrom, 1954). A sequence of heterogeneous sedimentary rocks is locally interlayered with the felsic to intermediate volcanic suite and underlies much of the western part of the area. Sub-concordant gabbro and feldspar porphyry dikes intrude the supracrustal rocks and are particularly abundant in the vicinity of the sheared contact between the mafic and felsic to intermediate volcanic suites.

The supracrustal rocks are intruded by a number of large hornblende granodioritic and quartz monzodioritic plutons. In addition, folded biotite granodiorite sheets are common in the vicinity of Snake Rapids. Pink to white, fine-grained to largely pegmatitic granite is abundant adjacent to the Sturgeon-Weir River and represents the latest igneous event.

The Precambrian rocks are unconformably overlain by flat-lying Paleozoic sandstones and dolostones to the south.

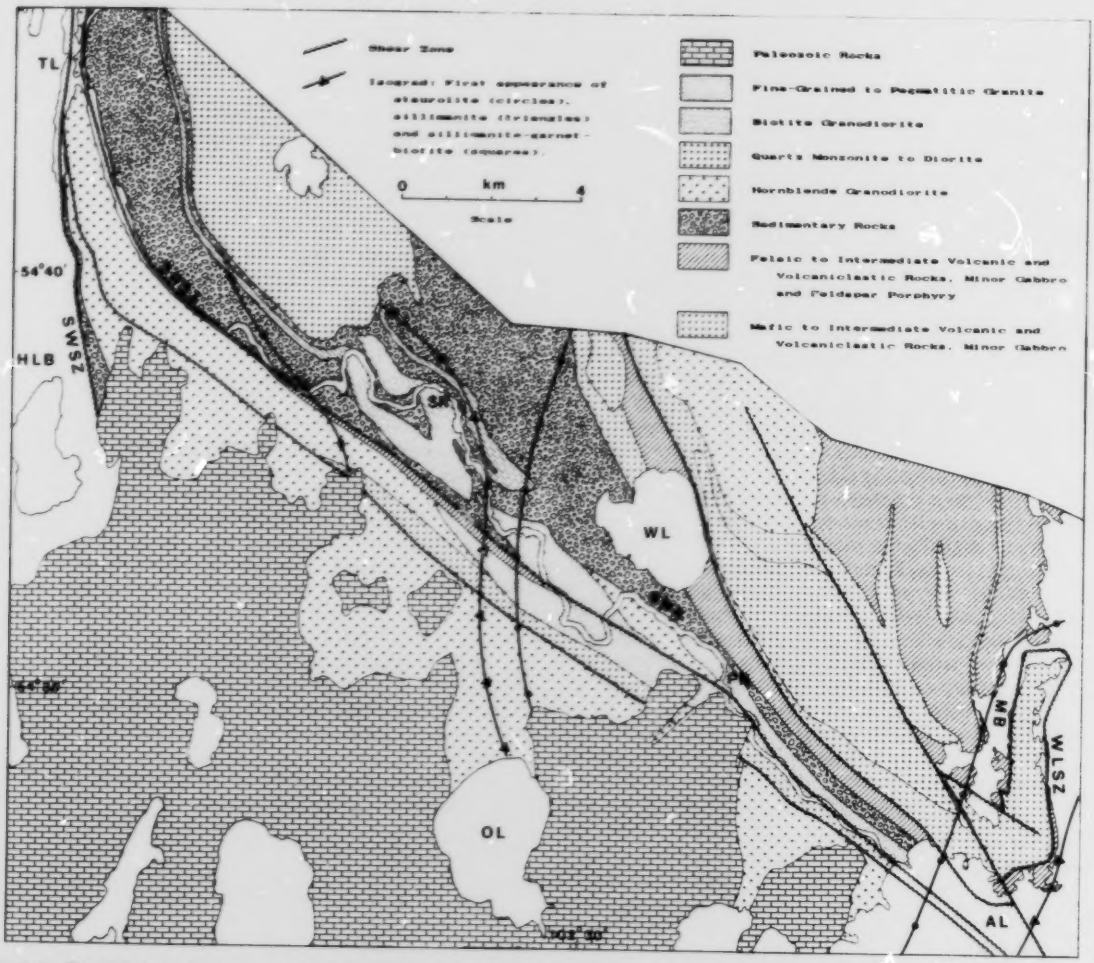

Figure 1 - Simplified geological map of the Snake Rapids area (AL - Amisk Lake, MB - Muskeg Bay, OL - Oskatukaw Lake, PR - Spruce Rapids, SR - Snake Rapids, SWR - Sturgeon-Weir River, TL - Attree Lake, WL - Wolf Lake, HLB - Hanson Lake Block, SRSZ - Spruce Rapids Shear Zone, SWSZ - Sturgeon-Weir Shear Zone, WLSZ - Wolf Lake Shear Zone).

All of the Precambrian rocks in the area have been metamorphosed and display an increase in grade from greenschist facies in the northeast to amphibolite facies in the southeast and northwest.

The first recognized period of deformation produced minor folding and a strong regional axial planar foliation. The early Wolf Lake Fold in the Muskeg Bay area (Figure 2) is attributed to this D_1 deformational event. The folded Wolf Lake Shear Zone is also thought to have formed during syn- to post-D_1 time. D_2 deformation is believed to have produced most of the northwest- and southeast-plunging minor and megascopic folds, as well as a number of apparently sinistral northeast-dipping shear zones. Rare outcrop-scale interference patterns in the north-central part of the area result from the interaction of D_2 folds with east-plunging D_3 minor folds. D_4 deformation is restricted to the oblique dextral-reverse Sturgeon-Weir Shear Zone.

2. Unit Descriptions

a) Mafic to Intermediate Volcanic and Volcaniclastic Rocks

Mafic volcanic and volcaniclastic rocks (Am) are best exposed in the core of the Wolf Lake Fold, but are also a minor component of the felsic to intermediate volcanic suite. Most weather dark green and are typical of greenschist facies rocks, containing locally preserved pillows and amygdules filled with epidote, plagioclase, quartz and/or carbonate. An apparent volcaniclastic texture characterizing several outcrops in the east-central Muskeg Bay area is attributed to patchy epidote alteration of mafic volcanic material which has also effected crosscutting gabbroic dikes. Traces of disseminated iron sulphides are common in most of the mafic volcanic and volcaniclastic rocks.

Highly strained outcrops of mafic volcanic rocks adjacent to the felsic to intermediate volcanic suite contain

an abundance of gabbro and feldspar porphyry dikes. Amphibolite-facies assemblages in black-weathering, locally garnetiferous amphibolites adjacent to the contact appear spatially related to occurrences of the feldspar porphyry and may have resulted from contact metamorphism.

Fox (1976b) conducted a geochemical study of mafic rocks in the western Amisk Lake area and concluded that they: 1) are tholeiitic, 2) display an upward evolution from olivine- to quartz-normative compositions and 3) exhibit juvenile island arc affinities. This is consistent with mafic rocks characterizing most of the Flin Flon Domain (Parslow and Gaskarth, 1988; Bailes and Syme, 1989), but distinct from the oceanic, rift-related suites of the east Amisk (Parslow and Gaskarth, 1988) and Athapapuskow (Syme, 1987) areas.

Intermediate volcanic and volcaniclastic rocks and intrusive equivalents (Ai) occur within both the mafic and felsic volcanic suites in the eastern part of the area and may broadly represent a stratigraphic transition.

Little is known about the units designated as intermediate rocks in the central part of the area due to limited exposure. The extensive intermediate unit south of the Sturgeon-Weir River is quite heterogeneous in the east where exposures of weakly layered to almost massive amphibolites along the southern shore of the river were previously mapped as sedimentary and mafic volcanic rocks (Byers and Dahlstrom, 1954). The western extension is based on rare garnetiferous outcrops containing minor interlayered felsic volcanic rocks.

b) Felsic to Intermediate Volcanic and Volcaniclastic Rocks

Felsic to intermediate volcanic and volcaniclastic rocks (Af) of the eastern part of the area include a wide range of rock types. Most are white- to grey-weathering biotite - quartz - feldspar ± hornblende ± white mica dacitic to

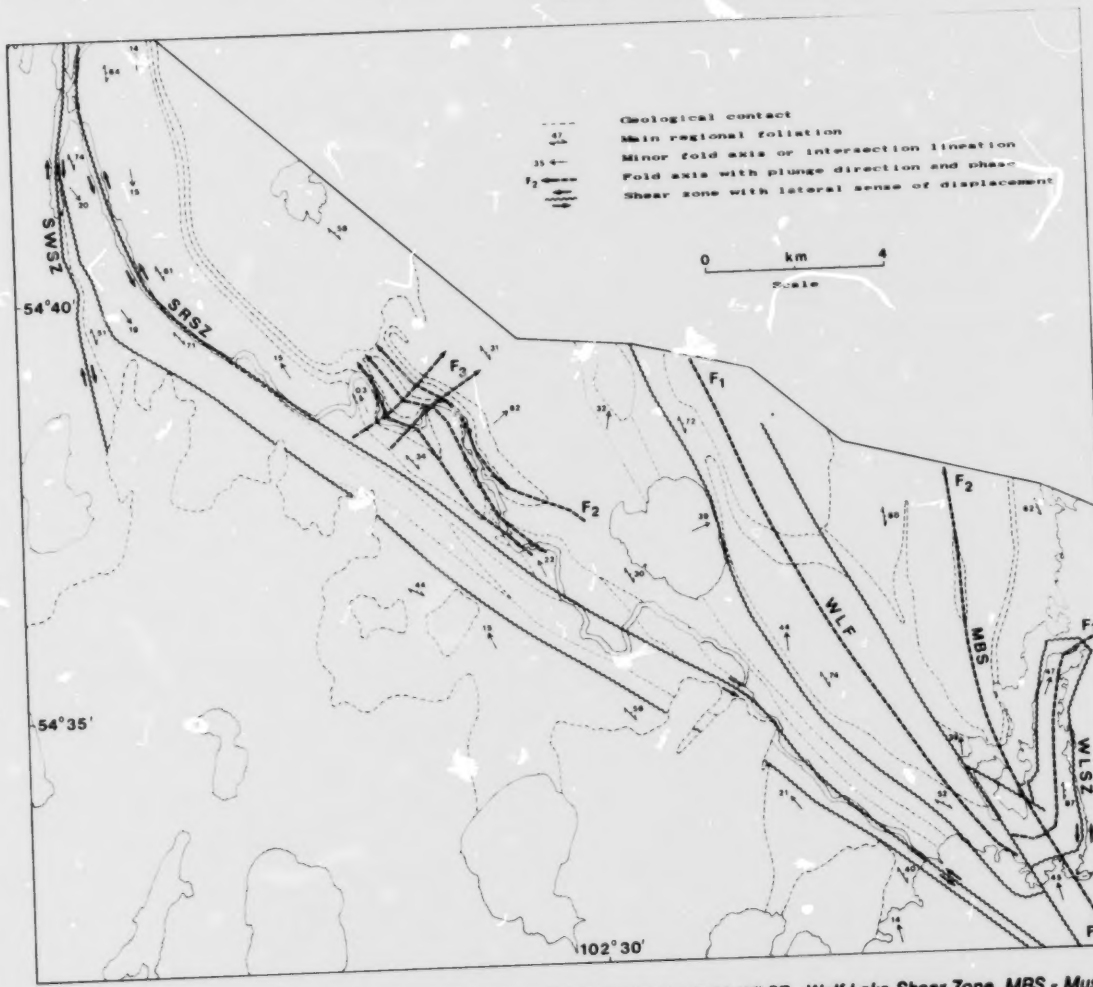

Figure 2 - Sketch map showing generalized structural features (WLF - Wolf Lake Fold, WLSZ - Wolf Lake Shear Zone, MBS - Muskeg Bay Synform, SRSZ - Spruce Rapids Shear Zone, SWSZ - Sturgeon- Weir Shear Zone).

andesitic flows and tuffaceous rocks. Accessory minerals include apatite, zircon, tourmaline, sphene, magnetite and iron sulphides. Many samples also contain minor carbonate, chlorite and epidote as late phases. Occurrences of garnet and staurolite in the Muskeg Bay area are broadly associated with zones of iron sulphide mineralization and are thought to result from pre-metamorphic hydrothermal alteration.

An extensively exposed plagioclase-phyric andesite north of Muskeg Bay and west of Barton Lake may be intrusive in origin. Apparent polygonal jointing locally preserved in fine-grained dacitic rocks of the central Muskeg Bay area also appears to indicate a shallow sub-volcanic origin.

Felsic to intermediate volcanic rocks are well layered, fine grained, heterogeneous and contain abundant iron sulphides in the Muskeg Bay area. Along the shore of Amisk Lake east and south of Muskeg Bay, the felsic to intermediate volcanic suite is difficult to trace due to the abundance of gabbro and feldspar porphyry dikes. Recognition of the felsic volcanic component of rocks in that area is further hindered by their highly strained nature, but locally preserved fragmental textures indicate that the unit is continuous. Lateral continuity of the felsic to intermediate suite further west is indicated by the recognition of volcaniclastic features north of the mouth of the Sturgeon-Weir River and along the eastern shore of Wolf Lake.

The poorly exposed westernmost occurrence of felsic to intermediate volcanic rocks outcrops along both sides of the river as highly strained hornblende - biotite - quartz - feldspar rocks containing several percent disseminated iron sulphides. They are thought to be conformable with the intermediate volcanic suite to the south.

Coarse volcaniclastic rocks (Ap), including predominantly heterolithologic volcanic breccias and extensive units of lithic tuffaceous rocks, are very common in the east. The best exposures are on the islands and shores of Amisk Lake and Muskeg Bay where locally preserved swallow-tail shapes and reaction rims around individual clasts indicate a pyroclastic origin for most occurrences. Most of the clasts are felsic to intermediate aphyric rocks and porphyries but rare mafic compositions were also noted. In some occurrences, clasts are more rounded and exhibit a wider range of compositions, possibly indicating epiclastic deposition as debris flows. Typical units of heterolithologic volcanic breccia on the islands of western Amisk Lake appear to be at least several tens of metres thick and are associated with lithic tuffs, rare felsic volcanic rocks and turbiditic wackes.

A detailed geochemical study in the adjacent area to the north led to the conclusion that felsic to intermediate volcanism in the western Amisk Lake area evolved as part of a calc-alkaline island arc succession (Walker and Watters, 1982).

c) Sedimentary Rocks

Epiclastic rocks include: heterogeneous calcic and aluminous wackes with minor argillite and siltstone (As), homogeneous aluminous wackes (Aw), and interlayered arenites and aluminous wackes (Aa). They are most extensive in the western and central parts of the area where their relationship to the volcanic rocks is unclear, but thin units of heterogeneous siltstone - argillite rhythmites and turbiditic wackes are interlayered with coarse pyroclastic and felsic volcanic rocks along the shore of Amisk Lake. Eastern occurrences of the epiclastic rocks are well preserved at greenschist facies metamorphic grade and locally display graded bedding, flame structures and channel fill.

The thinly layered siltstone - argillite weathers white and grey and commonly grades into interlayered calcic and aluminous turbiditic wacke. The calcic varieties contain about 30 percent combined amphibole and biotite with minor garnet in higher-grade rocks along the Sturgeon-Weir River. More aluminous compositions are biotite rich, many containing pink euhedral garnet characteristic of Amisk wackes in the Kisseynew Gneiss Belt to the north (Ashton and Wheatley, 1986). Staurolite-, sillimanite- and sillimanite - garnet - biotite assemblages characterize rocks of progressively higher grade. Apatite, zircon, tourmaline and opaque minerals occur as detrital grains in most rocks, and chlorite, white mica and sphene/rutile are generally present as late phases. Extensive areas in the central and western portions of the area are underlain by a more homogeneous sequence of these layered, grey- to rusty-weathering aluminous wackes.

Very fine-grained opaque material thought to be carbonaceous in composition is present in some thin sections of greenschist facies aluminous wackes but graphite is notably absent in rocks of higher metamorphic grade. This represents the main difference between these wackes and similar rocks of the Kisseynew Gneiss Belt (Ashton and Wheatley, 1986; Ashton *et al.*, 1987), and may indicate deposition in a proximal environment along the shallow-water flanks of volcanic edifices rather than in the deeper, more distal, basinal environment generally suggested for graphitic wackes of the Kisseynew Gneiss Belt (Gilbert *et al.*, 1980; Zwanzig, in press).

In the extreme northwest, resistant white-weathering arenaceous sediments are interlayered with calcic and aluminous wackes on a scale of a few centimetres to tens of metres. The arenites are mainly biotite - quartz - feldspar rocks but many contain abundant white mica and sillimanite in the form of thin fibrolitic sheets and faserkiesel. The presence of minor amounts of fine-grained, pink euhedral garnet characteristic of medium-grade Amisk sedimentary rocks, combined with the absence of magnetite, distinguish these rocks from Missi Group (Bruce, 1918; Wright, 1933) arenites which unconformably overlie the Amisk Group in the Flin Flon area and in the southern flank of the Kisseynew Gneiss Belt (Byers and Dahlstrom, 1954; Ashton and Wheatley, 1986; Ashton *et al.*, 1987).

d) Syn- to Post-Amisk Intrusions

Gabbro

Gabbroic dikes and small intrusions (Gb) are extremely common within the volcanic suite in the east. Most outcrops of mafic volcanic rocks contain at least a small component of intrusive material but small gabbroic bodies are also common in the felsic to intermediate suite. Most of the gabbros are homogeneous, dark green to black depending on metamorphic grade, and characterized by 1-3 mm amphibole porphyroblasts. Gabbroic dikes are particularly common along or adjacent to the sheared contact zone between the mafic and felsic to intermediate volcanic suites. Up to 30 percent carbonate in the form of centimetre-scale layers has been derived during shearing from some medium-grained black gabbroic amphibolites in that zone.

A distinctive intrusion of medium- to coarse-grained diorite or anorthositic gabbro (Ga) northeast of Wolf Lake consists of about 70 percent plagioclase and 30 percent green amphibole.

Feldspar Porphyry

Feldspar porphyry dikes (Pf), ranging in composition from granite to quartz diorite (Byers and Dahlstrom, 1954), are particularly common along the Wolf Lake Shear Zone, but also occur within the felsic to intermediate volcanic suite. Samples may be white or grey, fine to very fine grained and contain feldspar phenocrysts up to 6 mm. Quartz phenocrysts up to 10 mm occur in rare phases within porphyries of the southeastern part of the area. Phenocrysts are apparently absent in some felsite dikes but this may represent a recognition problem due to later deformation. Most of the porphyries are biotite - quartz - feldspar rocks containing small amounts of white mica and/or chlorite. More intermediate compositions contain minor hornblende. Accessory minerals include apatite, zircon, tourmaline, rutile/sphene and opaque minerals. Plagioclase phenocrysts are locally glomeroporphyritic and quartz phenocrysts are generally polygonized.

The feldspar porphyries clearly intrude the gabbros and at least some of the mixed sedimentary wackes suggesting that they represent the latest syn-volcanic magmatism.

e) Late Intrusions

Hornblende Granodiorite

A number of medium- to coarse-grained hornblende granodioritic plutons (Gdh), ranging from granodiorite to tonalite and quartz diorite in composition, intrude the volcanic suite in the east and also appear to intrude the supracrustal sequence south of the Sturgeon-Weir River where exposed contacts are rare. Most of the hornblende granodioritic rocks weather grey and contain 15-30 percent combined biotite and hornblende. Magnetite is locally present.

The hornblende granodiorite north of Wolf Lake, termed the Muskeg Bay Granodiorite, has a wide migmatitic margin containing layers and blocks of amphibolitic material and abundant granitoid dikes and pegmatite.

The hornblende granodioritic intrusion extending throughout much of the southern part of the area has been named the Oskatukaw Lake Granodiorite. It is only weakly deformed in the Amisk Lake area where it contains about 3 percent discrete subhedral epidote of possible igneous origin (Gdhe), and is intruded by white aplitic granodioritic dikes and late medium-grained to pegmatitic granite. The northwestward extension of the pluton largely consists of medium-grained hornblende - biotite - quartz - feldspar orthofoliates (see Ashton and Leclair, 1990). It is progressively more deformed approaching the Attree Lake area, taking on a finer-grained recrystallized appearance which caused previous workers to classify them as paragneisses (Johnson, 1967). Epidote is absent as a possible primary phase due to the higher metamorphic grade. Thin discontinuous units of fine-grained sheared gneiss within the orthofoliates (Gdhg) mark internal zones of high strain. Thicker units of sheared gneissic to migmatitic rocks appear to contain a large intermediate to mafic supracrustal component. Hornblende-free, medium-grained biotite granodiorite (Gdhb) characterizes both eastern and western contacts at the northwestern end of the pluton which are bounded by thin units of sheared paragneiss through the Sturgeon-Weir River and the river extending southward from Attree Lake. Along the western margin, the biotite granodiorite is in contact with well layered, heterogeneous paragneisses containing abundant shear-banded pegmatite and minor pseudotachylite. The eastern contact is characterized by a medium- to coarse-grained, weakly layered unit which is similar in appearance to the biotite granodioritic component of the pluton but contains abundant garnet and minor sillimanite porphyroblasts. The flanking biotite granodiorite pluton margins may represent zones of hornblende granodiorite which have undergone Ca depletion during shearing. Further Ca depletion could account for the appearance of garnet and sillimanite along the eastern pluton contact due to the associated relative aluminum enrichment. At present, the sillimanite-bearing rocks are considered to be paragneisses but the possibility that they are sheared and Ca-depleted granodiorites cannot be discounted.

Quartz Monzonite to Diorite

A suite of medium- to coarse-grained quartz monzodioritic plutons intrudes the Amisk supracrustal sequence north of the Sturgeon-Weir River. They differ from the hornblende granodiorites by having higher hornblende to biotite ratios and relatively low proportions of free quartz. Although there appears to be considerable compositional variation, most intrusions consist of an early grey-weathering phase of quartz monzodiorite to diorite (Md) and/or a later pink quartz monzonitic phase (Mz). In addition, medium-grained hornblende granodioritic and white tonalitic dikes and small irregular bodies (Mt) intrude the two main phases.

The largest of these quartz monzonite to diorite intrusions is the Snake Rapids Pluton (Eastwood, 1949; Johnson, 1967) in the northwestern part of the area. Its early mafic phase contains minor relict clinopyroxene, variable amounts of biotite, heterogeneous amphiboles resulting from the overprinting effects of metamorphism, and accessory sphene, apatite, tourmaline, zircon and opaque minerals. The abundance of quartz and K-feldspar is highly variable.

The quartz monzonitic to dioritic plutons are thought to be part of a more extensive suite of intrusions which include the ca. 1840 Ma (Ansdell and Kyser, this volume; Ashton and Hunt, in prep.) Neagle Lake Pluton (Pearson, 1951; Byers and Dahlstrom, 1954) and a similar but more deformed body on the western side of Granite Lake (Ashton *et al.*, 1987). Tectonic inclusions of similar rocks were also found in the Sturgeon-Weir Shear Zone to the north (Ashton, in prep.).

Biotite Granodiorite

White medium-grained biotite granodiorite (Gdb) forms a homogeneous resistant unit in the central and northwestern parts of the area. It has been tightly folded on a regional scale and locally exhibits evidence of high strain parallel to the main regional foliation. Typical rocks contain 5-10 percent biotite with minor amounts of accessory apatite, zircon, monazite(?) and opaque minerals.

Fine-Grained to Pegmatitic Granite

Fine-grained to pegmatitic granite occurs throughout the southern and western parts of the area as dikes and small plutons. Contacts between phases may be gradational or sharp in the case of crosscutting dikes. The granite generally exhibits a weak foliation or lineation, but in the Spruce Rapids and Sturgeon-Weir Shear Zones, it is intensely foliated and locally exhibits shear banding. Typical rocks contain 2-5 percent biotite, roughly equal proportions of quartz, plagioclase and microcline, and minor amounts of garnet, apatite, tourmaline, zircon, monazite and opaque minerals. Sheared samples also contain abundant white mica as well as chlorite and rutile and/or ilmenite resulting from biotite alteration.

f) Paleozoic Rocks

Nearly flat-lying Paleozoic strata (Od) unconformably overlie the Precambrian rocks to the south. The unconformity was not observed due to poor exposure but it is generally marked by an approximately 10 m high escarpment of fine-grained buff dolostone, the lower 5 m of which consists of a blocky talus slope. A basal sandstone up to 3 m thick was reported from the eastern side of Amisk Lake (Byers and Dahlstrom, 1954) but no exposures were found in the Snake Rapids area. Based on paleontological studies carried out in the Namew Lake - Ballantyne Bay area, Kupsch (1952) correlated the sequence with the Ordovician Winnipeg Sandstone and Red River Dolomite.

3. Metamorphism

The metamorphic grade ranges from upper greenschist facies in the Muskeg Bay - Wolf Lake area to lower amphibolite facies in the extreme southeast and middle to upper amphibolite facies in the northwest. Isograds marking the first appearance of staurolite, garnet and the assemblage garnet - sillimanite - biotite in aluminous rocks have been plotted on Figure 1. They are approximate due to the lack of appropriate compositions in the eastern and southern parts of the area and are subject to more detailed petrographic work. These observations led to three main conclusions:

1) The westward transition from low-grade rocks of the Flin Flon Domain into high-grade gneisses of the Hanson Lake Block does not take place along a sharp structural discontinuity but is gradational, extending over more than 10 km.

2) In addition, there is a gradational increase in metamorphic grade to the southeast as previously inferred from the recognition of stable amphibolite facies assemblages in altered rocks at the Coronation Mine located about 25 km east of Muskeg Bay (Froese, 1969). Together with the northward increase in metamorphic grade extending into the Kisseynew Gneiss Belt (Byers and Dahlstrom, 1954; Ashton *et al.*, 1987), the southeastward increase in grade implies that greenschist and sub-greenschist facies rocks are restricted to a roughly horseshoe-shaped area in Saskatchewan opening eastward towards the Flin Flon area. Evidence of variations in metamorphic pressure is scanty but sillimanite and rare relict kyanite in the central Snake Rapids area also indicate deeper levels of erosion than in the northern Amisk Lake area where andalusite is the stable Al_2SiO_5 polymorph (Byers and Dahlstrom, 1954; Ashton *et al.*, 1987).

3) Isograds are neither parallel to, nor appreciably displaced by the Spruce Rapids Shear Zone which approximately follows the northwest-striking portion of the Sturgeon-Weir River (Figure 1). The presence of garnet, staurolite, kyanite and sillimanite in a sheared granitic dike within the zone suggests that at least some of the shearing must have taken place prior to the peak of metamorphism in order to produce an aluminous composition from a granitic precursor. Therefore, variations in metamorphic grade cannot be strictly used as a basis of delineating the Flin Flon volcanic belt and Hanson Lake Block along the Spruce Rapids Shear Zone.

4. Structure

The earliest recognizable fabric in the area is the main regional foliation which has developed in an axial planar orientation to rare minor tight to isoclinal D_1 folds. The Wolf Lake Fold, which is defined by a core of mafic volcanic rocks in the Wolf Lake - Amisk Lake area, is thought to have formed as an isoclinal and possibly recumbent D_1 structure.

The layer-parallel Wolf Lake Shear Zone, which can be traced continuously around most of the contact between the mafic and felsic to intermediate suites, is also interpreted as resulting from D_1 deformation (Figure 1). Shearing has affected rocks from both of the volcanic suites and the heterogeneous sediments as well as gabbro and feldspar porphyry dikes. Most mafic rocks within the zone contain abundant free carbonate but hard glassy gabbroic dikes suggest that some rocks have also been subjected to minor silicification. Felsic rocks within the shear zone tend to be enriched in white mica. Minor pseudotachylite was noted in sheared to cataclastic felsic volcanic rocks along the eastern shore of Wolf Lake.

Most of the recognizable minor and megascopic folds in the area are attributed to D_2 deformation. Both the D_1 Wolf Lake Fold and Wolf Lake Shear Zone are refolded (Figure 2) by the Muskeg Bay Synform (Byers and Dahlstrom, 1954), a moderately north-plunging structure which is overturned to the west. Minor folds and intersection lineations plunge north-northwestward on the west limb of the synform and north-northeastward on the east limb possibly due to interference caused by the D_1 anticline geometry.

D_2 folds are tighter and more attenuated approaching the Spruce Rapids Shear Zone and in the west where the higher metamorphic grade allows for a more ductile response as exemplified by the tight folds defined by the biotite granodiorite (Figure 1). D_2 minor fold axes and intersection lineations plunge consistently northwestward in the east-central part of the area, southeastward in the vicinity of the northward bend in regional foliation, and northward in the extreme northwest (Figure 2). A non-penetrative east-northeast dipping D_2 foliation progressively overprints the near-parallel D_1 foliation.

The poorly exposed, moderately northeast-dipping Spruce Rapids Shear Zone is the most significant of a number of roughly parallel northeast-dipping high strain zones thought to have formed during D_2 time. The zone consists of heterogeneously strained aplitic to pegmatitic granite in the east and locally silicified, sheared to mylonitic supracrustal rocks containing rare pseudotachylite in the northwest. Shear bands in the granitic rocks, asymmetric pull-aparts in quartz veins and granitic dikes, and riedel shears consistently indicate a sinistral component of shear but no indication of the dip slip component was recognized (Figures 3 and 4).

D_2 structures can be most easily explained in their present orientation by east-northeast - west-southwest compression (Figure 2). This would explain the northwest plunge and southwest vergence of D_2 folds and predict oblique sinistral - reverse displacement on the Spruce Rapids Shear Zone. Continued shearing could account for the progressive rotation of D_2 axial planes and fold-related lineations toward the shear plane.

East-plunging D_3 mesoscopic folds, including the late east-trending folds defined by the biotite granodiorite, deform D_2 structures in the central and northwestern parts of the area.

D_4 deformation is restricted to the Sturgeon-Weir Shear Zone. Shear bands in pegmatitic rocks, pull-aparts within quartz veins and granitic dikes, and rotated quartz - feldspar segregations consistently indicate oblique dextral-reverse displacement.

A relatively young age for the Sturgeon-Weir Shear Zone is suggested by two independent lines of evidence.

1) A sharp increase in metamorphic grade approaching the shear zone (Ashton *et al.*, 1987; this work) implies syn- to post-metamorphic uplift of the eastern block which is consistent with the inferred dextral-reverse sense of displacement. This contrasts with the pre- to syn-metamorphic displacement along the Spruce Rapids Shear Zone as implied by the presence of a high grade metamorphic assemblage in granitoid rocks altered by shearing.

2) Oblique dextral-reverse displacement along the Sturgeon-Weir Shear Zone could account for the deflection of the regional foliation and the reversal in plunge direction of D_2 fold axes and intersection lineations in the northwestern part of the area. No evidence was found to support the suggestion that the Sturgeon-Weir Shear Zone is truncated by the Spruce Rapids Shear Zone south of Attree Lake as implied by Macdonald (1981). It appears more likely that the Spruce Rapids Shear Zone is deflected along with the regional foliation into the Sturgeon-Weir Shear Zone by subsequent dextral-reverse displacement.

5. Economic Geology

Disseminated iron sulphides and magnetite mineralization marked by gossans occur at several localities in the felsic to intermediate volcanic and volcaniclastic rocks in the Muskeg Bay area. On the northeastern side of the bay, iron staining in sheared felsic to intermediate tuffs and quartz-feldspar porphyries and/or crystal tuffs can be traced for about a kilometre along the shoreline. Up to 5 percent pyrrhotite characterizes much of the zone and disseminated chalcopyrite is described from an old trench by Byers and Dahlstrom (1954). Alteration associated with the mineralization includes extensive white mica in the felsic porphyry and garnet in the layered volcaniclastic rocks. Rare tourmaline - quartz - feldspar veins crosscut the shear fabrics. Gossans on several islands in northern Muskeg Bay also result from disseminated iron sulphides. Staurolite and garnet occurrences on the western shore of the bay are thought to represent pre-metamorphic hydrothermal alteration.

Disseminated iron sulphides and magnetite occur along the entire exposed length of the Wolf Lake Shear Zone. Therefore, it is not clear whether the mineralization is syngenetic and related to a possible stratigraphic break or is the result of fluids moving along the shear zone. It is most likely that shearing merely acted to locally concentrate mineralization already disseminated within the felsic to intermediate suite. Quartz veins associated with

Figure 3 - Shear band development in coarse-grained to pegmatitic granite at the mouth of the Sturgeon-Weir River indicating sinistral shear along the Spruce Rapids Shear Zone.

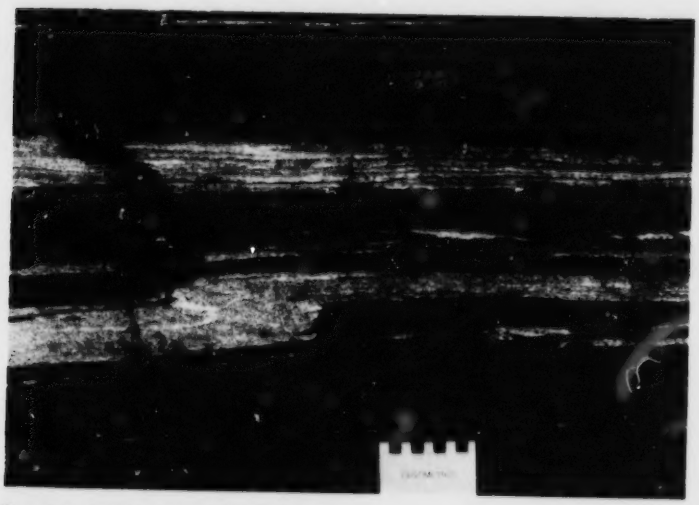

Figure 4 - Transposition of D_1 foliation and layering into the shear plane of the Spruce Rapids Shear Zone in sedimentary rocks along the northern shore of the Sturgeon-Weir River between Snake Rapids and Attree Lake. Continuous granitoid dike near top has undergone significant grain size reduction. Folding of the thin granitoid dike in lower right demonstrates the evolution of asymmetric pull-aparts by rotation of long thick fold limbs into the inferred flattening plane. Continued sinistral shear has resulted in boudinage of granitoid dike in centre of picture.

the early shear zone may be of interest for gold exploration.

Disseminated pyrite - pyrrhotite mineralization was reported from 'slates' and 'conglomerates' around the southern end of Seahorse Lake, located about 1 km east of Attree Lake (Eastwood, 1949; Johnson, 1967). Old trenches at the southwestern corner of the lake mark an area reputed to contain more massive iron sulphide mineralization.

Eastwood (1949) also reported traces of chalcopyrite in quartz veins within sheared granodiorite north of Snake Rapids. An old trench marks a similar occurrence containing trace chalcopyrite and pyrite in quartz veins within 'slates' 3 km west of Snake Rapids (Eastwood, 1949; Johnson, 1967).

6. Acknowledgements

Tracey Jungwirth and Danny Labelle provided cheerful and able assistance during the course of the field work. Discussions with John Lewry and Bob Macdonald during a brief visit to the field area were a great benefit. Bob Macdonald and Kent Wilcox provided valuable comments after reviewing an early version of the manuscript.

7. References

Ashton, K.E. (in prep.): Precambrian geology of the Mari Lake area, Saskatchewan; Geol. Surv. Can.

Ashton, K.E. and Hunt, P.A. (in prep.): U-Pb age constraints on the evolution of the Flin Flon Volcanic Belt and Kisseynew Gneiss Belt, Saskatchewan; *in* Radiogenic Age and Isotopic Studies, Geol. Surv. Can.

Ashton, K.E. and Leclair, A.E. (1990): Foliate: a useful term to complement the textural classification of foliated metamorphic rocks; Can. J. Earth Sci., v27.

Ashton, K.E. and Wheatley, K.J. (1986): Preliminary report on the Kisseynew gneisses in the Kisseynew - Wildnest Lakes area, Saskatchewan; *in* Current Research, Pt. B, Geol. Surv. Can., Pap. 86-1B, p305-317.

Ashton, K.E. and Wilcox, K.H. (1988): The Sturgeon-Weir shear zone: a thrusted boundary between the Flin Flon volcanic belt - Kisseynew gneiss terrain and Hanson Lake block, east-central Saskatchewan; Geol. Assoc. Can. Min. Assoc. Can., Jt. Annu. Meet., St. John's, Nfld., Prog. Abst., v13, pA3.

Ashton, K.E., Wilcox, K.H., Wheatley, K.J., Paul, D. and de Tombe, J. (1987): The boundary zone between the Flin Flon domain, Kisseynew gneisses and Hanson Lake block, northern Saskatchewan; *in* Summary of Investigations 1987, Sask. Geol. Surv., Misc. Rep. 87-4, p131-134.

Bailes, A.H. and Syme, E.C. (1989): Geology of the Flin Flon - White Lake area; Manit. Energy Mines, Geol. Rep. 87-1, 313p.

Bruce, E.L. (1918): Amisk - Athapapuskow Lake district; Geol. Surv. Can., Mem. 105, 91p.

Byers, A.R. and Dahlstrom, C.D.A. (1954): Geology and mineral deposits of the Amisk - Wildnest Lakes area, Saskatchewan; Sask. Dep. Miner. Resour., Rep. 14, 177p.

Eastwood, G.E.P. (1949): Snake Rapids, Saskatchewan; Geol. Surv Can., Pap. 49-18 (map with descriptive notes).

Fox, J.S. (1976a): Preliminary bedrock geology of west Amisk Lake area, 63L-9 (W) and 63L-16 (SW); Sask. Res. Counc., Geol. Div., Misc. Rep.

_____ (1976b): Volcanic stratigraphy and mineralization in the Amisk Group; Geol. Assoc. Can. Min. Assoc. Can., Jt. Annu. Meet., Edmonton, Alberta, Prog. Abstr., v1, p72.

Froese, E. (1969): Metamorphic rocks from the Coronation Mine and surrounding area; *in* Byers, A.R. (ed.), Symposium on the geology of Coronation Mine, Saskatchewan, Geol. Surv. Can., Pap. 68-5, p55-77.

Gilbert, H.P., Syme, E.C. and Zwanzig, H.V. (1980): Geology of the metavolcanic and volcaniclastic metasedimentary rocks in the Lynn Lake area; Manit. Energy Mines, Geol. Pap. 80-1, 118p.

Johnson, R.L. (1967): The geology of the Hanson Lake area (east half), Saskatchewan; Sask. Dep. Miner. Resour., Rep. 117, 18p.

Kupsch, W.O. (1952): Ordovician and Silurian stratigraphy of east central Saskatchewan; Sask. Dep. Miner. Resour., Rep. 10, 62p.

Macdonald, R. (1981): Compilation bedrock geology: Pelican Narrows and Amisk Lake areas (NTS 63M, 63L, part of 63N and 63K): Preliminary geological map; *in* Summary of Investigations 1981, Sask. Geol. Surv., Misc. Rep. 81-4, p16-23.

MacQuarrie, R.R. (1979): Geological re-investigation mapping, Birch Portage south, NTS area (63L-15S); *in* Summary of Investigations 1979, Sask. Geol. Surv., Misc. Rep. 79-10, p29-38.

Mawdsley, J.B. (1934): A brief outline of the geological history of the northwest shore of Lac la Ronge and the Beaver Lake areas; Sask. Dep. Nat. Resour., Annu. Rep. (1933), App. 2, 20p.

McInnes, W. (1914): The basins of the Nelson and Churchill Rivers; Geol. Surv. Can., Mem. 30, 146p.

Parslow, G.R. and Gaskarth, J.W. (1988): Proterozoic rocks of east-central Saskatchewan: geochemistry, structure and mineralization controls; *in* Summary of Investigations 1988, Sask. Geol. Surv., Misc. Rep. 88-4, p127-139.

Pearson, W.J. (1951): The origin and history of the Neagle Lake Pluton in the Amisk Lake area; unpub. M.A. thesis, Univ. Sask., 71p.

Syme, E.C. (1987): Athapapuskow Lake Project; *in* Report of Field Activities 1987, Manit. Energy Mines, p30-39.

Walker, D. and Watters, B.R. (1982): Geochemistry of metavolcanic rocks, Amisk Lake west area; *in* Summary of Investigations 1982, Sask. Geol. Surv., Misc. Rep. 82-4, p24-30.

Wright, J.F. (1933): Amisk Lake, Saskatchewan; Geol. Surv. Can., Summ. Rep. 1932, Pt. C, p73-110.

Wright, J.F. and Stockwell, C.H. (1934): West half of Amisk Lake area, Saskatchewan; Geol. Surv. Can., Summ. Rep. 1933, Pt. C, p12-22.

Zwanzig, H.V. (in press): The Kisseynew Gneiss Belt in Manitoba: stratigraphy, structure and tectonic evolution; *in* Lewry, J.F. and Stauffer, M.R. (eds.), The early Proterozoic Trans-Hudson Orogen of North America, Geol. Assoc. Can., Spec. Pap. 37.

New Perspective on the Amisk Group and Regional Metallogeny, Douglas Lake - Phantom Lake Area, Northern Saskatchewan

D. J. Thomas

Thomas, D.J. (1990): New perspective of the Amisk Group and regional metallogeny, Douglas Lake - Phantom Lake area, northern Saskatchewan; *in* Summary of Investigations 1990, Saskatchewan Geological Survey; Saskatchewan Energy and Mines, Miscellaneous Report 90-4.

Geological mapping at 1:12,500 scale aimed at improving the understanding of the Amisk Group stratigraphy, tectonic events and metallogenesis in the region continued into its second year. An area along the Saskatchewan - Manitoba provincial boundary from the townsite of Flin Flon to the north end of West Arm on Schist Lake (Figure 1) was mapped this year.

Previous reconnaissance and detailed geological mapping by the Geological Survey of Canada throughout the greater Flin Flon - Amisk Lake region include those by: Tyrrel (1902), McInnes (1909), Bruce (1918), Alcock (1923), Ambrose (1936a, 1936b), Tanton (1941a, 1941b), Stockwell (1960) and Heywood (1966). More recent federal and provincial investigations around the Douglas Lake - Phantom Lake area include those by

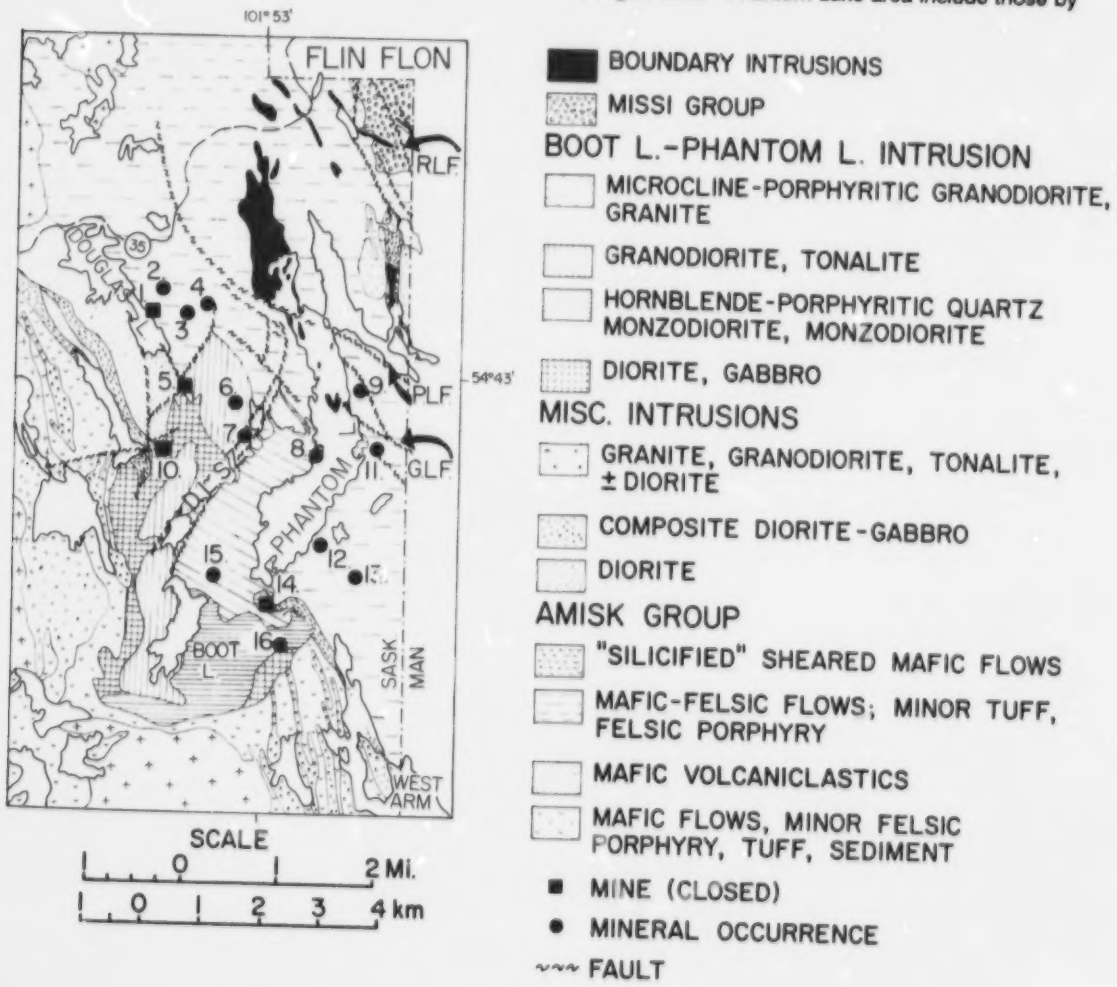

Figure 1 - Geological sketch of the Douglas Lake - Phantom Lake area and immediate adjoining areas. RLF = Ross Lake Fault; PLF = Phantom Lake Fault; GLF = Green Lake Fault. Numbers refer to mineral occurrences listed in Table 3.

Byers *et al.* (1965), Pearson (1979a, 1979b, 1981, 1984, 1985) and Galley and Franklin (1987). The regional geology and metallogeny of the Flin Flon area has been reviewed by: Stauffer and Mukherjee (1971), Stauffer *et al.* (1975), Price (1977), Coombe (1979, 1984), Pearson and Galley (1985), Pearson *et al.* (1986), Syme (1986, 1987, 1988), and Bailes and Syme (1987, 1989).

1. Regional Geology

The Douglas Lake - Phantom Lake area is within the Aphebian volcanoplutonic Flin Flon - Snow Lake Belt. This belt is transitional northwards into the higher grade Kisseynew Gneiss Belt (Ashton *et al.*,1986) and to the south is unconformably overlain by Ordovician dolomites. The Amisk Group, the oldest group of rocks in the region, comprises a metamorphosed assemblage of predominantly subaqueous mafic flows and flow breccias, subordinate felsic flows and porphyries, lesser volcaniclastic and sedimentary rocks, and a suite of syn- to post-volcanic dykes and sills. The group is unconformably overlain by metamorphosed alluvial sandstones and conglomerates of the Missi Group. Post-Missi intrusions include the Boundary intrusions, represented by a suite of ultramafic to felsic rocks, (Stockwell, 1946, 1960; Syme, 1975; Syme and Forester, 1977), and the younger Boot Lake - Phantom Lake Complex (Galley and Franklin, 1987), comprising a gabbro to granite composite intrusion (Figure 2).

Bailes and Syme (1987, 1989) recognize one phase of pre-Missi folding (P1) and four phases of post-Missi folding (P2 to P5) in the Flin Flon area. Strong north-, northeast- and northwest-trending fault systems are predominant features, and in some cases are identified as boundaries separating allocthonous blocks of distinctively different stratigraphic and metamorphic character (Bailes and Syme, 1987, 1989; Syme, 1986, 1987, 1988).

Several U-Pb zircon ages obtained from the Manitoba portion of the Flin Flon belt indicate an age of Amisk volcanism around 1886 Ma (Syme *et al.*, 1987), and deposition of Missi Group rocks around 1832 Ma (Gordon *et al.*, 1987). A U-Pb zircon age of 1820 Ma is reported from a granite dyke cutting the Missi Group (MacQuarrie, 1980).

2. Synopsis/Highlights of 1990 Field Work

a) Flin Flon Mine

The geological setting and Zn-Cu mineralization of the Flin Flon Mine have been described by numerous workers (Stockwell,1960; Byers *et al.*, 1965; Price, 1977; Bailes and Syme, 1989; Koo and Mossman, 1975; Gale and Eccles, 1988). The sulphide ore bodies are associated with rhyolitic flows and fragmentals occurring between the footwall South Main Basalts and hanging wall Hidden Lake Basalts (Bailes and Syme, 1987, 1989). Detailed mapping of the volcanic section near the South Main Shaft this summer shows that the trend of the footwall-hanging wall sequence may be displaced 700 m to the southwest of the South Main shaft where a similar stratigraphic sequence occurs at Mill Rock Hill (Gale, 1981). Bailes and Syme (1989, page 140, Figure 171) speculated that the westerly offset of the South Main - Hidden Lake contact was the result of a southwest-trending dextral fault. Mapping failed to confirm the presence of a fault, however, local reversals in facing direction within the volcanic stratigraphy strongly suggest that the 'ore horizon' has been deformed by a minor Z-fold along the east-facing limb of the larger Beaver Road Anticline (Figure 3). The axis of this Z-fold plunges moderately southeast and is coaxial with a southeast-plunging S1/S2 intersection lineation.

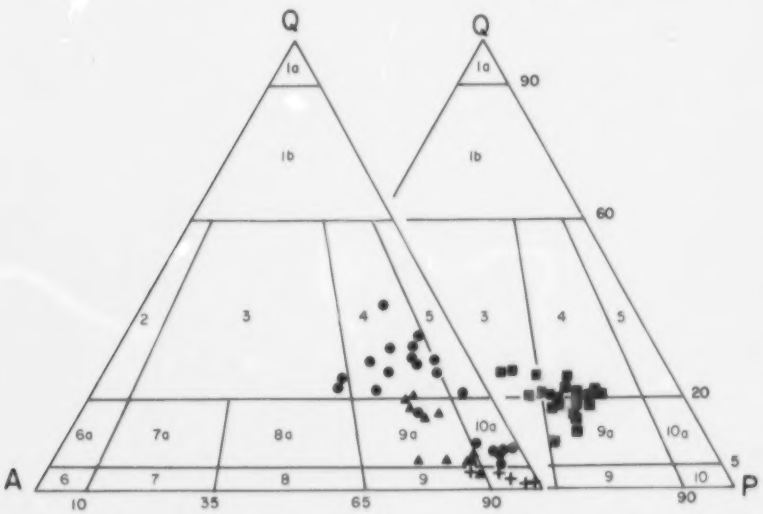

Figure 2 - Modal composition of rocks from the Boot Lake - Phantom Lake intrusion (phase 1 = crosses; phase 2 = circles; phase 4 = squares). Subdivisions represented after Streickeisen (1976): 3 = granite; 4 = granodiorite; 5 = tonalite; 8a = quartz-bearing monzonite; 9a = quartz-bearing monzodiorite; 10a = quartz diorite; 9 = monzodiorite/monzogabbro; 10 = diorite/gabbro.

Shearing is prevalent between major lithologic units along the limbs of the minor Z-fold structure. In particular, the footwall-hanging wall contact near the South Main Shaft and the stratigraphically equivalent rocks at Mill Rock Hill have been variably sheared. In the vicinity of the Flin Flon deposit, the shearing exhibits a left lateral reverse sense of displacement with the hanging wall (east side) having moved up and northwards to produce a moderately southeast-plunging stretching lineation (Brownell and Kinkell, 1935).

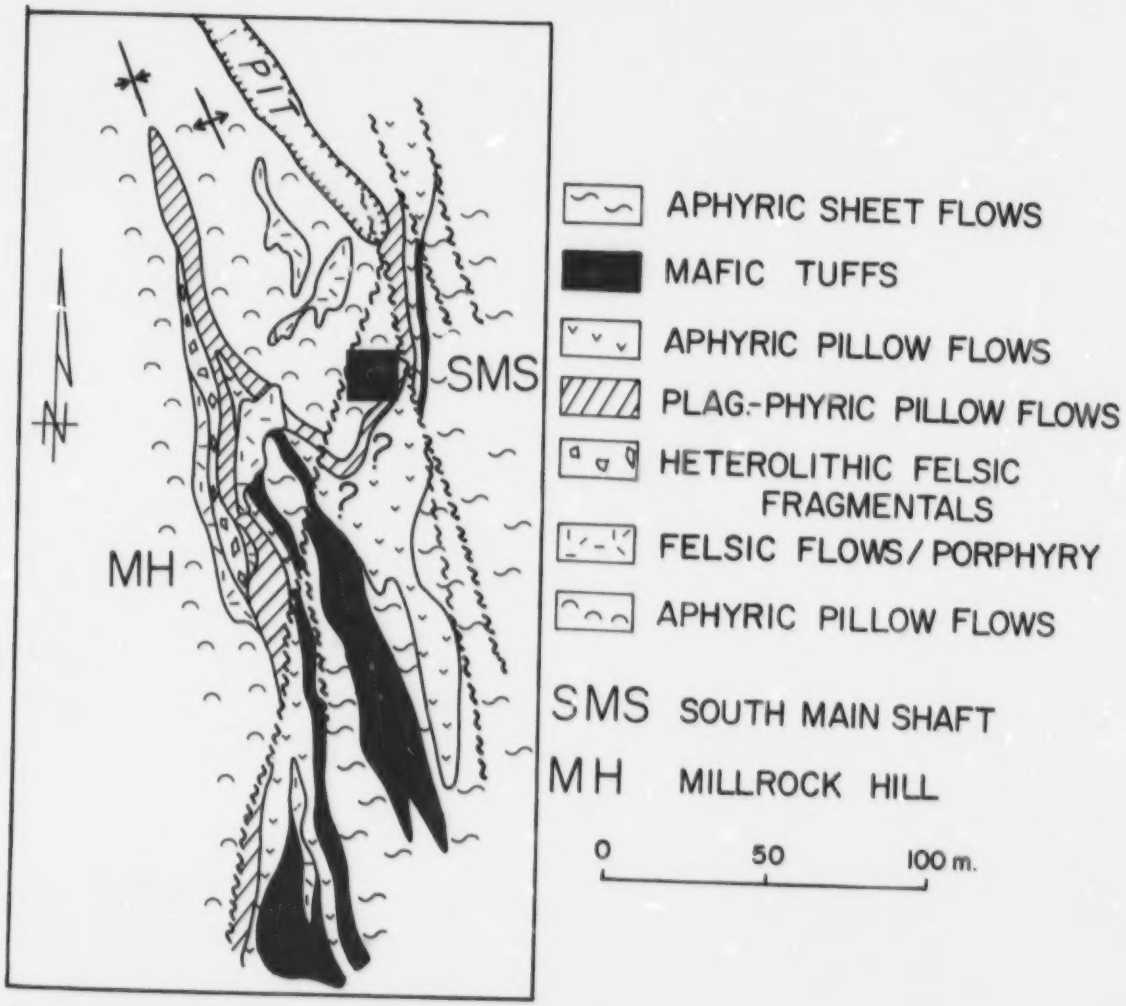

Figure 3 - Structural interpretation of the area around South Main Shaft (HBMS) and Mill Rock Hill area. Post-volcanic diorites and Boundary Intrusions omitted from sketch.

The deposit consists of six main sulphide lenses which plunge moderately southeast (Byers *et al.* 1965) parallel to the axis of the Beaver Road Anticline (Thomas 1989), S1/S2 intersection lineation and stretching lineation in the shears. The ore bodies were likely formed as a continuous to semicontinuous stratabound sulphide deposit which was rodded and boudinaged during regional folding (Beaver Road Anticline) prior to further attenuation during later shearing along the fold limbs.

b) Pre-Missi Deformation

An early episode of ductile shearing and associated alteration was recognized in the Amisk Group. This early structural event is tentatively interpreted as a period of major northeast-directed thrust imbrication within the Amisk Group prior to intrusion of the Boot Lake - Phantom Lake pluton and deposition of the Missi Group. Associated early structures were subsequently deformed by post-Missi folding and late faulting related to the Cliff Lake - Ross Lake Fault system.

Thrusting is thought to have occurred along two major shear zones located northwest of West Arm on Schist Lake and north of Potter Bay on Phantom Lake. The zones are characterized by intense silicification and feldspathization and for this reason have been previously interpreted as either rhyolites and/or interlayered mafic and felsic tuffs (Stockwell, 1960; Byers *et al.*, 1965; Pearson, 1981). They are reinterpreted as highly strained, largely mafic and commonly pillowed flow units which have been variably altered (silicified, carbonatized, epidotized and feldspathized). Pillow selvages and quartzofeldspathic amygdule-rich domains are commonly preserved even in the most intensely deformed and altered varieties. The rocks consist of felsic layers up to several tens of centimetres thick separated by mafic to intermediate layers of less than a few centimetres thick.

The West Arm (Schist Lake) Shear Zone is 50 to 100 m wide, southwest-dipping and is truncated to the northwest by the Boot Lake - Phantom Lake Intrusion. It forms a major break between two distinctive lithotectonic sequences. Volcanic rocks northeast of the zone are weakly to moderately deformed and are composed of subgreenschist to greenschist facies assemblages. In the vicinity of the shear zone they are predominantly quartz amygdaloidal mafic pillow flows, amoeboid pillow breccias and lesser mafic tuffs. This assemblage is probably the southeasterly continuation of the lithologically similar Newcor member which underlies the area northeast of Douglas Lake (Thomas, 1989). In marked contrast, rocks immediately southwest of the shear zone are strongly deformed and exhibit a well-developed regional penetrative fabric and have undergone somewhat higher metamorphic conditions (Reilly, this volume). Large heterogeneous sills of foliated metadiorite and metagabbro, commonly hosting extensive xenolithic screens and elongate bands of mafic volcanic material, intrude the metavolcanics southwest of the shear zone. Primary igneous layering is locally preserved in gabbroic phases.

Metavolcanic rocks to the northeast of the West Arm shear zone have been described as predominantly tholeiitic and show trace element features suggesting island arc affinities (Bailes and Syme, 1989; Thomas, 1989; Watters, 1989, Parslow and Gaskarth, 1988). The lithostructural character of the metavolcanic-intrusive sequence to the southwest is similar to that of rocks underlying the area between the east shore of Amisk Lake and the west margin of the Reynard Lake Pluton. Parslow and Gaskarth (1988) interpreted the geochemistry of the East Amisk Lake metavolcanic rocks as ..."tholeiitic, oceanic and rift related in character..." and suggested eruption took place in a MORB, ophiolitic, or back-arc rift setting. A comparison of the volcanics in the East Amisk Lake area with rocks southwest of the inferred West Arm thrust must await further geochemical analysis, however, if they are geochemically similar as suspected then the West Arm shear zone defines a major break between two fundamentally different volcanic environments (i.e. island arc vs. back-arc basin rift).

Although kinematic indicators are poorly developed and ambiguous within the main part of the West Arm structure, subsidiary shears within the hanging wall block indicate a reverse movement, by which more pervasively deformed and higher-grade rocks of possible oceanic or back-arc rift affinities were transported over lower-grade less deformed rocks of an island arc environment. It is interesting to note that massive sulphide deposits hosted by rocks of island arc affinity northeast of this structural break are generally Zn-Cu rich while deposits hosted by rocks of possible oceanic or back-arc affinity are smaller and generally Cu-dominant (Table 1).

The **Carlisle Lake shear zone**, immediately west of Carlisle Lake, is approximately 100 m wide and dips moderately to steeply east. Rocks within this zone have also been previously mapped as rhyolites (Stockwell, 1960), but highly attenuated 'ghosted' pillow selvages

Table 1 Selected massive sulphide deposits from the greater Flin Flon - Amisk Lake area.

Deposit*		Tonnes	%Cu	%Zn
1	FlinFlon	64,000,000	2.2	4.4
2	Callinan	2,400,000	1.55	4.0
3	SchistLake	2,000,000	4.22	7.01
4	Mandy	150,000	8.0	15.0
5	Coronation*	1,412,861	4.25	0.24
6	Birch*	300,819	6.21	–
7	Flexar*	337,300	3.77	0.47
8	WestArm**	700,000	4.63	0.6

* located in East Amisk Lake area
** located in Schist Lake area, southwest of the West Arm shear zone

and gradational contacts with mafic pillow flows to the west suggest that they are strongly silicified and feldspathized mafic flows. The zone is interpreted as an easterly-verging thrust which has been steeply overturned to the west by later folding about the Mandy Road Anticline (Figure 4). The footwall of the thrust, which is now structurally overlying, comprises a variety of plagioclase crystal-rich tuffs, mafic lapilli tuffs, and minor mafic ash tuffs and heterolithologic tuff - breccias, similar to upper units of the Douglas Lake Assemblage (Thomas, 1989) on the west limb of the Beaver Road Anticline. These stratigraphic and structural relationships suggest that the Carlisle Lake shear zone represents a thrust which has transported mafic flows of the Beaver Road Assemblage over volcaniclastic rocks of the Douglas Lake Assemblage.

c) Phantom Lake Fault

The southeasterly continuation of the Phantom Lake Fault was traced along the south shore of Potter Bay on Phantom Lake. Along Potter Bay the structure has an apparent sinistral horizontal component of displacement and a steep (70° to 80° northerly dip which reverses to the southwest on the west side of Phantom Lake (Thomas, 1989). Several subparallel faults form subsidiary splays up to 100 m into the hanging wall along the Potter Bay section of the fault .

Galley and Franklin (1987) interpret the Phantom Lake Fault as an easterly-trending, sinistral, P5 age structure which, together with north-northeast dextral faults (eg. Rio and Dion Lake Faults), form a conjugate set. The conjugate P5 structures are considered to be the product of a predominantly strike-slip system (Galley and Franklin, 1987), however, apparent horizontal displacement across the Phantom Lake Fault appears to be less than 200 m.

South of the Phantom Lake Fault, mafic volcanic rocks are typically dark greenish black, massive to poorly foliated and highly fractured. They commonly contain subconchoidal fracture surfaces and display moderate to intense carbonatization, epidotization and locally silicification. The degree of alteration increases and the rocks become increasingly massive and dense towards the northern margin of the Boot Lake - Phantom Lake Intrusion. In contrast, rocks immediately north of the fault

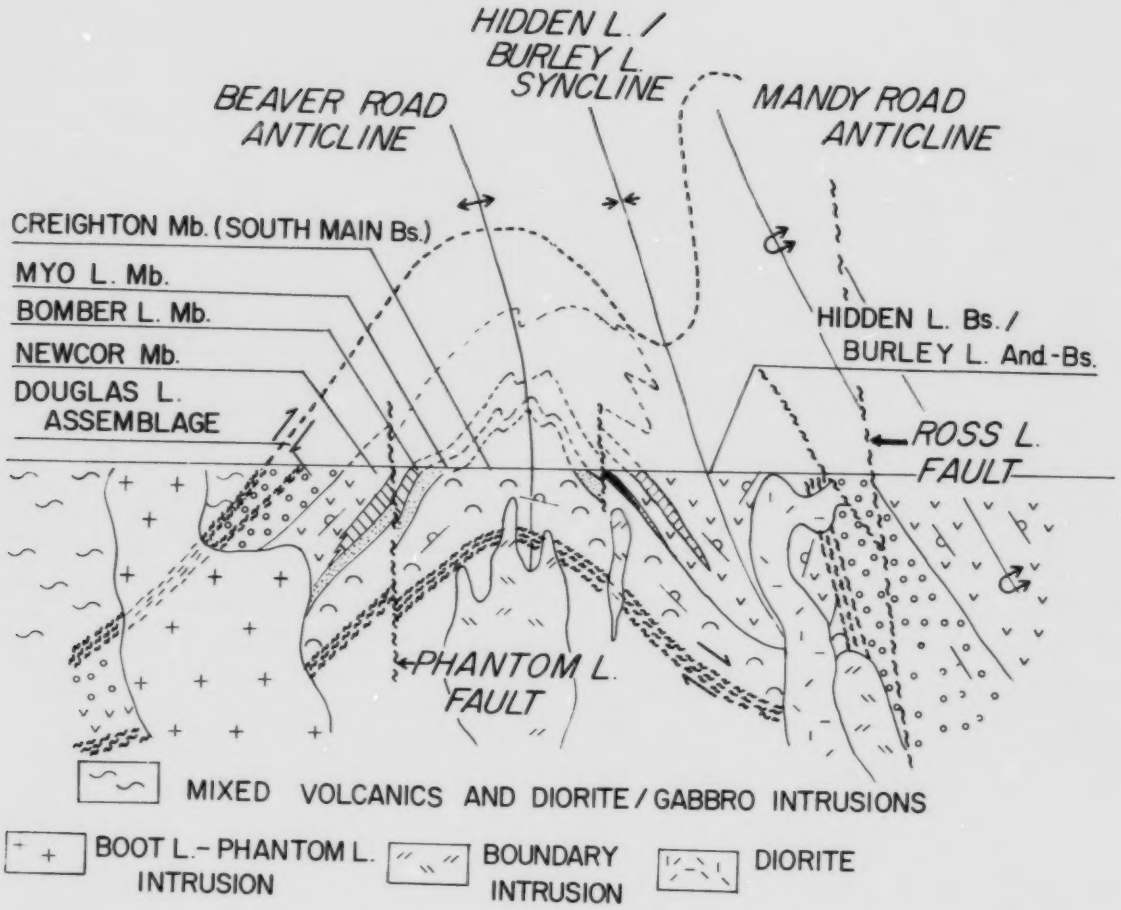

Figure 4 - Schematic structural cross-section, approximately southwest to northeast through the Douglas Lake - Phantom Lake area.

Table 2 - List of Au, Cu, W, Mo occurences in the Douglas Lake - Phantom Lake area. Modified from Galley and Franklin (1987).

	Deposit/Occurrence (principal commodity)	Reserve/ grade	Associated metals
1	Newcor (Au)	40,000t@13g/tAu	Zn,Cu
2	Cor (Au)		Cu
3	Unity (Au)		Cu
4	Douglas (W)		Cu
5	Bootleg/Rio (Au)	165,483t@12g/tAu	Cu,Zn,W
6	DionLake (Cu)		Au,Ag
7	Dion#7 (Cu)		Au,Ag,W
8	CBS766 (Ag)		Au,Mo
9	WO13 (W)		Cu
10	Henning-Maloney (Au)	13,500t@13.3g/tAu	Cu,Mo
11	Kar (W)		Cu,Mo
12	McMillan (Au)		Cu,Zn,Ag
13	Dee (Au)		Ag
14	Phantom (Au)		Ag,Cu,Mo,W
15	IMC-B (Au)		W
16	IMC-A (Au)		Ag,Cu

are typically pale green to greyish green, moderately-foliated, and exhibit minimal alteration. A marked contrast also occurs on the west side of Phantom Lake (Thomas, 1989) where more altered rocks south of the fault may represent a broad hornfels aureole around the Boot Lake - Phantom Lake Intrusion. The striking contrast between hornfels rocks immediately south of the fault and 'fresh' rocks north of the fault might indicate substantial vertical displacement with rocks to the south having moved up relative to the north side.

d) Gold Mineralization

Numerous mineral occurrences containing variable amounts of gold, copper, tungsten, and molybdenum are present in the Douglas Lake - Phantom Lake area (Pearson, 1981; Galley and Franklin, 1987, 1989) (Table 2). Two generations of gold-related mineralization and alteration are recognized; the earlier being directly related to the emplacement of the Phantom Lake granite

Table 3 - Geochemical analyses of grab samples from various mineral occurrences in the Phantom Lake area. Analyses by ACME Laboratories

ELEMENT SAMPLES	Mo ppm	Cu ppm	Pb ppm	Zn ppm	Ag ppm	Ni ppm	As ppm	Sb ppm	W ppm	Au* ppb
9012-0076	47	36	5	111	0.4	18	6	4	597	84
9012-0104	2	14	2	47	0.1	7	4	2	13	9
9012-0106	29	17	8	25	1.5	11	11	5	682	48
9012-0112	167	16	10	1	1.4	6	4	2	35	175
9012-0121	18	1079	2	8	0.3	25	2	2	7	19
9012-0123	1	522	5	26	0.1	10	2	2	1	10
9012-0135	731	13	14	33	1.2	18	2	6	18	480
9012-0139	229	82	6	53	0.3	11	11	38	591	22
9012-0168	10	54	2	26	1.6	9	8	13	5	1090
9012-0173	1	1086	5	46	0.1	13	3	2	1	30
9012-0194	6	92	91	442	36.2	88	12	39	216	72600
9012-0229	3	8	2	30	1.2	10	3	2	6	1060
9012-0241	2	47	12	115	0.6	47	7	7	46	470
9012-0263	5	5	4	17	0.3	17	4	2	382	85
9012-0278	4	834	10	43	1	27	2	2	11	98
9012-0283	84	43	2	29	2.2	27	3	2	15	580
9012-0299	2	54	5	57	0.7	9	2	2	4	510
9012-0303	6	14	18	23	8.1	10	2	2	1	3520
9012-0363	1012	38	13	24	3.6	19	15	5	26	920

-0076 fine-grained, greyish orange, quartz-ferrocarbonate-pyritic rock; east shore Phantom Lake
-0104 fine-grained, light grey, quartz-ferrocarbonate vein with quartz veinlets; WO13 occurrence
-0106 very fine-grained, light grey, cherty, quartz-ferrocarbonate rock, finely disseminated pyrite; WO13 occurrence
-0112 fine-grained, pale yellowish orange, altered brecciated feldspar porphyritic granitoid dyke; east shore Phantom Lake, Green Lake Fault
-0121 very fine-grained, medium bluish grey, cherty, quartz-ferrocarbonate rock, coarse pyrite stringers, ±chalcopyrite; Green Lake Fault
-0123 fine-grained, dark grey to greenish black, massive amphibolite, disseminated pyrite ± chalcopyrite; Green Lake Fault
-0135 very fine-grained, dark yellowish orange to medium light grey, cherty, quartz-ferrocarbonate rock, carbonate stringers and disseminated pyrite; 125 m north of KAR occurrrence
-0139 fine-grained, mottled light grey to yellowish orange, cherty quartz-ferrocarbonate rock, coarse quartz-ferrocarbonate veinlets, disseminated pyrite; KAR occurrence
-0168 fine-grained, light grey, cherty, quartz-ferrocarbonate rock, quartz-ankerite veinlets, disseminated pyrite; 400 m northeast of McMillian Mine
-0173 gossanous metagabbro with disseminated pyrrhotite-pyrite ± chalcopyrite; approx 425 m northeast of McMillian Mine
-0194 quartz vein, finely disseminated pyrite; McMillian Mine
-0229 medium-grained, light red, microcline-porphyritic granodiorite; southeast of Phantom Mine
-0241 fine-grained, silicified hornblende granodiorite/monzodiorite, disseminated pyrite pyrrhotite chalcopyrite; IMC-A
-0263 moderately silicified granodiorite/monzodiorite, disseminated pyrite; Phantom Mine area
-0278 moderately silicified granodiorite/monzodiorite in quartz-stockwork breccia zone; Phantom Mine
-0283 altered hornblende-porphyritic monzodiorite, cut by quartz-feldspar-chlorite-carbonate veinlets, disseminated pyrite-chalcopyrite; Phantom Mine
-0299 fractured, altered, microcline-porphyritic granodiorite; IMC-A
-0303 sericitized microcline-porphyritic granodiorite, diseminated pyrite ±chalcopyrite; IMC-A
-0363 quartz vein, disseminated pyrite ± chalcopyrite; south shore of Phantom Lake

(microcline-porphyritic granodiorite/granite/quartz monzodiorite phase; Phase 4) of the Boot Lake - Phantom Lake intrusion and the later to the development of a regional conjugate strike-slip fault system (Galley, pers. comm.). Mineralized grab samples collected from various occurrences in the Phantom Lake area are listed in Table (3).

Mineralization and associated alteration related to the emplacement of the Phantom Lake granite is characterized by two principal brittle fracture controlled types (Galley and Franklin,1987):

1) Au-Cu-W-Mo in quartz breccias and associated propylitic alteration (hematite - quartz - ferrodolomite - epidote).
2) Au-W-Cu mineralization in fracture-controlled phyllitic alteration zones (sericite-quartz-carbonate-pyrite).

Mineralization occurs either within the Phantom Lake granite (IMC-B), or more commonly, within the immediate country rocks such as the Phase 2 hornblende-porphyritic monzodiorite (Phantom, IMC-A), Phase 3 granodiorite/tonalite (Dion), or Amisk Group volcanics (Dion #7, WO13, Kar, Dee). In the metavolcanic country rocks mineralization is invariably found close to feldspar porphyritic granitic (*sensu lato*) dykes similar to the Phantom Lake granite. The overall character of the mineralization and the association with the calc-alkaline Boot Lake - Phantom Lake Intrusion suggests a possible Early Proterozoic porphyry-type system.

The later episode of gold mineralization is associated with a conjugate system of dextral NNE-trending and sinistral ESE-trending faults which post-date the emplacement of the Boot Lake - Phantom Lake intrusion. In these structurally-controlled deposits gold

mineralization occurs in quartz - carbonate (ankerite) veins displaying phyllitic alteration haloes (quartz - chlorite - ankerite - pyrite). Examples of this type include the Rio, Newcor and Henning Maloney mines.

3. References

Alcock, F.J. (1923): Flin Flon map area, Manitoba and Saskatchewan; Geol. Surv. Can., Summ. Rep., 1922, ptC, p1-36.

Ambrose, J.W. (1936a): Progressive kinetic metamorphism in the Missi Series, near Flin Flon, Manitoba; Am. J. Sci. (5th ser.), v32, p257-286.

_____ (1936b): Structures in the Missi Series near Flin Flon, Manitoba; Trans. R. Soc. Can. (3rd ser.), v30, sec4, p81-98.

Ashton, K.E., Wheatly, K.J., Moser, D., Paul, D. and Wilcox, K.H. (1986) : The Kisseynew Gneisses of Saskatchewan: Update; *in* Summary of Investigations 1986, Sask. Geol. Surv.; Misc. Rep. 86-4, p145-148.

Bailes, A.H. and Syme, E.C. (1987): Geology of the Flin Flon-White Lake area; Manit. Energy Mines, Map GR 87-1-1.

_____ (1989): Geology of the Flin Flon - White Lake area, Manit. Energy Mines, Geol. Rep. GR87-1, 313p.

Brownell, G.M. and Kinkell, A.R. (1935): The Flin Flon Mine, geology and paragenesis of the ore deposit: Trans. Can. Inst. Min. Metal., v38, p261-286.

Bruce, E.L. (1918): Amisk - Athapapuskow Lake District; Geol. Surv. Can., Mem. 105, 91p.

Byers, A.R., Kirkland, S.J.T. and Pearson, W.J. (1965): Geology and mineral deposits of the Flin Flon area, Saskatchewan; Sask. Dep. Miner. Resour., Rep. 62, 95p.

Coombe, W. (1979): Mineral deposits and regional metallogeny, southeastern Shield; *in* Summary of Investigations 1979, Saskatchewan Geological Survey; Sask. Miner. Resour., Misc. Rep. 79-10, p120-133.

_____ (1984): Gold in Saskatchewan; Sask. Energy Mines, Open File Rep. 84-1, 134p.

Gale, G.H.(1981): Mineral Deposit studies in the Flin Flon area; *in* Report of Field Activities 1981, Manit. Miner. Resour. Div., p45-55.

Gale, G.H. and Eccles, D.R. (1988): Mineral deposits and occurrences in the Flin Flon area NTS 63K/13SW: Part 2, Flin Flon area (63K/13SW); Manit. Energy Mines, Miner. Deposit Ser., Rep. 2, 98p

Galley, A.G. and Franklin, J.M. (1987): Geological setting of gold, copper, tungsten and molybdenum occurrences in the Phantom Lake region; *in* Summary of Investigations 1987, Sask. Geol. Surv., Misc. Rep. 87-4, p115-124.

_____ (1989): Setting of gold in the Phantom Lake region, Saskatchewan; *in* Investigations by the Geological Survey of Canada in Manitoba and Saskatchewan during the 1984-1989 Mineral Development Agreements, Geol. Surv. Can., Open File 2133, p33-44.

Gordon, T.M., Hunt, P.A., Loveridge, W.D., Bailes, A.H. and Syme, E.C. (1987): U-Pb zircon ages from the Flin Flon and Kisseynew belts, Manitoba: Chronology of Early Proterozoic crust formation; GAC-MAC Joint Annual Meeting, May 1987, Saskatoon, Prog. Abstr., v12, p48.

Heywood, W.W. (1966): Precambrian geology of the Ledge Lake area, Manitoba and Saskatchewan, Canada; unpubl. Ph.D. thesis, Univ. Wash.

Koo, J. and Mossman, D.J. (1975): Origin and metamorphism of the Flin Flon stratabound Cu-Zn sulphide deposit, Saskatchewan and Manitoba, Canada; Econ. Geol., v70, p48-62.

MacQuarrie, R. (1980): Absolute age of the Flin Flon deposit (abstract) CIM Bull. v73, no.820, p53.

McInnes, W. (1909): Explorations on the Churchill River and South Indian Lake; Geol. Surv. Can., Summ. Rep., 1908, p87-92.

Parslow, G.R. and Gaskarth, J.W. (1988): Proterozoic rocks of east-central Saskatchewan: Geochemistry, structure and mineralization controls; *in* Summary of Investigations 1988, Sask. Geol. Surv., Misc. Rep. 88-4, p127-139.

Pearson, J.G. (1979a): Flin Flon gold prospects: Douglas Lake - Wekach Lake area; 1:10 000 scale prelim. map with Summary of Investigations 1979, Sask. Geol. Surv., Misc. Rep. 79-10.

_____ (1979b): Flin Flon gold prospects; *in* Summary of Investigations 1979, Sask. Geol. Surv., Misc. Rep. 79-10, p145-151.

_____ (1980): Flin Flon gold project; *in* Summary of Investigations 1980, Sask. Geol. Surv. Misc. Rep. 80-4, p70-80.

_____ (1981): Gold metallogenic studies: Phantom Lake - Schist Lake area; *in* Summary of Investigations 1981, Sask. Geol. Surv., Misc. Rep. 81-4, p97-100.

_____ (1983): Gold metallogenic studies: Flin Flon - Amisk Lake area; in Summary of Investigations 1983, Sask. Geol. Surv., Misc. Rep. 83-4, p67-74.

_____ (1984): Gold metallogenic studies, the Rio deposit; *in* Summary of Investigations 1984, Sask. Geol. Surv. Misc. Rep. 84-4, p123-126.

Pearson, J.G. and Galley, A.G. (1985): Gold deposits of the Flin Flon - Amisk Lake area; *in* Summary of Investigations 1985, Sask. Geol. Surv. Misc. Rep. 85-4, p83-89.

Pearson, J.G., MacDougall, F.H., and Galley, A.G. (1986): Geology and evolution of gold occurrences in the Flin Flon - Amisk Lake area, Saskatchewan; *in* Clark, L.A. (ed.), Gold in the Western Shield; CIM Spec. Vol. 38, p399-411.

Price, D.P. (1977): Geology and economic potential of the Flin Flon - Snow Lake areas; Univ. Manit., Cent. Precambrian Stud., Annu. Rep., 1977, p52-83.

Sangster, D.F. (1972): Isotopic studies of ore-leads in the Hanson Lake - Flin FLon - Snow Lake mineral belt, Saskatchewan and Manitoba; Can. J. Earth Sci., v9, p500-513.

Stauffer, M.R. and Mukherjee, A. (1971): Superimposed deformations in the Missi meta-sedimentary rocks near Flin Flon, Manitoba; Can. J. Earth Sci., v8, p217-242.

Stauffer, M.R., Mukherjee, A.C. and Koo, J. (1975): The Amisk Group: an Aphebian(?) island arc deposit; Can. J. Earth Sci., v12, p2021-2035.

Stockwell, C.H. (1946): Flin Flon - Mandy area, Manitoba and Saskatchewan; Geol. Surv. Can., Pap. 46-14, 5p.

_____ (1960): Flin Flon - Mandy, Manitoba and Saskatchewan; Geol. Surv. Can., Map 1078A (with marginal notes), scale 1:12 000.

Streckeisen, A. (1976): To each plutonic rock its proper name; Earth Sci. Rev., v12, p1-33.

Syme, E.C. (1975): Petrogenesis of the boundary intrusions, Flin Flon area, Saskatchewan - Manitoba; unpubl. M.Sc. thesis, Univ. Sask.

_____ (1986): Schist Lake area, Athapapuskow Project; *in* Report of Field Activities 1986, Manit. Energy Mines, p36-42.

_____ (1987): Athapapuskow Lake Project; *in* Report of Field Activities 1987, Manit. Energy Mines, p30-39.

_____ (1988): Athapapuskow Lake Project; *in* Report of Field Activities, 1988, Manit. Energy Mines, p20-34.

Syme, E.C.; Bailes, A.H.; Gordon, T.M. and Hunt, P.A. (1987): U-Pb Zircon geochronology in the Flin Flon Belt: age of Amisk volcanism; *in* Report of Field Activities, 1987, Manit. Energy Mines, p105-107.

Syme, E.C. and Forester, R.W. (1977): Petrogenesis of the Boundary Intrusions in the Flin Flon area of Saskatchewan and Manitoba; Can. J. Earth Sci., v14, p444-455.

Tanton, T.L. (1941a): Flin Flon, Saskatchewan and Manitoba; Geol. Surv. Can., Map 632A (with marginal notes), scale 1:63 360.

_____ (1941b): Schist Lake, Saskatchewan - Manitoba; Geol. Surv. Can., Map 633A (with marginal notes), scale 1:63 360.

Thomas D.J. (1989): The geology of the Douglas Lake- Phantom Lake area (part of NTS 63K-12 and -13); *in* Summary of Investigations 1989, Sask. Geol. Surv., Misc. Rep. 89-4, p44-54.

Watters, B.R. (1989): Lithogeochemical studies in the Flin Flon - Amisk Lake area and the Glennie Domain; *in* Summary of Investigations 1989, Sask. Geol. Surv., Misc. Rep. 89-4 p55-57

Tyrrell, J.B. (1902): Explorations in the northeastern portion of the district of Saskatchewan and adjacent parts of the district of Keewatin; Geol. Surv. Can., Ann. Rep., Vol. VIII, 1900, Rep. F, 48p.

North Lake Gold Deposit: A Model for Arenite-hosted Gold

D. J. Thomas

Thomas, D.J. (1990): North Lake gold deposit: a model for arenite-hosted gold; *in* Summary of Investigations 1990, Saskatchewan Geological Survey; Saskatchewan Energy and Mines, Miscellaneous Report 90-4.

Gold exploration in northern Saskatchewan has been largely directed towards the major greenstone belts in the La Ronge and Glennie Domains (eg. Central Metavolcanic Belt, Nut Bay Belt, Laonil Lake Belt, Brownell Lake Belt). It has resulted in several discoveries, the majority of which occur in metavolcanic-plutonic terrains and are of shear zone-controlled quartz vein type. Significantly fewer metasedimentary-hosted gold occurrences have been documented in the La Ronge and Glennie Domains. The question which arises, is whether the relative abundance of gold occurrences in the greenstone belts is a function of a more favourable metallogeny than in the flanking metasedimentary belts, or whether it is simply due to an exploration bias towards greenstone belts.

Globally, there are several sedimentary environments which host economic gold mineralization. These include:

1) structurally-controlled vein systems in greywacke - turbidite sequences (eg. Archean Yellowknife Supergroup, Northwest Territories; Lower Paleozoic Meguma Group, Nova Scotia),

2) structurally-modified Lower Proterozoic paleoplacer Au-U-Cu deposits in conglomerates and arkosic arenites (eg. Witwatersrand, South Africa; Elliot Lake, Ont.; Jacobina, Brazil) and

3) finely disseminated gold in mixed carbonaceous, calcareous and argillaceous sedimentary rocks commonly referred to as Carlin-type deposits (eg. Nevada, United States).

Large portions of the La Ronge and Glennie Domains are underlain by metasediments, notably metagreywackes of the Crew Lake and MacLean Lake Belts, and to a lesser degree by mixed pelitic and calcareous metasediments in these belts, and feldspathic metaconglomerates and meta-arkoses of the McLennan Group. The most significant gold discoveries to date in the these metasedimentary belts have been: North Lake in the McLennan Group, Greywacke in the MacLean Lake Belt and Pine Lake in the Glennie Domain.

1. Property History

The North Lake property is located about 62 km north of La Ronge and 12 km south of Otter Lake in northern Saskatchewan. Highway 102 is located about 500 m east of the occurrence. The immediate area around the North Lake property was most recently mapped by Lewry (1986) for the Saskatchewan Geological Survey.

The North Lake occurrence is located on CBS 7396 which was staked for H. K. Fredrickson of Saskatoon. The property was optioned to Majorem Minerals Ltd. in 1985, and later assumed by Radcliffe Resources Ltd. In 1987, an airborne geophysical survey over the property identified linear magnetic and VLF anomalies which, in 1987, were prospected, stripped and sampled. A drilling program began in November 1987, with follow-up drill programs continuing through 1988. A zone of mineralization dipping 60° southwest was identified along the west side of a small lake informally named North Lake. Drilling has delineated a branching elongate structure with a strike length of about 600 m. The zone pinches and swells in plan view with surface widths varying between 5 and 40 m. Preliminary geological reserves are; "using a 0.04 oz./ton Au over 3 m cut-off indicate reserves of 2.6 million tons at 0.069 oz./ton Au for a total of 180,000 contained ounces of gold" (Stockwatch March 9, 1989).

2. Geology of the North Lake Gold Showing

The North Lake property is underlain by two main lithologic units; 1) meta-arkosic rocks of the McLennan Group, and 2) intercalated metavolcanic and metasedimentary rocks respectively of the Central Metavolcanic Belt and MacLean Lake Gneisses. Gross lithologic layering on the property dips moderately to steeply west (50°-75°). The contact between the meta-arkosic rocks of the McLennan Group and the mixed metavolcanic - metasedimentary unit is abrupt. Locally lithologic layering in the mixed unit is slightly discordant to that in the meta-arkoses suggesting that a low angle unconformity or disconformity may separate the two. Elsewhere in the region, the McLennan Group has been interpreted to unconformably overlie the Central Metavolcanic Belt and the MacLean Lake Gneisses, however, on the North Lake property original stratigraphic facing was not determined due to the poor preservation of primary depositional structures.

The rocks on the North Lake property are folded into a series of north-trending assymetric folds which are moderately overturned to the east. Figure (1) illustrates a schematic cross-section of the property geology.

The mixed metavolcanic - metasedimentary unit comprises rocks of both the Central Metavolcanic Belt and the MacLean Lake Gneisses. The two are complexly interleaved, however, the dominantly metavolcanic succession in the west contains progressively more metasediments eastwards. The lithologic gradation between the two belts suggests at least partial stratigraphic

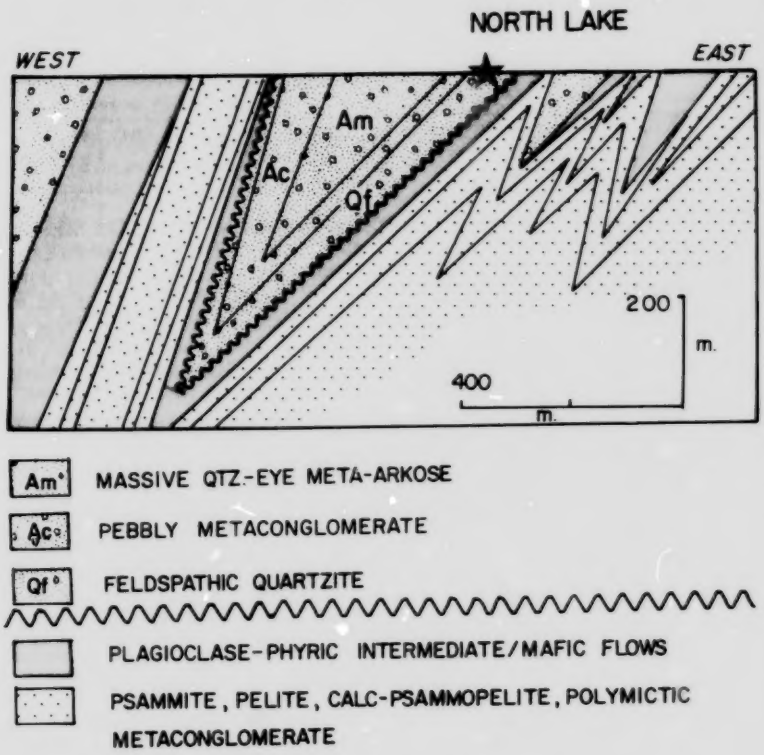

Figure 1 - Structural cross-section of the North Lake area looking north.

equivalence. The intricate interlayering and lateral transition (Figure 2) is then probably due to both primary facies variations and later folding and transposition of lithology.

a) McLennan Group

Meta-arkosic rocks of the McLennan Group outcrop along the west side of North Lake and extend further west for about 500 m. Their extent along strike was not determined. A second, narrow band, about 100 m wide, occurs 80 m east of the lake (Figure 1). The McLennan Group is composed of three main lithologic units: 1) a basal fine-grained feldspathic quartzite, 2) a pebbly meta-arkose and 3) massive 'granitic' quartz-eye meta-arkose.

The basal unit comprises pale red to moderate pink, equigranular, fine-grained feldspathic quartzite which commonly grades into aphanitic cherty varieties exhibiting a subconchodial fracture. These quartzites have a moderately developed cleavage and commonly display a faint centimetre-scale colour banding. They contain up to 5 percent fine-grained muscovite, generally concentrated along foliation planes. Small magnetite cubes, less than 1 mm in diameter, occur in traces amounts. Typically, in the vicinity of quartz veins, the rocks are bleached to a light greenish grey and contain up to 2 percent small reddish garnet (2 to 3 mm diameter) and pyrite cubes (2 to 10 mm diameter) in part enveloped by chlorite. Grit and pebble lenses, which are discontinuous and generally less than a metre thick, occur sporadically within the feldspathic quartzites.

Immediately west of North Lake the feldspathic quartzites are structurally overlain by a unit of pinkish grey to pale yellowish orange, pebbly metaconglomerate. The contact with the feldspathic quartzites is gradational and complexly interlayered on a scale of several tens of centimetres to metres. The metaconglomerate contains up to 15 percent clasts, ranging between 1 to 10 cm long, set in a fine- to medium-grained arkosic matrix. Clasts are predominantly psammopelitic to arkosic in composition although metavolcanic clasts are also present. Quartz granules (2 to 4 mm diameter) locally may comprise up to 30 percent in concentrations which define a crude layering. Up to 5 percent combined muscovite and biotite and locally up to 1 percent small magnetite and ilmenite are also present.

The metaconglomerate grades into a 'granitic' quartz-eye meta-arkose over several metres. The latter varies from moderate orange pink to greyish orange, and is poorly layered to massive. It typically contains from 20 to 35 percent quartz granules, less than 5 percent combined muscovite and biotite, and less than 1 percent magnetite and ilmenite.

b) Central Metavolcanic Belt[1] and MacLean Lake Belt

The unit is formed by trachytic-textured intermediate flows with narrow interflow metasediments and by a succession of calcareous to noncalcareous psammopelitic to pelitic schists and polymictic metaconglomerates. The trachytic-textured intermediate flows are particularly striking in that they contain from 10 to 30 percent plagioclase laths, which may exceed 5 cm in length. They are locally garnetiferous and gradational into intermediate to mafic schists and amphibolites by the loss of plagioclase phenocrysts. Psammopelitic and pelitic schists form narrow interflow beds ranging from 10 cm to several metres thick.

(1) The term Central Metavolcanic Belt is applied here in a lithostratigraphic sense.

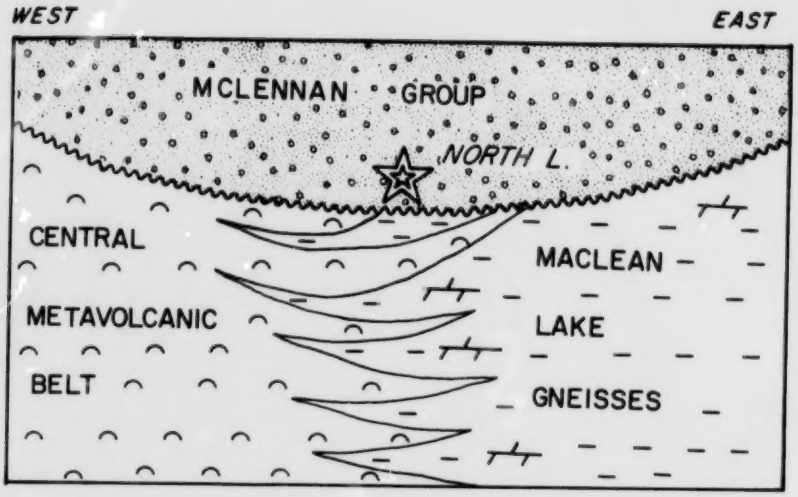

Figure 2 - Schematic section illustrating regional stratigraphic relationship between the McLennan Group, MacLean Lake Gneisses and Central Metavolcanic Belt.

The trachytic-textured flows become progressively interleaved to the east with a mixed succession of calcareous to noncalcareous psammitic to pelitic rocks, and polymictic metaconglomerate.

Calcareous psammite is typically greyish yellow to light greyish green, fine to medium grained, and varies from massive to faintly colour banded. The rocks contain up to 10 percent actinolite/tremolite, diopside, garnet, epidote, and carbonate. They are interlayered with amphibolitic biotite schist and pelitic gneiss. The rocks contain up to 5 percent finely disseminated magnetite. The distribution of magnetite may be in part stratigraphically-controlled with a progressive enrichment of magnetite towards the contact with the McLennan Group. Pelitic to psammopelitic rocks are typically dark greyish brown to dark olive, fine grained and possess a well-developed schistosity. They locally grade into amphibolitic biotite schist comprising 10 to 20 percent amphibole, greater than 35 percent biotite, and several percent free carbonate.

Polymictic metaconglomerate forms narrow discontinuous lenses generally less than 5 m thick and also larger wedge-like units up to several tens of metres thick within a dominantly psammopelitic sequence. The metaconglomerates are generally clast supported but locally possess a matrix-supported framework composed of biotite, chlorite, amphibole and lesser amounts of quartz and feldspar. Clasts range from pebble size (4 to 64 mm) through to cobble size (64 to 256 mm), and consist of various plutonic and volcanic rocks.

3. Structure and Metamorphism

All rocks in the area possess a strong penetrative fabric which is parallel to subparallel to transposed lithologic layering. The dominant foliation dips moderately west (50°-75°). Linear fabrics are locally developed and include mineral lineations, streaky quartz-feldspar aggregates and pebble elongation. Plunges are typically shallow to moderate (25°-45°) to the west. Locally, very high strain is indicated by clasts which display aspect ratios of 20:1, the highest degree of clast deformation occurring in the basal feldspathic quartzites immediately west of North Lake.

The repetition of stratigraphy across the North Lake property suggests tight folding on moderate west dipping axial planes and moderate to shallow southwesterly-plunging fold axes. Rocks of the McLennan Group immediately west of North Lake appear to occupy an easterly overturned synclinal core.

Upper greenschist to lower amphibolite metamorphic conditions are indicated by the presence of biotite, muscovite and garnet in meta-arkosic rocks, and actinolite, hornblende and epidote in metavolcanic rocks.

4. Characteristics of the Gold Mineralization

Gold mineralization is associated with pyritic quartz veins in the fine-grained feldspathic quartzite. The veins occur with greater frequency (locally up to 30 percent by volume) towards the contact with magnetite-rich metavolcanic flows and calcareous psammopelitic rocks. A few are present in the pebbly metaconglomeratic but quartz veins are rare in the 'granitic' quartz-eye meta-arkose.

The veins are typically straight-sided, remarkably uniform in thickness (0.1 to 10 cm) over several metres and show tapering wedge-shaped terminations. The majority appear subparallel to foliation on outcrop surfaces but dip more steeply (60°-70°) than foliation. High angle oblique quartz veins are uncommon.

Veins are enveloped by pale greenish grey bleached wallrock zones ranging in width from one to ten times vein thickness. The altered wallrock generally contains pinhead size garnet, small muscovite aggregates and small euhedral pyrite. Pyrite is the principal sulphide in the quartz veins, with crystals from 1 to 10 mm in diameter, and varying from euhedral cubes to elongated aggregates. Where gold precipitated, pyrite forms between 1 and 5 percent both in the quartz veins and immediate wall rock. Minor to trace amounts of pyrrhotite, chalcopyrite, galena and sphalerite are also present in

the veins. Visible gold is associated with chloritic seams along vein margins and less commonly within the veins.

The feldspathic quartzites appear to wrap around a fold closure to the southwest of North Lake and are less than 200 m thick on its western limb. Quartz veins occur in the same stratigraphic setting as at North Lake suggesting emplacement within the feldspathic quartzites prior to folding.

Immediately north of North Lake the quartz veins near the base of the feldspathic quartzites are more deformed (boudinaged, assymetrically folded, locally brecciated) than those lying structurally higher. Their more deformed state may reflect later shearing along the contact between the quartzites and structurally underlying trachytic-textured metavolcanic flows to the east. Alternatively, a more ductile deformational regime characterized this contact during vein emplacement.

5. Conclusions

1) Gold-bearing quartz vein systems at North Lake are hosted by feldspathic metasediments of the McLennan Group. In the North Lake area, the succession displays a coarsening upwards cycle from a basal feldspathic quartzite through pebbly metaconglomerate to massive quartz-eye metarkose. Contacts between major units are generally gradational over several tens of metres. The succession probably represented a prograding sequence of fluvatile sediments (McLennan Group) unconformably overlying an older succession of mixed volcanics and calcareous psammopelitic sediments (Central Metavolcanic Belt, MacLean Lake Gneisses).

2) The rocks are deformed into tight folds with moderately westerly-dipping axial planes and fold axes that plunge moderately to the west. The rocks appear to have undergone a high degree of strain, indicated by the deformed shapes of the clasts, either prior to or during folding.

3) Gold-bearing quartz veins are largely stratabound, occurring almost exclusively within the basal fine-grained feldspathic quartzites. The veins are increasingly important towards the contact of the quartzite with the structurally and stratigraphically underlying metavolcanic and/or psammopelitic rocks. They were emplaced prior to the last episode of folding.

4) Wall rock immediately adjacent to the veins is noticably altered to a pale greenish grey over widths of 1 mm to 1 m. Alteration halos typically contain garnet, muscovite, chlorite and pyrite. Magnetite, which is particularly prevalent throughout the arkosic succession as well as in the immediately adjacent metavolcanic and psammopelitic rocks, exhibits a significant decrease in abundance around the sulphide-bearing quartz veins.

The stratabound nature of the gold mineralization at North Lake may reflect an original syngenetic gold enrichment. Local iron-rich (magnetite) layers within the McLennan Group clastics are suggestive of heavy mineral accumulation during sedimentation. The depositional environment may have had similarities to that envisaged for Lower Proterozoic age gold-uranium placer deposits such as the Witwatersrand in South Africa (Pretorius, 1981).

During regional deformation the feldspathic quartzites behaved more competently than the surrounding rocks and developed abundant brittle fractures. The increasing abundance of quartz veins towards the base of the feldspathic quartzites reflects the general principle of focussing fluid activity in higher strain regimes, which commonly occur near major lithologic contacts. Metals from the immediate country rocks were mobilized by these fluids and precipitated with quartz in fracture-fillings in the feldspathic quartzites. This general model could apply elsewhere in the McLennan Group as well as to other meta-arkosic successions in northern Saskatchewan.

6. Acknowledgement

The writer would like to thank Mr. Victor Jones, Radcliffe Resources Ltd., for permission to use various maps and data from confidential assessment work submitted to Saskatchewan Energy and Mines. A special thanks is extended to Pamela Schawnn, SEM resident geologist in La Ronge, for constructive contributions and assistance.

7. References

Pretorius, D. (1981); Gold and uranium in quartz pebble conglomerates; *in* Skinner, E.J. (ed.), 75th Anniversary Volume 1981, Econ. Geol., p117-138.

Lewry, J.F. (1986): Bedrock geological mapping, MacKay Lake North; *in* Summary of Investigations 1986, Sask. Geol. Surv. Misc. Rep. 86-4, p48-53.

Bedrock Geological Mapping, Mystic - West Arm, Schist Lakes Area (Northwest part of NTS 63K-12)

B.A. Reilly

Reilly, B.A. (1990): Bedrock geological mapping, Mystic - West Arm, Schist Lakes Area (northwest part of NTS 63K-12); *in* Summary of Investigations 1990, Saskatchewan Geological Survey; Saskatchewan Energy and Mines, Miscellaneous Report 90-4.

Detailed mapping in 1990 of approximately 55 km^2 in the Mystic - West Arm-Schist Lakes area is part of a program to remap the Flin Flon - Amisk Lake region at a scale of 12,500. The objectives are to better understand the distribution and controls on gold and base metal deposits in this region. Emphasis is placed on the application of physical volcanology and lithogeochemistry in refining the Amisk Group stratigraphy and detailed structural analysis of the complex fault/shear systems transecting the region. The program was initiated in 1989, and continued in 1990, with mapping in the Douglas - Phantom Lakes area (Thomas 1989, and this volume).

1. Previous Work

The first reconnaissance geological surveys in the Flin Flon - Amisk Lake region are recorded by Tyrrell (1902), McInnes (1909) and Bruce (1916, 1918a, b). These surveys were followed with detailed mapping by Alcock (1923), Ambrose (1936a,b), Tanton (1941a, b), Stockwell (1946, 1960) and Heywood (1966). Froese (1968) analyzed garnet and biotite from the Mystic Lake, Coronation Mine and surrounding areas. The most recent geological mapping in the area was conducted by Byers *et al.* (1965) and on the Manitoba side by Bailes and Syme (1989) and Syme (1986). This list of previous work is far from exhaustive.

A geophysical series of maps was published in 1987 at various scales. These include aeromagnetic total field maps and vertical gradient maps at 1:20,000 and at 1:50,000. Earlier aeromagnetic series for the map area were published at 1:250,000 in 1971 and at 1:63,360 in 1963.

2. General Geology

The Mystic - West Arm-Schist Lakes area lies in the Flin Flon - Amisk Lake region of the Flin Flon - Snow Lake greenstone domain. The Flin Flon Domain comprises an assemblage of predominantly subaqueous and subordinate subaerial Aphebian metavolcanic rocks, associated metasedimentary rocks and dykes/sills of the Amisk Group. These are the oldest rocks in the belt at 1866 Ma (Syme *et al.* 1987). The Amisk Group is unconformably overlain by a sequence of terrestrial metasedimentary rocks of the Missi Group. The Missi Group is dated at 1830 Ma (Gordon *et al.* 1987) and does not crop out in the map area. The supracrustal rocks have been intruded by various intrusions between 1886 Ma and 1820 Ma (MacQuarrie 1980, Gordon *et al.* 1987). The Flin Flon Domain is bounded to the north by metasedimentary gneisses of the Kisseynew Domain. Flat-lying Ordovician dolomites unconformably overly the Precambrian rocks to the south.

The map area is essentially divided into two regions, namely the Mystic Lake area and the West Arm-Schist Lake area (Figure 1). These are separated by the Kaminis Lake Intrusion.

The Mystic Lake area is chiefly composed of layered metavolcanic rocks, with subordinate mafic metavolcanic rocks and is intruded by the Mystic Lake Intrusion. Layered metavolcanic rocks underly approximately 40 percent of the Mystic Lake area and exhibit sheared and mylonitic textures. Primary features are not observed and the layering is interpreted to be of tectono-metamorphic origin. Mafic metavolcanic rocks are concentrated along the west shore of Mystic Lake, including Woodsworth Bay, the south end of Spectral Lake and near Rochon Lake. They range from massive, pillowed, and plagioclase porphyritic flows to pyroclastic breccias. The Mystic Lake Intrusion is predominantly granodiorite to tonalite, underlies approximately 40 percent of the Mystic Lake area, extends at least 6 km from the north end of Mystic Lake to the south end of Spectral Lake and is approximately 1 km wide. Subordinate quartz diorite to monzodiorite and gabbro to diorite form the rest of the intrusion. The intrusion is highly strained, as are contacts with the country rocks.

The West Arm-Schist Lake area is chiefly underlain by mafic metavolcanic rocks which are intruded by synvolcanic gabbroic-dioritic sills. Pillow breccia flows are the dominant rock type. Massive, pillowed, plagioclase porphyritic and amygdaloidal flows comprise the rest of the mafic metavolcanic succession. Intermediate metavolcanic rocks, mainly pillow breccia flows, are found along the eastern margin of the Kaminis Lake Intrusion and are much less common than the mafic metavolcanic rocks. Undifferentiated synvolcanic gabbroic-dioritic sills comprise up to 40 percent of the metavolcanic succession. The sills extend from the McRobbie Lake area to Craig Lake and appear to be confined to the west side of the West Arm Shear Zone.

The Kaminis Lake Intrusion, first named the Kaminis Granite by Bruce (1918a), then renamed the Kaminis Granodiorite by Heywood (1966), is the largest intrusive body in the area, measuring approximately 5 km between Mystic Lake and West Arm-Schist Lake and extending beyond the area to the south. The Kaminis Lake Intrusion is arbitrarily separated from the Boot Lake - Phantom Lake Intrusion by a necking of the intrusions south of Boot Lake. The dominant component of the

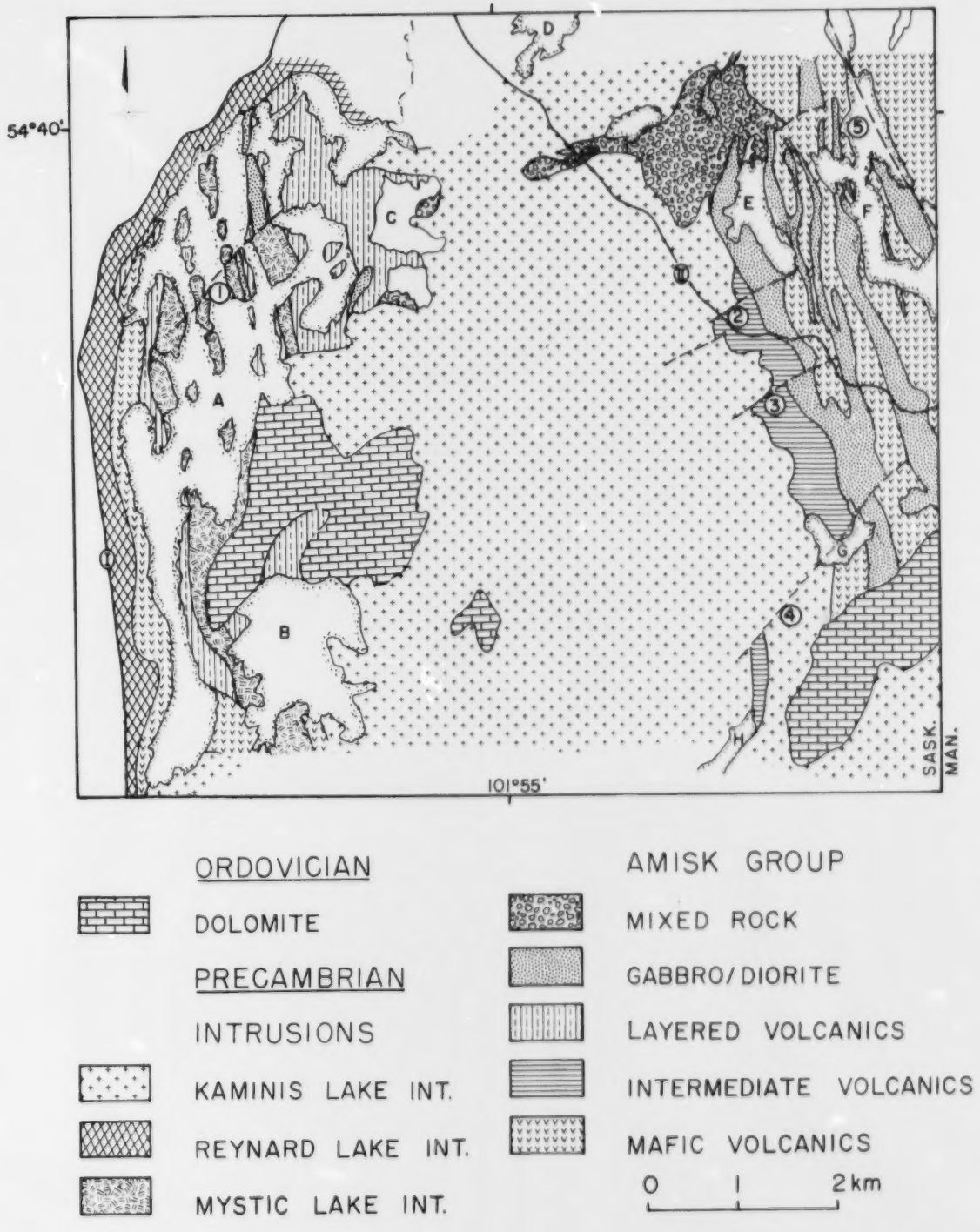

Figure 1 - Geological Sketch map of the Mystic Lake - West Arm-Schist Lake area. A, Mystic Lake; B, Spectral Lake; C, Rochon Lake; D, Boot Lake; E, McRobbie Lake; F, West Arm-Schist Lake; G, Craig Lake; H, Byklum Lake; (1) Mystic Lake Fault; (2) McRobbie Lake Fault; (3) Mine Road Fault; (4) Craig Lake Fault; (5) West Arm Shear Zone; (I) Mystic Lake Road; (II) West Arm Mine Road.

Kaminis Lake Intrusion is hornblende granodiorite, with subordinate biotite-hornblende granodiorite, plagioclase porphyritic granodiorite, quartz diorite to diorite, muscovite-biotite granite and a mixed zone. The margins of the intrusion are foliated and locally sheared, whereas the core of the intrusion is relatively undeformed to weakly foliated. The intrusion is variably fractured, the fractures being generally accompanied by a 2-3 cm hematite stained halo and less commonly infillings of epidote.

The Reynard Lake Intrusion is a large body along the western and northern sides of the map area. Two main components of the intrusion were recognized from a few outcrops mapped this season, namely gabbro and hornblende granodiorite. It also possesses a quartz- and locally plagioclase-porphyritic marginal phase similar to that observed in the Mystic Lake Intrusion. The heterogeneity of the Reynard Lake Intrusion was also observed by Thomas (pers. com.) in the Birch Lake area to the west.

3. Mystic Lake Area Rock Types

a) Mafic Metavolcanic Rocks

Massive and pillow flows weather medium-dark green to black, fresh surfaces are darker green. Mineral assemblages are dominated by hornblende ± actinolite and plagioclase. Minor chlorite, epidote and sericite occur locally. Massive and pillow flows are very fine-grained (< 1 mm) with a homogeneous and equigranular texture. Pillows range in size from 25 by 25 cm to 75 by 50 cm. with chilled selvages 1 to 2 cm wide. Plagioclase porphyritic flows consist of subhedral to euhedral phenocrysts from less than 1 to 10 mm; average size is 2 to 3 mm. Phenocrysts locally comprise up to 50 percent of this unit. In some cases, it is uncertain whether the plagioclase porphyritic rocks are extrusive or intrusive.

Heterolithic pyroclastic breccia at the south end of Woodsworth Bay contains two main types of intermediate composition fragments: plagioclase phyric fragments, which are more numerous, and aphyric fragments. Fragment size ranges from 3 by 1 cm up to 70 by 8 cm, averaging 15 by 3 cm. They are well-sorted, matrix-supported, more felsic than the matrix and variably deformed. Fragments comprise up to 80 percent of the breccia. Plagioclase crystal tuff layers are interbedded with the breccia locally and comprise up to 20 percent of this unit. This breccia is correlated with a pyroclastic breccia on the west shore of central Mystic Lake.

Amphibolite and hornblende-plagioclase gneiss are found adjacent to the major intrusions locally, and is best exemplified in the Rochon Lake area. Hornblende is the chief component of both rock types comprising most of the amphibolitic unit and alternating with plagioclase-rich layers in the hornblende-plagioclase gneiss unit. Layering within the gneiss averages 3 to 4 mm, ranging from 2 mm to 10 mm, and is discontinuous in strike length.

b) Layered Metavolcanic Rocks

These rocks typically weather pale grey green to orange brown, but fresh surfaces are slightly darker shades of grey and green. Grain size is generally fine grained to very fine grained (< 1 mm). Hornblende is the most common mineral, but actinolite and less commonly cummingtonite also occur. Biotite was observed in a few samples and chlorite and epidote are present locally. Plagioclase is variably sericitized and quartz occurs interstial to it and amphibole, or as discrete lenses. Opaque minerals, magnetite and pyrite, are accessory.

Layering is defined by discontinuous, alternating layers or lenses of very fine-grained mafic-rich (amphibole) and slightly coarser-grained felsic-rich (plagioclase) material which impart a streaky appearance. Thickness averages 0.5 mm to 2 mm, but some layers up to 5 cm thick were found. Remnant porphyroclasts comprise up to 20 percent of the rock locally. Primary features are not recognizable and the origin of layering is interpreted as tectono-metamorphic.

c) Mystic Lake Intrusion

Granodiorite to tonalite weathers buff cream to light grey, and fresh surfaces are medium grey to light green. Composition is dominated by quartz, plagioclase, biotite ± microcline and chlorite. Textures are generally porphyroclastic due to shearing. Quartz grains form augens or ribbons up to 3 cm long by 0.5 cm wide, but average 1 cm by 2 mm and comprise up to 50 percent of the rock. Plagioclase and microcline grains are generally smaller in size (1 to 2 mm), less abundant (20 to 30 percent), occur between the quartz augens and ribbons and commonly have porphyroclastic tails. Plagioclase is variably replaced by sericite. Dark green to brown biotite (± chlorite) comprises 10 to 15 percent of the rock and occurs as platy aggregates in discontinuous layers. A tectonic layering is present locally due to strain gradients. Mafic layers and discontinuous lenses represent inclusions of metavolcanic country rock, or mafic dykes/sills or mafic components of the same body. Some of these mafic layers/lenses contain pink euhedral garnet 1 to 3 mm in size that locally comprise up to 50 percent of the layers/lenses.

Gabbro to diorite forms concordant sill-like bodies which range from a few metres up to 70 m in width. Generally, there is a gradation from the gabbro to diorite phase through quartz diorite and monzodiorite to the main granodiorite to tonalite. Weathered surfaces range from a dark warty green to salt and pepper cream and dark green. Fresh surfaces are similar but darker, commonly greenish black. Hornblende is typically more abundant than plagioclase. Grain size ranges from fine to coarse but is generally medium. Although generally homogeneous in composition, the texture is locally heterogeneous. Relatively massive equigranular rocks found adjacent to and enveloped by strongly foliated rock represent heterogeneous strain during shearing. A bulk strain gradient is observed from relatively pervasive shearing in the granodiorite to tonalite to more heterogeneous shearing in the gabbro and diorite.

Quartz diorite to monzodiorite is less abundant than the other rock types with which it is generally gradational. The rock is composed of hornblende, plagioclase and up to 15 percent quartz. Weathered surfaces are buff white with speckled medium to dark green; fresh surfaces are slightly darker. The rock comprises hornblende, plagioclase and up to 15 percent quartz. Textures vary from porphyroclastic, similar to the granodiorite and tonalite, to more equigranular, similar to the gabbro and diorite.

d) Pre- to Syntectonic Minor Intrusions

Pre- to syntectonic felsic and mafic dykes and sills are abundant in the Mystic Lake area, especially in the layered metavolcanic rocks and the Mystic Lake Intrusion. They comprise up to 80 percent of the layered metavolcanic rocks locally. The intrusions are generally less than one metre thick, and rarely as much as five metres. Textures are sheared to mylonitic, similar to the host rocks. Contacts are concordant to weakly discordant and highly strained. The intrusions commonly display boudinage with quartz infilling the boudin necks.

Felsic intrusions are buff-white on weathered surfaces with fresh surfaces typically light grey. They are chiefly composed of quartzofeldspathic material with minor biotite, chlorite and epidote. Grain size ranges from aplitic to porphyritic to pegmatitic. Porphyries exhibit highly attenuated quartz and feldspar grains with tails which produce a streaky appearance. Pegmatites, on the other hand, possess sheared feldspar grains which produce a lapilli-size fragmental appearance.

Mafic intrusions weather dull grey to dark grey black; fresh surfaces are dark grey. Their composition is dominated by hornblende and plagioclase with subordinate actinolite, epidote and chlorite. Grain size ranges from very fine to medium and they are equigranular to plagioclase porphyritic. Shearing produces streaky to layered mylonitic textures.

e) Post-tectonic Minor Intrusions

Post-tectonic minor intrusions of mafic and felsic composition are less abundant than pre- to syntectonic minor intrusions. The late intrusions are typically < 1 m wide with contacts concordant to weakly discordant, similar to the early minor intrusions. Textures are homogeneous and range from massive to weakly foliated. They are equigranular but more commonly porphyritic with aphanitic to medium grain sizes. Post-tectonic intrusions include aphanitic to quartz-feldspar and feldspar-quartz porphyritic felsic intrusions and aphanitic to plagioclase porphyritic mafic intrusions.

4. West Arm-Schist Lake Area Rock Types

a) Mafic Metavolcanic Rocks

Mafic metavolcanic rocks generally possess a dull pale green weathered surface and medium green fresh surface at greenschist metamorphic facies. At amphibolite metamorphic facies, they are dark green and greenish black, respectively. Composition is chiefly chlorite (greenschist facies) or hornblende (amphibolite facies) plagioclase ± actinolite. Plagioclase is variably replaced by epidote and sericite.

Massive flows exhibit a homogeneous, massive equigranular texture. Grain size ranges from very fine (< 1 mm) to medium (2 to 3 mm), with the former more common. **Pillow flows** contain pillows that range from 40 by 20 cm up to 3 m by 75 cm, but average about 80 by 50 cm. Pillows are teardrop- to bun- with selvages that are 2 to 4 cm thick, dark green and weather recessively. The pillow texture varies from massive, plagioclase porphyritic, amygdaloidal and vesicular. Plagioclase phenocrysts, which comprise up to 20 percent of the pillows and 50 percent locally, range in size from 1 mm to 10 mm, but average 2 to 3 mm. They occur randomly in both the pillow and selvage, but are also core or rim concentrated. Pillow tops were discernable in only a few outcrops.

Pillow breccia flows are the most common rock type amongst the mafic metavolcanic sequence in the Schist Lake area. Fragments are essentially monolithic, similar in composition to the matrix and weather pale green due to epidote alteration. Like the pillow flows, fragments within the pillow breccia unit are variably plagioclase porphyritic, vesicular and most commonly quartz amygdaloidal. Fragments are generally amoeboid in shape, range in size from 3 by 1 cm up to 60 by 30 cm, but average 15 by 8 cm, are matrix-supported, comprise 60 to 80 percent of the rock and are generally well-sorted.

Silicified pillow and pillow breccia flow rock at the northwest end of the West Arm of Schist Lake is a product of silicification and contemporaneous shearing. Original textures and minerals are replaced by mylonitic layering and a quartz ± sericite ± calcite mineral assemblage, respectively. The texture is cherty and millimetre-scale mylonitic layering gives the rock a streaky appearance. Weathered surfaces are buff white and fresh surfaces are light grey. These silicified mafic metavolcanics were previously mapped as felsic metavolcanics, but their mafic metavolcanic protolith is identified in less deformed and silicified enclaves where pillows and pillow breccia can be recognized.

Although **amygdaloidal flows** are rare, amygdales are quite common inside pillows and fragments of pillow breccias. Quartz amygdales are the most abundant type; epidote and carbonate filled amygdales are less common. Average amygdale size is 2 to 3 mm but as large as 1.5 cm have been observed. Shape varies from spherical to lenticular. Amygdales typically comprise 10 to 15 percent of a rock and as much as 30 percent locally. Within pillows and pillow breccia fragments, amygdales are randomly distributed or concentrated in margins or cores.

Plagioclase porphyritic flows exhibit a homogeneous massive inequigranular texture. Phenocrysts are generally subhedral, equant shaped and range in size from 0.5

mm to 20 mm, averaging 2 to 3 mm. Matrix material is typically finer-grained and less than 1 mm in size. Phenocrysts generally comprise 25 to 30 percent and locally as much as 50 percent of the rock. Many pillows and pillow breccia flows are also plagioclase porphyritic.

A **mixed mafic metavolcanic and gabbroic-dioritic suite** forms a hybrid zone north of McRobbie Lake. Hornblende granodiorite rocks also occur locally. The mafic metavolcanics are very fine to medium grained (< 1 to 2 mm), generally foliated and occur as amphibolitized rafts and inclusions in the gabbro-diorite. The gabbroic-dioritic rocks are massive to foliated and range from fine to coarse grained (1 to 6 mm) and locally form an intrusion breccia.

b) Intermediate Metavolcanic Rocks

This unit is chiefly composed of pillow breccia in which fragments are similar to the mafic metavolcanic pillow breccia. The fragments are, amoeboid-shaped, matrix-supported, monolithic in composition, locally quartz amygdaloidal and preferentially epidotized. The essential difference is the presence of up to 20 percent quartz in the intermediate metavolcanic rock. Interbedded massive and pillow flows are found with the pillow breccia.

c) Gabbroic-Dioritic Sills

Gabbroic-dioritic sills weather orangish brown to medium-dark green and fresh surfaces are dark green. Hornblende, occurring in prismatic grains replacing pyroxene, is more abundant than plagioclase, which is variably replaced by sericite and epidote. Minor minerals are actinolite, chlorite, zoisite and magnetite. Grain size ranges from fine to more commonly medium (2 mm). The sills are typically equigranular but local plagioclase porphyritic varieties were also mapped. Decimetre-scale layering observed locally is defined by gradations between a hornblende-rich base and a plagioclase-rich top. Textures range from massive to sheared as foliation is heterogeneously developed and is best seen where relatively undeformed lithons are enveloped by highly strained rock. The width of the highly strained zones is typically less than 1 m. Contacts with the volcanic rocks are highly strained.

d) Post-Tectonic Mafic Intrusions

Plagioclase porphyritic mafic dykes, composed of a fine-grained matrix of hornblende and plagioclase and ranging in width from 1 to 10 metres, cross-cut the regional strike in a northeast orientation. Weathered surfaces are grey black and fresh surfaces dark grey. Euhedral plagioclase crystals average 5 mm and locally up to 4 cm in size, comprise about 15 percent of the rock. Textures are homogeneous and massive. Contacts with the metavolcanic rocks and gabbro-diorite sills are sharp and generally sheared.

5. Major Intrusions

a) Kaminis Lake Intrusion

Hornblende granodiorite comprises approximately 80 percent of the intrusion. Weathered surfaces exhibit a buff-cream and dark green salt and pepper texture; fresh surfaces are darker coloured. Grain size is generally medium (2 to 4 mm), but finer- and coarser-grained rocks are found locally. Plagioclase, variably replaced by sericite and epidote, comprises 30 to 40 percent, quartz 20 to 25 percent and potassium feldspar 5 to 15 percent of the rock, providing a generally equigranular texture. Prismatic hornblende comprises 20 to 30 percent and flakes of biotite less than 5 percent. The mafic minerals are in places weakly porphyritic. Accessory minerals include apatite, zircon, sphene, magnetite and pyrite. Inclusions of amphibolitized country rock, comprising up to 2 percent of the intrusion, are preferentially aligned parallel to foliation.

A **porphyritic hornblende granodiorite** variety outcrops south of Boot Lake. Subhedral plagioclase phenocrysts, ranging in size from 4 to 10 mm, comprise 15 to 20 percent of the rock.

Biotite-hornblende granodiorite contains 5 to 15 percent biotite and 0 to 30 percent hornblende. This component is mainly found east of Byklum Lake and locally where it is gradational with the main body.

Quartz diorite to diorite is found west of Green Bay, at the south end of Woodsworth Bay, north of McRobbie Lake and south of Craig Lake. These rocks consist of 50 to 60 percent plagioclase, 40 to 50 percent hornblende and 0 to 10 percent quartz. Texture and grain size is similar to that observed in the hornblende granodiorite described above.

A massive homogneous and medium-grained **muscovite-biotite granite** identified along the western most extremity of the Kaminis Lake Intrusion has pink weathered surfaces and light pinkish grey fresh surfaces. Microcline, quartz and plagioclase are found in approximately equal proportions. Platy flakes of biotite and muscovite comprise 10 and 5 percent, respectively. This granite is massive, homogeneous and medium grained (2 to 3 mm). Biotite crystals average 4 to 5 mm, and can be up to 10 mm to give an inequigranular, porphyritic texture.

A **mixed marginal zone** of hornblende granodiorite intrusions are quite heterogeneous in places. Highly sheared quartz, and locally plagioclase, porphyritic bodies are similar to the granodiorite to tonalite component of the Mystic Lake Intrusion both compositionally and texturally. A heterolithic intrusion breccia also occurs locally along the contact of the Kaminis Lake Intrusion. Fragments of mafic and intermediate metavolcanic rock, amphibolite, plagioclase-hornblende gneiss and gabbro are also included in this hornblende granodiorite. Late pink pegmatite dykes derived from the hornblende granodiorite truncate the country rocks as well as the intrusion along the contact zone. Mixed zones derived from various components of the Kaminis

Lake Intrusion, locally incorporating more than 50 percent of amphibolitized country rock, are found along the margins of the intrusion in places.

b) Reynard Lake Intrusion

Gabbro occurs immediately west of Mystic Lake where it intrudes the supracrustal rocks. Weathered surfaces exhibit salt and pepper texture and are buff-cream to dark green, similar to fresh surfaces. Grain size is medium (2 to 5 mm) and grains are equigranular. Hornblende is more abundant than plagioclase. Leucogabbro and melagabbro occur locally. The gabbro is highly sheared along the contact with the supracrustal rocks.

Hornblende granodiorite is the predominant phase of the Reynard Lake Intrusion along the north shore of Green Bay. The rock is heterogeneous in composition, and texture ranging from tonalite to gabbro and from foliated to massive. The hornblende granodiorite is mineralogically similar to the Kaminis Lake Intrusion.

c) Diabase Dykes

Diabase dykes up to 5 m in width, with local chilled margins 1 to 2 cm wide, cross-cut all rock units in the area. The dykes weather pale green and fresh surfaces are medium greyish green. They are chiefly mafic but locally intermediate in composition with a dominance of plagioclase and hornblende. Textures are generally massive, homogeneous, fine grained and equigranular although euhedral plagioclase grains up to 1.5 cm in size comprise up to 20 percent of the rock in places.

d) Dolomite

Outliers of flat-lying Ordovician dolomite unconformably overly the Precambrian rocks in the southern portion of the map area. They are located between Mystic and Spectral Lakes, between Craig and Byklum Lakes and east of Spectral Lake. The contact is typically marked by an escarpment of dolomite 10 to 20 m high which is flanked by a talus slope of angular dolomite blocks. The dolomite weathers a cream grey to a mottled reddish purple. Fresh surfaces are darker grey. Bedding within the dolomite is irregular often producing lenticular wedges several metres in length and typically a few centimetres to decimetres thick.

6. Metamorphic Geology

a) Regional Metamorphism

Mineral assemblages in the Mystic Lake area indicate an ambient metamorphic grade of lower amphibolite facies. Mafic and intermediate metavolcanic rocks in the Mystic Lake area predominantly comprise hornblende; actinolite and biotite are less common, and cummingtonite is rare. Plagioclase grains are variably replaced by sericite and epidote.

Mineral assemblages in the West Arm-Schist Lake area indicate at least two metamorphic facies terrains separated by the West Arm Shear Zone. On the east side of the shear zone, chlorite, epidote, zoisite and less commonly actinolite as well as local calcite indicate a lower greenschist facies. Rocks on the west side of the shear zone are similar in bulk composition, but are dominated by hornblende and plagioclase, indicating the attainment of lower amphibolite metamorphic facies. The presence of chlorite, epidote, zoisite and actinolite also indicates local areas where greenschist metamorphic facies grade were attained.

Further east, on the Manitoba side of the provincial boundary, prehnite-pumpellyite metamorphic facies rocks have been mapped and recorded southeast of Ledge Lake (Heywood, 1966; Syme, 1986; Digel and Gordon, 1990). Prehnite and pumpellyite have not, however, been found in this investigation.

In summary, there exists an apparent regional trend from sub-greenschist metamorphic facies in the area southeast of Ledge Lake, to greenschist metamorphic facies in the West Arm-Schist Lake area, to amphibolite metamorphic facies in the Mystic Lake area.

b) Contact Metamorphism

The Kaminis Lake Intrusion, and apparently the Reynard Lake Intrusion have produced a contact metamorphic aureole about 100 m wide. This is manifest by the presence of garnet porphyroblasts in the mafic and intermediate metavolcanic rocks. Locally, the metavolcanic rocks are also metamorphosed and deformed to produce amphibolites and hornblende-plagioclase gneisses. Up to middle amphibolite metamorphic facies is attained within the aureole.

c) Retrograde Metamorphism

Chlorite, epidote, zoisite, sericite and calcite are typically found associated with post-peak of metamorphism structures. These retrograde mineral assemblages are found within brittle-ductile shear zones and late faults throughout the area. This is best displayed in mafic rocks where amphibolite grade rocks are retrogressed to lower greenschist facies, chlorite-rich assemblages including chlorite schist. Felsic rocks have produced sericite-rich assemblages. Biotite within the Mystic Lake Intrusion retrogrades to chlorite where transected by late structures. Greenschist grade rocks are retrogressed to schists composed of chlorite $\pm$ calcite $\pm$ sericite. Carbonate is present within some of the shear zones.

7. Structural Geology

a) Mystic Lake Area

D1 Structures

The earliest recognizable structure in the Mystic Lake area is a strong to intense planar fabric. This foliation strikes north to northeast, dips steeply to the west, and is best developed in the layered metavolcanic rocks and Mystic Lake Intrusion. The foliation is enhanced by the

development of a tectono-metamorphic layering. The layered metavolcanic rocks and the Mystic Lake Intrusion exhibit sheared and mylonitic textures, as do many mafic and felsic dykes/sills. Mafic metavolcanic rocks along the west shore of Woodsworth Bay are unaffected by this fabric. A moderately to steeply south-plunging stretching lineation (L1) was observed in some localities.

Shallow to moderately north-plunging mesoscopic asymmetric folds are found associated with the D1 fabric. These folds typically exhibit a Z-shaped geometry and are tight to isoclinal, possibly representing asymmetric shear folds produced during a regional shearing event or parasitic folds produced in sheared fold limbs during a regional folding event. Rocks in the Mystic Lake area have been subjected to strong to intense shearing and localized folding under lower amphibolite grade metamorphism at an early stage in its deformation history. This D1 event post-dates the emplacement of the Mystic-Lake Intrusion.

Pluton Intrusion and Related D2 Structures

The Kaminis Lake Intrusion and the Reynard Lake Intrusion cross-cut the early D1 structure. The D1 foliation is folded within a zone of contact strain up to 100 m in width, coincident with contact metamorphism. Mesoscopic folds in this zone are close to open. Fold axes plunge moderately to steeply to the south and are coaxial with earlier L1 stretching lineation. The intersection of the axial plane of these folds with the D1 fabric in the contact metamorphic aureoles has produced an intersection lineation (L2) which is also coaxial, resulting in very high L:S ratios. Shearing and mylonitic textures are common in the contact zone.

D3 Brittle-Ductile Shear Zones

Localized brittle-ductile shear zones represent the third recognized deformational event in the area (D3). These zones are defined by zones of high strain, typically less than 1 m wide, and are commonly composed of discrete individual centimetre-scale shears within a broader zone. The shear zones are generally concordant to weakly discordant and in places exhibit an anastomosing geometry. The ductile component is dominant over the brittle component. Brittle-ductile shear zones are generally accompanied by retrogressive mineral assemblages. Brittle-ductile shear zones are found transecting the Kaminis Lake Intrusion. No mapping has been completed away from the margin of the Reynard Lake Intrusion to establish their presence.

D4 Late Faulting

The final deformation event is manifest as late faulting. Regionally, a conjugate set has developed in response to east-west shortening, comprising a dextral northeast set and a sinistral northwest set. Measured dips on the faults are vertical to subvertical and the dip slip component is unknown. Although essentially brittle structures, many show evidence for an earlier ductile component. The Mystic Lake Fault is a major fault, having an apparent dextral horizontal component of movement; but total displacement is unknown. Mesoscopic-scale predominantly brittle faulting is common in the area.

b) West Arm-Schist Lake Area

D1 Structures

The earlier deformation structures of the Mystic Lake area, namely the strong to intense planar fabric and asymmetric folds, are not represented in West Arm-Schist Lake. The earliest structure mapped in the West Arm-Schist Lake area is a weak to moderate penetrative planar flattening foliation which strikes north to northwest and dips steeply to the west, with no associated lineation. This foliation is associated with evidence of stratigraphic reversals. West of the West Arm Shear Zone, top determinations from pillow stacking in mafic metavolcanic rocks, and grading in layered gabbroic dioritic sills indicate younging predominantly to the west. East of the fault, top determination from pillows are more ambiguous; but there is an apparent predominantly easterly facing as shown by graded bedding within the matrix of pillow fragment breccias. This apparent reversal in younging direction may be explained by the presence of an overturned anticlinal fold with an axial plane parallel to the West Arm of Schist Lake. This, north to northwest-trending fold set may be related to the development of the regional weak to penetrative foliation. Alternatively, these relationships may be explained by the juxtaposition of oppositely younging successions during movement along the West Arm Shear Zone.

Pluton Intrusion and Related D2 Structures

The Kaminis Lake Intrusion superimposes a contact strain aureole on rocks in the West Arm-Schist Lake area similar to that observed in the Mystic Lake area described above.

D3 Brittle-Ductile Shear Zones: West Arm Shear Zone

The West Arm Shear Zone was first recognized by Heywood (1966). It extends south of the map area (Syme 1986) into Manitoba and north into the Douglas - Phantom Lakes area (Thomas this volume), and is essentially a zone of deformation striking in a northwest direction parallel to the West Arm of Schist Lake. It comprises a series of brittle-ductile shear zones (D3) similar to those described in the Mystic Lake area, except that they are typically wider, up to 10 m. The structure generally has strong penetrative planar fabric which is more intensely developed near the centre of the shear zones. Rocks of mafic composition have been transformed to chlorite ± calcite ± sericite schist. A strong stretching lineation (L3), which plunges moderately to steeply to the south, is defined by attenuated pillows and fragments of pillow breccia. C-C' fabric relationships indicate a west-side-up reverse movement along the shear zone.

The regional significance of the West Arm Shear Zone is not fully understood at this time. It demarcates a break

between a deeper rock package to the west which is predominantly amphibolite grade, west-younging metavolcanics with abundant gabbroic-dioritic sills, and a rock package to the east comprising predominantly greenschist grade, east-younging metavolcanics with no gabbroic-dioritic sills. Kinematic indicators are also consistent with the juxtaposition of a deeper package in the west against a shallower package in the east. Although present mineral assemblages indicate retrograde metamorphic conditions, movement along this structure may have been reactivated over time.

D4 Late Faulting

Late brittle faulting (D4) in the Mystic Lake area is also present in the Schist Lake area. The McRobbie Lake Fault, the Craig Lake Fault and the Mine Road Fault displace the metavolcanic succession and the Kaminis Lake Intrusion. Like the Mystic Lake Fault, these faults have an apparent dextral horizontal component of movement; however, the total amount of displacement is unknown.

8. Economic Geology

Mining companies have actively explored for base metals and gold in the Flin Flon - Amisk Lake region area since the early part of the century. The following notes are compiled from off-confidential data in the Saskatchewan Energy and Mines Mineral Assessment Files.

a) Summary of Industry Exploration in the Mystic Lake Area

Exploration activity in the Mystic Lake area is recorded from 1952 when Hudson Bay Exploration and Development Company Limited (Assessment File 63K12-0021) conducted a ground electromagnetic (EM) survey. Twelve conductors were identified. The following year twenty-two diamond drill holes were drilled for a total of 3335 m. Anomalous copper was detected in four holes.

Four trenches were dug by J.M. Jacobson (Assessment File 63 K12-0069) in 1971 on the west shore, central Mystic Lake. No assay results were recorded.

Hudson Bay Exploration and Development Company Limited (Assessment File 63K12-0068) identified two fair to excellent and two poor anomalies during a ground EM survey conducted in 1971 and 1972 in the central to north Mystic Lake area. Follow-up drilling revealed trace Au, Ag, Cu and Zn in 1971 (two diamond drill holes totalling 217 m) and trace Cu and Zn in 1972 (four holes totalling 239 m).

During 1977, Granges Exploration Aktiebolag (now Granges Exploration Limited) completed two ground EM surveys northwest of Mystic Lake (Assessment File 63K12-0098). One diamond drill hole (115 m) intersected low copper and nickel values in a pyrrhotitic-pyrite rich zone in a gabbroic phase of the Reynard Lake Intrusion. Another ground EM survey conducted by the company in 1987 delineated a weak extension of this mineralized zone (Assessment File 63K12-0149). Follow-up diamond drilling (three holes) was completed later that same summer (Assessment File 63K12-0159) and assay values remain confidential.

Granges Exploration Aktiebolag performed an EM survey and subsequent drilling from central Mystic Lake to north Spectral Lake in 1978 (Assessment File 63K12-0094). Three of the four diamond drill holes (totalling 205 m) intersected graphite, thus explaining the anomalies.

In 1979, Flin Flon Mines Limited conducted an EM and partial magnetometer survey, along the east shore, central Mystic Lake. One diamond drill hole, 168 m deep, revealed no economic mineralization (Assessment File 63K12-0107).

Flin Flon Mines Limited completed a ground EM and magnetic survey in 1980 on the east shore of Mystic Lake, between Rochon Lake and the West Arm Mine Road. Some rock samples were collected and analyzed for magnetite (Assessment File 63K12-0110). Several EM anomalies were identified. Earlier work, which included a ground EM survey (1969) and diamond drilling (1970), tested anomalies north of Rochon Lake.

In 1982, Wollex Exploration, at the request of Kenergy Resource Corporation, conducted a prospecting program in an area which includes north Mystic Lake and Wekatch Lake (Assessment File 63K12-0125). No outcrops containing significant gold mineralization were located. Ground EM surveys, geological mapping and sampling during 1983 concentrated on the Wekatch Lake area (Assessment File 63K12-0132). During 1984, Kenergy Resource Corporation conducted a geochemical survey of C-zone soils along with prospecting. Anomalous gold zones were found in the Boot Lake Intrusion and along the western shore of Wekatch/Meridian River (Assessment File 63K12-0139).

CAMECO conducted a geological mapping, prospecting and rock sampling program in the central Mystic Lake area in 1988 (Assessment File 63K12-0166). Results from this program remain confidential at this time.

Between 1989 and 1990, Coronation Mines Limited conducted a program in the central Mystic Lake area which included an EM survey, geological mapping, prospecting and drilling. The best assay results (L. Clark, Coronation Mines Limited, pers. comm.) for gold occurrences are as follows: Boys Showing - 0.32 oz/ton across a width of 8 cm, and Getz Showing - 0.99 oz/ton across a width of 5 cm. One of the two diamond drill holes intersected up to 1.8 percent zinc with significant amounts of copper and gold.

b) Summary of Industry Exploration in the West Arm-Schist Lake area

During 1946-47, Consolidated Mining and Smelting Company of Canada Limited (COMINCO) drilled six diamond drill holes totalling about 339 m in an area where the West Arm of Schist Lake straddles the Saskatchewan/Manitoba border. Gold mineralization was

detected apparently associated with iron formation at depth (Assessment File 63K12-0005).

In 1955, T.C. Meadows excavated twelve trenches in an area stretching from the West Arm of Schist Lake to Craig Lake. No details of rock analyses are given (Assessment File 63K12-0017).

Noranda Exploration Company completed a ground EM survey, seven trenches and five diamond drill holes (totalling 236 m) between 1961 and 1965 in an area along the Saskatchewan/Manitoba border between McRobbie Lake and Craig Lake (Assessment File 63K12-0026). Sulphide mineralization within chloritic and lesser graphitic schists did not yield ore value yet warranted further exploration based on their character, length and proximity to West Arm Mine.

In 1937, George M. Monson trenched an area believed to be located along the northern margin of the map area south of Phantom Lake (Assessment File 63K12-0039). No assays were recorded.

Hudson Bay Exploration and Development Company carried out an extensive exploration program in the West Arm-Schist Lake area since the 1950's. Between 1953 and 1954, they conducted a ground EM survey and drilled seven diamond drill holes totalling 3051 ft at the north end of the West Arm of Schist Lake (Assessment File 63K12-0019). Silicified metavolcanics were their prime target. Between 1969 and 1970, a ground EM survey was conducted from north of McRobbie Lake to south of Craig Lake (Assessment File 63K12-0056). Nine diamond drill holes (totalling 802 m) were drilled to test conductors, however, no economic mineralization was found. A second ground EM survey and a tenth hole drilled (136 m) in 1973 gave similar results (Assessment File 63K12-0075). Another four diamond drill holes (totalling 308 m) were completed in 1974 (Assessment File 63K12-0079) and two more (totalling 152 m) in 1975. Ground EM surveys were completed in 1975 (Assessment File 63K12-0085) and in 1976 (Assessment File 63K12-0087). Conductors from these surveys were tested in 1977 when four diamond drill holes were drilled for a total of 511 m (Assessment File 63K12-0008).

In 1979, a ground EM survey was done to test ambiguous anomalies from previous surveys and to check for any short anomalies which may have been missed. Two diamond drill holes totalling 159 m were drilled in 1978 (Assessment File 63K12-0091). Continued drilling in 1979 (Assessment File 63K12-0109) resulted in a total of 386 m from four diamond drill holes. Anomalies revealed by a ground EM survey in 1980 and 1981 (Assessment File 63K12-0115) had been located by earlier surveys. Two follow-up diamond drill holes at the West Arm Mine site area totalled 301 m in Saskatchewan and 482 m in Manitoba. Several EM check surveys were conducted in the Craig Lake area in 1982 from which one conductor was tested with a 72 m diamond drill hole (Assessment File 63K12-0127).

In 1984, a ground EM and magnetic survey was conducted along the West Arm of Schist Lake (Assessment File 63K12-0137). An EM target was defined and tested by a 48 m drill hole (Assessment File 63K12-0136). Five more targets were identified during a later ground EM survey in the same area in 1986 designed to define the northern extension of the West Arm Mine Horizon and locate additional gold-bearing pyritic shear zones (Assessment File 63K12-0145). Five diamond drill holes totalling 393 m were completed in 1987 (Assessment File 63K12-0151). All of the holes intersected a sequence of metavolcanic and igneous rocks with quartz-carbonate veining and some slight pyrite-arsenopyrite mineralization. Samples of the veining and mineralized sections failed to return economic values.

During 1987 and 1988, Hudson Bay Exploration and Development Company Limited and Mingold Resources Incorporated completed a humus biogeochemical survey and rock chip sample survey along the West Arm of Schist Lake (Assessment File 63K12-0156). Results from these surveys remain confidential. During 1987 and 1988, Mingold Resources Incorporated drilled seven diamond drill holes along the extension of the West Arm Mine, at the north end of the West Arm of Schist Lake (Assessment File 63K12-0154). Results from this program are confidential.

c) Base Metals

Base metal deposits, including the Flin Flon Mine, are the most abundant and significant mineral deposit type in the Flin Flon - Amisk Lake region. Much work has been completed including Sangster (1972), Koo and Mossman (1975), Stauffer *et al.* (1975), Price (1977), Coombe (1979), Bailes and Syme (1987) and Syme (1986, 1987, 1988). These deposits have been classified as volcanic-associated stratabound massive sulphide bodies. A comparative account of base metal deposits in the Flin Flon - Amisk Lake area has been compiled by Thomas (this volume).

Base metal deposits have not been found in the Mystic Lake - West Arm-Schist Lake area, although they occur in the West Arm Cu-Zn massive sulphide deposit nearby in Manitoba. The mine has estimated reserves of 710,000 tonnes of 4.63 percent copper and 0.6 percent zinc (Price 1977). The massive sulphide orebody is stratiform. Host rocks are black graphitic argillite, pyritic siltstone and banded chert-hematite (Syme 1986). This fine-grained sedimentary sequence is not exposed on the surface, nor is a stratigraphically equivalent sequence observed within the map area. Altered bleached and locally carbonatized and silicified plagioclase-phyric pillow flows and related pillow fragment breccias form the stratigraphic footwall for the deposit and are intruded by pale green fine-grained diorite (Syme 1986). The light colour is interpreted by Syme as a product of hydrothermal alteration and the original composition is presumed to be basaltic andesite. Similar flows and breccias found along the West Arm of Schist Lake this summer have also been variably deformed and altered, especially adjacent to the West Arm Shear Zone.

d) Gold

During the past ten years or so, detailed mapping by provincial and federal government geologists in the Flin Flon - Amisk Lake area has studied gold occurrences from deposit to camp scale. These workers include Pearson (1979, 1980, 1981, 1983, 1984), Coombe (1984), Pearson and Galley (1985), Pearson *et al.* (1986), and Galley and Franklin (1987). These studies have shown that the majority of gold occurrences in the Flin Flon - Amisk Lake area are structurally-controlled, many related to the Cliff Lake - Ross Lake Fault system (Thomas 1989). Zones of high strain were produced at various stages of the deformational history of the area. Early pervasive shearing is associated with the D1 event at Mystic Lake. Contact strain aureoles were produced in the margins of intrusions and in country rock during emplacement of the major intrusions (D2). Brittle-ductile shear zones associated with the D3 deformation are perhaps the most favourable targets for gold in the map area (e.g. West Arm Shear Zone). Alteration associated with many of these zones includes chloritization, carbonatization, silicification, sericitization and sulphidation. Late stage faulting, associated with the D4 event, may also serve as a favourable site for gold precipitation. The Mystic Lake Fault, for example, is enveloped by an extensive stockwork of quartz veining and hematite alteration along its exposed sections.

9. References

Alcock, F.J. (1923): Flin Flon map area, Manitoba and Saskatchewan; Geol. Surv. Can., Summ. Rep. 1922, ptC, p1-36.

Ambrose, J.W. (1936a): Progressive kinetic metamorphism in the Missi Series near Flin Flon, Manitoba; Am. J. Sci., (5th ser.), v32, p257-286.

_____ (1936b): Structures in the Missi Series near Flin Flon, Manitoba; Trans. R. Soc. Can. (3rd ser.), v30, sec4, p81-98.

Bailes, A.H. and Syme, E.C. (1989): Geology of the Flin Flon - White Lake area; Manit. Energy Mines, Geol. Rep. GR 87-1, 313p.

Bruce, E.L. (1916): Amisk - Athapapuskow Lake area, northern Saskatchewan and northern Manitoba; Geol. Surv. Can., Sum. Rep. 1915, p126-130.

_____ (1918a): Schist Lake district, northern Manitoba; Geol. Surv. Can., Sum. Rep. 1917, pt D.

_____ (1918b): Amisk - Athapapuskow Lake district; Geol. Surv. Can., Mem. 105, 91p.

Byers, A.R., Kirkland S.J.T., and Pearson, W.J. (1965): Geology and mineral deposits of the Flin Flon area, Saskatchewan; Sask. Dep. Miner. Resour., Rep. 62, 95p.

Coombe, W. (1979): Mineral deposits and regional metallogeny, southeastern Shield; *in* Summary of Investigations 1979, Sask. Geol. Surv., Misc. Rep. 79-10, p120-133.

_____ (1984): Gold in Saskatchewan; Sask. Energy Mines, Open File Rep. 84-1, 134p.

Digel, S. and Gordon, T.M. (1990): Low to medium-grade metabasites at Schist Lake, near Flin Flon, Manitoba; *in* Current Research, Part C, Geol. Surv. Can., Pap. 90-1C, p53-57.

Froese, E. (1968): Metamorphic rocks from the Coronation Mine and surrounding area; *in* Byers, A.R. (ed.), Symposium on the geology of the Coronation Mine; Geol. Surv. Can., Pap. 68-5, p55-77.

Galley, A.G. and Franklin, J.M. (1987): Geological setting of gold , copper, tungston and molybdenum occurrences in the Phantom Lake region; *in* Summary of Investigations 1987, Sask. Geol. Surv., Misc. Rep. 87-4, p115-124.

Gordon, T.M., Hunt, P.A., Loveridge, W.D., Bailes, A.H. and Syme, E.C. (1987): U-Pb zircon ages from the Flin Flon and Kisseynew belts, Manitoba: chronology of Early Proterozoic crust formation; Geol. Assoc. Can./Mineral. Assoc. Can., Joint Annual Meeting, Prog. Abst., v12, p48.

Heywood, W.W. (1966): Ledge Lake Area, Manitoba and Saskatchewan; Geol. Surv. Can., Mem. 337, 43p.

Koo, J. and Mossman, D.J. (1975): Origin and metamorphism of the Flin Flon stratabound Cu-Zn sulphide deposit, Saskatchewan and Manitoba, Canada; Econ. Geol., v70, p48-62.

MacQuarrie, R. (1980): Absolute age of the Flin Flon deposit; (abstract), CIM Bull. v73, no820, p53.

McInnes, W. (1909): Explorations on the Churchill River and South Indian Lake; Geol. Surv. Can., Summ. Rep., 1908, p87-92.

Pearson, J.G. (1979): Flin Flon gold prospects: Douglas Lake - Wekatch Lake area; 1:10,000 scale prelim. map with Summary of Investigations 1979, Sask. Geol. Surv., Misc. Rep. 79-10, p145-151.

_____ (1980): Flin Flon gold prospects; *in* Summary of Investigations 1980, Sask. Geol. Surv., Misc. Rep. 80-4, p70-80.

_____ (1981): Gold metallogenic studies: Phantom Lake - Schist Lake area; *in* Summary of Investigations 1981, Sask. Geol. Surv., Misc. Rep. 81-4, p97-100.

_____ (1983): Gold metallogenic studies: Flin Flon - Amisk Lake area; *in* Summary of Investigations 1983, Sask. Geol. Surv., Misc. Rep. 83-4, p67-74.

_____ (1984): Gold metallogenic studies, the Rio deposit; *in* Summary of Investigations 1984, Sask. Geol. Surv., Misc. Rep. 84-4, p123-126.

Pearson, J.G. and Galley, A.G. (1985): Gold deposits of the Flin Flon - Amisk Lake area; *in* Summary of Investigations 1985, Sask. Geol. Surv., Misc. Rep. 85-4, p83-89.

Pearson, J.G., MacDougall, F.H. and Galley, A.G. (1986): Geology and evolution of gold occurrences in the Flin Flon - Amisk Lake area, Saskatchewan; *in* Clark, L.A. (ed.), Gold in the Western Shield; CIM, Spec. Vol. 38, p399-411.

Price, D.P. (1977): Geology and economic potential of the Flin Flon - Snow Lake areas; Univ. Manit. Cent. Precam. Stud., Annu. Rep., 1977, p52-83.

Sangster, D.F. (1972): Isotopic studies of ore-leads in the Hanson Lake - Flin Flon - Snow Lake mineral belt, Saskatchewan and Manitoba; Can. J. Earth Sci., v9, p500-513.

Stauffer, M.R., Mukherjee, A.C. and Koo, J. (1975): The Amisk Group; an Aphebian(?) island arc deposit; Can. J. Earth Sci., v12, p2021-2035.

Stockwell, C.H. (1946): Flin Flon - Mandy area, Manitoba and Saskatchewan; Geol. Surv. Can., Pap. 46-14, 5p.

_____ (1960): Flin Flon - Mandy area, Manitoba and Saskatchewan; Geol. Surv. Can., Map 1078A (with marginal notes), scale 1:12,000.

Syme, E.C. (1986): Schist Lake area, Athapapuskow Project; *in* Report of Field Activities 1986, Manit. Energy Mines, Misc. Rep., p36-42.

_____ (1987): Athapapuskow Lake Project; *in* Report of Field Activities 1987, Manit. Energy Mines, Misc. Rep., p30-39.

_____ (1988): Athapapuskow Lake Project; *in* Report of Field Activities 1988, Manit. Energy Mines, Misc. Rep., p20-34.

Syme, E.C., Bailes, A.H., Gordon, T.M. and Hunt, P.A. (1987): U-Pb zircon geochronology in the Flin Flon belt: age of Amisk volcanism; *in* Report of Field Activities 1987, Manit. Energy Mines, Misc. Rep., p105-107.

Tanton, T.L. (1941a): Flin Flon, Saskatchewan and Manitoba; Geol. Surv. Can., Map 632A (with marginal notes), scale 1:63,360.

_____ (1941b): Schist Lake, Saskatchewan - Manitoba; Geol. Surv. Can., Map 633A (with marginal notes), scale 1:63,360.

Thomas, D.J. (1989): Geology of the Douglas Lake - Phantom Lake Area (Part of NTS 63K-12 and -13); *in* Summary of Investigations 1989, Sask. Geol. Surv., Misc. Rep. 89-4, p44-54.

Tyrrell, J.B. (1902): Explorations in the northeastern portion of the district of Saskatchewan and adjacent parts of the District of Keewatin; Annual Report, Geol. Surv. Can., v8, 48p.

Bedrock Geology, Tulabi - Church Lakes Area: Derivation and Significance of Porphyroclastic Gneisses in the Pelican Window

J.F. Lewry[1]

Lewry, J.F. (1990): Bedrock geology, Tulabi-Church Lakes area: derivation and significance of porphyroclastic gneisses in the southern part of the Pelican Window; *in* Summary of Investigations 1990, Saskatchewan Geological Survey; Saskatchewan Energy and Mines, Miscellaneous Report 90-4.

Recent re-evaluation of rocks of the 'Pelican Window', in the Hanson Lake Block, (Lewry and Macdonald, 1988; Lewry *et al.*, 1989), restricted mainly to lakeshore exposure around Pelican, Mirond and Jan Lakes, has shown that the Sahli and MacMillan Point Archean structural inliers are enveloped by a wide zone of early synkinematic, highly strained rocks of high metamorphic grade. This zone includes prominent feldspar-porphyroclastic gneisses, interpreted as fragmental metavolcanics by some earlier workers (e.g. MacQuarrie, 1979), which are reinterpreted as mylonitic gneisses (*sensu lato*) mostly derived from plutonic protoliths.

This summer, the author conducted more extensive 1:20,000 scale mapping of similar rocks in an area south of Jan Lake. The map area (Figure 1), parts of which were previously mapped by Kirkland (1958), Pyke (1966), Macdonald and Posehn (1976), Macdonald and MacQuarrie (1978) and MacQuarrie (1979), includes Tulabi and Church Lakes and is crossed by the Hanson Lake road (Highway 106).

1. Lithostructural Units

Map units recognized in the area (see accompanying map) are defined not only on the basis of petrography and probable protolith but also, in some cases, on the basis of strain-induced characteristics. Most of the area is underlain by heterogeneously strained rocks derived from plutonic protoliths. Rocks of volcanic or sedimentary derivation are of minor extent.

a) Supracrustal Rocks

Unit 1 - Layered Amphibolites

Layered mesocratic to mafic hornblende gneisses and amphibolites form two belts, one extending around the Tulabi Lake Synform (Figure 1), another trending northeastward across Highway 106 in the southeast.

The belt extending around the Tulabi Lake Synform comprises generally non-garnetiferous medium-grained mafic gneisses with laterally persistent, mafic and more felsic transposed compositional layering on a centimetre to ten-centimetre scale. These gneisses are broadly interpreted as mafic metavolcanics or volcaniclastics. The southeastern belt mainly comprises richly garnetiferous mafic to intermediate gneisses, commonly with garnet porphyroblasts up to 4 cm across forming 5 to 10 percent of the rock. Some components are well layered; others are more uniform, with only indefinite and discontinuous compositional banding, and are interpreted as mafic metalavas or minor intrusions. Possible pillow structures were seen in one outcrop.

Unit 2 - Garnetiferous Felsic Gneisses

Generally well-layered garnet-rich felsic to intermediate gneisses form a thin unit west of the garnetiferous mafic volcanics in the southeast. Some outcrops include very quartz-rich garnetiferous layers up to 50 cm thick. These rocks are interpreted as possible dacitic metavolcanics and proximal felsic volcanogenic sediments.

Unit 3 - Mixed Mesocratic to Felsic Gneisses

A very mixed and generally well-layered assemblage of mesocratic to felsic hornblende and biotite-hornblende gneisses with subordinate mafic interlayers is exposed mainly around Tulabi Lake. Non-hornblendic psammitic to pelitic gneisses with layered calc-silicate and impure marble subunits also occur in the sequence. The assemblage is probably derived from mixed volcaniclastics and volcanogenic sediments.

Unit 4 - Pelitic to Psammopelitic Biotite Gneisses

Biotite-rich sillimanite- and/or garnet-bearing pelitic-psammopelitic gneisses, with local subordinate psammitic layers, form minor mappable units in outcrops around east Tublabi Lake. Though separately defined, they are essentially part of the mixed assemblage of unit 3.

Unit 5 - 'Tonalitic' Biotite Felsic Gneisses

Biotite felsic gneisses or 'granoblastites' form a belt extending along the northwest side of west Tulabi Lake, adjacent to tonalites-leucotonalites of unit 13 . The gneisses are medium to fine grained, mid to light grey and locally brown-weathering. Definite to indistinct compositional layering, possibly representing transposed primary layering, was observed locally, but most of the belt comprises uniform fine-grained rocks. Although part or all of this unit may comprise psammitic to psammopelitic metasediments, evidence for a sedimentary protolith is inconclusive; thus some or all may be highly strained and recrystallized tonalite-leucotonalite (unit 13 protolith).

(1) Department of Geology, University of Regina, Regina, Saskatchewan

Unit 6 - Pelitic Diatexites

Pelitic diatexites are exposed west and north of Church Lake, and northwest of Tulabi Lake. Some of the rocks are sillimanite and/or garnet-bearing pelite diatexites similar to those in the Jan Lake area (e.g. Lewry *et al.*, 1989), with a subordinate well defined paleosome and up to 70 percent concordant to discordant seriate pegmatite to leucogranite anatectic leucosome which occurs as transposed lenses and discontinuous *lits* of variable size. The leucosome is commonly accompanied by selvages of ultramafic biotite-garnet melanosome. However, most of the unit is a more uniform, coarsely inequigranular biotite-rich granodioritic to tonalitic gneiss commonly containing prominent plagioclase megacrysts, traces of sillimanite, sporadic small isolated lenses and wisps of ultramafic biotite/garnet restite and no definable paleosome. This rock may represent *in situ* melt or it may have been mobilized and intruded into its present position.

b) Pre- or Early-Synkinematic Plutonic Rocks

Unit 7 - Gneissic Hornblende-Biotite Granodiorite Complex

Unit 7, located east of Highway 106, mainly comprises inhomogeneous medium- to coarse-grained weakly

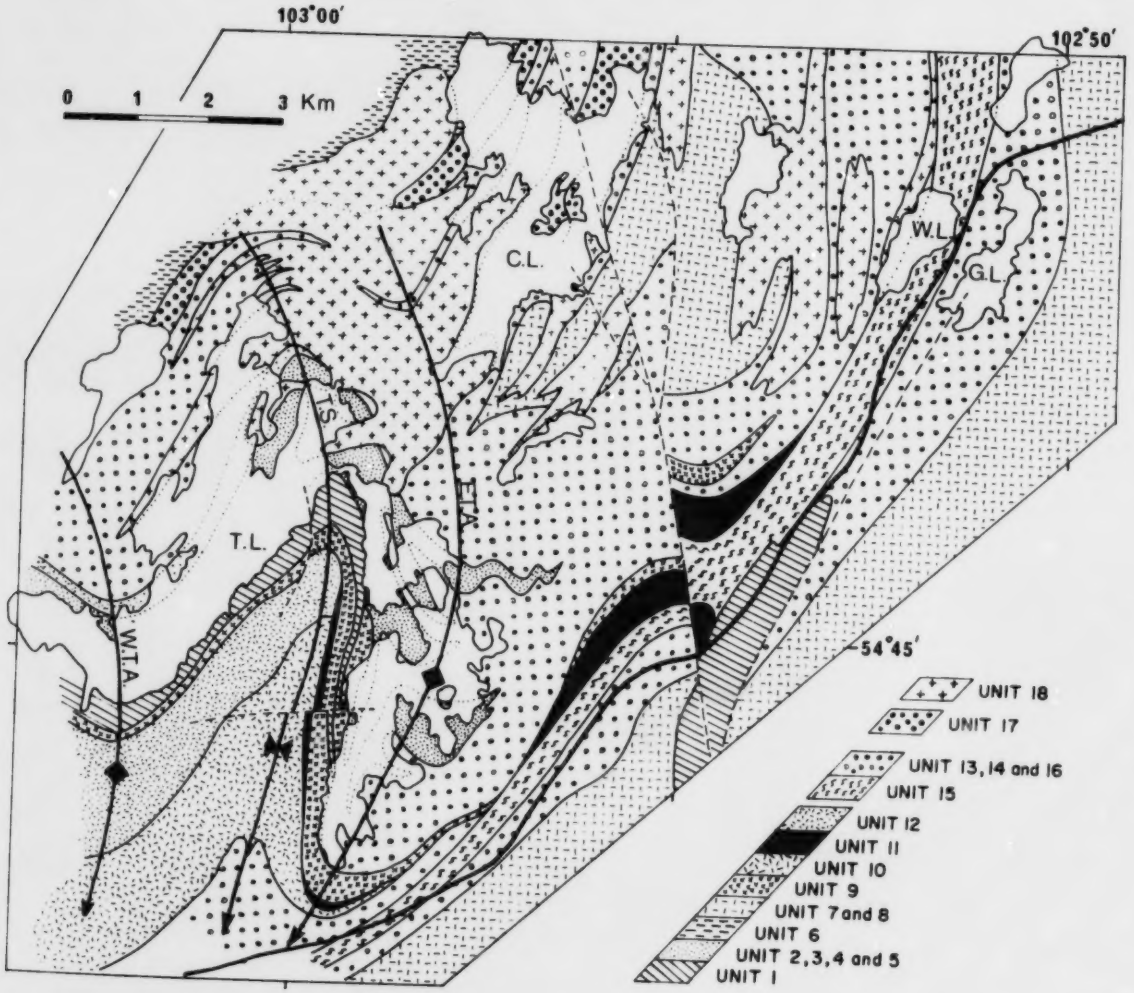

Figure 1 - Simplified geology of the Tulabi - Church Lakes area. T.L. = Tulabi Lake; C.L. = Church Lake; W.L. = Wintringham Lake; G.L. = Gillingham Lake; E.T.A. = East Tulabi antiform; T.L.S. = Tulabi Lake syform; W.T.A. = West Tulabi antiform. Lithologic units are: Unit 1, mafic supracrustals; Units 2,3,4 and 5, intermediate/felsic supracrustals; Unit 6, pelitic diatexite; Units 7 and 8, granodiorite/tonalite gneiss complexes; Unit 9, pink granite/granodiorite; Unit 10, garnet granodiorite; Unit 11, mafic/ultramafic metaplutonics; Unit 12, grey gneiss, uncertain protolith - possibly from unit 10; Unit 15, mylonitic prophyroclastic gneisses; Units 13, 14 and 16, high strain tonalitic and porphyroclastic gneisses (granodioritic/tonalitic profoliths); Unit 17, biotite-rich porphyroclastic gneisses; Unit 18, Jan Lake granite.

foliated to gneissic, variably megacrystic, grey hornblende-biotite granodiorite of unequivocal plutonic origin. The early, generally gneissic, relict foliation is locally deformed into tight to isoclinal minor folds. This fabric is variably overprinted and obscured by later granoblastic recrystallization and irregular patchy development of leucogranitic to leucogranodioritic neosome. Internally layered and unlayered amphibolite, 'metadiabase' and coarse 'metagabbro' inclusions of varied size and shape (angular blocks, tabular rafts, variably contorted lenses, ill-bounded schlieren and nebulitic mafic folia), occur sporadically throughout the complex. Some of these inclusions are metavolcanic xenoliths, but others may be disrupted intrusive sheets.

Much of the complex includes sparse to abundant pre-foliation sheets and lenses of pink granite pegmatite to which isolated potassium feldspar porphyroblasts are apparently related or coval. Larger subconcordant bodies of pre-foliation pink granite occur locally.

Unit 8 - Gneissic Biotite Tonalite Complex

Unit 8, occurring east and south of Church Lake, has many similar features as Unit 7 and the two may represent parts of the same compositionally gradational complex. Unit 8 is, however, generally more tonalitic, with low potassium feldspar content and little or no hornblende. It also differs in that it contains locally abundant sheets of uniform non-megacrystic leucocratic tonalite (unit 13) and a later pegmatoid trondhjemite phase. The unit is also intruded locally by variable quantities of pre-gneissosity pink granite similar to unit 9a. On average the unit contains less deformed pegmatite neosome than does unit 7.

Unit 9 - Pink Granite and Granodiorite

Subunit 9a is mainly a homogeneous, medium- to coarse-grained, reddish pink biotite-poor granite, locally with sparse potassium feldspar megacrysts up to 2 cm across. In places, such as east of the Tabbernor Fault, the granite appears to have been very coarse grained or pegmatitic prior to deformation. Typically, it is a non-gneissic L-S tectonite with dominant linear fabric and subordinate foliation. It may be of the same age as deformed leucogranite - pegmatite neosome components of units 7 and 8.

Unit 9b is a foliated grey pink biotite-hornblende granodiorite confined to the west side of east Tulabi Lake. It is generally slightly more mafic (commonly with subordinate hornblende as well as biotite) than unit 9a, and is locally intruded by unit 9a pink granite sheets. Its age relative to the gneissose megacrystic granodiorite (unit 7) was not established.

Unit 10 - Garnetiferous Granodiorite

Part of the area between east and west Tulabi Lake is underlain by a medium- to coarse-grained, unlayered, moderately to strongly foliated and migmatised biotite-hornblende granodiorite characterized by sparse to abundant red garnets. This unit can be discontinuously traced as a narrow belt extending northeastward to Gillingham Lake. It is characterized by widespread development of a coarser foliated leucocratic granodiorite - tonalite neosome which ranges in form, from isolated indefinitely-bounded irregular blebs and lensoid patches to anastomosing concordant to discordant veins which locally form 20 percent or more of the rock. In places, this leucosome is tightly to isoclinally folded axial planar to the main foliation. A younger richly garnetiferous unfoliated leucogranodiorite neosome occurs locally as veins crosscutting the foliation. In some localities, coarse garnetiferous granodiorite and a rather finer-grained poorly garnetiferous and somewhat more mafic quartz diorite occur as irregularly intermingled and indefinitely-bounded early phases.

The garnetiferous granodiorite commonly incorporates sparse to abundant blocks and schlieren of medium-grained mafic to ultramafic amphibolite and coarser metagabbro, ranging from fragments and strips a few centimetres across up to major rafts several tens of metres wide. Many are identifiable as remnants of unit 11 metagabbro, described below. In a few localities (e.g. one exposure at the south end of Gillingham Lake), extreme high-strain transposition of mafic inclusions and granodiorite has produced a spectacular 'pseudolayering'. A clear transition into less highly strained parts of the outcrop make it clear that this is not a primary (supracrustal) feature. Despite its unusual composition and character, the garnet granodiorite is interpreted as a metamorphosed plutonic rock, because of its general uniformity, absence of primary layering and incorporation of xenoliths.

Unit 11 - Metagabbro and Metapyroxenite

This unit includes weakly to strongly foliated and lineated, medium- to coarse-grained mafic metagabbro, and more intensely foliated, finer-grained unlayered mafic amphibolites (11a) considered, on the basis of field relations (e.g. visible strain gradation), to derive from metagabbro or mafic diorite protoliths. These rocks occur mainly in a discontinuously defined body, or series of bodies of variable width extending around the east Tulabi Antiform. The indicated discontinuity may be due to initial intrusive form, tectonic boudinage and dismemberment, or lack of exposure. Variably strained metagabbroic to metadiabasic inclusions typical of this unit occur in the garnetiferous granodiorite (unit 10) and more sporadically in other plutonic units.

Unit 11b is a body of coarse-grained, massive to poorly foliated ultramafic rock (possibly metapyroxenite) lying between Highway 106 and the old road, immediately east of the Tabbernor fault. Although evidently cut by the fault, its age in relation to other units is uncertain.

c) Highly Strained Rock Units

Unit 12 - Grey Felsic Gneiss

The core of the Tulabi Lake Synform is mostly underlain by mid to light grey, medium- to fine-grained, granoblastic felsic foliates of uncertain derivation. Their composition seems to range from granodioritic to quartz-dioritic,

although quartz content is difficult to estimate in finer grained variants. Total mafic content ranges from less than 5 percent to as much as 20 percent, and some exposures are finely garnetiferous. Most outcrops are uniform and unlayered; local faint ill-defined discontinuous compositional banding could not be definitively identified as of primary supracrustal origin. In some areas the felsic gneiss contains abundant mafic amphibolite and metagabbroic inclusions similar to those in the garnet granodiorite (unit 10).

Neither the protolith of the grey felsic gneiss nor its relation to the garnet granodiorite was unequivocally established. However, some clean outcrops show apparent strain gradation from coarse garnet granodiorite to more featureless finer-grained grey felsic gneiss. Such evidence, together with the occurrence of a similar inclusion suite, suggests that part or all of unit 12 may be highly-strained and dynamically recrystallized derivatives of unit 10.

Unit 13 - Non-Megacrystic Tonalite and Leucotonalite

Unit 13 broadly corresponds to the 'quartzofeldspathic gneisses' of Lewry *et al.* (1989), and unit 'Q' of Macdonald (1974, 1975) and MacQuarrie (1979). The main component is a generally uniform light grey to grey white, sparsely biotitic, non-megacrystic felsic foliate of tonalitic to leucotonalitic composition. Least strained variants are medium to coarse grained, locally xenolithic but otherwise extremely homogeneous rocks which can, with confidence, be interpreted as plutonic in origin. Elsewhere, the unit consists of medium- to fine-grained leucocratic felsic foliates and gneisses having a less clear protolith. However, abundant examples of unequivocal strain gradation from coarser-grained to finer-grained variants strongly indicate that the finer-grained phases are more highly-strained and dynamically recrystallized derivatives of the same plutonic protolith. This supports the conclusions of Lewry *et al.* (1989) with respect to similar rocks exposed in the Jan - Pelican - Mirond Lakes area.

Most outcrops of foliated tonalite include a variable amount of younger neosome. This is mostly coarse-grained to pegmatitic, grey white leucotonalite - trondhjemite. Less commonly it comprises pink granite or granite pegmatite. In low strain areas the trondhjemite neosome generally forms sharply to indefinitely bounded discontinuous patches, lenses and anastomosing veins, suggesting that it was derived *in situ* by partial remelting of the tonalite host. With increasing strain, the neosome is progressively transposed into the foliation, to form highly quartz-ribboned and prominently plagioclase-porphyroclastic gneissic folia with a progressively finer-grained dynamic recrystallization matrix. The pink granite neosome displays similar relationships, except that it generally has sharper contacts with the host rock and may represent locally injected material. In areas of high ductile strain, finely banded 'mylonitic' gneisses, easily mistaken for metasedimentary gneisses (cf. 'candy-striped' gneisses of Macdonald, 1974), have been produced by extreme transposition, dynamic recrystallization and grain-size reduction.

More mafic hornblendic variants of unit 13, with or without porphyroclastic trondhjemite neosome, occur locally. They seem to correspond in part to unit Wa of MacQuarrie (1979) but they could not be traced as the coherent units indicated on MacQuarrie's map.

As indicated above, unit 13 corresponds to similar rocks described by Lewry *et al.* (1989) however, in the present map area they contain few disrupted mafic dyke inclusions and typically incorporate a higher proportion of trondhjemitic neosome.

Unit 14 - Straight to Protomylonitic Porphyroclastic Granodioritic Gneisses

Unequivocal transitional field relations show that rocks of unit 14 are derived from the unit 7 hornblende-biotite granodiorite complex via gradational increase in ductile simple shear strain. In outcrop, the strain gradient is marked by progressive ribboning of quartz, rounding and 'beading' of groundmass plagioclase grains, and progressive replacement of a prior coarse crudely foliated groundmass fabric by a granoblastic to streaky, medium- to fine-grained dynamic recrystallization matrix. Neosomal pink pegmatite sheets are also progressively ribboned, disrupted and 'shredded', with consequent semi-isolation of large relict potassium feldspar porphyroclasts. Large plagiclase megacrysts and potassium feldspar porphyroclasts become rounded and commonly develop sigmoidal dynamic recrystallization tails (delta porphyroclasts).

The boundary between units 7 and 14 is irregularly gradational; exposures in the transition zone commonly show marked heterogeneous strain at the outcrop scale. The boundary indicated on the accompanying map approximately defines the locus at which increasing shear strain produces pervasive quartz ribboning and grain-size reduction.

Unit 15 - Protomylonitic to Mylonitic Porphyroclastic and Beaded Gneisses

Unit 15 rocks are also thought to derive mainly from hornblende-biotite granodiorite complex protoliths of unit 7, marking a further gradational increase in ductile shear strain from unit 14. The granodiorite protolith now posseses an entirely medium- to fine-grained dynamic recrystallization matrix which encloses sparse to plentiful small feldspar 'beads' and larger ovoidal to delta-tailed plagioclase and potassium feldspar porphyroclasts. Pegmatite neosome is more highly disrupted, intensely ribboned and locally mylonitic. A characteristic feature of the unit is widespread prominent post-high-strain hornblende blastesis in the recrystallized matrix.

Unit 16 - Tonalitic Porphyroclastic Gneiss Complex

Unit 16 also predominantly comprises highly-strained porphyroclastic and in part protomylonitic to mylonitic gneiss broadly similar in character to units 14 and 15. They are distinguished from these units because they seem to derive mainly from different, somewhat more varied and in some cases uncertain protoliths.

Much of this unit comprises more highly strained derivatives of the unit 8 megacrystic biotite tonalite complex. Well exposed strain gradation from one to the other was observed on traverses east and south of Church Lake. Elsewhere relict features seen in clean exposures of unit 16 constitute persuasive evidence of derivation from a plutonic and dominantly megacrystic tonalitic protolith. In other areas, however, it is clear that a major part of the assemblage was derived from predominantly non-megacrystic tonalite - leucotonalite (unit 13) incorporating an abundant, and locally dominant pegmatoid trondhjemite neosome. Many exposures of this unit are heavily lichened and it is difficult or impossible to determine whether porphyroclastic components were derived from megacrystic tonalite, trondhjemite pegmatite neosome or a mixture of the two. Thus, on the accompanying map, areas which appear to be underlain predominantly by clearly identifiable unit 13 tonalite - leucotonalite and associated trondhjemite pegmatite neosome are so indicated. Areas underlain either by clearly identifiable higher-strain derivatives of the megacrystic biotite tonalite complex (unit 8) or by prominently porphyroclastic gneisses of uncertain parentage are designated unit 16. Resultant apparent anomalies in indicated extent and continuity of the two units (e.g. either side of the Tabbernor Fault) are mainly an unavoidable artifact of variable outcrop quality.

Distinction between porphyroclastic gneisses of units 14 and 15, derived largely from the hornblende-biotite granodiorite complex, and those of unit 16, thought to derive mainly from units 8 and 13, is not always possible at the individual outcrop scale; accordingly the boundary between the two is indefinite in places. In general unit 16 is characterized by widespread incidence of components derived from the non-megacrystic tonalite - leucotonalite (which was not seen in the hornblende-biotite granodiorite complex). There is generally less potassium feldspar porphyroclasts and shredded pink pegmatite neosome (though this is abundant locally) and marked absence of the post-high strain hornblende blastesis which typifies rocks of unit 15 and, to a lesser extent, unit 14.

Unit 17 - 'Guncoat-type' Biotite-rich Porphyroclastic Gneiss

Rocks of this unit are mostly porphyroclastic and beaded biotite-rich gneisses which occur in proximity to unit 6 pelitic diatexites near Church Lake. The matrix is generally dark grey, medium to fine grained, granoblastic, relatively homogeneous to finely gneissose or streaky, and contains an estimated 15-20 percent or more biotite, as well as commonly incorporating abundant small rounded to lensoid white plagioclase beads. The average size of larger plagioclase porphyroclasts varies markedly from outcrop to outcrop, and even in individual outcrops. Some subunits are characterized by predominantly small ovoidal to lensoid porphyroclasts less than 1-2 cm across. Elsewhere heteroclastic subunits contain spectacular ovoidal white to blue grey plagioclase 'eggs' up to 5 cm or more across which form 10 percent or more of the rock.

Unit 17 is distinguished from units 14, 15 and 16 mainly on the basis of markedly higher biotite content and generally greater internal homogeneity. Unlike the other units, included plagioclase porphyroclasts are everywhere rounded and never show tails, a feature attributed to greater viscosity contrast between porphyroclast and biotite-rich matrix.

Some outcrops on the west shore of Church Lake display clear strain gradation from coarse-grained pelitic diatexite to finer-grained porphyroclastic gneisses of unit 17. On the basis of this evidence and the internal features described above, unit 17 porphyroclastic gneisses are interpreted largely or entirely as ductile high-strain 'mylonitic' derivatives of the pelitic diatexite, rather than derivatives of plutonic protoliths. Thus, they closely resemble the 'Guncoat Gneisses' (Lewry, 1981) in lithological and kinematic features, and in presumed protolith.

d) Late- to Post-Tectonic Intrusive Rocks

Unit 18 - 'Jan Lake' Granite and Pegmatite

Late- to post-tectonic intrusive rocks of the 'Jan Lake suite', including medium- to coarse-grained pink aplogranite, grey white leucogranite (possibly granodiorite) and abundant granite pegmatite, occur throughout much of the area as thin isolated sheets, anastomosing subconcordant to discordant 'net-vein' complexes and major intrusive bodies containing subordinate rafts of older gneisses. The pegmatites are unfoliated and clearly postdate significant ductile deformation; however, they locally display brittle fracturing in the vicinity of late faults. The aplogranite - leucogranodiorite is generally massive but locally has a weak subvertical north- to northeast-trending foliation.

On the accompanying map, larger areas designated as unit 18 denote **minimum** documented extent of at least 80 to 100 percent Jan Lake granite and pegmatite. The designated areas also include extensive sporadic zones of large and small rafts of older units, which in some areas permit tracing of 'ghost' lithological boundaries through the Jan Lake complex. Elsewhere, no attempt was made to extrapolate mappable sheets of Jan Lake granite - pegmatite encountered on traverse, since it is felt that control is insufficient to do this with confidence. Generally, presently reported work showed that Jan Lake granite - pegmatite in the area is much more abundant than indicated by MacQuarrie (1979). In particular, most of the area west of Church Lake and north of Tulabi Lake is underlain by a previously unmapped major plutonic complex which may be even more extensive than indicated here. Elsewhere, it is estimated that at least fifty percent of the northern half of the map area comprises Jan Lake material, occurring as individually unmappable anastomosing sheets.

2. Structure

Transposed primary layering and early synkinematic neosomal lenses and *lits* in supracrustal rocks are generally coplanar with a pervasive early foliation.

Coeval intrafolial/isoclinal D_1 minor fold closures are preserved locally. A pervasive moderate to strong and commonly gneissic early foliation is also evident in most plutonic rocks. Tight to isoclinal refolding of this early planar fabric is common in units 7 and 8. Earlier intrafolial isoclines, apparently coeval with the early foliation, were less commonly observed in these units. Early regional foliation and fold development thus seems to encompass at least two deformational episodes, perhaps representing a progressive strain continuum. All such early structures are overprinted by general granoblastic recrystallization.

Passage from generally coarse-grained foliated rocks of units 7 and 8 to higher-strain rocks of units 14, 15 and 16 is marked by intensification of a protomylonitic to locally ultramylonitic foliation typified by extreme ribboning of quartz and pegmatitic neosome, the development of a finer-grained dynamic recrystallization matrix which commonly incorporates slightly coarser feldspar 'beads', and by rolling of plagioclase and potassium feldspar porphyroclasts. Delta porphyroclasts, with asymmetrically curved tails, are ubiquitously developed in units 14 and 15 and less commonly in other high-strain units. These, and other shear-sense indicators such as asymmetric 'wrap-around' of mylonitic foliation adjacent to untailed porphyroclasts and rolled mafic inclusions, show that development of this high-strain fabric involved a significant component of simple shear. Shear-sense indicators exposed on subhorizontal outcrop surfaces of units 14 and 15, and locally of unit 17, overwhelmingly show dextral shear-sense throughout the area. However, only rare indefinite and indecisive preservation of coeval stretching lineation was observed. The regional significance of shear-sense data is accordingly indeterminate at present.

The relative age of the mylonitic foliation and kinematic fabric elements preserved in less strained plutonic rocks was not unequivocally established. In many places the high-strain fabric evidently overprints and transposes a prior gneissosity. It is far from certain, however, that all early structures in the less-strained plutonic complexes predate the high-strain foliation, as some fabric elements may be essentially coeval with the latter. In general, all of these early fabric elements, including the mylonitic foliation, are thought to represent components of a regional progressive strain continuum which involved gross partitioning of the simple shear strain component.

All structures described above are deformed by a younger set of major and minor folds developed about subvertical to steeply inclined and approximately north-trending axial surfaces. Three major south-southwest-plunging fold closures, the West Tulabi Antiform, Tulabi Lake Synform and East Tulabi Antiform (Figure 1), control structural trends in the western part of the area. These are moderate to tight asymmetric folds, overturned to the east, which reach maximum amplitude in the centre of the area and die away to lower amplitude open closures to the north and south. Their attitude suggests that they are coeval with the major south-plunging closure of the 'Pelican Window'.

Open to tight minor folds and coaxial intersection and mineral elongation lineation, cogenetic with the major Tulabi Lake folds, are ubiquitous. In most of the area lineation and minor fold hinges consistently plunge to the south-southwest, generally at 10 to 40°. Sub-horizontal to gentle north-northeast plunges occur locally in the area northeast of Tulabi Lake and south of Church Lake. Fold plunge appears to be largely a function of prior attitude of early planar structures.

a) Faults

Two late phases of faulting are recognized:

a) The eastern margin of unit 1b metavolcanics in the southeast is defined by a north-northeast-trending fault of unknown extent. Ductile mylonites and ultramylonites related to this fault, derived both from metavolcanics and adjacent granodiorite gneisses, are exposed in several places. The mylonite fabric developed under retrograde greenschist facies conditions and clearly postdates more extensive high-temperature mylonitic foliation typifying units 14, 15 and 16.

b) The youngest structures are north to north-northwest-trending splays of the Tabbernor fault system running through the central part of the area. Fault zone exposures in roadside outcrop on Highway 106 and north of the old Hanson Lake road show brittle cataclastic fabrics. Significant sinistral strike displacement is evident across the southern part of the main fault-line. Variation in thickness of some offset lithological units on either side of the fault suggests that there may also be significant downthrow to the east.

3. Metamorphism

Co-existing sillimanite and garnet in unit 6 pelitic diatexites and in pelitic gneisses around east Tulabi Lake indicate minimum middle to upper amphibolite facies conditions. Mineral assemblages in other rocks are less diagnostic. However, extensive anatexis of both supracrustal and plutonic protoliths, which took place prior to the northerly folding, indicates general attainment of high to very high grade conditions throughout much of the area. Most of the pelitic diatexite west of Church Lake comprises at least 70 percent anatectic melt: in many cases no remaining paleosome is evident. Throughout much of the rest of the area granodiorite - tonalite paleosome of units 7, 8 and 13, and their high-strain derivatives, show clear evidence of partial remelting both prior to and/or during development of the high-strain protomylonitic to mylonitic fabric. This suggests that most of the area was within uppermost amphibolite facies throughout the early deformational phases. Although low grade mineral assemblages are documented in the Hanson Lake area, just to the south, no clear indication of a marked southward decline in grade was seen in the area described here.

4. Discussion and Conclusions

Remapping of the Tulabi - Church Lakes area supports the conclusions of Lewry *et al.* (1989) regarding probable protoliths and geotectonic significance of major lithological units in the Pelican Window. The main differences between the results of this work and previous workers are:

1) Rocks formerly interpreted as 'psammites' (unit Q, Macdonald and MacQuarrie, 1978; MacQuarrie, 1979) are now clearly documented as variably strained and generally leucocratic tonalitic orthogneisses. In the Tulabi - Church Lakes area such rocks are generally more heterogeneously strained than in areas to the north, with more commonly preserved strain gradation into unequivocally plutonic coarser-grained variants. Moreover, high-strain derivatives of such rocks, incorporating a variable amount of porphyroclastic pegmatoid neosome, are more extensive than indicated by MacQuarrie (1979), and comprise a significant part of his unit Pb 'blastoporphyritic pyroclastic rocks'. The only felsic gneiss unit with a doubtful protolith (and which may be of sedimentary origin) is unit 4 of this report.

2) Unit Wa (biotite-hornblende gneiss) of MacQuarrie (1979) is not recognized as a mappable entity by the present author. Parts of units 13 and 16 of this report are sparsely hornblendic and/or contain abundant mafic gneiss schlieren and nebulitic folia but they could not be defined as continuous map units at the present scale of mapping.

3) The broad belt of unit Pb (blastoporphyritic pyroclastic rocks of MacQuarrie, 1979), which MacQuarrie conceded 'may be difficult to distinguish from porphyroblastic tonalites', are now conclusively documented as highly-strained and largely porphyroclastic orthogneisses derived variously from megacrystic and non-megacrystic tonalite and granodiorite, together with variable amounts of early (pre/syn-high strain) granitic and trondhjemitic pegmatoid anatectic neosome. These rocks correspond to and probably are continuous with mixed porphyroclastic gneisses recognized to the north (Lewry *et al.*, 1989).

4) Unit Ba ('feldspathoblastic biotite gneisses') of MacQuarrie (1979) are now documented as a more highly strained porphyroclastic derivative of coarse-grained pelitic diatexite (unit Bb, MacQuarrie, 1979; unit 6, this report).

Most of the porphyroclastic gneisses are not strictly 'mylonites'. Only a relatively narrow heterogeneously strained belt of rocks with rather ill-defined boundaries (unit 15, unit 14 in part) displays a fabric (pervasive medium/fine-grained dynamically recrystallized matrix; extreme ribboning of mineral subdomains; sparse retention of recognizable primary features, mainly feldspar porphyroclasts; extreme transposition) which justify designation as mylonitic and ultramylonitic gneisses. Rocks of unit 17 may also be termed mylonitic gneisses, in view of contrasts between their present state and that of their diatexite protoliths. The rest of the porphyroclastic gneiss assemblage are generally protomylonitic.

As indicated above, most high-strain gneisses show unequivocal evidence of a significant finite simple shear strain component (mainly rotated and tailed porphyroclasts) at relatively high strain rates (medium/fine-grained dynamic recrystallization fabric developed under high temperature conditions). Thus, these gneisses comprise a broad crustal 'package' which must have accomodated major lateral translation of structurally overlying crustal components. In the context of regional structural geometry it seems likely that this package represents exposure of a massive regional translational 'sole zone' which might underlie much of the adjacent allochthonous Kisseynew and Flin Flon domains, as postulated by Lewry *et al.*, in press). Unfortunately, general lack of preservation of coeval stretching lineation currently precludes any statement regarding direction of early nappe transport.

Although metamorphic conditions attending early high-strain are less well-constrained than those documented farther north (Lewry *et al.*, 1989), it seems clear that translation occurred under high temperature (and possibly relatively high pressure) anatectic conditions. Within certain limits of bulk strain rate, such conditions might favour dispersal of shear strain over a broad zone rather than concentration in a narrow well-constrained ductile 'shear zone'.

5. References

Kirkland, S.J.T. (1958): The geology of the Deschambault Lake area (east half), Saskatchewan; Sask. Dep. Miner. Resour., Rep. 31, 16p.

Lewry, J.F. (1981): La Ronge Project: II. Geology of the Stanley Shear Zone; *in* Summary of Investigations 1981, Sask. Geol. Surv., Misc. Rep. 81-4, p28-33.

Lewry, J.F. and Macdonald, R. (1988): Observations on deformation in the Glennie Domain and Hanson Lake Block; *in* Summary of Investigations 1988, Sask. Geol. Surv., Misc. Rep. 88-4, p35-41.

Lewry, J.F., Macdonald, R. and Stauffer, M.R. (1989): The development of highly strained rocks in the Pelican Window during high-grade metamorphism and pervasive anatexis; *in* Summary of Investigations 1989, Sask. Geol. Surv., Misc. Rep. 89-4, p58-65.

Lewry, J.F., Thomas, D.J., Chiarenzelli, J.R. and Macdonald, R. (in press): Structural relations in accreted terranes of the Trans-Hudson Orogen: telescoping in a collisional regime?; *in* Lewry, J.F. and Stauffer, M.R. (eds.), The Early Proterozoic Trans-Hudson Orogen of North America, Geol. Assoc. Can., Spec. Pap. 37.

Macdonald, R. (1974): Pelican Narrows (west) area; *in* Summary Report of Field Investigations by the Saskatchewan Geological Survey 1974; Sask. Dep. Miner. Resour., p30-37.

_____ (1975): Semi-reconnaissance in three areas, Pelican Narrows area; *in* Summary Report of Field Investigations by the Saskatchewan Geological Survey 1975; Sask. Dep. Miner. Resour., p35-43.

Macdonald, R. and MacQuarrie, R.R. (1978): Geological re-investigation mapping, Jan Lake area (part of NTS area 63M); *in* Summary of Investigations 1978, Sask. Geol. Surv., Misc. Rep. 78-10, p16-25.

Macdonald, R. and Posehn, G.A. (1976): Re-investigation of the Pickerel River and Limestone - Tulabi Lakes area; *in* Summary Report of Field Investigations by the Saskatchewan Geological Survey 1976; Sask. Dep. Miner. Resour., p44-52.

MacQuarrie, R.R. (1979): Geological reinvestigation mapping, Birch Portage South (NTS area 63L-15S); *in* Summary of Investigations 1979, Sask. Geol. Surv., Misc. Rep. 79-10, p29-38.

Pyke, M.W. (1966): The geology of the Pelican Narrows and Birch Portage areas, Saskatchewan; Sask. Dep. Miner. Resour., Rep. 93, 69p.

Lithogeochemical Studies in the Flin Flon - Amisk Lake Area

B.R. Watters[1]

Watters, B.R. (1990): Lithogeochemical studies in the Flin Flon - Amisk Lake area; *in* Summary of Investigations 1990, Saskatchewan Geological Survey; Saskatchewan Energy and Mines, Miscellaneous Report 90-4.

The geochemical study of metavolcanic rock units in the Flin Flon area, initiated in 1989, was continued during 1990. This study is being conducted in collaboration with the detailed bedrock remapping program being carried out in the Douglas Lake - Phantom Lake area (Thomas, 1989, and this volume) and the Mystic Lake area (Reilly, this volume).

Some aspects of geochemical data obtained for an initial suite of mainly metavolcanic rocks and lesser intrusive units from the Douglas Lake - Phantom Lake area (Thomas, 1989) are discussed below. Representative analyses from this suite were included in Watters (1989). Analysis of about 200 more samples has also recently been carried out, but these data have yet to be processed. Rare earth element (REE) data for some of the initial suite has also been obtained and preliminary interpretations based on these results are included in this report.

1. Discussion of Results

Although much of the work is still in a preliminary stage, data obtained so far has provided some clear indications regarding the compositional character and geotectonic setting of the metavolcanic rocks. As reported in Watters (1989), it can be demonstrated that silica has been mobile to varying degrees in the metavolcanic rock units, thus classifications and interpretations based on SiO_2 can be ambiguous. Although such alteration is common in the area, it is not ubiquitous. Such observations are consistent with the field evidence (Thomas, 1989) which indicates that many of the mafic pillowed volcanic units, for example, have been silicified.

Basaltic volcanic rocks from the Douglas - Phantom Lakes area, analyzed so far, are tholeiitic and of island arc affinity. This has been demonstrated by Watters (1989) and is also indicated by an AFM plot (Figure 1), various other interelement relationships and REE distribution patterns, to be discussed below. It can be argued that, in view of the possibility of alkali element mobility in these rocks, an AFM diagram would not produce a meaningful classification. The distribution of data points on this plot, with respect to the major classification fields, however, is very similar to that on a Jensen cation plot (Watters, 1989) which does not include the alkali elements. While this does not altogether rule out the possibility of alkali mobility, it does suggest that it did not occur to the same extent as with silica.

Wherever possible, those elements which are regarded as being generally immobile are being used in the interpretation of these rocks. It is also recognized that the introduction of varying amounts of silica into many of the basaltic flow units would have modified the absolute concentrations of other major (and trace) elements to an as yet undetermined extent. For this reason, an attempt has been made, so far as possible, to base interpretations on variations of element ratios and on three-component diagrams. For example on a ternary plot incorporating $Y+Zr$, $TiO_2 \times 100$ and Cr, the metabasalts clearly follow a tholeiitic trend as defined by Davies *et al.* (1979), having relatively lower $(Y+Zr)$:Ti ratios when compared with calc-alkaline basalts (Figure 2).

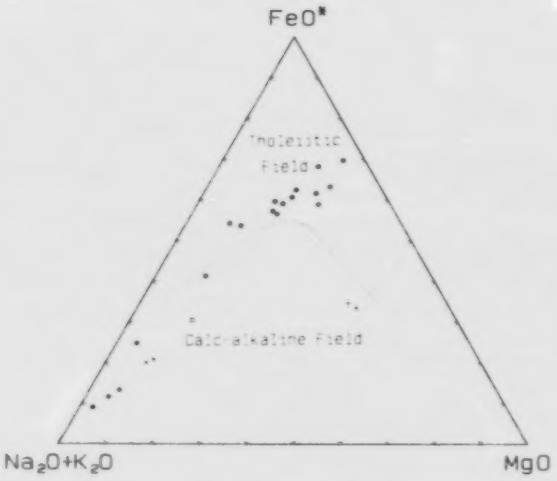

Figure 1 – AFM (Na_2O+K_2O - FeO - MgO) plot for some metavolcanic and intrusive rocks from the Douglas Lake - Phantom Lake area. Field boundaries are from Irvine and Barager (1971). Full circles, metavolcanics; crosses, Boundary Lake Intrusion; squares, Bootleg Lake Granodiorite; X, Phantom Lake Granite.*

The metavolcanic rocks are characterized by low Ti and low to moderate Zr contents and are confined almost exclusively to the volcanic arc field on Figure 3. Concentrations of the element Y are also typically low and, when plotted against Cr, provide further support for volcanic arc affinities (Figure 4).

The Zr-Ti-Sr discriminant plot (Figure 5), while including an element that may show a degree of mobility during metamorphism (i.e. Sr), provides an interpretation that is in agreement with the above, further suggesting that these mafic volcanic rocks are of arc tholeiitic character.

(1) Department of Geology, University of Regina, Regina, Saskatchewan

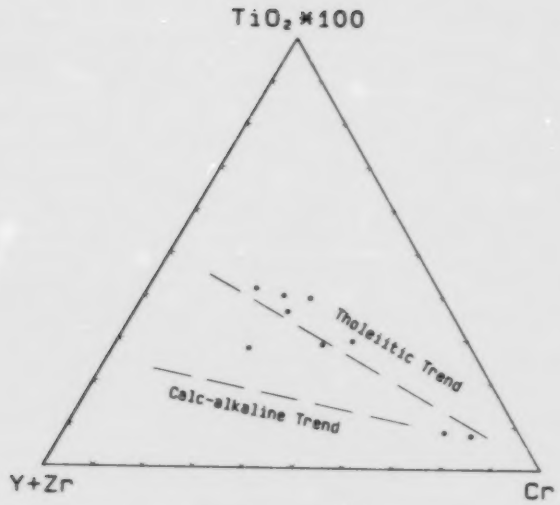

Figure 2 – Y+Zr - (TiO_2x100) - Cr plot for some metabasaltic rocks from the Douglas Lake - Phantom Lake area. Trend lines are from Davies et al. (1979).

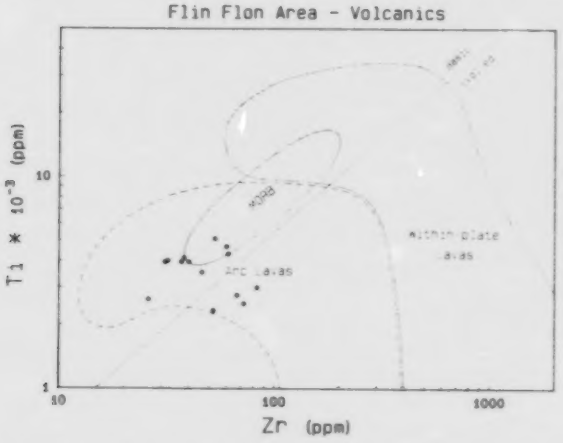

Figure 3 – Plot of Ti vs. Zr for metavolcanic rocks of the Douglas Lake - Phantom Lake area. Field boundaries are from Pearce and Norry (1979).

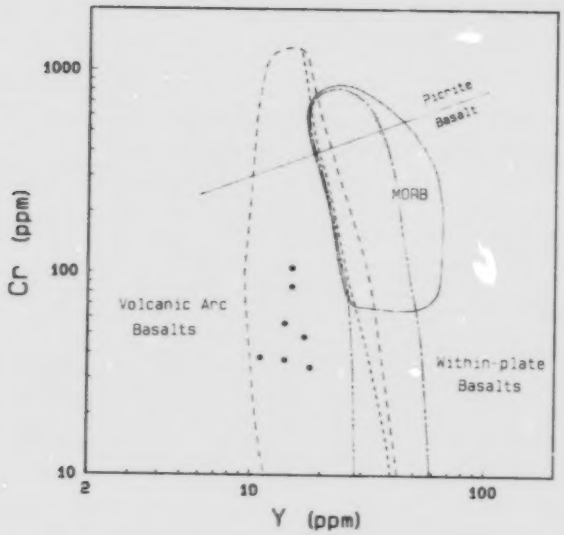

Figure 4 – Plot of Cr vs. Y for metabasaltic rocks of the Douglas Lake - Phantom Lake area. Field boundaries are from Pearce (1982).

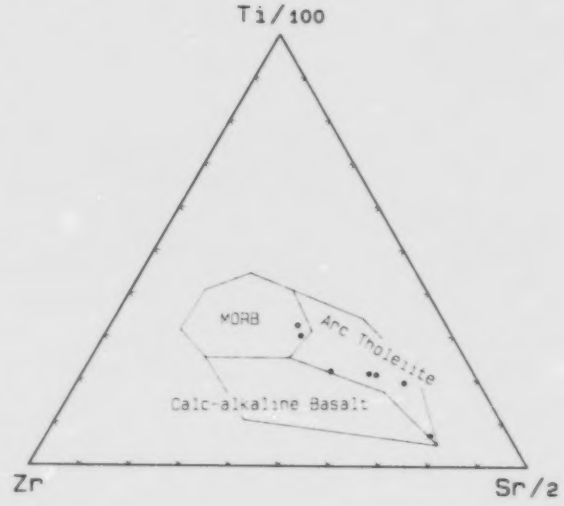

Figure 5 – Plot of Zr-Ti/100-Sr/2 for metabasaltic rocks of the Douglas Lake - Phantom Lake area. Field boundaries are from Pearce and Cann (1973).

Volcanic arc tholeiitic basalts typically have low concentrations of K (Jakes and White, 1972) and this characteristic is also shown by the basaltic rocks from the Douglas Lake - Phantom Lake area, which show a range of 0.22 to 0.60 percent K_2O.

REE distribution patterns for basaltic rocks from the area are presented in Figure 6. Profiles for individual flow units have been grouped according to which member they have been assigned on the basis of field evidence (Thomas, 1989). While the REE profiles from the three members have similarly shaped patterns, variable degrees of total REE content allow fairly clear distinctions to be made between them. All of the patterns are quite flat but the Creighton and Newcor Members' patterns are very mildly LREE depleted, whereas basaltic rocks of the Bomber Lake Member are slightly LREE enriched. The patterns displayed by the three Members are characteristic of island arc tholeiites and indicate an origin for the basaltic magmas by melting of primitive mantle peridotite (Jakes and White, 1972; Cullers and Graf, 1984a).

REE profiles of rhyolitic units of the Myo Lake Member (Millrock Hill locality) show moderately enriched, slightly

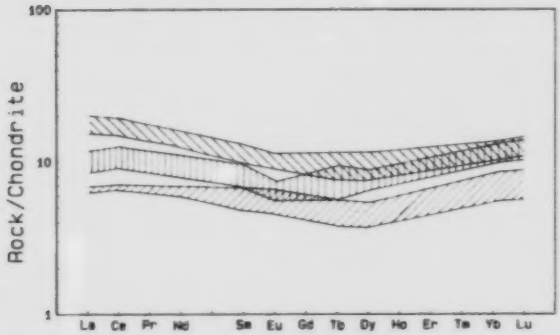

Figure 6 – Rare earth element distribution profiles for basaltic rock units in the Douglas Lake - Phantom Lake area. ///// = Creighton Member; ||||| = Newcor Member; \\\\\ = Bomber Lake Member.

concave-downwards patterns with no fractionation between the LREE and HREE, but with very strongly developed negative Eu anomalies (Figure 7). Such patterns may indicate derivation of these magmas by fractionation of a tholeiitic basic parent magma involving plagioclase and clinopyroxene as the major fractionating phases.

In view of the close spatial and temporal association between these rhyolitic units and the basic units of arc tholeiitic character it is suggested that such a genetic link existed between the two rock types, the felsic magmas being derived by extensive fractionation of the volumetrically more significant tholeiitic magmas. Such a process would explain the REE characteristics and the relatively low K_2O contents (2.10-2.62 percent) of the rhyolites is also consistent with their derivation from a low-K parent magma. Derivation of the felsic magmas by partial melting processes is considered much less likely because of the probable lack of intermediate to felsic crustal source rock in what is considered to have been an evolving island arc.

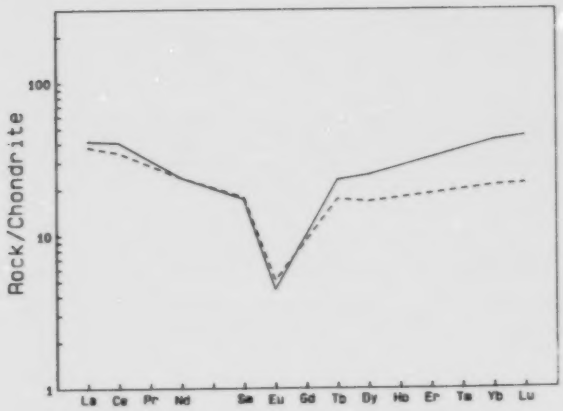

Figure 7 – Rare earth element distribution profiles for rhyolitic rock units of the Myo Lake Member in the Douglas Lake - Phantom Lake area.

REE distribution patterns for a single sample of the Phantom Lake Granite and for two samples of Boundary Intrusion, are presented in Figure 8. The former displays a strongly fractionated pattern with high LREE to HREE ratios and no Eu anomaly, a pattern typical of many granodioritic rocks (Cullers and Graf, 1984b). The two samples of Boundary Intrusion for which REE data have so far been obtained are basic in composition (48.10 percent SiO_2) and are strongly alkaline (5.24-5.29 percent total alkalis). The REE contents reflect these characteristics in that the profiles show moderately high total REE contents and moderately fractionated LREE to HREE with no Eu anomaly. Further data from a wider range of samples will be needed before reasonable interpretations can be made concerning the genetic significance of these characteristics.

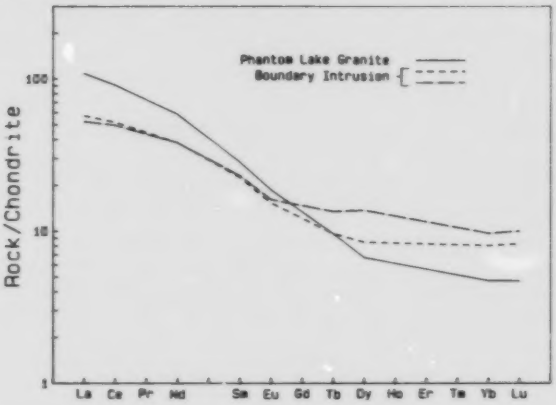

Figure 8 – Rare earth element distribution profiles for the Phantom Lake Granite and Boundary Intrusion.

2. Conclusions

1. Metabasaltic rock units in the Douglas Lake - Phantom Lake area, belonging to the Creighton Member, the Bomber Lake Member and the Newcor Member (after Thomas, 1989), display low potassium volcanic arc tholeiitic characteristics, and have been variably silicified.

2. REE distribution patterns for rocks from the three members are similar in that they are flat with little or no LREE to HREE fractionation, generally have low total REE and no Eu anomaly. Small, but quite distinct, differences in total REE contents, however, allow a distinction to be made between basalts from the different members.

3. Rhyolitic units of the Myo Lake Member display REE profiles consistent with an origin by fractionation of low-K tholeiitic parent magma of the type that gave rise to the basaltic flows of the other three members.

3. References

Cullers, R.L. and Graf, J.L. (1984a): Rare earth elements in igneous rocks of the continental crust: predominantly basic and ultrabasic rocks; *in* Henderson, P. (ed.), Rare Earth Element Geochemistry, Elsevier, New York, p237-274.

_____ (1984b): Rare earth elements in igneous rocks of the continental crust: intermediate and silicic rocks - ore petrogenesis; *in* Henderson, P. (ed.), Rare Earth Element Geochemistry, Elsevier, New York, p275-316.

Davies, J.F., Grant, R.W.E. and Whitehead, R.E.S. (1979): Immobile trace elements and Archean volcanic stratigraphy in the Timmins mining area, Ontario; Can. J. Earth Sci., v16, p305-311.

Irvine, T.N. and Baragar, W.R. (1971): A guide to the chemical classification of the common volcanic rocks; Can. J. Earth Sci., v8, p523-548.

Jakes, P. and White, A.J.R. (1972): Major and trace element abundances in volcanic rocks of orogenic areas; Geol. Soc. Am., Bull. v83, p29-40.

Jensen, L.S. (1976): A new cation plot for classifying subalkalic volcanic rocks; Ont. Geol. Surv., Misc. Pap. 66.

Pearce, J.A. (1982): Trace element characteristics of lavas from destructive plate boundaries; *in* R.S. Thorpe, (ed.), Andesites, J.Wiley and Sons, New York, p525-547.

Pearce, J.A. and Cann, J.R. (1973): Tectonic setting of basic volcanic rocks determined using trace element analysis; Earth Planet. Sci. Lett., v19, p290-300.

Pearce, J.A. and Norry, M.A. (1979): Petrogenetic implications of Ti, Zr, Y and Nb variations in volcanic rocks; Contrib. Mineral. Petrol., v69, p33-47.

Thomas, D.J. (1989): Geology of the Douglas Lake - Phantom Lake area (Part of N.T.S 63K-12 and -13); *in* Summary of Investigations 1989, Sask. Geol. Surv., Misc. Rep. 89-4, p44-54.

Watters, B.R. (1989): Lithogeochemical studies in the Flin Flon - Amisk Lake area and Glennie Domain; *in* Summary of Investigations 1989, Sask. Geol. Surv., Misc. Rep. 89-4, p55-57.

The Wollaston Group and Underlying Archean Basement in Saskatchewan: Subsurface and Bedrock Geological Mapping in 1990

Irvine R. Annesley[1] *and Catherine Madore*[2]

Annesley, I.R. and Madore, C. (1990): The Wollaston Group and underlying Archean Basement in Saskatchewan: subsurface and bedrock geological mapping in 1990; *in* Summary of Investigations 1990, Saskatchewan Geological Survey; Saskatchewan Energy and Mines, Miscellaneous Report 90-4.

Bedrock mapping and drill core logging of representative sections of the Wollaston Group and its Archean basement continued during the 1990 field season, and completed the field component of the project, initiated in 1988 by the Saskatchewan Research Council and Saskatchewan Energy and Mines. The project continued under a joint agreement between Cameco, CEGB Exploration (Canada) Ltd. (1 year support), Cominco Ltd., Interuranium Canada Ltd., PNC Exploration (Canada) Co. Ltd., Uranerz Exploration and Mining Ltd., Saskatchewan Energy and Mines, and the Saskatchewan Research Council. The major goals of the project are to characterize the field, petrographic, geochemical, and stratigraphic attributes of the various units of the Wollaston Group and its underlying Archean basement, and to determine the role of basement stratigraphy and tectonometamorphic events in the genesis of unconformity-type uranium deposits.

The area investigated includes the Wollaston Domain and eastern part of the Mudjatik Domain (Figure 1). It is part of a large region previously mapped on a reconnaissance scale by many workers (see 1:250,000 scale Compilation Bedrock Geology Map Series and references therein, Saskatchewan Energy and Mines). Results of recent bedrock mapping and drill core logging in this region were reported by Annesley and Madore (1988, 1989a and b), Annesley (1989a and b) and Quirt (1989).

This report mainly presents field observations by a two-person crew and preliminary conclusions from outcrops examined in 1990. Laboratory work will include examination of over 1000 rock thin sections, chemical analysis of several hundred samples, and U-Pb zircon geochemistry including zircon morphology studies. The final report of this project is scheduled for completion as an SRC publication in April of 1991, and released as a paper or series of papers after a two year period of confidentiality.

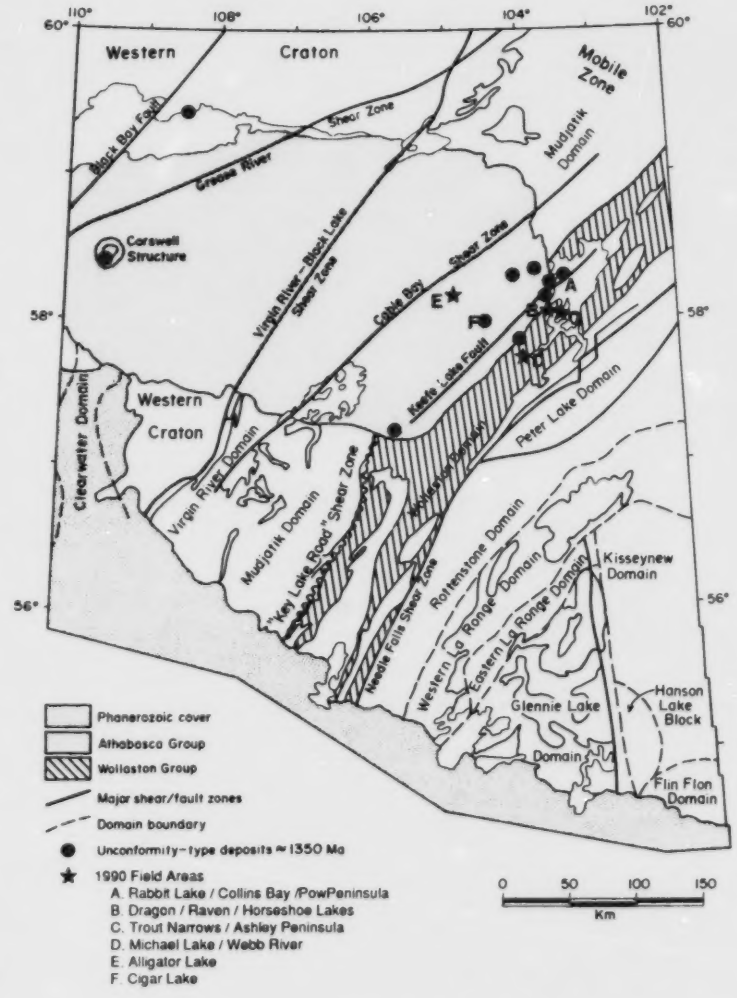

Figure 1 – Location of outcrops and drill holes visited during the summer of 1990.

(1) Minerals/Groundwater Program, Resources Technology Division, Saskatchewan Research Council, Saskatoon, Saskatchewan
(2) Department of Geology, University of Ottawa, Ottawa, Ontario

1. Trout Narrows/Hungry Bay/Ashley Peninsula Area

Six days of detailed mapping and sampling were carried out along the northwestern edge of the Trout Narrows granite and along the eastern shoreline of Ashley Peninsula. Exposures are generally excellent along the shorelines, but poor to fair inland. A recently burnt over area provided excellent exposure along the northwestern margin of the Trout Narrows granite (south of Deep Bay). Six distinct lithological units of Wallis (1971) were examined and three more units were identified at the margin of the Trout Narrows granite. The distribution of Wallis's units has not changed, but the authors have reinterpreted some quartzofeldspathic gneisses previously identified as meta-arkoses as calc-alkaline granitoid gneisses, on the basis of the preservation in these rocks of: 1) igneous minerals (e.g. igneous allanite and sphene, among other minerals); 2) igneous textures (see Percival and Girard, 1988; among others) and 3) preserved igneous mineral assemblages typical of calc-alkaline suites (i.e. hornblende, biotite, sphene, allanite, apatite, zircon, and magnetite with subordinate calcic clinopyroxene).

a) Trout Narrows Granite

The Trout Narrows granite is in part concentrically zoned with a relatively mafic-rich margin passing inwards to a more felsic and partly porphyritic core (cf. Wallis, p31, 1971). The margin ranges in composition from a garnet-biotite tonalite to a hornblende-biotite granodiorite (Figure 2). The major rock-forming minerals of the marginal rocks are plagioclase, K-feldspar, quartz, hornblende, biotite, and magnetite. Sphene, apatite, zircon, allanite, and garnet are common accessory minerals. The central core ranges from biotite monzogranite to biotite syenogranite. The biotite syenogranite and biotite monzogranite are dominated by K-feldspar (microcline and orthoclase, commonly perthitic), quartz, plagioclase, and biotite. Accessory minerals include apatite, zircon, sphene, and magnetite (altered to hematite). In general, the mineral assemblages of the Trout Narrows granite are higher temperature at the margins and lower temperature in the core. This is an example of Bowen's (1928) discontinuous reaction series in which a hornblende-rich outer zone is replaced by a biotite-rich central zone. The abundance of hornblende and the ubiquitous occurrence of magnetite and allanite in the marginal rocks indicate the I-type nature of the Trout Narrows granite. The mineralogy and textures of this granitoid body are similar to other I-type calc-alkaline granitoid intrusions, such as those of the Peninsular Ranges (Silver and Chappell, 1988) and the Central Andes (Pitcher *et al.*, 1985), among other examples.

The intensity of deformation increases in general from the core of the Trout Narrows granite to the northwestern margin. Three distinct foliations observed in the marginal zone are interpreted as S, C, and C' foliations.

Figure 2 – Tracing of photograph of thin section from the marginal hornblende-biotite granodiorite of the Trout Narrows granite (A90-021). Note the intricate growth of primary (igneous) biotite and hornblende crystals, and the presence of subhedral to anhedral apatite and magnetite grains partly to completely enclosed by biotite. At the bottom, a large magnetite crystal is surrounded by secondary granular sphene. Pl = plagioclase, Qtz = quartz, All = allanite, Ep = epidote, Bt = biotite, Spn = sphene, Chl = chlorite, Ap = apatite, Hbl = hornblende, Cpx = clinopyroxene, and Se = sericite.

The northwestern contact of the Trout Narrows granite is a high strain zone. Abundant kinematic indicators (i.e. rotated porphyroclasts, pull aparts, S-folds, quartz ribbons, mineral stretching lineations, etc.) give a consistent, sinistral strike-slip sense of shear. The layering is mylonitic in this zone. Boudinaged and attenuated quartzofeldspathic and mafic layers common in this zone are indicative of ductile strain at high metamorphic grade. The highly deformed amphibolite layers are comparable to those observed near the Raven/Horseshoe drill core camp (Figures 3a and 3b).

Varying proportions (along strike) of amphibolite, pegmatite, and aplite occur along the margin of the Trout Narrows granite. Drill hole observations confirm that these units occur at the contact of the granite and the overlying basal pelitic gneisses of the Wollaston Group.

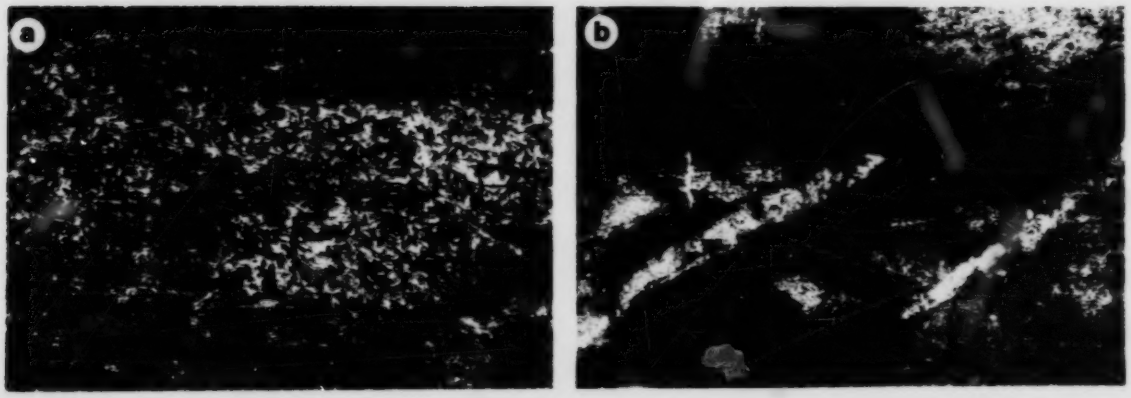

Figure 3 – a) Porphyroblastic amphibolite dyke. The center of the amphibolite dyke is composed of randomly oriented hornblende porphyroblasts up to 3.0 cm in length. The hornblende porphyroblasts cross-cut the earlier gneissosity. b) Details of the deformed equivalent of the porphyroblastic amphibolite dyke shown above. Note the well foliated and lineated nature (i.e. mylonitic) of the rock. This progressive mesoscopic transformation from a weakly to moderately deformed meta-igneous rock into a mylonitic rock is characteristic of ductile strain zones (for comparison, see Figure 6 of Tella and Annesley, 1988)

b) Reinterpretation of the Quartzofeldspathic Gneisses

Following careful examination of the field (Figure 4), textural and mineralogical characteristics, some quartzofeldspathic gneisses previously mapped as 'meta-arkose' (units 6a and 8a of Wallis, 1971), are now interpreted as calc-alkaline granitoid gneisses (i.e. I-type granodiorites, tonalites, quartz monzodiorites, and quartz diorites). These gneisses are similar to the mylonitic 'straight' quartzofeldspathic gneisses (Figure 5) seen west of Raven/Horseshoe drill core camp. The mineral assemblages are dominated by varying proportions of plagioclase, hornblende, biotite, calcic clinopyroxene, K-feldspar, and quartz. Zircon, allanite-epidote, sphene, apatite, and magnetite (in part Ti-rich) are the principal accessory minerals. The textural and mineralogical features of these rocks (Figures 6, 7, and 8; compare these features with those shown by Wilson, 1989, and Gromet and Silver, 1983) are typical of calc-alkaline granitoids observed elsewhere. Also consistent with the plutonic origin of these rocks are some of the field observations made by Wallis (1971), who for example stated "as a whole the psammites lack sedimentary structures", the psammites (units 6a and 6c) "are tough, massive rocks, and possess a well developed and persistent jointing", and "There is little difference between the recrystallized psammite and a medium-grained, foliated granodiorite".

Figure 4 – Fine- to medium-grained quartz dioritic gneiss (A90-006), composed of quartz (5%), feldspars (60%), aegirine-augite (10%), hornblende (10%), and biotite (7%). Accessory minerals include sphene, allanite-epidote, apatite, and zircon. The rock is relatively homogeneous in composition, and well lineated and layered. Outcrop is located on the eastern shoreline of Ashley Peninsula.

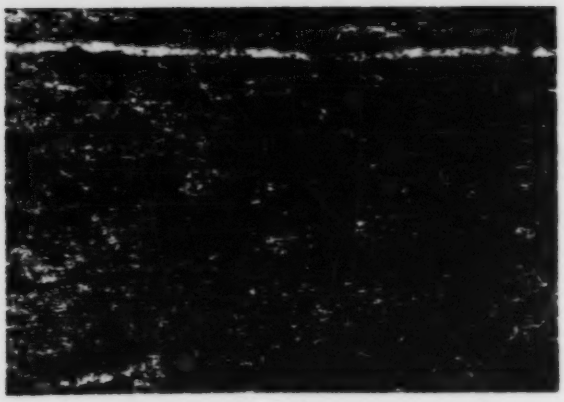

Figure 5 – Fine- to medium-grained, recrystallized, straight, quartz ribbony, mylonitic granodiorite (A89-116). The rock is composed of fine-grained quartz, plagioclase, microcline, biotite, hornblende with an accessory mineral assemblage of sphene, allanite, epidote, magnetite, apatite, and zircon. Rotated medium-grained K-feldspar porphyroclasts indicate the coarser nature of the rock prior to deformation. At least three generations of pegmatite are present in this rock. Outcrop located near the Raven/Horseshoe drill core camp.

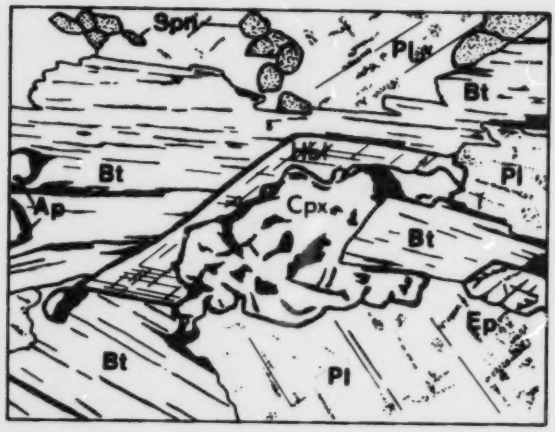

Figure 6 – Tracing of a photograph of a thin section from a quartz dioritic gneiss (A90-006, unit 6a of Wallis) displaying a resorbed calcic pyroxene grain mantled by euheral hornblende in contact with biotite. This is a typical texture of calc-alkaline granodiorites and tonalites.

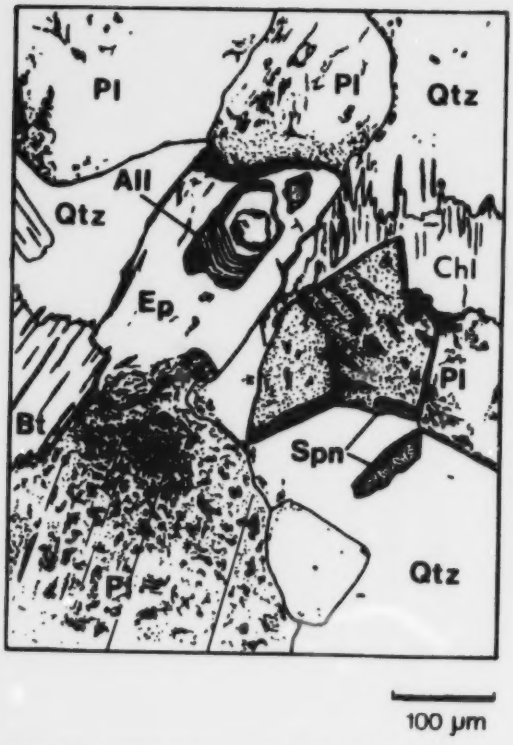

Figure 7 – Tracing of a photograph of a thin section from a tonalitic gneiss (A90-005b, unit 8a of Wallis) which shows a subhedral allanite core surrounded by a pale yellow epidote rim. The allanite core is reddish brown in colour and displays distinct, euhedral oscillatory zoned bands. The epidote overgrowth is commonly well developed around allanite where adjacent to biotite and plagioclase grains.

c) 'Polymictic Metaconglomerate'

The polymictic metaconglomerate (Figure 9) on Ashley Peninsula (unit 6g of Wallis, 1971) is intensely deformed. The authors were able on a few outcrops to structurally map out some of the lenticular masses of boulders and pebbles from high-strain zones to low-strain zones. The low-strain zones show boudinaged and partially pulled apart amphibolite layers and pegmatite veins. Therefore, some of the mafic and felsic clasts are the result of tectonic processes. Consequently, the authors question the identification of the metaconglomerate. We believe that derivation from a highly deformed granitoid gneiss with mafic and felsic dykes is equally plausible.

The aeromagnetic high that extends beyond the northern end of Ashley Peninsula can be explained by a significant amount of magnetite in quartzofeldspathic gneisses of that area.

2. Pow Peninsula Area

Detailed lithological mapping and sampling was carried out along the eastern shoreline of Pow Peninsula. Wallis (1971) mapped the geology of this area at a scale of 1:63,360.

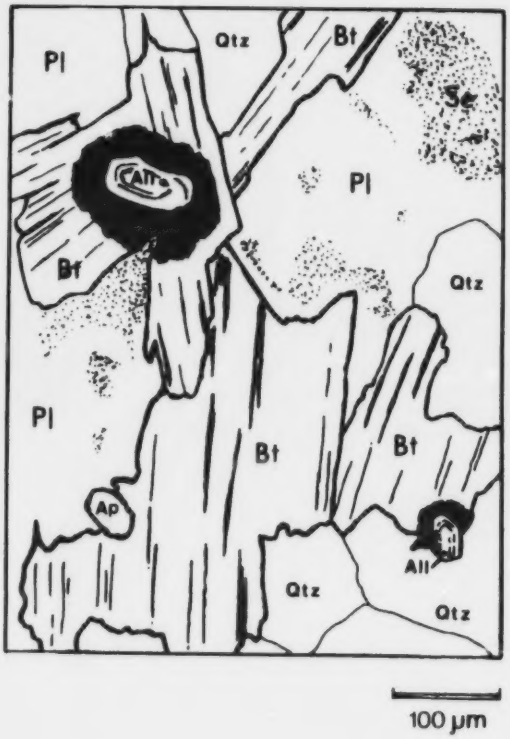

Figure 8 – Tracing of a photograph of a thin section from a granodioritic gneiss (A90-020, unit 8a of Wallis). Note the intimate intergrowth of subhedral to euhedral allanite and apatite crystals with biotite.

Figure 9 – Tectonized angular fragments and lenses of predominantly quartzofeldspathic composition within a highly deformed tonalitic gneiss. Note the late pegmatite vein cross-cutting the tonalitic gneiss and truncating some of the quartzofeldspathic lenses. This outcrop is characteristic of unit 6g of Wallis (1971), and is located on the eastern shoreline of Ashley Peninsula.

The distribution of rock units is the same as that reported by Wallis (1971). The metaquartzites, including the pseudo quartz-pebble conglomerate, are similar to those observed at the Raven - Horseshoe - Dragon Lakes area and also found in drill holes between Key and Rabbit Lakes. Original compositional layering was observed on a few outcrops, but no stratigraphic facing criteria were observed because of the extreme tectonic transposition of the rocks. At least two fold sets are common in the metaquartzites. Sheath folds and sheared-off fold limbs were also observed.

3. Michael Lake Area

The authors spent two days mapping and sampling between Dorward Lake and Michael Lake. The authors' interpretation of the lithological units and the structural and stratigraphic relationships of the region differs from Chadwick (1966).

The quartzofeldspathic gneisses are leucocratic light-coloured rocks that range from massive to strongly layered. All of these gneisses are granitic in composition. No primary sedimentary structures were recognized. Some of the quartzofeldspathic gneisses, mapped previously as 'meta-arkose' contain abundant K-feldspar megacrysts. The K-feldspar megacrysts are considered as reliable indicators of a granitic parentage (Vernon and Williams, 1988). In less deformed areas, the megacrystic quartzofeldspathic gneisses look similar to the megacrystic parts of the Trout Narrows granite. Although the field and petrographic evidence need additional support from geochemical and geochronological studies, at least some of the quartzofeldspathic gneisses are unequivocally plutonic igneous in origin. A porphyritic granite (unit 8 of Chadwick) similar to the one outcropping in the Rabbit Lake area is common at Michael Lake. In both areas xenoliths of tonalitic gneiss are found within the porphyritic granite. These xenoliths and the I-type calc-alkaline mineral assemblages of the granites are consistent with the derivation of the porphyritic granite by partial melting of older igneous rocks.

4. Conclusions

The field, petrographic, and geochemical work continues to focus on the two major geological problems; the identification of the protolith(s) of the quartzofeldspathic gneisses, and the division into Archean and/or Aphebian sequences remains, in places, questionable.

According to Windley (p.10, 1984) most researchers (e.g. Frish, 1988) in quartzofeldspathic gneiss terrains believe "that the bulk of the gneisses are metamorphosed and deformed calc-alkaline plutonic rocks, such as tonalites and granodiorites". Field, petrographic, and geochemical evidence from this study is demonstrating that a high proportion of the quartzofeldspathic gneisses so far examined to date, are indeed highly strained (i.e. tectonites) and metamorphosed calc-alkaline granitoids. This reinterpretation of the derivation of the quartzofeldspathic gneisses is similar to that proposed elsewhere in Saskatchewan (Hanmer, 1987; Lewry *et al.*, 1989) and in the southwestern Grenville Province (Davidson, 1986) (See also Barker, 990; Percival and Girard, 1988; Spry, 1969; Vernon and Williams, 1988).

The results of this study are broadly consistent with the model that Archean basement underlie allochthonous Early Proterozoic nappes (Bickford *et al.*, 1990). The U-Pb zircon study of this project will attempt to provide some constraints on crustal evolution in the Wollaston Domain.

5. Acknowledgements

Valuable discussions with K. Kogler, J. Murphy, and B. Tan (Uranerz Exploration and Mining Ltd.), B. Duncan, P. Ogryzlo, V. Sopuck, and D. Studer (Cameco), H. Quarch (Interuranium Canada Ltd.), N. Andrade (Cigar Lake Mining Corp.), S. Ahuja (PNC Exploration Co. Ltd.), and D. Quirt (Saskatchewan Research Council) were helpful. D. Quirt and V. Sopuck are especially thanked for sharing understanding and insights into unconformity-type uranium deposits. Review and critical comments by T.I.I. Sibbald are appreciated. The authors assume full responsibility for any speculative interpretation.

This work was funded by Cameco, Cominco Ltd., Interuranium Canada Ltd., PNC Exploration (Canada) Co. Ltd., Uranerz Exploration and Mining Ltd., Saskatchewan Energy and Mines and the Saskatchewan Research Council.

6. References

Annesley, I.R. (1989a): The Wollaston Group and its underlying Archean basement in Saskatchewan: an update; Sask. Res. Counc., Publ. R-855-5-E-89, 86p.

_____ (1989b): Whole-rock geochemistry from samples of Aphebian Wollaston Group metasediments and underlying Archean granitoid gneisses; Sask. Res. Counc., Publ. R-855-6-E-89, 70p.

Annesley, I.R. and Madore C. (1988): The Wollaston Group and its underlying Archean basement in Saskatchewan: preliminary report; *in* Summary of Investigations 1988; Sask. Geol. Surv., Misc. Rep. 88-4, p54-60.

_____ (1989a): A re-examination of the Wollaston Group and its underlying Archean basement in northern Saskatchewan; Geol. Assoc. Can./Mineral. Assoc. Can., Prog. Abstr., pA39.

_____ (1989b): The Wollaston Group and its underlying Archean basement in Saskatchewan: 1989 Fieldwork and preliminary observations; *in* Summary of Investigations 1989, Sask. Geol. Surv., Misc. Rep. 89-4, p87-91.

Barker, A.J. (1990): Introduction to Metamorphic Textures and Microstructures; Blackie, New York, 170p.

Bickford, M.E., Collerson, K.D., Lewry, J.F., Van Schmus, W.R. and Chiarenzelli, J.R. (1990): Proterozoic collisional tectonism in the Trans-Hudson Orogen, Saskatchewan; Geol., v18, p14-18.

Bowen, N.L. (1928): The evolution of the igneous rocks; Princeton University Press (reprinted by Dover Publications, New York, 1956), 334p.

Chadwick, B. (1966): The geology of the Nekweaga Bay area (west half), Saskatchewan; Sask. Dep. Miner. Resour., Rep. 116, 24p.

Davidson, A. (1986): New interpretations in the southwestern Grenville Province; *in* Moore, J.M., Davidson, A. and Baer, A.J. (eds.), The Grenville Province, Geol. Assoc. Can., Spec. Pap. 31, p61-74.

Frish, T. (1988): Reconnaissance geology of the Precambrian Shield of Ellesmere, Devon and Coburg Islands, Canadian Arctic Archipelago; Geol. Surv. Can., Mem. 409, 102p.

Gromet, L.P. and Silver, L.T. (1983): Rare earth element distributions among minerals in a granodiorite and their petrogenetic implications; Geochim. Cosmochim. Acta v47, p925-939.

Hanmer, S.K. (1987): Granulite facies mylonites: a brief structural reconnaissance north of Stony Rapids, northern Saskatchewan; *in* Current Research, Part A, Geol. Surv. Can., Pap. 87-1A, p563-572.

Lewry, J.F., Macdonald, R. and Stauffer, M.R. (1989): The development of highly strained rocks in the Pelican Window during high-grade metamorphism and pervasive anatexis; *in* Summary of Investigations 1989, Sask. Geol. Surv., Misc. Rep. 89-4, p58-65.

Percival, J.A. and Girard, R. (1988): Structural character and history of the Ashuanipi complex in the Schefferville area, Quebec-Labrador; *in* Current Research, Part C, Geol. Surv. Can., Pap. 88-1C, p51-60.

Pitcher, W.S., Atherton, M.P., Cobbing, E.J. and Beckinsale, R.D., eds. (1985): Magmatism at a plate edge: The Peruvian Andes; Blackie - Halsted Press, New York, 328p.

Quirt, D.H. (1989): Mineral deposit studies: Raven-Horseshoe uranium deposit, preliminary report; *in* Summary of Investigation 1989, Sask. Geol. Surv., Misc. Rep. 89-4, p92-94.

Silver, L.T. and Chappell, B.W. (1988): The Peninsular Ranges Batholiths: an insight into the evolution of the Cordilleran batholiths of southwestern North America; Trans., Roy. Soc. Edin., Earth Sci. v79, p105-121.

Spry, A. (1969): Metamorphic Textures; Pergamon Press, New York, 352p.

Tella, S. and Annesley, I.R. (1988): Hanbury Island Shear Zone, a deformed remnant of a ductile thrust, District of Keewatin, N.W.T.; *in* Current Research, Part C, Geol. Surv. Can., Pap. 88-1C, p283-289.

Vernon, R.H. and Williams, P.F. (1988): Distinction between intrusive and extrusive or sedimentary parentage of felsic gneisses: examples from the Broken Hill Block, NSW; Austral. J. Earth Sci., v35, p379-388.

Wallis, R.H. (1971): The geology of the Hidden Bay area, Saskatchewan; Sask. Dep. Miner. Resour., Rep. 137, 75p.

Wilson, M. (1989): Igneous Petrogenesis: A Global Tectonic Approach; Allen and Unwin, London, 466p.

Windley, B.F. (1984): The Evolving Continents; 2nd ed., John Wiley and Sons, Chichester, 399p.

U-Pb Sphene/Zircon Geochronological Investigations

G.D. Delaney, L.M. Heaman[1], S. Kamo[1], R.R. Parrish[2], W.L. Slimmon and B.A. Reilly

Delaney, G.D., Heaman, L.M., Kamo, S., Parrish, R.R., Slimmon, W.L. and Reilly, B.A. (1990): U-Pb sphene/zircon geochronological investigations; *in* Summary of Investigations 1990, Saskatchewan Geological Survey; Saskatchewan Energy and Mines, Miscellaneous Report 90-4.

This paper summarizes new U-Pb zircon and sphene ages obtained during 1990 and also reports on sampling initiatives that were undertaken this year.

1. New Geochronological Data

U-Pb dates were obtained from seven samples in two collaborative projects during 1990. Dr. Randy Parrish, Geochronology Section, Geological Survey of Canada, dated four specimens provided by G.D. Delaney from the Brownell Lake area, Glennie Domain. (Delaney, 1988). Dr. L. Heaman, Jack Satterly Geochronology Laboratory, Royal Ontario Museum dated two samples for W.L. Slimmon from the Gee Lake area, Glennie Domain and one sample for B. Reilly from the northern Mudjatik Domain.

2. Brownell Lake Area

A more comprehensive treatment of the data from the Brownell Lake area is planned for presentation in a forthcoming paper by Delaney and Parrish (in prep.) in the Radiogenic Age and Isotopic Studies report series by the Geological Survey of Canada. Consequently in this paper these dates will only be presented in Table 1.

3. Gee Lake Area

Deformation background: Complex polyphase deformation has affected rocks in the Gee Lake area (Slimmon, 1988). The dating program was designed to better understand the timing of the first two events:

1) D1 which resulted in the development of early schistose foliation (S1), generally parallel to primary layering, and coeval isoclinal folding.

2) D2 which caused the transposition of D1 structures into parallelism with a penetrative schistose foliation (S2) and associated down-dip stretching lineation (L2) which developed coeval to D2 thrusting and high strain zone formation

a) Sample 8930-GC1 (UTM co-ordinates 583710mE, 6123470mN)

Rock Unit: Intensely strained rhyolite from a felsic volcanic horizon in an interlayered felsic to intermediate metavolcanic succession. Collected by W.L. Slimmon.

Objective: To determine the age of volcanism and maximum age for D2 deformation.

Results: Preliminary discordant age of 1866 Ma for the extrusion age of the rhyolite obtained from three zircon fractions (Table 2; Figure 1). One more fraction is planned to be analyzed in an attempt to have at least three collinear zircon analyses. Age determination by L. Heaman, Royal Ontario Museum.

b) Sample 8930-GC2 (UTM Co-ordinates 580390mE, 6124810mN)

Rock Unit: Post-tectonic aplite intruding foliated granodiorite. Sample collected by W.L. Slimmon.

Objective: To determine the age of final intrusive activity and minimum age of D2 deformation.

Results: Three zircon fractions plot side-by-side and do not define a simple U-Pb discordia line (Table 2; Figure 2). Preliminary results constrain the intrusion age of the aplite by the minimum and maximum age estimates to be between 1835 and 1860 Ma respectively. It is planned to analyze titanite and an additional zircon fraction in order to better constrain these results. Age determination by L. Heaman, Royal Ontario Museum.

Table 1 - Summary of U-Pb Sphene/Zircon Dates Brownell Lake Area; all determinations by R. Parrish, Geological Survey of Canada.

Sample #	Rock Name and Unit[1]	UTM E[2]	UTM N	Mineral	$^{207}Pb/^{206}Pb$ age
8822-375	Granodiorite (gd3)	583570	6099590	zircon	1835±5 Ma
8822-375	Granodiorite (gd3)	583570	6099590	sphene	1830±5 Ma
8822-376	Arkose (WLr)	575820	6093250	zircon	1848-1888 Ma[3]
8822-377	Granite (BLgdp)	581760	6092940	zircon	1831 +9/-7 Ma
8822-378	Granodiorite (MLgd)	570640	6094800	zircon	1831 +6/-5 Ma

1. See Delaney (1988); 2. UTM Co-ordinates are for UTM zone 13; 3. dates are for individual detrital zircon grains.

(1) Jack Satterly Geochronology Laboratory, Royal Ontario Museum, 100 Queen's Park, Toronto, Ontario, M5S 2C6
(2) Geological Survey of Canada, 601 Booth Street, Ottawa, Ontario, K1A 0E8

Table 2 - U-Pb Isotopic Data for Zircons.

Zircon Fractions	Concentration			Common Pb (pg)	Atomic ratios					Apparent age (Ma)		
	Weight (mg)	U (ppm)	Pb (ppm)		$^{206}Pb/^{204}Pb$	$^{208}Pb/^{206}Pb$	$^{206}Pb/^{238}U$	$^{207}Pb/^{235}U$	$^{207}Pb/^{206}Pb$	$^{206}Pb/^{238}U$	$^{207}Pb/^{235}U$	$^{207}Pb/^{206}Pb$
8923-0149 Granodiorite, Mudjatik Domain												
1. NMO Ab Best needles	0.013	38	24	21	798	0.1805	0.5219	13.398	0.18617	2707	2708	2709
2. NMO Ab Multi-faceted	0.027	48	29	22	1981	0.1645	0.5211	13.363	0.18599	2704	2706	2707
3. NMO Equant, euhedral	0.185	42	24	19	12990	0.1350	0.5030	12.866	0.18553	2627	2670	2703
4. NMO Ab Large, euhedral	0.203	39	23	17	14500	0.1531	0.5025	12.950	0.18689	2625	2676	2715
8930-GC1 Rhyolite, Gee Lake												
5. NMO Ab Best equant	0.003	397	138	12	2081	0.0940	0.3318	5.222	0.11415	1847	1856	1866
6. NMO Ab 2nd best	0.004	671	228	17	3314	0.0802	0.3284	5.166	0.11409	1831	1847	1865
7. M1 Ab small cracks	0.020	563	193	15	15827	0.0989	0.3277	5.172	0.11446	1827	1848	1871
8930-GC2 Aplite, Gee Lake												
8. NMO+MO Ab 2nd best	0.171	201	71	25	28870	0.1208	0.3308	5.189	0.11375	1842	1851	1860
9. NMO Ab Best	0.037	194	69	13	11669	0.1216	0.3321	5.222	0.11403	1849	1856	1864
10. NMO Ab 2nd best	0.019	220	78	19	4723	0.1265	0.3318	5.240	0.11453	1847	1859	1872

Note: Ab = abraded fraction. $^{206}Pb/^{204}Pb$ corrected for spike; all other atomic ratios corrected for fractionation, blank and common Pb.

4. Mudjatik Domain

a) Sample 8923-149: UTM co-ordinates 578500 mE, 6638725 mN

Rock Unit: Inhomogeneous, inequigranular, medium- to coarse-grained, foliated, light grey granodiorite that weathers pinkish buff.

Objective: The granodiorite (unit Mg, Reilly, 1989) from the Mudjatik Domain intrudes the Ennadai-Rankin greenstone belt which has been dated by Chiarenzelli and Macdonald (1986) at 2682 ± 5.9 Ma. using U-Pb zircon methods. This Archean age is consistent with dates of 2697.5 ± 1.4 Ma and 2692 ± 1.0 Ma recorded by Mortensen and Thorpe (1987) in the same greenstone belt further north in the Northwest Territories. Dating the intrusion will establish whether the intrusion was emplaced during the Archean or Proterozoic and also provide the first age date from the Mudjatik Domain in the extreme northern part of Saskatchewan.

Results: The U-Pb age of 2708 +3/-2 Ma determined on four zircon fractions (Table 2; Figure 3), is older than anticipated based on the regional correlation of Archean volcanic units. Although there is a hint of inheritance in one fraction it is difficult to explain all the analyses as containing varying proportions of inherited component especially for the two nearly concordant analyses. Follow-up dating of the Ennadai volcanics in the vicinity of the granodiorite intrusion is warranted. Age determination by L. Heaman, Royal Ontario Museum.

5. 1990 Sampling Program

U-Pb dating of carefully selected units in the Reindeer Zone, Trans-Hudson Orogen, is critical in establishing or refining the detailed time framework within which to relate key phases in the geological and metallogenic

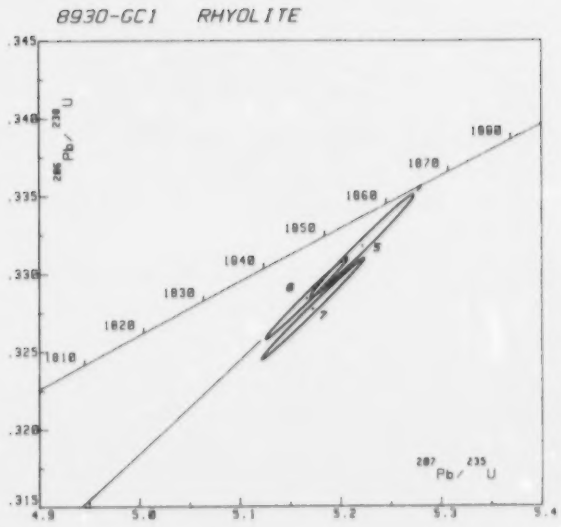

Figure 1 – U-Pb concordia diagram for zircons from sample 8930-GC1, rhyolite from Gee Lake area.

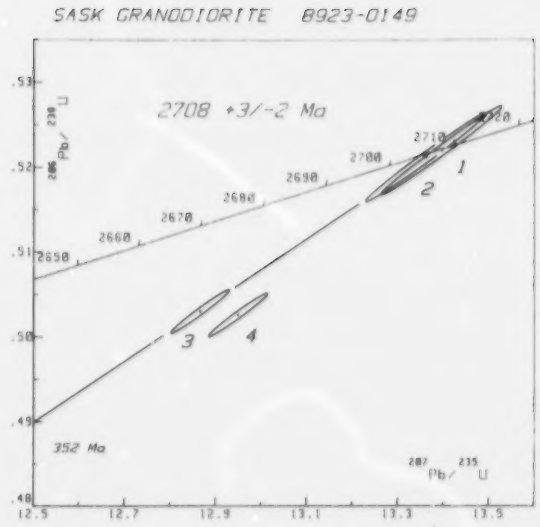

Figure 3 – U-Pb concordia diagram fro zircons from sample 8923-0149, granodiorite from Hattie Lake area. Fraction 4, which plots to the right of the discordia line, may contain a small inherited lead component.

evolution of the orogen (ie. Gordon, *et al.*, in press). Excellent candidates for dating have been identified during the past few years in the course of 1:20,000 mapping in the Saskatchewan part of the Reindeer Zone. In order to fill this void, the Saskatchewan Geological Survey has entered into a collaborative contract with the Jack Satterly Laboratory of the Royal Ontario Museum, represented by Dr. L. Heaman and S. Kamo, to date a minimum of 10 samples this year. During August 1990 a suite of 28 samples was collected for dating. Most of this suite was collected from the Glennie and La Ronge Domains to resolve geological problems identified during earlier detailed mapping projects. Other samples such as those from Hanson and Flin Flon Domains, were collected to resolve timing problems in areas that are currently being mapped (see Thomas and Reilly, this volume). From the suite of 28 samples, a priority group of 10 will be selected for dating this year; the other samples will be used to supplement the priority suite should any samples from that group prove unsuitable for dating. The remaining samples will be considered for dating during future years. All geochronological data from this program are expected to be in hand by March 31, 1991.

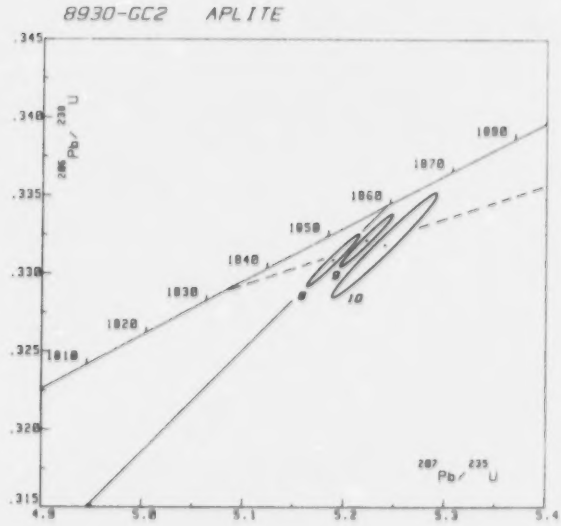

Figure 2 – U-Pb concordia diagram for zircons from sample 8930-GC2, aplite from Gee Lake area.

6. References

Chiarenzelli, J.R. and Macdonald, R. (1986): A U-Pb zircon date for the Ennadai Group; *in* Summary of Investigations 1986, Sask. Geol. Surv., Misc. Rep. 86-4, p112-113.

Delaney, G.D. (1988): Bedrock geological mapping, Brownell Lake Area (part of NTS 64M and 63L-13); *in* Summary of Investigations 1988, Sask. Geol. Surv., Misc. Rep. 88-4, p8-19.

Delaney, G.D. and Parrish, R.R. (in prep): New U-Pb data from the Brownell Lake area, southern Glennie Lake Domain, Trans-Hudson Orogen, Saskatchewan; *in* Radiogenic Age and Isotopic Studies: Report 4, Geol. Surv. Can., Pap. 90-4.

Gordon, T.M., Hunt, P.A., Bailes, A.H. and Syme, E.C. (in press): U-Pb ages from the Flin Flon and Kisseynew belts, Manitoba: Chronology of crust formation at an Early Proterozoic accretionary margin; *in* Lewry, J.F. and Stauffer, M.R. (eds.), The Early Proterozoic Trans-Hudson Orogen of North America, Geol. Assoc. Can., Spec. Pap. 37.

Mortensen, J.K. and Thorpe, R.I. (1987): U-Pb zircon ages of felsic volcanic rocks in the Kaminak Lake area, District of Keewatin; *in* Radiogenic Age and Isotopic Studies: Report 1, Geol. Surv. Can., Pap. 87-2, p123-128.

Reilly, B.A. (1989): Bedrock Geological Mapping Hatie Lake Area (Part of NTS 64M-13 and -14); *in* Summary of Investigations 1989, Sask. Geol. Surv., Misc. Rep. 89-4, p11-16.

Slimmon, W.L. (1988): Bedrock Geological Mapping, Gee Lake Area (Part of 63M-3 and -14); *in* Summary of Investigations 1988, Sask. Geol. Surv., Misc. Rep. 88-4, p26-31.

Structural Controls on Gold Deposits in the Star Lake and Island Lake Plutons

R.G. Roberts[1]

Roberts, R.G. (1990): Structural controls on gold deposits in the Star Lake and Island Lake Plutons; *in* Summary of Investigations 1990; Saskatchewan Geological Survey, Saskatchewan Energy and Mines, Miscellaneous Report 90-4.

A study of the structural controls of gold mineralization in the Star Lake and Island Lake Plutons, which was initiated in 1989 (Roberts and Schwann, 1989) was continued in 1990. The geology and the structure of the plutons have been described by Poulsen *et al.* (1985), Poulsen (1986a,b) and Ames *et al.* (1987).

The present field work was directed towards an examination of the relationship between the regional structural fabric (foliation and lineation) and the structures in the deposit hosting shear zones.

1. The Shear Zones

Gold deposits in the Star Lake and the Island Lake Plutons are controlled by mylonitic shear zones. In the Star Lake Pluton, at least seven shear zones have been defined by Ames *et al* (1987). The shears strike 060°, dip steeply, are up to 30 m thick, and their strike lengths vary from 1 to 4 km. They are characterized by a pronounced down-dip lineation defined by aggregates of biotite and rod-like feldspar grains. At least six gold occurrences have been located in the shears, including the Jolu, Star Lake, and Decade mines.

The attitude of shear zones in the Island Lake Pluton is similar to that of shears in the Star Lake Pluton in that they are steeply dipping to the north, strike in the northeast quadrant, and contain the same down-dip lineation; but the strike directions are more variable, and the shears are less persistent along strike. The strikes of discrete, or isolated shears in the Broedder Lake area vary from 025° to 070°. The shear systems that hosts the Jasper and Roxy deposits strike approximately 040° and 030° respectively, but the Roxy shear zone is made up of shears that strike between 010° and 040°.

2. Regional Fabric (S Foliation)

Following the 1989 field season, the writer concluded that the regional foliation was formed under conditions of rotational strain (Roberts and Schwann, 1989). The following observations from the 1990 field season support this conclusion: 1) in any outcrop, it is common to find two or more foliations, which cannot be differentiated except on the basis of their attitude, 2) curving foliations are quite common and may be deflected into a narrow zone of strong foliation (a shear) a few centimetres wide; two or more such shears may occur in any outcrop, and 3) strain in the rocks may be represented entirely by layers, less than a centimetre wide, exhibiting grain size reduction and foliation.

The regional foliations were defined by measuring the zones of high strain described in 2) and 3) above. The foliations are subvertical, and are classified into the following six groups, based on the direction of strike; 350°, 020°, 060°, 098°, 125° and 150°. The foliations contain the same mineral lineation that characterizes the shear zones. The lineation lies on the foliation and plunges steeply towards the north. Consequently the precise attitude of the lineation varies according to the attitude of the foliation with which it is associated.

3. Discussion

The model that best explains the relationship between the regional foliation and the shear zones is that both types of structures belong to the same deformation or strain regime, and that the shear zones simply represent zones of higher strain. Thus the evidence of the regional foliations is that the plutons deformed by the development of small shears which have the range of attitudes noted above. In the shear zones, the same planes of deformation can be recognized, but the amount of strain is greater, and is most intense along the shears that strike in the northeast quadrant. This last observation leads to the conclusion that the bulk strain for the region is rotational. The model is particularly significant in interpreting the relationship between the various shears that make up a shear zone. One of the shear directions is generally significantly stronger, and transects and deforms the other shears. Consequently the system cannot be interpreted as a principal shear with secondary or subordinate shears such as Reidel structures. Furthermore, the line formed by the intersection of the shears does not relate to the sense of movement on the shears. Such an interpretation by the author (Roberts and Schwann, 1989) lead to the conclusion that there was a significant horizontal component to the direction of slip in the shear zones. This is not correct; the slip direction on the shears is given by the attitude of the mineral lineation.

The model also provides an explanation for the attitudes of the folds within the shear zones. Where one shear, is deformed by a second shear, the resulting fold is steeply plunging. This is because the two planes are subvertical. Where the folds are developed in a shear plane, by the action of shearing along the plane, the axes of the resulting folds are very close to being perpendicular to

(1) Department of Earth Sciences, University of Waterloo, Waterloo, Ontario, N2L 3G1

the direction of shearing, and therefore have a shallow plunge, because the direction of shearing is steeply plunging.

The morphology of the ore zones is controlled essentially by the direction of shearing, and consequently their long axes are generally steep. However, this shape may be modified by folding of the shear zone and the ore in the manner described above. It is likely that the Jolu deposit has been affected this way.

4. References

Ames, D.E., Poulsen, K.H. and Galley, A.G. (1987): Geology and gold deposits, Star Lake Pluton, La Ronge Domain, Saskatchewan; Geol. Surv. Can., Open File 1469, 1:10,000 scale map with marginal notes.

Poulsen, K.H. (1986a): Controls on gold mineralization in the Star Lake Pluton, La Ronge Domain; *in* Summary of Investigations 1986, Sask. Geol. Surv., Misc. Rep. 86-4, p139-140.

_____ (1986b): Gold mineralization in the Star Lake Pluton, La Ronge belt, Saskatchewan; a preliminary report; *in* Current Research, Pt. A, Geol. Surv. Can., Pap. 86-1A, p205-212.

Poulsen, K.H., Ames, D.E. and Galley, A.G. (1985): Structural studies of gold mineralization in the La Ronge area; *in* Summary of Investigations 1985, Sask. Geol. Surv., Misc. Rep. 85-5, p96-98.

Roberts, R.G. and Schwann, P.L. (1989): Structural controls on gold deposits in the La Ronge Domain, Saskatchewan: a progress report: *in* Summary of Investigations 1989, Sask. Geol. Surv., Misc. Rep. 89-4, p36-40.

Field Observations on the Corner Lake and Tower Lake East Gold Showings, Byers Fault Area

P.L. Schwann

Schwann, P.L. (1990): Field observations on the Corner Lake and Tower Lake East gold showings, Byers Fault area; *in* Summary of Investigations 1990, Saskatchewan Geological Survey; Saskatchewan Energy and Mines, Miscellaneous Report 90-4

Documentation of the lithologic and structural characteristics of gold mineralization located along the Byers Fault began in 1989 with investigations at Weedy Lake and Oven Lake - Corner Lake (Schwann, 1989). The study was continued in 1990 at the Corner Lake and Tower Lake East occurrences. The Corner Lake property (CBS 5205), located in NTS 64D-4, is operated by CAMECO and has geological reserves of 136,000 t of 16.1 g/t gold (150,000 tons of 0.47 oz/ton gold). The Tower Lake East property (S-96833 to 96836, CBS 5205), located in NTS 74A-1, is operated by Golden Rule Resources and has geological reserves of 538,000 t of 6.9 g/t (593,000 tons of 0.20 oz/ton gold).

Previous work in the area by the Saskatchewan Geological Survey was carried out by Byers (1948), Kirkland (1959), Johnston (1969), and more recently by Harper (1984, 1985). Coombe (1984), Coombe *et al.* (1985), and Thomas (1987) presented overviews of gold deposits in the La Ronge Domain and results of a structural study of gold mineralization in the area is reported by Poulsen *et al.* (1987).

1. Regional Geology

The Byers Fault area is situated within the La Ronge Domain and is located near Waddy Lake, about 150 km northeast of La Ronge. The geology has been described by Harper (1984, 1985). The metavolcanic succession comprises ultramafic to intermediate subaqueous flows which are overlain by felsic flows and pyroclastics. Intravolcanic metagreywackes, meta-argillites and iron formation occur locally above the felsic metavolcanics. This metamorphosed volcanosedimentary assemblage is unconformably overlain by metaconglomerates. The supracrustal rocks are intruded by a variety of gabbro to granite plutons and stocks ranging in age from synvolcanic through syn- to post-tectonic.

The dominant structural feature of the area is the Byers Fault, a 26 km long east to northeasterly-trending, early discordance. Ancillary subparallel faults (eg. Oven Lake - Corner Fault) are located to the south of the Byers Fault. Harper (1985) related development of these faults to an early folding event (D1) accompanied by faulting parallel to intrusion margins. The faults appear as prominent, positive linear anomalies on regional (1:50,000) vertical gradiometer maps (GSC Maps: C41119 G and C41117 G). Regionally the area exhibits features similar to those identified in gold producing areas of the Superior Province (Colvine *et al.* 1988) as follows:

i) within or immediately adjacent to volcanic belts intruded by felsic plutons,

ii) within regional-scale deformation zones,

iii) close to faults and fault splays and

iv) within greenschist to middle amphibolite facies rocks.

The Byers Fault was first recognized as a major gold-bearing structure in the early sixties as a result of work done by the Augustus Concession (SEM Assessment Files 64D4-NE-0001-0005). Numerous showings occur along the Byers and ancillary faults (Figure 1), the majority being epigenetic sulphide-quartz (± carbonate) shear and tension veins within metavolcanics and felsic to mafic intrusions (Coombe *et al.*, 1985).

2. Corner Lake Property

Mapping at 1:5000 scale of an area west of Corner Lake to Boundary Lake continued this season. The area comprises predominantly intermediate and felsic metavolcanics intruded by the Boundary Lake Pluton and subsequently by the Corner Lake and Oven Lake granodiorite stocks. The Corner Lake Stock outcrops along the southwest and southeast shores of Corner Lake. A stripped area (70 by 30 m) immediately southwest of the lake was mapped in detail at 1:100 scale (see map). The Oven Lake - Corner Lake Fault and the contact of the stock with adjacent intermediate and felsic metavolcanic rocks is exposed by the overburden stripping.

a) Description of Rock Types

Metavolcanic Rocks

Intermediate metavolcanics are blue grey weathering, dark grey, fine-grained, equigranular rocks comprising predominant plagioclase and up to 40 percent hornblende and 15 percent biotite. Outcrop surfaces in part weather recessively and appear pitted. Where in contact with the granodiorite stock the intermediate metavolcanics are transformed into biotite schists composed of biotite (60 to 65 percent) and plagioclase (30 to 35 percent) with disseminated pyrite (5 to 7 percent). Quartz veinlets occur subparallel to the schistosity.

Felsic metavolcanics are fine-grained porphyritic rocks containing up to 15 percent plagioclase phenocrysts (2 mm). They weather pale pink and are dark bluish grey on fresh surfaces. A trace of pyrite can be present.

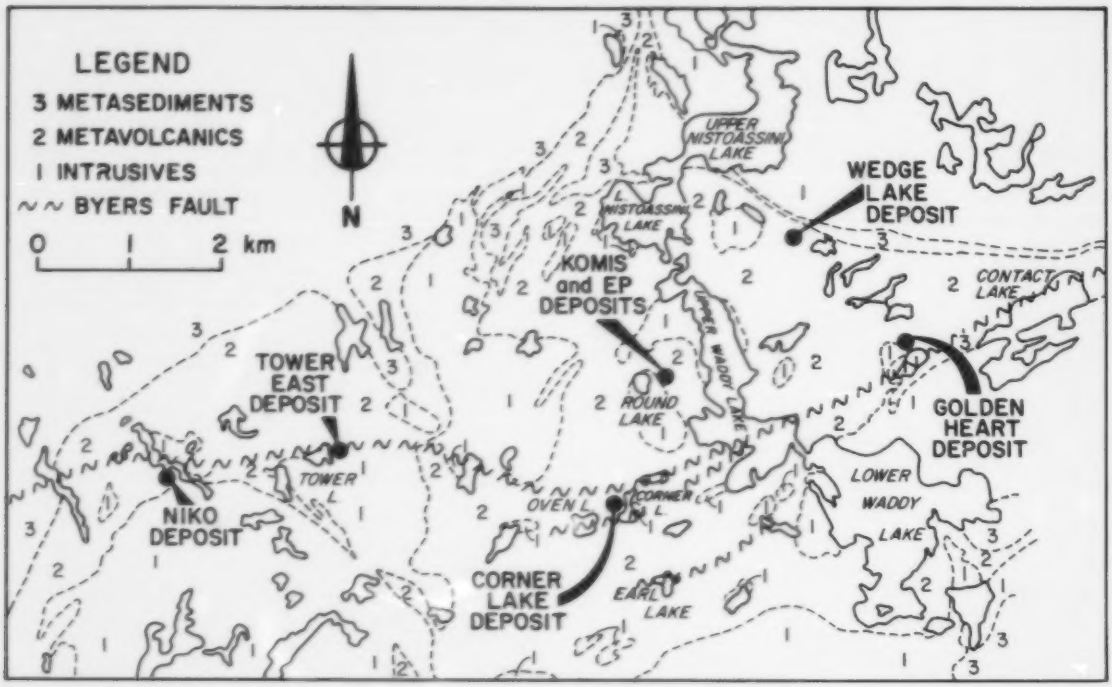

Figure 1 - Geological Sketch map of the Byers Fault area.

Intrusive rocks

The Corner Lake Stock is a pink weathering, grey, medium- to coarse-grained, equigranular homogeneous granodiorite comprising plagioclase, potassium feldspar, quartz and brown biotite (10 to 15 percent). A quartz-feldspar porphyry dyke intrudes the felsic and intermediate metavolcanics but not the granodiorite. It weathers creamy white while fresh surfaces are typically dark bluish grey. Plagioclase phenocrysts (25 to 30 percent) range between 3 and 6 mm in length, while quartz phenocrysts (5 to 10 percent) are generally 2 mm in diameter.

b) Structure

The Oven Lake - Corner Lake Fault, which is subparallel to the intrusive contact of the Corner Lake Stock, strikes east-northeast (065° - 075°) and dips steeply south (75° - 85°). The structure has been identified by diamond drilling over a 1.5 km strike length as a zone of strongly deformed granodiorite containing quartz veins and sulphides. Within the fault zone, the granodiorite has a mylonitic foliation defined by ribboned quartz and beaded feldspar grains. Biotite and quartz-feldspar aggregates form a strong subvertically southward-plunging lineation interpreted as a stretching direction.

c) Mineralization

An auriferous quartz vein occurs in the centre of the deformation zone and is flanked by granodiorite. Its width varies from 0.5 to 5 m. The hanging wall of the vein contains fragments of mylonitic granodiorite and the hanging wall granodiorite is cherty, pyritic and mylonitic over a width of 0.5 to 1.0 m. Deformation in the hanging wall decreases rapidly outside this zone.

Footwall granodiorite is strongly deformed over widths ranging between 1 and 6 m. Granodiorite in the immediate footwall is typically cherty, pyritic and mylonitic. Discrete shears (2 to 5 cm wide) envelope losenges of relatively undeformed to moderately foliated granodiorite.

d) Alteration

Sericite, potassium feldspar and epidote are common as fracture fillings and coatings within and adjacent to the main auriferous quartz vein. Quartz-tourmaline veins occur in the granodiorite at the east end of the stripped outcrop. Intermediate volcanics in contact with the granodiorite are altered to a pyritic and silicified biotite schist.

3. Tower Lake East

Mapping at 1:2500 scale was carried out around Tower Lake (see map) primarily to the south of the Byers Fault, where mafic to intermediate, finely layered tuffs are intruded by a mafic to intermediate layered intrusion. These rocks are in turn cut by felsic dykes. Mafic pillowed flows outcrop to the north (footwall) of the fault.

Exploration has concentrated on the northeastern shore of Tower Lake and extended westward under the lake.

There is virtually no outcrop in the immediate drilled area. The Byers Fault, which occupies a linear muskeg that runs parallel to the northern edge of Tower Lake, is unexposed. Nine drill holes were logged to examine the style of gold mineralization at Tower Lake.

a) Description of Rock Types

Metavolcanic Rocks

Mafic flows outcrop on the north side of Tower Lake and occur in drill core in the footwall of the Byers Fault. They are dark green to black weathering, dark grey, fine-grained, massive rocks comprising predominant hornblende (chlorite), plagioclase and minor sulphides (1 percent). Quartz-carbonate amygdales form up to 2 percent of the rock and small (20 by 8 cm) pillow structures are common. Outcrop surfaces are typically fractured and carbonate-veined.

Mafic tuffs outcrop over a small area immediately south of the Byers Fault and east of Tower Lake, as well as occurring towards the top of one of the logged drill holes. They are olive to dark green, fine-grained to aphanitic and delicately layered and comprise variable amounts of hornblende, biotite and plagioclase and minor quartz. Textural (grainsize) and compositional layering occurs on a millimetre to metre scale. Primary structures include soft-sediment slumping, cross-bedding, and truncated surfaces. Metamorphic recrystallization has locally obliterated primary textures producing a medium-grained amphibolite.

Felsic tuffs are uncommon in outcrop but relatively abundant in drill core. They weather to buff-white, tan and rust colour and typically display pitted outcrop surfaces. Felsic tuffs are bluish grey, fine-grained to aphanitic, locally feldspar-phyric and layered on a millimetre to centimetre scale. Bedding is commonly defined by alternating lapilli-rich, feldspar phyric and aphanitic layers. The tuffs are of dacitic composition and comprise plagioclase, potassium feldspar, quartz and up to 15 percent biotite and 5 percent sulphides.

Intrusive Rocks

Layered igneous rocks form a zoned multiple intrusion composed of gabbro, diorite, quartz diorite, tonalite and granodiorite, which is part of the Tower Lake Phase of the Brindson Lake Pluton (Harper, 1985, 1986). Primary igneous textures are often preserved, although plagioclase is partially saussuritized, and mafic minerals are altered to amphibole, biotite and chlorite. Sulphide contents vary from a trace to 5 percent.

Gabbroic rocks commonly display metre-scale layering between melanocratic, mesocratic and leucocratic members. Contacts between layers are sharp and straight. The gabbros are typically medium-grained, massive, equigranular rocks comprising variable proportions of green amphibole and white plagioclase. Locally, there is a grading from fine to coarse units. A spectacular coarse to pegmatitic unit containing euhedral clinopyroxene crystals up to 5 cm in diameter, in a matrix of clinopyroxene and plagioclase, outcrops southwest of Tower Lake.

Diorite is a brownish grey weathering, greenish grey, medium-grained, massive, equigranular rock comprising hornblende and clinopyroxene (60 percent) and plagioclase (40 percent). Plagioclase is euhedral and shows a subparallel orientation. Locally, up to 15 percent bluish quartz phenocrysts (1 to 2 mm diameter) are present.

Tonalite is a white weathering, greyish white, medium-grained, massive, inequigranular rock. Euhedral plagioclase crystals are set in a finer-grained felsic matrix containing around 10 percent hornblende and biotite. Up to 5 percent blue quartz phenocrysts may be present as small (1 to 2 mm diameter) subhedral crystals. Gabbro and diorite xenoliths make up 10 percent of tonalite outcrops.

Granodiorite is pinkish grey weathering, greenish grey, leucocratic, medium-grained, massive and equigranular. It comprises predominant plagioclase and potassium feldspar, with up to 15 percent blue quartz and 15 percent biotite. The granodiorite contains up to 20 percent xenoliths of gabbroic, dioritic and tonalitic compositions.

Aplite and quartz porphyry dykes intrude all the above rock types. The aplites weather a distinctive salmon colour and are pale pinkish grey on fresh surface. They are fine-grained, equigranular rocks essentially barren of mafic minerals. Quartz porphyry is pale pink weathering, bluish grey, fine grained, inequigranular and characterized by up to 15 percent blue quartz phenocrysts (1 to 2 mm diameter) set in a nondescript felsic matrix containing a few percent sulphides.

b) Structure

Both the metavolcanics and layered igneous rocks retain primary layering (So). The former dips steeply (70° to 85°) to the southwest whereas layering in the igneous rocks dips steeply (77° to 85°) to the west. In outcrop, rocks generally lack distinct deformational fabrics although a weak stretching lineation marked by the long axes of tonalite-hosted diorite xenoliths plunges steeply southwest.

In drill core, deformation features are most commonly developed in granodiorite, occurring as up to 10 m wide zones of cataclasis showing brecciation and granulation. Within these zones the granodiorite is finer-grained and darker coloured than the undeformed protolith. Proximal to the Byers Fault, the deformation fabric is more strongly developed and often accompanied by silicification. The Byers Fault itself is a zone characterized by hematization, chloritization and carbonate veining and poor core recovery. Ductile fabrics in the hanging wall granodiorite are overprinted by later brittle structures, such as open-spaced fractures lined with quartz, hematite and limonite. In footwall mafic metavolcanics, carbonate veining and chlorite are prominent. Hematization persists for 5 to 10 m below the Byers Fault.

c) Mineralization

Gold mineralization at Tower Lake East is hosted by a variety of rock types:

(i) pyritized and silicified felsic metavolcanics,

(ii) pyritized and silicified diorite, quartz-porphyritic diorite and granodiorite,

(iii) quartz-carbonate-pyrite veins in quartz-porphyritic tonalite - granodiorite,

(iv) fine-grained mafic metavolcanics,

(v) microbrecciated, limonitic, hematitic diorite - granodiorite adjacent to the Byers Fault and

(vi) pyrite-bearing quartz porphyry dykes.

Pyrite, carbonate, quartz, limonite and hematite are prominent alteration minerals associated with gold mineralization. Visible gold is prevalent in quartz-carbonate veins and in apparently unaltered and undeformed fine-grained mafic volcanics as isolated millimetre-sized flecks. Mineralized zones are relatively narrow, but wider intersections occur within a pyritized, silicified and carbonatized halo in the felsic metavolcanics and intrusives. Subhedral pyrite forms up to 10 percent of the rock. Individual quartz veins are narrow and discontinuous. Limonite and hematite coat fracture surfaces in microbrecciated intrusive rocks.

4. Summary

i) Gold mineralization at Corner Lake is associated with a mylonitic, pyritized and silicified granodiorite and a quartz vein structure. Pyritic, silicified, biotite schists proximal to the granodiorite are also mineralized.

ii) Gold mineralization at Tower Lake East occurs in virtually all rock types ranging in age and composition from the oldest mafic metavolcanics to the youngest felsic dykes, although there is likely more than one gold mineralizing event. Alteration of the host rocks is also varied and includes silcification, pyritization, carbonatization, and hematization. Mineralization is not controlled by a discrete structure as at Corner Lake.

5. Acknowledgements

Terri Uhrich provided efficient and conscientious assistance. The cooperation of CAMECO and Golden Rule Resources is appreciated.

6. References

Byers, A.R. (1948): The geology of the Waddy Lake area, Rottenstone Mining Division, Saskatchewan; Sask. Dep. Miner. Resour., Rep. 1, 36p.

Colvine, A.C., Fyon, J.A., Heather, K.B., Marmont, S., Smith, P.M. and Troop, D.G. (1988): Archean lode gold deposits in Ontario: Part 1, A depositional model; Part 2, A genetic model; Ont. Geol. Surv., Misc. Pap. 139, 136p.

Coombe, W. (1984): Gold in Saskatchewan; Sask. Energy Mines, OF Rep. 84-1, 134p.

Coombe, W., Lewry, J.F. and Macdonald, R. (1985): Regional geological setting of gold in the La Ronge Domain, Saskatchewan; *in* Clark L.A. (ed.), Gold in the Western Shield, C.I.M. Spec. Vol. 39, p25-56.

Harper, C.T. (1984): Geological mapping, Waddy Lake area (part of NTS 64D-4 and -5): *in* Summary of Investigations 1985, Sask. Geol. Surv., Misc. Rep. 84-4, p6-20.

_____ (1985): Bedrock geological mapping, Waddy - Tower Lakes Area (part of NTS 64D-4 and -5 and 74A-1 and -8); *in* Summary of Investigations 1985, Sask. Geol. Surv., Misc. Rep. 85-4, p6-17.

_____ (1986): Bedrock geological mapping, Windrum Lake area (part of NTS 64D-4, 73P-16 and 74A-1); *in* Summary of Investigations 1986, Sask. Geol. Surv., Misc. Rep. 86-4, p8-17.

Johnston, W.G.Q. (1969): The geology of the eastern portion of the Waddy Lake area, Saskatchewan; Sask. Dep. Miner. Resour., Rep. 127, 43p.

Kirkland, S.J.T. (1959): The geology of the Brabant Lake area, Saskatchewan; Sask. Dep. Miner. Resour., Rep. 33, 31p.

Poulsen, K.H., Ames, D.E., Galley, A.G., Derome, I., and Brommecker, R. (1987): Structural studies in the northern part of the La Ronge Domain: *in* Summary of Investigations 1987, Sask. Geol. Surv., Misc. Rep. 87-4, p107-115.

Schwann, P.L. (1989): La Ronge Gold Belt geology: Gold deposits in the Byers Fault area (part of 64D-4); *in* Summary of Investigations 1989, Sask. Geol. Surv., Misc. Rep. 89-4, p41-43.

Thomas, D.J. (1987): Gold deposits of the La Ronge Domain; GAC/MAC Field Trip No. 4 Guidebook, GAC/MAC Joint Annual Meeting, 1987, Saskatoon, Sask.

Oxygen, U-Pb and Pb-Pb Isotope Systematics in Uraninite from Complex U-Au-PGE Vein-Type and Unconformity-type Uranium Deposits in Northern Saskatchewan[1]

T.K. Kyser [2], T. Kotzer [2] and T.I.I. Sibbald

Kyser, T.K, Kotzer, T. and Sibbald, T.I.I. (1990): Oxygen, U-Pb and Pb-Pb isotope systematics in uraninite from complex U-Au-PGE vein-type and unconformity-type uranium deposits in northern Saskatchewan; *in* Summary of Investigations 1990, Saskatchewan Geological Survey, Saskatchewan Energy and Mines, Miscellaneous Report 90-4.

Stable isotopic, fluid inclusion and petrographic studies on alteration mineral assemblages occurring with high-grade unconformity-type uranium mineralization in the Athabasca Basin indicate that the early (ca. 1400 to 1100 Ma), high grade uranium ore formed as a result of interaction between high temperature basement and saline basin fluids in highly faulted areas (Kotzer and Kyser, 1990; Wallis *et al.*, 1983; Wilson and Kyser, 1987). Fluid inclusion studies on gangue minerals associated with mineralogically and chemically complex U±Ni±As±S±Au±PGE vein-type deposits in the Beaverlodge area (Rees, unpubl. data; Sassano *et al.*, 1972) yield temperatures and salinities similar to those of the fluids in the Athabasca Basin associated with unconformity-type uranium mineralization (Kotzer and Kyser, this volume; Pagel *et al.*, 1980). That similar fluids and structural controls are responsible for ore formation in the complex vein-type in the Beaverlodge area and the Athabasca unconformity-type uranium deposits has been suggested by numerous workers (Hoeve and Sibbald, 1978; Peiris and Parslow, 1988; Sibbald, 1988) on the basis of geochemical similarities of alteration associated with uranium mineralization, similar sulphide and arsenide mineralogies, proximity of uranium mineralization to the sub-Athabasca unconformity, and similarity of Pb-Pb and U-Pb ages of uranium minerals from both areas (Koeppel, 1968; Hoeve and Sibbald, 1978; Peiris and Parslow, 1988; Sibbald, 1988).

Since the initial suggestions that the complex vein-type and unconformity-type uranium deposits may have formed by the same mechanism and from the same fluid events, many fluid inclusion data have been acquired from the alteration minerals in both the Athabasca unconformity-type (Pagel *et al.*, 1980; Kotzer and Kyser, 1990 and this volume) and the Beaverlodge complex vein-type uranium deposits (Quirt and Rees, 1987; Rees, unpubl. data). These data indicate inclusions of similar paragenesis and microthermometric properties in both areas.

1. Objectives and Methodology

The present investigation is to determine (1) pitchblende and uraninite from both complex and simple vein-type deposits in the Beaverlodge area have had a fluid history similar to uraninites from unconformity-type deposits in the Athabasca Basin and, (2) to what extent oxygen, lead and uranium isotopic compositions of uraninites record the timing, origin, and expanse of fluids in the basin.

Uraninite and pitchblende samples from vein-type and unconformity-type uranium deposits (Figure 1) were examined by reflected light microscopy and with an electron microprobe. Areas showing minimal effects of later alteration were selected in the most pristine samples to determine the oxygen, lead, and uranium isotopic compositions and hence assess the type and timing of the fluid events associated with uranium formation. Pb-Pb and U-Pb isotopic systematics in the uraninites are also compared to the Pb-Pb isotopic systematics in paragenetically late Fe, Ni-As and Pb sulphide minerals occurring in the Athabasca Basin (Cumming *et al.*, 1984; Kotzer and Kyser, 1990) to determine if the Pb isotope ratios in the sulphides are the result of alteration by later fluids of the earlier-formed uranium mineralization.

2. Oxygen Isotope and Electron Microprobe Results

Uraninite and pitchblende samples from both the Beaverlodge and Athabasca Basin have $\delta^{18}O$ values from -27 to -2.3 per mil (Table 1). Samples which show the least petrographic alteration and have SiO_2 contents of less than 1 wt. percent have the lowest $\delta^{18}O$ values, from -27 to -22.3 per mil (Figure 2). Other samples having similar optical reflectivities, but exhibiting a greater degree of fracturing and chemical heterogeneity as shown by a general increase in Si and Ca contents and higher U/Pb ratios, have $\delta^{18}O$ values greater than -20 per mil (Figure 2). Those uraninites having similar $\delta^{18}O$ values of -27 to -23 per mil (Table 1) are the least petrographically altered in both the Beaverlodge and Athabasca areas and may have formed from similar fluids. The increase in $\delta^{18}O$ values with SiO_2 content of the more altered uraninites is exactly the behaviour expected from simple addition of SiO_2 (enriched in $\delta^{18}O$ relative to most fluids) to uraninite (depleted in $\delta^{18}O$ relative to most fluids).

(1) Project funded under Canada-Sask. Subsidiary Agreement on Mineral Development 1984-1990
(2) Department of Geological Sciences, University of Saskatchewan, Saskatoon, Sask., S7N 0W0

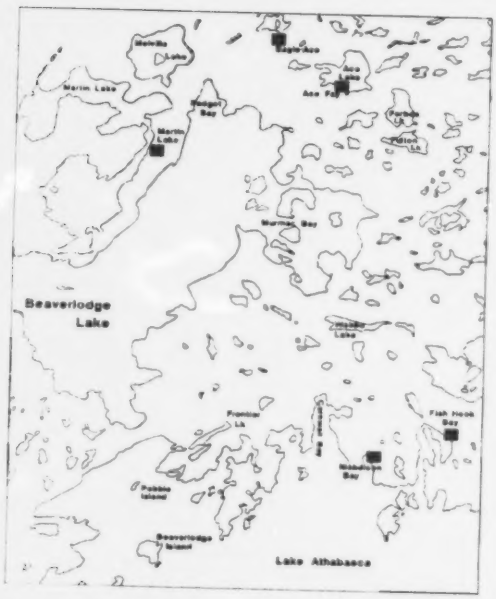

Figure 1 – Map of northern Saskatchewan showing lithostructural domains, the extent of the Athabasca Basin (shaded area), location of the uranium deposits, and uraninite samples used in this study (black squares). Enlargement for the Beaverlodge (Uranium City) area to show sample locations. MD, Mudjatik Domain; WD, Wollaston Domain; PLD, Peter Lake Domain; and RD, Rottenstone Domain.

Theoretical oxygen isotope fractionations between water and uraninite calculated by Hattori and Halas (1982) indicate that between temperatures of 25° to 200°C, uraninite will have $\delta^{18}O$ values which are 2 to 8 per mil lower than coexisting water. In the Athabasca Basin, the $\delta^{18}O$ values of co-existing quartz-illite assemblages and characteristics of fluid inclusions in euhedral quartz present in the alteration zones surrounding unconformity-type uranium deposits indicate formation at temperatures of 200°C from fluids having $\delta^{18}O$ values near 4 per mil. Fluids with similar temperatures and $\delta^{18}O$ values are suggested by analyses of gangue minerals associated with the complex, vein-type uranium

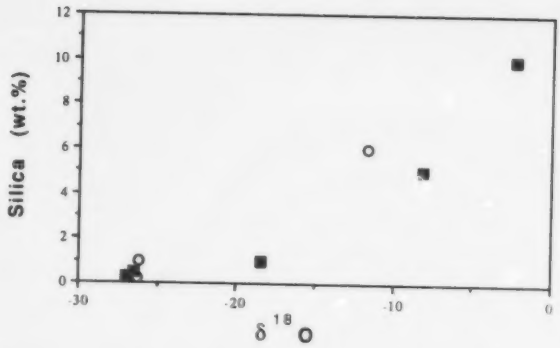

Figure 2 – Relation between $\delta^{18}O$ values of uraninites and silica content. Squares represent samples from Beaverlodge vein-type uranium deposits and open circles are samples from Athabasca unconformity-type uranium deposits. Data from Table 1.

deposits in the Nicholson-Fish Hook area. (Rees, unpubl. data).

Using the theoretical fractionation factor for uraninite-water and $\delta^{18}O$ values of 4 per mil and temperatures of 200°C for fluids associated with uranium mineralization, the $\delta^{18}O$ value of uraninite in both the Athabasca and Nicholson-Fish Hook areas could be from 2 to -4 per mil. None of the uraninites analyzed have $\delta^{18}O$ values this high, except for a sample of highly-fissile uraninite from the Ace-Fay mine. However, this sample also has a high SiO_2 content, which would suggest its initial chemical composition has been substantially altered. Accordingly, either the fractionation factor for uraninite is larger than has been originally calculated or the uraninites have undergone oxygen isotope exchange with fluids other than the high-temperature Athabasca fluids.

It is unlikely that the theoretical fractionation factors are in error, especially by the magnitude needed to produce uraninites having such low $\delta^{18}O$ values from high temperature Athabasca fluids with $\delta^{18}O$ values near 4 per mil. However, modern meteoric waters in the Athabasca Basin have $\delta^{18}O$ values of about -20 per mil, and recrystallization of uraninite with this meteoric water could produce the low $\delta^{18}O$ values of less than -20 per mil measured in the uraninites. That such meteoric waters have affected fault controlled uranium deposits in the Athabasca Basin is substantiated by the hydrogen isotopic compositions of clay minerals proximal to unconformity-type deposits, which indicate interaction between the clays and large quantities of low-temperature, meteoric water (Kotzer and Kyser, 1990 and this volume; Wilson and Kyser, 1987). Thus, the oxygen isotopic composition of the uraninites suggest that most samples have been extensively recrystallized in the presence of relatively modern meteoric waters.

3. U-Pb and Pb-Pb Ages of Uraninite

Chemical ages of the uraninites have been calculated using U and Pb contents measured with an electron

Table 1 – Petrologic Descriptions, Chemical and Isotopic Analyses, and Ages of Uranium for Uranium Minerals (see Figure 1 for locations). U/Pb chemical ages are determined by microprobe analysis (Cameron-Schimann, 1978).

Sample	Description	Remarks	U-Pb chemical age (Ma) electron microprobe	$^{207}Pb/^{206}Pb$ age (Ma)	^{18}O
8730-1	aniso. pitchblende + carbonate in vein Nicholson #4 (complex vein-type)	variable Si, Ca, Pb	802 - 1870	1214 ± 15	-8.2
8730-7	aniso. pitchblende intergrown with rammels + nicco. Nicholson #4 (complex vein-type)	homogenous Si, Ca, Pb	730 - 1120	1260 ± 10	-26.5
8730-24	weakly iso. pitchblende + quartz in vein Fish Hook 'B' (complex vein-type?)	variable Si, Ca, Pb	204 - 705.2	1018 ± 24	
Ea 26	massive, aniso.-iso. uraninite + carbonate + pyr./cpy/galena cubes Eagle Ace Mine (simple vein-type)	high Si, Ca, and homo. Pb - highly altered areas near fracs. (galena cubes)	252 - 312	———	-18.6
Ea 24	——————same as Ea 26 ——————		261 - 282	393 ± 22	-18.5
ML 19	massive, aniso. uraninite + carbonate Martin Lake Mine (complex vein-type)	homo. Ca, Si, Pb v. little alteration	1050 - 1294	1144 ± 16	-27.0
Ace Fay 1	fissile, massive uraninite aniso. - iso. Ace Fay Mine (simple vein-type)	variable Si, Ca, Pb high SiO_2 contents appears v. heterogeneous	383 - 626	519 ± 29	-2.3
KL 478-14	massive, aniso. uraninite in vein x-cutting Athabasca Sst. Key Lake (uncon.-type)	v. homo. Si, Ca, Pb contents	1314	1207 ± 10	-26.3
M208-519.7	aniso. uraninite w/cpy. in silicified sst. x-cut by pyr. Bermuda Lake, McArthur River area (uncon.-type)	slightly variable Ca, Pb	~ 100 - 929	1371 ± 13 (possible qtz. contamination)	-11.7
M212-516.2	massive, botryoidal pitchblende Bermuda Lake, McArthur River area (uncon.-type)	———	———	1120 ± 6	-22.3
HL20-563.3	aniso., massive uraninite near unconformity, McArthur River area (uncon.-type)	v. homo. Si, Ca, Pb	~ 200 - 740	1428 ± 10	-26.2

aniso. = anisotropic; iso. = isotropic; pyr. = pyrite; cpy = chalcopyrite; homo. = homogeneous; fracs. = fractures; uncon. = unconformity; qtz. = quartz

microprobe (Cameron-Schimann, 1978), assuming that no Pb loss or gain has occurred and no thoranogenic Pb is present (Table 1). In some uraninite samples, a range of ages results from analyzing a number of areas which are only a few microns apart (Table 1). However, in nearly all cases, the U-Pb chemical age is younger than the $^{207}Pb/^{206}Pb$ age of the uraninites indicating Pb loss has occurred. The large range of chemical ages in some of the samples provides a qualitative indication of the amount of alteration by later fluids. The U-Pb chemical ages do not correlate well with $\delta^{18}O$ values because the $\delta^{18}O$ values are increased by the addition of SiO_2 to some of the samples.

The $^{207}Pb/^{206}Pb$ ages of the uranium minerals range from 393±22 to 1428±10 Ma (Table 1) with the bulk of the ages occurring between 1018±24 to 1428±10 Ma. Uraninite from the Beaverlodge complex vein-type uranium deposits have $^{207}Pb/^{206}Pb$ ages of 1018±24 to 1260±10 Ma, which overlap the $^{207}Pb/^{206}Pb$ ages of uraninites from the Athabasca unconformity-type deposits, suggesting that the complex vein-type uranium formed at the same time as did the high-grade uranium deposits in the Athabasca Basin.

Two samples from the Beaverlodge simple vein-type deposits, have $^{207}Pb/^{206}Pb$ ages of 393±22 and 519±29 Ma (EA 24; Ace-Fay - Table 1). As these samples are fractured and contain chemical evidence for later alteration, they most likely represent a highly-altered, recrystallized early uraninite which has undergone complete lead loss. A comparison of the $^{207}Pb/^{206}Pb$ ages and $\delta^{18}O$ values of all the uraninites shows that some of the oldest ages are associated with the lowest $\delta^{18}O$ values (Figure 3). Inasmuch as low $\delta^{18}O$ values represent recrystallization of the uraninites by low-temperature meteoric waters, the $^{207}Pb/^{206}Pb$ ages indicate that this recrystallization event occurred relatively recently and that not all of the lead was removed from the uraninite during recrystallization. If the uraninite recrystallized completely and lead loss was complete, young $^{207}Pb/^{206}Pb$ ages would result, as is the case for the simple vein-type uraninites from the Beaverlodge area (EA 24; Ace-Fay - Table 1).

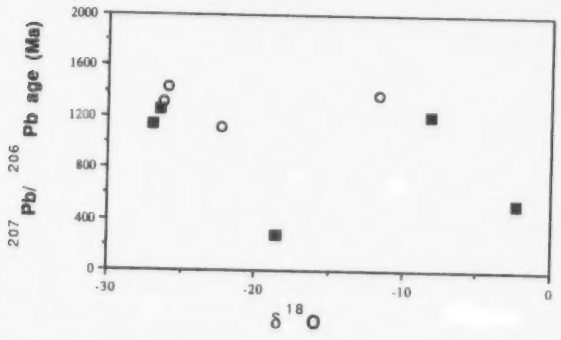

Figure 3 – Relation between $^{207}Pb/^{206}Pb$ age and $\delta^{18}O$ value of uraninites (squares represent samples from Beaverlodge complex and simple vein-type uranium deposits and open circles represent samples from Athabasca unconformity-type uranium deposits). Data from Table 1.

The U-Pb isotopic analyses of the uraninites from the Beaverlodge vein-type deposits yield a regression age of 1549±89 and a lower intercept age of 214±28 Ma from samples that are highly discordant (Figure 4a). As with many of the U-Pb ages previously reported for uraninites in the Athabasca Basin, the age obtained by regression of the Beaverlodge samples is probably not significant given the high degree of discordancy. Uraninite from the simple vein-type Eagle Ace Deposit (Ea 24) plots very close to the lower intercept with the concordia curve. As this sample has high Si, Ca, and low Pb contents and young $^{207}Pb/^{206}Pb$ and U/Pb chemical ages, it represents a sample of uraninite which has undergone complete lead loss during recrystallization by a later fluid event similar to what occurred at many of the unconformity-type deposits in the Athabasca Basin (Cumming and Rimsaite, 1978; Phillipe and Lancelot, 1988; Ruhlmann, 1985; Trocki *et al.*, 1984). Samples of petrographically and chemically unaltered uraninite from both the Athabasca and Beaverlodge areas yield a U-Pb regression line with intercepts of 1444±255 and 169±90 Ma (Figure 4b). Most samples are very discordant as a result of extensive recrystallization by a modern fluid, which is consonant with the oxygen isotopic compositions that indicate most uraninites have been recrystallized in the presence of relatively modern meteoric waters. Despite the extensive recrystallization reflected by the U-Pb ages and $\delta^{18}O$ values, most samples have retained an old age of formation in their $^{207}Pb/^{206}Pb$ ratios because not all of the lead was lost during recrystallization.

4. Implications of Pb-Pb Ages from Sulphides in the Athabasca Basin

The $^{207}Pb/^{204}Pb$ and $^{206}Pb/^{204}Pb$ ratios from the late-stage sulphides occurring in the basement rocks and sandstones of the unconformity-type uranium deposits at Key Lake, McArthur River and Eagle Point (this study) and Midwest Lake (Cummings *et al.*, 1984) plot on secondary isochrons (Figure 5) which are discordant with a crustal Pb growth curve (Stacey and Kramers, 1975). Slopes of the secondary isochrons from sulphides in the Athabasca Basin indicate formation relatively late in the history of the basin. At Key Lake, late sulphides and sulphate minerals plot on a secondary isochron yielding an actual age of 444 Ma for the sulphides using a radiogenic Pb source age of 1406 Ma (Figure 5a). Late sulphides in the Athabasca Basin occur as pyrite and marcasite on re-activated high angle fractures at Eagle Point and McArthur River. The $^{207}Pb/^{204}Pb$ and $^{206}Pb/^{204}Pb$ isotopic compositions of lead in these sulphides plot on a secondary isochron yielding an actual age of 130 Ma for sulphide formation on the high angle fractures using a radiogenic Pb source age of 904 Ma (Figure 5b). These ages are similar to the galena ages associated with uranium at Midwest Lake (Cummings *et al.*, 1984) and to the lower intercept U-Pb age of uraninites. Such young ages suggest that the entire Athabasca Basin was affected by late stage fluids which mobilized lead from uranium mineralization into sulphides.

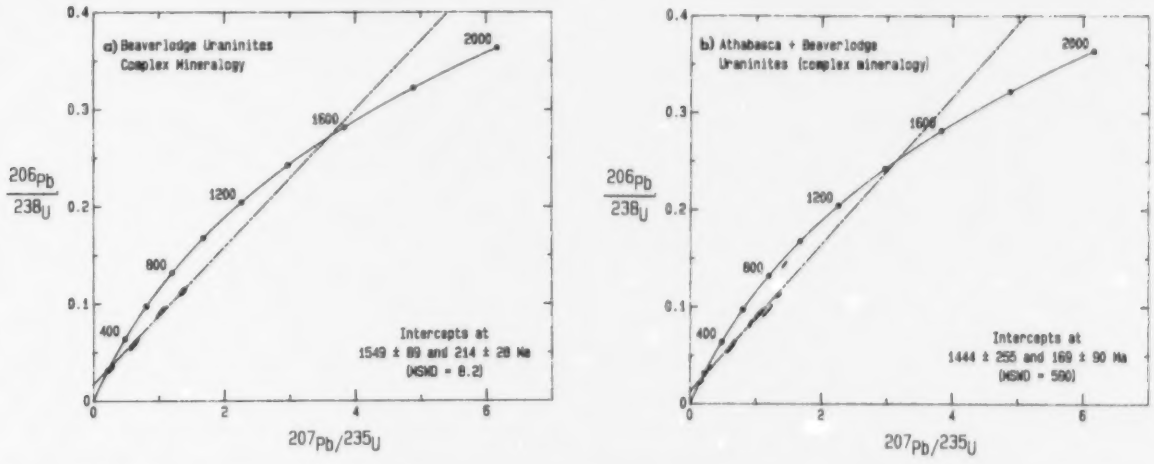

Figure 4 – a) U-Pb concordia plot of uraninite samples from the complex vein-type uranium deposits in the Beaverlodge area. Highly discordant points yield a regression line with intercepts at 1549±89 and 214±28 Ma. b) U-Pb concordia plot of uraninite from both the Beaverlodge vein-type and the Athabasca unconformity-type uranium deposits. Large MSWD indicates that all samples are not from the same fluids.

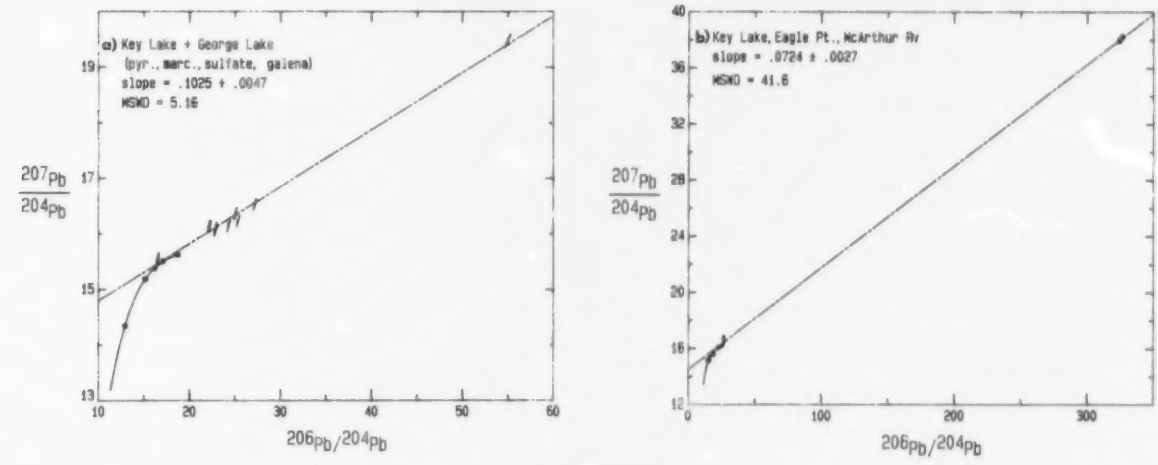

Figure 5 – Pb isotopic compositions of sulphides and sulphates of varying paragenesis in the Athabasca Basin. a) $^{207}Pb/^{204}Pb$ and $^{206}Pb/^{204}Pb$ secondary isochron plot of sulphides and sulphates having a similar paragenesis at the Key Lake deposit and nearby George Lake. b) $^{207}Pb/^{204}Pb$ and $^{204}Pb/^{204}Pb$ secondary isochron plot of late Fe-sulphides from Key Lake, McArthur River, and Eagle Point.

5. Conclusions

1) The $\delta^{18}O$ values and Pb-Pb isotope systematics of the most pristine uraninites (generally those with $\delta^{18}O$ values below -22 per mil) from both the Athabasca unconformity-type and vein-type Beaverlodge uranium deposits are similar and indicate that both areas have been affected by similar fluid events.

2) $^{207}Pb/^{206}Pb$ ages of uraninites from both the complex vein-type deposits in the Beaverlodge area and unconformity-type deposits in the Athabasca Basin are older than the U-Pb ages of the uraninites indicating that various degrees of Pb loss have recently occurred. On the basis of the $^{207}Pb/^{206}Pb$ ages, uranium mineralization in both the Beaverlodge complex vein-type and Athabasca unconformity-type deposits is temporally related.

3) Using the oxygen isotope fractionation factor calculated for the system uraninite-water (Hattori and Halas, 1982), most uraninites have equilibrated with

a fluid having a $\delta^{18}O$ value similar to modern meteoric water. Obvious petrographic alteration of uraninites affected by this fluid event are absent, but the Pb-Pb isotope systematics suggest that uraninite can recrystallize and retain some of the $^{207}Pb/^{206}Pb$ isotope systematics.

4) The general agreement between the lower intercept ages from the U-Pb concordia plots (Figures 4a and b) and the Pb-Pb ages of sulphide formation (Figures 5a and b) indicates that the U-Pb and Pb-Pb systematics in the uranium minerals and sulphides in both the Athabasca Basin and the Beaverlodge areas are coupled systems that reflect large scale fluid processes.

6. References

Cameron-Schimann, M. (1978): Electron microprobe study of uranium minerals and its applications to some Canadian deposits; unpubl. Ph.D. thesis, Univ. Alberta.

Cumming, D.B. and Rimsaite, J. (1979): Isotopic studies of lead-depleted pitchblende in secondary radioactive minerals and sulphides from the Rabbit Lake uranium deposit, Saskatchewan; Can. J. Earth Sci., v16, p1702 - 1715.

Cummings, G., Krstic, D., Worden, J. and Baadsgaard, H. (1984): Isotopic composition of lead in galenas and Ni-arsenides of the Midwest Deposit, northern Saskatchewan; Can. J. Earth Sci., v21, p649-656.

Hattori, K. and Halas, S. (1982): Calculation of oxygen isotope fractionation between uranium dioxide, uranium trioxide and water; Geochim. Cosmochim. Acta, v46, p1863-1868.

Hoeve, J. and Sibbald, T.I.I. (1978): On the genesis of Rabbit Lake and other unconformity-type uranium deposits in northern Saskatchewan, Canada; Econ. Geol., v73, p1450-1473.

Koeppel, V. (1968): Age and History of the Uranium Mineralization of the Beaverlodge Area, Saskatchewan; Geol. Surv. Can., Pap. 67-31, 111p.

Kotzer, T.G. and Kyser, T.K., (1990): The use of stable and radiogenic isotopes in the identification of fluids and processes associated with unconformity-type uranium deposits; *in* Beck, L.S. and Harper, C.T. (eds.), Modern Exploration Techniques, Sask. Geol. Soc., Spec. Publ. 10, p115-131.

Pagel, M., Poty, B. and Sheppard, S.M.F. (1980): Contributions to some Saskatchewan uranium deposits mainly from fluid inclusion and isotopic data; *in* Ferguson, S. and Goleby, A.B. (eds.), Uranium in the Pine Creek Geosyncline; IAEA, Vienna, p639-654.

Peiris, E. and Parslow, G. (1988): Geology and Geochemistry of the Uranium-Gold mineralization in the Nicholson Bay-Fish Hook Bay Area; *in* Summary of Investigations 1988, Sask. Geol. Surv., Misc. Rep. 88-4, p70-77.

Phillipe, S. and Lancelot, J. (1988): U-Pb geochronological investigation of the Cigar Lake uranium deposit, Saskatchewan; Chem. Geol., v70 #1/2, p135.

Quirt, D. and Rees, M. (1987): Current research in mineral deposits at the Saskatchewan Research Council; *in* Summary of Investigations 1987, Sask. Geol. Surv., Misc. Rep. 87-4, p160-166.

Ruhlmann, F. (1985): Mineralogy and metallogeny of uraniferous occurrences in the Carswell Structure; *in* Laine, R., Alonso, D., and Swab, M. (eds.), The Carswell Structure Uranium Deposits, Saskatchewan, Geol. Assoc. Can., Spec. Pap. 29, p105-120.

Sassano, G., Fritz, P. and Morton, R. (1972): Paragenesis and isotopic composition of some gangue minerals from the uranium deposits of Eldorado, Saskatchewan; Can. J. Earth Sci., v9, p141-157.

Sibbald, T.I.I. (1988): Nicholson Bay uranium-gold-platinum group element deposit studies; *in* Summary of Investigations 1988, Sask. Geol. Surv., Misc. Rep. 88-4, p77-81.

Stacey, J. and Kramers, J. (1975): Approximation of terrestrial lead isotopic evolution by a two-stage model; Earth Planet. Sci., v26, p207-221.

Trocki, L., Curtis, D., Gancarz, J. and Banar, J. (1984): Ages of major uranium mineralization and lead loss in the Key Lake uranium deposit, northern Saskatchewan, Canada; Econ. Geol., v79, p1378-1386.

Wallis, R.H., Saracoglu, N., Brummer, J.J. and Golightly, J.R. (1982): Geology of the McClean uranium deposits; Geol. Surv. Can., Pap. 82-11, p71-110.

Wilson, M.R. and Kyser, T.K. (1987): Stable isotope geochemistry of alteration associated with the Key Lake uranium deposit, Canada; Econ. Geol., v82, p1540-1557.

Reconnaissance Geological Study of the Seabee Gold Deposit, Glennie Domain

D.J. Schultz[1]

Schultz, D.J. (1990): Reconnaissance geological study of the Seabee gold deposit, Glennie Domain; *in* Summary of Investigations 1990, Saskatchewan Geological Survey; Saskatchewan Energy and Mines, Miscellaneous Report 90-4.

The Seabee property, 120 km northeast of La Ronge, is located on the north end of Laonil Lake. The property, originally staked in 1949, was the focus of sporadic trenching and diamond drilling by Cominco Ltd. over a 35 year period. Claude Resources, in 1984, purchased the Seabee property and continued exploration by undertaking more diamond drilling, and preparing a preliminary ore reserve estimate. In 1985, Placer-Dome, with an agreement to acquire a 55 percent interest in Seabee, completed additional diamond drilling and surface work. An underground exploration and a bulk sampling program was commenced to confirm estimated reserves. The joint venture was terminated in 1988 and Claude Resources proceeded independently with the underground work, which appeared to verify reserve grade and increased ore potential. An independent feasibility study, conducted by Cominco Engineering Services, reported an ore reserve (all classes) of 1.14 million tons, grading 0.4 oz/ton, which could support a 400 tpd mine for 5 years. This information led Claude Resources to announce a production decision in May of 1990.

1. Regional Geology

The Laonil Lake Intrusive Complex (Delaney, 1936), which is transected by the mylonitic shear zones hosting the Seabee deposit, is situated within the northern part of the Glennie Domain of the early Proterozoic Trans-Hudson Orogen (Hoffman, in press; Lewry and Collerson, in press). Lewry (1981) suggested that the Glennie Domain was a remnant Archean micro-continent that collided with the La Ronge volcanic arc. Subsequent U-Pb dating (Bickford and Van Schmus, 1985; Van Schmus and Bickford, 1984; Van Schmus *et al.*, 1987; Chiarenzelli, 1989) has revealed that the only Archean rocks are found in the Iskwatikan Dome near the western margin of the Glennie Domain. As further detailed structural studies have been completed, the northern part of the domain has been interpreted to be a stack of southeastward directed, refolded allochthonous thrust sheets formed during terminal collision in the Trans-Hudson Orogen (Lewry *et al.*, in press).

The Laonil Lake Intrusive Complex comprises dominantly meta-gabbro and meta-diorite with minor phases being granodiorite, feldspar porphyry, mafic dykes ('green dyke'), and intermediate dykes ('grey dykes'). Remnants or xenoliths of metavolcanic and metasedimentary rocks are also present. A sample of diorite collected by Delaney has been dated at 1889 + 8.7 Ma (Chiarenzelli 1989). The multi-phase complex, which intrudes the supracrustal Pine Lake Metavolcanics to the north-east, is bounded by apparently early granodioritic - dioritic gneiss to the west and by the late Eyahpaise (1859±5 Ma) granodioritic pluton to the south. The Laonil Lake Shear Zone (Delaney, 1986), a zone of intensive deformation represented by mylonites occurs between the Eyahpaise Pluton and the Laonil Lake Intrusive Complex (Figure 1).

2. Objectives

In order to understand the geology, geodynamic setting and controls on gold mineralization at Seabee, a surface mapping and sampling program was initiated during June, 1990. This program included:

1) structural measurements of contacts, foliations, mineral lineations, and kinematic indicators,
2) identification of major rock types, shear zones and associated mineralization,
3) identification of quartz veining, including vein types, mineralogy, and structural relationships, and
4) representative sampling of major rock types.

In addition to this field program the following analytical work will be carried out during the fall and winter of 1990-91:

1) Fluid inclusion studies to discriminate 2-phase, water rich, and immiscible 3-phase, water - liquid CO_2 - vapour CO_2 inclusions; immiscibility is an excellent indicator of conditions appropriate for gold precipitation.
2) Sulphur isotope determinations to monitor CO_2 immiscibility: H_2S becomes immiscible from the initial homogeneous fluid and, the residual aqueous phase undergoes oxidation. Consequently, there is a drastic change in the S isotopic composition of pyrite within the vicinity of gold enrichment, since pyrites and other sulphide minerals are sensitive to the oxidation state of the fluid.
3) Determination of the relationship between S/Se, pyrite and gold mineralization; S/Se systematics vary as a function of redox state and pH.
4) Major and trace element lithogeochemistry: potassic alteration is the dominant characteristic of most mesothermal gold deposits. Distribution patterns of lithophile elements, such as K, Rb, Ba, Li, and U, should identify possible source areas for gold, the origin of the potassium, and therefore of the gold itself.

(1) Department of Geological Science, University of Saskatchewan, Saskatoon, Saskatchwan

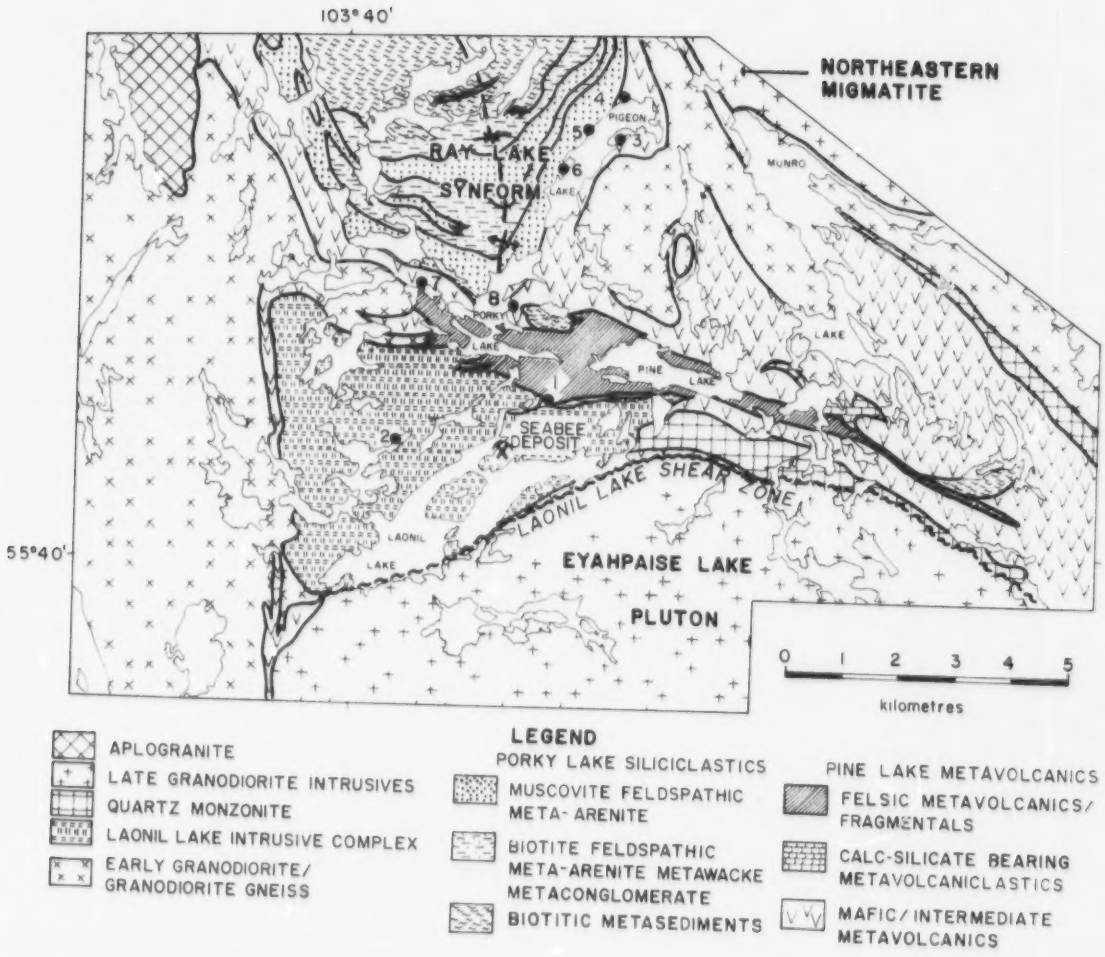

Figure 1 - Geological sketch map of Laonil Lake map area (after Delaney 1986).

3. Field Mapping and Sample Collection

Four separate and distinctive localities, Zones 20, 2, 5 and 14, were the focus of initial investigations in June 1990. A total of 173 foliations and 123 mineral lineations were measured, as well as refining the trench mapping completed by Placer Dome during the 1985 and 1986 field seasons. A summary of information is presented in Figure 2.

In late August of 1990, after careful evaluation of the property, additional sampling was conducted. Sample suites included three diamond drill hole intersections from Zone 2 and one intersection from Zone 5. Among the surface specimens taken were oriented feldspar porphyry samples from Zone 2 and granodiorite from Zone 20. Thin section analyses and hand sample slabbing of these will assist identification of any small scale kinematic indicators, such as C-S fabrics and rotated clasts, which were not macroscopically distinct. It has been suggested that gold precipitation at Seabee may be enhanced in shear zones at localities where both pure and simple shear occurred. Analysis of kinematic indicators will assist in evaluating this hypothesis.

In total 213 samples were collected from the Seabee Property as follows:

Location	Number of samples
Zone 20	60
Zone 2	110
Zone 5	35
Zone 14	5
East boundary	8

Unfortunately, Zone 14 could not be completely sampled due to mine construction.

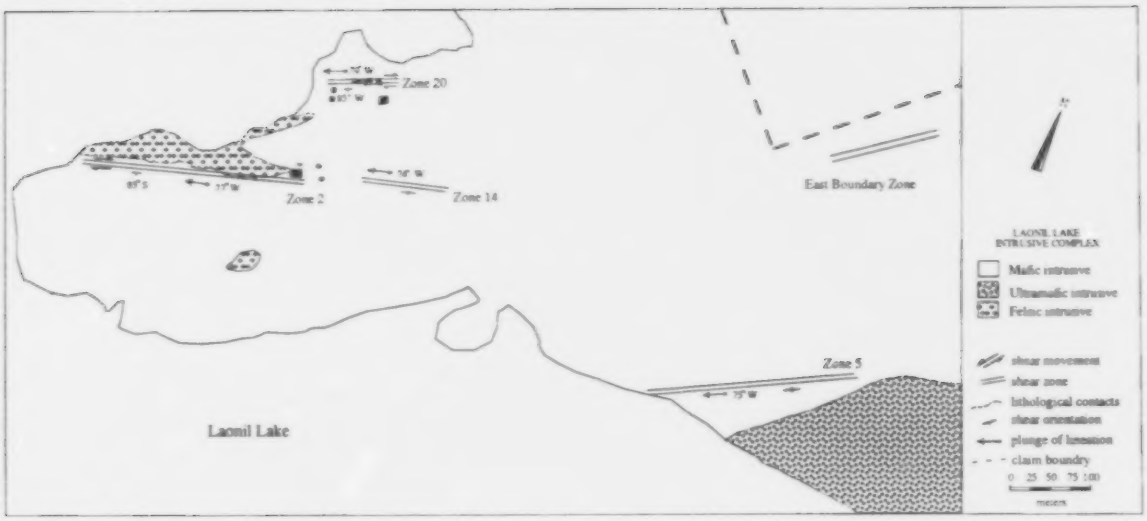

Figure 2 - Simplified geological map of the Seabee property.

4. Geological Relationships

The brittle - ductile shear zones that host the Seabee deposit comprise protomylonitic and mylonitic equivalents of the dominant meta-dioritic and meta-gabbroic wall rocks. Mafic and felsic mineral segregations are common within the shear zones. In addition, zones proximal to felsic intrusives, may show abundant quartz veining, strong biotite alteration and pyrite mineralization.

Zone 2, with a strike length of 300 m, strikes 065° to 075°, dips steeply south, and is located at the contact between feldspar porphyry and meta-gabbro. This zone contains an inter-connecting network of folded, deformed and boudinaged quartz veins.

Zone 5 demonstrates similar structural relationships to Zone 2, although it strikes between 050° and 080° and dips near vertically. Feldspar porphyry, logged in drill core, was not observed in surface outcrops, but quartz - biotite - staurolite - garnet rocks were observed and sampled.

Zone 14 is considered a vein extension of Zone 2. Surface outcrops, which have been silicified and subjected to strong potassic alteration, contain a network of highly brecciated quartz veins.

Zone 20 strikes 062°, dips steeply south, contains multiple felsic intrusives, and is similar in its structural characteristics to Zones 2 and 5. In Zone 20, segregations of felsic and mafic composition characterize the shear zone.

At the East Boundary Zone, recent outcrop stripping, adjacent to the Currie Rose claim boundary, has revealed a strongly foliated biotite - garnet - staurolite lithology and a layered, banded, iron-rich, mafic 'flow'. Further analysis and mapping is needed to determine the geological significance of these rocks.

5. Movement History

At some localities well preserved angular or ruptured gabbro fragments are hosted by diorite to form an intrusion breccia. Adjacent to the shear zone, these gabbroic fragments become elongated and flattened (or oblate) and, within the centre of the shear zone, oriented subparallel to the plane of shearing. Thus, they provide a record of the finite, rotational strain within the shear zone (see Figure 3). The deformed fragments are best seen at Zone 20, although they are also present at Zone 2. At both locations, the sense of shear indicated is right lateral or dextral.

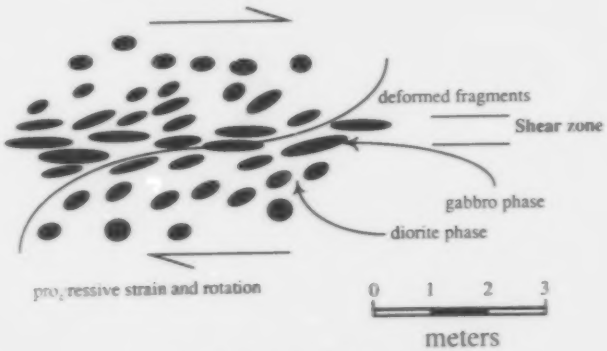

Figure 3 - Ruptured gabbro fragments

6. Quartz Veins

Four distinct sets of quartz veins were observed in surface mapping (Figure 4):

1) parallel to foliation and boudinaged, striking at 060° - 070°,
2) sub-parallel to foliation and folded with axial plane striking 065° - 085°,
3) parallel or sub-parallel to foliation and associated with the feldspar porphyry, and
4) oblique to foliation and proximal to the shear zone, striking at 090° - 120° (late stage veins).

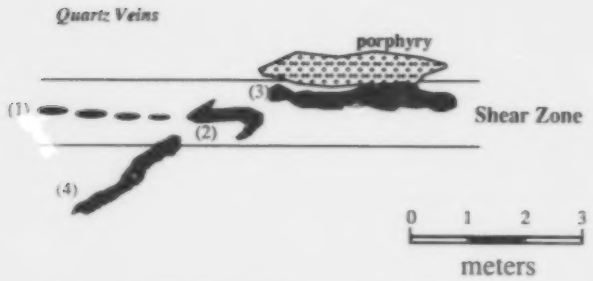

Figure 4 - Varieties of quartz veining observed in surface mapping. See text for explanation.

Tourmaline is ubiquitous to all generations of veins. At surface, pyrite and other sulphide minerals are, at best, present only in trace abundance. Veins and quartz masses associated with the feldspar porphyry, generally are more deformed, mineralized and altered and contain a higher percentage of tourmaline.

7. Future Work

Future work will attempt to:

1) discern and identify controls on mineralization, i.e. the relationship between wall rock chemistry, alteration, structure, geodynamic setting and quartz veining,
2) develop an understanding of the movement history of the shear zones, through hand sample description and thin section analysis,
3) determine if there is a relationship between the feldspar porphyry and gold mineralization,
4) continue with prior analytical objectives, and
5) construct a geodynamic model for the Seabee gold deposit, i.e. the relationship between the gold-quartz vein shears, the Laonil Lake Shear and the regional Tabbernor Fault Zone.

8. Acknowledgments

This project is funded by Saskatchewan Energy and Mines. The author is grateful to Peter Gummer and Gary Billingsley of Claude Resources for general support and appreciated the incisive field supervision by Tom Sibbald and Tracey Hurley.

9. References

Bickford, M.E. and Van Schmus, W.R. (1985): Preliminary U-Pb age data for the Trans-Hudson Orogen in northern Saskatchewan: new and revised results; *in* Summary of Investigations 1985, Sask. Geol. Surv., Misc. Rep. 85-4, p63-66.

Chiarenzelli, J.R. (1989): The Nistowiak and Guncoat Gneisses: implications for the tectonics of the Glennie and La Ronge Domains, northern Saskatchewan, Canada; unpubl. Ph.D. Thesis, Univ. Kansas, 229p.

Delaney, G.D. (1986): Bedrock Geological Mapping, Laonil Lake Area; *in* Summary of Investigations 1986, Sask. Geol. Surv., Misc. Rep. 86-4, p32-41.

Gummer, P.K. (1986): Geology of the Seabee gold deposit, Tabbernor Lake Greenstone Belt, Saskatchewan; *in* Clark, L.A. (ed.), Gold in the Western Shield, CIM Spec. Vol. 38, p272-284.

Hoffmann, P.F. (in press): Subdivision of the Churchill Province and extent of the Trans-Hudson Orogen; *in* Lewry, J.F. and Stauffer, M.R. (eds.), The Early Proterozoic Trans-Hudson Orogen of North America; Geol. Assoc. Can., Spec. Pap. 37.

Lewry, J.F. (1977): The geology of the Glennie Lake area; Sask. Dep. Miner. Resour., Rep. 143, 59p.

_____ (1981): Lower Proterozoic arc - microcontinent collisional tectonics in the western Churchill Province; Nature, v294, no. 5836, p69-72.

Lewry, J.F. and Collerson, K.D. (in press): The Trans-Hudson Orogen: Extent, subdivision, and problems; *in* Lewry, J.F. and Stauffer, M.R., (eds.), The Early Proterozoic Trans-Hudson Orogen of North America; Geol. Assoc. Can., Spec. Pap. 37.

Lewry, J., Thomas, D.J., Macdonald, R. and Chiarenzelli, J. (in press): Structural relations in accreted terranes of the Trans-Hudson Orogen, Saskatchewan: telescoping in a collisional regime; *in* Lewry, J.F. and Stauffer, M.R. (eds.), The Early Proterozoic Trans-Hudson Orogen of North America; Geol. Assoc. Can., Spec. Pap. 37.

Northern Miner (1990): Claude's Seabee may be next Saskatchewan mine; May 21, p1 and 23.

Van Schmus, W.R. and Bickford, M.E.(1984): Preliminary age data for the Trans-Hudson Orogen in Northern Saskatchewan; *in* Summary of Investigations 1984, Sask. Geol. Surv., Misc. Rep. 85-4, p63-66.

Van Schmus, W.R., Bickford, M.E., Lewry, J.F. and Macdonald, R. (1987): U-Pb zircon geochronology in the Trans-Hudson Orogen in northern Saskatchewan, Canada; Can. J. Earth Sci., v24, p407-424.

Bedrock Geological Mapping, Nielsen Lake Area, Tabbernor Fault Zone

K.H. Wilcox

Wilcox, K.H. (1990): Bedrock geological mapping, Nielsen Lake area, Tabbernor Fault Zone; *in* Summary of Investigations 1990, Saskatchewan Geological Survey; Saskatchewan Energy and Mines, Miscellaneous Report 90-4.

The Tabbernor Fault Zone is exposed for over 600 km from the Phanerozoic cover between Hanson and Limestone Lakes through the Wollaston Lake area, to the northern boundary of Saskatchewan and beyond. It is characterized by a braided or branching network of linear depressions, faults and mylonite zones (Byers, 1962). The Tabbernor Fault Zone has been used to separate the Glennie Domain on the west from the Hanson Lake Block and Kisseynew Domain on the east (Lewry and Sibbald, 1977; MacQuarrie, 1979). The fault zone was initially interpreted as a transform fault representing a microplate boundary (Lewry, 1981), however, recent interpretation has downplayed its early tectonic significance (Lewry *et al.*, in press). Nonetheless, the extensive strike length and apparent continuation of the fault zone beneath the Phanerozoic cover (Byers, 1962) suggests that the Tabbernor Fault Zone is an integral part of any dynamic reconstruction of the Trans-Hudson Orogen.

During the summer of 1990, a three person, 1:20 000 scale mapping project was initiated along the trace of the Tabbernor Fault in the region of Nielsen and Prongua Lakes. The objectives of this mapping were to: 1) establish a kinematic framework for the Tabbernor Fault zone by documenting kinematic indicators, 2) determine the regional extent of strain features associated with the Tabbernor Fault zone, 3) attempt to establish the relationship between metamorphism and deformation, 4) determine the context of mineralization and its timing relative to deformation and metamorphism and 5) establish a framework for future investigations.

1. Background and General Geology

Previous geological mapping and other relevant studies in the southern region of the Tabbernor Fault zone include Budding and Kirkland (1956), Kirkland (1957, 1958 and 1976), Byers (1957), Pyke (1966), Padgham (1968), Coleman, Gaskarth and Smith (1970), Macdonald (1975, 1976), Macdonald and Posehn (1976), Sibbald (1978) and Delaney (1987). The study area forms part of a larger area mapped at 1:63 360 scale in 1972 by Sibbald (1978).

Previous kinematic interpretations based primarily on mesoscopic (drag) folds, veins and slickenside lineations have suggested two kinematic components in the Tabbernor Fault Zone: 1) oblique sinistral reverse displacement of the eastern block up and to the north and 2) strike-slip sinistral shear-sense (Budding and Kirkland, 1956; Padgham, 1968).

2. Lithologic Units

Nine main lithologic units were identified during current mapping and are listed below in inferred chronological order from oldest to youngest: 1) mafic to intermediate volcanic rocks and related intrusives, 2) mafic to intermediate volcaniclastic rocks, 3) psammo-pelitic to pelitic sedimentary rocks, 4) felsic rocks and intermediate volcaniclastic rocks, 5) tonalite and diorite, 6) mafic gneiss, 7) grit, 8) leucogranodiorite and 9) pegmatite. The prefix meta should precede all units except for leucogranodiorite and pegmatite but has been omitted for brevity.

a) Mafic to Intermediate Volcanic Rocks and Related Intrusives

A heterolithic package underlying a large percentage of the study area consists of mafic intrusives, mafic volcanic rocks and rare possibly dacitic horizons. Lateral continuity of units within this package is not common and extrusive features rare.

Most of the area north and west of Prongua Lake is underlain by a featureless fine-grained dark green unit interpreted as a mafic volcanic (Figure 1). This area was intruded by a number of mafic phases interpreted as subvolcanic sills and dykes and include: 1) a mafic plagioclase porphyry with 1 to 5 mm euhedral plagioclase phenocrysts in an aphanitic green matrix, containing 1 to 10 mm stubby amphibole porphyroblasts, 2) a distinctive mafic unit, containing orbicular plagioclase nodules in a fine-grained green matrix, intrudes mafic units north and west of Prongua Lake and 3) foliated fine- to medium-grained diorite to gabbro.

Recrystallization due to deformation and metamorphism obliterated many primary features, but the lack of flow features and abundance of phaneritic material suggests a predominantly subvolcanic intrusive origin for most of the mafic suite north and west of Prongua Lake. A number of intermediate units crop out in the mafic volcanic package in this area. For the most part, these compositions result from feldspathic and silicic alteration of mafic material.

Rare pillows are preserved in volcanic rocks at localities east of the north arm of Lariviere Lake, immediately west of Prongua Lake and on Wood Lake, east of Indian Reserve number 184D.

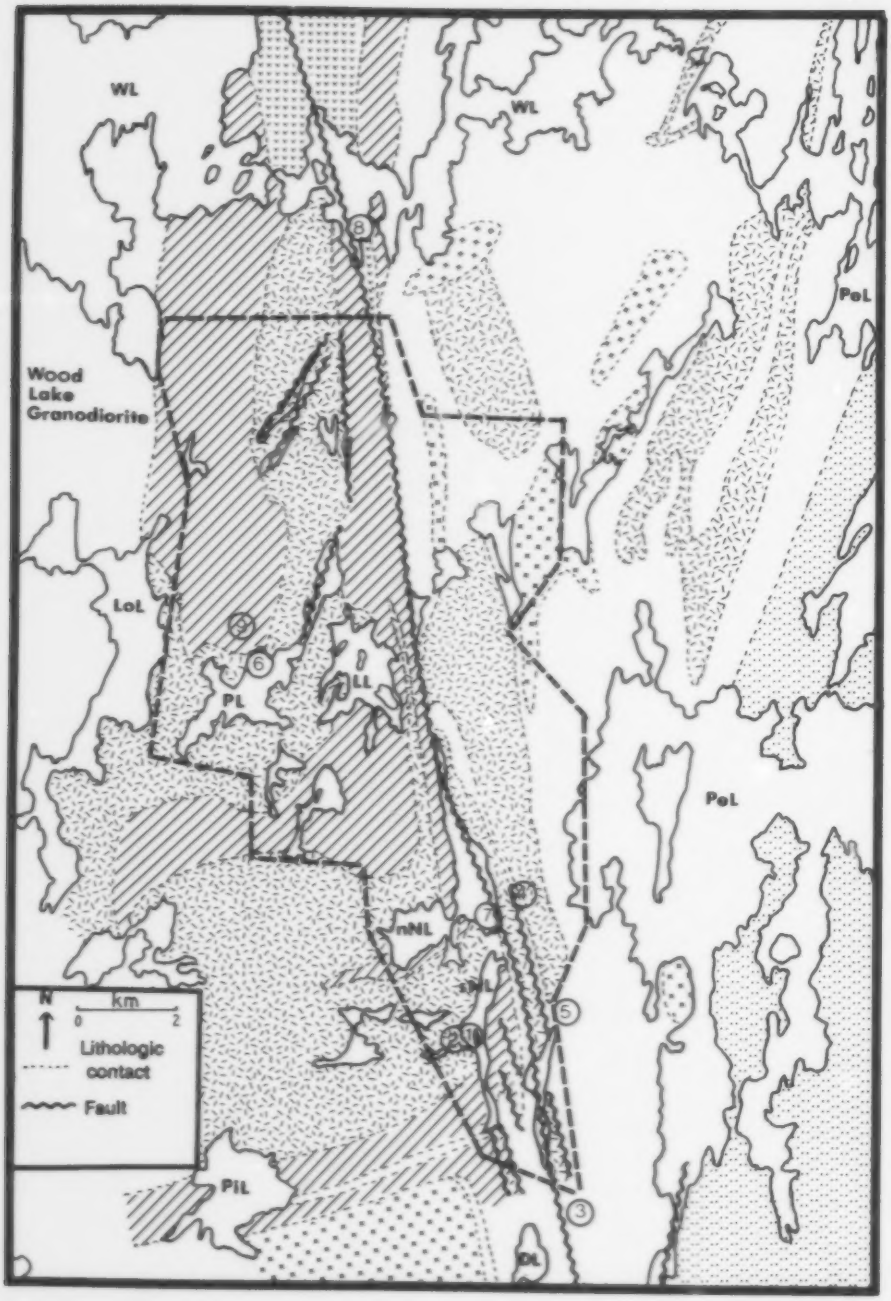

Figure 1 - General geology of the Nielsen - Prongua Lakes area. Numbers refer to localities mentioned in the text. PL - Prongua Lake; WL - Wood Lake; LL - Lariviere Lake; nNL - north Nielsen Lake; sNL - south Nielsen Lake; DL - Deschambault Lake; LoL - Lovell Lake; PeL - Pelican Lake; PiL - Piney Lake. Area mapped in 1990 is indicated by line. Additional geology from Sibbald (1978). Diagonal lines - mafic to intermediate volcanic and volcaniclastic rocks; clear - pelitic to psammopelitic sedimentary rocks; V pattern - felsic volcaniclastic rocks (Sibbald, 1978); dotted pattern - hornblende gneiss series (Sibbald, 1978); random stick pattern - tonalite to diorite; cross pattern - leucogranodiorite and pegmatite.

b) Mafic to Intermediate Volcaniclastic Rocks

Volcaniclastic units underlie most of the area south of Prongua and Lariviere Lakes and occur rarely as thin discontinuous horizons north and west of Prongua Lake.

Coarse heterolithologic fragmental units contain elliptical clasts up to 20 by 60 cm. Tentatively identified clast types include: fine-grained grey feldspar porphyry, epidosite, plagioclase phyric mafics, fine-grained mafics of unknown protolith, amygduloidal mafic volcanic rocks and diorite. Aspect ratios on flat surfaces depend upon clast type, relationship to early structural features and later superimposed strain, and range from 2:1 for epidosite to 20:1 for mafic clasts. The matrix, which is composed of fine-grained granular hornblende and plagioclase with lesser chlorite is homogeneous and unlayered. Metamorphic recrystallization has made it locally difficult to distinguish clasts from matrix.

Lapilli and ash tuff horizons are interlayered with the coarse units. Plagioclase grains were the only clasts identified in the field. The matrix in the lapilli tuff layers is similar to the matrix in coarse horizons as described above. Layering is defined by grain size and composition and occurs on a millimetre, centimetre and metre scale. In ash tuffs, layering is generally planar, but locally displays normal and reverse graded bedding over 5 to 10 cm sequences. Normally graded sequences contain massive basal layers of granule to coarse sand-sized clasts, middle layers of weakly-layered sand-sized clasts and upper very finely-laminated horizons of fine sand-sized clasts.

c) Felsic to Intermediate Volcaniclastic Rocks, Arenite and Felsic Intrusives

A heterolithic package containing felsic to intermediate volcaniclastic rocks, clastics and related intrusions is confined to areas immediately adjacent to the trace of the Tabbernor Fault from Nielsen Lake to Wood Lake. Felsic volcaniclastic rocks are more extensive to the north (Sibbald, 1978) where they are in contact with Ourom meta-arenite (Kirkland, 1976; Delaney, 1987).

The west to east succession of units in the area east of a thin sliver of tonalite to the trace of the Tabbernor Fault at Nielsen Lake is described below. Identification of protoliths in this area is difficult locally due to superimposed strain.

Adjacent to the tonalite is a discontinuous fine-grained mafic unit about 5 m wide. Hornblende-rich tonalite and mafic inclusions in the tonalite suggest an intrusive contact. The mafic unit appears to grade into a finely-layered assemblage interpreted as intermediate volcaniclastic rocks, which are characterized by centimetre-scale interlayering of barrel-boudinaged amphibolitic layers, feldspathic layers and rare greywacke bands containing metamorphic chlorite and muscovite in addition to detrital quartz and feldspar. Magnetite porphyroblasts up to 1.5 mm in diameter are common and impart a high magnetic signature to the intermediate volcaniclastic unit (see Aeromagnetic Series, Map 4584 G, Sandy Narrows, 63M3).

The number and width of clastic layers increases concomitantly with quartz content until the unit can be classified an arenite. Sand-sized quartz and feldspar grains are enveloped by muscovite and chlorite. Aphanitic dark laminae in the arenite possibly represent heavy mineral concentrates. Magnetite is rare or absent in contrast to the interlayered intermediate volcaniclastic rocks. Local pebble horizons contain clasts of granitoid, jasper, epidosite, quartz and aphanitic grey-black material. Sibbald (1978) interpreted similar rocks in the Wood Lake area as felsic volcaniclastic rocks.

Tonalite sills and feldspar porphyry dykes and concordant sheets occur in intermediate volcaniclastic rocks and arenite in the Nielsen Lake area. Contact relationships between arenites and intrusives are uncertain.

The apparent continuity of rock types from mafic to intermediate volcaniclastic to arenite may indicate that sedimentation was concomitant with volcanism, as described elsewhere in the Glennie Domain (Delaney, 1988; Thomas, 1988; Slimmon, 1988).

d) Pelites to Psammopelites

Pelitic to psammopelitic sedimentary rocks crop out in a northerly expanding prism east of the trace of the Tabbernor Fault and in linear belts in the southern map region. At Wood Lake, there appears to be a continuous succession over 40 m wide from mafic volcanic to mafic volcaniclastic to pelitic sedimentary rocks.

In the sedimentary rocks, the occurrence and distribution of chlorite, biotite, andalusite, fibrolite, muscovite and rare garnet and staurolite porphyroblasts depend on the metamorphic grade. Accessory metamorphic minerals include apatite, tourmaline and rarely graphite. Quartz-tourmaline sweats occur locally where fibrolite is the stable aluminosilicate polymorph. Asymmetrically boudinaged and folded quartz veins up to 5 cm wide are common throughout the sedimentary units.

e) Tonalite to Diorite

Tonalite

Medium-grained tonalite underlies large areas on both sides of the Tabbernor Fault and intrudes the mafic volcanic and pelitic sedimentary suite. It is unconformably overlain by a clastic sediment on south Nielsen Lake. The tonalite contains all of the strain features associated with the Tabbernor Fault Zone.

In the Prongua Lake area in regions of low strain, the tonalite has pinkish weathering, 1 to 5 mm quartz and plagioclase, rare alkali feldspar and locally, weakly-lineated amphibole crystals. The lineation may represent an emplacement fabric. Mafic inclusions, xenolithic layers and residual rafts are abundant and commonly sites of strain and sulphide mineralization. Where a fabric is penetrative, amphibole is replaced by biotite and chlorite . The foliation west of the Tabbernor Fault is heterogeneously developed but becomes penetrative east of the Tabbernor Fault. Magnetite content is highly

variable west of the Tabbernor Fault but is virtually absent east of the Tabbernor Fault.

Diorite

A medium-grained diorite to hornblende quartz diorite, considered to have been intruded as a phase of the tonalite crops out at a lake immediately north of Prongua Lake and just east of Lariviere Lake. Hornblende-bearing quartz diorites appear to have been produced by contamination of the tonalite by mafic volcanic units and commonly grade into the tonalite.

A multiphase and highly xenolithic diorite plug intrudes mafic volcanic rocks in the Prongua Lake area and contains a copper showing (Sibbald, 1978). A strong moderately westerly plunging mineral lineation exists locally. The plug is composed of at least eight intrusive phases having variable hornblende, plagioclase and quartz content. Angular fine-grained mafic, gabbroic and dioritic xenoliths up to 30 cm long are abundant.

A large multiphase quartz diorite to diorite pluton crops out northwest of Long Lake, and extends farther south than previously mapped (Sibbald, 1978). It is tentatively correlated with the xenolithic diorite described above. The pluton has a fine-grained border and consists of 0.5 mm equant interlocking quartz and plagioclase, and rare stubby 3 mm amphibole phenocrysts which appear to be partially replaced by chlorite. The grain size increases away from the margin to an average of 1 mm concomitantly with a decrease in quartz content and a slight increase in the abundance of amphibole phenocrysts. Additional phases in this body include a salt and pepper textured dioritic to gabbroic rock and a mafic unit with a matrix of green amphiboles separating isolated plagioclase laths 0.2 to 10 mm in size. Contacts between these phases were not observed. The pluton is foliated in narrow recessively weathering northerly-striking zones which correspond to biotite- and locally chlorite-rich alteration and possible high strain zones. Foliated sedimentary rocks which envelope the body and rarely observed crosscutting pegmatite dykes suggest that the diorite is similar in age to the tonalite.

f) Mafic Gneiss

Mafic gneiss defined by centimetre-scale variably hornblende- and plagioclase-rich layers occurs on the western bay of north Nielsen Lake and along south Nielsen Lake. The gneissosity is highlighted by 1 cm to 50 m wide tonalite sills. Chlorite is a minor constituent compared to mafic volcanic rocks in the Prongua Lake area.

g) Grit

A small outlier of quartz pebble conglomerate to grit lies in apparent unconformity on tonalite at locality 1 (Figure 1). Rounded to elliptical and weakly lineated quartz clasts are wrapped by muscovite. Garnet is rare. The isolated position of this unit makes direct correlation with other units difficult, however, the pebbly nature, quartzofeldspathic composition, presence of a fabric and being located near the trace of the Tabbernor Fault suggest that these rocks may correlate with sedimentary rocks on north Nielsen Lake. Alternatively, the clastic assemblage on north Nielsen Lake appears to be part of an uninterrupted succession from mafic volcanic to sedimentary rocks. Since the grit rests unconformably on tonalite and tonalite intruded mafic volcanic units, a post-volcanic deposition is suggested.

h) Leucogranodiorite

White to light orange leucogranodiorite forms pods and dykes exclusively on the east side of the Tabbernor Fault where it is generally associated with elevated regional metamorphic grade. Leucogranodiorite intrudes all rock types. It contains quartz and feldspar averaging 1.5 mm in length, minor amounts of muscovite and garnet, and trace biotite. A weak foliation is defined by slightly elliptical quartz grains and locally planar-parallel micas.

i) Pegmatite

Pink pegmatite sheets, dykes and pods intrude all units east of the trace of the Tabbernor Fault but are most abundant in leucogranodiorite and sedimentary rocks. The dykes are composed of: perthitic alkali feldspar up to 18 cm long with graphic intergrowths of quartz, grey plagioclase, isolated flakes and books of biotite and muscovite, minor euhedral tourmaline up to 4 cm long and rare buff coloured beryl. Garnet is a common accessory. Pegmatite dykes vary from unfoliated to weakly foliated and are locally boudinaged and folded. Foliations in the supracrustal units envelope pegmatite boudins. Variably-strained pegmatite dykes possibly indicate a syntectonic injection.

White plagioclase-rich pegmatites in the sedimentary rocks are thought to represent metamorphically derived melts. They exhibit similar features to the pink pegmatites but have lower alkali feldspar content.

3. Structure

Sibbald (1978) outlined structural elements believed to have been created during three fold forming movements. Only two deformational events (P_1 and P_2) were recognized in the vicinity of the Tabbernor Fault during current mapping. The first created a foliation and associated minor high strain zones and the second deflected P_1 fabrics and formed new features. Early fabrics are preserved west of the Tabbernor Fault where foliations have a regional westerly strike and variable northerly dip. The early fabric is deflected to a northerly strike as the Tabbernor Fault is approached. Foliations east of the Tabbernor Fault have a regional northerly strike.

The Tabbernor Strain Zone refers to the area adjacent to the Tabbernor Fault where early fabrics are deformed and overprinted and newly formed features are confined.

Kinematic features in the Tabbernor Strain Zone suggest that high angle reverse N-S striking strain zones were formed initially and then evolved into oblique

sinistral reverse zones with upthrow on the eastern block to the north and finally into strike-slip sinistral faults and strain zones.

a) Phase One Strain Features

Phase one features are heterogeneously developed west of the Tabbernor Fault and are defined by synkinematic cleavage, locally flattened clasts, variably developed gneissosity and local mineral lineations.

The foliation, depending upon rock type, is defined by the planar parallel alignment of chlorite, biotite, muscovite, amphibole and quartz. It is commonly parallel to bedding where bedding was recognized. Tonalite may have been intruded synkinematic with this deformation as it varies from unfoliated and intrusive into foliated supracrustals to locally foliated parallel to the surrounding supracrustals.

A heterogeneously developed mineral lineation defined by amphibole and quartz occurs in a inclusion-riddled tonalite west of south Nielsen Lake. Its variable orientation is due to subsequent crenulation but commonly it plunges to the north.

Isolated higher strain zones west of the Tabbernor Fault range from less than 50 cm to 15 m wide and are concordant with the foliation. In the tonalite, they are defined by well-foliated horizons containing highly-flattened to ribbony quartz. Protoliths are always recognizable in these higher strain zones. S-C fabric (Berthé *et al.*, 1979) and asymmetric extension cleavage (shear bands) together with a northerly plunging mineral lineation at locality 2 (Figure 1) possibly indicate a southerly vergent thrust zone. Strain zones are commonly crenulated about a northerly striking hinge surface in the Tabbernor Strain Zone.

The regional extent and kinematic interpretation of P_1 strain zones have important implications for tectonic reconstructions in the Glennie Domain. Lewry *et al.* (in press) have postulated south-southeasterly directed nappe emplacement with concomitant foliation and concordant high strain zone formation. They also suggested that mylonites in the southern section of the Tabbernor Fault Zone may represent an early refolded high strain zone. Therefore, recognition of early strain zones and kinematic interpretations are fundamental to an understanding of the tectonic history of the region. Preliminary indications from the study area are consistent with both ideas presented by Lewry *et al.* (in press) however, more detailed work is required.

b) Strain Features in Tonalite, East of the Tabbernor Fault

East of Nielsen Lake

A 200 to 750 m wide strip of variably deformed tonalite parallels the east side of the Tabbernor Fault extending from north Nielsen Lake to the southern limit of the map area. S-C fabric, asymmetric extension cleavage, rare quartz veins and asymmetric folds were used in conjunction with mineral lineations to define the sense of shear in this area. In general, three divisions of texture can be made representing low, intermediate and high strain.

In regions of low strain, tonalite is medium-grained and contains equant interlocking quartz, feldspar, hornblende and biotite. A weak fabric defined by the planar parallel alignment of biotite is developed locally.

In regions of moderate strain, tonalite has a 'flaggy' protomylonitic texture as a result of spaced asymmetric extension cleavage deflecting flattened quartz grains, recrystallized plagioclase aggregates and biotite. Quartz varies from flattened to rodded, commonly with 5:1 to 10:1 X:Y (X - longest, Z - shortest) aspect ratios. A lineation defined by either quartz rods, feldspar ridges or biotite streaks and alignment was observed in many places.

In regions of high strain the tonalite is a fine-grained straight gneiss and considered mylonitic. Quartz is progressively more ribboned and feldspar aggregates flattened and dismembered. Mylonitic bands are grey on the weathered surface and locally resemble finely-laminated sedimentary rocks. Felsic laminations to lenses can be correlated to progressively flattened individual feldspars. Aphanitic ultramylonitic bands occur but do not exhibit mesoscopic kinematic indicators.

Gradual to abrupt strain gradients on the centimetre, metre and ten metre scale are unique to the area and represented by losanges and layers containing the three textures described above (Plate 1).

Southern Mylonite

A 50 to 75 m wide mylonite zone occurs in tonalite at the southern end of the map area (locality 3, Figure 1). Grain size grades from an average of 3 mm in foliated regions outside the zone to locally aphanitic in the zone. Two sets of mutually exclusive high strain layers exhibiting separate sense of shear occur in this zone. Layers ranging from 10 to 100 cm wide document either westwardly vergent reverse displacement or sinistral strike-slip displacement.

A possible explanation for the relative timing of reverse and strike-slip displacement was observed in tonalite at locality 4 (Figure 1). A mineral lineation changing from subvertical to shallow southeasterly plunging can be seen along successively exposed subvertical foliation planes. Steeply plunging lineations occur in a 'flaggy' protomylonite exhibiting westwardly vergent thrust shear-sense. The shallowly plunging lineations occur in a mylonitic layer exhibiting oblique sinistral shear-sense where the eastern block has moved up and to the north. The change in shear sense and lineation plunge is consistent with dip slip followed by strike-slip displacement. Individual strain layers commonly contain one consistent mineral lineation although regionally they exhibit a dispersal (Figure 2) similar to locality 4. A moderately southerly plunging maximum (Figure 2) reflects the predominance of oblique displacement in this zone.

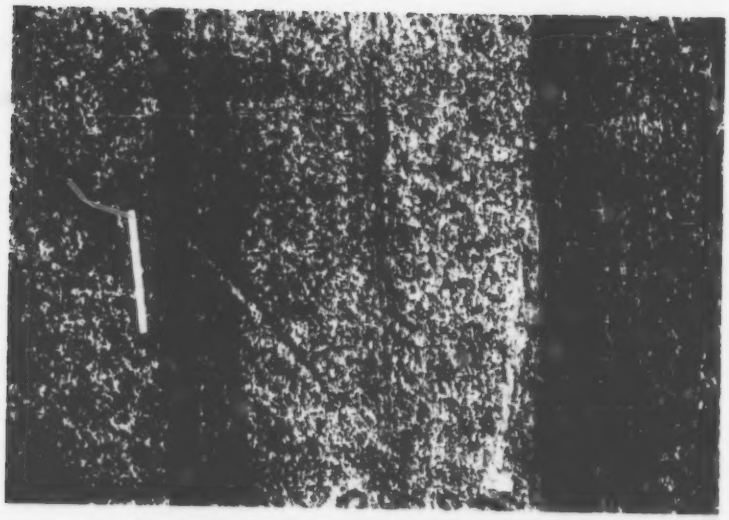

Plate 1- Light coloured 'flaggy' protomylonitic tonalite in central section flanked by dark coloured straight gneiss mylonitic tonalite layers. Pen is 15 cm long, points 350°, and is colinear to sub-horizontal lineation in the outcrop.

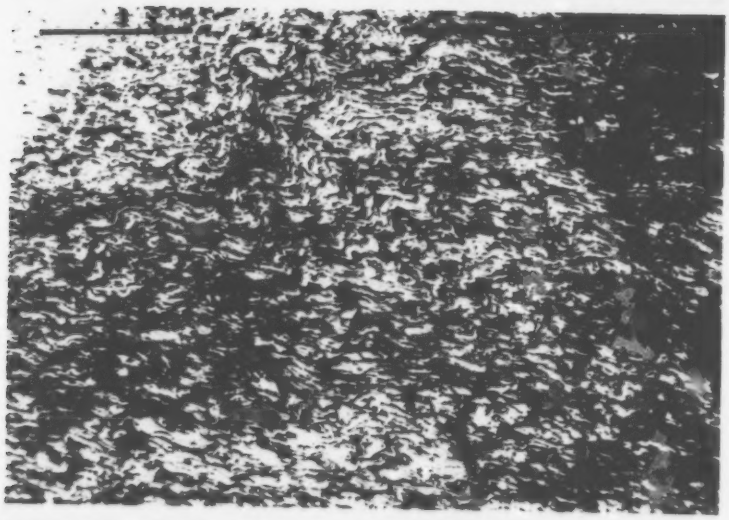

Plate 2 - Asymmetric S crenulations in protomylonitic tonalite. Black bar in upper left corner is 2.5 cm long and strikes 350°. Crenulation hinges are sub-vertical.

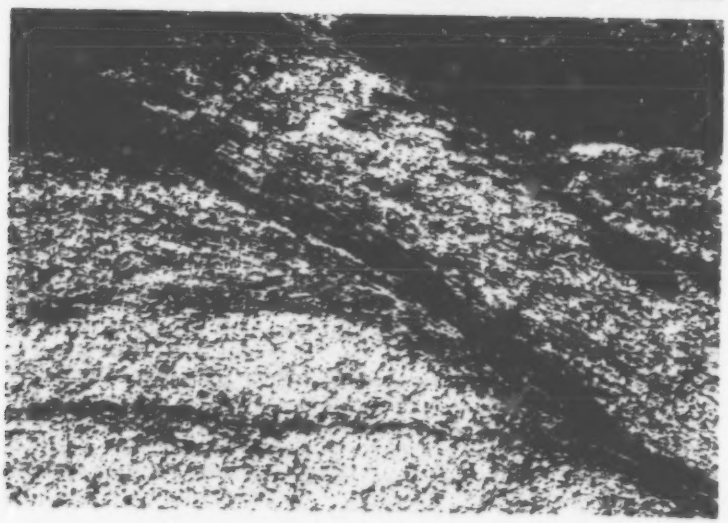

Plate 3 - Mesoscopic dextral strain layer in tonalite, northwest of Prongua Lake. Pen cap is 6.5 cm long and trends 037°.

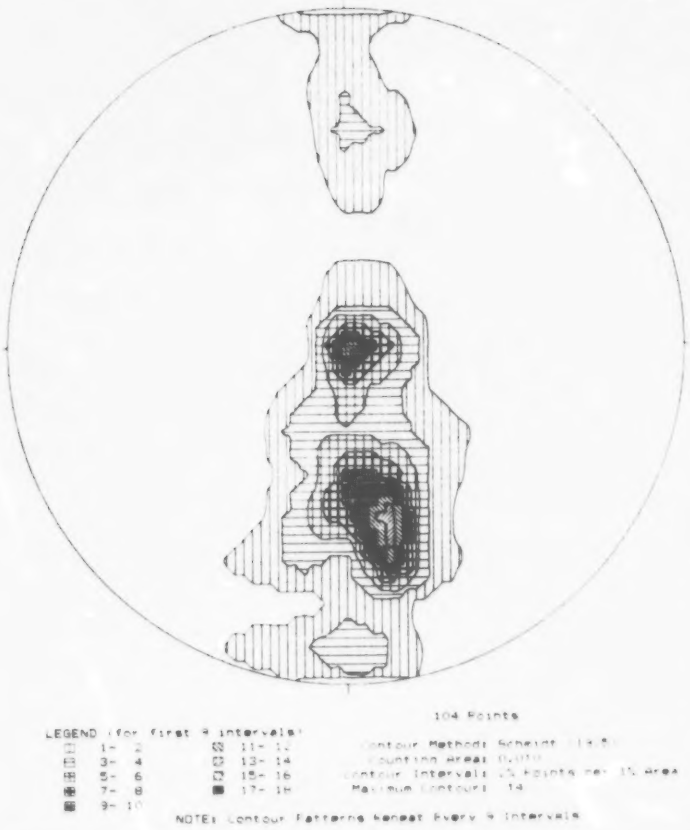

Figure 2. Contoured stereonet plot of mineral lineations in tonalite east of Nielsen Lake. Point maximum occurs at 45° →165° outlining the predominace of oblique displacement.

Pegmatite Thrust

An approximately 15 m wide oblique reverse high strain zone informally termed the Pegmatite Thrust is defined by a straight gneiss in tonalite east of the trace of the Tabbernor Fault (locality 5, Figure 1). A thrust fault has been placed between tonalite on the west side and a thin layer of sedimentary rocks on the east side. The western footwall has a strain gradient from heterogeneously strained tonalite containing centimetre-wide high strain zones to penetratively mylonitic tonalite where mesoscopic strain zones have merged. Pegmatite dykes are absent in the footwall. The eastern hanging wall is marked by a thin layer of sedimentary rocks which is intruded on the east side by tonalite. Both rock types in the hanging wall contain well-foliated pegmatite dykes and sills which locally contain feldspar porphyroclasts and ribbony quartz. The sedimentary rocks do not appear highly strained in contrast to the pegmatite. Elsewhere, pegmatites are generally less strained.

Thrusting occurred after pegmatite emplacement as evidenced by strained pegmatites and restriction of pegmatite-bearing rocks to the east side of the zone. Pegmatite occurrence also suggests that lower structural levels have been brought up on the east side and emplaced adjacent to colder higher level material. Similar strain features were not recognized east of this zone. However, metamorphic grade increases easterly towards the Sahli Granite (Sibbald, 1978) which may suggest undetected thrust faults in that area.

Tabbernor Strain Zone

A 200 to 1500 m wide strain zone occurring on either side of the Tabbernor Fault comprises the Tabbernor Strain Zone. Strain features are heterogeneously developed and depend upon the host rock. In general, features exhibiting the evolution from a plastic thrust zone to a brittle sinistral strike-slip zone are best observed in tonalite, whereas supracrustal rocks commonly record strike-slip displacement. Regional deflection of lithologic units on the west side into the Tabbernor Fault (Sibbald, 1978) indicate an apparent horizontal component of sinistral shear sense.

Adjacent to the Tabbernor Fault

A late shallowly plunging slickenside lineation is common adjacent to the trace of the Tabbernor Fault (<300 m). It is generally confined to foliation planes and small scale faults on the west side of the Tabbernor Fault and in many cases overprints a mineral lineation. Plunge is variable but is always less than 45° to the north or south.

Crenulated zones confined to mylonitic tonalite and micaceous sedimentary rocks occur immediately adjacent to the Tabbernor Fault. Crenulation hinge surfaces are generally subvertical, although chaotically oriented in the sedimentary rocks. In tonalite, crenulations commonly exhibit mesoscopic S asymmetry with upright northeasterly striking hinge surfaces and subvertical plunge (Plate 2).

Asymmetrically boudinaged and folded quartz veins appear similar to type 2B asymmetric pull aparts (Hanmer, 1986) and are ubiquitous in the pelitic sedimentary rocks adjacent to the Tabbernor Fault. Long axes of quartz boudins are oriented approximately 15° northeasterly divergent from the foliation which suggests sinistral strike-slip sense of shear.

A number of other features proximal to the Tabbernor Fault that indicate strike-slip displacement and sinistral shear-sense include:

1) sinistral asymmetric extension cleavage striking 330° occurs in arenite along Nielsen Lake,

2) a set of 305°/90° dextral kink bands and a set of 230°/90° sinistral kink bands with subvertical hinges, and

3) a set of 340°/steep sinistral fault zones and faults with centimetre to metre displacement possibly correlate to Riedel R shears.

The trace of the Tabbernor Fault at the south end of north Nielsen Lake is defined by a silicified breccia locally containing pyrite mineralization. Penetrative mesoscopic faults cutting mylonitic foliation are associated with late quartz flooding defined by stockwork quartz veins and breccias containing mylonitic fragments.

Features West of the Tabbernor Fault

Lineaments

Several prominent as well as numerous subsidiary arcuate valleys occur north of Nielsen Lake. Valleys change strike from southeasterly to northerly as the Tabbernor Strain Zone is approached. Some of the valleys correspond to recessively weathered high strain zones and faults locally containing chlorite schist, chlorite veinlets, calcite and more rarely pyrite and epidote. Subhorizontal dextral as well as oblique dextral deflection (the northwestern side has been displaced up and to the northeast) of the schistosity was observed immediately adjacent to the northeasterly-striking faults in some locations. Subhorizontal sinistral displacement on the northerly-striking continuation of these lineaments is indicated locally by foliation deflection, S-C fabric, asymmetric extension cleavage and a slickenside lineation. The change in shear sense and orientation is possibly due to progressive rotation by a dominant sinistral strike-slip system. Early features were reactivated when in a favourable orientation to facilitate sinistral slip. Northeasterly-striking valleys are confined to the outer margins of the Tabbernor Strain Zone.

Mesoscopic Strain Zones

Discrete centimetre-scale mylonite bands occur in weakly foliated tonalite north of Prongua Lake (see Plate 3). Kinematic indicators observed in the mesoscopic zones include foliation deflection, S-C fabric and asymmetric extension cleavage in conjunction with a mineral or slickenside lineation. Locally, lineaments (see above) are marked by a gradual increase in the number of mesoscopic plastic strain zones and the appearance of a penetrative foliation.

Approximately 1 km from the Tabbernor Fault mesoscopic strain zones can be classified into three contemporaneous sets:

1) 085°/steeply dipping dextral or southerly vergent reverse,

2) 035°/steeply dipping dextral strike-slip, and

3) 350°/steeply dipping sinistral strike-slip.

The first set was only observed at distances greater than 750 m from the Tabbernor Fault. The second set becomes less abundant as the trace of the Tabbernor Fault is approached. The third set is most abundant in the map area.

Pseudotachylite

Apparent pseudotachylite was observed in three localities (6,7,8 on Figure 1); the largest is on Prongua Lake, where apparent offset along a fault associated with pseudotachylite generation is on the order of metres. The pseudotachylite is a grey black aphanitic mass in 1 mm to 10 cm wide veins with N-S strike and orthogonal offshoots. Veins commonly have internal zoning exhibited by colour banding and individual feldspar xenoliths are common.

c) Conclusion

Deformation features associated with the Tabbernor Strain Zone indicate a high angle thrust system which evolved to an oblique reverse, through a sinistral wrench system and finally to a brittle sinistral fault. Deformation occurred during and after pegmatite emplacement.

4. Metamorphism

West of the Tabbernor fault metamorphic grade is relatively uniform in volcanic rocks. At the southern edge of the map area west of the Tabbernor Fault, isograds appear to strike easterly in sedimentary rocks (Sibbald, 1978). From Nielsen Lake northward, isograds in the sedimentary rocks strike northerly and indicate a steep metamorphic gradient east of the Tabbernor Fault.

a) West of the Tabbernor Fault

Amphibole and chlorite are common matrix constituents in volcanic rocks and impart a green colour to the rocks. Regional hornblende blastesis occurred syn- to post-P_1 as evidenced by fabric overgrowths and deflections. Amphibole porphyroblasts are progressively deformed and replaced by chlorite as the Tabbernor Fault is approached and chlorite commonly lines minor fault planes throughout the area. Schistose and finely cleaved mafic rocks are common immediately west of the Tabbernor Fault. Greenschist to lower amphibolite facies conditions prevailed for both deformation events with greenschist facies conditions accompanying late brittle deformation.

Quartzofeldspathic sedimentary rocks west of the Tabbernor Fault contain muscovite, chlorite and locally incipient biotite. Idioblastic garnet occurs in a quartz-pebble conglomerate on south Nielsen Lake.

Late hornblende blastesis and recrystallization is common around minor faults in mafic volcaniclastic units west of the Tabbernor Fault. Rare garnet occurs in association with feldspathic, calc-silicate and sulphide alteration in this area.

b) East of the Tabbernor Fault

East of the Tabbernor Fault three isograds delineating the appearance of andalusite, fibrolite and andalusite pseudomorphs occur over approximately 350 m in sedimentary rocks.

Outcrops immediately adjacent to the Fault are highly crenulated chlorite-muscovite ± biotite schists. The first occurrence of andalusite is in 0.5 to 3 cm subidioblastic porphyroblasts containing inclusions and inclusion trails of quartz and rare biotite. Andalusite grains are wrapped by the foliation and chiastolite crosses are rare. Fibrolite first occurs as foliation-parallel intergrowths with biotite and plagioclase apparently concomitant with the breakdown of andalusite to fine-grained muscovite. In some localities, andalusite and fibrolite occur together at the first appearance of an aluminosilicate polymorph. Fibrolite is locally lineated colinear to minor folds. Complete pseudomorphing of andalusite by coarse unfoliated intergrowths of muscovite, quartz, plagioclase, and less commonly biotite define the third isograd. Fibrolite is always observed in these rocks.

Garnet is rare in the sedimentary rocks and most commonly occurs adjacent to garnetiferous pegmatite and leucogranodiorite dykes.

Andalusite and sillimanite assemblages together with a lack of garnet suggest low pressure metamorphism in this area.

c) Southern Map Area

Sibbald (1978) mapped a continuous zone of E-W striking sedimentary rocks from Piney Lake to the study area but did not recognize garnet - staurolite occurrences at the southern tip of south Nielsen Lake. Current mapping has also defined a fault truncation of this unit. Metastable staurolite is indicated by xenomorphic to subidioblastic grains with felsic haloes. Wine-coloured garnet is subidioblastic and part of a prograde assemblage differing from the sporadic occurrences north of Nielsen Lake.

Andalusite occurs in a layer of sedimentary rocks on the west side of the Tabbernor Fault but was not observed in the northern continuation of this unit at north Nielsen Lake.

The newly recognized occurrences will modify the isograd distribution outlined by Sibbald (1978).

5. Mineralization

Gold mineralization is the prime exploration target in the area. Several vein-associated copper occurrences described by Sibbald (1978) were re-examined to determine their regional context. One occurrence west of Prongua Lake (locality 9, Figure 1) is summarized below.

a) Prongua Lake Occurrence (SMDI #0335)

Sibbald (1978) assayed three grab samples containing irregular thin stringers of pyrite and chalcopyrite with secondary malachite staining. The veins are hosted by volcanic relicts in a diorite plug. The samples contained up to 1.62% Cu and 0.010 oz/ton Au (Sibbald, 1978).

In addition to chalcopyrite and pyrite, pyrrhotite, bornite, magnetite and an unknown copper-coloured metallic mineral occur. Mineralization occurs within or adjacent to quartz veins in 1 to 10 mm wide vein-parallel discontinuous stringers or nodular masses. The sulphides are accompanied by calcite and locally epidote. The dominant veins are generally less than 10 cm wide and are composed of grey to white sugary masses of quartz. A rusty stain is common on the weathered surface. Veins have a slight left stepping *en echelon* arrangement in an overall northerly strike. Chlorite haloes with a subhorizontal ridging lineation locally surround the quartz veins. The host diorite is generally unfoliated but locally contains a well developed westerly plunging hornblende lineation. Small-scale strain zones exhibiting strike-slip sinistral shear also occur in the diorite in this area. Mineralization probably occurred during the waning stages of deformation as suggested by weakly boudinaged quartz veins, lineated chlorite linings around quartz veins and associated small-scale strain zones.

b) Regional Generalizations

There are numerous sulphide occurrences throughout the area and a number of generalizations can be made at this time: 1) many of the mineralized zones are related to fluid infiltration during deformation associated with the Tabbernor Strain Zone, 2) pyrite is the most common sulphide, 3) tourmaline is a common accessory forming up to 75 percent of some veins and 4) mineralization is generally confined to rock types west of the Tabbernor Fault.

6. Summary

Possibly syntectonic tonalite intrusion occurred after deposition of the volcano-sedimentary package; tonalitic bodies were subsequently unroofed and unconformably overlain by a clastic sediment. Pegmatite and leucogranodiorite intrusion occurred syn-metamorphically in regions of elevated metamorphic grade. All features were subsequently deformed in the Tabbernor Fault Zone.

7. Acknowledgements

Myles Loydl and Joey Wright provided able field assistance. Special thanks are extended to Gary Wong and Placer Dome for their hospitality and discussions. I would also like to express thanks to Wayne Fisher for fireside discussions.

8. References

Berthé, D., Choukroune, P. and Jegouzo, P. (1979): Orthogneiss, mylonite and non-coaxial deformation of granites, the example of the South Armorican shear zone; J. Struct. Geol., v1, p31-42.

Budding, A.J. and Kirkland, S.J.T. (1956): The geology of the Reindeer River area; Sask. Dep. Miner. Resour., Rep. 22, 42p.

Byers, A.R. (1957): The geology and mineral deposits of the Hanson Lake area; Sask. Dep. Miner. Resour., Rep. 30, 47p.

_____ (1962): Major faults in the western part of the Canadian Shield with special reference to Saskatchewan; *in* Stevenson, J.S. (ed.), The Tectonics of the Canadian Shield, Roy. Soc. Can., Spec. Publ. No. 4, p40-59.

Coleman, L.C., Gaskarth, J.W. and Smith, J.R. (1970); Geology and geochemistry of the Hanson Lake area; Sask. Res. Counc., Geol. Div., Rep. 10, 156p.

Delaney, G.D. (1987): Bedrock geological mapping, Carruthers - Uskik Lakes area; *in* Summary of Investigation 1987, Sask. Geol. Surv., Misc. Rep. 87-4, p8-17.

_____ (1988): Bedrock geological mapping, Brownell Lake area; *in* Summary of Investigation 1988, Sask. Geol. Surv., Misc. Rep. 88-4, p8-19.

Hanmer, S.K. (1986): Asymmetrical pull aparts and foliation fish as kinematic indicators; J. Struct. Geol., v8, p111-122.

Kirkland, S.J.T. (1957): The geology of the Manawan Lake area (north half), Saskatchewan; Sask. Dep. Miner. Resour., Rep. 27, 22p.

_____ (1958): The geology of the Deschambault Lake area (east half), Saskatchewan; Sask. Dep. Miner. Resour., Rep. 31, 16p.

_____ (1976): The geology of the Manawan Lake area (south half), Saskatchewan; Sask. Dep. Miner. Resour., Rep. 175, 24p.

Lewry, J.F. (1981): Lower Proterozoic arc-microcontinent collisional tectonics in the Western Churchill Province; Nature, v294, no5836, p69-72.

Lewry, J.F. and Sibbald, T.I.I. (1977): Variation in lithology and tectonometamorphic relationships in the Precambrian basement of northern Saskatchewan; Can. J. Earth Sci., v14, p1453-1467.

Lewry, J.F., Thomas, D.J., Macdonald, R. and Chiarenzelli, J. (in press): Structural relations in accreted terranes of the Trans-Hudson, Saskatchewan: telescoping in a collisional regime?; *in* Lewry, J.F. and Stauffer, M.R. (eds.), The Early Proterozoic Trans-Hudson Orogen of North America: Geol. Assoc. Can., Spec. Pap. 37

Macdonald, R. (1975): Compilation geology, Pelican Narrows (63M) and Amisk Lake (63L) areas, *in* Summary of Investigations 1975, Sask. Geol. Surv., p44-47.

_____ (1976): Compilation geology, Pelican Narrows (63M) and Amisk Lake (63L) areas; *in* Summary of Investigations 1976, Sask. Geol. Surv., p53-57.

Macdonald, R. and Posehn, G.A. (1976): Re-investigation in the Pickerel River and Limestone-Tulabi Lakes (63L) area; *in* Summary of Investigations 1976, Sask. Geol. Surv., p44-52.

MacQuarrie, R. (1979): Geological re-investigation mapping, Birch Portage south (NTS area 63L-15(S)); *in* Summary of Investigations 1979, Sask. Geol. Surv., Misc. Rep. 79-10, p29-38.

Padgham, W.A. (1968): The Geology of the Deschambault Lake district; Sask. Dep. Miner. Resour., Rep. 114, 92p.

Pyke, M.W. (1966): The geology of the Pelican Narrows and Birch Portage areas, Saskatchewan; Sask. Dep. Miner. Resour., Rep. 93, 68p.

Sibbald T.I.I. (1978): Geology of the Sandy Narrows (east) area, Saskatchewan; Sask. Dep. Miner. Resour., Rep. 170, 50p.

Slimmon, W.L. (1988): Bedrock geological mapping, Gee Lake area; *in* Summary of Investigations 1988, Sask. Geol. Surv., Misc. Rep. 88-4, p26-31.

Thomas, D.J. (1988): Bedrock geological mapping, Paif Lake area; *in* Summary of Investigations 1988, Sask. Geol. Surv., Misc. Rep. 88-4, p20-25.

Petrogenetic Aspects of the Goldfields Granites, Saskatchewan

Edward C. Appleyard[1]

Appleyard, E.C. (1990): Petrogenetic aspects of the Goldfields Granites, Saskatchewan; *in* Summary of Investigations 1990, Saskatchewan Geological Survey; Saskatchewan Energy and Mines, Miscellaneous Report 90-4.

Gold mineralization is known to occur in association with three small, similar and contiguous granite bodies in the Goldfields (Lodge Bay) area on the north shore of Lake Athabasca. These deposits have been known since the mid-1930s and subjected to a number of episodes of exploration and evaluation (Sibbald and Buller, 1984). The Box Mine, hosted in the Box Granite, produced about 60,000 oz. of gold from 1939 to 1942 but never reopened following World War II. The Athona property was explored by two shafts and two levels of underground workings but never entered production. The Frontier occurrence was explored by an adit and several drifts but likewise never entered production. Rises in the price of gold in the past decade and the resultant renewal of exploration interest in this commodity have prompted the current study of the petrology and geochemistry of these rocks as well as a parallel, complementary study of their structural history and patterns conducted by R.G. Roberts, University of Waterloo (Roberts and Tyedmers, 1988; Roberts, 1990).

The granites are poorly dated with ages ranging from ca. 2350 to 2000 Ma (Persons, 1983; Macdonald, 1987). They share a suite of common petrographic and geochemical characteristics that relate them to a common origin. On the question of genesis, however, there is no agreement and thus there is no single genetic model to help guide exploration strategy.

This report presents some petrographic observations and lithogeochemical data that pertain to the genesis of the granites.

1. Previous Work

Regional studies by Alcock (1936), Cooke (1937), Christie (1953), Sibbald (1984) and Sibbald and Jiricka (1986), structural studies by Roberts and Tyedmers (1988) and Roberts (1990), technical studies by Byrne (1937) and Swanson (1945), property studies by Beavon (1938), Jewitt and Gray (1940), Dawson (1956), Jiricka (1984), Mason (1989) and Appleyard (1989), and geochemical studies by Quirt (1987), Quirt and Rees (1987), Appleyard (1988) and Quirt (1988) provide a background to this report.

2. Proposed Genetic Theories

Genetic theories for the Goldfields granites have been reviewed by Sibbald (1984) and Appleyard (1989) and will only be identified briefly here. Conventional magmatic, intrusive origins have been proposed by Cooke (1937), Beavon (1938) and Jewitt and Gray (1940). Another group of authors concluded that the granites formed by granitization or feldspathization of the enclosing metasediments; among these are Swanson (1945, referenced by Mason, 1989), Christie (1953), Sibbald (1984), Sibbald and Jiricka (1986) and Quirt and Rees (1987). Jiricka (1984) identified hydrothermal activity, with solution ponding beneath amphibolite sills, as a variant of the granitization model. Mason (1989) suggested that the granites originated by essentially isochemical anatexis *in situ* of arkosic metasediments with initial compositions close to the Qz-Ab-Or ternary minimum. Appleyard (1988, 1989) preferred a hybrid origin involving a magmatic, intrusive phase associated with extensive granitization.

3. General Geological Relationships

a) Host Rocks

The Lower Proterozoic supracrustals which host the Goldfields Granites are now considered to be part of the miogeosynclinal Murmac Bay Group (Macdonald, 1983). In the vicinity of Lodge Bay they have been mapped and described most fully by Sibbald who describes them as "characterized by a quartzite - carbonate succession metamorphosed under lower to middle amphibolite conditions to yield quartzites, quartz - mica schists, dolomitic marbles, diopsidic calc-silicate rocks and amphibole schists" (Sibbald, 1984, p116). Many of the quartzites are substantially feldspathic and termed arkosic by some authors.

Conformable amphibolite sheets are found within the supracrustal rocks and are closely associated with each of the three granite occurrences, forming parts of the enclosing country rocks.

b) Granites

In the Lodge Bay area four subdivisions of granite identified by Sibbald (1984) may be described as follows:

1. **'Older granite'** complex. This unit comprises a texturally, structurally and lithologically varied suite of gneisses with an abundance of supracrustal inclusions ('relics') attributable to the Murmac Group and its intrusive amphibolites. Feldspar augen and lineated mafic clots are considered to be characteristic. The rocks frequently have a migmatitic (venitic) appearance and in many cases the granitic fraction (leucosome) may closely resemble some of the other granite types listed

(1) Department of Earth Sciences, University of Waterloo, Ontario, N2L 3G1

Table 1 - Mean compositions of the Goldfields Granites. $\bar{x}$ = mean; arithmetic mean calculated for major elements (SiO_2-S; expressed in wt.%), logarithmic mean calculated for trace elements (Li - U; expressed in p.p.m.). c = coefficient of variation (standard deviation/mean).

	Box Granite		Frontier Granite		Athona Granite			
					"Mine Granite"		"Cataclastic Albite Granite"	
n	6		8		5		4	
	$\bar{x}$	c	$\bar{x}$	c	$\bar{x}$	c	$\bar{x}$	c
S.G.	2.64	0.01	2.63	0.00	2.62	0.00	2.65	0.01
SiO_2	77.20	0.01	81.6*	0.04	76.60	0.02	78.34	0.02
TiO_2	0.10	0.26	0.05	0.32	0.06	0.10	0.04	0.13
Al_2O_3	11.48	0.06	8.4	0.14	11.80	0.07	12.14	0.02
Fe_2O_3	0.89	0.19	0.85	0.30	0.33	0.51	0.35	0.72
FeO	0.3	0.47	0.5	0.48	0.6	0.20	0.6	0.39
ΣFeO	1.08	0.12	1.30	0.35	0.89	0.06	0.89	0.17
MnO	<0.01	—	0.003	0.47	0.02	0.46	0.02	0.67
MgO	0.31	0.28	0.24	0.82	0.41	0.04	0.26	0.33
CaO	0.06	0.25	0.08	0.72	0.35	0.51	0.52	0.70
Na_2O	2.97	0.16	0.31	0.13	3.48	0.05	4.97	0.21
K_2O	4.45	0.09	6.35	0.13	4.29	0.11	2.69	0.61
P_2O_5	<0.02	—	0.03	0.29	<0.02	—	<0.02	—
LOI	1.09	0.18	—	—	0.89	0.17	0.64	0.33
S	0.061	0.32	0.049	1.16	0.013	0.76	0.053	0.56
Li	2	0.65	4	0.74	4	0.13	2	0.23
Be	<1	—	<1	—	2	0.18	2	0.22
B	27	0.72	20	0.52	6	2.07	11	1.33
Sc	1.6	0.10	—	—	1.2	0.08	1.9	0.15
V	14	0.40	10	0.76	9	0.80	11	0.35
Cr	94	0.18	143	0.99	120	0.06	89	0.13
Co	0.7	1.14	3	0.39	1.0	0.18	0.4	0.69
Ni	3	0.26	6	1.13	2	0.50	1	0.55
Cu	12	0.59	7	0.71	5	0.66	3	0.23
Zn	16	0.66	5	0.47	34	0.43	51	0.85
As	3	0.60	2.4	0.65	1	0.61	4	0.23
Se	<0.5	—	0.2	0.31	<0.5	—	<0.5	—
Br	0.8	0.28	—	—	0.7	0.62	0.9	0.14
Rb	140	0.11	170	0.12	152	0.23	102	0.84
Sr	21	0.17	35	0.24	17	0.31	30	0.32
Y	32	0.19	4	0.44	29	0.21	46	0.58
Zr	133	0.21	82	0.45	79	0.17	100	0.08
Nb	12	0.14	—	—	14	0.21	28	0.10
Mo	2	0.90	<5	—	1	0.39	1	0.58
Ag	0.2	0.84	0.2	—	0.1	1.07	0.4	0.45
Cd	<1	—	—	—	<1	—	<1	—
Sn	7	0.61	—	—	4	0.68	11	0.34
Sb	0.4	0.24	—	—	0.3	0.13	0.1	0.41
Cs	0.4	0.54	—	—	0.4	0.66	<0.5	—
Ba	320	0.18	726	0.91	128	0.21	62	0.16
La	25	0.48	16	0.52	16	0.14	10	0.34
Ce	57	0.42	35	0.46	38	0.13	28	0.33
Hf	5.0	0.10	—	—	3.4	0.11	4.6	0.18
W	3	0.92	—	—	<1	—	2	1.25
Au	0.068	1.18	0.062	3.51	0.015	5.83	0.333	0.56
Hg	0.005	—	—	—	0.006	0.32	0.006	0.35
Pb	17	0.92	16	0.11	11	1.51	42	0.97
Th	21	0.12	7	0.77	23	0.22	28	0.14
U	7.6	0.30	1.8	1.44	6.8	0.64	13	0.14

below. The metamorphic fraction (melanosome) has been identified in this study as a paragneiss, possibly derived from a protolith of psammopelite, at least in the vicinity of the Box and Athona Granites.

2. **Pink leucogranite.** This unit ranges from a fine-grained, felsitic granite to medium to coarse grained with strongly colour contrasted white to grey quartz and pink to brick-red feldspar. Quartz-filled gash veins occur wherever veinlets are more than 1 or 2 cm in thickness. Granitic veinlets of this character were observed in this study as comprising a significant part of the 'granitic' fraction in the Frontier occurrence and as parts of the leucosome of the "older granites" where they are marginal to the Athona and Box granites.

3. **Feldspar augen granite.** This is a mesocratic, biotite granite with weakly developed foliation and rodding. The biotite is usually retrograded to chlorite. Sibbald (1984) notes it is intermixed with and transitional with the leucogranite in places.

4. **'Mine Granite'.** This unit comprises the most characteristic rock of the Box and Athona Granites and the most 'granitic-looking' phase of the Frontier 'granite'. It is typically pyritic, brick-red, pink, buff or yellowish to greenish in colour, and marked by an exceptional abundance of quartz veins which may contain visible gold. In the Box occurrence the 'mine' granite comprises a linked pair of thin lensoid sheets of medium to coarse-grained granite roughly conformable to the regional strike and the bedding and foliation of the enclosing metasediments and gneisses. Slab-like xenoliths and screens of host rocks of several lithologies are present in marginal locations. The unit is remarkably homogenous and geochemically uniform except where contaminated by assimilated xenolithic material. The Athona 'mine' Granite is described by Mason (1989) as having granodiorite, diorite, monzodiorite, monzonite and quartz syenite phases as well as granite (*sensu stricto*). The current study also recognized variable K-feldspar/plagioclase ratios in

these rocks but the most abundant variety is remarkably uniform and similar to the Box Granite.

In the present study, only the 'older granite' was regarded as a unique genetic unit. The other three lithologies can be distinguished arbitrarily and as such comprise useful mapping units but they appear to be coproducts of the same genetic process.

c) Metamorphic/Tectonic History

Sibbald (1984) and Roberts and Tyedmers (1988) have recognized two major deformation events in the area. The first is associated with the development of a foliation (S_1) which is generally parallel or subparallel to bedding (S_0). Where S_0 and S_1 intersect, a southeast plunging lineation and rodding results. The second deformation folds both S_0 and S_1 and created the Goldfields Syncline, a major structure whose axial surface passes through the Athona Granite. The associated S_2 foliation is variable in the intensity of its development but it is commonly weakly developed.

The 'older granite' exhibits evidence of both D_1 and D_2 whereas the other three granitic units only preserve evidence of the later deformation.

4. Petrology and Lithogeochemistry

One hundred and forty-five specimens of the granites and their host rocks were collected during the field study and 50 of these were analyzed for 12 major constituents plus LOI (Loss on Ignition) and 34 trace elements by Activation Laboratories Ltd, Ancaster, Ontario. Fifteen analyses are of the Athona and Box Granites *per se* and eight analyses of the Frontier Granite were available from an earlier study (Appleyard, 1988). The

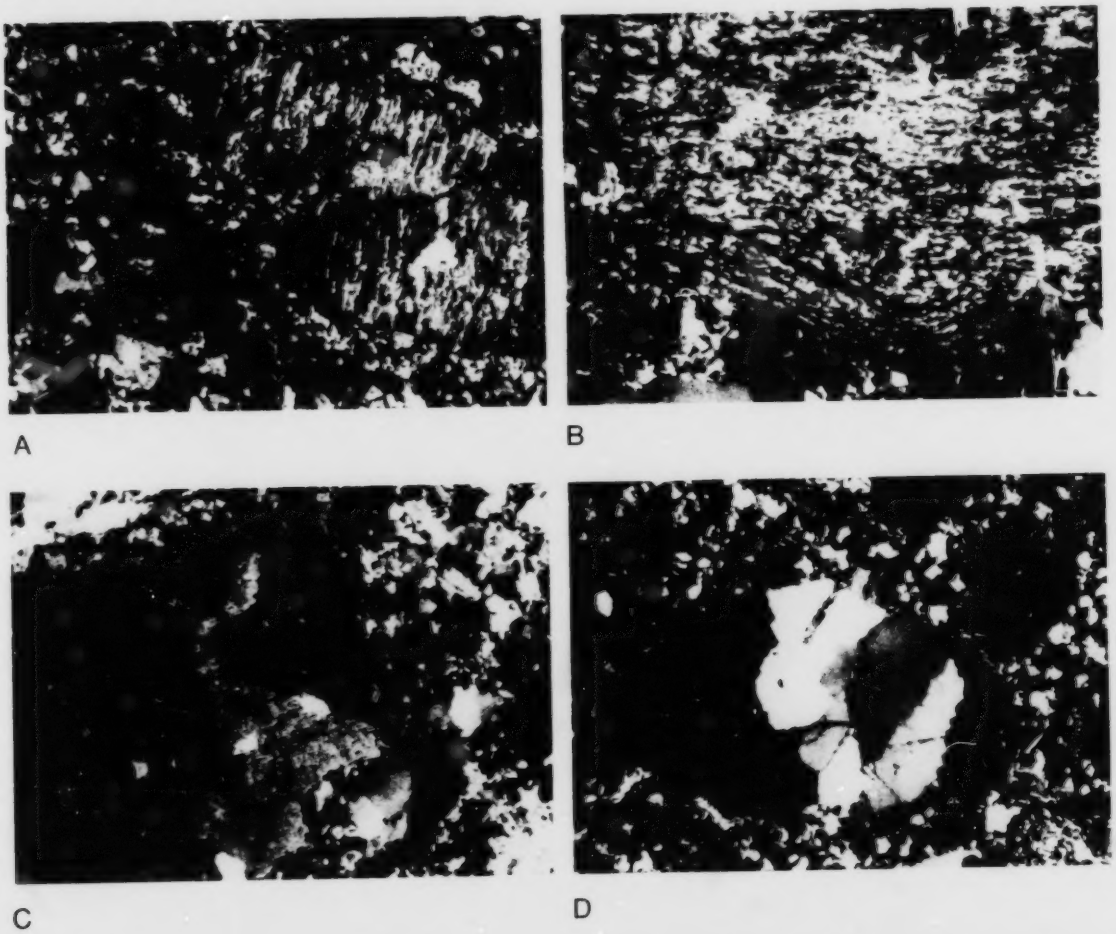

Plate 1 - A) Euhedral megacryst of mesoperthitic alkali feldspar in fine-grained granoblastic matrix. Box Granite, specimen 89-157; 25 X. B) Margin of large alkali feldspar megacryst with relict oscillatory zoning picked out by exsolution films. Grain also exhibits simple contact twinning, probably on the Carlsbad law. Box Granite, specimen 89-134; 40 X. C) Square section of alkali feldspar microperthite megacryst showing Baveno twinning. Box Granite, specimen 89-150; 25 X. D) Euhedral, slightly corroded, doubly terminated, bipyramidal quartz megacryst. Box Granite, specimen 89-134; 25 X.

remainder of the analyses represent host rocks and hybrid granitized rocks. Thirty-nine of the analyzed samples were from surface exposures and 11 were from two drill cores from the Box and Athona properties respectively. A summary of the analytical results on the granites is presented in Table 1.

a) Box Granite

The margins of the Box Granite can be mapped quite precisely if the arbitrary decision is made to exclude material that appears like a migmatitic admixture of granite and country rocks. Beyond these limited boundaries, however, is a broad aureole, exceeding 70 m in thickness on the hanging wall (southeast) side, where a granitic phase which resembles the Box Granite has permeated, veined and replaced the gneisses.

Within the confines of the Box Granite, as defined above, there are also areas, particularly near the margins, where mafic streaks and patches, i.e. schlieren, appear to represent ingested and assimilated fragments of country rocks. Angular xenoliths of a more refractory nature, such as quartzite, are also present and support the xenolithic origin of the more highly assimilated schlieren. Granite with a significant mafic content is largely restricted to the margins of the body and to where screens of country rocks are enclosed within the granite, as at the extreme northeast end of the body. The main body of the granite is virtually completely leucocratic. This facies obviously represents the pristine character of the granite while the mafic phases have been contaminated by wall rock assimilation.

Petrology

The Box Granite has a distinctly bimodal grain size population comprising a suite of megacrysts enclosed within a much finer grained matrix. The megacrysts consist predominantly of alkali feldspar with a lesser proportion of quartz and albite. The matrix comprises a granoblastic assemblage of the same three minerals with muscovite as a minor, erratically distributed phase. Pyrite is the only widely distributed trace mineral commonly observed.

The origin of the megacrysts has been a problem to many of those who have studied these rocks. Some have identified them as igneous phenocrysts and others as metamorphic or metasomatic porphyroblasts. A number of observations relate to this question.

1. All the megacrystic minerals occur in euhedral (or idioblastic) forms with this tendency being most strongly developed in the alkali feldspars (Plate 1A) and least developed in the quartz megacrysts.

2. The megacrysts do not appear to overgrow matrix minerals but individuals are commonly replaced by polygonal or granoblastic aggregates of unstrained daughter grains apparently formed by a strain recovery, i.e. annealing, mechanism. These grains differ from matrix grains in degree of freedom from strain and in size. This process is generally concentrated at the megacryst margin, along fractures that cut the grain or in other zones where strain energy was available to drive the recrystallization process.

3. The alkali feldspar phase appears, on the basis of optical tests, to range from orthoclase cryptoperthite through a transition series to microcline mesoperthite. Some crystals appear to be homogenous (cryptoperthite), others have tiny exsolution lamellae (microperthite) while others have prominent albite exsolution patches, veins, marginal segregations and 'swapped rims' (Ramberg, 1962). There is a tendency for the more unmixed varieties to be found in samples with greater amounts of post-consolidation crushing, cataclasis, brecciation or foliation development, i.e. in samples where lattice strain is available to drive the diffusion necessary for exsolution. The alkali feldspars appear to represent a typical high to low temperature Si/Al ordering sequence derived from hypersolvus K-Na alkali feldspar. Although late albitization effects are reported in the literature and have been recognized in other rocks in the area, the lack of correlation between rock Na_2C and the abundance of albite in the Box Granite points to exsolution rather than metasomatism being the principal process responsible for these textures.

4. Oscillatory compositional zoning can be recognized in a few alkali feldspar megacrysts as multiple concentric layers of perthitic albite (Plate 1B).

5. Alkali feldspar megacrysts possess twinning according to a number of twin laws. Amongst the simple twins to be observed are Carlsbad (Plate 1B), Baveno (Plate 1C), and possible Manebach twins, the first two of these being relatively common. Intersecting polysynthetic albite and pericline twins merge into the familiar cross-hatched twinning of low temperature microcline.

6. Albite megacrysts are always much less abundant than those of alkali feldspar, are absent in some specimens and are usually smaller in size. They are easily recognized by prominent multiple albite and occasionally pericline twins.

7. Quartz megacrysts range from ovoid through blocky to squat hexagonal bipyramidal in form (Plate 1D). Some have irregular margins suggestive of the effects of corrosion. All have an internal structure of fractures and possess subgrains with strongly divergent orientations and undulose extinction suggestive of crystals that have undergone the β/α quartz transition. In some examples quartz megacrysts with undulose extinction composed of sub-parallel or low-angle radiating deformation bands are clearly the product of later deformation.

8. Megacrysts have no preferred orientation within the specimen. Many are isolated from each other but it is also common for clumps of megacrysts to occur in which outer individuals mold over inner crystals.

9. Most samples, but not all, show some cataclastic effects such as granulation of matrix grains, cracking and bending of megacrysts and wispy trails of mus-

covite and, rarely, chlorite following high strain zones. In the latter case, the occurrence of relatively unstrained phyllosilicates in association with cataclastic tectosilicates identifies muscovite and chlorite as overprinted upon the strain zone.

10. Samples with mafic minerals contain either biotite or chlorite. If the mafic mineral is biotite, it nearly always shows some retrogression to chlorite. As in the hand specimen and in outcrop the mafic minerals are always irregularly distributed in thin section.

11. The relatively homogenous pattern of megacrsts and matrix is disrupted in most samples by irregular 'pools' or veinlets of quartz. This generation appears to be younger in age than the megacrysts.The petrographic observations are interpreted as indicating a phenocrystic origin for the megacrysts.

Lithogeochemistry

The mean of six new analyses of Box Granite is listed in Table 1. Some compositional characteristics are illustrated in Figures 1 to 3. The implications of these compositional patterns will be discussed below. All samples were free of discrete quartz veins but nevertheless contain quartz 'pools' and veinlets intimately permeating the matrices. Four analyses of the Box Granite were previously published by Sibbald (1984); they are not included in the above figures.

All samples are remarkably uniform in compositional attributes. Of note are the very high SiO_2, S, Cr and Au values and the relatively low values of elements such as Li, Be, B, Sr and Ba. All are peraluminous (Table 2) with Al/(Ca + Na + K) (mol. prop.) ratios in the range 1.14 to 1.22.

Table 2 - Compositional parameters of the Goldfields granites. $\bar{x}$ = mean; δ = standard deviation. Or, Ab and Qz expressed in molecular percentages.

	Box Granite		Frontier Granite		Athona Granite			
					"Mine Granite"		"Cataclastic Albite Granite"	
n	6		8		5		4	
	$\bar{x}$	σ	$\bar{x}$	σ	$\bar{x}$	σ	$\bar{x}$	σ
Al/(Ca+Na+K)	1.18	0.03	1.13	0.08	1.11	0.02	1.05	0.05
K/(K+Na)	0.50	0.06	0.93	0.01	0.45	0.03	0.26	0.16
$Fe^{3+}/(Fe^{3+}+Fe^{2+})$	0.74	0.11	0.61	0.10	0.32	0.15	0.35	0.26
Or	28.1	2.5	39.6	5.8	27.1	3.2	16.7	10.4
Ab	26.8	4.2	2.8	0.4	31.4	1.5	44.0	9.2
Qz	45.2	2.7	57.6	6.1	41.3	3.9	39.3	1.7

b) Frontier "Granite"

The Frontier occurrence is poorly exposed on a talus covered northwest-facing slope of the topographic ridge created by a 100 to 120 m thick metagabbro north of Frontier Lake. Three trenches provide the best opportunity to observe and sample the sequence. These were created by Saskatchewan Mining Development Corporation in 1982-83 (Jiricka, 1984).

Granitic rocks are much less extensive here than at either the Box or Athona occurrences and are found more or less concordantly developed within a sequence of quartzite, feldspathic quartzite, micaceous quartzite and fine-grained muscovite/biotite (chlorite) schist (metasiltstone). The sequence immediately beneath the base of the metagabbro sheet has been variably silicified, feldspathized, hematitized, chloritized and pyritized. Appleyard (1989) attributed all these phenomena to metasomatic processes.

Petrology

Thin sections confirm the classification of the rocks into the three categories defined in earlier work by Quirt (1987) and Quirt and Rees (1987), i.e. (1) quartzite, (2) transitional, and (3) 'granite'. In the latter category, however, two 'granitic' facies must be distinguished.

One is usually very coarse grained, very rich in quartz and contains brick-red alkali feldspar anhedral megacrysts. This granite phase occurs in semiconcordant veins and these tend to be fractionated like pegmatites with cores of massive gray-white quartz with finer grained feldspar-rich margins. Veins range from a few centimetres to a maximum of about 1 m in thickness and appear to inject and wedge apart foliation/layering in the host rocks. This granitic phase appears to be identical to Sibbald's (1984) 'pink leucogranite'.

In outcrop and in thin section, transverse quartz chlorite 'ladder' veins cut the 'granite' veins described above. In general, however, thin sections of the 'granite' veins are much richer in quartz than would be expected for normal igneous granite.

The second facies of granitic rock is much finer grained and is aplitic or saccharoidal in texture. It is generally massive and lacks relict sedimentary structures but appears in outcrop to have been derived from the sediment hosts

by processes that introduced feldspar, pyrite and a reddish colour (Appleyard, 1989). A more irregular quartz veining than the ladder veins of the first granite type is often present in this facies.

Wedging of the coarse pegmatoid granitic veins between sedimentary folia and disruption of micaceous layers by pegmatoid granite veins are consistent with injection of a magmatic phase. The close spatial association of these veins with the *in situ* metasomatic 'granite' ties the two types together in a related genetic model.

Lithogeochemsitry

Thirty-six whole rock and trace element analyses of the Frontier 'granite', its host metasediments, and the 'transitional' granitized psammites obtained from D.H. Quirt (Saskatchewan Research Council) were discussed in terms of a metasomatic assessment in an earlier paper (Appleyard, 1988). Only two additional analyses were obtained in the current study; both would be identified as 'transitional' in Quirt's (1987) classification. Each comprises tongues of granitic material wedging into bedded psammite or metasiltstone. Each also displays areas of penetrative alkali feldspar and muscovite development throughout the metasedimentary groundmass. The average composition of eight 'granite' samples taken from Quirt's analyses is listed in Table 1. These analyses appear to be from the aplitic (metasomatic) phase of granite.

c) Athona Granite

The Athona Granite appears as a sheet-like body emplaced into the unit mapped as 'Older Granite' by Sibbald (1984). It is situated in the axial zone of the Goldfields Syncline (Sibbald, 1984; Roberts and Tyedmers, 1988). Footwall contacts between the Athona Granite and the gneisses are exposed on the western and northern margins of the body and have been intersected by drilling over the east-central part of the area of granite outcrop.

Contacts can also be observed in a number of places between Athona Granite and amphibolite. The mafic rocks contain structures not found in the granite (Roberts and Tyedmers, 1988), xenoliths of amphibolite are found in the granite and amphibolite is locally veined by granite; the latter rock type is clearly younger. Whether all the amphibolite bodies are parts of a single sheet or whether several sheets are involved is uncertain but two layers of amphibolite have been intersected in drilling in the northwest part of the area strengthening the possibility that at least two sheets may be present.

Petrology

Thin sections from the Athona Granite are similar in most respects to those of the Box Granite. Several differences can be noted but are not fundamental. The megacrystic habit of alkali feldspar and albite is the same as in the Box Granite but there is relatively more albite in the Athona than in the Box Granite. Alkali feldspar megacrysts appear to be partly ordered and variably unmixed from high temperature forms. Occasional individuals with Baveno and Carlsbad twinning can be found. All the feldspar, whether megacrystic or matrix grains and whether alkali feldspar or albite, is turbid and usually strongly altered to sericite and clay. Megacrystic quartz is abundant but undoubted euhedral forms have not been observed. This lack of hexagonal bipyramidal shapes may be a result of a fairly strong cataclastic overprint in all the samples observed to date. The existing quartz megacrysts are consequently strongly fractured and strained. Muscovite is not as prominent in the Athona Granite as in the Box Granite except where micaceous country rock has been assimilated.

An area on the east side of the Athona peninsula was identified during mapping as 'quartzite' (Appleyard, 1989) instead of Athona Granite as previously mapped (Sibbald, 1984; Roberts and Tyedmers, 1988). The rock is equigranular, relatively fine grained, with a siliceous or 'cherty' appearance. It ranges from grey, through yellowish to pink and rusty red and closely resembles in colour, granularity and texture some of the massive hematitic feldspathic quartzites from the Frontier occurrence. Ovoid feldspathic spots can be seen in many hand specimens. These spots were interpreted as porphyroblastic growths. Pyrite is common as an accessory mineral. Seven thin sections cut from samples of this unit do not however support its identification as a metasediment. No blastopsammitic textures are present. The rock consists of a mixture of quartz, albite and alkali feldspar with very rare wisps of chloritized biotite and occasional pyrite cubes; quartz is unusually abundant and albite predominates over alkali feldspar. The most obvious textural element is an ubiquitous and relatively intensive cataclasis which has broken and disaggregated the megacrysts to varying degrees. These fractured megacrysts represent the misidentified porphyroblasts of hand specimens. The 'quartzite' unit is therefore now interpreted as being a textural and compositional variant of the Athona 'mine' Granite and is classified as a cataclastic albite-rich granite.

Lithogeochemistry

Ten new analyses of the main facies of the Athona Granite have been made which augment the three analyses previously published by Sibbald (1984). The mean composition of the 5 least contaminated samples is listed in Table 1.

Compositional parameters of these granites are plotted on Figures 1 to 3 and are discussed below. The Athona Granite is peraluminous like the Box Granite with Al/(Ca + Na + K) (mol. prop.) ratios for the 5 least contaminated samples falling in the range 1.08 to 1.13 (Table 2).

The same unique compositional characteristics that were noted for the Box Granite also apply to the Athona Granite. In all major aspects the two granites are very similar. A few subtle differences can, however, be noted as follows:

1. the Athona Granite has higher CaO than the Box Granite by a factor of 5.8 X although it is still low in an absolute sense;

2. the ratio of K/(K + Na) is a little lower in the Athona than in the Box Granite (Table 2);

3. the Athona Granite is 30 percent enriched in Cr compared with the Box Granite; both granites are much higher in this element than so - called 'normal' granites;

4. the Box Granite is richer in Ba than the Athona Granite by a factor of 2.5 X and

5. the background Au in the Box Granite is higher by a factor of 4.5 X in comparison with the Athona Granite (in view of the well known difficulty in estimating mean values of Au in rocks, this comparison should be treated with some caution).

Four analyses of the unit previously identified as 'quartzite' were made and their mean composition is included in Table 1. This unit is more siliceous than either the Box or the Athona 'mine' Granites and has higher SiO_2 in absolute terms than would be present in any 'normal' igneous granite. Its peraluminous index is slightly lower than that of the Box and Athona Granites reflecting the lower abundance of muscovite. The relatively higher content of Al_2O_3 in the 'quartzites' than in the other granites results in a lower normative Qz content but the very high Ab composition is very different from that of a residua system granite melt. Another way of illustrating this difference from the Athona 'Mine' Granite is seen in the K/(K + Na) ratio (Table 2) which illustrates the strong emphasis on Na over K by a ratio of 3:1.

Lower Rb and Ba, higher Nb, Au, Pb, Th and U represent subtle differences between this unit and the Athona Granite but the overall similarity of many other elements is striking.

5. Commentary

The petrographic evidence corroborates the field observations (Appleyard, 1989) that the granites are fundamentally of igneous origin. The evidence pointing to this interpretation can be summarized as follows:

1. The granites enclose a small number of xenoliths of country rocks ranging from slightly granitized refractory compositions like quartzite, to very strongly granitized amphibolite to almost totally assimilated quartzofeldspathic gneisses. Some of the larger of these inclusions can be referred to as "screens" inasmuch as they appear to have been enclosed by tongues of granite emplaced on either side of them without much spatial disorientation.

2. The granites are megacrystic and the megacrysts are interpreted as phenocrysts for these reasons:(a) megacrysts include quartz, alkali feldspar and albite; (b) the megacrysts are subhedral to euhedral shapes characteristic of crystallization from a melt; (c) the feldspar megacrysts display twin laws that are common in igneous but not in metamorphic settings; (d) some feldspar megacrysts preserve evidence of oscillatory zoning;(e) the alkali feldspar megacrysts appear to comprise a transition series from mixed K - Na, high temperature disordered forms to extensively unmixed, more ordered perthites.

3. the Athona Granite contains comagmatic veins of aplitic and pegmatitic character.

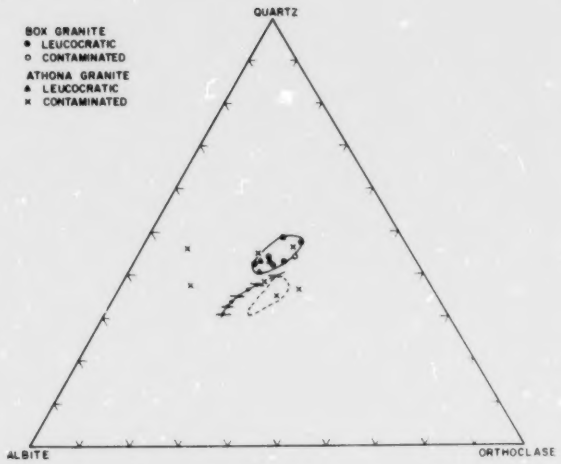

Figure 1 - Normative Qz-Ab-Or plot for samples of Athona and Box Granites. The solid line outlines the field of least altered Athona and Box Granites. The dashed line outlines the centre of the normal granite compositional field (571 analyses). Trend line shows path of ternary minima for pressures from 4000 kg/cm^2 to 500 kg/cm^2 (Tuttle and Bowen, 1958).

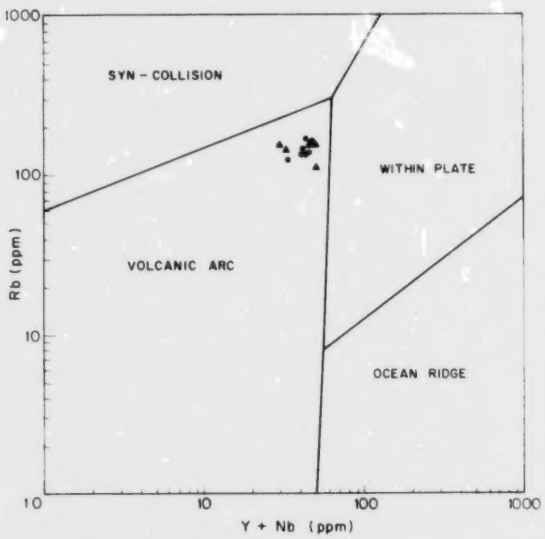

Figure 2 - Rb/Y + Nb discrimination plot for the Athona (triangles) and Box (circles) Granites. Diagram after Pearce et al. (1984).

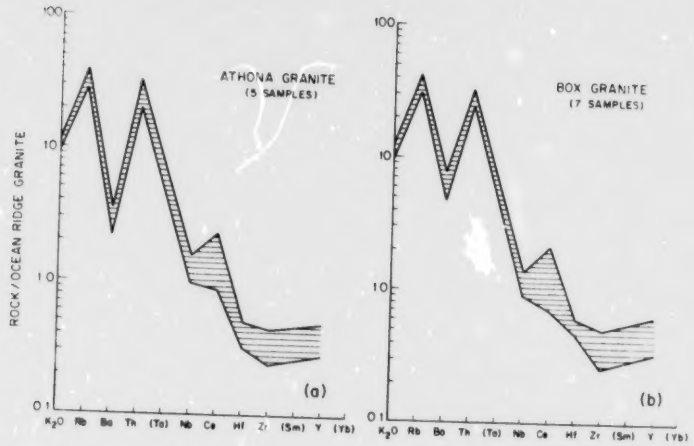

Figure 3 - Plot of geochemical parameters for the Athona (a) and Box (b) Granites normalized against the 'ocean ridge granite' values defined by Pearce et al. (1984). Patterns can be compared with representative plots in Pearce et al. (1984, Fig. 1).

Along with the magmatic indicators there is, however, abundant evidence of granitization which will be detailed in another report.

Another question arising from the compositional differences amongst the four granitic phases singled out in this study centres on the reasons for the occurrence of both K-rich and Na-rich facies. The Box and Athona 'mine' granites have remarkably restricted compositional ranges but differ slightly in K/(K + Na) ratios (Table 2) although not sufficiently to displace the analyses from the thermal minimum for low pressure melts in the Qz-Ab-Or system (Figure 1). The Frontier 'granite', on the other hand, is not only strongly enriched in SiO_2 but is also characterized by an extremely high K/(K + Na) ratio (Table 2). Conversely, the Athona 'cataclastic albite-rich granites' are strongly enriched in Ab with respect to Or. An explanation may reside in the presence of the late hydrothermal fluid, its composition and its effect on feldspar equilibrium, i.e. the development of albite may be a metasomatic effect but unequivocal textural evidence of this possibility was not observed. The relationship of possible albitization to the granitization event is one that will have to be established with further study. Albitization is a widely reported phenomenon in the region and is thus not restricted to the granites. It would be useful to know the amount of time which elapsed between these processes. This question will be further addressed in a mass balance study of the respective rocks.

Systematics of the equilibrium between hydrothermal fluids and feldspars under the mesozonal conditions of the emplacement of Goldfields granites are much less well known than magmatic crystallization phenomena, but it is known that the anionic composition of the late fluids can significantly affect alkali exchange equilibria (Manning and Pichavant, 1985). If the late fluids were predominately aqueous and their alkali exchange behaviour not influenced significantly by the presence of F, B etc., it is perhaps more likely that progressive changes in fluid composition as reactions occurred may have been the operative control.

For example, as muscovite and orthoclase/microcline formation fixes K in the rocks at the expense of Na-bearing phases, the fluids would become more Na-rich and ultimately produce albitization reactions further along their flow paths.

In terms of the current practise of classifying granitic rocks according to their probable source material and depth of melting, the Goldfields granites are S-type (Chappell and White, 1974). This interpretation is consistent with their very restricted range of melt compositions (excluding contamination effects, of course), the relatively high K/(K + Na) ratios for the pristine igneous phases of both the Box and Athona Granites, the low oxygen fugacity of the melts as expressed in relatively low $Fe^3/(Fe^3 + Fe^2)$ ratios (Table 2) at least in the Athona Granite, and the peraluminous character (Table 2) (White and Chappell, 1977; Hine *et al.*, 1978). S-type granites are characteristic, though not exclusive to Hercynotype orogenies (Pitcher, 1979) which are characterized by a thickened sialic crust and a compressional tectonic regime, possibly even an ensialic mega shear environment (Strong, 1985). This setting would be found, for example, in an intracontinental or 'back-arc' basin. Magmas in these settings are derived by anatexis of miogeosynclinal sediments, accompanied by an abundance of migmatite, are harmonious with low pressure regional metamorphism and emplaced in a tectonic regime of crustal shortening with upright folding and cleavage (Pitcher, 1979). Magmas are typically generated and remain within the regional heat plume and are emplaced dominantly by diapiric or tectonic forces.

A somewhat different indication of the tectonic setting is derived from plots constructed according to the methods of Pearce *et al.* (1984) (Figures 2 and 3). These authors subdivided granites into four tectonic settings as indicated on Figure 2. The Athona and Box Granites plot within the field characteristic of 'volcanic arc granites' though at a position very close to its confluence with the 'syn-collision granites' and 'within plate granite' fields. Hercynotype granites would be expected to plot in the 'syn-collision' field with higher Rb contents than are found within the Goldfields granites. Pearce *et al.*, however, caution users of their diagrams to be wary when applying them to Precambrian rocks, especially where crustal melting may be significant. Specifically they predict a blurring of the 'syn-collision' and 'volcanic arc' discrimination. This may indeed be the situation in this case for the spidergrams of elements illustrated in Figure 3 are most similar to patterns Pearce *et al.* illustrate from 'syn-collision' and 'post-collision' granites,

although there are similarities with the Chilean suite of 'active continental margin volcanic arc granites'.

Relatively little is known about the orogenic history of this part of the Canadian Shield. It lies within the Rae tectonic province which is becoming known as having undergone high grade metamorphism and deformation about 2.0 Ga (Bickford *et al.*, 1990). These authors speculate that the orogenic event responsible was related either to the development of the 1.91 to 2.0 Ga Taltson magmatic zone involving collision of the Slave and the Rae provinces (Hoffman, 1988) or to a collision between the Rae and the Hearne provinces along the Snowbird tectonic zone (Hoffman, 1988) concurrent with the activity on the Taltson zone. Each model would involve collisions between pre-existing Archean continental blocks; granites generated during the event would be expected to have the character of the Pearce *et al.* (1984) 'syn-collision' group. The present interpretation of the nature of the Goldfields granites supports such a setting.

6. Conclusions

It is concluded on the basis of the evidence presented and previously reported (Appleyard, 1988; 1989) that the Goldfields granites are fundamentally of igneous origin. They are part of a continuum of magmatic and hydrothermal events of possibly protracted duration. The later hydrothermal fluids, which were active after deformation of the granites, imposed feldspathization, silicification, muscovitization, chloritization, hematitization, pyritization and quartz veining effects on both the granites and their country rocks. It is inferred that the magmas were generated by crustal anatexis of metasediments during a collision between Archean/Early Proterozoic continental blocks.

7. References

Alcock, F.J. (1936): The gold deposits of Lake Athabasca; Trans., Can. Inst. Min. Metall., v39, p531-546.

Appleyard, E.C. (1988): The origin of the Frontier Granite, Goldfields area, Saskatchewan: a metasomatic assessment; *in* Summary of Investigations 1988, Sask. Geol. Surv.; Misc. Rep. 88-4, p161-167.

_____ (1989): Field observations on the Frontier, Box and Athona granites, Goldfields area, Saskatchewan; *in* Summary of Investigations 1989, Sask. Geol. Surv., Misc. Rep., 89-4, p82-86.

Beavon, A.P. (1938): The geology and gold deposits of Goldfields, Lake Athabasca, Saskatchewan; unpubl. Ph.D. thesis, Princeton Univ., 158p.

Bickford, M.E., Collerson, K.D., Lewry, J.F., Van Schmus, W.R. and Chiarenzelli, J.R. (1990): Proterozoic collisional tectonism in the Trans-Hudson Orogen, Saskatchewan; Geol., v18, p14-18.

Byrne, N.W. (1937): Diamond drilling at Lake Athabasca; Trans., Can. Inst. Min. Metall., v40, p165-184.

Chappell, B.W. and White, A.J.R. (1974): Two contrasting granite types; Pacific Geol., v8, p173-174.

Christie, A.M. (1953): Goldfields - Martin Lake map-area, Saskatchewan; Geol. Surv. Can., Mem. 269, 126p.

Cooke, H.C. (1937): Preliminary report, Goldfields area, Saskatchewan; Geol. Surv. Can., Pap. 37-3, 22p.

Dawson, K.R. (1956): Petrology and red colouration of wallrocks, radioactive deposits, Goldfields region, Saskatchewan; Geol. Surv. Can., Bull. 33, 46p.

Hine, R., Williams, I.S., Chappell, B.W. and White, A.J.R. (1978): Contrasts between I- and S-type granitoids of the Kosciusko batholith; J. Geol. Soc. Australia, v25, p219-234.

Hoffman, P.F. (1988): United plates of America, the birth of a craton: Early Proterozoic assembly and growth of Laurentia; Ann. Rev. Earth Planet. Sci., v16, p543-603.

Jiricka, D.E. (1984): Saskatchewan Mining Development Corporation, Exploration 1983, Lodge Bay Project, CBS 5664, 5665 and 5677, S-98948, Athabasca Mining District, Saskatchewan, NTS-74-N-07, -08; Sask. Energy Mines, Assess. Rep. 74N-07-0315, 59p.

Jewitt, W.G. and Gray, S. (1940): The Box Mine of the Consolidated Mining and Smelting Company of Canada, Limited; Trans., Can. Inst. Min. Metall., v43, p447-467.

Macdonald, R. (1983): Geology and regional context of the Oldman Lake area; *in* Summary of Investigations 1983, Sask. Geol. Surv.; Misc. Rep. 83-4, p19-23.

_____ (1987): Update on the Precambrian geology and domainal classification of northern Saskatchewan; *in* Summary of Investigations 1987, Sask. Geol. Surv.; Misc. Rep. 87-4, p87-104.

Manning, D.A.C. and Pichavant, M. (1985): Volatiles and their bearing on the behaviour of metals in granitic systems; *in* Taylor, R.P. and Strong, D.F. (eds.), Recent advances in the geology of granite-related mineral deposits; CIM, Spec. Vol. 39, p13-24.

Mason, I.M. (1989): Goldfields project, geology and drilling; private internal report prepared for R.J.K. Mineral Corporation, 58p.

Pearce, J.A., Harris, N.B.W. and Tindle, A.G. (1984): Trace element discrimination diagrams for the tectonic interpretation of granitic rocks; J. Petrol., v25, p956-983.

Persons, S.S. (1983): U-Pb geochronology of Precambrian rocks in the Beaverlodge area, northwestern Saskatchewan; unpubl. M.Sc. thesis, Univ. Kansas, 68p.

Pitcher, W.S. (1979): Comments on the geological environments of granites; *in* Atherton, M.P. and Tarney, J. (eds.), Origin of granite batholiths, geochemical evidence; Shiva Publishing Ltd., Orpington, Kent, p1-8.

Quirt, D.H. (1987): Frontier prospect - lithogeochemistry and mass balance calculations; unpubl. rep., Sask. Res. Counc., 8p.

_____ (1988): Reconnaissance investigation of Pt, Pd and Au in host rocks of Saskatchewan uranium deposits; *in* Summary of Investigation 1988, Sask. Geol. Surv.; Misc. Rep. 88-4, p176-178.

Quirt, D.H. and Rees, M. (1987): Current research in mineral deposits at the Saskatchewan Research Council; *in* Summary of Investigations 1987, Sask. Geol. Surv., Misc. Rep. 87-4, p160-163.

Ramberg, H. (1962): Intergranular precipitation of albite formed by unmixing of alkali feldspar; Neues Jahrb. Mineral., Abh., v98, p14-34.

Roberts, R.G. (1990): Structural controls of the Box and Athona deposits, Goldfields area, Saskatchewan; unpubl. rep., Sask. Energy Mines, 51p.

Roberts, R.G. and Tyedmers, P.H. (1988): Structural controls of the Box and Athona deposits, Goldfields, Saskatchewan: progress report; *in* Summary of Investigations 1988, Sask. Geol. Surv., Misc. Rep. 88-4, p82-83.

Sibbald, T.I.I. (1984): Gold metallogenic studies, Goldfields area; *in* Summary of Investigation 1984, Sask. Geol. Surv., Misc. Rep. 84-4, p116-121.

Sibbald, T.I.I. and Buller, G. (1984): Biogeochemical investigations, Goldfields area; *in* Summary of Investigations 1984, Sask. Geol. Surv., Misc. Rep. 84-4, p108-114.

Sibbald, T.I.I. and Jiricka, D.E. (1986): Geology of the gold deposits, Goldfields, Saskatchewan; *in* Clarke, L.A. (ed.), Gold in the Western Shield; CIM, Spec. Vol. 38, p412-414.

Strong, D.F. (1985): A review and model for granite-related mineral deposits; *in* Taylor, R.P. and Strong, D.F. (eds.), Recent advances in the geology of granite-related mineral deposits; CIM, Spec. Vol. 39, p424-445.

Swanson, C.O. (1945): Probabilities in estimating the grade of gold deposits; Trans., Can. Inst. Min. Metall., v48, p323-350.

Tuttle, O.F. and Bowen, N.L. (1958): Origin of granite in the light of experimental studies in the system $NaAlSi_3O_8$-$KAlSi_3O_8$-SiO_2-H_2O; Geol. Soc. Am., Mem. 74, 153p.

White, A.J.R. and Chappell, B.W. (1977): Ultrametamorphism and granitoid genesis; Tectonophysics, v43, p7-22.

Reconnaissance Isotopic P-T-t Study of Hydrothermal Fluid History in the Tabbernor Fault Zone, Saskatchewan: Progress Report

M.P. Field[1] *and R. Kerrich*[1]

Field, M.P. and Kerrich, R. (1990): Reconnaissance isotopic P-T-t study of hydrothermal fluid history in the Tabbernor Fault Zone, Saskatchewan: Progress report; *in* Summary of Investigations 1990, Saskatchewan Geological Survey, Saskatchewan Energy and Mines, Miscellaneous Report 90-4.

The Tabbernor Fault Zone has been recognized as a pronounced continuous northwest-striking structure. It transects the Reindeer Zone of the Trans-Hudson Orogen along a strike length of approximately 600 km in Saskatchewan (Byers, 1962). Its width is unknown (Padgham, 1968). Interpreted as a crustal structure (Green *et al.*, 1885) with a dominant left lateral displacement (Furnival, 1941; Macdonald, 1976), the Tabbernor Fault Zone separates the Glennie Domain on the west from the Kisseynew Domain and Hanson Lake Block on the east (Lewry and Sibbald, 1977; MacQuarrie, 1979). It has been recognized that deep crustal structures may act as conduits for ascending metal laden fluids that mineralize second and third order splays (Kerrich, 1989). Therefore characterizing the fluids which travel through major structures such as the Tabbernor Fault Zone may aid in interpretation of deformation history relative to fluid infiltration. It is the aim of this study to determine the composition of fluids in syn- to post-tectonic features and to document P-T-t fluid histories. The project is co-sponsored by the University of Saskatchewan and Saskatchewan Energy and Mines and is part of a Master's thesis to be completed by M.P. Field. The work is part of a complementary effort with K. Wilcox (this volume) to geologically map, and document the kinematic, metamorphic, chronological and fluid evolution of the Tabbernor Fault Zone.

1. Sample Collection

Forty-three samples were collected from the Nielsen Lake area southwest of Pelican Narrows, Saskatchewan and along the Hanson Lake Road (Highway 106) where the Tabbernor Fault divides into several splays.

Quartz veins, wall rocks and host units were sampled from a mylonitized chloritic rock of uncertain protolith (approximate UTM coordinate 619400mE, 6104200mN) and from a highly strained tonalite to granodiorite (approximate UTM coordinate 619500mE, 6104800mN) at Nielsen Lake. A number of small discontinuous quartz veins ranging from 1 cm wide by 5 cm long to 15 cm wide and 100 cm long cutting both rock types can be divided into two sets:

1) those which appear internally strained and lie parallel to the fabric and
2) veins which crosscut the foliation and comprise a multi-stage evolution.

Syn- to post-tectonic quartz veins and wall rocks were sampled from a splay of the Tabbernor Fault located near the intersection of the Tulabi River and Hanson Lake Road (approximate UTM coordinate 626600mE, 6065400mN).

2. Short Term Objectives

All samples have been prepared for polished thin sectioning. The initial objective is to attempt to differentiate fluids and fluid events affecting the Tabbernor Fault Zone. This will be based on: 1) field relationships, 2) petrography and 3) $\delta^{18}O$ systematics of vein quartz and host rock quartz and feldspars.

3. Long Term Objectives

Once distinct fluids are identified, P-T-t fluid histories can be constrained and compared to the fluids in mineralized second and third order splays. This information will be derived using: 1) compositional data from the electron microprobe, 2) stable isotope data on mineral triplets, 3) radiogenic isotope pairs where applicable and 4) chemical mass balance using ICP-MS.

4. References

Byers, A.R. (1962): Major faults in western part of Canadian Shield with special reference to Saskatchewan; *in* Stevenson, J.S. (ed.), Tectonics of the Canadian Shield, R. Soc. Can., Spec. Publ. 4, p40-59.

Furnival, G.M. (1941): Porcupine River, northern Saskatchewan; Geol. Surv. Can., Map 658A with marginal notes.

Green, A.G., Hajnal, Z. and Wever, W. (1985): The evolutionary model of the western Churchill Province and western margin of the Superior Province in Canada and the north central United States; Tectonophysics, v116, p281-322.

Kerrich, R. (1989): Geochemical evidence on the sources of fluids and solutes for shear zone hosted mesothermal gold deposits; *in* Bursnall, J.T. (ed.), Mineralization and Shear Zones, p129-198.

Lewry, J.F. and Sibbald, T.I.I. (1977): Variation in lithology and tectonometamorphic relationships in the Precambrian basement of northern Saskatchewan; Can. J. Earth Sci., v14, p1453-1467.

(1) Department of Geological Sciences, University of Saskatchewan, Saskatoon, Saskatchewan, S7N 0W0

Macdonald, R. (1976): Compilation geology: Pelican Narrows (63M) and Amisk Lake (63L); *in* Summary of Investigations 1976, Sask. Geol. Surv., p53-57.

_____ (1987): Update on the Precambrian geology and domainal classification of northern Saskatchewan; *in* Summary of Investigations 1987, Sask. Geol. Surv., Misc. Rep. 87-4, p87-104.

MacQuarrie, R.R. (1979): Geological re-investigation mapping, Birch Portage south (NTS area 63L-15(s)); *in* Summary of Investigations 1979, Sask. Geol. Surv., Misc. Rep. 79-10, p29-38.

Padgham, W.A. (1968): The geology of Deschambault Lake district, Saskatchewan; Sask. Dep. Miner. Resour., Rep. 114, 92p.

Metallogenic Environments: Deception Lake Area

Charlie Harper

Harper, C.T. (1990): Metallogenic environments: Deception Lake area: *in* Summary of Investigations 1990, Saskatchewan Geological Survey, Saskatchewan Energy and Mines, Miscellaneous Report 90-4.

In early September 1989, prospector David Partridge discovered galena - sphalerite mineralization, with associated silver and gold values, in the Northeast Bay area of Deception Lake, 200 km north-northeast of La Ronge (Figure 1). News of the discovery in this little explored part of the Rottenstone Domain resulted in a flurry of claim staking. The present project was undertaken to determine the nature and geological setting of this new multi-element base metal discovery and the necessity for further studies in the region.

Field investigations included: reconnaissance-style traversing across a 2 by 12 km zone on the northwest side of Northeast Bay (shown at 1:20,000 scale on the accompanying map), detailed mapping around the discovery itself (shown at 1:10,000 scale on the accompanying map), logging of selected drill core from the initial phase of diamond drilling and examination of other reported occurrences of sulphide mineralization and gossans (Shklanka, 1962) elsewhere on Deception Lake (Figure 1).

1. General Geology

The Deception Lake area was previously mapped by McMurchy (1938), Shklanka (1962) and Gilboy (1982) at scales of 1:253,440, 1:63,360 and 1:100,000 respectively. The northeast strike extension of the rocks hosting the lead-zinc mineralization was mapped by Lewry, Curry and Roberts (1980) also at 1:100,000 scale.

The Rottenstone Domain is one of several lithostructural subdivisions of the Early Proterozoic Reindeer Zone which forms part of the larger Trans-Hudson Orogen (Hoffman, in press). The domain comprises granitoid and migmatitic metasedimentary gneisses and the regionally extensive Wathaman Batholith. The boundaries of the domain are marked by major regional shear zones, the Needle Falls and Paull River Shear Zones along the northwest and southeast sides respectively. To the southeast the Rottenstone Domain borders the metasedimentary gneiss-dominated Crew Lake Belt of the La Ronge Domain.

Shklanka (1962) described the geological setting of Deception Lake as lying at the regional contact between trondjhemitic granitoid rocks to the northwest and migmatitic metasedimentary rocks to the southeast. The migmatites comprise psammitic to pelitic, calc-silicate and amphibolitic paleosomes with variable granitic neosomes including pegmatite, pegmatitic trondjhemite, trondjhemite or quartz diorite. Northeast Bay lies in a transitional zone between the two major lithologies, where paleosomal remnants rarely compose more than twenty-five percent by volume.

The author's investigations indicate that the migmatites along the north side of Northeast Bay occupy an extremely elongate, locally doubly plunging, overturned synformal fold. In addition to the metasedimentary paleosomes mentioned above, the most economically significant lithology is a mixed calcareous silicate - sulphide facies iron formation which hosts the lead-zinc-silver-gold mineralization.

2. Migmatites

Metasedimentary paleosomes typically occur as wispy schlieren or highly disrupted, boudinaged pods and lenses that rarely exceed 3 m in thickness. Definition of discrete paleosomal units is hampered by their interlayered character. Compositional variants include: biotite-quartz-feldspar gneiss; garnetiferous, biotitic quartzofeldspathic gneiss; garnetiferous biotite-hornblende gneiss and the calcareous silicate - sulphide facies iron formation assemblage.

a) Biotite-Quartz-Feldspar Migmatite (Bqf)

Biotite-quartz-feldspar migmatite is typically grey, medium to coarse grained and well foliated. Biotite, averaging 30 percent by volume, commonly occurs in 1 to 2 cm diameter clots. White plagioclase (60 percent) and quartz (10 percent) form elongate grains oriented in the plane of the prominent foliation, which is also marked by a biotite orientation. Alternation of biotite-rich and biotite-poor layers, of 1 to 10 cm thickness, is also characteristic.

Lit-par-lit pegmatites, from 1 to 10 cm thick, comprising plagioclase and quartz with minor biotite, form a major component of the unit. These felsic granitoids predate the generally coarser-grained pegmatitic trondjhemite and are always folded. The biotite-quartz-feldspar migmatite is so strongly invaded by pegmatitic trondjhemite that distinction of the two rock types on the accompanying map is somewhat arbitrary.

b) Garnet-Biotite-Quartz-Feldspar Gneiss (Gqf)

Garnet-bearing layers occur within the biotite-quartz-feldspar migmatites and are more readily distinguishable. They are generally fine-grained (< 1.5 mm), equigranular, granoblastic, and thinly layered (< 5 cm thick) rocks, containing less than 10 percent biotite, from 5 to 30 percent garnet in addition to about equal amounts of quartz and feldspar (both plagioclase and microcline). Although highly disrupted by the pegmatitic trondjhemites, several zones, up to 150 m thick in places, are mappable and indicated on the accompany-

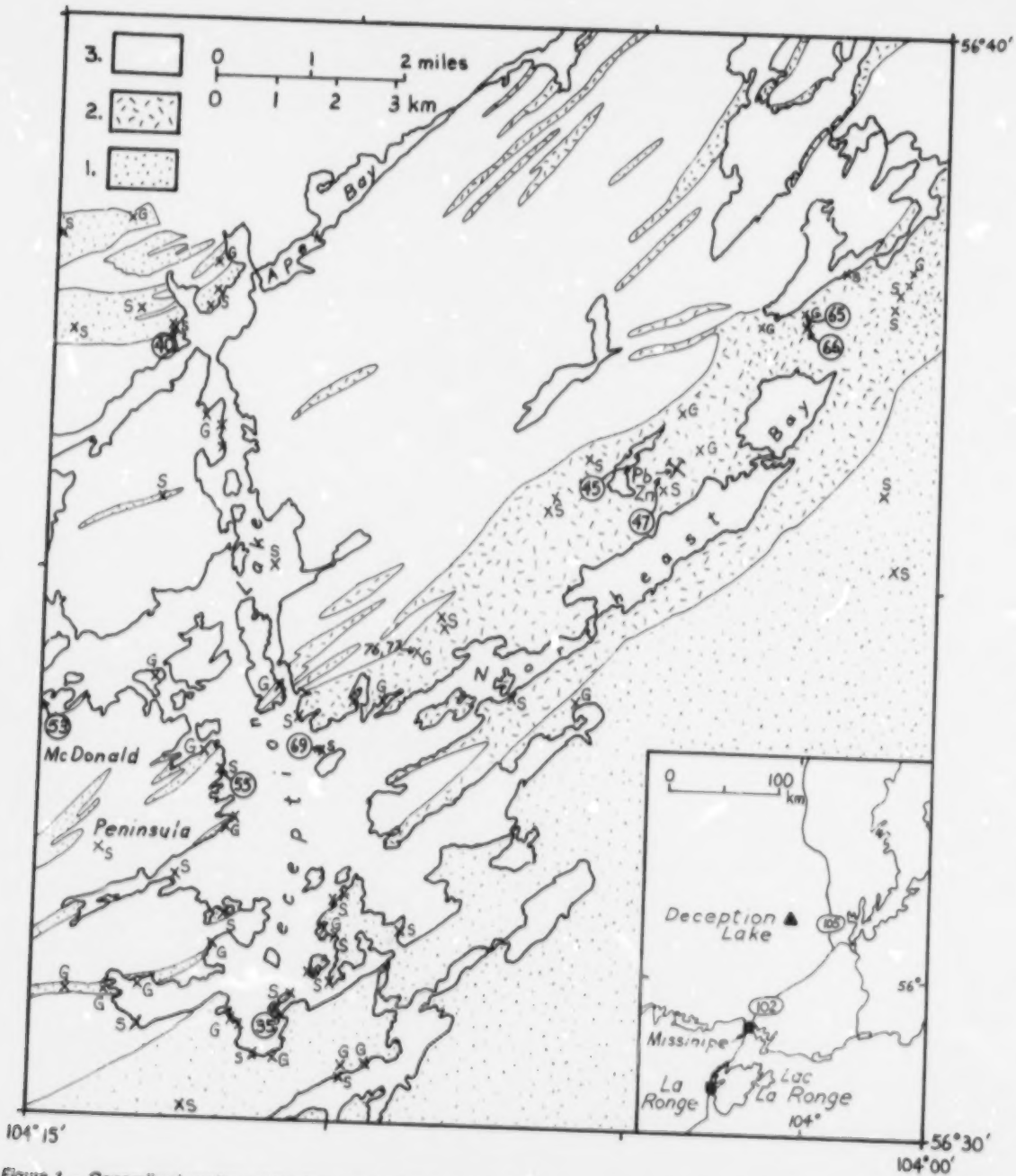

Figure 1 – Generalized geology of the Deception Lake area showing the location of the lead-zinc-silver-gold mineralization (crossed hammers symbol). Also shown are the location of other sulphide (S) and gossan (G) occurrences; the numbers correspond to samples collected for geochemical analysis. Lithologies are: 1) predominantly metasedimentary migmatite; 2) Northeast Bay transitional zone with abundant pegmatite trondjhemite and 3) predominantly biotite trondjhemite and granitoid gneiss. Modified from Shklanka (1962).

ing map. The garnet-biotite-quartz-feldspar gneiss is interlayered with the more mafic garnet-biotite-hornblende gneiss, and may in part be in gradational contact with each other.

c) Garnet-Biotite-Hornblende Gneiss (Bh)

Garnet-biotite-hornblende gneiss is dark grey to black, fine to medium grained (<2 mm) inequigranular and generally granoblastic textured. Biotite and hornblende

compose up to 90 percent of the rock; the remainder being plagioclase and minor quartz. Pale pink to red anhedral garnet porphyroblasts, up to 10 mm diameter, but typically less than 4 mm, compose up to 40 percent of these rocks. As garnet content increases, so does quartz and plagioclase, so that garnet is commonly surrounded by a light coloured felsic rim. In one outcrop near the southwest end of the exploration grid, garnet size and abundance decrease away from the contact of a pegmatitic trondjhemite dyke, suggesting a contact metamorphic effect related to the dyke.

Thin, pale green, rusty weathering calc-silicate layers are interlayered locally. The rusty weathering is caused by a few percent disseminated pyrrhotite. In some places the garnet-biotite-hornblende gneiss is found in close proximity to the iron formation; however, this spatial association is not necessarily a guide to locating unexposed parts of the iron formation unit.

d) Calcareous, Silicate-Sulphide Facies Iron Formation (If)

The iron formation unit consists of a number of interlayered lithologies principally biotite-pyrrhotite±garnet± graphite-quartz-feldspar and biotite-pyrrhotite-diopside± graphite-quartz-plagioclase rocks, both of which locally grade into semi-massive to massive pyrrhotite±pyrite. Minor lithologies include: pyrrhotite-magnetite-garnet-hornblende-quartz-feldspar rocks, amphibole and biotite schists, biotitic and sulphide-bearing diopsidites (calc-silicates) and impure marble. Pegmatite is equally common in the iron formation, as in the other units, but commonly has a greenish tint.

The principal lithologies are found throughout the Deception Lake area and exhibit little variation from one locality to another. The minor lithologies are more restricted in their distribution with the amphibole and biotite schists and diopsidites most closely associated with the lead-zinc mineralization.

The iron formation rocks are moderately to very strongly iron stained and are responsible for most of the reported gossanous zones. Weathering of the sulphide-bearing rocks can reach several metres depth, so that good exposures are normally only found along shorelines, steep slopes or escarpments.

The biotite-pyrrhotite±garnet±graphite-quartz-feldspar unit is typically grey to dark grey, fine grained, equigranular, and granoblastic. Relict primary layering, marked by disseminated variations in garnet, graphite and sulphide content is common and developed on a 1 to 100 cm scale. Biotite content ranges from 10 to 40 percent and decreases with a corresponding increase of garnet, quartz and feldspar. Pyrrhotite content is typically about 10 percent, but can reach 30 percent. The garnetiferous varieties, with up to 30 percent garnet, are more resistant, because of their higher felsic mineral content. Graphite is present locally in concentrations of up to 5 percent.

The biotite-pyrrhotite-diopside±graphite-quartz-plagioclase unit is generally the most resistant weathering of the iron formation lithologies and therefore most commonly exposed. It is light grey to pale green, medium to coarse grained (2 to 5 mm diameter), relatively massive and consistently contains from 10 to 20 percent pyrrhotite. Compositional layering is best seen in thin section where diopside-rich and -poor layers alternate with plagioclase±quartz layers on a millimetre to centimetre scale. Biotite is a minor component typically associated with diopside. Pyrrhotite is disseminated throughout the rock as amoeboid to skeletal-shaped grains, commonly flattened in the plane of the foliation. Up to 3 percent graphite is present locally. At the north end of Deception Lake, near the mouth of Apex Bay, green, glassy grains, up to 3 mm diameter, of the zinc spinel, gahnite, compose a percent or two of the rock.

Pyrrhotite-magnetite-garnet-hornblende quartz-feldspar rocks were found only in one locality, on a small point at the north tip of MacDonald Peninsula. They represent silicate facies iron formation with a minor sulphide and oxide component (< 10 percent).

The remaining rock types, **amphibole and biotite schists, sulphide-bearing diopsidites and impure marble** are found along the Northeast Bay iron formation horizons. As a group they are commonly coarser grained than the other types, nearly monomineralic in places and closely associated with the lead-zinc mineralization. They are interlayered with each other and the main iron formation lithologies.

The **amphibole schists** are dark green to black where hornblende is the principal amphibole or pale brown where a fibrous amphibole, believed to be anthophyllite, dominates. Radiating aggregates of the latter reach 10 to 15 cm long. Plagioclase and quartz are normally minor components. In some places the hornblende schist is replaced almost completely by coarse dark brown biotite and forms a **biotite schist**. The highest lead values are associated with the hornblende/biotite schists. Galena occurs in millimetre to centimetre thick layers in the schist, suggesting that the original character of the mineralization was bedded. The euhedral galena grains range from 1 to 10 mm in size, the coarsest galena occurring in low pressure boudin necks. Sphalerite is also present as disseminated grains and layers.

The anthophyllite schists do not appear to contain any of the base metal mineralization. They may represent the manifestation of an alteration zone.

The **diopsidites** (calc-silicates) are pale brown to pale green weathering, relatively massive textured, and in part brecciated. Brecciation is marked by green to dark green amphibole, which has crystallized along the fractures and partially replaced the diopsidite fragments. The amphibole appears to be actinolite, suggesting a retrograde origin. Diopside composes 50 to 95 percent by volume; plagioclase is the other main component. In some plagioclase-rich portions, light green to blue green apatite is an abundant accessory. Apatite crystals up to 2.5 cm long and 0.75 cm diameter are well developed at one locality on the north limb of the

western-most iron formation horizon near the southwest end of Northeast Bay.

Flat ellipsoidal biotite/hornblende clots, from 1 to 5 cm long and up to 1 cm thick, impart a rather distinctive texture to parts of this rock type. The apparent alignment of the clots is suggestive of disrupted sedimentary layers. Black sphalerite has a similar form in these rocks, possibly also representing original layering.

Impure marble is a very minor component of the iron formation unit. Thin (< 5 cm) recessively weathering layers are mottled white, pale green and pale brown. The marble is grey, medium to coarse grained and generally equigranular. In thin section serpentine occurs as pseudomorphs of roundish olivine grains. Layering visible in samples consists of alternating calcite-plagioclase±quartz+(olivine), diopside and plagioclase-quartz layers.

3. Pegmatitic Trondjhemite (Pt)

Pegmatitic trondjhemite is the most abundant rock type for the most part occurring as narrow (generally <3 m thick) sheets that are boudinaged and typically subparallel to compositional paleosomal layering and to small and regional scale fold axial surfaces. Only in a few places are cross-cutting relations apparent. The sheets are anastomosing, probably a result of the strong deformation and contacts with the metasedimentary units and migmatites are both sharp and gradational, particularly with the biotite-quartz-feldspar migmatite. In places pegmatitic trondjhemite and the earlier *lit par lit* neosome are almost indistinguishable. A few of the more coherent bodies of this unit are shown on the accompanying map.

The pegmatitic trondjhemite is normally white weathering, but splotchy to extensive rusty weathering is common, with no apparent cause visible in surface exposures. In drill core the presence of pyrite coating late fractures explains the rusty weathering. The rocks have a variable grain size, but average 2 to 3 cm and tend to be moderately foliated. The foliation is defined by the elongation of the felsic minerals, the alignment of the little biotite present and the alignment of biotite-rich schlieren, which comprise up to 10 percent of the rock. Plagioclase and quartz are the principal components, with generally less than 10 percent biotite, In the vicinity of or where it intrudes the iron formation, the pegmatite commonly has a greenish colouration. Shklanka (1962) reported that the colour was caused by the presence of very fine disseminated chlorite. From outcrop, drill core and thin section observations the author suggests that some of the pale green to yellow green colouration is caused by very fine to flaky sericite.

4. Structure and Metamorphism

The migmatite - trondjhemite complex of Northeast Bay forms a major, elongate, undulating northeast-trending, moderately northwest-dipping, overturned synform. Small scale folds generally plunge northeasterly at 15° to 45°, although there are local reversals in plunge of equal magnitude to the southwest.

An early phase of deformation (D1) produced the dominant foliation, which for the most part appears to have been parallel to the original layering. Folds related to this early deformation are difficult to recognize but were probably isoclinal. Formation of the early *lit par lit* anatectic neosomal layers contributes to this difficulty. Subsequent northwesterly compression produced the dominant regional northeast trend. The abundant small scale folds, which fold the foliation and help define the regional synform, are related to this phase of deformation (D2). The pegmatitic trondjhemites were emplaced subparallel to the northeast-trending D2 axial surfaces probably syn- to late-tectonically, because they are boudinaged and possess a weak to moderate D2 foliation.

The presence of anatectic granitoids in the metasedimentary gneisses and the preserved mineral assemblages indicate that upper amphibolite grade metamorphism was attained. Subsequent retrograde metamorphism resulted in the development of greenschist facies minerals.

5. Economic Geology

McMurchy (1938) reported that exploration activity had taken place in 1928-29 around the base and platinum group metal occurrences at Rottenstone Lake, 45 km southwest of Deception Lake, but it is not known whether this exploration included the latter area. At the time of Shklanka's (1962) mapping in 1957 no claims had been staked in the Deception Lake area and there was no record of any exploration activity.

In 1966, Don Fisher Syndicate, apparently following up Shklanka's (1962) sulphide and gossan occurrences, carried out a number of Self-Potential and Dual Frequency Magnephase E.M. surveys across portions of the sulphide zones. Two of these surveys tested the iron formation units north of Northeast Bay; one was actually conducted over the main lead-zinc showing. Several trenches were excavated at widely scattered locations elsewhere on Deception Lake, but with negative results, no further work was done (SEM Assessment File 74A09-SE-0004).

In 1967 Sherritt Gordon Mines Ltd. followed up several E.M. conductors between the northeast part of the area investigated by the author and Buss Lake, 5 km further northeast (SEM Assessment File 64D12-NW-0001). Restricted magnetic surveys were conducted over favourable zones revealing coincident magnetic and E.M. anomalies. A single diamond drill hole, 86 m long, tested a zone of sulphide mineralization about 2 km northeast of the northeastern-most part of Northeast Bay. Sections of core gave consistently low nickel and copper values, from 4 to 41 percent iron and traces of silver and gold. Lead and zinc were not included in the assays. No further work was carried out on the property.

In 1969 Scurry Rainbow Oil Ltd. prospected an area at the north end of Deception Lake near the mouth of Apex Bay. Ground magnetic and geological surveys in two separate areas identified several pyrrhotite-bearing horizons in the migmatitic gneisses. Several trenches

were excavated and at least two short diamond drill holes were completed; unfortunately one of these holes was drilled down dip. In 1973 Scurry Rainbow followed up their earlier work in the western area with more ground geophysics, but did no further work on the property (SEM Assessment Files 74A09-0002 and 74A09-SE-0005).

The area lay virtually dormant until 1989 when prospector David Partridge discovered the galena-sphalerite mineralization while checking out Shklanka's (1962) reported sulphide occurrences north of Northeast Bay. A number of trenches were excavated and the property optioned to Pine Channel Gold Corp. and then Northair Mines Ltd., who carried out an airborne magnetic and E.M. survey and completed a 24 hole, 2200 m diamond drill program by the end of February, 1990.

Initial trench sampling had given exciting results, with up to 11.2 percent Pb, 3.44 percent Zn, 1.88 oz/ton Ag and 0.12 oz/ton Au (Stewart, 1989). The prospect was described as being at least 250 m long and 10 m wide with the possibility of having parallel zones (*ibid*). A later news release stated that grab samples from a site 210 m east of the initial discovery contained up to 28.39 percent Pb, 4.72 percent Zn, 3.4 oz/ton Ag and 0.01 oz/ton Au as well as anomalous platinum and palladium values (Kilburn, 1989). At this time mineralization was reported to have been identified over a 760 m strike length along a 2500 m ground geophysical anomaly.

However Northair decided to drop their option because of poor drill results (Northern Miner, 1990a and b). Pine Channel continued to evaluate the property, and recently Noranda Exploration optioned it and plans to do further diamond drilling (Northern Miner, 1990c). No results have yet been released from this work.

Mineralization of potential economic interest is almost exclusively related to the iron formation sequence which is found at numerous locations around Deception Lake. Most of the examined sulphidic iron formation comprises disseminated to weakly layered and locally massive pyrrhotite with minor pyrite and rare magnetite. Chalcopyrite has been noted in a few places (Shklanka, 1962). Galena-sphalerite mineralization with low silver and gold values accompany the iron formation where amphibole- and diopside-rich rocks (calcareous silicate facies) occur. Chemical analysis of mineralized grab samples confirms the calcareous nature of these rocks; they also contain elevated MgO concentrations (Table 1). Sample 9011-78, with the highest lead concentration (63,900 ppm), has the highest and anomalous values for gold and silver (536 ppb and 25 ppm, respectively), which indicates a Au-Ag association with galena. Zinc-rich samples do not show the same association.

Currently the only known lead-zinc mineralization is within the Northeast Bay area iron formation horizons, however, this should not preclude its development elsewhere in the region. This is demonstrated in grab samples of the pyrrhotite-bearing diopsidic variety which consistently contain high concentrations of zinc (Table 2). Sample 9011-40, the gahnite-bearing rock from the north end of Deception Lake, has 842 ppm Zn which may suggest the presence of nearby sphalerite mineralization. This group of samples also contain high CaO but typically less MgO than the mineralized samples. Two of these regional samples (9011-47 and 55) contain elevated to anomalous gold values (25 and 96 ppb respectively), but are not associated with lead. Copper values are about the same for the regional and mineralized samples.

Table 1 - Northeast Bay Pb-Zn-Bearing Samples. Major oxides (in percent) and selected trace elements (in ppm; gold in ppb).

Sample No.	9011	9011	9011	9011	9011	9011	9011
Oxides	-4	-50	-78	-80	-85	-76	-77
SiO_2	52.60	42.10	47.00	39.30	67.80	51.20	48.30
Al_2O_3	5.86	11.70	13.40	18.80	10.00	3.41	12.30
Fe_2O_3	5.58	13.90	6.50	11.60	9.30	9.93	5.56
MgO	11.90	8.19	11.80	15.20	2.13	11.70	9.07
CaO	19.90	14.20	15.30	2.79	5.30	17.80	16.50
K_2O	0.19	1.59	0.80	7.22	0.56	0.48	1.81
Na_2O	0.69	0.50	0.62	0.28	0.59	0.31	0.50
TiO_2	0.05	0.81	0.11	0.17	0.10	0.12	0.16
MnO	1.14	0.18	0.21	0.17	0.06	0.90	0.79
P_2O_5	0.08	0.20	0.20	0.13	0.13	1.20	0.31
LOI	1.40	4.68	2.97	2.87	2.89	2.56	3.10
Total	99.39	98.05	98.91	98.53	98.86	99.61	98.40
Trace Elements							
Au	5	16	536	22	13	2	<1
Ag	1.8	<0.2	25	1.2	2.0	0.2	<0.2
Cu	14	233	163	81	127	340	19
Pb	178	15	63,900	1341	1881	11	23
Zn	3739	345	1085	4089	33,200	802	635
Cd	10	<1	9	12	102	<1	<1
Ba	49	166	65	357	56	52	198

9011-4	sphalerite-bearing diopsidic rock
9011-50	pyrrhotite in anthophyllitic rock, near main zone
9011-78	galena-bearing biotite quartzofeldspathic gneiss
9011-80	sphalerite-bearing biotite schist
9011-85	layered sphalerite in amphibole-diopside rock
9011-76	pyrrhotite-bearing amphibolite, B conductor
9011-77	calc-silicate, B conductor

6. Discussion

There is a growing recognition that many "stratiform base metal deposits are either components or close associates of iron formation

Table 2 - Regional Samples of Pyrrhotite-Bearing Calcareous Iron Formation. Major oxides (in percent) and selected trace elements (in ppm; gold in ppb).

Sample No. Oxides	9011 -35	9011 -40	9011 -45	9011 -47	9011 -53	9011 -55	9011 -65	9011 -66	9011 -69
SiO_2	51.70	45.90	41.70	43.20	46.50	52.00	47.40	46.10	50.30
Al_2O_3	14.90	12.20	11.60	27.90	12.70	10.60	12.30	14.40	12.70
Fe_2O_3	14.30	14.90	19.80	4.28	18.20	16.50	10.10	13.60	10.10
MgO	2.86	3.26	8.69	2.53	0.98	4.02	11.30	2.44	7.36
CaO	5.81	16.20	8.85	11.00	13.60	8.27	12.60	11.90	13.30
K_2O	1.46	1.03	0.32	3.91	0.63	0.78	0.30	0.29	1.37
Na_2O	0.51	0.43	0.61	0.38	1.97	0.61	0.66	0.62	0.94
TiO_2	0.42	0.58	0.84	0.55	1.02	0.73	0.95	0.78	0.62
MnO	0.10	0.49	0.15	0.09	1.05	0.12	0.19	0.09	0.25
P_2O_5	0.16	0.23	0.17	0.23	0.24	0.13	0.28	0.28	0.18
LOI	6.77	4.15	6.22	5.28	1.99	5.94	2.70	7.93	1.48
Total	98.99	99.37	98.95	99.35	98.88	99.07	98.78	98.43	98.60
Trace Elements									
Au	2	<1	6	25	7	96	5	9	1
Ag	<0.2	1.1	1.1	0.6	0.9	09.	09	<0.2	0.8
Cu	110	81	138	32	349	307	65	228	96
Pb	3	<2	8	11	16	12	21	7	<2
Zn	121	842	381	128	153	71	247	83	74
Cd	4	<1	<1	<1	<1	<1	<1	<1	<1
Ba	44	90	57	737	161	77	36	61	234

9011-35	pyrrhotite-bearing calcareous IF
9011-40	pyrrhotite bearing calcareous IF
9011-45	pyrrhotitic amphibolite
9011-47	pyrrhotite bearing calcareous IF; SW end of main zone
9011-53	layered pyrrhotite + magnetite silicate facies; McDonald Peninsula
9011-55	pyrrhotite-bearing amphibolite; McDonald Peninsula
9011-65	pyrrhotitic amphibolite
9011-66	pyrrhotite-bearing calcareous IF
9011-69	calc-silicate layer in amphibolite gneiss

units that developed as chemical members of the clastic ...sequences in which the ores occur." (Vaughan and Stanton, 1986, pB94). Oxide and sulphide facies varieties are well known and easily recognized, but the silicate facies iron formations are less conspicuous. The iron silicate mineral assemblages are similar to skarn assemblages or calc-silicate rocks. The common silicate minerals in amphibolite grade metamorphic rocks are: almandine garnet, iron-rich pyroxenes and amphiboles, epidote, grunerite, olivine and if sufficient quantities of Mg and Al are available, cordierite and anthophyllite. The iron-rich rocks, that also contain notable amounts of Ca, Mg, Al and Mn, develop skarn type mineral assemblages, not by contact metamorphism, but during regional metamorphism, Notable world class base metal deposits which belong to this type of silicate iron formation are the Broken Hill deposit, Australia and the Aggenays and Gamsberg deposits of Namaqualand to name a few (*ibid*).

The Northeast Bay area iron formation sequence has many of the same chemical and mineralogical characteristics. Similar pyrrhotite-bearing calcareous iron formation and the associated sediments occur throughout the Rottenstone Domain, in the adjacent Crew Lake Belt of the La Ronge Domain (Harper, 1986; Thomas, 1985), the McLean Lake Belt and in the Kisseynew Domain. Examples of base metal mineralization (lead-zinc or copper-zinc), similar to Northeast Bay, elsewhere in the Reindeer Zone of Saskatchewan and Manitoba include: the zinc-copper Brown mineral claim at Paskwachi Bay on Reindeer Lake (Stockwell, 1929); the Borys Lake zinc-lead-silver prospect (Coombe, 1975); the Brabant Lake zinc-copper mineralization (Coombe, 1975) and possibly the Sherritt-Gordon deposit at Kississing Lake, Manitoba.

A potential exists for economic concentrations of base metals in this type of environment. The difficulty is identifying targets along the many hundreds of kilometres of strike length of these peculiar iron formations.

7. References

Coombe, W. (1975): La Ronge - Wollaston base minerals project; *in* Summary of Investigations 1975, by the Saskatchewan Geological Survey, Sask. Dep. Miner. Resour., p101-109.

Gilboy, C.F. (1982): Geology of an area around Rottenstone and Dobbin Lakes (part of NTS area 74A); Sask. Miner. Resour., Rep. 193, 68p.

Harper, C.T. (1986): Bedrock geology of the Windrum Lake area (part of NTS 64D-4, 73P-16 and 74A-1) *in* Summary of Investigations 1986, Sask. Geol. Surv., Misc. Rep. 86-4, p8-17.

Hoffman, P.F. (in press): Subdivision of the Churchill Province and extent of the Trans-Hudson Orogen; *in* Lewry, J.F. and Stauffer, M.R. (eds.), The Early Proterozoic Trans-Hudson Orogen of North America, Geol. Assoc. Can., Spec. Pap.

Kilburn, J. (1989): Northair plans program for Saskatchewan find; Northern Miner, Dec. 25, 1989, p1.

Lewry, J.F., Curry, A. and Roberts, K. (1990): Geology of an area around Ghana Lake; Sask. Miner. Resour., Rep. 192, 29p.

McMurchy, R.C. (1938): Foster Lake Sheet (east half), northern Saskatchewan; Geol. Surv. Can., Map 433A.

Northern Miner (1990a): Deception Lake drilling comes up short; Feb, 19, 1990, p12.

_____ (1990b): Northair drops Deception Lake; Apr. 9, 1990, p24.

_____ (1990c): Noranda options Deception Lake bet; Oct. 15, 1990, p13.

Shklanka, R. (1962): The geology of the Deception Lake area (east half), Saskatchewan; Sask. Dep. Miner. Resour., Rep. 57, 32p.

Stewart, P. (1989): High amounts of lead and zinc found near Deception Lake; Prince Albert Herald, Oct. 4, 1989.

Stockwell, C.H. (1929): Reindeer Lake area, Saskatchewan and Manitoba: Geol. Surv. Can., Summ. Rep., ptB, p46B-72B.

Thomas, D.J. (1985): Bedrock geological mapping, Roundish - Bervin Lakes area (part of NTS 73P-15 and -16); *in* Summary of Investigations 1985, Sask. Geol. Surv., Misc. Rep. 85-4, p18-27.

Vaughan J.P. and Stanton, R.L. (1986): Sedimentary and metamorphic factors in the development of the Pegmont stratiform Pb-Zn deposit, Queensland, Australia; Trans. Inst. Min. Metall., Sect. B, Appl. Earth Sci., v95, pB94-B121.

Rare Earth Element Mineralization in the Athabasca Group - Maw Zone

D. G. MacDougall

MacDougall, D.G. (1990): Rare earth element mineralization in the Athabasca Group - the Maw Zone; *in* Summary of Investigations 1990, Saskatchewan Geological Survey; Saskatchewan Energy and Mines, Miscellaneous Report 90-4.

The Maw Zone rare earth element (REE) occurrence was discovered near Williams Lake, 5.5 km northwest of Russell Lake - Wheeler River by Agip Canada Ltd., during a 1982 uranium exploration program in the Athabasca Basin (Figure 1). Yttrium values of 300 to 5000 ppm were obtained together with significant values for the heavy rare earth elements in drill core samples. Dravitic tourmalinization and drusy quartz silicification associated with the anomalous REE content is apparent both in core and outcrop (Agip Canada Ltd., 1982-1984). The zone is described as containing 336,000 tonnes of 0.25 percent yttrium oxide (Agip Canada Ltd., 1985; Energy Mines and Resources, 1989).

1. Geological Setting

The Maw Zone lies in an area of moderately well exposed quartz sandstones of the Athabasca Group, Manitou Falls Formation. Exposures are small, but evenly distributed. Surrounding glacial overburden consists of drumlins of sandstone debris. The Maw Zone itself occupies the northern end of a northeast-trending ridge of intermittent outcrop that coincides with the crest of a low amplitude anticline. Stripped of its overburden, the zone forms a prominent and conspicuous landmark.

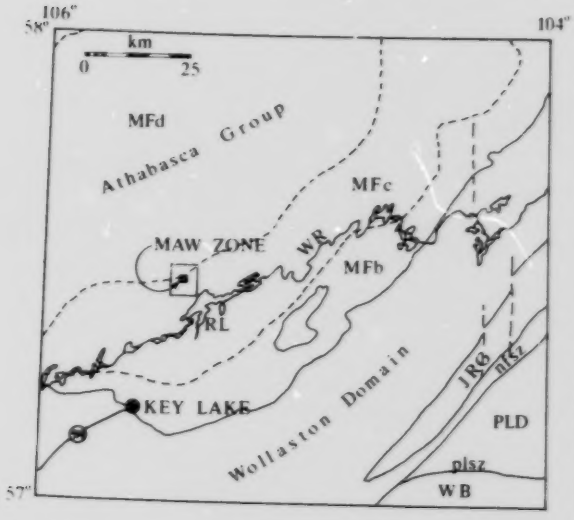

Figure 1 – Regional setting of the Maw Zone: MF - Manitou Falls Formation; MFb - fluviatile conglomerate; MFc - clean sandstone member; MFd - intraclast-rich member; RL - Russell Lake; WR - Wheeler River; JRG - Johnson River Granite; PLD - Peter Lake Domain; WB - Wathaman Batholith; nfsz - Needle Falls Shear Zone; plsz - Parker Lake Shear Zone.

The Manitou Falls Formation in the eastern part of the Athabasca Basin comprises basal fluviatile conglomerates, a middle clean sandstone member and an upper intraclast-rich member (Ramaekers, 1990). The Maw Zone is within the middle clean sandstone member, near its transition to the overlying intraclast-rich member. At Williams Lake, most of the outcrop on the northeast-trending ridge is of cross-bedded, commonly ripple marked and lightly silicified quartz sandstones, whereas away from the ridge, the outcrop consists of unsilicified, cross-bedded quartz sandstones. Outcrop at the Maw Zone shows the greatest degree of silicification and variety of sedimentary features and lithologies. The sandstones are remarkably uniform in appearance except for single grain-diameter grit bands.

The most striking lithology at the Maw Zone is a white to pink to reddish breccia-conglomerate which is not recognized anywhere else in the region. Texturally it varies from breccia, made up of 2 to 40 cm angular quartz sandstone fragments set in a slightly lighter coloured and less durable matrix, to conglomerate, in which the well-rounded fragments are of banded siltstone or hematite stained quartz sandstone lithologies foreign to the immediate area. The breccia ranges from one extreme - "jigsaw breccia" in which the original fit of the fragments can be seen, to a jumbled mass of angular material that includes large (40 to 90 cm) cross-bedded slabs.

Elsewhere the quartz sandstones form a regular, near horizontal stratigraphic sequence bedded at 10 to 30 cm intervals; the bedding planes being marked by either rip-up clay clasts or ripple marks. Rip-up clay clasts about 1 cm thick and 4 cm diameter are composed of white to grey, moderately hard amorphous material which weathers out relatively easily to leave a pock-marked bedding surface. Where weathering has removed the clay, the quartz grains that originally surrounded the clast are seen to be olive green, perfectly spherical and frosted.

The breccia-conglomerate is not confined to any definite narrow linear zones that could be interpreted as faults, but generally forms part of the stratigraphic sequence as continuous beds or as small (60 x 30 cm) discontinuous pockets. In one place breccia containing large slabs of ripplemarked quartz sandstone or sandstone with rip-up clay clasts, and smaller angular sandstone fragments set in a cross-bedded matrix, is banked against regularly stratified outcrop.

Evidence concerning the origin of the breccia-conglomerate is equivocal as one or more of the following interpretations may be applicable: a) talus slope breccia, b) solution collapse breccia, c) frost-shattered or desert pavement and d) shoreline pavement.

2. Alteration and Mineralization

Alteration is expressed as pervasive silicification and by a subtle green colouration along hairline fractures lined with dravite and drusy quartz, and in the matrix of the sandstone and breccia-conglomerate. The REE mineralization is not obvious; rare drusy quartz-lined cavities up to 10 cm across, yellow-brown limonite and clay-coated fractures and clay-filled cavities which occur within the mineralized zone may or may not be related to the mineralization. A weak radioactivity gives readings of 140 to 440 cps (4 to 11 times background) over the strongly stained and clay-altered fractures. In thin sections of the silicified sandstones the original boundaries of the well-rounded quartz grains are outlined by a fine opaque dusting. Needles of dravite (0.05 to 0.1 mm) radiate from the old grain surfaces into the former pore space and are themselves overgrown by quartz that completely fills the interstices and is in optical continuity with the original grains. Clay that fills cavities, coats fractures and forms rip-up clasts, is largely composed of a meshwork of microscopic radiating 'snowflake' dravite clusters and minor randomly oriented illite flakes.

In the breccia, the "snowflake" dravite is concentrated in the matrix, where it composes up to 50 percent of the groundmass. Smaller quartz grains in the matrix are angular and do not have a surface dusting of opaque to mark the position of former grain boundaries. Breccia cracks do not cut across quartz grains, showing that brecciation occurred prior to silicification and before the rock was well-cemented. Some interstices are filled with aggregates of dravite needles and a granular golden to brown, translucent isotropic, unidentified mineral (monazite?).

The greatest concentration of dravite occurs at the Maw Zone where it makes up a significant proportion of the breccia-conglomerate matrix and in some cases the clasts themselves. Lesser amounts of dravite occur in quartz sandstones from other parts of the northeast-trending ridge and decreases to negligible amounts away from the ridge and to the southwest. Outcrops west of Williams Lake contain no dravite needles. Silicification follows the same pattern as dravite.

Geochemical results show that the dravite alteration can be readily detected by boron analysis (Table 1). Boron values of up to 3200 ppm (the Maw Zone) and 1410 ppm (southwest along the ridge) coincide with those samples showing the most dravite in thin section. Yttrium values do not echo those of boron, so that the local degree of dravitization is not a guide to the distribution of yttrium. Yttrium values at the Maw Zone reach 4270 ppm; elsewhere they only reach a maximum of 20 ppm.

Table 1 - Trace Element Analyses Maw Zone & Williams Lake Area

Sample Number	P_2O_5 %	B ppm	Y ppm
90106	0.02	406	10
90107	0.03	236	6
90108	0.02	429	7
90109	0.02	3200	218
90110	0.03	707	991
90111	0.02	215	17
90112	0.02	561	31
90114	0.03	767	4270
90115	0.02	635	29
90116	0.02	502	29
90117	<0.01	124	12
90125	0.01	1410	20
90127	0.01	242	6
90130	0.01	295	8
90131	0.02	230	12
90133	0.01	61	15
90135	0.01	45	9

3. Conclusions

More than one event may have formed the breccia-conglomerate. Its coincidence with mineralization may be fortuitous and thus the lithology may be more widespread, but was made obvious by the silicification that accompanied mineralization. Given the shallow-water fluvial nature of much of the Manitou Falls Formation, it is reasonable to suppose that the deposits were in part exposed and subjected to various fragmentation processes, both soon after deposition and later when more consolidated. Solution collapse processes are more difficult to account for as it is uncertain what would have dissolved to allow the collapse.

The current model for unconformity type uranium deposits (Sibbald, 1985; Sibbald *et al.*, 1990) invokes a low temperature hydrothermal circulation system in the Athabasca sandstones as the conveyor of many elements, particularly uranium, that ended up in the deposits. Key ingredients in their precipitation are the interaction with a basement-derived fluid emanating from faults that disturb the unconformity and the presence of basement graphitic pelites. Developed above the uranium deposits are alteration envelopes typified by illite, chlorite, kaolinite, hematite, silica and dravite. Hoeve and Quirt (1984) envisage Maw Zone type quartz precipitation and REE phosphate mineralization as the outermost, near surface effect of the diagenetic-hydrothermal convective system above developing unconformity-type uranium deposits.

4. References

Agip Canada Ltd. (1982-1984): Assessment File 74H06-NW-0080, Sask. Energy Mines (confidential until 1st May 1991).

_____ (1985): 1985 Annual Report, 13p.

Energy Mines and Resources (1989): Canadian mineral deposits not being mined in 1989; National Mineral Inventory, Mineral Policy Sector, Mineral Bulletin MR 223, (Sask. 47).

Hoeve, J. and Quirt, D.H. (1984): Mineralization and host-rock alteration in relation to clay mineral diagenesis and evolution of the middle Proterozoic Athabasca Basin, northern Saskatchewan, Canada; Sask. Res. Counc., Tech. Rep. No. 187, 187p.

Ramaekers, P. (1990): Geology of the Athabasca Group (Helikian) in northern Saskatchewan; Sask. Energy Mines, Rep. 195, 49p.

Sibbald, T.I.I., (1985): Geology and genesis of the Athabasca Basin uranium deposits; *in* Summary of Investigations 1985, Sask. Geol. Surv., Misc. Rep. 85-4, p133-156.

Sibbald, T.I.I., Quirt, D.H. and Gracie, A.J. (1990): Uranium deposits of the Athabasca Basin, Saskatchewan (field trip 11); 8th IAGOD Symposium Field Trip Guidebook; Geol. Surv. Can., Open File 2166, 56p.

Pyett Lake Pegmatites and Fluoritic Granites, Peter Lake Domain, NTS Area 64E-5

D. G. MacDougall

MacDougall, D.G. (1990): Pyett Lake pegmatites and fluoritic granites, Peter Lake Domain, NTS area 64E-5; *in* Summary of Investigations 1990, Saskatchewan Geological Survey, Saskatchewan Energy and Mines, Miscellaneous Report, 90-4.

The beryl pegmatite[1] sill in dioritic rocks west of Pyett Lake was discovered during regional mapping of the Combe Lake area (Scott, 1970). Scott describes the beryl pegmatite as containing 30 percent each of quartz, plagioclase and microcline, 9 percent muscovite and biotite and 1 percent garnet and beryl, and quotes the assayed beryllium oxide content of the beryl as 10.75 percent. Significantly, several of the felsic plutonic rock units described have syenitic or monzonitic compositions (Scott's, (1970) unit 10, table 10, specimen 2; unit 12a, table 12a, specimen 2; unit 12b, table 12b, specimen 4) or contain sodic amphibole (unit 12a, table 12a, specimen 3).

The present work was aimed at: checking the Be, Li, REE, Nb, Ta, Sn potential of the Pyett Lake beryl pegmatite, investigating its relationship with nearby felsic plutonic rocks, looking for similar pegmatites and determining the nature and extent of the syenitic and monzonitic rocks.

1. Geological Setting

Pyett Lake lies within the Peter Lake Domain, a shear-bounded block between the Wathaman Batholith to the southeast and the Wollaston Domain to the northwest. In the domain Lewry (1976) recognized an older dioritic-gabbroic suite intruded by syenomonzonitic and granitic plutons.

The map-area (Figure 1) is predominantly one of low relief glacial outwash and boulder pavement covered with sparsely treed sphagnum bog, interspersed with well wooded low hills composed mainly of glacial till and moraine, dumped and shaped into ridges in the lee of resistant outcrops. Exposed bedrock, which forms the up-ice edges of the hills, is minimal. An attempt has been made to supplement the previous mapping by using frost heave, disjointed outcrop and other angular material that could be safely judged to be near to source. The rocks in the area belong to three groups: a predominant felsic plutonic suite, a gabbroic-dioritic suite and pegmatites.

2. Felsic Plutonic Suite

The felsic plutonic suite is equivalent to Scott's (1970) units 12a (fine-grained granite), 12b (medium- to coarse-grained granite), 12c (coarse-grained porphyritic granite and 10 (gneissic granite gradational to augen gneiss). Modal analyses of the main rock types recognized here are shown in Table 1; a summary of the chief petrographic features is given in Table 2.

Adamellite (Adm, Adl) outcrops mainly east and south of Pyett Lake as oval bodies less than 1 km^2 in size. It is a salmon-pink, fine-grained to coarse-grained megacrystic rock. Pink and cream mottling of potassic feldspar megacrysts is due to their high content of inclusions. Accessory fluorite occurs as colourless, pale purple to deep purple anhedral interstitial grains, some concentrated in mafic clots; 0.1 mm pale purple cubes, spindles in biotite cleavage planes, small inclusions in apatite and as coatings with biotite on hairline fractures.

The mafic-rich foliated variety (Adm) is composed of a groundmass mosaic of 0.1 to 0.5 mm equant polygonal grains of quartz, untwinned plagioclase and potassic feldspar, and 4 mm megacrysts of quartz, plagioclase and rare potassic feldspar. The quartz megacrysts have been recrystallized into elongate mosaics. Those of plagioclase are irregular anhedral, interlocking, zoned untwinned grains with sericitized cores and exsolved patches of potassic feldspar. Potassic feldspar megacrysts contain carbonate and biotite inclusions and show evidence of crushing and recrystallization to

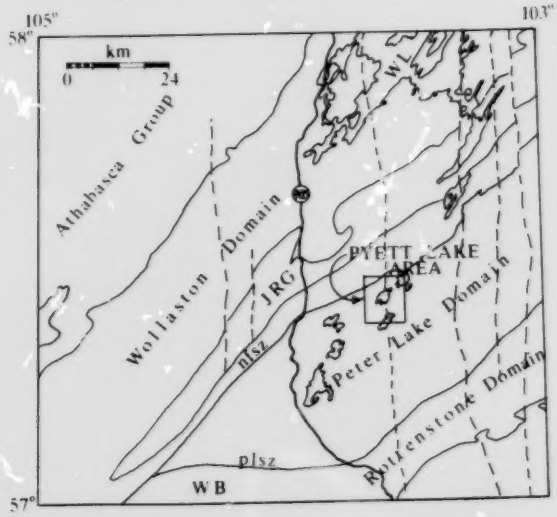

Figure 1 - Regional setting of the Pyett Lake area: WL - Wollaston Lake; JRG - Johnson River Granite; nfsz - Needle Falls Shear Zone; plsz - Parker Lake Shear Zone; WB - Wathaman Batholith.

(1) Pegmatite is used in the sense of granitic pegmatite throughout the text.

Table 1 - Modal Analyses of Felsic Plutonic Rocks

	Adamellite		Granite			Quartz -Syenite	Monzo-nite
Unit	*Adm*	*Adl*	*Ghb*	*G*	*Ga*	*Sq*	*Mz,Mzq*
Mineral%							
Quartz	20-23	20-35	20-35	25-30	25	17-25	0-10
Plagioclase	30-50[1]	35-60	25-35[1]	20[1]	-	15-25[1]	30-48[1]
Composition	An 5	An 4-20	An 0-20	An 10	-	An 15-25	An 5-42
K-spar	10-25	15-30	32-44	48-55	70	40-60	25-50
Hornblende	0-3	-	0-5	-	-	7-10	15
Hastingsite	7-10	tr-3[2]	tr-42	-	2[2]	1-3[2]	7-10
Pyroxene	-	-	-	-	-	-	0-15[3]
Biotite	5-40	1-7	0-7	tr-2	3	2-7	0-10
Muscovite	-	-	tr	-	-	-	-
Chlorite	-	-	-	tr	-	-	-
Carbonate	tr-<1	tr-1	tr	-	-	-	tr
Epidote	tr-1	tr-1	tr-2	tr	tr	tr-1	tr-5
Allanite	tr	-	-	-	-	tr	0-tr
Zoisite	-	-	-	-	-	-	0-5
Apatite	tr	tr	tr	tr	-	tr	0-tr
Fluorite	0-<1	tr-1	tr	-	-	-	0-tr
Zircon	-	tr	tr	-	tr	-	-
Opaque	tr[4]	tr	tr-5[5]	tr-<1[5]	-	tr	-
Sphene	-	-	-	-	-	tr	-
Hematite	-	-	tr	-	-	-	-
No. of thin sections	5	8	13	3	1	4	3

Adm - Mela-adamellite
Adl - Leuco-adamellite
Ghb - Hornblende-biotite granite
G - Granite
Ga - Alkaline Granite

1 - mainly untwinned
2 - ferrohastingsite
3 - diopsidic augite
4 - some pyrite
5 - mainly magnetite

Granite (Ghb, G, Ga) is the predominant underlying bedrock, occupying most of the area north and west of Pyett Lake. Hornblende-biotite granite (Ghb) is salmon-pink weathering, grey to pink, fine grained saccharoidal to coarse grained generally equigranular, unfoliated to weakly foliated and strongly magnetic. The degree of segregation of mafic and felsic constituents increases with the degree of foliation and in extreme cases the rock is a potassic feldspar augen gneiss. Numerous hairline fractures coated with magnetite or biotite are common.

Quartz, plagioclase and potassic feldspar form 2 to 6 mm megacrysts set in a 0.2 to 0.6 mm groundmass made up of a polygonal mosaic of quartz, untwinned sericitized plagioclase and untwinned potassic feldspar.

Quartz megacrysts have been recrystallized to 0.5 to 2 mm granular ribboned mosaic. Untwinned tabular plagioclase megacrysts have undulose extinction and cloudy sericitized cores. Inclusion-filled perthitic potassic feldspar megacrysts in places form 15 mm aggregates and have myrmekitic boundaries with quartz. The inclusions of anhedral plagioclase in potassic feldspar form stringers. Biotite is concentrated at feldspar boundaries, or forms clots, the cores of which are occupied by corroded sieve-textured anhedral to euhedral hornblende or ferrohastingsite laths.

polygonal mosaic. Mafic minerals comprise subhedral 1 to 3 mm corroded amphibole laths, commonly filled with quartz and feldspar inclusions ("sieve-texture") and a variety of brown biotite with strong absorption that forms segregations or 2 mm clots.

The partly gneissic leucocratic variety (Adl) consists of 2 to 12 mm megacrysts of quartz, plagioclase and potassic feldspar set in a groundmass mosaic of 0.2 to 0.6 mm equant polygonal grains of quartz and plagioclase, and interstitial twinned and untwinned potassic feldspar. Quartz megacrysts have been recrystallized into composite mosaics, some drawn out into elongate ribbons parallel to the foliation. Zoned anhedral plagioclase megacrysts are poorly to patchily twinned, have slightly to intensely altered cores, fresh rims, contain exsolved patches of potassic feldspar and are commonly filled with inclusions. Some show distorted twin lamellae and evidence of crushing and recrystallization to polygonal mosaic. Perthitic potassic feldspar megacrysts contain up to 30 percent quartz and plagioclase inclusions. Mafic minerals comprise anhedral to euhedral brown (strong absorption) or green (weak absorption) varieties of biotite and 1 to 2 mm clots of anhedral to subhedral ferrohastingsite laths.

Granite (G) is pink, coarse grained to aplitic, commonly megacrystic, moderately to weakly magnetic, and commonly has segregated mafic streaks or clots. Some hairline fractures are coated with carbonate or contain pyrite.

The 0.1 to 0.4 mm groundmass mosaic consists of polygonal quartz (in some cases forming ribbons), polygonal and lathshaped plagioclase and polygonal potassic feldspar. Set in this are 5 to 10 mm megacrysts of plagioclase and potassic feldspar. Tabular subhedral untwinned plagioclase megacrysts are lightly sericitized. Perthitic potassic feldspar megacrysts are anhedral to subhedral, tabular, inclusion-filled and show crosshatch or Carlsbad twinning and patches of exsolved plagioclase.

Alkali granite (Ga) is a minor pale pink, coarse-grained megacrystic variety represented by only a small area of frost heaved foliated rock near the beryl pegmatite west

Table 2 - Felsic Plutonic Suite; Chief Petrographic Features Summary

Unit		Adm	Adl	Ghb	G	Ga	Sq	Mz
Petrographic feature								
Foliation	-yes	x	some	weak	-	x	-	weak
	-no	-	x	x	x	-	x	x
Gneissosity	-yes	-	some	rare	x	-	-	-
	-no	x	x	x	-	x	x	x
Groundmass polygons	-Plagioclase	x	x	x	-	-	x	x
	-K-spar	x	x	x	x	x	x	x
	-Quartz	x	-	-	-	-	-	x
Megacrysts	-Plagioclase	x	x	x	x	-	x	x
	-K-spar	rare	x	x	x	x	x	x
Cataclasis of megacrysts		x	x	x	-	-	-	-
Quartz ribbons		-	x	x	x	x	x	-
Plagioclase	-Antiperthite	x	x	-	-	-	-	-
	-Zoning	x	x	-	-	-	-	x
	-Sericitic cores	x	x	x	-	-	x	-
	-Twinning	-	patchy	-	-	-	-	x
K-spar	-Perthite	-	x	x	x	x	-	-
	-Inclusions zoned distrib.	-	-	-	-	-	x	-
	-Crosshatch tw.	-	-	-	x	x	x	x
	-Carlsbad tw.	-	-	-	x	x	-	-
Fluorite		x	x	-	-	-	-	x

of Pyett Lake. Anhedral quartz and tabular perthitic potassic feldspar (4 to 8 mm) megacrysts showing crosshatch and Carlsbad twinning are set in a 0.2 to 0.6 mm groundmass mosaic consisting of quartz ribbons and potassic feldspar grains with altered cores. The anhedral ferrohastingsite is filled with inclusions.

Quartz Syenite (Sq) forms small oval or round bodies southwest and north of Pyett Lake. It is a pink, coarse- to fine-grained, commonly megacrystic, unfoliated magnetic rock containing biotite-rich xenoliths and unevenly distributed mafic-rich patches.

Quartz and plagioclase (1 to 3 mm) and potassic feldspar (up to 8 mm) megacrysts are set in a 0.1 to 0.4 mm equant groundmass of polygonal quartz, plagioclase and twinned and untwinned potassic feldspar.

Quartz megacrysts have been recrystallized and drawn out to form elongate composite ribbons consisting of 1 to 3 mm subsidiary grains. The untwinned subhedral plagioclase megacrysts have sericitized cores; the subhedral potassic feldspar megacrysts show crosshatch twinning and zoned distribution of inclusions. Sieve-textured, subhedral to anhedral hornblende or ferrohastingsite laths are, in some samples, segregated into layers with biotite and epidote.

Monzonite (Mz, Mzq) occurs as small pinkish grey to dark grey, fine- to medium-grained, megacrystic feldspathized and epidotized outcrops southwest of Pyett Lake and west of Dunnett Lake, and as angular boulders near the beryl pegmatite.

The monzonite (Mz) groundmass consists of 0.2 to 0.4 mm untwinned, heavily sericitized, polygonal plagioclase and 0.05 to 0.1 mm interstitial potassic feldspar. Set in it are anhedral 1 to 1.5 mm potassic feldspar megacrysts with crosshatch twinning and diopsidic augite as pale green pleochroic, anhedral grains intergrown and overgrown with 2 to 3 mm inclusion-filled hornblende. Ferrohastingsite, where present, forms 0.5 mm euhedral laths. Deep Purple fluorite forms 0.1 mm interstitial patches.

The quartz monzonite (Mzq) groundmass consists of 0.2 mm polygonal quartz grains. Set in this are 1 to 3 mm subhedral tabular zoned plagioclase megacrysts with pericline and lamellar twinning and 4 to 6 mm subhedral tabular potassic feldspar megacrysts having 1 mm plagioclase rims and crosscutting lines of 0.5 mm polygonal plagioclase inclusions.

3. Gabbroic - Dioritic Suite

Modal analyses of the main rock types are shown in Table 3. The suite, which is equivalent to Scott's (1970) units 1 (hornblende gneiss, granulite and amphibolite), 11 (dioritic gabbro) and 13 (trap rocks), outcrops west of Pyett Lake and between Pyett and Dunnett Lakes, where it coincides with a pronounced magnetic high (aeromagnetic map 2760G). Layering is evident in outcrop and from the disposition of the constituent rock types. The various isolated mafic bodies probably represent fragments of one large layered mafic intrusion, dismembered by folding, faulting and intrusion of felsic plutonic rocks. Showings of disseminated chalcopyrite occur in gabbro-diorite on the south shore of the northeast arm of Pyett Lake (Scott 1970) and in leucodiorite on the west shore of Dunnett Lake.

Gabbro - Diorite (GbD) is a dark grey green to black, fine-grained to coarse-grained, nonmagnetic to weakly magnetic rock, in places showing 15 cm scale felsic/mafic layering and ophitic texture. It is composed of predominant hornblende, grey to pinkish or creamy brown plagioclase (some with green sericitized cores) and reddish bronzy biotite. Finer-grained varieties contain conspicuous 5 to 10 mm euhedral plagioclase megacrysts. Near contacts with the felsic plutonic suite it contains granitic clots; microgranitic, aplitic and feldspathic veins and feldspathized fractures. A very fine-

Table 3 - Modal Analyses of Gabbroic - Dioritic Rocks

	Gabbro-Diorite	Norite-Diorite	Leuco-Diorite	Quartz-Diorite
Unit	*Gbd*	*Nrd*	*Dl*	*Dq*
Mineral%				
Quartz	0-8	0-<2	<1-5	15-20
Plagioclase	15-55	53-70	70-90[1]	35-50
Composition				
Unzoned	An 26-48	-	-	An 38-45
Zoned (core)	An 44-67	An 44-58	-	-
Zoned (rim)	An 11-44	An 18-38	-	-
K-spar	0-1	-	-	-
Hornblende	40-80	0-40	3-25	15-50[2]
Orthopyroxene	-	5-25[3]	-	-
Biotite	0-10	1-3	<1-15	0-10
Muscovite	tr	-	-	-
Chlorite	0-tr	-	-	-
Carbonate	0-tr	-	-	tr
Epidote	tr-1	-	tr	0-5
Apatite	0-2	0-tr	tr	-
Opaque	tr-3[4]	0-3	tr[5]	tr
No. of thin sections	15	3	2	3

1-untwinned
2-some actinolite
3-hypersthene in one section
4-some pyrite
5-some chalcopyrite

grained variety forms late stage dykes (equivalent to Scott's unit 13) cutting the coarser phase.

Hornblende is present in two generations in roughly equal proportions; primary zoned, sieve-textured to poikilitic, equant 2 to 3 mm anhedral grains and 0.2 to 0.4 mm euhedral to subhedral, inclusion-free laths in a groundmass aggregate with fresh untwinned polygonal plagioclase. Inclusions in the primary hornblende consist of sericitized plagioclase laths and quartz. Exsolved opaque material parallel to the cleavages is especially abundant in the cores. Subhedral to euhedral, tabular, zoned and twinned plagioclase megacrysts have moderately to severely sericitized cores. Biotite is poikilitic.

Leucodiorite (Dl) is found as very minor layers within the gabbroic - dioritic body west of Dunnett Lake. It is a light grey to dark grey, very fine- to medium-grained rock composed of predominant plagioclase, hornblende and minor biotite. Centimetre to metre scale layering parallel to the foliation is evident in some outcrops.

Hornblende is present as primary 1 to 2 mm anhedral inclusion-filled grains, secondary overgrowth of 0.5 mm euhedral laths and as fracture coatings. Plagioclase forms slightly sericitized, untwinned, polygonal grains and interlocking subophitic 0.5 to 1 mm laths.

Quartz-Diorite (Dq) forms greenish black to black, very fine- to fine-grained dykes cutting the felsic plutonic suite and fine- to medium-grained component layers within the gabbroic-dioritic suite. It is composed of hornblende, plagioclase, quartz and bronzy biotite. The dykes are internally banded parallel to their contacts. Their age relationships with the felsic plutonic rocks are ambiguous; contacts are cleancut, but ptygmatic and linear granitic veins are present in the dyke.

Plagioclase forms a 0.05 to 0.2 mm groundmass of equant polygonal, fresh, twinned and untwinned grains. In this are set 4 mm equant subhedral, sericitized plagioclase and hornblende as anhedral equant megacrysts aligned parallel to a weak foliation or as euhedral to subhedral, interlocking laths forming an overgrowth meshwork.

Noritic Diorite (NrD) forms several thin, medium- to coarse-grained layers in the less altered core of the gabbroic-dioritic suite southwest of Dunnett Lake. The rocks are equigranular, medium grey, strongly magnetic, and composed of predominant greenish grey feldspar, hornblende and minor poikilitic biotite. West of Charles Lake adamellite is chilled against and veins a sill-like body of olive green, very fine-grained megacrystic, noritic diorite.

In the coarser-grained rock, hornblende, where present, forms anhedral to subhedral twinned laths containing numerous inclusions. Orthopyroxene (zoned hypersthene in one example) is present as 0.1 to 0.3 mm equant anhedral, corroded scattered grains, some of them twinned. Plagioclase occurs as 0.3 to 2 mm anhedral, equant, well-twinned, subophitic laths with sericitized cores, some containing biotite and orthopyroxene inclusions.

The sill-like body comprises 1 to 3 mm clusters of inclusion-filled, interlocking, equant, anhedral hornblende megacrysts, set in a groundmass of 0.1 to 0.2 mm euhedral secondary hornblende laths and fresh untwinned polygonal plagioclase. Hornblende is also present as fracture coatings. Orthopyroxene forms remnant cores in amphibole clots.

4. Pegmatites

Three types of pegmatite are recognized; beryliferous, amazonstone-bearing and allanitic. Their modal analyses are listed in Table 4.

Beryl Pegmatite (Pbe) occurs in a 60 m long lens in a north-northeast-trending cliff face of gabbro-diorite west of Pyett Lake. The lens is 1.5 m thick at its maximum, tapering at both ends to splayed 10 to 30 cm thick veins. The cliff face possibly parallels a regional fault along the western shore of Pyett Lake, so that a downthrown southeast extension of the sill may lie under the lake.

The pegmatite lens is symmetrically zoned. An outer 10 cm thick (2 to 4 cm grain size) plagioclase-rich margin gives way to coarser quartz-potassic feldspar-plagioclase core comprising grey to smokey quartz and 20 cm subhedral square sections of white, pinkish or greenish perthitic microcline, in part rimmed with white plagioclase, and rare 4 cm diameter, 4 to 8 cm thick biotite books. Euhedral beryls 10 to 20 cm in diameter are present in the core zone; more numerous 1 to 3 cm diameter and up to 10 cm long, commonly fractured

Table 4 - Modal Analyses of Pegmatites

Unit	Beryl Pegmatite Pbe				Amazonstone Pegmatite Paz	Allanite Pegmatite Pal
Sample Position	*outer margin*	*central margin*	*inner margin*	*core*		
Mineral %						
Quartz	5	5	30-38	25	2-30	25
Plagioclase	90-92	87-95	62-70	5	10-15	15[1]
Composition	An 8-17	An 10-33	An 4-5	An 8	An 12	-
K-spar	tr	0-3	-	70	60-83	60
Biotite	tr	tr	tr	tr	tr	tr
Muscovite	tr	tr	tr	-	tr	tr
Chlorite	tr	tr	-	-	-	-
Carbonate	-	-	tr	-	-	-
Epidote	tr	tr	tr	-	tr	-
Allanite	tr	-	tr	-	-	tr
Zoisite	tr	tr	-	-	-	-
Fluorite	tr	-	-	-	tr	-
Beryl	-	0-10	-	-	-	-
Tourmaline	tr	tr	-	-	-	-
Garnet	tr	tr	-	tr	tr	-
Opaque	-	-	-	-	-	tr
Hematite	-	-	-	-	tr	tr
Diopside	-	tr	-	-	-	-
No. of thin sections	3	2	2	1	2	1

1-untwinned

and impure beryls, partially altered to potassic feldspar, are concentrated in the margin. A black non-magnetic mineral (probably ilmenite), minor sulphide and 0.2 to 0.4 mm pinhead garnets are also present.

In the marginal zone, plagioclase occurs as an interstitial mosaic of 0.1 mm polygonal grains, as 1 to 2 mm interlocking laths and up to 8 mm anhedral irregular grain aggregates made up of 0.2 to 0.6 mm grains with subparallel crystallographic orientations. At the pegmatite contact and at quartz plagioclase boundaries, plagioclase is highly sericitized. Minute needles of opaque material in it form a Widmanstatten pattern. Muscovite forms up to 4 mm poikilitic flakes; biotite is altered to chlorite and is full of opaque exsolved material. Dark brown, red and yellow, anhedral to euhedral and in some cases zoned metamict allanite grains are surrounded by a characteristic halo of radial cracks. Tourmaline occurs as fine needles in groundmass and fractures.

In the pegmatite core, potassic feldspar forms very large perthitic grains containing euhedral quartz and plagioclase inclusions. Plagioclase is present as polygonal fracture fillings in quartz and myrmekite is typically developed at plagioclase/potassic feldspar boundaries.

The sill contains a 50 to 100 cm thick, 3 m long xenolith, which is part of a late stage mafic dyke cutting the gabbro-diorite.

Amazonstone Pegmatite (Paz) is found west of the beryl pegmatite as veins up to 30 cm thick in fluoritic adamellite (Adl) and south of Dunnett Lake as a series of *en echelon* 1.5 to 2 m dykes occupying a 600 m by 200 m zone in granite (G). The rock consists of smokey to intensely black, euhedral bipyramidal quartz, sparse 2 cm biotite books and accessory pinhead garnets set in pale blue amazonstone, brecciated and coated with pink feldspar. Fluorite fills fractures in the quartz.

Potassic feldspar forms 20 to 40 mm perthitic, crosshatch twinned, anhedral grains containing abundant anhedral, crystallographically aligned quartz and plagioclase inclusions. Abundant unidentified, extremely fine opaque inclusions are concentrated in parallel ribbons; platey hematite inclusions parallel the cleavage. Plagioclase forms an interstitial mosaic of 0.4 to 2 mm polygonal grains or subhedral to euhedral interlocking radiating laths, and fracture fillings in potassic feldspar.

Allanite Pegmatite (Pal) occurs as 30 to 60 cm thick veins in xenolithic hornblende-biotite granite (Ghb) frost heave south of Pyett Lake. It comprises very coarse (10 to 20 cm) pink feldspar and quartz set in a medium- to fine-grained (in places aplitic) groundmass of smokey grey quartz and pink and white feldspar. Allanite is present as rare but large (up to 10 cm by 4 cm) euhedral crystals with marked radial fracture haloes up to 20 cm in diameter, and as fine disseminated aggregates in the groundmass.

Large megacrysts of potassic feldspar and smaller ones of plagioclase are set in an interstitial groundmass consisting of 0.2 to 0.6 mm polygonal grains of quartz, plagioclase and untwinned potassic feldspar. Potassic feldspar megacrysts are untwinned, perthitic (up to 20 percent exsolved plagioclase) and contain plagioclase inclusions and fractures filled with quartz. Untwinned round plagioclase megacrysts 2 to 3 mm across have sericitized cores.

Radiometric readings up to 1000 cps are obtained over the pegmatite, and up to 1950 cps over the larger allanites.

5. Geochemistry

Table 5 shows whole rock major oxide and trace element analyses[2] for quartz-syenite, adamellite, gabbro-diorite and the three types of pegmatite. The adamellite and quartz-syenite are distinguished by enhanced lithium and tungsten; anomalous barium, lanthanum and zirconium, and highly anomalous fluorine. Sporadic anomalous tantalum occurs in adamellite.

Beryl pegmatite contains only background lithium, sporadic anomalous tantalum and tin and some anomalous zirconium. Amazonstone pegmatite contains highly anomalous yttrium and fluorine and sporadic anomalous tantalum. Allanite pegmatite is distinguished only by enhanced barium values; despite the presence of allanite (a sample of which returned 3031 ppm yttrium), yttrium values in the pegmatite are background.

6. Conclusions

Relationships of the felsic plutonic rocks to each other and to the gabbroic-dioritic suite are unknown, as unambiguous contacts and cross-cutting veining are not exposed. Of the felsic plutonic rocks, the adamellite and monzonite are marked as the most unusual by their content of accessory fluorite and carbonate. Evidence in both indicates that the original magmas had a high fluorine and CO_2 content that persisted as a volatile phase after consolidation.

The undeformed, post-tectonic pegmatites that intrude representatives of both the felsic plutonic (Adm, Mz, Ghb) and the gabbroic-dioritic suites (GbD) are the youngest rocks in the area. The fluorite content of the beryl and amazonstone pegmatites could be evidence that they are related to the adamellites and monzonite, but there is little similarity in the trace element geochemistry.

Although rare metal values in the quartz-syenite, adamellite and beryl pegmatite are anomalous, they are generally below the range that would be expected if discrete Li, Nb, Ta and Sn mineral phases were present. However, the values are significant because they are equal to or greater than rare metal values reported from pegmatites and granites in the Manitoban Cat Lake - Winnipeg River and Wekusko Lake pegmatite fields (Cerny *et al.*, 1981) and from Red Sucker Lake (Chackowsky and Cerny, 1984). Granitic and pegmatitic rocks in those areas contain, or are closely associated with, highly fractionated pods bearing concentrations of Be, Li, Ta, Sn and REE minerals. In view of this, the Pyett Lake area may be considered to have potential for rare metal mineralization.

7. References

Cerny, P., Trueman D.L., Ziehlke, D.V., Goad, B.E. and Paul, B.J. (1981): The Cat Lake - Winnipeg River and Wekusko Lake pegmatite fields, Manitoba; Manit. Energy Mines; Miner. Resour. Div., Econ. Geol. Rep. ER80-1, 216p (in particular p50-68).

Chackowsky, L.W. and Cerny, P. (1984): Mineralized pegmatitic granites at Red Sucker Lake, Manitoba; *in* Report of Field Activities 1984, Manit. Energy Mines, p184-190.

Geological Survey of Canada (1963): Aeromagnetic map, Combe Lake (NTS 64E-5); Geol. Surv. Can., Map 2760G, scale 1:63,360.

Lewry, J.F. (1976): Reindeer Lake north (SW quarter) area, reconnaissance geological mapping of 64E-3, -4 and -6; *in* Summary of Investigations 1976, Sask. Geol. Surv., p29-35.

Scott, B.P., (1970): The geology of the Combe Lake area, Saskatchewan; Sask. Dep. Miner. Resour., Rep. 135, 32p.

(2) Analyses by Bondar-Clegg and Co. Ltd., Vancouver. Whole rock analysis of major oxides by borate fusion/DC plasma emission; loss on ignition by gravimetry. Trace element analyses as follows: all except B, F and Rb by $HF-HNO_3-HClO_4-HCl$ extraction and induction coupled plasma; B by potassium hydroxide fusion/DC plasma emission; F by potassium hydroxide fusion/specific ion analysis; Rb by potassium hydroxide fusion/X-ray flourescence

Table 5 - Whole Rock and Trace Element Analyses

UNIT	Sq	Adl	Adl	Adl	GbD	Pbe	Pbe	Pbe	Pbe	Pbe	Pbe	Pbe	Paz	Paz	Paz	Paz	Paz	Pal	Pal
SAMPLE	85143	85146	85148	90092	85150	85152	85153	85158	90003	90004	90051	90055	90012	90039	90040	90042	90074	90097	90099
%																			
SiO_2	69.50	69.40	70.40	74.20	49.80	74.70	75.80	68.20	66.60	72.80	75.60	67.00	73.00	78.70	70.10	80.20	74.20	73.70	74.40
Al_2O_3	13.00	13.00	12.50	11.70	16.00	12.20	12.70	19.60	17.70	15.70	13.10	18.80	16.00	11.80	16.10	10.80	14.40	13.60	13.40
TiO_2	0.61	0.51	0.41	0.32	1.19	0.20	0.05	0.12	0.02	0.02	0.09	0.03	0.02	0.01	0.01	0.01	<0.01	0.04	0.04
Fe_2O_3	5.02	4.60	3.47	2.42	12.40	3.13	0.73	1.9	0.56	0.54	1.38	0.53	0.59	0.63	0.30	0.60	0.47	0.69	0.77
MnO	0.10	0.09	0.09	0.04	0.17	0.02	0.01	0.02	0.01	0.11	0.01	0.02	0.26	0.05	0.02	0.02	0.08	<0.01	<0.01
MgO	0.74	0.71	0.52	0.31	6.42	0.78	0.16	0.37	0.09	0.06	0.25	0.13	0.03	0.10	0.03	0.07	0.02	0.09	0.12
CaO	1.95	1.23	1.23	0.86	8.28	1.93	1.61	1.77	0.46	0.43	1.42	0.97	0.45	0.21	0.15	0.55	0.19	0.54	0.33
N2O	3.45	3.76	3.12	3.68	2.89	4.12	5.95	4.73	5.09	6.27	6.41	9.53	8.78	5.52	4.26	5.17	5.91	3.81	3.12
K2O	5.04	4.32	5.58	4.71	1.02	0.41	0.36	0.57	6.90	4.18	0.30	0.32	0.80	2.44	8.16	1.99	4.17	5.63	7.02
P_2O_5	0.21	0.16	0.17	0.20	0.20	0.18	0.24	0.15	2.48	0.08	0.08	0.56	0.25	0.06	0.19	0.02	0.09	0.23	0.26
LOI	0.45	0.75	0.73	0.30	0.77	0.95	0.75	0 30	0.15	0.15	0.64	0.58	<0.05	<0.05	0.34	0.19	0.15	0.48	0.45
TOTALS	100.07	98.53	98.22	98.74	99.14	98.62	98.36	98.30	100.06	100.34	99.28	98.47	100.18	99.52	99.66	99.62	99.68	98.81	99.91
ppm																			
Li	41	91	74	9	18	15	11	8	8	5	10	8	7	6	12	8	5	6	5
Rb	196	277	312	215	30	42	24	20	1293	762	31	45	169	321	1016	248	601	250	391
Sr	103	113	97	25	452	192	233	242	26	18	165	61	<1	3	2	<1	<1	54	27
Ba	821	844	768	365	358	125	100	138	54	27	95	27	<1	11	13	<1	19	175	287
Y	31	39	55	39	12	14	12	69	7	15	23	14	46	34	138	321	19	15	9
La	26	44	34	52	<1	2	<1	21	<1	<1	2	<1	<1	<1	<1	2	<1	<1	<1
Zr	287	308	276	277	49	202	73	102	16	30	31	63	50	29	20	28	36	43	41
Nb	32	28	25	31	15	25	18	38	27	29	27	27	25	9	11	4	10	24	12
Ta	26	21	105	67	<1	21	16	90	38	89	<1	<1	70	81	46	<1	32	30	<1
W	59	16	<10	<10	14	19	16	<10	<10	<10	<10	<10	<10	12	<10	<10	<10	<10	<10
Sn	<20	<20	<20	<20	<20	<20	<20	<20	<20	26	<20	45	<20	<20	<20	<20	<20	<20	<20
B	43	44	38	17	31	1990	46	532	14	10	143	20	12	16	14	18	14	25	22
Ga	11	15	24	7	<2	18	8	15	32	29	12	36	33	11	20	10	25	22	15
F	1283	2969	5080	1165	334	126	51	75	40	48	92	129	1875	67	264	1041	45	76	73

Geochemistry of Miscellaneous Pegmatites in the Wollaston, Peter Lake and Glennie Domains

D. G. MacDougall

MacDougall, D.G. (1990): Geochemistry of miscellaneous pegmatites in the Wollaston, Peter Lake and Glennie Domains; *in* Summary of Investigations 1990, Saskatchewan Geological Survey; Saskatchewan Energy and Mines, Miscellaneous Report 90-4.

Five pegmatite bodies were chosen for geochemical analysis on the basis of unusual mineral content or associations described in the literature. They include three from the Wollaston Domain (Figure 1) and one each from the Peter Lake (Figure 1) and Glennie Domains (Figure 2).

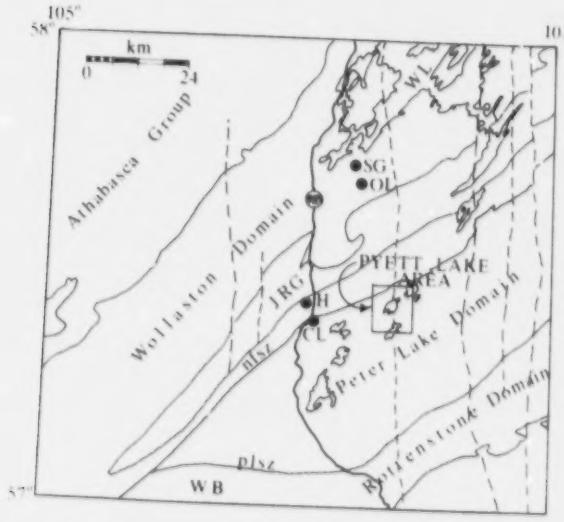

Figure 1 – Regional setting of the Wollaston and Peter Lake Domain miscellaneous pegmatites: SG, Salaba Lake - Geikie River; OL, Oriordan Lake; H, Hill 462; CL, Courtenay Lake; WL, Wollaston Lake; JRG, Johnson River Granite; nfsz, Needle Falls Shear Zone; plsz, Parker Lake Shear Zone; WB, Wathaman Batholith.

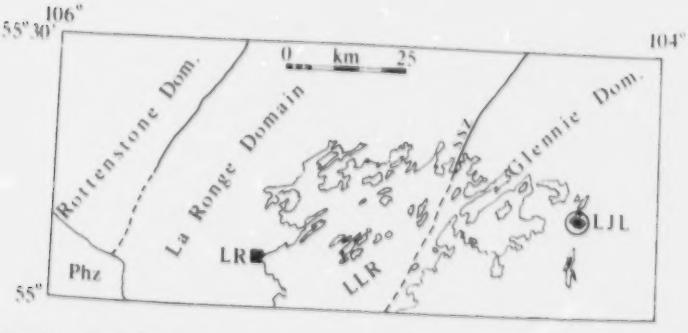

Figure 2 – Regional setting of the Lee - Jahala Lake pegmatite; LJL, Lee - Jahala Lake; Phz, Phanerozoic cover; LR, La Ronge; LLR, Lac La Ronge; ssz, Stanley Shear Zone.

1. Wollaston Domain

a) Salaba Lake - Geikie River (NTS 64E-12)

Chadwick (1967) described a plagioclase-quartz-biotite pegmatite containing rare interstitial fluorite in contact with fluoritized biotite paragneiss north of a small lake between Salaba Lake and the Geikie River. Great Plains Development Company of Canada Ltd. (1969) trenched and drilled the outcrop, reporting radiometric readings of up to 6000 cps and uranium values of up to 0.243 percent U_3O_8 in trench 2. The rock is typically pink, medium-grained (1 to 3 mm) unfoliated granite containing little visible quartz or mica. Fresh material from trench 2 is white and contains disseminated carnotite, uranophane, allanite, purple fluorite, and possibly monazite. Fracture-bound allanite is also present. Drill core shows that the metasedimentary succession to the north of the granite comprises plagioclasite, biotite-quartz-feldspar gneiss containing traces of pyrrhotite, chalcopyrite and pyrite, and biotite-quartz-pink feldspar gneiss.

b) Oriordan Lake (NTS 64E-12)

Chadwick's (1967) map shows a 1.5 km outcrop of diopside-plagioclase pegmatite northeast of Oriordan Lake. In fact exposure in this area is very poor, and the rock is not a pegmatite, but is a pinkish grey medium-grained (2 to 4 mm) gneissic calc-silicate rock made up of pink feldspar, greenish grey feldspar, possibly some scapolite, quartz, biotite and ilmenite. No diopside is present. Glacial debris and frost heaved material shows a variety of calcareous meta-arkosic rocks are present in the area, all containing obvious ilmenite. Some of the meta-arkose is foliated and contains 1 to 2 cm orbicular feldspar porphyroblasts rimmed with quartz.

c) Hill 462 (NTS 64E-5)

Scott (1970) records white pegmatite containing rose muscovite or lithium mica, in mixed Wollaston Group metasediments 3.5 km north of Courtenay Lake. The occurrence consists of frostheaved slabs of rusty-weathering, white, but locally medium- to coarse-grained (4 to 8 mm), two-mica granite. Thin section shows the muscovite to be a pale green variety as radiating clusters or as poikilitic flakes. Biotite contains spindles of zoisite and is chloritized.

2. Peter Lake Domain

a) Courtenay Lake (NTS 64E-5)

The beryl pegmatite sill reported by Scott (1970) is a poorly exposed, pink, coarse-grained granitic rock comprising smokey to black, subhedral quartz, pink anhedral feldspar, green muscovite and fairly common 5 to 10 mm diameter euhedral pale green beryls. Thin sections show interstitial purple fluorite and garnet in the pegmatite with fluorite also in the quartz-muscovite host rock. The green muscovite is concentrated in a 1 to 3 cm thick zone in the pegmatite margin. Angular quartz-rich ilmenite-bearing pegmatite debris close to the exposed pegmatite possibly represents material from the core of the sill.

3. Glennie Domain

a) Lee - Jahala Lake (NTS 73P-1)

Radioactive pegmatites were discovered on the east shore of Lee - Jahala Lake in 1949 (Sabina, 1987; Forsythe, 1981). There are two groups of showings; the main northern one, in which an inclined shaft was sunk in 1954, contains large uraninite crystals (Saskatchewan Mineral Deposits Index No. 0720) and a southern group (SMDI No. 0721) which were trenched and contain uranophane and pitchblende. Samples reported here were taken from two large north-northeast-trending pegmatite dykes, one occupying the ridge of land separating Lee - Jahala Lake from Tagseth Lake to the east (the Ridge pegmatite) and the other outcropping along the west shore of Tagseth Lake itself (the Tagseth pegmatite). The pegmatites are near vertical, greater than 5 m thick and over 70 m in strike length. Both contain xenoliths of biotite-hornblende granulite host rock. The Ridge pegmatite consists of coarse (> 10 cm) pink feldspar graphically intergrown with quartz; minor smokey quartz and sparse thin lath-shaped plates of biotite. Its eastern margin, which has been extensively trenched and pitted, is highly fractured and radioactive (up to 2400 cps compared to 140 cps in the interior). The Tagseth pegmatite is composed of coarse (up to 20 cm) subhedral to euhedral pink feldspar graphically intergrown with quartz, minor smokey quartz and accessory garnet, muscovite and biotite. Quartz lenses 30 cm thick and 3 m long are present parallel to the pegmatite contacts. Radiometric readings range from 180 to 450 cps.

4. Geochemistry

The only geochemical data[1] available from the Salaba Lake - Geikie River pegmatite is for yttrium, which is high in one sample (82 ppm) and elevated in the other three (21 to 22 ppm). In the other pegmatites, strontium, tungsten, tin, boron and gallium are low in all samples (Table 1).

Table 1 - Whole Rock and Trace Element Analyses

	COURTENAY LAKE						HILL 462				LEE-JAHALA LAKE					
ROCK TYPE	Beryl Pegmatite						Quartz-rich Pegmatite				Ridge Pegmatite			Tagseth Pegmatite		
SAMPLE	90136	90137	90138	90140	90141	90142	90144	90147	90150	90153	90158	90159	90163	Garn 90164	Musc 90166	Biot 90167
%																
SiO2	71.20	71.20	75.00	74.60	74.60	73.40	92.50	84.20	70.00	78.70	72.80	72.00	73.70			
Al2O3	15.40	15.40	13.20	13.50	13.30	14.20	2.57	7.49	15.60	12.10	13.70	13.80	14.40			
TiO2	<0.01	<0.01	0.07	0.15	0.01	0.02	0.06	0.02	<0.01	0.04	<0.01	<0.01	0.02			
Fe2O3	0.54	0.48	1.19	2.56	0.98	0.74	0.79	0.52	0.40	0.65	0.24	0.25	2.19			
MnO	0.21	0.09	0.23	0.15	0.62	0.38	0.01	0.01	0.08	0.07	<0.01	<0.01	0.52			
MgO	0.02	0.03	0.09	0.19	0.04	0.05	0.09	0.08	0.05	0.15	0.03	0.02	0.09			
CaO	0.33	0.60	0.31	0.31	0.19	0.18	0.01	0.06	0.03	0.39	0.04	0.05	0.94			
N2O	4.67	4.07	1.89	0.34	5.58	4.59	0.28	0.87	2.72	4.31	1.89	1.95	5.00			
K2O	5.88	6.57	5.74	4.72	2.49	4.42	1.85	5.62	9.89	2.19	9.63	9.74	1.59			
P2O5	0.46	0.81	0.91	0.42	0.36	0.75	0.28	0.17	0.18	0.16	0.18	0.09	0.19			
LOI	0.69	0.34	0.99	1.73	0.39	0.54	0.20	0.24	0.30	0.58	0.15	0.44	0.39			
TOTALS	99.40	99.59	99.62	98.67	98.56	99.27	98.64	99.28	99.25	99.34	98.66	98.34	99.03			
ppm																
Li	2	12	4	16	2	43	1	3	1	5	2	2	16	24	145	694
Rb	909	1013	867	704	420	699	75	174	547	134	302	330	112	25		
Sr	<1	<1	7	4	<1	<1	17	66	3	<1	16	14	10	6		
Ba	22	19	231	567	22	14	596	1873	160	42	75	38	<1	<1		
Y	<1	1	6	15	2	<1	2	<1	3	3	4	<1	74	329		
La	<1	<1	17	74	<1	<1	<1	<1	<1	<1	<1	<1	7	16		
Zr	26	14	85	163	47	87	18	96	42	30	21	16	56	24		
Nb	20	34	24	32	22	73	3	29	45	85	16	11	32	13		
Ta	<1	<1	<1	<1	32	157	22	<1	122	25	78	92	43	<1		
W	<10	<10	<10	<10	<10	<10	10	<10	<10	<10	<10	<10	<10	<10		
Sn	<20	<20	<20	<20	<20	<20	<20	<20	<20	<20	<20	<20	<20	<20	190	32
B	21	21	26	40	20	16	14	13	13	16	10	10	15			
Ga	2	12	4	16	2	7	<2	<2	14	19	6	10	14	6		
F	40	318	468	923	2300	330	268	58	41	155	32	29	299			

(1) Analyses by Bondar-Clegg & Co. Ltd., Vancouver. Whole rock analysis of major oxides by borate fusion/DC plasma emission; loss on ignition by gravimetry. Trace element analyses as follows: all except B, F and Rb by HF-HNO_3-$HClO_4$-HCl extraction and induction coupled plasma; B by potassium hydroxide fusion/DC plasma emission; F by potassium hydroxide fusion/specific ion analysis; Rb by potassium hydroxide fusion/X-ray fluorescence.

Rubidium and fluorine are high in the Courtenay Lake beryl and quartz-rich pegmatites, which also contain sporadic high barium, lanthanum, zirconium, niobium, tantalum and lithium. The Courtenay Lake quartz-rich pegmatite contains unusually high barium (maximum 1873 ppm). The trace element anomalies in the Courtenay Lake beryl pegmatite, which classify it as well-fractionated, may be significant because they are in the same order of magnitude as those values reported from the Manitoban Cat Lake - Winnipeg River and Wekusko Lake pegmatite fields (Cerny *et al.*, 1981) and from Red Sucker Lake (Chackowsky and Cerny, 1984). Granitic and pegmatitic rocks in those areas contain, or are closely associated with, highly fractionated pods bearing concentrations of Be, Li, Ta, Sn and REE minerals.

In the Hill 462 pegmatite niobium and tantalum values are high. The low lithium content rules out the presence of lithium mica.

The Lee - Jahala Lake pegmatites show moderately elevated tantalum. Low yttrium values from the Ridge pegmatite dictate also low heavy REE content, however high yttrium and elevated fluorine in the Tagseth pegmatite show the neighbouring pegmatite to be geochemically different, raising the possibility of a systematic variation in composition across the pegmatite field. Lithium and tin are concentrated in the micas; lithium in the biotite and tin in the muscovite. Yttrium is concentrated in the garnet (Table 1).

5. References

Cerny, P., Trueman D.L., Ziehlke, D.V., Goad, B.E. and Paul, B.J. (1981): The Cat Lake - Winnipeg River and Wekusko Lake pegmatite fields, Manitoba; Manit. Dep. Energy Mines; Miner. Resour. Div., Econ. Geol. Rep. ER80-1, 216p (in particular p50-68).

Chackowsky, L.W. and Cerny, P. (1984): Mineralized pegmatitic granites at Red Sucker Lake, Manitoba; *in* Report of Field Activities 1984, Manit. Energy Mines, p184-190.

Chadwick, B. (1967): The Geology of the Morell Lake area (west half) Saskatchewan; Sask. Dep. Miner. Resour., Rep. 116, 24p.

Forsythe, L.H. (1981): Geology of the Lac La Ronge - Hunter Bay - Cartier Lake Area, Saskatchewan; NTS area 73P-1, -2, -3(E); Sask. Miner. Resour., Open File Rep. 81-1, 20p.

Great Plains Development Company of Canada Ltd. (1969): Assessment File 74H-0006, Sask. Energy Mines.

Sabina, A.P. (1987): Rocks and minerals for the collector; La Ronge - Creighton, Saskatchewan; Flin Flon - Thompson, Manitoba; Geol. Surv. Can., Misc. Rep. 42, p9.

Saskatchewan Mineral Deposits Index; Sask. Energy Mines computer file.

Scott, B.P. (1970): The geology of the Combe Lake area, Saskatchewan; Sask. Dep. Miner. Resour., Rep. 135, 32p.

Aeromagnetic Anomaly Ground Check for Kimberlite Exposures in the Precambrian Shield

W.L. Slimmon

Slimmon, W.L. (1990): Aeromagnetic anomaly ground check for kimberlite exposures in the Precambrian Shield; *in* Summary of Investigations 1990, Saskatchewan Geological Survey; Saskatchewan Energy and Mines, Miscellaneous Report 90-4.

This summer two days were spent ground checking four aeromagnetic anomalies determined by M. Gent to be favorable for the possible existence of kimberlitic rocks. The anomalies were picked from Geological Survey of Canada (1971) 1:250,000 scale aeromagnetic map 8190G and are underlain by the Precambrian Shield east of Lac La Ronge (Figure 1). The circular to oval shaped aeromagnetic anomalies range from 0.4 to 1.2 km in diameter and from 80 to 200 gammas above background aeromagnetic values. In the field, a hand-held flux-gate magnetometer was used to determine the area of highest magnetic signature which was then searched for signs of kimberlitic outcrops or boulders. Soil samples were taken from the centre of each anomaly for later analysis.

1. Regional Geology

All four anomalies are situated in the west-central part of the Glennie Domain of the Trans-Hudson Orogen. Anomalies A, B and C are underlain by granitoid gneisses, and anomaly D is underlain by mafic to mafelsic amphibolitic supracrustal rocks of probable volcanic origin (Lewry and Slimmon, 1985).

2. Anomaly A: (UTM - 560750mE, 6131600mN)

Background magnetometer value: 59,800 gamma maximum magnetometer value: 63,050 gammas

Country rock consists of granodiorite gneiss containing a few mafic hornblendic pod-like layers and granitic sweats. The anomaly is strongest in a topographic low with no outcrop and only a few exposed granodioritic boulders. A few metres to the south, on the edge of the topographic low, a medium- to coarse-grained amphibolite is exposed along the margin of the granodioritic country rock.

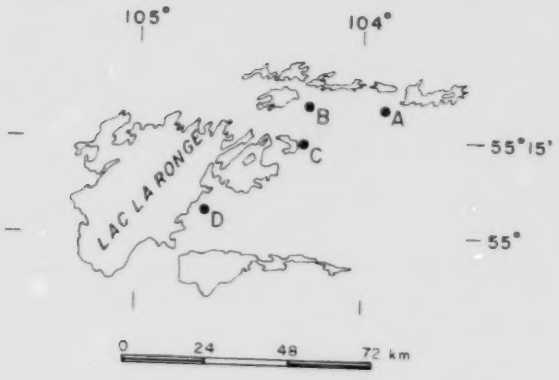

Figure 1 - Location of aeromagnetic anomalies investigated.

3. Anomaly B: (UTM - 546300mE, 6132500mN)

Background magnetometer value: 59,400 gammas
Maximum magnetometer value: 60,700 gammas

Highest magnetic values were obtained in a low swampy area with no evidence of outcrop or boulders in the immediate vicinity. Country rock is exposed within 25 m of the anomaly and consists of granodiorite gneiss.

4. Anomaly C: (UTM - 546200mE, 6122000mN)

Background magnetometer value: 59,700 gammas
Maximum magnetometer value: 65,125 gammas

Highest readings occur on the edge of a muskeg where no outcrop or boulders are present. Approximately 10 m south of the magnetic high, a highly magnetic fine- to medium-grained amphibolite is exposed along the margin of a large granodioritic outcrop.

5. Anomaly D: (UTM - 519800mE, 6102250mN)

Background magnetometer value: 58,800 gammas
Maximum magnetometer value: 59,700 gammas

Country rock consists of fine-grained intermediate to mafic amphibolite gneiss. The highest magnetic values are on the edge of a boulder strewn hill with no outcrop exposed for several tens of meters. The boulders range from granitic to dioritic in composition.

6. Conclusions

No kimberlitic outcrops or boulders were found in the vicinity of the four aeromagnetic anomalies checked. Anomalies A and C are possibly caused by unexposed magnetite-bearing amphibolite plugs similar to the material exposed close to the margins of both anomalies. The cause of anomalies B and D is open for speculation since there is no exposed outcrop in their

immediate vicinities. Boulders in these two areas are neither kimberlitic nor show high concentrations of magnetite.

7. References

Geological Survey of Canada (1971): Aeromagnetic map, Lac La Ronge (NTS 73P), Saskatchewan; Geol. Surv. Can., Map 8190G, scale 1:253,330.

Lewry, J.F. and Slimmon, W.L. (1985): Compilation bedrock geology, Lac La Ronge, NTS area 73P/73I; Sask. Energy Mines, Rep. 225.

Mineralized Core Collection

A.J. Gracie

Gracie A.J. (1990): Mineralized Core Collection; *in* Summary of Investigations 1990, Saskatchewan Geological Survey; Saskatchewan Energy and Mines, Miscellaneous Report 90-4.

The Mineralized Core Collection has been previously described (Gracie, 1984, 1985, 1986, 1987, 1988, 1989) and a revised index for the collection (Gracie and Scutt, 1990) was published. The index identifies the location of all cores by latitude and longitude on 1:250,000 scale maps, and gives full particulars of each hole: company, mineral dispositions, exploration commodity, year, hole number, core size, hole bearing and inclination, length of sample, reference to other exploration data and storage location.

The mineralized core is housed in the Precambrian Geological Laboratory in La Ronge. Contributions totalling some 3287.4 m in 1990 (Table 1) were made up of cores from mineral properties drill tested for uranium (61 percent), base metals (29 percent), REE (8 percent) and gold (3 percent). The collection is augmented by suites of rock samples from numerous mineral properties in northern Saskatchewan. Important stratigraphic cores such as deep holes in the Athabasca Basin, are housed in the Subsurface Geological Laboratory in Regina. No additions of these cores were made last year.

Mineralized uranium cores were exhibited to participants in the International Association on the Genesis of Ore Deposits: IAGOD Symposium, Uranium Deposits of the Athabasca Basin, Saskatchewan field trip and to trainees of an International Atomic Energy Agency uranium geology and exploration program at the University of Regina. Also, a variety of mineralized cores were examined and sampled by research and exploration geologists.

1. References

Gracie, A.J. (1984): Mineralized core collection; *in* Summary of Investigations 1984, Sask. Geol. Surv., Misc. Rep. 84-4, p127-128.

Table 1 - Mineralized Core Acquistions (September 1, 1989 to August 31, 1990).

Company or Joint Venture Operator	Commodity	NTS Area	No. of Holes	Core Size	Property/Deposit Location by Lake	Length (m)
Asamera Oil Corp. Ltd.	U	64-L-05	2	NQ	Dawn Lake	259.6
AGIP(Canada) Ltd.	REE	74-H-06	1	NQ	Maw Zone	272.8
Cameco	(Cu,Zn)	63-L-10	4	NQ,BQ	Miskat Lake	170.1
	(Zn,Pb,Ag,Cu,Au)	63-L-10	1	BQ	Old Hanson Lake Mine Zone	148.5
	(Cu,Zn,Ag)	63-L-10	1	NQ	McIlvenna Bay	126.1
	U	64-L-05	1	NQ	Eagle Point North	301.7
	U	64-L-05	1	NQ,BQ	Eagle Point South	224.6
	U	74-H-10	1 Incomplete	NQ,BQ	BJ Zone	462.2
	U	74-H-11	1 Incomplete	BQ	P2 Main	307.1
Cigar Lake Mining Corp.	U	74-I-02	1	NQ	Cigar Lake Mine	433.0
Corona Corp.	Au	63-M-06	1	NQ	Manawan Lake	59.8
Gamsan Resources Ltd.	(Zn,Cu,Pb,Ag)	64-D-04	2	NQ	McKenzie Orebody, Brabant Lake	491.0
Newmont Mining Corp. of Canada Ltd.	Au	74-B-13	1	BQ	Ithingo Lake	30.2

_____ (1985): Mineralized core collection; *in* Summary of Investigations 1985, Sask. Geol. Surv., Misc. Rep. 85-4, p82.

_____ (1986): Mineralized core collection; *in* Summary of Investigations 1986, Sask. Geol. Surv., Misc. Rep. 86-4, p121-122.

_____ (1987): Mineralized core collection; *in* Summary of Investigations 1987, Sask. Geol. Surv., Misc. Rep. 87-4, p80-81.

_____ (1988): Mineralized core collection; *in* Summary of Investigations 1988, Sask. Geol. Surv., Misc. Rep. 88-4, p125-126.

_____ (1989): Mineralized core collection; *in* Summary of Investigations 1989, Sask. Geol. Surv., Misc. Rep.89-4, p110-111.

Gracie, A.J. and Scutt A.G. (1990): Index to La Ronge core collection; Sask. Energy and Mines, Data File 15, 228p.

Contributed Northern Geoscience Reports

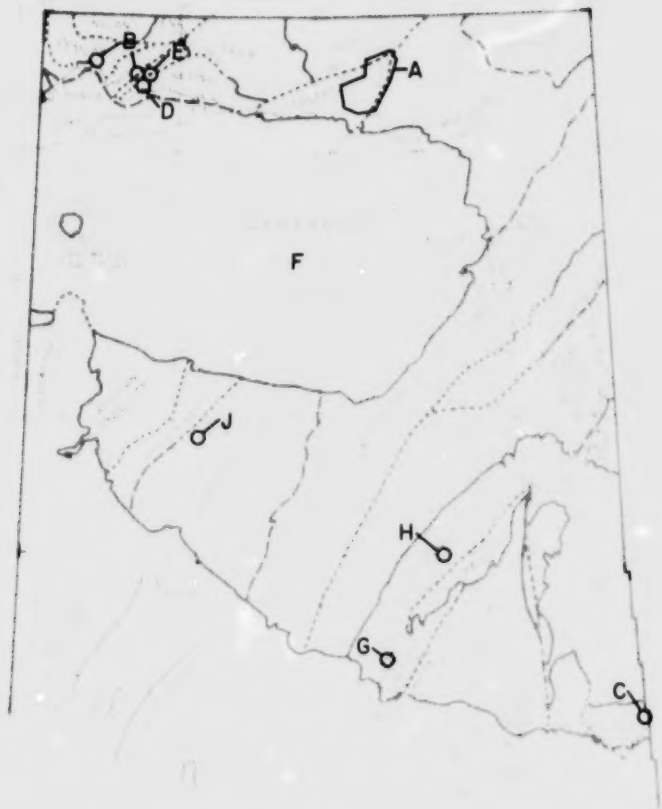

Location of projects for papers contributed to this volume. The base map shows in abbreviated form the location of the main lithostructural domains in northern Saskatchewan.

A The Snowbird Tectonic Zone, Stony Rapids Area, Northern Saskatchewan
Simon Hanmer, Shao Chengji, Mark Darrach and Chris Kopf (F)

B Lithogeochemistry and XRD Mineralogy of the Martin Group and Related Rocks, Greater Beaverlodge Area
David H. Quirt

C Age of Granitoids from the Flin Flon Domain: An Application of the Single-zircon Pb-evaporation Technique
Kevin M. Ansdell and T.K. Kyser

D Rb-Sr Geochronology of the Lodge Bay Granite, a ca. 3.0 Ga Basement in the Beaverlodge Area
Michael Bikerman, Keith Bell and John Blenkinsop (X)

E Metasomatic Host-rock Alteration at the Frontier Gold Prospect, Goldfields Area
David H. Quirt

F Fluid History of the Athabasca Basin and its Relation to Uranium Deposits
T. Kotzer and T.K. Kyser

G Site Investigation of a Biogeochemical Gold Anomaly near Wadin Bay, Lac La Ronge
C.E. Dunn and P.L. Schwann (F,J)

H Fluid Inclusion, Stable Isotope and Microprobe Data from the Jasper Zone Lode Gold Deposit, La Ronge Domain
F. Hrdy, T.K. Kyser and R.T. Kusmirski

I Petrology of Some Mafic Gneisses, Black Birch Lake, Saskatchewan
S. Orrell and J. Tangeman (X)

F Field component in 1990
J Joint venture with SEM in 1990
X Derived from earlier joint venture study

The Snowbird Tectonic Zone, Stony Rapids Area, Northern Saskatchewan

Simon Hanmer[1], *Shao Cheng Ji*[1], *Mark Darrach*[2] *and Chris Kopf*[3]

Hanmer, S., Cheng Ji, S., Darrach, M. and Kopf, C. (1990): The Snowbird Tectonic Zone, Stoney Rapids area, northern Saskatchewan; *in* Summary of Investigations 1990, Saskatchewan Geological Survey, Saskatchewan Energy and Mines, Miscellaneous Report 90-4.

A high amplitude linear anomaly in the horizontal gravity gradient map of the Canadian Shield extends from the Canadian Rocky Mountains to the coast of Hudson Bay, near Baker Lake and beyond. Low amplitude anastomosing linear elements in the magnetic field also occur along the trend of the gravity anomaly and define an elliptical area (300 by 100 km) to the southwest of Stony Rapids. This geophysical feature, the Snowbird tectonic zone (Hoffman, 1988), has been considered as a possible Early Proterozoic suture (Thomas *et al.*, 1988; Hoffman, 1988). Others considered that it reflects a fundamental intra-plate boundary, related to the Trans-Hudson Orogen (Lewry *et al.*, 1978; Lewry and Sibbald, 1980; Thomas and Gibb, 1985). However, the geological nature of this important tectonic line is little known. In this contribution, we treat the Tantato Domain (Figure 1) as a segment of the Snowbird tectonic zone. The interested reader is referred to an expanded version of this report which will appear elsewhere (Hanmer *et al.*, in prep.).

1. Principal Elements

Within the areas we have examined, the principal results of our field work are:

1) Geometrically, the Tantato Domain can be divided into two parts. A hanging wall panel of shallowly to steeply dipping granulite mylonites between Clut Lakes and the Fond du Lac River (Figures 2 and 3), and a footwall of steeply dipping granulite to amphibolite facies mylonites. Lineations in the granulite panel trend northeast-southwest to east-west; those in the footwall trend northeast-southwest and 'porpoise' about the horizontal.

2) Kinematically, the eastern half of the footwall contains sinistral shear features, whereas the western half contains dextral shear features. No evidence for earlier shearing of opposite sense has been observed anywhere within the footwall. Qualitatively, the volumes of rock affected and intensity of the deformation are of equal importance in both the sinistrally and dextrally sheared parts of the footwall. Taken as a whole, the progressive deformation of the footwall appears to reflect large-scale boundary conditions approximating to pure shear.

(3) Shear sense deduced in the granites at the contact between the hanging wall panel and the footwall (Figure 3) indicate post-granulite extensional displacement of the hanging wall, down towards the west. No visible shear features were observed within the granulite panel itself, but the occurrence of granulite facies mylonites in the hanging wall overlying amphibolite facies mylonites in the footwall suggests that the granulite panel may have been initially thrust emplaced.

4) Petrologically, the Tantato Domain comprises 5

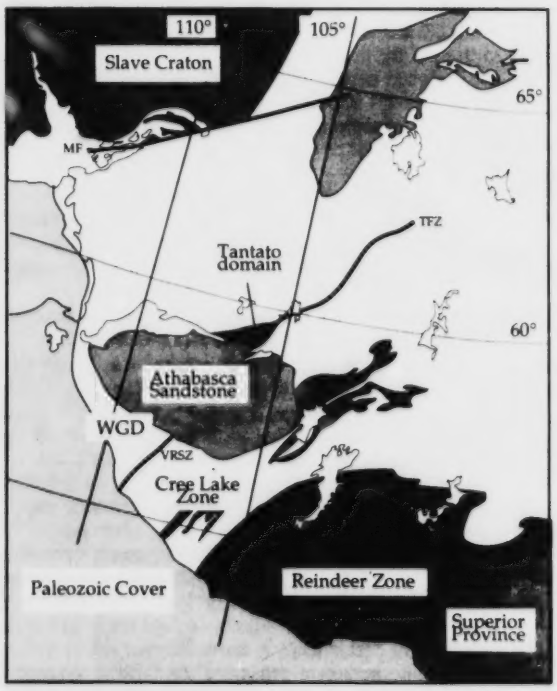

Figure 1 - Location of the Tantato Domain, northern Saskatchewan, with respect to other tectonic elements of the western Canadian Shield. WGD = Western Granulite Domain; MF = MacDonald Fault. The Virgin River Shear Zone (VRSZ) and Tulemalu Fault Zone (TFZ) are components of the Snowbird tectonic zone (Hoffman, 1988).

(1) Geological Survey of Canada, 601 Booth Street, Ottawa, Ontario
(2) University of Massachusetts, Boston, Massachusets
(3) University of California, Santa Cruz, California

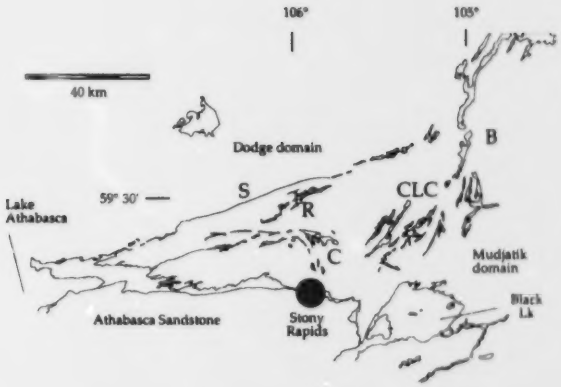

Figure 2 - A location map for the triangular-shaped Tantato Domain. B, Bompas Lake; C, Clut Lakes; CLC, Core-Lytle-Chipman Lakes; R, Reeve Lake; S, Straight River.

major map units (Figures 3 and 4): (i) amphibole - clinopyroxene tonalite intruded by biotite - hornblende granites in the eastern footwall; (ii) a strongly garnetiferous granite to granodiorite in the western footwall; (iii) graphitic and aluminous, strongly garnetiferous diatexite with (iv) sheets of coronitic metagabbro and mafic granulite in the hanging wall to the south; and (v) coarse equigranular to megacrystic biotite - hornblende granites along the hanging wall - footwall interface. A large volume of strongly garnetiferous diatexite also occurs throughout the footwall.

5) The tonalite and the spatially associated later granites in the eastern part of the Tantato Domain (Figure 4) contain abundant mafic and ultramafic inclusions, at least in part derived from a layered mafic or anorthositic complex, and may have been emplaced relatively close to their respective sources. The tonalite is apparently intrusive into the garnetiferous diatexite, itself derived at the expense of aluminous and graphitic metasediments.

6) A swarm of mafic dykes (Chipman Sill Swarm of Macdonald (1980)), emplaced during the period spanning granulite facies metamorphism to the end of low temperature crystal plastic deformation, occurs throughout the tonalite of the eastern part of the footwall (Figure 4). Mafic dykes are conspicuously absent from the wall rocks to the east of the Tantato Domain. Spectacular garnet - hornblende, garnet - clinopyroxene - plagioclase and hornblende - plagioclase metamorphic assemblages within the dykes may represent preservation of both prograde and retrograde assemblages, close to the amphibolite - granulite facies transition.

7) Mylonites are penetratively developed throughout the Tantato Domain. Nevertheless, the preservation of quartz ribbon fabrics within the footwall is variable. Spectacular mylonitic ribbon structure is well preserved in the central and western parts, whereas an extensive volume of annealed mylonites occurs in the east where it is spatially coincident with the densest concentration of late-tectonic Chipman dykes (Figure 4).

8) There is a consistent relationship between metamorphic grade and width of the zone of active mylonitization, in that mylonite zones formed at lower metamorphic grade tend to be narrower. Granulite mylonites of the hanging wall panel show evidence for local post-mylonite retrogression to amphibolite facies. Granulite facies mylonites are locally well preserved throughout the central and western parts of the footwall. However, the footwall mylonites are extensively retrogressed from granulite to amphibolite facies mineral assemblages. In places retrogression is post-mylonitization, but amphibolite facies mylonites are penetratively developed in belts 1 to 10 km wide. Upper greenschist facies mylonites have been mapped in three narrow belts up to several hundreds of metres wide. One of these belts occupies the length of the eastern boundary of the Tantato Domain. The other two are relatively minor structures within the domain and their displacements probably represent late adjustments.

9) Belts of porphyroclastic granulite facies mylonite form an anastomosing network around poorly foliated lenses from 10 to 1000 m wide, in a discrete corridor adjacent to the northwest boundary of the Tantato Domain (Figure 3). Within this corridor there is an intimate interlayering of several lithologies of different rheology.

10) A suite of homogeneous and relatively leucocratic, biotite ± hornblende granites is the protolith to extensional mylonites at the hanging wall - footwall interface (Figure 3). Major post-granulite granite sheets were emplaced along this interface. Lesser volumes of granites were emplaced in the footwall, adjacent to the trailing edge of the extensional shear zone.

11) Other biotite - hornblende ± garnet granites were emplaced syntectonically in a corridor adjacent to and along the eastern boundary of the Tantato Domain, spatially coincident with the densest concentration of Chipman dykes (Figure 4). Away from the eastern boundary these granites have been penetratively mylonitized under amphibolite facies conditions. Along the eastern boundary, the granites were emplaced during upper greenschist mylonitization.

12) The wall rock to the east (Mudjatik Domain, Figure 2) comprises garnet - sillimanite metatexites of metapelitic and semipelitic origin passing westwards into layered garnet - cordierite - muscovite metapelites and garnetiferous quartzites. The metatexites are retrogressed and tectonically reduced to porphyroclastic biotite - muscovite schists adjacent to the eastern boundary of the Tantato Domain. The wall rock to the west (Dodge Domain, Figure 2) comprises coarse biotite - muscovite schists and granitic segregations or veins in sharp fault contact with the mylonites of the Tantato Domain.

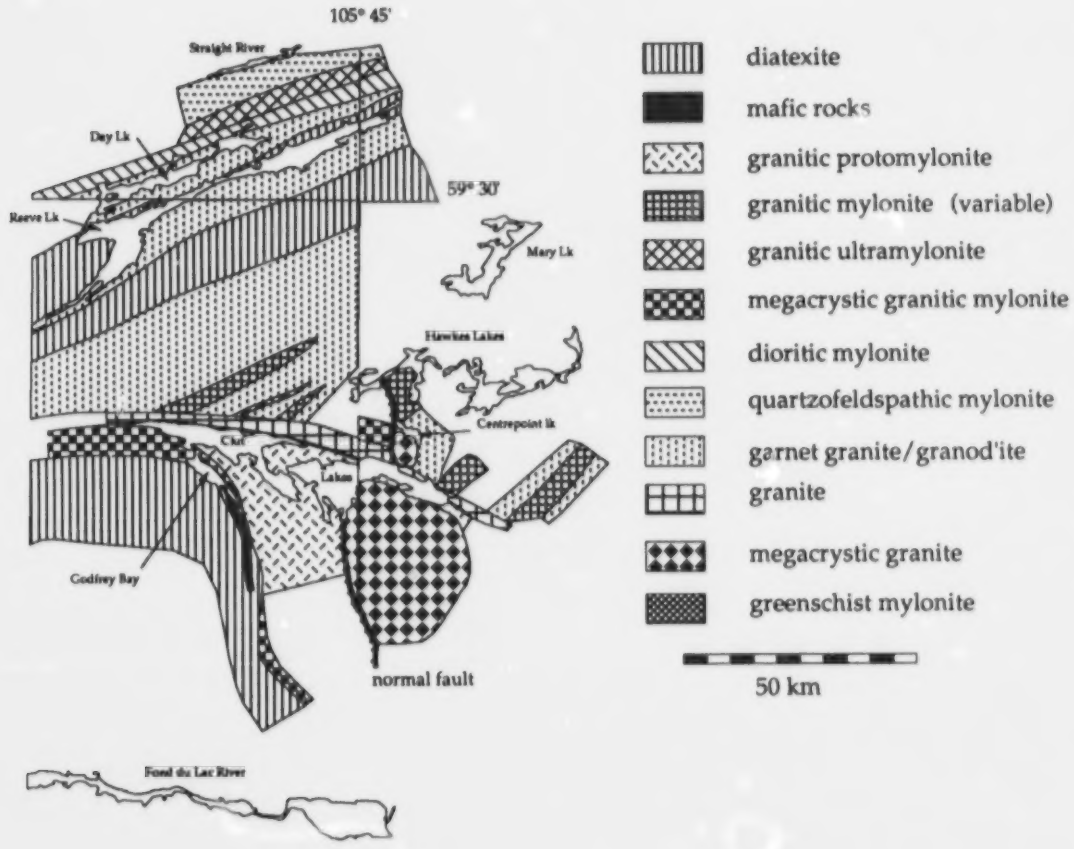

Figure 3 - Summary of the geology in the Clut Lakes to Reeve Lake area. The hanging wall - footwall interface zone goes through Clut Lakes.

2. Discussion

a) Stony Rapids Area

The protoliths to the mylonites of the Snowbird tectonic zone in the Tantato Domain comprised a tonalite batholith intruded into a dismembered layered mafic complex, monotonous pelitic metasediments, widespread minor iron-rich impure psammites and possible mafic volcanics. According to one possible interpretation of sheeted intercalated contacts, the pelitic metasediments may also be intruded by an I-type (*sensu lato*) granite - granodiorite batholith and gabbros. During mylonitization, significant volumes of I-type (*sensu lato*) granite and mafic dykes were emplaced into the eastern part of the tonalite batholith. Combined with granulite to upper amphibolite facies metamorphic conditions, the lithological association of the Snowbird tectonic zone is suggestive of the deep roots of a magmatic arc.

Metamorphic mineral assemblages in granulite facies mylonites of both the hanging wall and footwall correspond to the lower part of bathozone 6 (Carmichael, 1978; Davidson *et al.*, 1990) i.e. temperatures close to 800°C and, given the absence of kyanite, pressures of 700-800 MPa. Syntectonic metamorphic mineral assemblages in the mafic dykes in the tonalite batholith are transitional between the upper amphibolite and granulite facies and could represent comparable PT conditions to those just cited (Newton, 1985).

A large volume of high grade mylonites with very little low grade mylonite, cataclasite and brittle fault products, such as pseudotachylite and quartz veining, indicates that most deformation in the Snowbird tectonic zone occurred at crustal depths of circa 30 km. Later uplift was accompanied by relatively minor ductile deformation. Granulite facies diatexitic mylonites in the hanging wall panel are identical to those present throughout much of the footwall. The footwall mylonites are variably reworked and retrogressed to amphibolite facies in the central and western parts of the footwall and either formed at, or were retrogressed to, upper amphibolite facies in the eastern part. The important point here is that, if the granulite mylonites of the hanging wall are contemporaneous with the granulite and amphibolite facies mylonites of the footwall, then the hanging wall

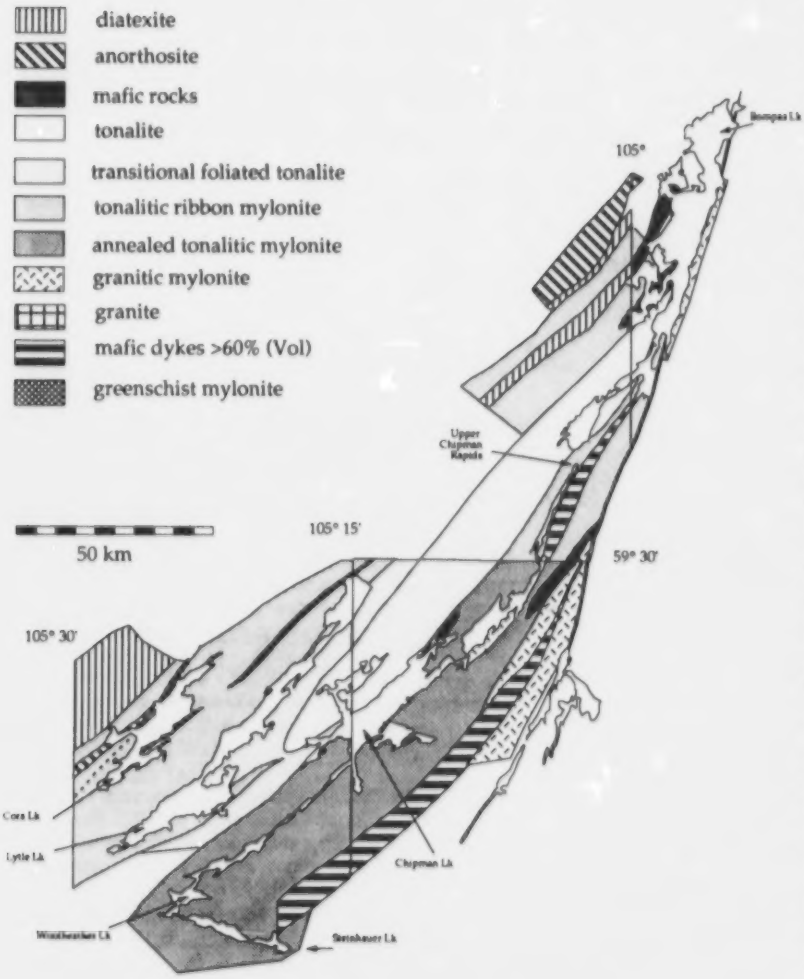

Figure 4 - Summary of the geology in the Chipman River - Bompas Lake area. Greenschist mylonites are restricted to a very narrow band along the eastern boundary of the Tantato Domain.

mylonites are thrust related. If the extension lineation is approximately parallel to the transport direction, then thrusting was from either the east or the west.

A qualitative geometrical balance between sinistral and dextral sectors within the high grade strike-slip footwall mylonites suggests that, if they are contemporaneous, they formed in response to pure shear boundary conditions, at the scale of the Tantato Domain. Truncation of the mylonitized tonalite batholith by tonalitic ribbon mylonites adjacent to the eastern margin of the Snowbird tectonic zone (Figure 4) indicates that there were local, but significant, adjustments to those boundary conditions during progressive deformation. Given that the adjacent rocks of the Dodge and Mudjatik Domains have not significantly participated in this progressive deformation, tectonic flow within the footwall must have led to a relative southwestward displacement of the footwall rocks with respect to the wall rocks on either side. Clearly, the relationship between flow in the footwall and thrust-related progressive deformation in the hanging wall is not simple.

Demonstrably extension-related mylonites formed at the expense of syntectonic granites at the base of the hanging wall panel. Magmatic intrusion along the trailing edge of the upper plate of an extensional shear zone suggests a causal relationship between the locus of emplacement and the locus of progressive deformation. Deformation would create a zone of potential dilation and the soft, recently emplaced granites would localize continued tectonic displacement.

In the eastern part of the Snowbird tectonic zone, there is a coincidence between the distribution of extensive strongly annealed mylonites, the absence of anhydrous mafic metamorphic minerals, a gravity high and the presence of a relatively densely packed mafic dyke swarm. If there is a genetic relationship between these various elements, it is unlikely to be due to a thermal anomaly related to the mafic intrusions. Rather, we might speculate on the possibility that the mafic magmas could have played a role in the introduction of hydrous fluids into hot tonalitic and granitic mylonites.

b) Regional Context

As has been suggested by other workers, there appear to be a number of lithological and structural similarities between the northern rocks described here and rocks of the Western Granulite Domain in the region south of the Athabasca Basin. The lithological assemblage of the tonalite batholith in the Tantato Domain resembles the eastern part of the Western Granulite Domain (Figure 1; Lewry and Sibbald, 1977; Crocker and Collerson, 1988). The western margin of the Tantato Domain (Grease River - Straight River shear zone of authors; see Gilboy, 1980) has been equated with the Clearwater Domain (Wallis, 1970a; Lewry *et al.*, 1978). The eastern margin (Black Lake shear zone of authors; see Gilboy, 1980) has been correlated with the Virgin River Shear Zone to

the south (Figure 1; Wallis, 1970a,b; Lewry *et al.*, 1978; Lewry and Sibbald 1980). Descriptions of the Virgin River Domain so closely resemble the western part of the Mudjatik Domain north of the Athabasca Basin (see also Gilboy, 1978) as to suggest extension of the former into the northern region. Possible correlation of megacrystic granites in the eastern part of the tonalite batholith with the Junction Granite in the south was pointed out by Gilboy (1978). Mafic dykes in the Virgin River Shear Zone, as now described by Carolan and Collerson (1988, 1989) were equated with the dykes in the tonalite batholith by Macdonald (1980). Note also that Carolan and Collerson found that mafic dykes are absent in the wall-rocks immediately east of the Virgin River Shear Zone.

To the northeast of the Tantato Domain, Gilboy and Ramaekers (1981) identified a narrow low grade 'cataclastic' zone, the Gaste Lake Shear Zone. Our observation that the eastern margin of the Snowbird tectonic zone truncates both the tonalite batholith and the trend of the western margin of the tectonic zone, suggests that the Gaste Lake structure is probably the extension of the eastern margin.

In light of the foregoing, it is interesting to note that, whereas the eastern margin of the Snowbird tectonic zone is associated with sinistral shear along a southward plunging extension lineation in the Stony Rapids area, the upper greenschist to lower amphibolite facies Virgin River Shear Zone shows dextral shear along a northward plunging lineation (Carolan and Collerson, 1988, 1989). Furthermore, the sinistral and dextral mylonites of the Tantato Domain, the Virgin River Shear Zone and the Clearwater domain occupy the four quadrants located at the ends of the large elliptical area apparent in the magnetic field of northern Saskatchewan. While noting that the Virgin River Shear Zone is a relatively minor low grade structure, and that the internal magnetic structure of the elliptical area is abruptly truncated by the trend of the Clearwater Domain, we speculate that the geophysically defined ellipse represents a continental scale 'island' of stiff material, subjected to a major component of regional scale pure shear.

c) Age Constraints

There are no direct age constraints on the geological history of the Snowbird tectonic zone, north of the Athabasca Basin. However, in light of the above noted similarities on either side of the basin, the 1.82 Ga magmatic age of the Junction Granite and the circa 2.0-2.3 Ga metamorphic ages of Mudjatik domain gneisses (U/Pb in zircon; Bickford *et al.*, 1986, 1987, 1988) are indicative of the importance of Early Proterozoic events in the tectono-thermal history of the region.

3. References

Bickford, M.E., Collerson, K.D. and Lewry, J.F. (1988): U-Pb geochronology and isotopic studies of the Trans-Hudson orogen in Saskatchewan; *in* Summary of Investigations 1988, Sask. Geol. Surv., Misc. Rep. 88-4, p112-116.

Bickford, M.E., Van Schmus, W.R., Collerson, K.D. and Macdonald, R. (1987): U-Pb zircon geochronology project: New results and interpretations; *in* Summary of Investigations 1987, Sask. Geol. Surv., Misc. Rep. 87-4, p76-86.

Bickford, M.E., Van Schmus, W.R., Macdonald, R., Lewry, J.F. and Pearson, J.G. (1986): Trans-Hudson Orogen: current sampling and recent results; *in* Summary of Investigations 1986, Sask. Geol. Surv., Misc. Rep. 86-4, p101-107.

Carmichael, D.M. (1978): Metamorphic bathozones and bathograds: a measure of the depth of post-metamorphic uplift and erosion on the regional scale; Am. J. Sci., v278, p769-797.

Carolan, J. and Collerson, K.D. (1988): The Virgin River Shear Zone in the Careen Lake area: Field relationships and kinematic indicators; *in* Summary of Investigations 1988, Sask. Geol. Surv., Misc. Rep. 88-4, p92-96.

_____ (1989): Field relationships and kinematic indicators in the Virgin River Shear Zone; *in* Summary of Investigations 1989, Sask. Geol. Surv., Misc. Rep. 89-4, p98-101.

Crocker, C.H. and Collerson, K.D. (1988): Archean and Early Proterozoic field relationships in the Careen Lake area of the Western Granulite Domain; *in* Summary of Investigations 1988, Sask. Geol. Surv., Misc. Rep. 88-4, p97-102.

Davidson, A., Carmichael, D.M. and Pattison, D.R.M. (1990): Metamorphism and geodynamics of the southwestern Grenville Province, Ontario; IGCP Project 235-30, Field Trip #1 guidebook, 123p.

Gilboy, C.F. (1978): Reconnaissance geology, Stony Rapids area (Parts of NTS area 74P); *in* Summary of Investigations 1980, Sask. Geol. Surv., Misc. Rep. 78-10, p35-42.

_____ (1980): Reconnaissance Bedrock Geology: Chambeuil Lake East Area (Part of NTS 74P); *in* Summary of Investigations 1980, Sask. Geol. Surv., Misc. Rep. 80-4, p14-16.

Gilboy, C.F. and Ramaekers, P. (1981): Compilation Bedrock Geology: Stony Rapids Area (NTS 74P); *in* Summary of Investigations 1981, Sask. Geol. Surv., Misc. Rep. 81-4, p6-11.

Hanmer, S., Darrach, M., Kopf, C. and Ji, S. (in prep.): Snowbird tectonic zone, N. Saskatchewan: a geological window into a 3000 km long geophysical anomaly; *in* Current Research Part A, Geol. Surv. Can., Pap. 91-1A.

Hoffman, P.F. (1988): United plates of America, the birth of a craton: Early Proterozoic assembly and growth of Laurentia; Ann. Rev. Earth Planet. Sci., v16, p543-603.

Lewry, J.F. and Sibbald, T.I.I. (1977): Variation in lithology and tectonometamorphic relationships in the Precambrian basement of northern Saskatchewan; Can. J. Earth Sci., v14, p1453-1467.

_____ (1980): Thermotectonic evolution of the Churchill Province in northern Saskatchewan; Tectonophysics, v68, p45-82.

Lewry, J.F., Sibbald, T.I.I. and Rees, C.J. (1978): Metamorphic patterns and their relation to tectonism and plutonism in the Churchill Province in northern Saskatchewan; Geol. Surv. Can., Pap. 78-10, p139-154.

Macdonald, R. (1980): New edition of the geological map of Saskatchewan, Precambrian Shield area; *in* Summary of Investigations 1980, Sask. Geol. Surv., Misc. Rep. 80-4, p19-21.

Newton, R.C. (1985): Temperature, pressure and metamorphic fluid regimes in the amphibolite facies to granulite facies transition zones; *in* Tobi, A.C. and Touret, J.L.R. (eds.), The Deep Proterozoic Crust in the North Atlantic Provinces, p75-104.

Thomas, M.D. and Gibb, R.A. (1985): Proterozoic plate subduction and collision: processes for reactivation of Archean crust in the Churchill Province; Geol. Assoc. Can., Spec. Pap. 28, p264-279.

Thomas, M.D., Grieve, R.A.F. and Sharpton, V.L. (1988): Gravity domains and the assembly of the North American continent by collisional tectonics; Nature, v331, p333-334.

Wallis, R. H. (1970a): A geological interpretation of gravity and magnetic data, northwest Saskatchewan; Can. J. Earth Sci. v7, p858-868.

_____ (1970b): The geology of the Dufferin Lake area (west half), Saskatchewan; Sask. Dep. Miner. Resour., Rep. 132, 59p.

Lithogeochemistry and XRD Mineralogy of Martin Group and Related Rocks, Greater Beaverlodge Area, Saskatchewan

David H. Quirt[1]

Quirt, D.H. (1990): Lithogeochemistry and XRD mineralogy of the Martin Group and related rocks, greater Beaverlodge area, Saskatchewan; *in* Summary of Investigations 1990, Saskatchewan Geological Survey; Saskatchewan Energy and Mines, Miscellaneous Report 90-4.

Along the north shore of Lake Athabasca are found the remnants of several Proterozoic red-bed clastic successions: the Athabasca, Martin, and Thluicho Groups (Langford, 1980, 1981). These rocks were initially grouped together as a single unmetamorphosed to weakly metamorphosed sedimentary unit overlying the highly deformed and metamorphosed Tazin Group rocks (Hale, 1953, 1954, 1955; Koster, 1968, 1970). Mapping of this area by Scott (1978) allowed the subsequent subdivision of these cover rocks into the Athabasca, Martin, and Thluicho Groups.

The Martin Group in general has been extensively studied (Tremblay, 1972; Macey, 1973) and detailed sedimentological studies on this unit have also been carried out by researchers at the University of Saskatchewan (Langford, 1980, 1981; Elliot, 1982; Hendry, 1983; Mazimhaka and Hendry, 1984, 1985, 1986). The nomenclature and subdivision of the Martin Group rocks in this report follows that suggested by Langford (1981) and used in Mazimhaka and Hendry (1984, 1985, 1986). The Thluicho Group has not been covered as exhaustively as the Martin Group, with rocks of this group having been mapped by Koster (1968) and Scott (1978) and a reconnaissance sedimentological investigation having been conducted on these rocks during the Martin Group study of Mazimhaka and Hendry (1985).

As uranium is associated with the Martin Group (Hoeve, 1982) as well as with the overlying Athabasca Group (Hoeve and Quirt, 1984), a lithogeochemical study was initiated to evaluate the major and trace element content and distribution in the Martin Group rocks. In addition, whole-rock and $<5\mu m$ fraction mineralogical analyses were carried out using x-ray diffraction (XRD) with the aim of correlating the geochemical data with mineralogy, stratigraphic position, and possible sediment source areas. P. Mazimhaka of the University of Saskachewan supplied 102 samples of powdered rock. Partial funding for the geochemical analyses was provided by the Saskatchewan Geological Survey. The samples represent all of the Martin Group formations, as well as the underlying Thluicho Group.

1. General Geology

The Martin Group rocks are found in several isolated basins within a 50 km radius of Uranium City, the best exposed being in the immediate vicinity of the townsite. These rocks lie unconformably on the highly deformed and metamorphosed basement rocks of the Tazin Group which consist primarily of metasedimentary and metavolcanic units. A number of igneous complexes are also present in the region.

The Martin Group consists of up to 6000 m of texturally immature sediments (Tremblay, 1972). A basal conglomerate up to 750 m thick is followed by up to 2400 m of arkosic sandstone which contains up to 1000 m of volcanic flows intercalated with the upper portion of the unit. Overlying these volcanic rocks is up to 2100 m of arkosic sandstone, in turn being overlain by up to 1800 m of siltstone. Only in the Martin Lake area is a complete section preserved.

Conditions of deposition were continental as indicated by the presence of cross-bedding, raindrop imprints, mudcracks, and grain size variations (Tremblay, 1972). Transport distances were short and deposition was rapid into several basins having a rugged, block-faulted terrain. Basin deepening, controlled by active faults, occurred as the basin filled, allowing the accumulation of great thicknesses of material (Tremblay, 1972; Hendry, 1983). The typical red colour of most of the Martin Group rocks is due to hematite, which is found in several forms including cement in siltstone and arkosic sandstone, as coloring in feldspar grains, and in the matrix of the conglomerate. Conglomerate clast compositions in the Martin and Tazin Lake areas indicate that the main sediment source was the unweathered granitic basement immediately underlying the Martin rocks or in adjacent fault blocks (Tremblay, 1972; Mazimhaka and Hendry, 1986). Clasts in the Charlot Point Formation were mainly derived from sedimentary sources.

The Martin Group has been divided into a number of formations by Langford (1981) and Mazimhaka and Hendry (1985). Four formations are found in the Martin Lake area while only the basal succession remains in areas away from the Martin Lake basin. For detailed descriptions of the Martin Group rocks, see Tremblay (1972), Langford (1981), Elliot (1982), Hendry (1983), and Mazimhaka and Hendry (1984, 1985, 1986), and for the Thluicho Group rocks, see Scott (1978) and Mazimhaka and Hendry (1985).

(1) Minerals/Groundwater Program, Resources Technology Division, Saskatchewan Research Council, Saskatoon, Saskatchewan

2. X-ray Diffraction Mineralogy

Mineralogical data were obtained using XRD techniques. Whole-rock bulk mineralogy is tabulated by formation and rock type (Table 1). The mineralogy of the <5μm fraction was determined from the remaining material following centrifugal extraction of the >5μm fraction (Table 2).

The Martin, Charlot Point, and Thluicho sediments are composed of quartz and feldspar with minor mica/clays, carbonate, and ubiquitous hematite (Table 1). Potassium feldspar generally exceeds plagioclase with quartz and feldspar being approximately equal in abundance, as for most arkoses (Pettijohn *et al.*, 1972; van de Kamp *et al.*, 1976). This relationship is likely due to inheritance of the feldspar ratio present in the source area. The carbonate is predominantly calcite but dolomite is present in some samples. The clays are composed of illite/sericite and Fe-Mg trioctahedral chlorite. Only trace amounts of aluminous di,trioctahedral chlorite (sudoite), as found in the Athabasca Basin, and kaolinite have been detected in these rocks. Mixed-layer illite-smectite is rare. Trace amounts of pyrite have been noted in several hand samples of grey sandstone. Two samples of Beaverlodge Formation (grey sandstone and breccia) contain traces of hornblende. Rock fragments and conglomerate clasts include sandstone as well as metamorphic and igneous lithologies.

The clay content in the arkoses is generally less than 10 percent of the rock. Most of the clay minerals are in the matrix as siltstone fragments are sparse. Biotite is rare, likely having been chloritized, and the presence of amphibole was not detected by XRD. Calcite cement is locally present.

Rock fragments are variably present, usually in lesser quantity than feldspar. As the quartz content is far less than 75 percent, the rocks are predominantly arkoses according to the Pettijohn classification scheme (Pettijohn *et al.*, 1972). The low matrix content of the arkose classification separates this lithology from that of greywacke.

Table 1 – Whole-rock mineralogy for formation and rock type. Pl, plagioclase; Ct, trioctahedral chlorite; K, kaolinite; Do, dolomite; Kf, potassium feldspar; Cc, calcite; I, illite; Cd, di,trioctahedral chlorite; nd, not detected.

Formation or rock - type	n	Q	Pl	Kf	Q/F	Pl/Kf	Cc	Do	H	I	Cd	Ct	K
Thluicho	4	42	14	24	1.11	0.58	2	nd	7	7	nd	4	nd
Taz Bay	7	26	25	29	0.48	0.86	2	nd	7	4	nd	7	nd
Beaverlodge	36	41	17	23	1.03	0.74	3	2	5	3	<1	4	<1
Charlot Point	18	46	15	14	1.59	1.07	<1	5	10	8	<1	2	1
Gillies Channel	13	38	17	23	0.95	0.74	8	nd	4	5	<<1	4	2
Seaplane Base	15	32	22	29	0.63	0.76	3	nd	11	3	<1	1	nd
Melville Lake	9	36	12	25	1.33	0.48	7	2	13	3	<<1	1	nd
Siltstone/fine - grained sandstone	13	32	15	27	0.76	0.56	6	2	12	5	nd	3	nd
Sandstone	43	41	18	22	1.03	0.82	3	1	7	4	<1	3	1
Coarse - grained sandstone	9	38	24	11	1.09	2.18	5	4	8	8	<1	3	nd
Conglomerate/breccia	31	41	17	22	1.05	0.77	3	2	8	4	<1	3	<1
Coarse - grained conglomerate/breccia	5	31	7	51	0.53	0.14	2	1	3	<1	nd	5	nd
Volcanic	1	15	2	42	0.24	0.05	nd	10	19	8	nd	4	nd

Table 2 – Clay mineralogy of the <5μm fraction for formation and rock type. I, illite; K, kaolinite; C, total chlorite; Ir, illite I002/I001 peak area ratio; Ki, Kubler index; PC, percentage of sample in fraction; nd, not detected; nc, not calculated.

Formation or rock - type	n	I	C	K	Ir	Ki	PC
Thluicho	4	54	46	nd	0.27	2.5	3.3
Taz Bay	7	23	77	nd	0.40	3.7	3.3
Beaverlodge	36	32	66	2	0.33	4.9	3.2
Charlot Point	18	67	27	6	0.33	4.3	4.4
Gillies Channel	13	52	42	6	0.30	4.3	4.2
Seaplane Base	15	61	39	nd	0.35	4.4	2.8
Melville Lake	9	80	20	nd	0.28	3.7	3.3
Siltstone/fine-grained sandstone	13	62	38	nd	0.32	3.7	3.7
Sandstone	43	49	47	4	0.35	4.6	3.4
Coarse-grained sandstone	9	50	50	nd	0.30	4.7	3.4
Conglomerate/breccia	31	53	44	3	0.31	4.2	3.6
Coarse-grained conglomerate/breccia	5	8	92	nd	0.45	3.1	2.2
Volcanic	1	17	83	nd	nc	nc	5.0

The preservation of the feldspars, as illustrated by the low quantity of clay minerals present, indicates that only mild chemical weathering of the source rocks had occurred. This evidence agrees with the interpretation of Hendry (1983) and Mazimhaka and Hendry (1984) that the arkoses were derived from areas of high relief such as occurs during long periods of scarp retreat in a fault-bounded graben environment. The abundance of feldspar and the relatively low amount of quartz indicates that the arkoses are likely a result of first-cycle sedimentation.

On the basis of formation, a number of differences in mineralogy appear between the samples used in this study. Samples of Charlot Point formation tend to be more quartz-rich (Q/F >1.5), dolomitic, hematitic, illitic, and less chloritic than the other basal, sandstone formations (Taz Bay, Beaverlodge), but are similar to those of the silty Melville Lake formation in some aspects. The plagioclase to potassium feldspar ratio (1.07) is also distinctly different from the other formations, indicating that the source area for the Charlot Point sediments was likely different than for the other formations.

The Taz Bay Formation is quartz-poor (Q/F <0.50) relative to the other formations. It is distinctly different from the Beaverlodge formation, having less quartz, more plagioclase and no dolomite.

The Gillies Channel and Melville Lake formations are distinctly more calcic than the other formations. The significances of the differences between the formations are low due to small sample populations.

Minor amounts of dolomite are only found in the Beaverlodge, Melville Lake, and to a somewhat greater degree, Charlot Point formations. The Thluicho rocks are similar in bulk mineralogy to the basal Martin lithologies. Both the Thluicho and Charlot Point formations appear to be more illitic than the Martin lithologies.

The clay-size fraction mineralogy of these formations are also similar (Table 2) although Thluicho Group illite tends to be less aluminous (lower Ir value) and slightly more crystalline (lower Ki value). The minor amounts of kaolinite present may be due to pre-Athabasca Group paleoweathering. In general, the clay mineralogy of the Martin Group appears to become increasingly illitic up section from the Beaverlodge formation, through the Gillies Channel and Seaplane Base formations, to the Melville Lake formation.

For the fine- to medium-grained clastic classifications, the Q/F ratio is approximately unity. This feature appears to be typical of arkose derived from unweathered sources (van de Kamp *et al.*, 1976). The very fine-grained and very coarse-grained sediments contain substantially less quartz than feldspar, with Q/F values of less than 0.76. Only one volcanic rock was included in the sample set. This sample revealed a very low Q/F ratio (0.34). Both quartz and plagioclase contents are low, while the potassium feldspar content is high (Pl/Kf = 0.05), as are the dolomite and hematite proportions. The high Pl/Kf value (2.18) for the coarse-grained sandstone remains unexplained as no control on sampling was available. The bulk clay mineralogy appears to be consistent between rock types with only the poorly represented very coarse-grained sediment group differing by having a relatively low illite proportion.

The clay mineralogy of the clay-size fraction (Table 2) reveals a trend of decreasing illite proportion with increasing grain size. Total chlorite proportion varies inversely to that of illite. Only minor kaolinite was detected. The sample of Martin Group volcanic material showed a dominance of illite over chlorite in the whole rock analysis yet revealed a much higher proportion of chlorite than illite in the clay-size fraction. This trend, also observed to a lesser extent for the clastic rocks, is likely due to the presence of coarser-grained muscovite in these samples in addition to illite/sericite. The chlorite is likely an alteration product of biotite and hornblende. Crystallinity and composition of illite appears to be similar for the clastic rock types, but the amount of clay-size fraction material is significantly lower in the very coarse-grained sediments.

3. Lithogeochemistry

All rock samples were analyzed by several methods following crushing by steel jaw crusher and grinding using an motorized agate mortar. Most elements were analyzed by atomic absorption spectrophotometry (AAS) or inductively coupled plasma emission spectroscopy (ICP) following total digestion using $HF/HNO_3/HClO_4$. Exceptions are as follows: FeO analysis was by titration following HF/H_2SO_4 digestion; LOI was determined after heating to 900°C; CO_2 and S by use of an induction furnace; As and Se by hydride generation and AAS analysis; U by fluorometry; Au by fire assay with AAS completion; Pt and Pd by instrumental neutron activation analysis (INAA). Only selected samples underwent analysis for S, Pt, and Pd. The oxides SiO_2, Fe_2O_3, and H_2O were calculated by difference. Group mean values by formation and rock type are presented in Tables 3 and 4, respectively.

Clastic rocks can be classified by chemical composition in order to show relationships between elemental composition, mineralogy, and rock type (Pettijohn *et al.*, 1972). A number of classification schemes to relate chemical compositions to common sandstone classifications have been devised, with the most commonly used being the log (Na_2O/K_2O) versus log (SiO_2/Al_2O_3) plot of Pettijohn *et al.* (1972). Herron (1988) has proposed a similar plot (Sand Class format) using (total iron as Fe_2O_3/K_2O) rather than (NaO/K_2O) as the ordinate parameter. The SiO_2/Al_2O_3 ratio is used as an indicator of mineralogical maturity (Pettijohn *et al.*, 1972) while the Na_2O/K_2O ratio is used to differentiate lithic sandstone from arkose and greywacke. The Fe_2O_3/K_2O ratio is used as an indicator of mineralogical stability (Herron, 1988). As the use of the Sand Class format better classifies these analyses with respect to their petrographic classification (Quirt, 1990), only the Sand Class format was used in this study for classification purposes.

The chemistry of the Martin arkoses does not vary greatly with respect to the SiO_2/Al_2O_3 ratio, most of the variation on the Sand Class plot being in Fe_2O_3/K_2O. The samples fall primarily into the arkose field, however, a number fall into the wacke, litharenite, Fe-sand, and Fe-shale fields with increasing Fe_2O_3/K_2O ratios (Quirt, 1990). This feature is likely due to the abundant hematite present in the majority of these samples. No differentiation can be made on the basis of rock type, as each rock type reveals a substantial spread of Fe_2O_3/K_2O values. A similar situation prevails for the values of the Na_2O/K_2O ratio. Grouping of the samples by formation tends to reveal the same situation as for

Table 3 – Average Chemical Compositions by Formation.

	Thluicho	Taz Bay	Beaverlodge	Charlot Point	Gillies Channel	Seaplane Base	Melville Lake
SiO_2c	71.23	70.40	73.28	74.11	71.12	75.40	68.68
Al_2O_3	11.80	12.61	10.43	10.62	10.46	10.74	10.16
Fe_2O_3t	3.40	3.55	3.33	2.84	2.97	2.26	2.74
FeO	1.15	2.02	1.95	0.78	1.47	0.72	0.50
Fe_2O_3c	2.12	1.30	1.16	1.97	1.32	1.46	2.19
MgO	2.03	1.52	1.92	1.77	1.35	0.67	1.11
CaO	1.70	1.33	1.84	1.39	3.55	1.59	4.95
K_2O	3.66	4.49	2.83	3.77	3.00	3.42	2.90
Na_2O	2.36	3.22	2.54	1.55	2.64	3.41	3.17
TiO_2	0.27	0.21	0.26	0.32	0.35	0.19	0.25
P_2O_5	0.11	0.11	0.10	0.18	0.15	0.09	0.13
LOI	3.27	2.32	3.22	3.25	4.16	2.00	5.61
CO_2	1.40	0.84	1.65	1.49	2.37	1.12	4.41
H_2Oc	1.87	1.48	1.57	1.75	1.78	0.88	1.20
Ni	22.5	22.5	19.8	16.4	18.4	11.4	25.1
Cr	49.2	38.7	41.5	45.0	47.0	23.8	53.0
Ba	532.2	758.8	647.9	664.9	879.6	851.6	696.6
Sr	81.7	85.4	105.2	118.1	174.3	148.1	181.6
V	54.2	45.8	47.0	47.7	39.2	25.1	34.2
Zr	198.5	156.0	138.3	154.3	180.6	1344	162.5
Th	33.0	15.4	13.7	13.6	17.4	14.8	13.7
U	4.7	3.6	3.6	2.6	3.5	3.1	4.2
Au	10	4	7	3	7	6	9
Pt	5	5	5	5	5	5	5
Pd	5	5	5	33	5	6	5

Table 4 – Average Chemical Compositions by Rock Type. A, siltstone and fine-grained sandstone; B, sandstone; C, coarse-grained sandstone; D, conglomerate and fine-grained breccia; E, coarse-grained conglomerate and breccia; F, volcanic.

	A	B	C	D	E	F
SiO_2c	69.65	74.22	73.45	73.12	70.00	49.02
Al_2O_3	11.09	10.40	9.73	10.82	12.54	13.80
Fe_2O_3t	3.38	2.72	2.26	3.09	3.91	9.92
FeO	1.24	1.35	0.83	1.22	2.54	5.20
Fe_2O_3c	2.00	1.22	1.33	1.73	1.08	4.14
MgO	1.52	1.38	1.66	1.54	1.79	6.76
CaO	3.16	1.98	2.79	1.86	1.56	5.20
K_2O	3.28	3.27	3.95	3.37	1.17	2.81
Na_2O	3.01	2.49	1.61	2.42	5.48	2.10
TiO_2	0.31	0.23	0.18	0.27	0.34	1.98
P_2O_5	0.14	0.11	0.09	0.10	0.19	1.26
LOI	4.18	2.98	4.07	3.19	2.74	6.50
CO_2	2.73	1.60	2.44	1.59	1.28	3.30
H_2Oc	1.45	1.38	1.63	1.60	1.46	3.20
Ni	26.4	17.9	14.4	16.2	13.2	83.0
Cr	58.3	38.4	34.6	39.8	22.2	151.0
Ba	753.1	656.3	674.0	674.8	1011.6	3160.0
Sr	146.7	121.8	88.3	103.3	163.2	1000.0
V	44.9	35.6	37.5	46.2	42.6	184.0
Zr	158.5	145.2	153.8	144.7	207.4	256.0
Th	13.2	21.8	17.6	16.1	21.8	18.0
U	4.4	3.0	3.9	3.3	5.4	3.6
Au	6	5	8	6	8	3
Pt	5	5	5	5	5	na
Pd	5	5	5	23	5	na

the grouping by rock type, however, Fe-shale and Fe-sands are found only in the Beaverlodge and Gillies Channel formations. The Seaplane Base and Melville Lake formation samples tend to cluster in and close to the arkose field, not having a large range of Fe_2O_3/K_2O ratio values.

Major oxide concentrations are similar to those of common granitic and metamorphic rocks (cf. Taylor, 1972; Ross, 1972). Values for SiO_2, CO_2, and H_2O appear to be elevated in the Martin Group arkoses with respect to average Canadian Shield material (cf. Shaw, 1967), whereas concentrations of Al_2O_3, and to a lesser extent CaO and Na_2O, are lower. The lower CaO and Na_2O values probably result from plagioclase alteration and non-incorporation in clay minerals. Elevated CO_2 and H_2O values are a result of matrix mineral formation. When plotted on an AFM diagram, commonly used to illustrate trends in igneous differentiation series, the study samples plot along and in the vicinity of a calc-alkaline trend line. This might suggest that the source rocks were calc-alkaline plutonic rocks.

Trace element concentrations are similar to those given for granitic to granodioritic rocks (Taylor, 1972; Ross, 1972) and to those given for the average composition of the Canadian Shield (Shaw, 1967). Strontium content is low (80 to 180 ppm), likely a reflection of the Pl/Kf ratio (Table 1). The TiO_2 content is also low due to the relatively small quantities of clay minerals in these lithologies.

Ni and Cr are strongly correlated and show a scattered but positive relationship to the Niggli mg parameter [= mol. MgO/(mol. MgO + FeO + MnO + 2 Fe_2O_3)] (Quirt, 1990), which are to be expected in igneous rocks (van de Kamp *et al.*, 1976). The lack of, or low negative correlation between SiO_2 and Niggli mg is also characteristic of igneous suites (van de Kamp *et al.*, 1976). The independent behavior of Zr with increasing SiO_2 that these rocks exhibit (Quirt, 1990) does not fit the fan-like sedimentary Zr-SiO_2 pattern (van de Kamp *et al.*, 1976) of the maximum Zr value rising and the minimum Zr value falling with increasing silica content. Tarney's (1976) discriminant plot of TiO_2 versus SiO_2 indicates that most of

the study samples fall within the field representing an igneous origin (Quirt, 1990). Those samples that do fall into the sedimentary field are close to the boundary with the igneous field. The slightly higher SiO_2 values of these samples possibly result from quartz enrichment caused by minor mechanical and chemical reworking of the detritus, which may also explain the relatively low CaO and Na_2O values.

Shaw (1972) developed a discriminant function (DF) to distinguish between igneous and sedimentary protoliths of an amphibolite facies biotite-quartz-feldspar gneiss. Positive values of this function indicate an igneous origin, negative values a sedimentary origin. This function classified only approximately half of the samples as igneous. For the Martin rocks, the relatively high SiO_2 and Fe_2O_3t values, and low Na_2O values found for these samples are reflected in low, commonly negative, values for the DF. Increasing 'igneous' signature upwards in the Martin stratigraphy appears to reflect reworking of the detrital inflow to the basin. Van de Kamp *et al.* (1976), do not consider this function to be a reliable means of determining the origin of arkosic rocks and the ambiguous results from the Martin rocks appear to confirm this opinion. However, the data in Table 5 do appear to allow some discrimination of the uppermost Martin formations from the basal lithologies, likely due to an increased volcanic component in these formations.

Table 5 – Mean values for Shaw's (1972) discriminant function.

Formation	Mean value of function	Percentage of samples classified as 'igneous'
Thluicho	-1.1	25
Taz Bay	0.9	86
Beaverlodge	-1.6	31
Charlot Point	-2.6	17
Gillies Channel	0.6	46
Seaplane Base	0.9	80
Melville Lake	2.9	89

The sedimentary source strongly indicated by the DF for the Charlot Point formation is in agreement with the sedimentological evidence. For Charlot Point rocks, illite correlates well with K_2O (as does potassium feldspar) and H_2O. Chlorite correlates well with MgO, FeO, Al_2O_3, TiO_2, and a number of trace elements including Mn, Zn, Ni, Co, and U. Chlorite also correlates with plagioclase and correlates negatively with hematite and quartz. Illite correlates negatively with plagioclase. Both K and Rb are present in the clay minerals, likely illite, but variations in the feldspar compositions that dominate the mineral assemblage cause scatter in the illite-K_2O relationship. As expected CaO correlates well with CO_2 with both occurring in calcite, and a good CaO and P_2O_5 correlation indicative of apatite. Dolomite is represented by a strong MgO and CO_2 correlation. The dolomite-CO_2 relationship has two trends because CO_2 is in dolomite and calcite, these minerals being negatively correlated. Similarly, the dolomite-MgO relationship has of two trends with MgO present in both dolomite and chlorite. Ferric iron correlates strongly with hematite and negatively with ferrous iron, which correlates well with S in pyrite. Zinc also correlates with S and chlorite. Copper is associated with As, Ni, Co, MgO, FeO, and TiO_2 in chlorite, kaolinite, and potassium feldspar. Heavy minerals are represented by correlations between Zr-U-Pb-REE (zircon) and TiO_2-Zr (rutile).

The range of mean gold values obtained for the groups of Martin samples (0.003 to 0.010 ppm) is similar to that for shales as well as for felsic plutonic rocks (0.001 to 0.050 ppm and 0.002 to 0.061 ppm, respectively: Mason, 1966; Garett, 1983). The highest gold value obtained was 46 ppb (M-11-1), however, the formations with the highest mean Au values (Thluicho: 9.6 ppb, Melville Lake: 8.8 ppb) had relatively narrow ranges, with no values greater than 18 ppb. Gold correlates with only U and Cu, and correlates negatively with Pb. Mineral associations with Au are poor with only low positive correlations with potassium feldspar and calcite.

Similar to gold, the range of mean uranium values for the Martin formations is similar to those for shales and felsic plutonic rocks. Uranium correlates well with Zr and Al_2O_3 and to a lesser degree with MnO, FeO, TiO_2, Zn, Co and P_2O_5. The U-Zr association reflects uranium present in zircon and that of U-P_2O_5 reflects uranium included in apatite. A moderate U-chlorite correlation is supported by the U-FeO-TiO_2-Zn-Co-MnO association.

Only a few representative samples were analysed for Pt and Pd, most of which were at or below the detection limit of 5 ppb. One sample of hematitic Charlot Point conglomerate (M4022) had 60 ppb Pd. The low concentration levels precluded element correlations.

Limited sampling of Martin formations allows only generalizations to be made on the geochemical characterization of the individual formations (Table 3). The Thluicho Group rocks, with lower Ba values and higher Th and Au values, appear to reflect a different source area than the other units. The Taz Bay formation tends to contain substantially more K_2O than the others and tends to have more FeO than Fe_2O_3. Samples of the Gillies Channel and Melville Lake formations are CaO-CO_2-Sr-Ba-rich due to calcite cement, whereas the Seaplane Base formation samples tend to have less clay matrix than the other formations. The lack of clay is reflected in lower H_2O, MgO, Ni, Cr, and V contents relative to the other units. The Charlot Point formation does not appear to be geochemically distinguishable from the other formations, except through Shaw's (1972) discriminant function.

4. Summary

The Proterozoic clastic successions found along the north shore of Lake Athabasca exhibit many similarities in mineralogy and lithogeochemistry. In general, the mineral assemblage consists of quartz and feldspar with minor mica/clays, carbonate and hematite. Potassium feldspar content usually exceeds that of plagioclase, both being typically well preserved. Quartz content approximates that of total feldspar, indicating a relatively unweathered source area. This mineral assemblage is typical of an arkose. The Charlot Point assemblage differs from the other units with respect to quartz and

dolomite contents, as well as the plagioclase to potassium feldspar ratio.

The clay minerals present are illite (sericite), chlorite, kaolinite, and mixed-layer illite-smectite. Illite content normally exceeds that of chlorite, while kaolinite is only locally present. Most chlorite is Fe-Mg-rich trioctahedral chlorite, likely a result of degradation of biotite, with only trace amounts of aluminous di,trioctahedral chlorite (sudoite) being observed. Generally speaking, Martin Group clay mineralogy becomes increasingly illitic up section. Thluicho Group illite is less aluminous and more crystalline than that of the other formations.

Accessory minerals are scarce and include trace amounts of pyrite, noted in greyish, reduced sandstone, and carbonate (calcite, dolomite) which forms the cementing agent in some samples.

Major oxide and trace element concentrations and trends are similar to those described for common granitic and meta-igneous rocks of calc-alkaline character. Shaw's (1972) discriminant function indicates that the Charlot Point formation is probably derived from a sedimentary source, perhaps second-cycle sedimentation. Thluicho Group material differs from the other formations with respect to Ba, Th, and Au content, probably reflecting a different source. Gold, uranium, platinum and palladium are found in low concentration in all the rocks. Au is poorly correlated with other elements and minerals (U, CaO, potassium feldspar, calcite), but U correlates well with the heavy minerals zircon (Zr) and apatite (P_2O_5), and with chlorite (Al_2O_3, MgO, FeO, TiO_2, Zn, Co).

5. Conculsions

From this investigation it is concluded that the formations of the Martin Group possess minor differences in mineralogy and geochemistry which reflect variations in source relief and depositional processes, as noted in previous sedimentological studies. Both the Charlot Point formation and the Thluicho Group are distinguishable from the other units with respect to mineralogy and geochemistry.

The relative lack of clay minerals and the presence of unaltered feldspars in these rocks indicates that the source area for the Martin Group and related rocks had undergone only mild chemical weathering before erosion. First-cycle sedimentation is indicated by the quartz to feldspar ratio.

The minor quantities of kaolinite found in the samples taken for this study possibly relate to pre-Athabasca Group paleoweathering. Minor quantities of sudoite in the Martin Group rocks may be an indication of the proximity of these rocks to the sub-Athabasca unconformity and related basement - Athabasca sandstone fluid interaction associated with uranium mineralization. Martin Group formations become increasingly illitic up-section.

Shaw's (1972) discriminant function does not appear to be of great use in determining the provenance of these arkoses. The strong indication of sedimentary source area given by this function for the Charlot Point formation does, however, indicate some utility for discriminators of this type.

Gold, uranium, platinum and palladium are not seen to be anomalous in the Martin arkoses. Due to the lack of diagenetic alteration exhibited by these rocks and the ubiquitous, albiet low concentrations of these elements, the possibility that the Martin lithologies may host syngenetic gold and uranium mineralization in the area is discounted. Later epigenetic processes have, however, formed mineralization in these rocks (eg, uranium at the Martin Lake Adit).

6. References

Elliot, C. G. (1982): A description of the Gillies Channel Formation, Martin Group; *in* Summary of Investigations 1982, Sask. Geol. Surv., Misc. Rep. 82-4, p31-38.

Garett, G.J.S. (1983): Handbook of Exploration Geochemistry, Volume 3: Rock Geochemistry in Mineral Exploration; Elsevier, New York, 461p.

Hale, W. E. (1953): Black Bay map area, Saskatchewan (preliminary report); Geol. Surv. Can., Pap. 53-15, 18p.

_____ (1954): Gulo Lake, Saskatchewan; Geol. Surv. Can., Pap. 54-6.

_____ (1955): Forcie Lake map area, Saskatchewan; Geol. Surv. Can., Pap. 55-4.

Hendry, H. E. (1983): Sedimentological study of the Martin Group; *in* Summary of Investigations 1983, Sask. Geol. Surv., Misc. Rep. 83-4, p46-48.

Hoeve, J. (1982): Perspective on uranium mineralization at Beaverlodge; Sask. Res. Counc., Publ. No. G7451E82, 23p.

Hoeve, J. and Quirt, D. H. (1984): Mineralization and hos trock alteration in relation to clay mineral diagenesis and evolution of the middle Proterozoic Athabasca Basin, northern Saskatchewan, Canada; Sask. Res. Counc., Tech. Rep. No. 187, 187p.

Koster, (1968): The geology of the Zin Bay area, Saskatchewan; Sask. Dep. Miner. Resour., Rep. 121, 40p.

_____ (1970): The geology of the Burchnall Lake area, Saskatchewan; Sask. Dep. Miner. Resour., Rep. 131, 24p.

Langford, (1980): Successor basins in the Beaverlodge area; in Summary of Investigation 1980, Sask. Geol. Surv., Misc. Report 80-4, p29.

_____ (1981): The Martin Group in the greater Beaverlodge area; *in* Summary of Investigation 1981, Sask. Geol. Surv., Misc. Rep. 81-4, p38-43.

Macey, G. J. (1973): A sedimentological comparison of two Proterozoic red-bed successions (the South Channel and Kazan Formations of Baker Lake, NWT, and the Martin Formation at Uranium City, Saskatchewan); unpubl. M.Sc. thesis, Carleton University, Ottawa, Ontario.

Mason, B. (1966): Principles of Geochemistry, third ed., John Wiley & Sons, New York, 329p.

Mazimhakam P. and Hendry, H.E. (1984): The Martin Group, Beaverlodge area; In Summary of Investigation 1984, Sask. Geol. Surv., Misc. Rep. 84-4, p53-62.

_____ (1985): The Martin Group: Tazin Lake, Charlot Point and Jug Bay areas; *in* Summary of Investigation 1985, Sask. Geol. Surv., Misc. Rep. 85-4, p67-80.

_____ (1986): Conglomerate composition, source areas and dispersal in the depositional basin of the Martin Group; *in* Summary of Investigation 1986, Sask. Geol. Surv., Misc. Rep. 86-4, p114-120.

Pettijohn, F.J., Potter, P.E. and Siever, R. (1972): Sand and Sandstone; Springer-Verlag, New York, 618p.

Quirt, D.H. (1990): Mineralogy and lithogeochemistry of samples from the Martin and Thluicho Groups, Beaverlodge area, Saskatchewan; Sask. Res. Counc., Publ. No. R12301E90.

Ross, D.C. (1972): Petrographic and chemical reconnaissance study of some granitic and gneissic rocks near the San Andreas Fault from Bodega Head to Cajon Pass, California; U.S. Geol. Surv., Prof. Pap. 698.

Scott, B.P. (1978): The geology of an area east of Thluicho Lake, Saskatchewan; Sask. Dep. Miner. Resour., Rep. 167, 51p.

Shaw, D.M. (1967): An estimate of the chemical composition of the Canadian Precambrian Shield; Can. J. Earth Sci., v4, p829-835.

_____ (1972): The origin of the Apsley gneiss, Ontario; Can. J. Earth Sci., v9, p18-35.

Tarney, J. (1976): Geochemistry of Archean highgrade gneisses, with implications as to the origin and evolution of the Precambrian crust; *in* Windley, B.E. (ed.), The early history of the earth John Wiley & Sons, London, p405-417.

Taylor, S.R. (1972): Geochemistry of andesites: origin and distribution of the elements; *in* Ahrens, L.H. (ed.), Physics and chemistry of the earth Pergamon Press, New York, p559-583.

Tremblay, L.P. (1972): Geology of the Beaverlodge mining area, Saskatchewan; Geol. Surv. Can., Mem. 367, 265p.

van de Kamp, P.C., Leake, B.E. and Senior, A. (1976): The petrography and geochemistry of some Californian arkoses with application to identifying gneisses of metasedimentary origin; J. Geol., v84, p195-212.

Age of Granitoids from the Western Flin Flon Domain: An Application of the Single-zircon Pb-Evaporation Technique[1]

Kevin M. Ansdell[2] and T. Kurtis Kyser[2]

Ansdell, K.M. and Kyser, T.K. (1990): Age of granitoids from the western Flin Flon Domain: an application of the single-zircon Pb-evaporation technique; *in* Summary of Investigations 1990, Saskatchewan Geological Survey; Saskatchewan Energy and Mines, Miscellaneous Report 90-4.

This project forms part of ongoing research at the University of Saskatchewan into the relationship between mesothermal gold mineralization and the tectonic development of the Trans-Hudson Orogen. The western Flin Flon Domain hosts numerous occurrences of epigenetic gold mineralization (Coombe, 1984). These have been the subject of geological studies by Saskatchewan Energy and Mines and the Geological Survey of Canada, and have led to the construction of preliminary genetic models (Pearson, 1987; Galley and Franklin, 1987). Recent research at the University of Saskatchewan has provided new data on the structural setting and fluid chemistry of the Tartan Lake deposit, Manitoba (Fedorowich *et al.*, in prep.) and a number of other smaller deposits, e.g. Rio deposit and Laurel Lake deposit, Saskatchewan (Ansdell and Kyser, 1990), and has provided new constraints on the genesis of epigenetic gold mineralization in the region. In order to relate gold mineralization to the tectonic development of the area, the timing of mineralization is determined relative to igneous, deformational, and metamorphic events.

The objective of this study is to provide ages for a number of granitoid plutons in the western Flin Flon Domain using a new geochronological tool, the single-zircon Pb-evaporation technique (Kober, 1986; 1987). Field relationships are reasonably well-accepted (Byers and Dahlstrom, 1954; Stauffer, 1984; Galley and Franklin, 1987; Thomas, 1989; Wilcox, 1989), and so the age of these plutons should constrain the timing of molasse sedimentation, deformation, metamorphism, and gold mineralization.

1. Geological Setting

The Flin Flon Domain lies in one of the lithotectonic elements of the Reindeer Zone (Stauffer, 1984) of the Trans-Hudson Orogen, northern Saskatchewan and Manitoba (Hoffman, 1988). The oldest rocks in the western part of the domain (Figure 1) include tholeiitic to calc-alkaline volcanic and volcaniclastic rocks (Amisk Group) that were deposited in an oceanic island-arc setting (Stauffer *et al.*, 1975; Gaskarth and Parslow, 1987; Bailes and Syme, 1989; Thom *et al.*, in press). Unconformably overlying the Amisk Group is a sequence of synorogenic molasse deposits of the Missi Group (Stauffer, 1990). These supracrustal rocks have been metamorphosed and variably deformed during the Hudsonian Orogeny. The deformation terminology used by previous authors and in this study are correlated in Table 1. These rocks are intruded by a variety of gabbroic to granitic rocks, which range in age from syn-volcanic to late-tectonic.

Although the rocks have been interpreted as Aphebian in age and affected solely by the Hudsonian Orogeny (Mukherjee *et al.*, 1971; Sangster, 1978), it is only recently that the first precise U-Pb zircon ages have been obtained from the area (Gordon *et al.*, in press). Felsic volcanic and intrusive rocks in the Manitoba part of the Flin Flon Domain have been the focus of these geochronology studies, which indicate the age of Amisk Group volcanism in the Bear Lake Block (Bailes and Syme, 1989) is 1886±2 Ma, and the pre-Missi, Cliff Lake pluton (Figure 1) is 1874 +32/-25 Ma.

2. Sampling Rationale

The selection of granitoids was based on field and structural relations, so that the ages of major geological events in the area could be determined. Large (10-20 kg) samples were collected from all the locations in Figure 1, except for sample 484 which was a hand sample. Because the Pb-evaporation technique requires individual zircons, a hand sample may provide a suitable sample. Zircons were separated from the crushed samples using standard Wilfley Table, heavy liquid, and magnetic separation techniques. Non-magnetic, 125 to 250 micron zircons were then hand-picked prior to analysis. No pre-treatment is required.

3. The Single-zircon Pb-Evaporation Technique

The single-zircon Pb-evaporation technique was developed for routine zircon analysis by Kober (1986; 1987). The procedure involves heating a single zircon, which has been loaded directly on a rhenium evaporation filament, in a Finnigan MAT 261 mass spectrometer. As the zircon is heated, loosely-held Pb, which is evident from the presence of ^{204}Pb or low $^{204}Pb/^{206}Pb$ ratios, is emitted from the surface or cracks. This represents the Pb that would be removed by cleaning or abrading zircons prior to conventional U-Pb zircon dissolution procedures. The zircon is usually held at this temperature (about 1250°C) for about 15 minutes to 'clean' it. The temperature of the zircon is then increased to about 1400°C. At this temperature Pb

(1) Project funded under NSERC Cooperative Research and Development Project with CAMECO
(2) Department of Geological Sciences, University of Saskatchewan, Saskatoon, S7N 0W0

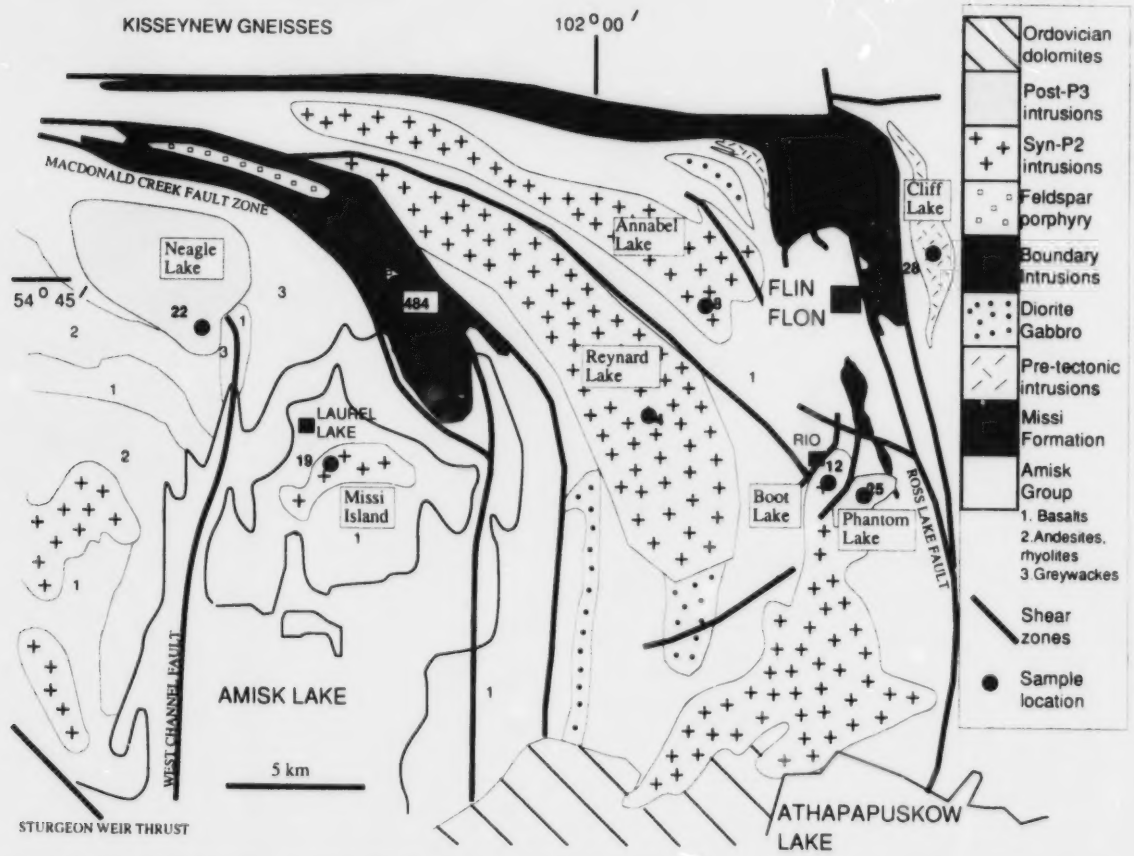

Figure 1 - Geological map of the western Flin Flon Domain (modified after Byers and Dahlstrom, 1954; Stauffer, 1984) showing the granitoid rocks sampled in this study (sample location and number). Phantom Lake granite dykes are too small to mark on the map, but radiate from the Phantom Lake granite and crosscut the Boot Lake pluton. The Rio, and Laurel Lake gold deposits are also shown.

starts to diffuse out of the crystal structure and emitted Pb is deposited on a cold ionization filament which faces the evaporation filament. Deposition of Pb is allowed to continue for about 10 to 15 minutes and the temperature of the evaporation filament is then reduced to about 800°C. The temperature of the ionization filament is increased to about 1250° to 1300°C and the Pb emitted from this filament is then analyzed by peak hopping using a secondary electron multiplier. After each analysis, the ionization filament is cleaned by raising its temperature to about 2200°C. The Pb deposition procedure is then repeated, although the evaporation filament is heated to a slightly higher temperature. In a perfect concordant zircon, the Pb isotopic composition

Table 1 - Correlation of Deformation Events in the Western Flin Flon Domain.

Stauffer and Mukherjee (1971)	Bailes and Syme (1989)	Wilcox (1989) N.E. Amisk Lake	Fedorowich et al (in prep) Flin Flon area	This study
P1 folding	P1 pre-Missi folding	pre-Missi folding	P1 pre-Missi folding	pre-Missi folding
	P2 folding	P1 folding	P2 folding	P1 folding
P2 folding	P3 folding P4 folding	P2 folding	P3 early - ductile shear zones and folding	P2 ductile shear zones and folding
		P3 folding, ductile-brittle shear zones	P3 late - folding, dominantly ductile shear zones	P3 folding, dominantly ductile shear zones
P3 Embury Lake fold, ductile and brittle faulting	P5 Embury Lake fold, ductile and brittle faulting	P4 Embury Lake fold	P4 Embury Lake fold, reactivated ductile-brittle shear zones	P4 Embury Lake fold, reactivated ductile-brittle shear zones
		P5 brittle strike-slip faults	P5 brittle strike-slip faults	P5 brittle strike-slip faults

measured after each evaporation step should be the same. However, many zircons contain metamict domains which release their Pb at lower temperatures than the more crystalline parts of the zircon. In these cases, only the higher temperature evaporation steps derive their Pb from the concordant parts of the zircon. In this study, the ages reported (Table 2) are calculated using the $^{207}Pb/^{206}Pb$ ratios taken from the highest temperature evaporation step unless otherwise indicated.

Table 2 - Ages of Zircons from Granitoids in the Western Flin Flon Domain, Saskatchewan.

Sample No.	Intrusion	No. Zircons	Age (Ma±2 sigma)
89-28	Cliff Lake tonalite	See Results section	
89-8	Annabel Lake granodiorite	5	1860±6
89-4	Reynard Lake granite	3	1853±8
89-19	Missi Island trondhjemite	2	1848±11
484	Graham Trail feldspar-porphyry	1	1841±18
89-22	Neagle Lake granodiorite	3	183±75
74-T-12	Boot Lake granodiorite	1	1842±13
89-25	Phantom Lake granite	2	1840±7
89-18	Phantom Lake granite dyke	1	1834±13

The analysis at each step was usually continued until the relative deviation in the $^{207}Pb/^{206}Pb$ ratio within a given block of data exceeded 1 percent. Data taken when the Pb signal was either unstable, or poor were screened using the technique outlined by Kroner and Todt (1988). The $^{204}Pb/^{206}Pb$ was continuously monitored, and a common Pb correction was only applied if the ratio exceeded 0.00005. The $^{207}Pb/^{206}Pb$ ages are quoted at the 95 percent confidence level, and in most cases represent the average of a number of zircons (Table 2). From a given intrusion, only zircons that have similar $^{207}Pb/^{206}Pb$ and $^{208}Pb/^{206}Pb$ ratios are used to calculate the average age. As described in a later section, the $^{208}Pb/^{206}Pb$ ratio may be used to detect xenocrystic zircons, which are not used in determining the age of the intrusion.

During the course of this study the accuracy and precision of the method was tested using zircons previously dated using high-precision U-Pb techniques at the Royal Ontario Museum (Otto Stock; Corfu *et al.*, 1989) and using the ion microprobe at the Australian National University (Nord Pascalis; Claoue-Long *et al.*, 1990). Three zircons from the Otto Stock yielded $^{207}Pb/^{206}Pb$ ages of 2675±4, 2683±4 and 2671±8 Ma (Table 3), which compare extremely favourably with the conventional U-Pb age of 2680±1 Ma (Corfu *et al.*, 1989). Two zircons from the Nord Pascalis mesothermal gold deposit, Abitibi, yielded $^{207}Pb/^{206}Pb$ ages of 2683±20 and 2727±36 Ma (Table 3) which agree well with the weighted mean age of 2697±19 obtained with the ion microprobe (Claoue-Long *et al.*, 1990). The Pb evaporation technique and the ion microprobe produce very similar results, and the imprecision in both cases is considered to result from the low U content (< 100 ppm) of the zircons. Overall, the accuracy of the single-zircon Pb-evaporation technique is comparable to other techniques, and so it is suggested in this study that the ages quoted are representative of the age of crystallization of the intrusions.

Table 3 - Comparison of ages (Ma) obtained using the single-zircon Pb-evaporation technique with high-precision U-Pb and ion microprobe techniques.

OTTO STOCK (Corfu *et al.*, 1989)		(This study)
High-precision U-Pb zircon dissolution		Single-zircon Pb-evaporation
Intercept:	2680±1	2683±4 2675±4 2671±8
NORD PASCALIS (Claoue-Long *et al.*, 1990)		(This study)
Ion microprobe		Single-zircon Pb-evaporation
$^{207}Pb/^{206}Pb$ ages (±2 sigma):	2697±30 2685±38 2711±38 2693±52	(±2 sigma) 2683±20 2727±36
Weighted mean $^{207}Pb/^{206}Pb$ age (± 2 sigma)	2697±19	

4. Results

a) Cliff Lake Tonalite

The Cliff Lake pluton is generally considered to be a pre-Missi intrusive from field relations (Stauffer, 1984; Bailes and Syme, 1989), and an imprecise age of 1874 +32/-25 Ma has been used to support this conclusion (Gordon *et al.*, in press). The zircon population separated is complex, and consists of long prismatic (length/width = 15/1), cracked zircons and light brown, subhedral zircons that yield ages of 1897±12 and 1896±17 Ma, respectively. Another brown, subhedral, partly broken and cracked zircon yields an imprecise age of 1859±22 Ma. These data suggest that this pluton is one of the oldest although older zircons probably represent xenocrystic zircons from either Amisk Group volcanic rocks or a slightly older unknown source (Figure 2). Further work on zircons from the Cliff Lake pluton will determine whether the age of 1859±22 is representative of the age of crystallization, and thus whether the Cliff Lake pluton is coeval with the Annabel Lake and Reynard Lake pluton. A mixture of zircon populations also explains the imprecise age measured by Gordon *et al.* (in press).

b) Annabel Lake Granodiorite

Five euhedral, prismatic, light pink zircons with fine magmatic zoning, collected from the granodioritic phase of the composite diorite-granodiorite-granite Annabel Lake pluton, yield an average age of 1860±6 Ma (Table 2). The Rb/Sr whole-rock isochron age of 1765±14 Ma obtained by Mukherjee *et al.* (1971) probably records the

time of Rb and Sr resetting during the latter stages of the Hudsonian Orogeny.

c) Reynard Lake Granite

Field relationships suggest that the Reynard Lake composite pluton is approximately the same age as the Annabel Lake pluton. Two flat, long prismatic zircons, and one stubby prismatic zircon were analyzed from the central granitic phase of the Reynard Lake pluton, and yield an average of 1853±8 Ma (Table 2).

d) Missi Island Trondhjemite

Two brown stubby prismatic zircons from the Missi Island trondhjemite yield identical ages of 1848±11 Ma (Table 2). This is interpreted as the age of crystallization, which indicates that the Missi Island Intrusion formed about 30 to 40 million years after Amisk Group volcanism. Chute and Ayres (1977) suggested that the trondhjemite represents the intrusive core of an Amisk Group vent complex, but the $^{207}Pb/^{206}Pb$ ages indicate that the intrusion was probably time-equivalent to many of the other post-Amisk intrusions in the area.

e) Graham Trail Feldspar-Porphyry

This highly-sheared feldspar-porphyry is enclosed by Missi Group rocks and is considered to intrude them (Wilcox, 1989). A light pink, euhedral zircon yields an age of 1841±18 Ma (Table 2).

f) Neagle Lake Granodiorite

The timing of the Neagle Lake pluton relative to deformation is ambiguous. Byers and Dahlstrom (1954) and Stauffer (1984) considered it to be a late tectonic intrusion that post-dates the north-south trending West Channel Shear Zone. However, the pluton contains a fabric that parallels the S2 schistosity in the surrounding supracrustal rocks, and the northwest part of the pluton appears to have been attenuated during P3 (K. Ashton, pers. comm.). The zircons analyzed are from the granodioritic phase of the pluton, and are translucent, prismatic, and contain opaque inclusions. The 'cleaning' stage, and the lower temperature evaporation steps yielded a large amount of Pb. However, the highest temperature evaporation steps yielded consistent ages, which average 1837± 5 Ma (Table 1).

g) Boot Lake - Phantom Lake Intrusive Complex

These intrusions are considered together, although there has been some discussion as to whether the contacts between various phases of the Boot Lake and Phantom Lake intrusions are gradational, or whether the Boot Lake and Phantom Lake are distinct entities separated in time (Galley and Franklin, 1987; Thomas, 1989). Field relations indicate that the Phantom Lake granite intrudes the Boot Lake granodiorite. A subhedral brown zircon from the Boot Lake granodiorite yields an age of 1842±13 Ma (Table 2), while two colourless, long prismatic zircons from the Phantom Lake granite give an average of 1840±7 Ma (Table 2). Their ages are indistinguishable within analytical error. The Phantom Lake pluton, like the Neagle Lake pluton, is considered to be late in the tectonic evolution of the area.

h) Phantom Lake Granite Dyke

From field relationships, the youngest magmatic event is the intrusion of the Phantom Lake feldspar-porphyritic granite dykes (Galley and Franklin, 1987; Thomas, 1989). The age of 1834±13 Ma (Table 2) was derived from the lowest temperature evaporation step from a zircon with a visible core and rim. The highest temperature evaporation step yielded an age of 1845±10 Ma, and is interpreted as the age of the core. The core and rim also have distinct $^{208}Pb/^{206}Pb$ ratios of 0.0497 and 0.0355, respectively. The possible significance of these $^{208}Pb/^{206}Pb$ ratios will be discussed in the following section.

5. Detection of Xenocrystic Zircons

The ability to detect xenocrysts in a suite of zircons is important in any U-Pb zircon study. The measured $^{208}Pb/^{206}Pb$ ratios are related to the Th/U ratio of the zircon, which should be a function of the Th/U ratio of the magma from which the zircon crystallizes. Thus, zircons that form simultaneously from a magma of constant composition should have identical $^{208}Pb/^{206}Pb$ and $^{207}Pb/^{206}Pb$ as do most of the zircons from the majority of intrusions in the Flin Flon area (Figure 2). The Cliff Lake, and Missi Island plutons are notable exceptions, and their variable $^{208}Pb/^{206}Pb$ ratios suggest that at least some of the zircons in these plutons are inherited. The core of a zircon from a Phantom Lake granite dyke yielded an age of 1845±10 Ma with a $^{208}Pb/^{206}Pb$ ratio of 0.0497. The age and $^{208}Pb/^{206}Pb$ ratio are characteristic of zircons from the Phantom Lake granite itself (Figure 2), and so it is suggested that this zircon may be a xenocryst from the Phantom Lake granite overgrown by zircon crystallizing from the slightly younger Phantom Lake granite dyke magma. Another zircon from the Phantom Lake granite dyke yielded an age of 1850±9 Ma, and a $^{208}Pb/^{206}Pb$ ratio of 0.0636, similar to zircons from the Reynard Lake pluton (Figure 2).

6. Constraints on the Timing of Tectonic and Fluid Events

The aim of this study is to provide constraints on the timing of molasse sedimentation, deformation, metamorphism, and gold mineralization, as well as the age of plutonism. The paragenesis of the western Flin Flon Domain is shown in Figure 2, and the constraints on the timing of events outlined below.

a) Missi Group Sedimentation

The Missi Group is crosscut by the Graham Trail feldspar-porphyry, which yielded an age of 1841±18 Ma (Table 2). In the vicinity of Flin Flon, the Missi Group is crosscut by one of the Boundary Intrusions, which are themselves cut by the Phantom Lake granite (1840±7)

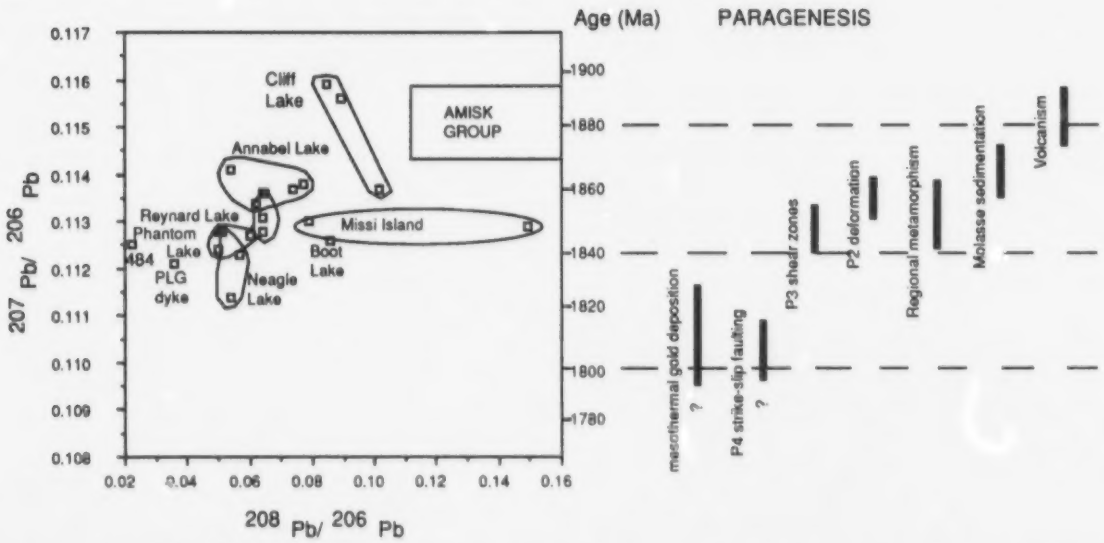

Figure 2 - Plot of $^{207}Pb/^{206}Pb$ versus $^{208}Pb/^{206}Pb$ ratios for zircons in granitoids and their relation to the paragenetic sequence of the Flin Flon Domain. The Amisk Group field is compiled from the data of Gordon et al. (in press) and R. McQuarrie (unpublished data).

(Syme and Forrester, 1977; Galley and Franklin, 1987). These relations indicate that Missi Group sedimentation must have been completed prior to 1840 Ma. This contrasts with an age of 1832±2 Ma for Missi felsic volcanic rocks near Snow Lake. Missi Group sedimentary rocks have also been metamorphosed and deformed during P2 and P3 (Stauffer and Mukherjee, 1971; Wilcox, 1989) and so any constraints on the timing of these events will provide further limits on the timing of molasse sedimentation. A study of detrital zircons in the Missi Group, to be started shortly, will further constrain the timing of sedimentation.

b) P2 and P3 Deformation, and Regional Metamorphism

The two most distinct foliations in the western Flin Flon Domain developed during P2 and P3 (Table 1), and are mainly defined by phyllosilicates that grew during regional metamorphism. The Boot Lake (1842±13 Ma), and Phantom Lake (1840±7 Ma) plutons are considered to post-date or be approximately contemporaneous with P3 shear zones (Byers and Dahlstrom, 1954; Thomas, 1989). The timing of the Neagle Lake pluton (1837±5 Ma) is ambiguous, but appears to predate P3 (K. Ashton, pers. comm.). Peak low-grade regional metamorphism was attained during P2, and was probably maintained up to and during P3 (Stauffer and Mukherjee, 1971; Bailes and Syme, 1989; Wilcox, 1989). An amphibolite grade halo around the Reynard Lake pluton (Longiaru, 1980) suggests that these intrusions locally elevated the thermal gradient during regional metamorphism. This amphibolite grade halo is offset by the P3 Robinson Creek shear zone.

Gordon *et al.* (in press) determined an age of 1815 Ma for peak regional metamorphism in high grade rocks in the central Kisseynew Domain. The zircon data in this study indicate that peak temperatures in the lower grade Flin Flon Domain were attained earlier, during the emplacement of the main intrusions. The Graham Trail feldspar-porphyry and the Neagle Lake pluton are metamorphosed, and so peak metamorphic temperatures were maintained locally to beyond 1837 Ma. However, in the Phantom Lake area, the Phantom Lake granite has a contact metamorphic aureole that post-dates regional metamorphism (Galley and Franklin, 1987; Thomas, 1989). Peak regional metamorphism was thus attained at about 1860 Ma, and peak metamorphic temperatures appear to have been maintained longer in higher grade metamorphic rocks (Figure 2).

c) Mesothermal Gold Mineralization

The timing of gold mineralization is presently unknown, but deposits such as Tartan Lake and Rio are spatially associated with reactivated P3 shear zones and P4 strike-slip faults. The best constraint on the timing of gold mineralization is provided in the vicinity of the Boot Lake - Phantom Lake complex. Gold mineralization and associated alteration overprints a Phantom Lake granite dyke (Andsell and Kyser, 1990), and thus must be younger than 1834 Ma. The mineralization was deposited from metamorphic fluids (*ibid*). Gordon *et al.*, (in press) determined an age of 1815 Ma for peak regional metamorphism in the Kisseynew Domain, and it is possible that continued degassing of amphibolite and granulite grade rocks adjacent to, or underlying the presently exposed Flin Flon Domain may represent the source of the metamorphic fluids associated with mesothermal gold deposits. Thus an age of about 1815 Ma may be reasonable for the age of gold mineralization in this region.

7. Conclusions

Zircons separated from granitoids in the western Flin Flon Domain have been dated using the single-zircon Pb-evaporation technique (Kober, 1987). The results indicate that the main plutons in the area were intruded between 1860 and 1834 Ma and are similar in age to other plutons in the Reindeer Zone of the Trans-Hudson Orogen (Van Schmus *et al.*, 1987). The age of the plutons provide constraints on the timing of other events in the region (Figure 2). P2, P3, and low-grade regional metamorphism took place within a 20 million year period from about 1860 to 1840 Ma, and are closely related in time with the intrusive activity. Peak metamorphic temperatures were probably maintained in adjacent higher grade terrains until 1815 Ma (Gordon *et al.*, in press), and these areas may represent the source of metamorphic fluids from which the mesothermal gold deposits in the Flin Flon area formed (Ansdell and Kyser, 1990).

This study indicates that the single-zircon Pb-evaporation technique can differentiate between closely-spaced magmatic events, and the accuracy and precision of the single-zircon Pb-evaporation technique are comparable to the ion microprobe and conventional U-Pb zircon techniques. However, the main advantages of the technique are as follows:

1) a hand sample may provide enough zircons to determine the age of a rock,
2) no chemical dissolution, or pretreatment is required, and so there is no problem with Pb contamination in the laboratory. Surface contamination is removed during the early part of the analysis.
3) analyses are cheap, and the analytical procedure now well-developed,
4) xenocrystic zircons can be detected, which will be masked in conventional multi-grain analyses, and
5) concordant ages can be obtained, through careful analysis, from highly metamict zircons.

8. Acknowledgements

Financial support is provided by NSERC and CAMECO to TKK, and a University of Saskatchewan Graduate Scholarship to KMA. F. Corfu and R. King kindly provided zircons from the Otto Stock and Nord Pascalis, respectively. Zircons from the Boot Lake pluton were provided by R. McQuarrie and M. Stauffer. A. Vuletich and D. Wyman are thanked for analytical assistance. K. Ashton is thanked for his critical review of the manuscript.

9. References

Ansdell, K.M. and Kyser, T.K. (1990): Epigenetic gold mineralization in the Flin Flon Domain: Fluid characteristics; *in* Beck, L.S. and Harper, C.T. (eds.), Sask. Geol. Soc., Spec. Publ. 10, p219-234.

Bailes, A.H. and Syme, E.C. (1989): Geology of the Flin Flon - White Lake area; Manit. Energy Mines, Geol. Services Branch, Geol. Rep. 87-1, 313p.

Byers, A.R. and Dahlstrom, C.D.A. (1954): Geology and mineral deposits of the Amisk - Wildnest Lakes area, Saskatchewan; Sask. Dep. Miner. Resour., Rep. 14, 177p.

Chute, M.E. and Ayres, L.D. (1977): Missi Island volcanic centre; *in* Report of Activities, Part B, Geol. Surv. Can., Pap. 77-1B, p29-31.

Claoué-Long, J.C., King, R.W. and Kerrich, R. (1990): Archaean hydrothermal zircon in the Abitibi greenstone belt: constraints on the timing of gold mineralisation; Earth Planet. Sci. Lett., v98, p109-128.

Coombe, W. (1984): Gold in Saskatchewan; Sask. Energy Mines, Open File Rep. 84-1, 134p.

Corfu, F., Krogh, T.E., Kwok, Y.Y. and Jensen, L.S. (1989): U-Pb zircon geochronology in the southwestern Abitibi greenstone belt, Superior Province; Can. J. Earth Sci., v26, p1747-1763.

Fedorowich, J.S., Stauffer, M. and Kerrich, R. (in prep): Structural and fluid characteristics of the Proterozoic Tartan Lake deposit, Trans-Hudson Orogen, northern Manitoba.

Galley, A.G. and Franklin, J.M. (1987): Geological setting of gold, coper, tungsten and molybdenum occurrences in the Phantom Lake region; *in* Summary of Investigations 1987, Sask. Geol. Surv., Misc. Rep. 87-4, p115-124.

Gaskarth, J.W. and Parslow, G.R. (1987): Proterozoic volcanism in the Flin Flon greenstone belt, east-central Saskatchewan, Canada; *in* Pharoah, T.C., Beckinsale, R.D., and Rickard, D. (eds.), Geochemistry and Mineralization of Proterozoic Volcanic Suites, Geol. Soc. London, Spec. Publ. 33, p183-200.

Gordon, T.M., Hunt, P.A., Bailes, A.H. and Syme, E.C. (in press): U-Pb ages from the Flin Flon and Kisseynew belts, Manitoba: Chronology of crust formation at an Early Proterozoic accretionary margin; *in* Lewry, J.F., and Stauffer, M.R. (eds.), The Early Proterozoic Trans-Hudson Orogen, Geol. Assoc. Can, Spec. Pap. 37.

Hoffman, P.F. (1988): United Plates of America, the birth of a craton: Early Proterozoic assembly and growth of Proto-Laurentia; Annu. Rev. Earth Planet. Sci. Lett., v16, p543-603.

Kober, B. (1986): Whole-grain evaporation for $^{207}Pb/^{206}Pb$ age investigations on single zircons using a double-filament thermal ion source; Contrib. Mineral. Petrol., v93, p482-490.

_____ (1987): Single-grain evaporation combined with Pb^+ emitter bedding for $^{207}Pb/^{206}Pb$ investigations using thermal ion mass spectrometry, and implications for zirconology; Contrib. Mineral. Petrol., v96, p63-71.

Kober, B., Pidgeon, R.T. and Lipolt, H.J. (1989): Single-zircon dating by stepwise Pb-evaporation constrains the Archean history of detrital zircons from the Jack Hills, Western Australia: Earth Planet. Sci. Lett., v91, p286-296.

Kröner, A. and Todt, W. (1988): Single zircon dating constraining the maximum age of the Barberton greenstone belt, southern Africa; J. Geophys. Res., v93, p15329-15337.

Longlaru, S.J. (1980): Structure and metamorphism of the northeast Amisk Lake area, Saskatchewan; unpubl. M.Sc. thesis, Univ. Sask., 119p.

Mukherjee, A.C., Stauffer, M.R. and Baadsgaard, H. (1971): The Hudsonian Orogeny near Flin Flon, Manitoba: a tentative interpretation of Rb/Sr and K/Ar ages; Can. J. Earth Sci., v8, p939-946.

Pearson, J.G. (1987): Gold mineralization in the Flin Flon - Amisk Lake area, Saskatchewan; *in* Gilboy, C.F. and Vigrass, L.W (eds.), Economic Minerals of Saskatchewan; Sask. Geol. Soc., Spec. Publ. 8, p37-43.

Sangster, D.F. (1978): Isotopic studies of ore-leads in the circum-Kisseynew volcanic belt of Manitoba and Saskatchewan; Can. J. Earth Sci., v15, p1112-1121.

Stauffer, M.R. (1984): Manikewan: an Early Proterozoic ocean in central Canada, its igneous history and orogenic closure; Precamb. Res., v25, p257-281.

_____ (in press): The Missi Formation: an Aphebian molasse deposit in the Reindeer Lake zone of the Trans-Hudson Orogen, Canada; *in* Lewry, J.F., and Stauffer, M.R. (eds.), The Early Proterozoic Trans-Hudson Orogen, Geol. Assoc. Can., Spec. Pap. 37.

Stauffer, M.R. and Mukherjee, A.C. (1971): Superimposed deformations in the Missi metasedimentary rocks near Flin Flon, Manitoba; Can. J. Earth Sci., v8, p217-242.

Stauffer, M.R., Mukherjee, A.C. and Koo, J. (1975): The Amisk Group: an Aphebian(?) island arc deposit; Can. J. Earth Sci., v12, p2021-2035.

Syme, E.C. and Forester, R.W. (1977): Petrogenesis of the Boundary intrusions in the Flin Flon area of Saskatchewan and Manitoba; Can. J. Earth Sci., v14, p444-455.

Thorn, A., Arndt, N.T., Chauvel, C. and Stauffer, M. (in press): Flin Flon and western La Ronge Belts, Saskatchewan: Products of Proterozoic subduction-related volcanism; *in* Lewry, J.F., and Stauffer, M.R. (eds.), The Early Proterozoic Trans-Hudson Orogen, Geol. Assoc. Can., Spec. Pap. 37.

Thomas, D.J. (1989): Geology of the Douglas Lake - Phantom Lake area (part of NTS 63K-12 and -13); *in* Summary of Investigations 1989, Sask. Geol. Surv., Misc Rep. 89-4, p44-54.

Van Schmus, W.R., Bickford, M.E., Lewry, J.F., and Macdonald, R. (1987): U-Pb geochronology in the Trans-Hudson Orogen, northern Saskatchewan, Canada; Can. J. Earth Sci., v24, p407-424.

Wilcox, K.H. (1989): Investigation of Missi metasedimentary rocks in the Amisk-Welsh lakes area, Saskatchewan; *in* Current Research, Part C, Geol. Surv. Can., Paper 89-1C, p165-171.

Rb-Sr Geochronology of the Lodge Bay Granite, a ca. 3.0 Ga Basement in the Beaverlodge Area, Saskatchewan

Michael Bikerman[1], *Keith Bell*[2] *and John Blenkinsop*[2]

Bickerman, M., Bell, K. and Blenkinsop, J. (1990): Geochronology of the Lodge Bay Granite, a ca. 3.0 Ga basement in the Beaverlodge area, Saskatchewan; *in* Summary of Investigations 1990, Saskatchewan Geological Survey; Saskatchewan Energy and Mines, Miscellaneous Report 90-4.

As part of a program of remapping of the geology of the Beaverlodge area north of Lake Athabasca, geochronological determinations were carried out on a number of plutons. This paper reports on the unusual results of Rb-Sr analyses on the Lodge Bay Granite.

The Lodge Bay Granite, generally a uniform massive leucogranite, was originally mapped by Christie (1953) as a plutonic intrusion emplaced within low grade metasediments of the 'Tazin Series' of unknown Precambrian age. These supracrustals were subsequently identified as part of the Murmac Bay Group (e.g. Tremblay, 1972; Macdonald and Slimmon, 1984) – a mixed assemblage of quartzites, conglomerates, carbonates, pelites and pillowed basaltic flows and epiclastics – which covers an area of about 600 km^2 along the north shore of Lake Athabasca. In the area of the Lodge Bay Granite, Murmac Bay rocks have attained lower amphibolite facies grade and generally retain original depositional structures such as cross bedding. The granite and some of the contiguous supracrustals contain thick gabbroic sheets, which appear to be sills on the map; Christie (1953), and Sibbald and Lewry (1980) regarded these as intruded by the granite.

Macdonald (1984) in company with Roscoe (pers. comm.) noted an apparent unconformity in the Elliot Bay locality, at the south end of the granite, between granite and overlying granite/quartz pebble conglomerate of the Murmac Bay Group. In 1985 an exposure of a suspected deformed unconformable junction between quartzite and granite was identified on the northeastern flank of the Lodge Bay Granite by Van Schmus *et al.* (1986), who collected samples for U-Pb zircon determination from which they derived an imprecise U-Pb upper intercept of 3072±41 Ma. Samples for Rb-Sr determinations had been collected previously from the Lodge Bay Granite by the present authors which also indicated a comparable age, but the results were not published earlier due an apparent discrepancy in the initial ratios.

A few kilometres east of the Lodge Bay Granite small granitic bodies known as the 'Mine Granites' have been interpreted to be derived by feldspar metasomatism of pre-existing supracrustal rocks of the Murmac Bay Group (Sibbald, 1984; Sibbald and Jiricka, 1985). Still farther east are the larger Mackintosh Bay and Cameron Island plutons. Bell *et al.* (in press) using Rb-Sr determinations and incorporating U-Pb zircon results from some of these granites (Van Schmus *et al.*, 1986) present a model in which an intrusive event at ca. 2350 Ma has been succeeded by the feldspar metasomatising event at ca. 2000 Ma

In this paper we present corroborative evidence that the Lodge Bay Granite is significantly older than any of these granites, and that it is part of the basement underlying the Murmac Bay Group, and may have been part of the crust from which the later granites were derived.

1. Procedures

Whole rock samples of the Lodge Bay Granite were pulverized to less than 100 mesh in a Beuhler mill. Aliquots were pressed into 32 mm boric acid-backed briquets for X-ray fluorescence analysis for Rb and Sr. The XRF analyses were carried out using a modified version of the Norrish and Chappell (1967) method with a U.S. Geological Survey standard G-2 run before and after each sample. Baseline counts were made before and after each peak count, and each was counted for 40 seconds. Each sample was run twice and the average values are reported. Precision of the Rb/Sr ratios is about one percent.

All isotopic analyses were carried out following chemical preparation and ion-exchange chromatography on chlorides using single Ta filaments for Sr and double Re filaments for Rb on a Finigan-MAT 261 multicollector solid-source mass spectrometer. On this machine ^{85}Rb, ^{86}Sr, ^{87}Sr and ^{88}Sr are measured simultaneously. Internal precision for Sr isotopic ratios is considered to be 5 parts in 70,000. Isotope dilution mass-spectrometric checks on two samples show variances in Rb and Sr contents from XRF determinations as shown in Table 1. ^{87}Rb and ^{84}Sr spikes were used.

The isochron plot (Figure 1) shows the measured points and the calculated values of the date and intercept using York's (1969) method. The Steiger and Jäger (1977) Rb half life value of 48.8 x 10^9 yrs. was used. Table 2 shows the XRF chemical analyses for four samples from the Lodge Bay Granite.

Thirteen XRF determinations for Rb and Sr, and two duplicates run by isotope dilution (marked ID in Table 1) and their corresponding Sr isotope analyses give a date of 2839±67 Ma, an initial ^{87}Sr/^{86}Sr intercept ratio of

(1) Department of Geology and Planetary Science, University of Pittsburg, Pittsburg, Pennsylvania
(2) Ottawa-Carleton Geoscience Centre, Department of Earth Sciences, Carleton University, Ottawa, Ontario

Table 1 - Lodge Bay Rubidium And Strontium Isotopic Data

Sample	Rb ppm	Sr ppm	Rb/Sr	$^{87}Rb/^{86}Sr$	$^{87}Sr/^{86}Sr$
SK-1	124	114	1.09	3.175	0.82449
SK-2	108	111	0.98	2.861	0.81041
SK-3	120	129	0.94	2.768	0.81125
SK-4	63	134	0.47	1.368	0.75026
SK-710	73	124	0.59	1.721	0.76208
SK-711	67	132	0.51	1.467	0.75061
SK-745	123	76	1.63	4.790	0.89084
SK-746	111	71	1.57	4.616	0.87739
SK-747	97	36	2.72	8.078	0.98146
SK-748	103	40	2.55	7.591	1.00892
SK-749	150	41	3.63	10.960	1.15338
SK-750	99	64	1.55	4.557	0.88266
SK-751	91	74	1.23	3.608	0.84590
SK-711ID	61.27	125.1	0.49	1.423	0.75058
SK-749ID	132.7	37.19	3.57	10.772	1.14894

ID-Isotope dilution Rb and Sr contents; rest by XRF

Table 2 - Lodge Bay Granite Chemical Analyses - XRF

Major elements in weight %

OXIDE	SK-711	SK-745	SK-746	SK-749
SiO2	72.32	75.12	76.66	75.19
Al2O3	14.28	13.87	13.12	14.09
Fe2O3	1.14	0.53	0.39	0.5
MgO	1.44	0.5	0.35	0.28
CaO	0.89	0.39	0.28	0.37
Na2O	3.9	3.11	3.86	4.2
K2O	3.87	5.41	4.26	4.59
TiO2	0.11	0.04	0.04	0.02
P2O5	0.03	0.022	0	0.01
MnO	0.09	0.01	0.01	0.02
TOTAL	98.07	99.002	98.97	99.27
Trace elements in ppm				
Ba	596	441	168	181
Cr	21	13	11	17
Zr	74	22	21	16
Sr	124	66	30	33
Rb	61	111	88	135
Y	3	3	5	6
Nb	1	2	2	6
Zn	20	7	8	15
V	2	2	0	0

0.69276±0.00239 and an MSWD of 0.726. Eliminating the point for SK-746 which lies well off the line changes the values slightly to 2896±73 Ma, 0.69134±.00253 and 0.154.

2. Discussion

Since the points are well spread out along the isochron, the differences between the variations described above is small, and no matter how the data in Table 1 is interpreted, it seems that a date of ca. 2900 Ma and an intercept significantly less than 0.700 is obtained. The date is significantly older than any other of the plutons in the region. The intercept seems too low as it is lower than the meteorite values of BABI (0.69898), Allende (0.69877) and ADOR (0.69883) (Wasserburg *et al.*, 1977; Birck and Allègre, 1978; Wasserburg, 1987), the 3.8 Ga Amîtsoq Gneiss value of 0.6973±0.0006 (Baadsgaard *et al. 1976) or the 0.698*±0.014 of the 1.18 Ga Tugtutôq central complex of south Greenland (van Breeman and Upton, 1972). If the meteorite values set the actual constraints on terrestrial initial Sr ratios - i.e. if all terrestrial rocks must have some excess of ^{87}Sr above meteoritic values - then our determination can be considered to reflect some geological event(s) which rotated the isochron.

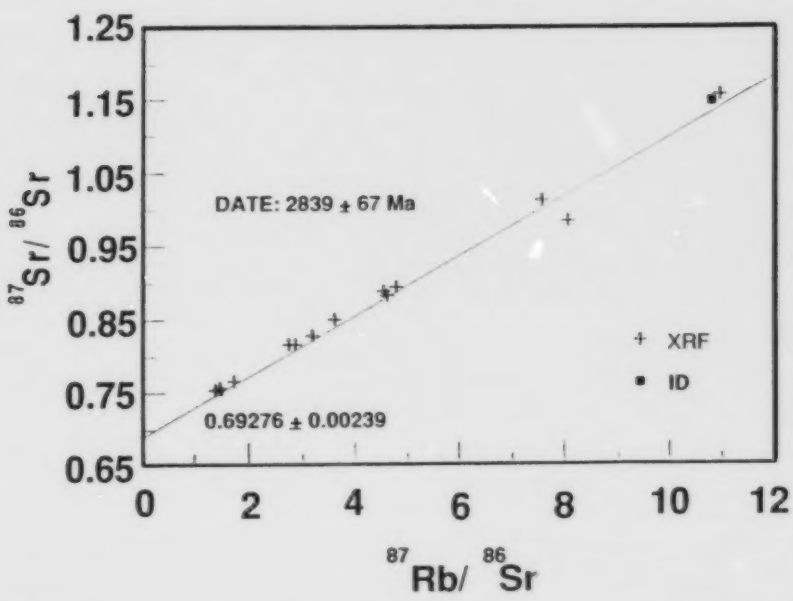

Figure 1 - Rb-Sr isochron of the Lodge Bay Granite. The date of all points (including two duplicates run by isotope dilution - marked 1D here and in Table 1) is 2839±67 Ma, with an initial $^{87}Sr/^{86}Sr$ intercept ratio of 0.69276±0.00239 and an MSWD of 0.726. Eliminating the point of SK-746 gives 2896±73 Ma, 0.69134±0.00253 and 0.154.

It is proposed that the Lodge Bay Granite is a parent to the Cameron Island and Mackintosh Bay granites and their metasomatic progenies the Mine Granites (Bell *et al.*, in press). The Cameron Island and Mackintosh Bay granites give well-constrained isochrons at ca. 2010 to 2020 Ma, with high initial $^{87}Sr/^{86}Sr$ ratios. However, since the average Rb/Sr value for the Lodge Bay Granite is 1.77, it is too deficient in Rb to serve as the source for metasomatism of the Mine Granites.

The date of ca. 2.9 Ga for the Lodge Bay Granite gives a lower bracket for the age of the overlying Murmac Bay Group. An upper

bracket appears to be set by the ca. 2.35 Ga U-Pb zircon date (Van Schmus *et al.*, 1986) of the intruding Mackintosh Bay and Cameron Island plutons. One may speculate that the Murmac Bay Group correlates with the Prince Albert Group (Schau, 1977) and other quartzite-carbonate-volcanic assemblages now known in the Canadian Shield which have been dated within this interval.

3. References

Baadsgaard, H., Lambert R. St.J. and Krupicka, J. (1976): Mineral isotopic relationships in the polymetamorphic Amitsoq gneisses, Gothaab District, West Greenland; Geochim. Cosmochim. Acta, v40, p513-527.

Bell, K., Blenkinsop, J., Sibbald, T.I.I. and Macdonald, R. (in press): Rb-Sr Geochronology of the auriferous North Shore Plutons, Lake Athabasca, Saskatchewan; Can. J. Earth Sci.

Birck, J.L. and Allègre, C.J. (1978): Chronology and chemical history of the parent body of basaltic achondrites studied by the ^{87}Rb-^{86}Sr method; Earth Planet. Sci. Lett., v39, p37-51.

Christie, A.M. (1953): Goldfields-Martin Lake map-area, Saskatchewan; Geol. Surv. Can., Mem. 269, 126p.

Macdonald, R. (1984): Bedrock compilation, greater Beaverlodge area (NTS-74N-6 to -11) *in* Summary of Investigations 1984, Sask. Geol. Surv., Misc. Rep. 84-4, p42-44.

Macdonald, R. and Slimmon, W.L. (1984): Bedrock geology of the greater Beaverlodge area, NTS 74N-6 to -11; Sask. Energy Mines, Map 241A, scale 1:100,000.

Norrish, K. and Chappell, B.W. (1967): X-Ray fluorescence spectrography; *in* Zussman, J. (ed.), Physical Methods in Determinative Mineralogy, Academic Press, New York, p161-214.

Schau, M. (1977): Komatiites and quartzites in the Archean Prince Albert Group; *in* Baragar, W.R.A, Coleman, L.C. and Hull, M.J. (eds.), Volcanic regimes in Canada, Geol. Assoc. Can., Spec. Pap. 16, p341-354

Sibbald, T.I.I. (1984): Gold metallogenic studies, Goldfields area; *in* Summary of Investigations 1984, Sask. Geol. Surv., Misc. Rep. 84-4, p116-121.

Sibbald, T.I.I. and Jiricka, D.E. (1985): Geology of the gold deposits, Goldfields, Saskatchewan; *in* Gold in the Western Shield (Program and Abstracts); CIM Geology Division Gold Symposium and Field Tours, Saskatoon, Sept. 7-12, p33-35.

Sibbald, T.I.I. and Lewry, J.F. (1980): Uranium metallogenic studies: Lodge Bay area, Lake Athabaska; *in* Summary of Investigations 1980, Sask. Geol. Surv., Misc. Rep. 80-4, p44-48.

Steiger, R. and Jäger, E. (1977): Subcommission on geochronology: Convention on the use of decay constants in geo- and cosmochronology; Earth Planet. Sci. Let.t, v36, p359-362.

Tremblay, L.P. (1972): Geology of the Beaverlodge mining area, Saskatchewan; Geol. Surv. Can., Mem. 367, 165p.

van Breemen, O. and Upton, B.G.J. (1972): Age of some Gardar Intrusive Complexes, South Greenland; Geol. Soc. Am. Bull., v83, p3381-3390.

Van Schmus, W.R., Persons, S.S., Macdonald, R. and Sibbald, T.I.I. (1986): Preliminary results from U-Pb zircon geochronology of the Uranium City Region; *in* Summary of Investigations 1986, Sask. Geol. Surv., Misc. Rep. 86-4, p108-111.

Wasserburg, G.J. (1987): Isotopic abundances: inferences on solar system and planetary evolution; Earth Planet. Sci. Lett., v86, p129-173.

Wasserburg, G.J., Tera, F., Papanastassiou, D.A. and Huneke, J.C. (1977): Isotopic and chemical investigations on Angra dos Reis; Earth Planet. Sci. Lett., v35, p294-316.

York, D. (1969): Least-squares fitting of a straight line with correlated errors; Earth Planet. Sci. Lett., v5, p320-324.

Metasomatic Host-rock Alteration at the Frontier Gold Prospect, Goldfields Area, Saskatchewan

David H. Quirt[1]

Quirt, D.H. (1990): Metasomatic host rock alteration at the Frontier gold prospect, Goldfields area, Saskatchewan; *in* Summary of Investigations 1990, Saskatchewan Geological Survey; Saskatchewan Energy and Mines, Miscellaneous Report 90-4.

Numerous investigations have been carried out in the Goldfields area since the discovery of gold mineralization in 1934 at the location of the former Box Mine, located on the north shore of Lake Athabasca, approximately 25 km southeast of Uranium City, Saskatchewan. The earliest of these (see references listed in Quirt, 1990) were spurred on by this and other discoveries nearby, the next generation by the discovery of uranium in the Beaverlodge area and the latest group of studies by a renewed interest in precious metal mineralization. In addition, regional mapping, bedrock compilation, and geochronology projects have been carried out by the Saskatchewan Geological Survey. An overview of the geology, structure and gold mineralization of the Goldfields region can be found in Sibbald (1984) and Sibbald and Jiricka (1986).

The 'Mine Granites' hosting the gold mineralization at the Box and Athona Mines and the Frontier prospect have been variously interpreted as magmatic and metasomatic in origin. Lithogeochemical investigations have been performed both by Quirt (1987, 1990) and by Appleyard (1988, 1989) to evaluate these hypotheses and to determine the history of the gold mineralization. The conclusions offered by these two studies concerning the Frontier 'granite' are quite different with respect to the alteration process and to the amount of volume change associated with this alteration. This report has been prepared in order to deal with two points. The first is to amplify the data and interpretations of Quirt (1987), which was a preliminary interpretation of field and lithogeochemical data. The second is to address the interpretations proposed by Appleyard (1988, 1989), whose 1988 report was not based on field or lithologic criteria but strictly on evaluation of Quirt's geochemical data.

1. Geological Setting

The area around Goldfields belongs to the Nevins Lake Block (Macdonald, 1983, 1984, 1987) of the Western Craton (Lewry and Sibbald, 1977). The Nevins Lake Block is an Archean basement complex that is part of the western foreland to the Trans-Hudson Orogen located to the southeast. The basement rocks are overlain by the Lower Proterozoic Murmac Bay Group, a miogeosynclinal supracrustal assemblage consisting of metasedimentary and metavolcanic lithologies which have been intruded by gabbroic sills. This assemblage has been, in turn, intruded by a number of small granitoid bodies, the 'North Shore Plutons' (Macdonald, 1983, 1987).

In the Frontier Lake area, quartzites of the Murmac Bay Group, cut by intrusive metagabbro, predominate. The mafic intrusive rocks form thin sill-like bodies usually less than 25 m in thickness (Tremblay, 1972) that form the resistant caps on the higher hills in the area. Rocks which have been loosely termed 'granitic' host the Frontier prospect and also the Box and Athona gold mines.

Several varieties of quartzite are recognized (Jiricka, 1984; Quirt, 1987), including siliceous quartzite, ferruginous quartzite, and arkosic quartzite. Siliceous quartzite is white to off-white in color, well-jointed and fractured, with bedding planes locally visible. This layer is rarely pebbly. The dominant mineral component is quartz which comprises greater than 95 percent of the rock. Potassium feldspar is a minor component in this rock and minor to trace quantities of sericite, chlorite, and hematite are also present. Ferruginous quartzite is similar to siliceous quartzite but contains up to 20 percent hematite. The hematite is present as a stain along fractures or joint planes and, locally, as part of a quartz-hematite cement in brecciated quartzite. Jiricka (1984) postulated that this hematization may be related to pre-Athabasca Group paleoweathering. Arkosic quartzite is common in the area immediately around Frontier Lake, occurring as a distinct grey to pinkish unit within the siliceous quartzites. Potassium feldspar is present in amounts of up to 60 percent with quartz making up most of the remainder of the rock, along with sericite, hematite, chlorite, and rare pyrite. Contacts with the siliceous quartzite appear to be gradational.

The gabbroic sills are generally dark green to black, massive, weakly foliated and comprise hornblende megacrysts in a matrix of feldspar, amphibole, and chlorite. Foliation is pronounced at contacts with the metasediments, dipping moderately to the southeast. A mineral and rodding lineation plunges moderately south-southwesterly parallel to the axis of the Goldfields synclinorium (Sibbald, 1984).

Lineaments that likely represent fault zones form a conjugate set related to the Goldfields synclinorium and trend northeast and northwest. Jiricka (1984) noted the presence of a major north to north-northwesterly-trending structure that passes immediately to the southeast of the Frontier prospect, just east of the adit.

(1) Minerals/Groundwater Program, Resources Technology Division, Saskatchewan Research Council, Saskatoon, Saskatchewan

Lenticular zones of a more or less massive 'granite' comprising potassium feldspar and quartz with significant disseminated pyrite and cut by numerous quartz veins occur in the arkosic quartzite. One of these zones is the Frontier Granite.

Several distinct sets of quartz veins are recognized within the massive 'granitic' rocks (Jiricka, 1984). Two are known to host gold mineralization. The veins are dilational in nature and are ubiquitous, from microscopic size to centimetre-scale widths.

'Granite' at the Frontier Prospect is cut by numerous quartz veins containing gold and sulphides. Quartz veins, within the 'granite' and the 'granitic' portions of transitional rocks, die out rapidly, within 1 cm, upon encountering quartzite. Sulphides, pyrite and traces of chalcopyrite, are present both in the quartz veins, and in the 'granite' host rock. Chalcopyrite is only rarely found as specks associated with pyrite. Chlorite is locally present in the veins, while tourmaline is only rarely noted.

Vein mineralization is geochemically simple with Au ± S, Cu (Quirt, 1990). This association compares well with the Au ± Ag, Zn, Pb, Cu, Mo mineralization of the Box and Athona deposits (Sibbald and Jiricka, 1986), however, the absolute copper concentration at Frontier is low (Table 1). Gold is found as specks of free gold and as native gold along fractures in pyrite. Neither gold nor pyrite appear to be spatially associated with chlorite. The Au-S, Cu, (U) correlation, while not extremely high, is present in both unaltered (quartzite) and altered ('granite') material (Quirt, 1990) implying that the source for the elevated Au and S contents in the 'granite' may have been the quartzite protolith (Sibbald and Jiricka, 1986; Quirt, 1990).

2. The Frontier 'Granite'

The Frontier 'Granite' forms a conformable unit in arkosic quartzite over an outcrop width of 25 to 65 m and a total strike length of 600 m (Jiricka, 1984). It is quite homogeneous on a small scale but relatively inhomogeneous on outcrop scale. A number of field identifiable features of this zone, including quartz veining, silicification, feldspathization, pyritization, transitional contacts with the host quartzite, and the variability of the zone, indicate that a metasomatic origin is likely. Further observations that support this origin have been listed in Quirt (1987) and amplified in Appleyard (1989). These observations are:

1. Sedimentary bedding and layering become progressively blurred in the transition from quartzite to 'granitic' rock which is additionally marked by a reddening of the rock, a more massive appearance, and an apparent increase in feldspar content such that the sericitic and foliated host quartzite becomes feldspathic and granular textured.

2. Slightly altered foliated, white to brown to green arkosic quartzite may contain reddish, granular quartzofeldspathic zones that follow foliation, or may show patches and spots of reddish feldspathization.

3. Rocks transitional between quartzite and 'granite', while being reddish and relatively massive, show color banding, which is due to the alignment of fine chloritic streaks, parallel to layering in adjacent quartzites.

4. Strongly altered 'granite' is a massive, reddish, feldspathic granulite which contains finely disseminated pyrite only rarely seen in the unaltered quartzite.

3. Sampling, Geochemical Data, and Data Analysis

Samples taken for this study have been subdivided into three groups (quartzite, transitional, granite) using the criteria listed in Quirt (1987) and apparent from the descriptions above. The mineral assemblages contained by the three groups were determined by x-ray diffraction (Table 1) and by thin section microscopy (Quirt, 1990). The quartzite is composed of an assemblage of quartz and potassium feldspar with minor biotite + sericite + chlorite + monazite/zircon. Quartz and feldspar megacrysts are set in a fine-grained foliated matrix of sericite (± chlorite). Grain size is variable but commonly from 0.5 to 1 mm. Biotite, and rarely chlorite, form detrital flakes lying parallel to bedding. Rounded grains of monazite/zircon tend to occur with biotite and also, occasionally, ilmenite/rutile/hematite. Most samples of quartzite have undergone recrystallization following cataclasis, as shown by the common but variable occurrence of mortar texture in quartz.

'Granite' resembles recrystallized quartzite and is composed of an assemblage of mortar-textured quartz, potassium feldspar, and rare sericite. Grain size is fine, around 0.4 mm, although there are also extremely fine-grained aggregates of recrystallized grains which are around 0.02 mm in diameter. Due to ubiquitous cataclasis and recrystallization, the precursor lithology cannot be determined except by the field evidence of lateral gradation of this rock into quartzite.

Data available include major and trace element geochemical analyses, specific gravity determinations, and whole rock mineralogical analyses. Samples were not analyzed for SiO_2, therefore silica was calculated by difference and is used only in an illustrative fashion. A number of other elements (Ag, Se, Be, Lu, Tb, Eu, Mo, Cd) were not used in the mass balance calculations as many of the analytical values are at or close to the analytical detection limit.

Sixty-seven samples were available for study, however, only 51 were selected for use in the mass balance calculations. Summary data for the three sample groups is presented in Table 1. The 16 samples omitted showed evidence of shearing and/or were considered to be non-representative based on mineralogy. The spread of mineralogical variations in the selected samples was evaluated using a triangular diagram representing quartz, potassium feldspar, and total phyllosilicate mineral content. The change from arkosic quartzite to 'granite' is marked by a reduction in the phyllosilicate

Table 1 - Analyses of quartzite and altered equivalents in the Frontier area. Major element and mineralogical data are expressed in percent and are represented by the arithmetic mean. Trace element data are expressed in parts per million (parts per billion for Au) and are represented by the arithmetic mean of the log-transformed data. Coefficient of variation (CV) represents the relative dispersion from the mean.

	Quartzite n = 14		Transitional n = 12		Granite n = 25	
	mean	*CV*	*mean*	*CV*	*mean*	*CV*
Quartz	25.07	0.46	32.16	0.35	31.60	0.19
K-feldspar	60.71	0.20	52.50	0.16	65.88	0.09
Sericite	12.57	0.64	3.91	0.54	1.80	0.69
Chlorite	1.64	1.11	1.41	0.76	0.72	1.10
Specific Gravity	2.676	0.016	2.651	0.010	2.623	0.006
SiO_2c	72.23	0.12	74.48	0.08	79.82	0.05
Al_2O_3	14.25	0.32	12.98	0.24	10.18	0.21
Fe_2O_3t	1.63	0.52	1.52	0.61	0.72	0.46
FeO	0.47	0.41	0.89	0.63	0.50	0.40
Fe_2O_3c	1.11	0.72	0.54	0.78	0.19	1.12
CaO	0.15	1.64	0.15	0.87	0.10	0.52
MgO	1.17	0.89	0.83	0.47	0.27	0.60
K_2O	8.11	0.39	8.06	0.18	7.75	0.21
Na_2O	0.48	1.03	0.39	0.27	0.30	0.37
TiO_2	0.24	0.53	0.20	0.69	0.08	0.68
P_2O_5	0.06	0.78	0.08	0.59	0.06	0.56
MnO	0.02	1.05	0.01	0.54	<0.01	0.50
LOI	1.40	0.37	1.03	0.53	0.44	0.62
CO_2	0.17	0.57	0.24	0.75	0.18	0.54
H_2Oc	1.22	0.43	0.81	0.69	0.27	0.78
Au	3.42	0.81	5.99	1.46	15.62	3.22
S	110.00	1.69	50.00	2.97	190.00	2.85
Ni	8.99	0.56	13.09	1.08	6.71	0.73
Pb	16.87	0.77	14.42	0.47	14.12	0.30
Cu	4.71	0.77	5.23	1.02	6.08	0.88
Co	4.70	0.66	5.33	1.00	2.16	0.56
Ag	0.17	0.45	0.20	0.27	0.20	0.36
As	2.04	1.37	3.29	2.32	2.32	1.33
Se	0.22	0.82	0.12	0.34	0.18	0.49
U	3.13	0.78	2.06	0.36	1.77	0.71
V	25.20	0.55	20.96	0.63	9.94	0.63
Th	18.46	0.75	13.92	0.48	9.90	0.64
Cr	81.45	0.99	82.26	1.65	48.61	2.01
Be	1.81	0.54	1.12	0.46	0.80	0.44
Zr	183.64	0.58	121.14	0.45	95.39	0.54
Y	11.31	0.55	8.06	0.49	5.46	0.54
Rb	229.29	0.32	206.64	0.24	188.10	0.18
Sr	40.60	0.40	45.74	0.21	36.96	0.24
Ba	945.77	0.30	1197.51	0.18	1163.28	0.27
B	25.28	1.13	11.89	0.31	12.69	0.37
Li	9.32	0.99	8.69	0.96	3.86	0.82
Mo	5.74	0.39	6.24	0.32	5.78	0.20
Zn	19.24	0.88	11.14	0.42	5.70	0.56
Cd	1.08	0.29	1.41	0.48	1.16	0.33
La	44.52	0.55	31.00	0.54	22.48	0.56
Lu	0.54	0.17	0.52	0.13	0.50	0.00
Yb	1.40	0.60	1.20	0.50	0.62	0.54
Er	0.99	0.93	1.35	1.06	0.83	0.70
Tb	2.34	0.34	2.66	0.48	2.00	0.00
Dy	2.30	0.46	1.48	0.71	1.27	0.48
Eu	0.98	0.38	0.80	0.44	0.68	0.37
Nd	32.36	0.52	23.33	0.68	12.46	0.99
Ce	86.83	0.50	63.56	0.56	44.43	0.54

proportion and a narrowing of the range of the quartz to potassium feldspar ratio, factors which both result in increasing homogeneity of the mineralogy of the rocks. Accordingly, there is a progressive reduction in variance of density and elemental abundances in the transition from quartzite to 'granite'.

Probability plots (Wilkinson, 1988) of the major elements typically show distributions that are close to normal while trace elements are log-normally distributed. Some elements, such as Au, Cu and U show some deviation from a log-normal distribution but they appear to be sufficiently close to allow the use of log-transformed statistics for description.

The mean values for the three sample groups, 'parent quartzite', 'transitional rock', and 'granite' (Table 1) are not recalculated to a 'constant average amount of the immobile elements' as in Appleyard (1988) because this procedure assumes conclusions on the immobility of the elements before the results of the mass balance calculations were interpreted.

4. Element Correlations

Interelement correlations were examined to determine the elements associated with the phyllosilicate minerals, sericite and chlorite. Studies have established phyllosilicates as having a high capacity for binding metals (e.g., Chester, 1965; O'Conner, 1974; van de Kamp *et al.*, 1975; Zielinski *et al.*, 1983) and that some of the first mineralogic sites to be leached of absorbed metals are the exchangeable sites on phyllosilicates (Zielinski *et al.*, 1983). Zielinski *et al.* (1983) also noted that Mo, Co, V, Ni, and Cu tend to be easily absorbed onto, and leached from, phyllosilicate mineral surfaces, and that these heavy metals, and others such as Pb, Zn, and U, can also reside in structural sites within the phyllosilicates. Similarly, van de Kamp *et al.* (1975) observed that Zn, Li, Rb, Nb, Ni, Co, Cr, Zr, and TiO_2 are dominantly carried in the phyllosilicate minerals in arkosic sediments. Bailey (1980) noted that Mn, V, Ba, Cr and Li can substitute into the structural sites of illite and/or chlorite.

Pearson correlation coefficients calculated on the suite of 14 relatively phyllosilicate-rich quartzite samples reveal the association of (a) K_2O with Al_2O_3-TiO_2-Rb-Ce-La-Yb-Zr-V-Y and to some extent with H_2O and Dy and (b) MgO with Zn-Co-Li-H_2O-MnO-Fe_2O_3. In the quartzite, K_2O is shared between sericite and potassium feldspar, however, the correlation coefficients calculated using the potassium feldspar-rich, sericite-poor granite suite, as well as sericite-poor quartzite samples, identify the potassium feldspar element association. This information has been used to screen out the contribution of potassium feldspar to the K_2O association in the quartzite in order to reveal the contribution by sericite, namely: K_2O-TiO_2-H_2O-Ca-Dy-V-Y-Zr-Yb-La. This screening must be considered to be qualitative only, as the K_2O correlations in quartzite represent sericite and potassium feldspar while those in granite represent potassium feldspar plus an unknown contribution from the metasomatic fluid. Based on the above, the elements related to the sericite and/or chlorite proportion in the rocks are as follows: TiO_2, MnO, FeO, Fe_2O_3, H_2O, MgO, Al_2O_3, V, Yb, Zn, Be, B, Y, La, Lu, Nd, Ce, Se, and, to some extent, Rb, Li, Dy and Zr.

5. Mass Balance Calculations

The approach taken in this study on the Frontier 'Granite' was to evaluate the effects of pervasive metasomatism of the arkosic quartzite by comparing relatively unaltered, parental material with its altered equivalent, 'granite'. Absolute elemental gains, losses, and immobilities were evaluated using Pearce element ratios (e.g., Davies *et al.*, 1979) as well as the mass balance techniques described by Gresens (1967), Grant (1987), and others. The mass and/or volume changes that took place during alteration were evaluated by using multi-element whole rock geochemical analyses in conjunction with specific gravity determinations.

Pearce element ratios (PER's: Pearce, 1968; Beswick and Soucie, 1978; Stanley and Russell, 1989) were used to evaluate alteration gains and losses. On X/Z-Y/Z mole ratio diagrams, metasomatically related rocks produce trends which are colinear with the origin and the protolith (parent) composition, where X and Y are conserved (immobile) elements and Z is mobile (Davies *et al.*, 1979; Grant, 1987; MacLean and Kranidiotis, 1987). Diagrams using ratios of three immobile elements (conserved element plots; e.g., Russell and Halleran, 1990) will result in a cluster of data points for a cogenetic suite of samples whose dispersion is consistent with analytical uncertainty.

PER diagrams derived from quartzite samples typically reveal poorly defined trends and mean ratio values with high associated coefficients of variation. These patterns are consistent with the suggestion that the quartzite in the Goldfields area is not homogeneous, at least on the scale of sampling. Field observations indicate that the character of the quartzite changes noticeably both laterally and vertically within several metres with respect to lithology and sedimentary features.

Alteration superimposed on this parent rock will tend to further complicate the search for immobile elements using PER's. As a result, no conserved elements were identified using PER diagram analysis.

Composition-volume (C-V) diagrams (Gresens, 1976) can be used to determine a possible value for the volume factor (f_v) by showing the volume change necessary to account for the concentration of each element in the altered rock relative to its parent. The gain or loss of each component is plotted as a function of f_v. If volume remains constant, elements with values of $f_v > 1$ have been removed while those with values < 1 have been enriched. In the general case where volume change occurs in the metasomatic process (because some components are immobile), they will show similar values of f_v (where the curves for several components cluster in crossing the zero gain-loss line) and thereby identify the volume factor together with the gain or loss behaviour of mobile elements.

Some 'false' clusters that are generated can be eliminated by their lack of consistency within a sequence of C-V diagrams representing various parent-altered pairs. Other 'false' trace element clusters may result from the elimination or formation of a mineral phase in which elements were or become concentrated. The equation for the alteration reaction can be derived once a 'geologically probable' f_v value is obtained by inspection. An example of this clustering occurs at Frontier because of the loss of sericite and gain of feldspar with accompanying loss of trace elements.

Several elements (TiO_2, MnO, FeO, Fe_2O_3, H_2O, MgO, V, Yb, Zn, B, Y, La, Nd, Ce, Li, Dy, Zr) may be suspect based on their common association with the phyllosilicate minerals. As the alteration from quartzite, through transitional material, to 'granite' involved a significant loss of phyllosilicate minerals, elements associated with these minerals may have been lost to the alteration fluid.

The following elements identified as being associated with the phyllosilicates reveal a cluster of zero-change f_v values substantially greater than 1 (Table 2) indicating removal from the system: TiO_2, Li, U, Y, Dy, Zr, Nd, La, Th, Yb, Ce, V and B. A number of other elements, also associated with phyllosilicate minerals, show f_v values indicative of even greater degrees of removal from the system, namely: Fe_2O_3, MgO, MnO, Zn, H_2O. Their elimination, because of a potential to generate 'false' clusters, leaves a substantially reduced choice for selection of immobile elements: Al_2O_3, SiO_2, CaO, K_2O, Na_2O, P_2O_5, CO_2, Au, S, Ni, Pb, As, U, Co, Cr, Cu, Th, Sr, Ba, Er, and Rb.

Only SiO_2(c), Au, S, CO_2, FeO, Ba, and Cu show absolute enrichment in the 'granite' ($f_v < 1$), in harmony with both field observation and elemental correlation analysis. The widely varying values of f_v (most significantly greater than 1) for all of the other elements precludes the possibility that the apparent addition of Au, S, Cu, Ba, CO_2, and Si is a result only of the depletion of the remainder of the elements.

Table 2 - F_v at zero - change

	Quartzite to Transitional	Transitional to Granite	Quartzite to Granite
SiO_2c	0.99	0.94	0.91
TiO_2	1.17	2.73	3.19
Al_2O_3	1.11	1.29	1.43
CaO	1.01	1.52	1.53
K2O	1.01	1.05	1.07
MgO	1.41	3.13	4.42
FeO	0.53	1.80	0.95
Fe_2O_3	2.05	2.82	5.78
H_2Oc	1.51	2.96	4.48
CO_2	0.72	1.33	0.96
Na_2O	1.27	1.28	1.61
P_2O_5	0.76	1.38	1.02
MnO	1.65	2.78	4.59
Au	0.58	0.39	0.22
S	2.22	0.27	0.59
Cu	0.91	0.87	0.77
Zn	1.74	1.98	3.44
Co	0.89	2.49	2.22
Li	1.08	2.28	2.46
U	1.54	1.17	1.80
Th	1.34	1.42	1.90
Zr	1.53	1.28	1.96
V	1.21	2.13	2.59
B	2.15	0.95	2.03
Y	1.42	1.49	2.11
La	1.45	1.39	2.02
Nd	1.40	1.89	2.65
Dy	1.56	1.18	1.84
Yb	1.18	1.94	2.28
Ce	1.38	1.45	2.00
Ba	0.80	1.04	0.83
Rb	1.12	1.11	1.24
Sr	0.90	1.25	1.13
Cr	1.00	1.71	1.71

The field evidence of (a) dilational quartz veining (estimated at 10 percent by volume in the 'granite'), and (b) gain of potassium feldspar at the expense of phyllosilicate minerals, constrains the selection of a geologically reasonable value for f_v. The range of f_v values from approximately 0.95 to 0.75 corresponds to a 5 to 25 percent volume decrease for the 'granite'. Using these values, only SiO_2(c), FeO, CO_2, Ba, and Cu have been immobile or relatively immobile and indicate a volume decrease of from 4 to 23 percent. As quartz is the filling mineral for the dilational veins, the presumption that SiO_2(c) remained immobile on a local scale may be justifiable. SiO_2(c) values indicate a volume decrease of approximately 9 percent, however, as SiO_2 was not analyzed directly, this value can only be taken as an estimate. In any event, the range of volume decrease caused by alteration of parent quartzite to 'granite' of from 4 to 23 percent appears to this author to be geologically reasonable. As noted in Quirt (1987) and Appleyard (1988), the transitional samples display little or no change in volume relative to the quartzite.

6. Interpretation

There likely was little or no volume change associated with the alteration from quartzite to transitional material as f_v values for SiO_2, Al_2O_3 and K_2O, the three most common elements in these rocks, are approximately 1.00 (Table 2). Only the mean values for FeO, P_2O_5, and CO_2 show any significant change in value from quartzite to transitional, however, CO_2 and P_2O_5 values are close to the detection limit in all cases and the FeO mean value for the transitional group is strongly influenced by one or two samples which contain somewhat more FeO (1.5 to 2.5 percent) than the remainder of the group, which have values similar to those of the quartzite. Most trace elements do, however, appear to have been depleted, in concert with phyllosilicate loss (Table 1).

A volume reduction of approximately 10 percent is suggested to have accompanied the alteration of quartzite to 'granite'. The 0.91 f_v value for SiO_2 (Table 2) indicates that at zero volume change, the SiO_2 content in the 'granite' must be increased by 9 percent with respect to the quartzite or that there was a constant SiO_2 content with a 9 percent decrease in volume. The latter scenario appears to better fit the field evidence of quartzofeldspathic 'granitic' rock containing microscopic to macroscopic dilational quartz veining.

F_v values at zero-change for TiO_2, MgO, Fe_2O_3t, H_2O and MnO are very high (>3) and geologically unrealistic, indicating strong depletion of these elements in the 'granite' due to phyllosilicate mineral loss. Values for Na_2O, CaO, and Al_2O_3 are also high (>1.4) and those for both P_2O_5 and K_2O are greater than 1.00, also indicating depletion, or a volume gain that does not correspond to the field evidence. Of the three oxides, SiO_2(c), Al_2O_3, and K_2O, present in host and altered rock in amounts greater than 5 percent, the f_v value of 0.91 for SiO_2 appears to be the most geologically reasonable. On this basis, both Al_2O_3 and K_2O appear to have been released into the alteration fluid, along with most of the other major elements, as a consequence of the destruction of sericite.

No significant differences are apparent in the mean values for FeO, CO_2, CaO, and Na_2O between quartzite and granite, however, all of these elements are present in amounts less than 0.65 percent and all show a substantial amount of within-group variation (Table 1). Irrespective of this, all of these elements are present in lower concentrations in the altered material relative to quartzite. All other major elements, except K_2O, show significant differences in mean values, with SiO_2(c) being higher in the granite and the others being much lower. K_2O does not show a significant reduction in mean value from quartzite to 'granite', however, a trend of K_2O reduction from quartzite through transitional material to 'granite' is present.

Using $KAl_2Mg0.5Si_3.5O_{10}(OH)_2$ as a general representation of a slightly magnesian sericite, the conversion of sericite to potassium feldspar would release Al, Mg, and some Si. In the conditions present during alteration at Frontier, Si may have reprecipitated as quartz while Al and Mg were lost from the system. Some quartz may also have been introduced during a later event of quartz veining, however this matter is purely conjecture at this point.

Trace elements occurring at low levels in the quartzite (Zn, Pb, Ni, Li, V, Co, As, Ag, U, Mo, Th, Y, Se, Cd, Be, Eu, Tb, Dy, Yb, Lu, Er, Nd) remained at low levels during alteration to 'granite'. Other trace elements occurring at moderate levels (Mn, Cr, Rb, Sr, B, Zr, La, Ce) were released due to destruction of phyllosilicate minerals. The only trace elements to show higher concentrations in the 'granite' than in the quartzite are Au, S, Ba, and As. Mean values and ranges for both Au and S show dramatic increases in the 'granitic' material as compared to either the quartzite or transitional material. Barium appears to follow potassium feldspar while arsenic in the 'granite' only shows a minor increase with respect to quartzite that appears to be due to a few moderately high erratic values. Gold generally follows sulphur but high sulphur content does not appear to be a requirement.

These data suggest that the alteration of quartzite to 'granite' was not due to potassium metasomatism but to redistribution and recrystallization during cataclasis leading to the disappearance of sericite and the appearance of potassium feldspar. Sufficient potassium is present in the host quartzite to account for that in the 'granite'. Potassium feldspar stability and the destabilization of the hydrous phyllosilicate minerals during alteration requires that the alteration fluid has a relatively low activity of H^+ relative to that of K^+ (e.g., Rose and Burt, 1979; Beane and Titley, 1982). This change in mineralogy was accompanied by a depletion in many major and trace elements, however, it is not certain whether the gold and sulphur enrichment occurred at this time.

7. Conclusions

The conclusions reached by this study are similar to those proposed earlier (Quirt, 1987) with only minor differences brought about by the addition of new sample data. A minor volume decrease for the alteration of arkosic quartzite to 'granite' through destabilization of sericite and chlorite and redistribution of K_2O, Al_2O_3, and SiO_2 into potassium feldspar and quartz during cataclasis is proposed. These conclusions differ significantly from Appleyard's (1988, 1989) interpretation. By concluding Ti, P, V, Y, Zr, La, Ce, Dy, and Yb to be immobile, Appleyard (1988) determined that metasomatism of the arkosic quartzite resulted in "an approximate doubling of the mass and volume of the Frontier 'granite' with respect to the host quartzite". In doing so he erroneously assumed the phyllosilicate mineral-related element cluster to be immobile, although he did state that "all the elements identified as being immobile would be primarily resident within these 'other' minerals rather than in the quartz-feldspar framework", i.e., the phyllosilicate minerals.

A number of genetic models for the origin of the Goldfields area 'Mine Granites' have been proposed (see Appleyard, 1989 for brief summaries). The models proposed by Jiricka (1984) [ponded hydrothermal fluids (after Kerrich and Fryer, 1979)] and by Appleyard (1988, 1989) [magmatic infiltration] appear to be conceptually similar. The main difference between these concepts is the character of the hydrothermal fluid (Jiricka, 1984), or highly fluid hydrous magma (Appleyard, 1988, 1989) that caused the 'granitization' phenomena. Jiricka (1984) prefers a hydrothermal solution consisting primarily of water, while Appleyard (1988, 1989) prefers a fluid similar to a pegmatitic fluid. Both believe that the ultimate fluid source was a late granitic intrusion located at depth.

Classical potassic silicate alteration (Guilbert and Park, 1986), as opposed to potassic alteration, is proposed as the most likely hydrothermal alteration process to have formed the Frontier alteration assemblage. This process, yielding a quartz + potassium feldspar + pyrite + Au assemblage, is typical of the lower levels of epithermal vein systems (Berger and Eimon, 1982; Guilbert and Park, 1986). Jiricka's (1984) model appears to be similar in many ways, however, the concept that 'ponding' of the hydrothermal fluids beneath competent amphibolite (metagabbro) units occurred is questioned. The sheared nature of the gabbro-'granite' contact, the shearing and cataclasis of the 'granite', and the presence of sheared quartzite in the immediate vicinity suggests an alternative possibility, namely that the channelway for the hydrothermal fluids was structurally controlled as in other lode gold deposits. This argument is supported by the restriction of gold-quartz vein systems to the 'granite', although quartz vein systems are widespread (Sibbald and Jiricka, 1986), and, additionally, by the presence of pyrite and gold in the 'granite', not confined to quartz veins.

The hypothesis provided above fits well with the interpretation of Rees (in Quirt and Rees, 1987; Rees, in prep.) that the fluids that formed the Box and Athona veins, and likely the Mine Granites, were CO_2-rich with characteristics similar to those of Archean lode gold veins. The available data for the Frontier prospect are not sufficient to define a source for the gold although derivation from the precursor supracrustals is suggested. Evidence does point, however, to a hydrothermal mechanism of deposition which ultimately may have been magmatic, as Jiricka (1984) believed, or metamorphic.

8. Acknowledgements

I am grateful to Dr. T. Sibbald of Saskatchewan Energy and Mines for critically reviewing the text of this contribution.

9. References

Appleyard, E. C. (1988): The origin of the Frontier Granite, Goldfields area, Saskatchewan: A metasomatic assessment; *in* Summary of Investigations 1988, Sask. Geol. Surv., Misc. Rep. 88-4, p161-167.

_____ (1989): Field observations on the Frontier, Box and Athona Granites, Goldfields area, Saskatchewan; *in* Summary of Investigations 1989, Sask. Geol. Surv., Misc. Rep. 89-4, p82-86.

Bailey, S.W. (1980): Structures of layer silicates; *in* Crystal structures of clay minerals and their x-ray identification; Miner. Soc. Mono. No. 5, p1-123.

Beane, R.E. and Titley, S.R. (1982): Porphyry copper deposits, Part II, Hydrothermal alteration and mineralization; Econ. Geol., 75th Anniv. Vol., p235-269.

Berger, B.R. and Elmon P.J. (1982): Comparative models of epithermal silver-gold deposits; Am. Inst. Min. Metal. Petrol. Eng., Reprint 82-83, 25p.

Beswick, A.E. and Soucie, G. (1978): A correction procedure for metasomatism in an Archean greenstone belt; Precam. Res., v6, p235-248.

Chester, R. (1965): Adsorption of zinc and cobalt on illite in sea water; Nature, v206, p884-886.

Davies, J.F, Grant, R.W.E., and Whitehead, R.E.S. (1979): Immobile trace elements and Archean volcanic stratigraphy in the Timmins mining area, Ontario; Can. J. Earth Sci., v16, p305-311.

Grant, J.A. (1987): The Isocon Diagram-a simple solution to Gresens' equation for metasomatic alteration; Econ. Geol., v81, p1978-1982.

Gresens, R.L. (1967): Composition-volume relationships of metasomatism; Chem. Geol., v2, p47-65.

Guilbert, J.M. and Park, C.F. (1986): The Geology of Ore Deposits; W.H. Freeman and Company, New York, 985p.

Jiricka, D. E. (1984): Exploration 1983, Lodge Bay Project, CBS 5664, 5665, and 5677, S98948, Athabasca Mining District, Saskatchewan, NTS 74N07,08; Saskatchewan Mining Development Corporation Assessment Report; Sask. Energy Mines, Assessment File 74N07-0315, 59p.

Kerrich, R. and Fryer, B.J. (1979): Archean precious metal hydrothermal systems, Dome Mine, Abitibi greenstone belt, II. REE and oxygen isotope relations; Can. J. Earth Sci., v16, p440-458.

Lewry, J.F., and Sibbald, T.I.I. (1977): Variation in lithology and tectonometamorphic relationships in the Precambrian basement of northern Saskatchewan; Can. J. Earth Sci., v14, p1453-1467.

MacLean, W.H. and Kranidiotis, P. (1987): Immobile elements as monitors of mass transfer in hydrothermal alteration: Phelps Dodge massive sulphide deposit, Matagami, Quebec; Econ. Geol., v82, p951-962.

Macdonald, R. (1983): Geology and regional context of the Oldman Lake area; *in* Summary of Investigations 1983, Sask. Geol. Surv., Misc. Rep. 83-4, p19-23.

_____ (1984): Bedrock compilation, Greater Beaverlodge area; *in* Summary of Investigations 1984, Sask. Geol. Surv., Misc. Rep. 84-4, p42-44.

_____ (1987): Update on the Precambrian geology and domainal classification of northern Saskatchewan; *in* Summary of Investigations 1987, Sask. Geol. Surv., Misc. Rep. 87-4, p87-104.

O'Conner, T.P. (1974): The adsorption of copper and cobalt from aqueous solution onto illite and other substrates; unpubl. Ph.D. thesis, Univ. Rhode Island, 188p.

Pearce, T.H. (1968): A contribution to the theory of variation diagrams; Contrib. Mineral. Petrol., v19, p142-157.

Quirt, D.H. (1987): Frontier prospect - lithogeochemistry and mass balance calculations; Sask. Res. Counc., Publ. No. R 8554E87, 12p.

_____ (1990): The Frontier granite and the Frontier Au prospect, Goldfields area, northern Saskatchewan; Sask. Res. Counc., Publ. No. R12302A90.

Quirt, D. H. and Rees, M. (1987): Current research in mineral deposits at the Saskatchewan Research Council; *in* Summary of Investigations 1987, Sask. Geol. Surv., Misc. Rep. 87-4, p160-163.

Rees, M. (in prep.): Fluid history of the Beaverlodge area; M.Sc. thesis, Univ. Sask.

Rose, A.W. and Bert, D.M. (1979): Hydrothermal alteration; *in* Barnes, H.L (ed.), Geochemistry of Hydrothermal Ore Deposits, 2nd ed., Wiley, New York, p173-235.

Russell, J.K. and Halloran, A. (1990): Trace elements formulated as Pearce element ratio's (PER), I: Insights into magma differentiation; *in* Theory and application of Pearce element ratios to geochemical data analysis, Geol. Assoc. Can., Short Course, v8, p55-72.

Sibbald, T.I.I (1984): Gold metallogenetic studies, Goldfields area; *in* Summary of Investigations 1984, Sask. Geol. Surv., Misc. Rep. 84-4, p116-121.

Sibbald, T.I.I. and Jiricka, D. (1986): Geology of the gold deposits, Goldfields, Saskatchewan; *in* Clark, L.A. (ed.), Gold in the Western Shield, CIM, Spec. Vol. 38, p412-414.

Stanley, C.R. and Russell, J.K. (1989): Petrologic hypothesis testing with Pearce element ratio diagrams: Derivation of diagram axes; Contrib. Mineral. Petrol., v108, p78-89.

Tremblay, L.P. (1972): Geology of the Beaverlodge mining area, Saskatchewan; Geol. Surv. Can., Mem. 367, 285p.

van de Kamp, P.C., Leake, B.E., Senior, A. (1976): The petrography and geochemistry of some Californian arkoses with application to identifying gneisses of metasedimentary origin; J. Geol., v84, p195-212.

Wilkinson, L. (1988): SYSTAT: The System for Statistics; SYSTAT, Inc., Evanston, IL.

Zielinski, R.A., Block, S. and Walker, T.R. (1983): The mobility and distribution of heavy metals during the formation of first cycle red beds; Econ. Geol., v78, p1574-1589.

Fluid History of the Athabasca Basin and Its Relation to Uranium Deposits[1]

T. Kotzer[2] and T.K. Kyser[2]

Kotzer, T. and Kyser, T.K. (1990): Fluid history of the Athabasca Basin and its relation to uranium deposits; *in* Summary of Investigations 1990, Saskatchewan Geological Survey, Saskatchewan Energy and Mines, Miscellaneous Report 90-4.

Studies of clays and other minerals in and around unconformity-uranium deposits of the Athabasca Basin have resulted in genetic models that involve interaction between high-temperature basin and basement fluids at the unconformity between Aphebian metasedimentary and overlying Helikian sedimentary rocks (Hoeve and Sibbald, 1978; Hoeve and Quirt, 1984 and 1986). These models have been furthur refined by isotopic and fluid inclusion studies (Pagel *et al.*, 1980; Bray *et al.*, 1988; Wallis *et al.*, 1983; Wilson and Kyser, 1987; Kotzer and Kyser, 1990), which indicate that uranium mineralization has resulted from mixing of a high salinity, metal-bearing basinal brine with a reducing basement fluid at temperatures of 200°C along well-developed fault zones. Zones of fluid mixing are marked by well-developed geochemical haloes containing illite, tourmaline, Mg-chlorite, euhedral quartz and Ni-Co-As and Cu sulfides. A regional diagenetic assemblage of illite and kaolinite occurring within the Manitou Falls Formation throughout the basin attests to the high permeability of the sediments in the basinal aquifers that allowed large-scale fluid flow.

Late-stage incursion of low-temperature meteoric fluids into the basin along the fault zones which host the uranium deposits has altered the isotopic and chemical compositions of both the clay and uranium minerals. Relatively young K-Ar ages of illite and U-Pb ages of uranium minerals, formation of kaolinite in the fault zones, remobilization of uranium into fractures in the re-activated fault zones (Wilson and Kyser, 1987; Kotzer and Kyser, 1990) and formation of secondary sulphides with highly variable $\delta^{34}S$ and Pb isotopic compositions (Kyser *et al.*, this volume) are all indicative of these late-stage fluid events.

The various types of fluids and fluid-flow events have characteristic mineralogical and geochemical signatures, so that it is likely that the metallogenic and mineralogic evolution of the Athabasca Basin has been controlled by large scale fluid events associated with prograde and retrograde basin diagenesis. The association between fluid flow events, basin diagenesis, and uranium ore formation in the Athabasca Basin is similar to the mechanism of ore formation in other types of sediment-hosted mineral deposits (Gustafson and Williams, 1981).

This report summarizes data from stable and radiogenic isotope and fluid inclusion analyses obtained mainly from uranium deposits in the southeastern portion of the Athabasca Basin (Figure 1) and places them within a fluid evolution framework.

1. Fluid Inclusion and Isotopic Evidence for Fluid Movements in the Athabasca Basin

The results of petrographic work carried out by CAMECO combined with stable and radiogenic isotopic compositions, fluid inclusion and scanning electron data allow formulation of a fluid-mineral-age paragenesis of the Athabasca Basin (Figure 2).

Correlations between the petrographic and geochemical data indicate that many of the basin-wide events which

Figure 1 – Map indicating the present extent of the Athabasca Basin, locations of uranium deposits and major lithostructural domains in the crystalline basement of Saskatchewan (after Hoeve and Sibbald, 1978). MD = Mudjatik Domain, WD = Wollaston Domain, PLD = Peter Lake Domain, RD = Rottenstone Domain.

(1) Project funded under NSERC Cooperative Research and Development Project with CAMECO
(2) Department Geological Sciences, University of Saskatchewan, Saskatoon, Saskatchewan, S7N OWO.

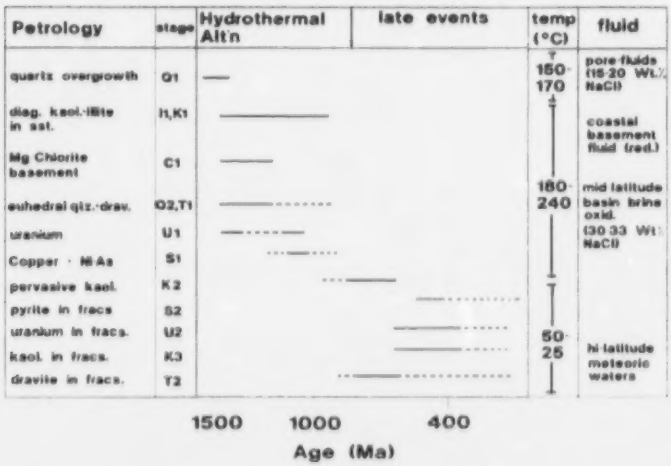

Figure 2 – Fluid-mineral-age relationships for various minerals within the Athabasca Basin developed from petrographic work, stable and radiogenic isotopes and fluid inclusion analyses. Data used for correlations are from drill core and hand specimens from Key Lake, McArthur River (Bermuda and Phoenix Lake), Eagle Point and Midwest Lake.

are seen petrographically have distinct temperatures and stable isotopic composition. Initial diagenesis (Q1), evolved to high-temperature basin diagenesis, basin-basement fluid mixing, and polymetallic uranium mineralization (I1-K1, C1, Q2-T1, U1, S1), followed eventually by uplift and fracturing of the basin resulting in incursion of oxidizing meteoric fluids producing retrograde mineral assemblages and destruction of the previously formed unconformity-type uranium deposits (K2, S2, U2, K3, T2). Some of the later events, such as late kaolinite formation and remobilization and destruction of uranium deposits, are a continuum of events which began around 800 Ma and have persisted periodically until the past few million years (Figure 2).

a) Fluid Inclusions

Microthermometric analysis of fluid inclusions in paragenetically distinct mineral phases from the McArthur River Area (Bermuda and Phoenix Lake) and Eagle Point North indicate that there was an increase in the salinity and temperature during early prograde diagenesis and a subsequent decrease in temperature and salinity of the fluids involved with late retrograde diagenesis. The temperatures and salinities of fluids determined in the fluid inclusions from the McArthur River Area and Eagle Point are similar to the fluids in inclusions measured in equivalent phases at Cluff Lake and Rabbit Lake (Pagel *et al.*, 1980) thereby indicating that these fluids were basinal in extent.

Primary, two-phase, H_2O fluid inclusions (representative of the earliest diagenetic fluid within the basin) occurring along the interface between the original detrital quartz grain and the quartz overgrowth (Q1), have homogenization temperatures of 80 to 180°C and salinities from 5 to 28 wt.% NaCl equivalents (Figure 3 a+b). The large range of homogenization temperatures and salinities of the inclusions reflects heterogeneities in the composition of the fluids during the initial stages of basin diagenesis.

Primary, three-phase, H_2O fluid inclusions, containing halite, hematite and phyllosilicate daughter minerals, are found along well-developed growth planes in euhedral quartz (Q2) associated with the fluid producing the uranium deposits. Primary fluid inclusions in the euhedral quartz yield homogenization temperatures of 120 to 340°C and salinities of 29 to 36 wt.% NaCl equivalent (Figure 3 a+b). In addition, the fluids within the inclusions have a δD value of -53 per mil. This value is similar to the δD value of the basinal fluid calculated to be in equilibrium with early diagenetic illite (I1) which is found pervasively throughout the sandstones in the Athabasca Basin (Wilson and Kyser, 1987; Kotzer and Kyser, 1990).

Two-phase, H_2O fluid inclusions having homogenization temperatures of 40 to 60°C and salinities of 2 to 5 wt.% NaCl equivalent are found in siderite having a similar paragenesis to the late kaolinite (K3) in fractures in the McArthur River Area (Figure 3a). These low temperatures and salinities represent late-stage meteoric waters which infiltrated the basin and destroyed some of the uranium deposits.

b) Stable Isotopes

Stable isotopic compositions (O and H) of clay minerals and silicates at Key Lake, Midwest Lake, Eagle Point and McArthur River (Wilson *et al.*, 1987; Kotzer and Kyser, 1990) indicate uranium and other metals were deposited by mixing of high salinity basinal brines, represented by the three-phase fluid inclusions in euhedral quartz (Q2) and diagenetic illite and kaolinite (I1, K1), with reducing basement fluids which produced Mg-chlorite (C1) (Figure 4). The occurrence of an illite alteration halo in the sandstones, a Mg-chlorite halo in the basement pelites and gneisses, and uranium which is concentrated in fault zones at the unconformity where fluids can be channelled suggest fluid interaction of these two fluids are a necessary pre-requisite for sufficient quantities of uranium to form. Although differences exist between the Athabasca Basin deposits, such as the amount and types of metals in the arsenides and sulfides with uranium ore and the degree of clay formation and silicification around the ore, the occurrence of two fluids mixing in structurally controlled areas appears to be the dominant control on uranium mineralization.

Late-stage kaolinite, having δD and $\delta^{18}O$ values similar to modern meteoric waters in the Athabasca Basin, occurs in reactivated fault zones hosting the uranium deposits (Figure 4). The amount of kaolinite formation depends upon the integrated water/rock ratio of the late meteoric fluids in the re-activated fault zones, and ranges from extreme in highly permeable, fractured areas to negligible in areas where early silicification, clay

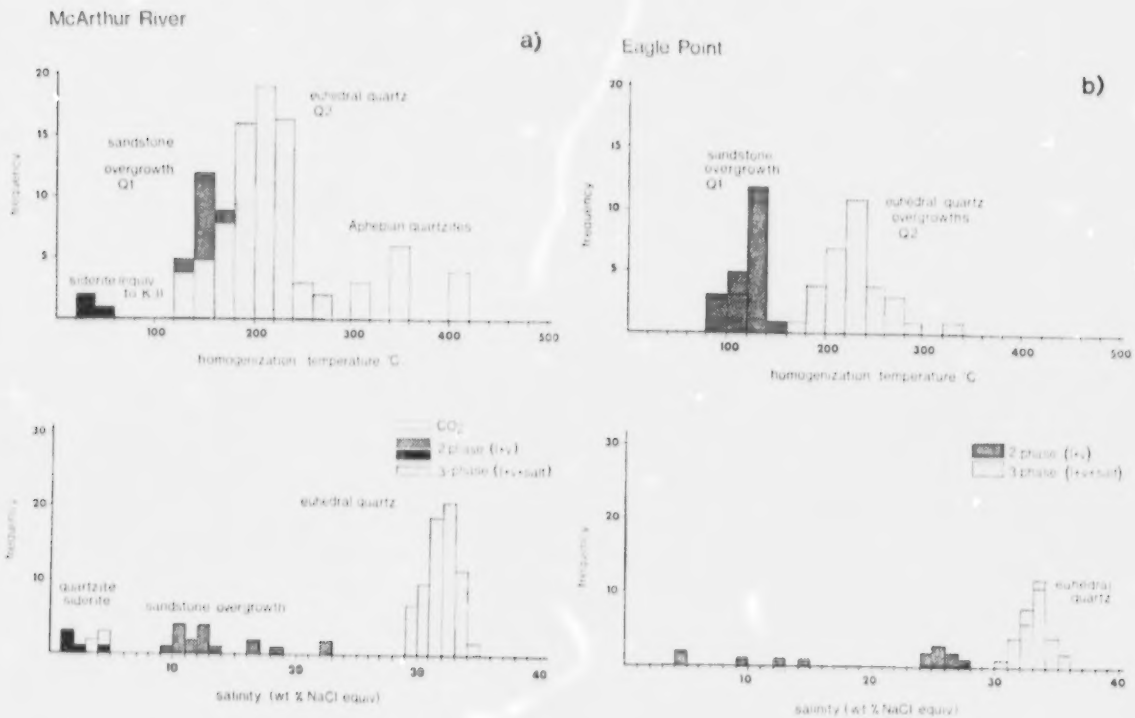

Figure 3 – Fluid inclusion histograms indicating the homogenization temperatures and salinities of fluid inclusions occurring in paragenetically distinct minerals at a) McArthur River (Bermuda and Phoenix Lake) and b) Eagle Point North. Similar fluid inclusion temperatures and salinities in euhedral quartz at both McArthur River and Eagle Point North suggest the basinal fluid was quite pervasive.

development or restricted fault movements have impeded permeability. As most of the uranium deposits examined so far in the Athabasca Basin show some evidence of retrograde alteration, it can be concluded that the later, low-temperature fluid event was widespread. Therefore, the condition of the uranium ore deposits today is dependant upon the amount of permeability existing around the uranium deposits at the time of incursion of the later, oxidizing fluids.

Sulphur isotopes from sulphides occurring with uranium ore lend furthur support to the model involving mixing of reducing basement fluids and oxidizing basinal fluids in fault structures that have focussed fluid flow. Nickel arsenide and sulphide at Key Lake and copper sulphide minerals at Bermuda Lake, directly associated with uranium minerals, and considered to be paragenetically equivalent (S1), have $\delta^{34}S$ values indicative of mixing between two isotopically distinct sources and sulphide formation during relatively closed-system, reducing conditions (Kotzer *et al.*, in prep.). Later formed iron sulphides peripheral to the uranium have a large range of $\delta^{34}S$ values which indicate sulphide formation during highly variable fO_2 conditions resulting from incursion of meteoric waters along re-activated fault structures hosting the uranium deposits.

The occurrence of highly variable, anomalously high $^{207}Pb/^{204}Pb$ and $^{206}Pb/^{204}Pb$ ratios in most of the sulphide minerals analyzed in the Athabasca Basin suggests high lead mobility due to alteration of uranium mineralization by the numerous fluid events which have affected the Athabasca Basin (Kotzer *et al.*, in prep).

c) Radiometric Age Determinations

The wide range of ages from the uranium mineralization and sediments (Tremblay, 1982) reflects the complex fluid history of the Athabasca Basin. However, the general overlap of U-Pb ages from uranium mineralization and Rb-Sr ages of diagenetic clay minerals in the Athabasca sediments suggests that uranium mineralization and high temperature basin diagenesis are closely linked (Kotzer and Kyser, 1990).

The timing of the high temperature diagenesis event in the sediments of the Manitou Falls Formation has been determined using Rb-Sr systematics on interstitial illites having similar $\delta^{18}O$ and δD values. A Rb-Sr isochron

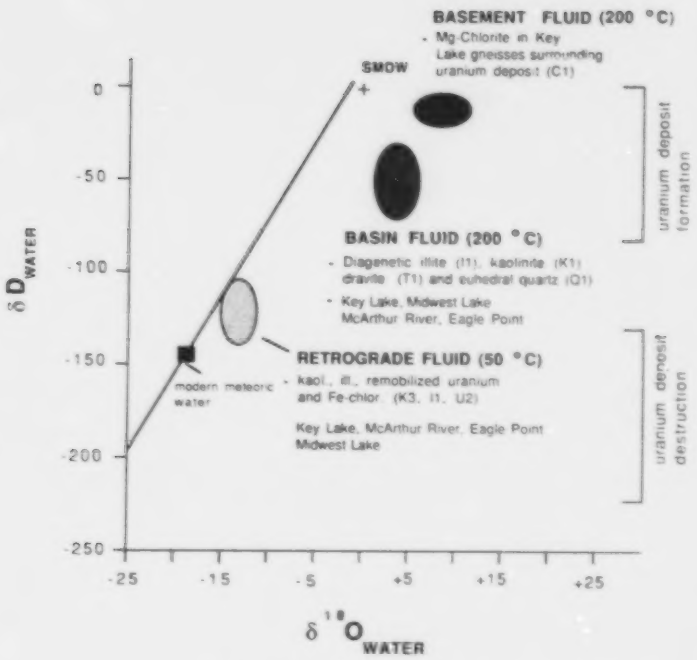

Figure 4 – Calculated $\delta^{18}O$ and δD values for various fluids associated with unconformity-type uranium deposits in the Athabasca Basin. Shaded areas represent fluids in equilibrium with: 1) Mg-chlorite formed at approximately 200°C in basement rocks at Key Lake (Wilson and Kyser, 1987) and Bermuda Lake in the McArthur River area (Basement Fluid), 2) diagenetic illite at 200°C from Key Lake, Midwest Lake (Wilson and Kyser, 1987), McArthur River and Eagle Point (Kotzer and Kyser, 1990) (Basin Fluid) and, 3) kaolinite associated with remobilized uranium in fractures which is similar to the fluids measured in fluid inclusions in siderite. Also shown are the values for modern meteoric waters in the Athabasca Basin, the meteoric water line (MWL) and ocean water (SMOW).

age of 1477 ± 57 Ma (Figure 5a) for diagenetic illite formation in the Athabasca sediments pre-dates the earliest age for uranium emplacement at 1406 Ma (Carl *et al.*, 1988) in the basin and suggests that large-scale fluid flow occurred before uranium mineralization. The time difference of approximately 50 Ma between high temperature diagenesis and uranium emplacement would allow the fluids to leach sufficient quantities of uranium from heavy minerals in the Athabasca sediments.

Euhedral quartz-dravite (Q2-T1) assemblages occur in the hydrothermally altered sediments associated with the uranium deposits in the Manitou Falls Formation. In some areas of the Athabasca Basin, strongly developed zones of euhedral quartz-dravite breccias are evident and appear to be the result of early dissolution of Athabasca sandstones. An Rb-Sr age of approximately 1270 Ma (Figure 5b) has been determined for this event using the Rb-Sr and $^{87}Sr/^{86}Sr$ ratios from both the tourmaline and fluids extracted from the fluid inclusions in coexisting euhedral quartz. The age determined from this event is similar to the ages of much of the uraninite at Key Lake (Ruhrmann, 1987) and some of the diabase dikes (Armstrong and Ramaekers, 1985) in the Athabasca Basin and possibly represents a major pulse of basement fluids out of the fault zones to mix with basinal fluids and further the production of high-grade uranium ore.

At the Eagle Point North uranium deposit, an Rb-Sr model age of 957 Ma has been calculated from illite in altered pegmatite (Figure 5c). The younger age for the illite at Eagle Point may indicate that the high temperature diagenetic fluids in the Athabasca Basin persisted for some time or that the nature of the hydrothermal system was episodic because the illite at Eagle Point has similar δD and $\delta^{18}O$ values to the illites having an age of 1477 Ma.

2. Conclusions

Stable isotopic, fluid inclusion, and radiometric age determinations on mineral phases having an identifiable paragenesis in the Athabasca Basin suggest a long and protracted fluid history. Fluid inclusion and stable isotopic compositions indicate that the Athabasca Basin was affected by early, high salinity diagenetic fluids having temperatures near 200°C and by later, meteoric fluids having temperatures less than 100°C. Coincident with the high and low-temperature fluid events are periods of uranium deposit formation and destruction, respectively, with the magnitude of uranium formation and destruction directly dependant on the quantities of reactive fluids involved. The late, meteoric fluid event has remobilized much of the uranium and has had the most pronounced effect on the current state of some of the uranium deposits in the Athabsca Basin. The magnitude of uranium deposit destruction is directly related to the permeability developed within the sediments and fault structures hosting the uranium deposits.

3. References

Armstrong, R.L. and Ramaekers, P. (1985): Sr isotopic study of Helikian sediment and diabase dikes in the Athabasca Basin, northern, Saskatchewan; Can. J. Earth Sci., v22, p399-407.

Bray, C., Spooner, E.T.C. and Longstaffe, F.J. (1988): Unconformity-related uranium mineralization , McClean deposits, northern Saskatchewan, Canada: Hydrogen and oxygen isotope geochemistry; Can. Mineral., v26, p249-268.

Carl, C., Hoehndorf, F., Pechmann, E.V., Strnad, J.G., and Ruhrmann, G. (1988): Geochronology of the Key Lake uranium deposit, Saskatchewan, Canada (abstract); J. Chem. Geol., v70, p133.

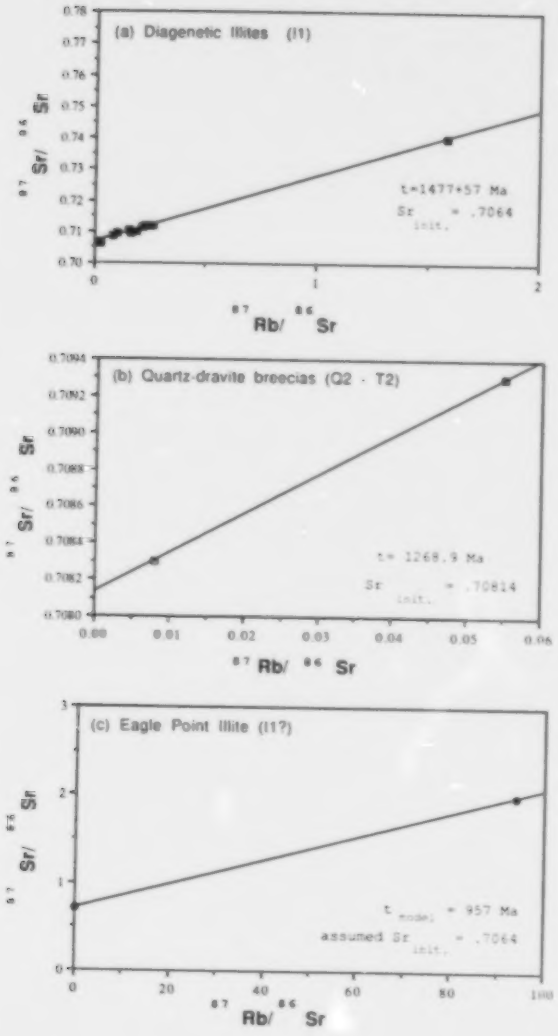
(a) Diagenetic Illites (I1)
t=1477±57 Ma
Sr init. = .7064
(b) Quartz-dravite breccias (Q2 - T2)
t= 1268.9 Ma
Sr init. = .70814
(c) Eagle Point Illite (I1?)
t model = 957 Ma
assumed Sr init. = .7064

Figure 5 – Rb-Sr isochrons of: a) interstitial, diagenetic illite in the Athabasca sandstones give an age of 1477 ± 57 Ma, b) the euhedral quartz-dravite event gives an age of approximately 1270 Ma and, c) diagenetic illite at Eagle Point gives an Rb-Sr model age of 957 Ma assuming an initial $^{87}Sr/^{86}Sr$ ratio of 0.7064. Varying the assumed initial $^{87}Sr/^{86}Sr$ ratio would have little affect on the model age.

Gustafson, L.B. and Williams, N. (1981): Sediment-hosted stratiform deposits of copper, lead and zinc; *in* Skinner, B.J. (ed), Econ. Geol. (Seventy-fifth Anniversary Volume), p139-179.

Hoeve, J. and Sibbald, T.I.I. (1978): On the genesis of Rabbit Lake and other unconformity-type uranium deposits in northern Saskatchewan, Canada; Econ. Geol., v73, p1450-1473.

Hoeve, J. and Quirt, D. (1984): Mineralization and host-rock alteration in relation to clay mineral diagenesis and evolution of the middle-Proterozoic Athabasca Basin, northern Saskatchewan, Canada; Sask. Res. Counc., Tech. Rep. #187, 187p.

_____ (1986): A common diagenetic-hydrothermal origin for unconformity-type uranium and stratiform copper deposits; Sask. Res. Counc., Publ. R-8555-5-A-81.

Kotzer, T.G. and Kyser, T.K., (1990): The use of stable and radiogenic isotopes in the identification of fluids and processes associated with unconformity-type uranium deposits; *in* Beck, L.S. and Harper, C.T. (eds.), Modern Exploration Techniques, Sask. Geol. Soc., Spec. Publ. 10, p115-131.

Kotzer, T.G., Kyser, T.K. and Ruhrmann, G., (in prep): Sulphur and lead isotopic constraints on the sources and ages of the fluids involved with unconformity-type uranium deposits; Can. J. Earth Sci.

Pagel, M., Poty, B. and Sheppard, S.M.F. (1980): Contributions to some Saskatchewan uranium deposits mainly from fluid inclusion and isotopic data; *in* Ferguson, S. and Goleby, A.B. (eds.), Uranium in the Pine Creek Geosyncline; IAEA, Vienna, p639-654.

Ruhrmann, G. (1986): The Gaertner uranium orebody at Key Lake (northern Saskatchewan, Canada) - After three years of mining: An update of the geology; *in* Gilboy, C.F. and Vigrass, L.W. (eds.), Economic Minerals of Saskatchewan, Sask. Geol. Soc., Spec. Publ. 8, p120-137.

Tremblay, L.P. (1982): Geology of the uranium deposits related to the sub-Athabasca unconformity, Saskatchewan, Canada; Geol. Surv. Can., Pap. 81-20, 56p.

Wallis, R.H., Saracoglu, N., Brummer, J.J. and Golightly, J.R. (1983): Geology of the McClean uranium deposits; Geol. Surv. Can., Pap. 82-11, p71-110.

Wilson, M.R. and Kyser, T.K. (1987): Stable isotope geochemistry of alteration associated with the Key Lake uranium deposit, Canada; Econ. Geol., v82, p1540-1557.

Wilson, M.R., Kyser, T.K., Mehnert, H. and Hoeve, J. (1987): Changes in the H-O-Ar isotopic composition of clays during retrograde alteration; Geochim. Cosmochim. Acta, v51, p869-878.

Site Investigation of a Biogeochemical Gold Anomaly Near Wadin Bay, Lac La Ronge

C.E. Dunn[1] *and P.L. Schwann*

Dunn, C.E. and Schwann, P.L. (1990): Site investigation of a biogeochemical gold anomaly near Wadin Bay, Lac La Ronge; *in* Summary of Investigations 1990, Saskatchewan Geological Survey; Saskatchewan Energy and Mines, Miscellaneous Report 90-4.

A reconnaissance biogeochemical survey of the southern part of the La Ronge Domain found several areas with anomalous levels of gold in plant tissues (Dunn, 1984). One anomaly is 32 km northeast of La Ronge, south of Aikenhead Lakes and east of the road to the abandoned Anglo-Rouyn copper mine (Figure 1) that produced gold as a by-product. The survey area lies in pristine forest far from possible sources of contamination. In the 1984 regional survey, samples of outer bark of jack pine and spruce, and twigs of shrub alder yielded up to 71 ppb Au in ash. These concentrations represent enrichment of about five times normal background levels for the La Ronge Domain. The following year vegetation sampling focused on 46 sites within a 1 km^2 area and delineated a zone yielding gold concentrations in jack pine bark of up to 270 ppb Au, associated with enrichment of As, Sb and Cs. Data from black spruce bark substantiated the evidence from the jack pine, whereas weaker Au enrichment was noted in the alder twigs (Figures 2 and 3 in Dunn, 1985) The gneiss which dominates the area shows no sign of mineralization.

In June, 1990, one day was spent investigating the anomaly. Samples of rock, B-horizon soil, and tissues from several species of tree and shrub were collected from 14 sites, and detailed geological observations were recorded. No species of plant was available at all the desired sample sites, therefore several species were collected at each site in order to obtain a complete coverage of the area, and to augment a data base on site specific differences in plant chemistry. Species collected were the outer and middle layers of bark from paper birch (*Betula papyrifera*), the outer bark of jack pine (*Pinus banksiana*), the outer bark of black spruce (*Picea mariana*), the most recent three years growth of twigs from mountain alder (*Alnus crispa*), and the entire stems of Labrador tea (*Ledum groenlandicum*).

Figure 1 - Location of survey area.

1. Physical Setting and Geology

The area is well-drained upland with locally steep 3 to 5 m high ridges, that follow the bedrock strike. Between the ridges there are moist densely-forested hollows and valleys, and an east-west trending bog at the southern part of the survey area (Figure 2). Most ridges are rock outcrop with sparse growth of jack pine, with poorly developed soils in small depressions. Glacial deposits are thin, sandy, and restricted to the valleys between the ridges.

Bedrock comprises part of the Jepson Lake pluton, contained within the Nut Bay Belt of the La Ronge Domain (Lewry, 1984). In the survey area the pluton is a pale to medium grey, pink weathering, medium-to coarse-grained, homogeneous biotite granite gneiss containing potassium feldspar megacrysts. Alteration has resulted in local chloritization of biotite, saussuritization of plagioclase feldspar and hematite dusting of potassium feldspar. Adjacent to joint surfaces the alteration is more pronounced. The gneiss is intruded by minor quartz veins, and by a later phase of coarse-grained quartz-feldspar dykes.

A consistently strong, locally protomylonitic, fabric (S1) is defined by a preferred orientation of biotite, stretched quartz grains, and feldspar porphyroclasts. The foliation trends eastward and dips 50° to 60° to the north. Quartz veins are sub-parallel to S1, and a prominent jointing forms a spaced cleavage subparallel to S1 and to the trend of outcrop ridges. Small scale folding of foliation is common and appears to predate vein emplacement. Small-scale displacement of veins and other features indicates sinistral movements.

The east-west-trending bog shown on Figure 2 is flanked to the north by a near vertical wall of bleached

(1) Mineral Resources Division, Geological Survey of Canada, Ottawa, Ontario, K1A 0E8

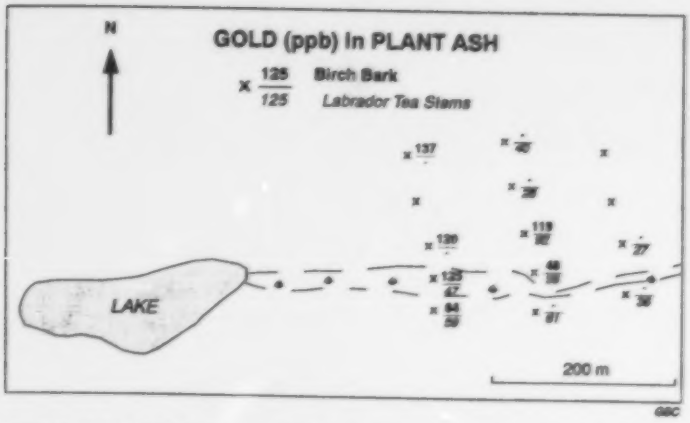

Figure 2 - Gold (ppb) in the ash of birch bark (papery layers) and Labrador tea stems.

and friable granite suggesting that the bog may occupy a zone of structural weakness. The southern flank is less steep and less intensely altered.

2. Geochemistry

Rocks were crushed, and ground in a tungsten carbide disk mill; soils were sieved through a -150 mesh and the fine fraction analyzed, and vegetation samples were ashed overnight at 470 C in a kiln. Thirty gram samples of the rocks and soils, and 0.1 - 0.7 g samples of ash (depending on the yield of the different media) were analyzed by instrumental neutron activation for approximately 35 elements. The range of elements determined was similar for all sample media, except Sn results were obtained on the rocks and soils only, and K data were provided for the vegetation. These differences are limitations on the analytical technique imposed by the different sample matrices.

Summary statistics of the rock analyses (Table 1) show no unusual enrichments of elements and analyses are typical of rocks of granitic affinity. The close similarity between mean and median values attests to the normal distribution for all elements. One sample contained 13 ppb Au, but 10 of the 14 sites yielded less than the detection limit of 5 ppb Au. B-horizon soils were collected at 9 of the sites, and in general the analyses closely resemble those of the rocks (Table 1). Concentrations of a few elements (Cr, Hf, Sc, Th, U, Yb, Lu) are higher in the soils than rocks because of the resistate nature of the minerals in which they occur, and the concentrating effect of rock weathering. Monazite is the probable host of most of these elements. Conversely the alkali metals (Na, Rb) are depleted in the soils owing to their relatively high solubilities.

Analyses of vegetation ashes show appreciably higher element concentrations than in the rocks or soils, because the ashing process removes organic components (which comprise 95 to 99.7 percent of the plant tissues) and effectively enhances subtle element differences in the bedrock that are not detectable by normal analytical procedures for silicate samples. There are, however, complications with vegetation analyses that need to be taken into account, such as the element requirements and tolerances of different plant species. A good example of these differences is that of Zn, which is an essential element for plant metabolism, but concentrations among species vary greatly. Table 2 shows that the samples of birch bark contain from 9000 to 23000 ppm Zn, whereas the other species have an order of magnitude less. Conversely, Sr and Rb levels in the birch are appreciably lower than in the alder.

A comparison of element concentrations in pine and spruce bark with data obtained from earlier studies (Dunn, 1985, Table 1) shows that they are close to normal background levels for conifers on granitic rocks of the Precambrian Shield. There is slight enrichment in the jack pine of Au, Cs, Cr, Fe, Hf, Sc, Th, and the rare earth elements. Except for the Au and Cs, this suite of elements is a typical association with Fe enrichment in vegetation. Trees that yielded high Au concentrations five years previously were not resampled, because it is virtually impossible to identify a tree from which only a few bark scales have been removed. In effect, the conifers sampled on this occasion did not indicate mineralization.

The deciduous species (alder, birch, and Labrador tea) were, however, all enriched in several elements, notably Au, Cs, Rb, Sr, REE, and to a lesser extent As. Figure 2 shows the distribution of Au in samples of birch bark and Labrador tea. Although the values for birch are substantially higher than in the other sample media, it must be remembered that the ash yield from the birch bark is low, and therefore the concentration factor is high. Notwithstanding this fact, birch is able to effectively concentrate traces of Au in the substrate, and values in this area are appreciably higher than the background levels of 20 to 50 ppb Au in birch bark ash. By way of comparison, a sample of the same medium collected from a tree rooted in a mineralized shear zone adjacent to the Anglo-Rouyn copper/gold mine 5 km to the southwest yielded 130 ppb Au. It should be noted that it is only the thin papery layers of the bark that are enriched in Au - the inner bark from the tree sampled at Anglo-Rouyn contained only 10 ppb Au in ash.

Labrador tea is also capable of absorbing and concentrating traces of Au, which in the study area contained up to 92 ppb (Figure 2), whereas background levels are commonly 10 to 20 ppb Au. For comparison stems from Labrador tea growing in the bog down slope from the discovery outcrop at the Jasper gold deposit yielded up to 779 ppb Au, with a mean concentration of 129 ppb (Dunn *et al.*, 1990). Similarly, in the bog above subcropping mineralization at Star Lake, Labrador tea collected prior to any mine development contained 110 ppb Au (Dunn, 1985).

Gold concentrations in alder (Table 2) are two to three times background, and similar to levels recorded pre-

Table 1 - Elemental Content of Granitic Gneisses and B-horizon Soils from Survey Area near Wadin Bay, Lac La Ronge.

	SOILS	ROCKS		
	Range	Range	Mean	Median
Au ppb	<5	<5-13	<5	<5
Ag ppm	<2	<5		
As ppm	<3	<2		
Ba ppm	300-820	500-1300	900	840
Br ppm	<1-5	<1		
Ca %	1-3	<1-3	2	2
Co ppm	<1-12	n.d.		
Cr ppm	10-82	<10		
Cs ppm	<2	<2		
Fe %	0.9-3.7	0.8-2.3	1.3	1.3
Hf ppm	7-10	2-4	3	3
Mo ppm	<5	<5		
Na %	1.6-3.0	2.8-3.9	3.3	3.3
Ni ppm	<50-70	<50		
Rb ppm	<30-43	<30-75	58	58
Sb ppm	0.1-0.3	<0.2		
Sc ppm	7-14	1-7	3	3
Sr ppm	<500-800	<500-900	<500	<500
Ta ppm	<2	<1-2	<1	<1
Th ppm	3-8	2-5	2.8	2.6
U ppm	2-11	1.3-3.3	1.9	1.7
Zn ppm	<50-100	<50-80	<50	<50
La ppm	4-24	5-22	10	9
Ce ppm	10-49	11-43	20	20
Nd ppm	6-19	<5-18	8	8
Sm ppm	1.3-3.3	0.6-2.9	1.3	1.2
Eu ppm	0.5-1.0	<0.2-0.9	0.5	0.5
Yb ppm	1.6-2.1	0.5-0.9	0.7	0.7
Lu ppm	0.27-0.37	0.08-0.15	0.12	0.12

All samples contained <1 ppm Hg, <5 ppb Ir, <5 ppm Se, <100 ppm Sn, <0.5 ppm Tb, and <2 ppm W.
n.d. = not determined.
Mean values for elements yielding concentrations below detection were calculated by taking a value of half the detection level.

Table 2 - Element Concentrations in Ashed Plant Tissues from Survey Area near Wadin Bay, Lac La Ronge.

	JACK PINE BARK (n = 10)	SPRUCE BARK (n = 5)	BIRCH BARK (n = 6)	ALDER TWIGS (n = 4)	LAB. TEA TWIGS (n = 9)
Ash %	1.3 - 2.1	2.1 - 4.7	0.3 - 0.6	1.4 - 2.2	1.1 - 1.6
Au ppb	6 - 25	<5 - 10	48 - 137	29 - 37	27 - 92
As ppm	6 - 10	3 - 7	8 - 24	1 - 3	2 - 5
Ba ppm	580 - 850	420 - 3600	1200 - 2500	800 - 2700	4400 - 6000
Br ppm	21 - 40	14 - 32	45 - 75	10 - 14	6 - 40
Ca %	8 - 18	22 - 29	6 - 18	22 - 27	19 - 25
Co ppm	7 - 11	4 - 5	8 - 17	6 - 14	2 - 6
Cr ppm	26 - 48	9 - 29	13 - 46	<1 - 3	<1 - 13
Cs ppm	3 - 7	<0.5 - 3	2 - 6	6 - 25	6 - 19
Fe %	1.4 - 2.2	0.5 - 1.1	0.5 - 1.6	0.16 - 0.19	0.5 - 0.9
Hf ppm	3 - 4	1 - 3	1 - 4	<0.5	<0.5 - 2
K %	2.8 - 4.3	1.0 - 3.0	2.4 - 6.5	17 - 20	9 - 17
Mo ppm	<5	<5	<5	<2 - 10	<5
Na ppm	0.6 - 0.9	0.2 - 0.6	0.2 - 0.8	0.04	0.16 - 0.26
Ni ppm	<50	<50	<50	<50	<50 - 100
Rb ppm	94 - 190	26 - 68	40 - 200	650 - 980	350 - 620
Sb ppm	1.1 - 3.4	0.5 - 0.8	0.5 - 1.8	0.1 - 0.4	0.3 - 1.2
Sc ppm	5 - 8	2 - 4	1 - 6	0.2 - 0.3	1.4 - 2.3
Sr ppm	<300 - 1200	<300 - 1300	<300 - 1500	1500 - 3800	600 - 1300
Ta ppm	<0.5	<0.5	<0.5	<0.5	<0.5 - 0.7
Th ppm	2.6 - 4.5	1.1 - 2.2	0.9 - 2.8	<0.1 - 0.4	0.5 - 1.3
U ppm	1.1 - 2.3	<0.1 - 1.0	<.2 - 3.0	<0.1	<0.1 - 0.7
Zn ppm	1700 - 2600	590 - 1800	9000 - 23000	1000 - 2000	1100 - 1400
La ppm	16 - 26	6 - 11	5 - 16	2 - 17	5 - 13
Ce ppm	28 - 45	10 - 20	8 - 30	<3 - 22	9 - 22
Nd ppm	12 - 30	<5 - 13	<5 - 7	<5 - 7	<5 - 7
Sm ppm	2.6 - 4.2	0.9 - 1.8	0.6 - 2.1	0.1 - 0.6	0.8 - 1.7
Eu ppm	<.02 - 0.97	<0.02 - 0.30	<0.05	<0.02 - 0.11	<0.02 - 0.7
Yb ppm	1.1 - 2.1	0.4 - 0.9	0.5 - 1.3	<0.05	0.38 - 0.79
Lu	0.23 - 0.39	0.08 - 0.18	<0.05 - 0.26	<0.05	0.06 - 0.12

All samples contained <1 ppm Ag, <1 ppm Hg, <5 ppb Ir, <2 ppm Se, <2 ppm W, and <0.5 ppm Tb

viously (Dunn, 1985). The Cs enrichment observed previously is confirmed, and may be an indication of gold mineralization. Coincident Cs and Au enrichment in alder has been observed at a number of localities, and Cs is known to occur in association with some gold deposits, notably Hemlo and at sites of hydrothermal activity in New Zealand (Dunn *et al.*, 1990).

3. Conclusions

Gold enrichment has been confirmed in several species of vegetation from the vicinity of a previously identified biogeochemical gold anomaly. Concentrations are highest in birch bark and Labrador tea stems and are associated with higher than normal levels of As, Cs, Rb, Sr, and REE.

Rocks and soils are not enriched in gold, and field observations have not found any sign of gold or sulphide mineralization. The rocks are, however, strongly foliated and possibly sheared, which would provide the potential for leakage of metals to the surface by hydromorphic or gaseous dispersion from a mineralized source at depth. The boggy valleys between the granite gneiss ridges could be the sites of more intensely deformed zones with a potential to host structurally controlled gold mineralization. The trees and shrubs could be absorbing traces of metals transported in solution along fracture zones.

4. References

Dunn, C.E. (1984): Biogeochemical methods and surveys, southern La Ronge Belt; *in* Summary of Investigations, 1984, Sask. Geol. Surv., Misc. Rep. 84-4, p95-103.

_____ (1985): Biogeochemical exploration for gold in the La Ronge Belt, 1985; *in* Summary of Investigations, 1985, Sask. Geol. Surv., Misc. Rep. 85-4, p37-49.

Dunn, C.E., George, H., and Spirito, W. (1990): Patterns of metal enrichment in vegetation in relation to geology and gold mineralization: Star Lake area, Saskatchewan; *in* Beck, L.S. and Harper, C.T. (eds.), Modern Exploration Techniques, Sask. Geol. Soc., Spec. Publ. No. 10, p12-26.

Lewry, J.F. (1984): Bedrock compilation, Lac la Ronge and Wapawekka areas (NTS 73P/7 3I); *in* Summary of Investigations, 1984, Sask. Geol. Surv., Misc. Rep. 84-4, p34-41.

Fluid Inclusion, Stable Isotope and Microprobe Data from the Jasper Zone Lode Gold Deposit, La Ronge Domain[1]

F. Hrdy[2], T.K. Kyser[2] and R.T. Kusmirski[3]

Hrdy, F., Kyser, T.K. and Kusmirski, R.T. (1990): Fluid inclusion, stable isotope and microprobe data from the Jasper Zone lode gold deposit, La Ronge Domain; *in* Summary of Investigations 1990, Saskatchewan Geological Survey; Saskatchewan Energy and Mines, Miscellaneous Report 90-4.

The Jasper gold zone is situated within the southern portion of the Island Lake Intrusive, located approximately 155 km northeast of La Ronge, Saskatchewan. The Island Lake intrusive is a zoned pluton displaying a dioritic margin and a granitic central core. Lewry *et al.* (1987) have obtained a U-Pb zircon age of 1855 ± 22 Ma for this pluton. Mineralization is hosted within a late stage northeast-trending brittle-ductile shear structure which is well exposed on surface. Underground mining is currently in progress.

This report summarizes fluid inclusion, stable isotope, and tourmaline compositional data, which, together with petrographic and field relations, can be used to constrain the geochemical characteristics of fluids responsible for gold deposition at the Jasper zone.

1. Petrography

The Jasper zone is a shear structure hosted within a predominantly granitic phase of the zoned Island Lake Intrusive. Mineralized portions are dominated by quartz veining and flooding and display a ribbony 'crack and seal' texture indicative of a ductile environment. Associated minerals include: sericite, chlorite, potassium feldspar, tourmaline, pyrite, sphalerite, marcasite, galena, chalcopyrite, and gold. Macroscopic gold, in the form of blebs and veins, is locally abundant and tends to occur within late brittle fractures implying a remobilization of gold deposited from an earlier event. Microprobe analyses of the gold reveal a significant silver and tellurium content. Sphalerite, galena, chalcopyrite, tourmaline, sericite, chlorite, and pyrite are locally in textural equilibrium with gold, although the paragenesis of these minerals has not yet been established. As with most of the vein-type gold deposits in northern Saskatchewan, wallrock alteration is minimal.

2. Fluid Inclusions and Microthermometry

Fluid inclusion studies provide insight into fluid temperatures, pressures, and compositions. Several polished fluid inclusion wafers have been prepared of representative samples taken from surface exposures of the Jasper zone. Petrographic observations of fluid inclusion distributions reveal at least three fluid events. A fluid responsible for quartz deposition, which may have had associated gold, is preserved in primary fluid inclusions. These inclusions occur as isolated individuals and as irregular clusters, well removed from any fractures or planar features. Secondary inclusions, related to later hydraulic events, are identified by the presence of generally conjugate planar and curviplanar inclusion sets, representing healed microfractures. The pattern of secondary inclusions suggests a relatively pervasive 'crack and seal' mechanism active during this period. Unhealed open fractures, cross-cutting all other observed features, typify a third phase of fluid permeation. These late-phase open fractures often display mineral overgrowths and are the sites of macroscopic gold development. Appropriate inclusions for thermometric measurements are rare for this later phase of fluid permeation.

No differences have as yet been observed between primary and secondary inclusions present at Jasper. Homogenization temperatures, which represent minimum temperatures of trapping, are between 175 and 300°C. Salinities of the fluids in the inclusions range from 1.64 wt% NaCl equivalent to 10.58 wt% NaCl equivalent, but typically average 7wt% NaCl equivalent. CO_2 mole fractions and densities are from 0.041 to 0.059 and from 0.716 to 0.928 g/cc, respectively. Minimum temperatures of homogenization, salinities, and CO_2 densities measured at Jasper are similar to those measured at Star Lake (Ibrahim, 1990). The range of CO_2 mole fractions in the inclusions at Jasper are however, more restricted than those from the Star Lake deposit where CO_2 mole fractions are from <0.01 to 0.9 (Ibrahim, 1990), and are consistent with variable ratios expected from CO_2 immiscibility during inclusion formation.

3. Stable Isotope Compositions

Quartz samples were collected from the pluton, the main Jasper mineralized structure, and late generation quartz veins also hosted by the same structure (Figure 1). Preliminary $\delta^{18}O$ data suggest that the three types of quartz are isotopically distinct and probably formed from separate fluids. $\delta^{18}O$ values of quartz from the Island Lake Intrusive are similar to the values obtained from the Star Lake pluton by Kyser *et al.* (1986). $\delta^{18}O$ values of auriferous and barren quartz at Jasper range from 11.8 to 13.3 per mil and 9.8 to 11.8 per mil, respectively. These ranges are the reverse of those at Star

(1) This project is supported by University - Industry grant from Cameco and NSERC
(2) Department of Geological Sciences, University of Saskatchewan, Saskatoon, Saskatchewan, S7N 0W0
(3) Cameco, 122 3rd Ave. N., Saskatoon, Saskatchewan, S7K 2H6

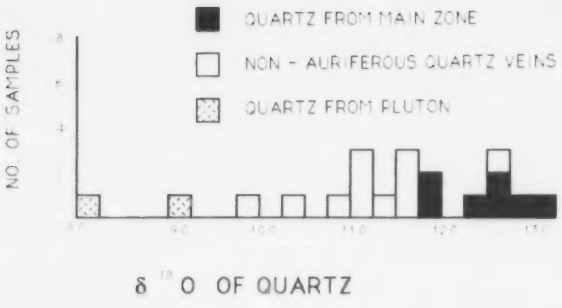

Figure 1 - Histogram of $\delta^{18}O$ values of quartz associated with the Jasper deposit. The three types of quartz sampled at Jasper are isotopically distinct. Both the relatively late non-auriferous quartz veins and auriferous quartz from the main zone are hosted by the main Jasper structure.

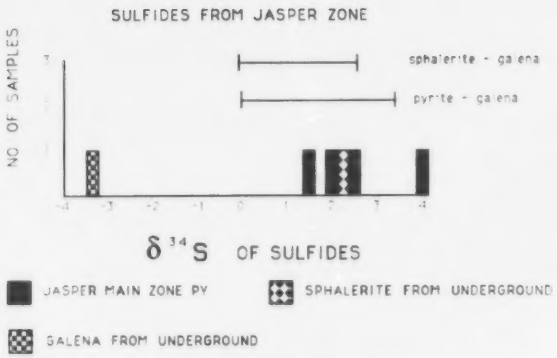

Figure 2 - Histogram of $\delta^{34}S$ data gathered from pyrite, sphalerite and galena of representative ore samples obtained from Jasper. The scale bar illustrates the separation necessary between the various sulfides, at 300°C, to indicate isotopic equilibrium (Kyser, 1987).

Lake where only the veins with $\delta^{18}O$ Values of quartz greater than 12 per mil are barren (Ibrahim, 1990).

Sulphides, including pyrite, galena, sphalerite, marcasite and chalcopyrite are present in the Jasper ore zone. $\delta^{34}S$ values obtained from pyrite, galena and sphalerite indicate that the sulfides are not in isotopic equilibrium (Figure 2). Variable $\delta^{34}S$ H_2S values of the hydrothermal fluid during the period when minerals, especially pyrite, were precipitated, and the effect of later metamorphism on the $\delta^{34}S$ value of galena are likely mechanisms that resulted in sulphur isotopic disequilibrium (Ohmoto and Rye, 1979; Kyser, 1987). Unlike Jasper, where $\delta^{34}S$ values of pyrite are variable, $\delta^{34}S$ values of sulphur at Star Lake are 2.0 to 3.3 per mil (Ibrahim, 1990), suggesting an essentially homogeneous source, whereas at Jasper, sulphur was remobilized.

4. Tourmaline Compositions

Tourmaline is a refractory mineral showing substantial major and trace-element compositional variation, which will retain these elements during alteration and weathering. Elemental analysis of tourmaline associated with ore zones may, therefore, provide clues concerning fluid chemistries responsible for ore deposition.

From electron microprobe analyses, tourmalines, that occur in textural equilibrium with gold mineralization at Jasper are enriched in magnesium and chromium relative to tourmalines from Archean mesothermal lode gold deposits (King and Kerrich 1986), but are more compositionally similar to tourmalines found in volcanogenic massive sulphide deposits (Figure 3). Chrome and magnesium enrichments in tourmalines from the Jasper zone suggest the fluid, from which the tourmalines precipitated, interacted with ultramafic rocks.

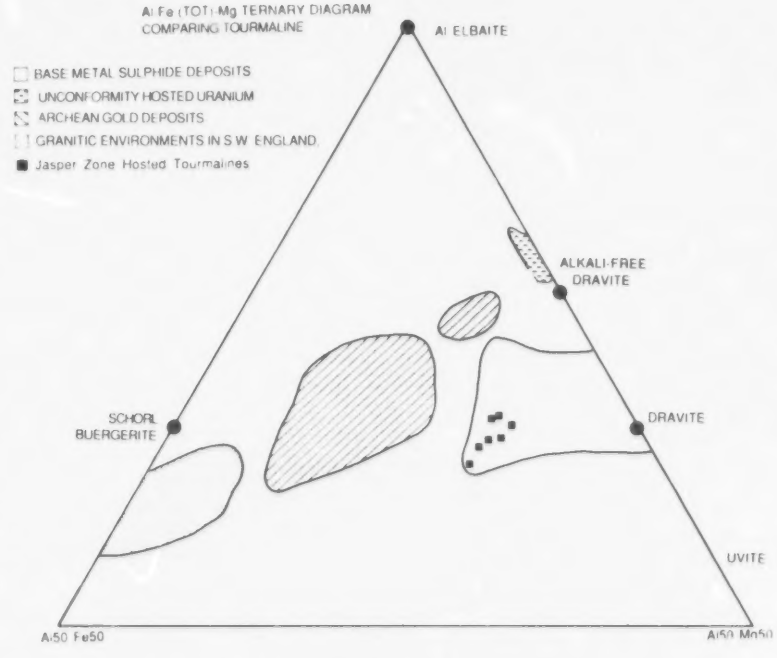

Figure 3 - A ternary plot shows the compositional range of tourmalines from base metal sulphide deposits, unconformity type uranium deposits, Archean gold deposits, granitic environments in S.W. England and Jasper Zone-hosted tourmalines (modified after King and Kerrich, 1986).

5. Conclusions

Moderate salinities measured from fluid inclusions, and the restricted range of CO_2 mole fractions observed at the Jasper gold mineralized zone contrast with fluid inclusions in Archean lode-gold deposits, which have lower salinities, and variable CO_2 contents (Fyfe and Kerrich, 1982). More variable CO_2 contents and slightly higher temperatures of homogenization also typify fluid inclusions of the Star Lake gold deposit, however, the high $\delta^{18}O$ values of quartz in conjunction with the moderate to high fluid temperatures measured from fluid inclusions at Jasper and Star Lake suggest a metamorphic fluid source for both deposits (Kyser *et al.*, 1986; Ibrahim, 1990).

6. References

Fyfe, W.S. and Kerrich, R.W. (1982): Gold: Natural Concentration Processes; *in* Gold '82: The Geology, Geochemistry and Genesis of Gold Deposits, Geol. Soc. Zimbabwe, Spec. Publ. No.1, p99-127.

Ibrahim, M.S. (1990): History of the fluids associated with the Proterozoic Star Lake lode-gold deposit, northern Saskatchewan, Canada; unpubl. MSc. thesis, Univ.Sask., 124p.

King, R.W. and Kerrich, R.W. (1986): Tourmaline in Archean lode gold deposits: Geochemical characteristics; Geol. Soc. Am. , Prog. Abstr. v18, p675.

Kyser, T.K. (1987): Equilibrium fractionation factors for stable isotopes; *in* Kyser, T.K., (ed.), Stable Isotope Geochemistry of Low Temperature Fluids, Mineral. Assoc. Can., short course v13, p1-84.

Kyser, T.K., Janser, B.W., Wilson, M.R. and Hattie, I. (1986): Stable isotope geochemistry related to gold mineralization and exploration in the western shield; *in* Clark, L.A. (ed.), Gold in the Western Shield, CIM, Spec. Vol. 38, p470-498.

Lewry, J.F., Macdonald, R., Livesey, C., Meyer, M., Van Schmus, W.R. and Bickford, M.E. (1987): U-Pb zircon geochronolog of accreted terranes in the Trans-Hudson Orogen, northern Saskatchewan; *in* Geol. Soc. London; Spec. Publ. 33, p147-166.

Ohmoto, H. and Rye, R.O. (1979): Isotopes of Sulfur and Carbon; *in* Barnes, H.L. (ed.), Geochemistry of Hydrothermal Ore Deposits, 2nd ed., J. Wiley and Sons, New York, p509-567.

Petrology of Some Mafic Gneisses, Black Birch Lake, Saskatchewan

S. Orrell[1] *and J. Tangeman*[2]

Orrell, S. and Tangeman, J. (1990): Petrology of some mafic gneisses, Black Birch Lake, Saskatchewan; *in* Summary of Investigations 1990, Saskatchewan Geological Survey; Saskatchewan Energy and Mines, Miscellaneous Report 90-4.

The Black Birch Lake area is underlain by granites and high-grade metamorphic rocks of the Cree Lake Zone, part of the early Proterozoic Hearne Province. Metamorphic rock types include an older sequence of tonalitic to granitic gneisses not discussed here, and a younger package of mafic to quartzofeldspathic gneisses of probable supracrustal origins. Mafic gneisses subdivide further into amphibolites and garnet amphibolites, commonly associated with aluminous assemblages. The current paper focusses on the petrochemisty and tectonic significance of a part of the lowest coherent mafic unit

1. Field Relations

Supracrustal rocks comprise a very small proportion of all rocks exposed in the Cree Lake Zone (Lewry and Sibbald, 1977, 1980), where they are preserved in synformal keels between much larger areas of tonalitic and granitic gneisses. Mafic gneisses comprise a small portion of the supracrustal rocks, and occur at a number of structural levels within the supracrustal sequence (Figure 1).

The structurally lowest mafic unit (Mafic Unit I) is immediately underlain by quartzites and pelites, and overlain by psammitic gneisses. It comprises variably deformed amphibolites, intimately interlayered with aluminous gneisses and calc-silicate rocks. The rocks are both layered and foliated, but late grain growth in amphibolites is typically random in orientation and obscures earlier fabrics. Metamorphism occurred at temperatures of at least 65° C at low pressures (2.5 kbar, Orrell, unpublished data) and it is assumed that igneous parageneses have been completely eradicated, although it may turn out that some of the pyroxenes are relics. Structures resembling pillows have been observed (Orrell *et al.*, 1988 and Orrell and Bickford, 1989), leading Tangeman (1990) to conclude that at least some of the amphibolites developed from submarine flow basalts. This is consistent with the development of ortho-amphiboles in interlayered subunits, as ortho-amphiboles commonly develop in argillaceous sediments at high grades. Garnet amphibolites and aluminous gneisses are also interlayered with the metabasalts.

2. Petrochemistry of Mafic Unit I Amphibolites

Tangeman (1990) studied the whole-rock chemistry of gneisses from a single large outcrop of Mafic Unit I (see Figure 1 and Orrell *et al.*, 1988), on the premise that the rocks represent metamorphosed basalts as suggested by field observations. Her data are reproduced in Table 1, in order of increasing silica content.

Both fine-grained and porphyritic amphibolites are included. As no systematic chemical differences between the two are distinguished, textural differences must be related to local strain histories. Silica concentration ranges from 43.4 to 49.6 wt. percent with no apparent systematic covariation of other major elements. In view of the small outcrop area, grade of metamorphism, and intensity of deformation, this lack of covariation is not surprising. Silica contents are slightly lower than those of most Proterozoic amphibolites (Macedo, 1978; Clough and Field, 1980; and Sivell and Foden, 1985, among others), indicating perhaps the removal of a small amount of siliceous partial melt. Like many Precambrian metavolcanic rocks, Black Birch Lake amphibolites are very low in potassium, and relatively low in magnesiun. The rocks are uniformly metaluminous and typically hypersthene-olivine-diopside normative (Figure 2), although a few are nepheline normative.

Despite thorough deformation and recrystallization, some original chemical characters of these Black Birch Lake metavolcanics may have been perserved. Zirconium is thought to be immobile under all but the highest metamorphic grades (Floyd and Winchester, 1975) and is used here to discriminate between elements whose concentrations have been altered and those whose concentrations have remained unchanged. Magnesium and iron show no correlation to Zr, but the mg# shows a fairly strong negative linear correlation (Figure 3), suggesting variation due to fractional crystallization. Supporting this hypothesis, incompatible trace elements, Ti and Y show good linear correlations with Zr, while P and Nb show correlations that are less marked (Figure 4). As expected, K and Rb (not shown) show no correlation to Zr, and are considered to have been altered during metamorphism. However, a poor curved correlation of K/Rb vs. Rb does exist (Figure 5), and this again suggests that sample compositions were related by fractional crystallization.

3. Tectonic Interpretations

In order to make tectonic interpretations of Unit I mafic rocks, Tangeman (1990) avoided those elements known to be mobile under metamorphic conditions, such as the alkalies, and applied tectonic discrimination diagrams developed for mafic volcanic rocks (Pearce and Cann, 1973; Pearce *et al.*, 1974; Floyd and

(1) Department of Geology, University of Kansas, Lawrence, KS 66045
(2) Current address: Department of Geological Sciences, University of Michigan, Ann Arbor, MI 48109-1063

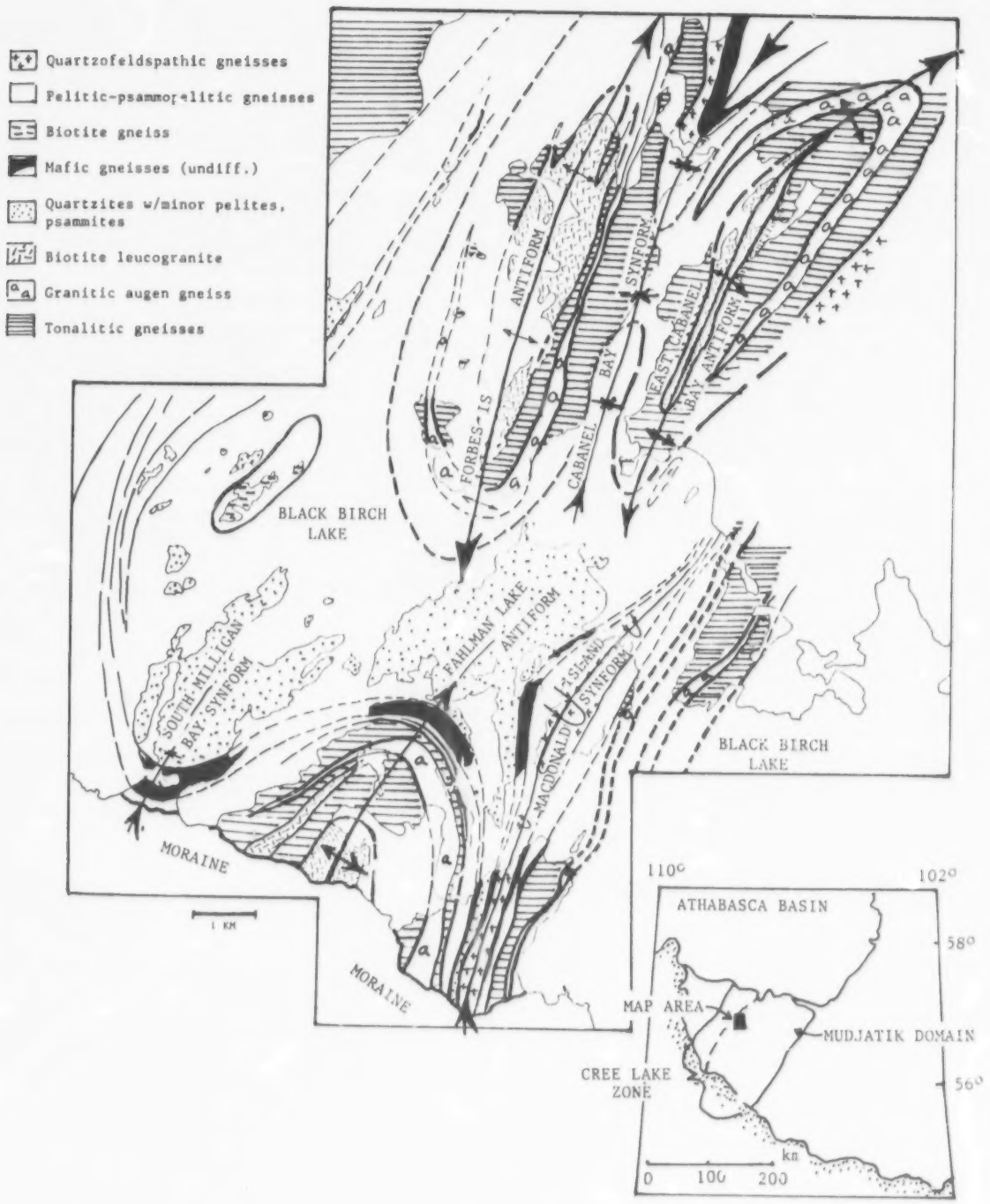

Figure 1 - Sketch map showing major structures and rock types in the Black Birch Lake area, from Orrell and Bickford (1989). Note location of current study.

Table 1 - Whole - Rock Chemistry of Metabasites, Black Birch Lake.

Sample	T88-20 b	T88-19	T88-34	T88-46 porph.	T88-20 a	T88-5	T88-12 b	T88-41 porph.	T88-42	T88-39	T88-21 a	T88-40	T88-10 porph.	T88-15	AVERAGES NE norm	HY norm
(wt. %)																
SiO2	43.38	43.39	45.66	45.87	46.29	47.83	48.83	48.98	49.03	49.09	49.14	49.40	49.42	49.57	45.12	48.54
Al2O3	16.63	16.69	16.02	15.91	14.63	15.97	14.94	14.67	15.18	15.19	16.07	15.21	15.23	15.24	16.30	15.24
TiO2	1.57	1.61	1.70	1.20	1.39	1.44	1.64	1.54	1.26	1.39	1.09	1.37	1.23	1.54	1.46	1.42
Fe2O3*	3.07	3.11	3.20	2.70	2.89	2.94	3.14	3.04	2.76	2.89	2.59	2.87	2.73	3.04	2.96	2.92
FeO	10.73	10.62	11.18	9.81	8.87	9.38	9.93	10.12	8.94	8.95	8.29	9.22	8.80	9.93	10.14	9.42
MgO	9.53	9.68	8.40	10.86	8.43	8.29	8.14	8.12	8.87	8.67	9.25	8.86	9.28	8.17	9.59	8.62
CaO	11.83	11.87	10.57	10.10	10.35	9.96	10.19	9.72	10.18	10.31	11.99	10.35	9.64	9.65	10.94	10.30
Na2O	2.01	1.89	2.52	2.39	2.62	3.05	2.82	2.99	2.99	3.17	2.12	2.62	3.08	3.02	2.34	2.80
K2O	0.24	0.24	0.21	0.52	0.22	0.22	0.27	0.49	0.46	0.18	0.21	0.38	0.17	0.22	0.31	0.28
P2O5	0.17	0.18	0.19	0.12	0.16	0.12	0.19	0.16	0.13	0.16	0.10	0.14	0.20	0.15	0.15	0.16
LOI	0.94	0.79	0.23	0.74	0.58	0.74	0.45	0.33	0.70	0.43	0.39	0.80	0.58	0.47	0.80	0.50
Total:	100.1	100.07	99.88	100.22	96.43	99.94	100.54	100.16	100.50	100.43	101.24	101.22	100.36	101.00	100.08	100.18
(ppm)																
Rb	11	11	10	15	7	6	4	10	9	5	6	8	2	4	11	7
Sr	251	249	236	179	258	291	319	281	247	266	341	248	285	209	243	269
Th	1	1	1	1	3	2	1	0	0	0	2	1	1	1	1	1
Pb	2	2	5	2	2	8	2	1	1	3	1	3	3	2	4	2
Nb	8	9	8	7	7	7	8	8	7	7	6	7	6	8	8	7
Y	21	22	24	16	20	21	22	21	18	19	15	18	18	21	20	20
Zr	82	86	84	62	77	78	85	79	67	71	58	70	64	81	77	74
K2O+Na2O	2.25	2.13	2.73	2.91	2.84	3.27	3.09	3.48	3.45	3.35	2.33	3.00	3.25	3.24	2.64	3.08
FeO+MgO	20.26	20.30	19.58	20.67	17.30	17.67	18.07	18.24	17.81	17.62	17.54	18.08	18.08	18.10	19.73	18.04
mg#	0.47	0.48	0.43	0.53	0.49	0.47	0.45	0.45	0.50	0.49	0.53	0.49	0.51	0.45	0.49	0.48
A/CNK	0.66	0.67	0.68	0.70	0.63	0.68	0.64	0.63	0.63	0.63	0.63	0.65	0.67	0.67	0.68	0.65
A/NK	4.11	4.36	3.25	3.06	2.85	2.70	2.68	2.35	2.45	2.51	3.83	2.82	2.59	2.60	3.43	2.75
Rb/Sr	0.04	0.04	0.04	0.08	0.03	0.02	0.01	0.04	0.04	0.02	0.02	0.03	0.01	0.02	0.04	0.02
CIPW Norm																
an	0.74	0.74	0.60	0.62	0.55	0.53	0.53	0.50	0.51	0.50	0.67	0.56	0.51	0.52	0.70	0.54
(wt.%)																
AN	35.66	36.36	31.77	31.13	27.51	29.24	27.29	25.18	26.65	26.71	33.75	28.63	27.24	27.40	34.38	28.31
AB	12.38	12.53	21.34	18.88	22.18	25.80	23.86	25.28	25.28	26.80	16.99	22.18	26.06	25.54	14.60	23.76
OR	1.39	1.39	1.22	3.06	1.28	1.28	1.61	2.89	2.73	1.06	1.17	2.23	1.00	1.28	1.95	1.61
MT	4.44	4.52	4.63	3.91	4.19	4.26	4.56	4.41	4.01	4.19	3.75	4.17	3.96	4.40	4.29	4.23
IL	2.97	3.07	3.23	2.28	2.64	2.73	3.11	2.93	2.40	2.64	2.06	2.59	2.34	2.93	2.77	2.69
AP	0.40	0.44	0.44	0.27	0.37	0.27	0.44	0.37	0.30	0.37	0.24	0.34	0.47	0.37	0.37	0.36
DI	17.83	17.36	15.94	14.76	19.33	16.41	17.99	17.97	18.67	18.99	20.31	17.71	16.68	15.86	16.65	17.81
OL	21.56	21.76	17.71	24.42	12.38	15.36	8.57	11.21	14.03	12.93	5.84	9.57	13.66	8.14	22.58	11.76
HY	0.00	0.00	3.96	0.00	6.13	3.95	12.66	9.59	5.75	6.33	16.44	12.58	8.05	14.61	0.00	9.10
NE	2.50	1.88	0.00	0.74	0.00	0.00	0.00	0.00	0.00	0.00	0.00	0.00	0.00	0.00	1.70	0.00
	99.13	99.31	100.24	99.45	96.01	99.30	100.09	99.82	99.82	100.02	100.55	100.00	99.46	100.53	99.29	99.62

Fe2O3*-- Fe2O3 is calculated as TiO2 + 1.5, after Irvine and Baragar, 1971.

Winchester, 1975) and for metamorphosed metavolcanic rocks (Winchester and Floyd, 1976). Results are shown graphically in Figure 6a to d. The rocks plot in fields with low-potassium tholeiites and ocean-floor basalts.

Given the field relations of these rocks, especially the relict pillows and lithologic assemblage, we feel these rocks are best interpreted as a cogenetic suite of tholeiitic basalts, erupted onto thin tonalitic crust in a (possibly shallow) marine setting, in response to rifting.

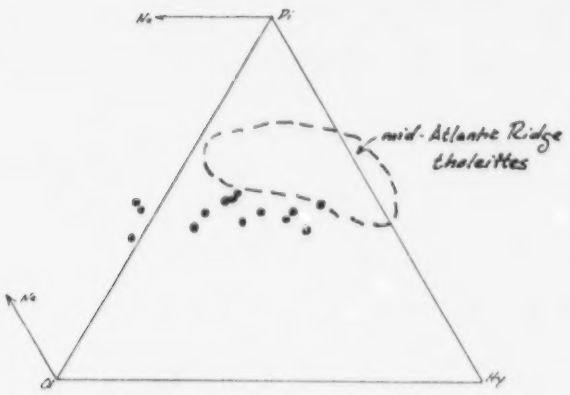

Figure 2 - Normative characteristics of Unit 1 amphibolites shown on basalt tetrahedron of Yoder and Tilley (1962). The field of Mid-Atlantic tholeiites (Shilling, 1975) is also shown.

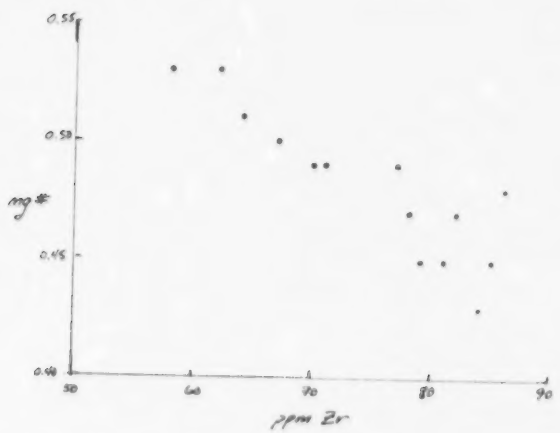

Figure 3 - Plot of mg# vs. Zr for Black Birch Lake amphibolites.

This hypothesis is identical to that proposed for early Proterozoic amphibolites of the Harts Range meta-igneous complex in Australia (Sivell and Foden, 1985) and for the Pan-African Ilesha amphibolites of southwest Nigeria (Olade and Elueze, 1979). The Black Birch Lake amphibolites compare well with Harts Range amphibolites in terms of age, chemistry and tectonic setting. In this model, pelites and ortho-amphibole-bearing samples at Black Birch Lake represent argillaceous sediments, possibly hemipelagic, or perhaps developed by weathering of the basalts themselves. Garnet-amphibolites may represent basalts from separate magma lineages, as in the Harts Range, but further chemical study is required to prove this.

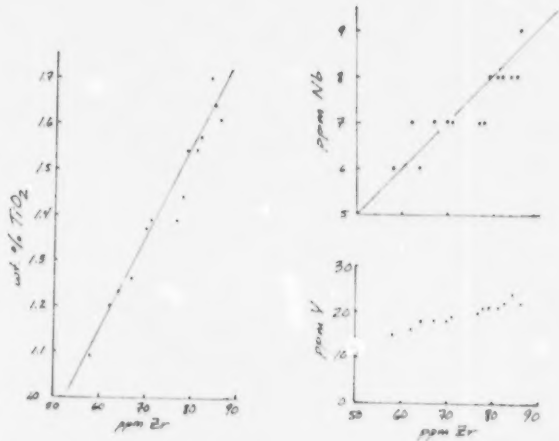

Figure 4 - Plots of incompatible trace elements Ti (as TiO_2), Nb and Y against Zr.

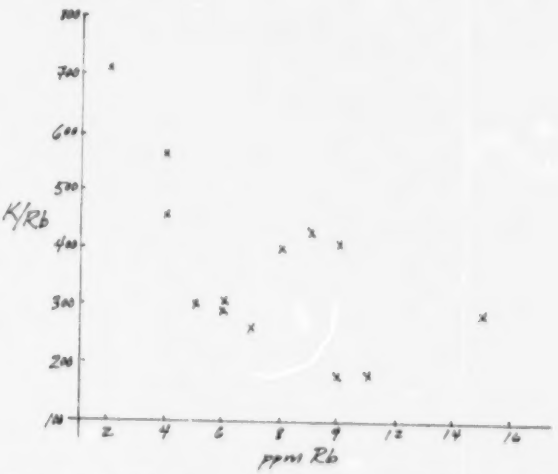

Figure 5 - Plot of K/Rb vs. Rb showing curved negative correlation.

4. Acknowledgements

This research was supported by Saskatchewan Energy and Mines, and by U. S. National Science Foundation, Grant # EAR-8719998. Discussion with W. R. Van Schmus and J. D. Walker improved the content, and critical review by J. D. Walker improved the text of this paper.

5. References

Clough, P.W.L. and Field, D. (1980): Chemical variation in metabasites from a Proterozoic amphibolite-granulite transition zone, South Norway; v73, p277-286.

Floyd, P.A. and Winchester, J.A. (1975): Magma type and tectonic setting discrimination using immobile elements; Earth Planet. Sci. Lett., v27, p211-218.

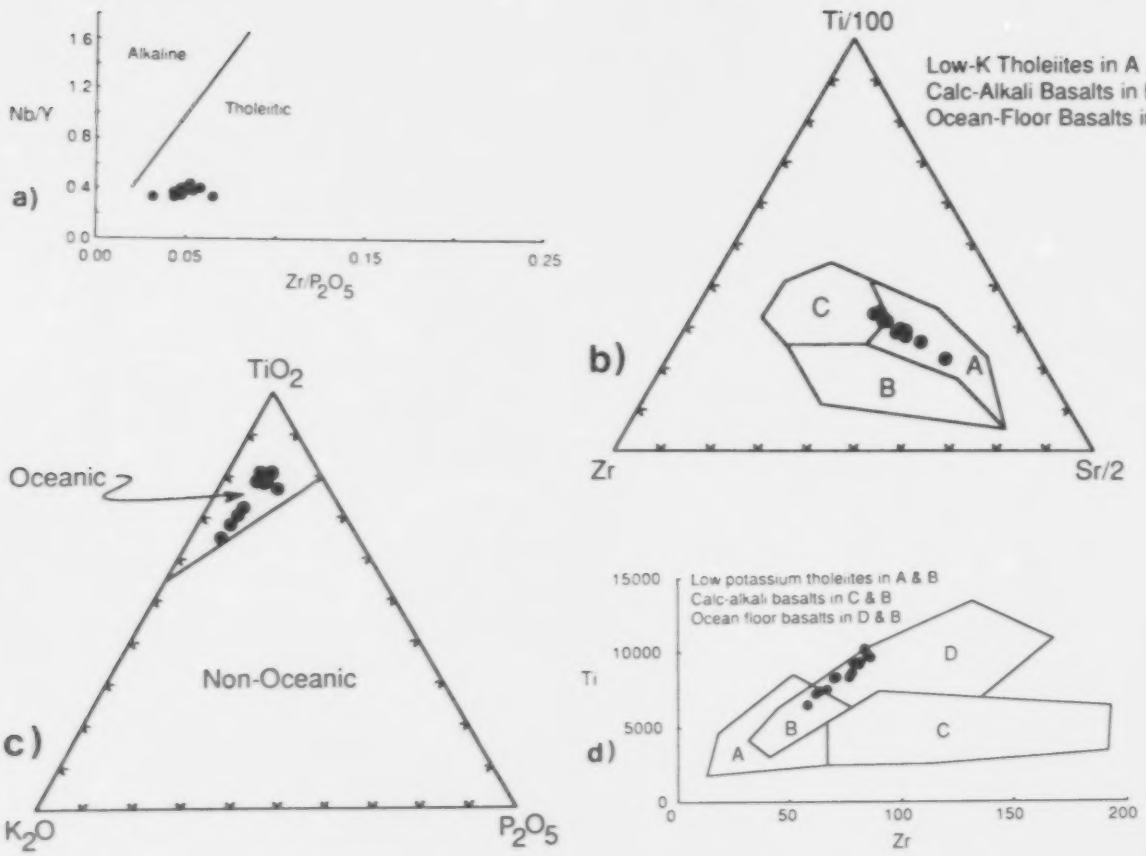

Figure 6 - a) Plot of Nb/Y vs. Zr/P_2O_5 (from Winchester and Floyd, 1976), illustrating tholeiitic character of Black Birch Lake amphibolites. b) The (Ti/100)-Zr-(Sr/2) ternary of Pearce and Cann (1973) illustrates similarity of Black Birch Lake amphibolites to low potassium tholeiites. c) The (TiO_2) - (K_2O) - (P_2O_5) ternary of Pearce et al. (1974) illustrates oceanic affinity of Black Birch Lake amphibolites. Note that metamorphic reduction of potassium would alter the affinity. d) The Ti vs Zr plot of Pearce and Cann (1973) reiterates the oceanic character of Black Birch Lake amphibolites.

Irvine, T.N. and Baragar, W.R.A. (1971): A guide to the chemical classification of the common volcanic rocks; Can. J. Earth Sci., v8, p523-548.

Lewry, J.F. and Sibbald, T.I.I. (1977): Variation in lithology and tectonometamorphic relationships in the Precambrian basement of northern Saskatchewan; Can. J. Earth Sci., v14, p1453-1467.

_____ (1980): Thermotectonic evolution of the Churchill Province in northern Saskatchewan; Tectonophysics, v68, p45-82.

Macedo, D.C. (1978): Geoquimica dos anfibolitos. I. Elementos maiores; Anais Do XXX Congresso Brasileiro de Geologia, Recife, v5, p2121-2133.

Olade, M.A. and Elueze, A.A. (1979): Petrochemistry of the Ilesha amphibolites and Precambrian crustal evolution in the Pan-African domain of SW Nigeria; Precam. Res., v8, p303-318.

Orrell, S. and Bickford, M. (1989): Geology of Early Proterozoic gneissic rocks, Black Birch Lake area: Progress Report 2; *in* Summary of Investigations 1989, Sask. Geol. Surv., Misc. Rep. 89-4, p105-109.

Orrell, S., Tangeman, J. and Bickford, M. (1988): Geology of Early Proterozoic gneissic rocks, Black Birch Lake area; *in* Summary of Investigations 1988, Sask. Geol. Surv., Misc. Rep. 88-4, p84-91.

Pearce, J.A. and Cann, J.R. (1973): Tectonic setting of basic volcanic rocks determined using trace element analysis; Earth Planet. Sci. Lett., v19, p290-300.

Pearce, T.H., Gorman, B.E. and Birkett, T.C. (1974): The TiO2-K2O-P2O5 diagram: A method of discriminationg between oceanic and non-oceanic basalts; Earth Planet. Sci. Lett., v24, p419-426.

Schilling, J.G. (1975): Azores mantle blob: Rare earth evidence; Earth Planet. Sci. Lett., v25, p103-115.

Sivell, W.J. and Foden, J.D. (1985): Banded amphibolites of the Harts Range meta-igneous complex, central Australia; An early Proterozoic basalt-tonalite suite; Precam. Res., v28, p223-252.

Tangeman, J.A. (1990): Petrographic and geochemical analysis of Precambrian amphibolites from the Mudjatik Domain, Saskatchewan; unpubl. BSc. thesis, Univ. Kansas, 9p.

Winchester, J.A. and Floyd, P.A. (1976): Geochemical magma type discrimination: Application to altered and metamorphosed basic igneous rocks; Earth Planet. Sci. Lett., v28, p459-469.

Yoder, H.S. and Tilley, C.E. (1962): Origin of basaltic magmas. An experimental study of natural and synthetic rock systems; J. Petrol., v3, p342- 532.

Petroleum Geology

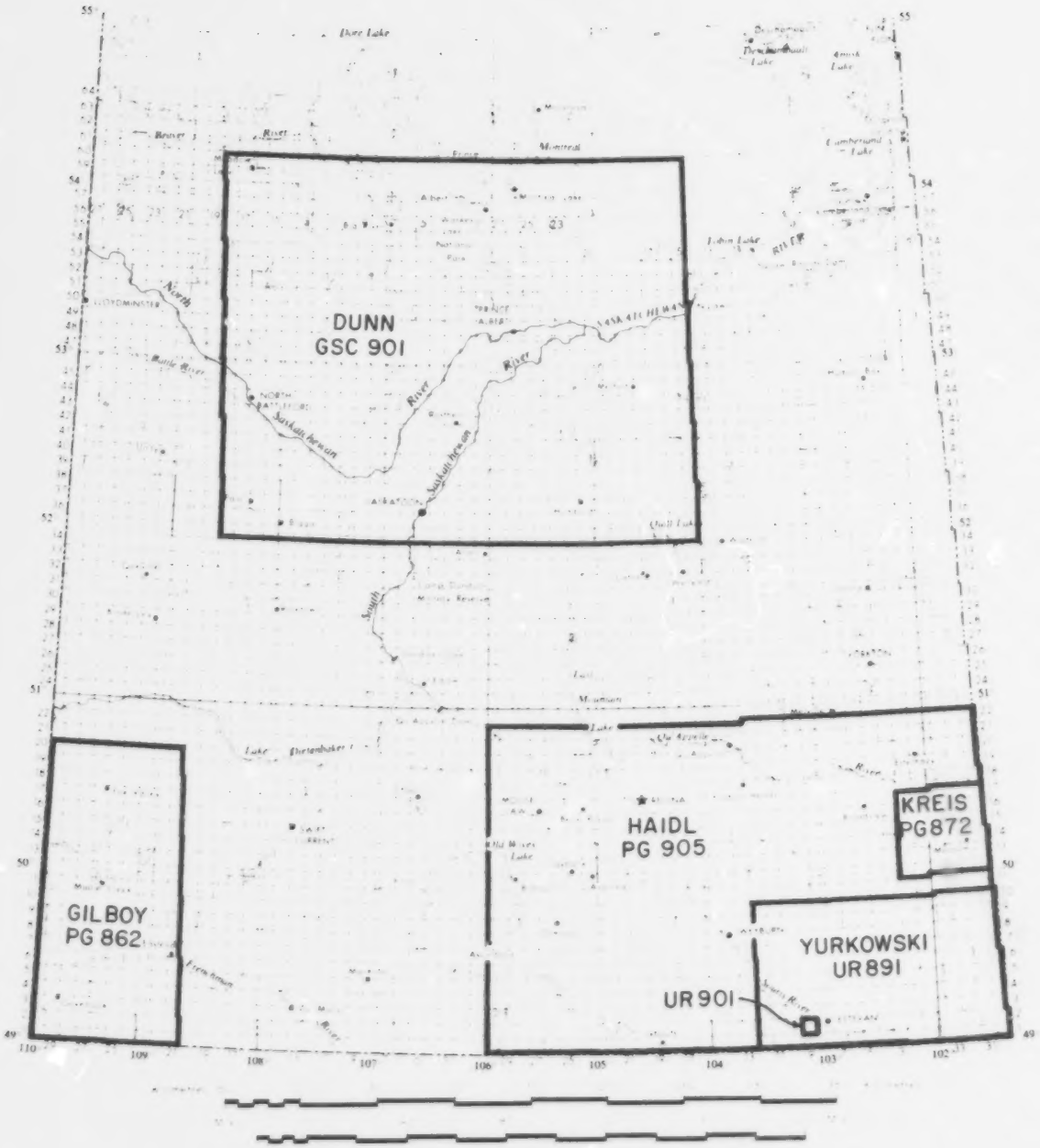
DUNN
GSC 901
HAIDL
PG 905
KREIS
PG872
GILBOY
PG 862
YURKOWSKI
UR891
UR901

Projects Supported by Petroleum Geology Branch in 1990

No.	Researcher	Title	Area	Status
*GSC901	Dunn, C.E.	Lithogeochemical Study of the Cretaceous in Central Saskatchewan	Ranges 15W2 to 18W3 inclusive; Townships 35 to 60 inclusive	Ongoing Oct. 1990. Feasibility study Feb 1990. Preliminary Report submitted for Summary of Investigations, Nov. 1990
PG861	Haidl, F.M.	Geology of the Silurian Interlake Formation, Saskatchewan	Townships 1 to 60 inclusive.	Ongoing in Oct. 1990
PG862	Gilboy, C.F.	Geology of the Upper Colorado Group and the Milk River Formation (Upper Cretaceous), Southwestern Saskatchewan.	Ranges 21 to 29W3 inclusive; Townships 1 to 20 inclusive	Ongoing in Oct. 1990
PG871	Christopher, J.E.	Geology of the Mannville Group (Lower Cretaceous), Saskatchewan.	Townships 1 to 100 inclusive	Contract. In final study phase Oct. 1990
PG872	Kreis, L.K.	Stratigraphy of the Jurassic System in the Wapella - Moosomin Area, Southeastern Saskatchewan	Ranges 30W1 to 2W2 inclusive; Townships 12 to 17 inclusive.	Study completed March 1990 as Master's Thesis. Successfully defended April 1990. Report in preparation in Oct. 1990
PG901	Gilboy, C.F.	Regional Cross-Sections of Strata above the Mannville Group (Lower Cretaceous) in Saskatchewan	Townships 1 to 25 inclusive.	Ongoing Oct. 1990
PG902	Leckie, D.A., Gilboy, C.F. et al.	Colorado/Alberta Group Strata of the Western Canada Sedimentary Basin	Townships 1 to 65 inclusive (in Saskatchewan).	Completed and presented at 'Basin Perspectives' Meeting, Calgary, May 1990. Will be incorporated into 'Geological Atlas of the Western Canada Sedimentary Basin' in 1991
PG903	Slind, O.L., Paterson, D.F. et al.	Middle Cambrian - Ordovician Strata of the Western Canada Sedimentary Basin	Lower Townships 1 to 70 inclusive (in Saskatchewan).	Completed and presented at 'Basin Perspectives' Meeting, Calgary, May 1990. Will be incorporated into 'Geological Atlas of the Western Canada Sedimentary Basin' in 1991
PG904	Norford, B.S., Haidl, F.M., Paterson, D.F. et al.	Middle Ordovician - Silurian Strata of the Western Canada Sedimentary Basin	Townships 1 to 66 inclusive (in Saskatchewan).	Completed and presented at 'Basin Perspectives' Meeting, Calgary, May 1990. Will be incorporated into the 'Geological Atlas of the Western Canada Sedimentary Basin' in 1991
*PG905	Haidl, F.M.	Ordovician Hydrocarbon Reservoirs, Herald and Yeoman Formations (Red River), Southeastern Saskatchewan	Ranges 30W1 to 30W2 Townships 1 to 22 inclusive;	Completed and prepared for Summary of Investigations, Nov. 1990
*UR891	Yurkowski, M.	Pore Geometry Reservoir Model Study for the Devonian Upper; Winnipegosis Member in Southeast Saskatchewan	Ranges 30W1 to 12W2 Townships 1 to 10 inclusive.	Ongoing Master's Study at University of Regina in Oct. 1990. Preliminary Report in Summary of Investigations, Nov. 1989 Progress Report in March 1990 and in Summary of Investigations, Nov. 1990.
*UR901	Qiang, N. and Kent, D.M.	A Paleo flow Model for a Winnipegosis Reef (Devonian), Southeastern Saskatchewan	Range 9W2; Township 2.	Ongoing study at University of Regina, Oct. 1990. Progress Report in Summary of Investigations, Nov. 1990.

Note: Only the asterisked projects are reported on in this volume.

Ordovician Hydrocarbon Reservoirs, Herald and Yeoman Formations (Red River), Southeastern Saskatchewan

F.M. Haidl

Haidl, F.M. (1990): Ordovician hydrocarbon reservoirs, Herald and Yeoman Formations (Red River), southeastern Saskatchewan; *in* Summary of Investigations 1990, Saskatchewan Geological Survey; Saskatchewan Energy and Mines, Miscellaneous Report 90-4.

Saskatchewan's first commercial oil production from rocks of Ordovician age was obtained in 1958 from Imperial Hummingbird 6-13-2-19W2. This well produced only 625 m^3 of oil before being shut in due to excessive water production (Table 1). In the following three decades only seven wells, with a cumulative production of 78,749 m^3, were successfully completed in the Ordovician. The Mark *et al.* Minton 11-2-3-21W2 well has, however, on its own, produced over a quarter of this oil and it provided the key to the current highly successful development of Ordovician and Devonian hydrocarbon resources in the Minton area where Mark Resources, in partnership with Saskoil, has drilled nine wells to the end of September, 1990 (Figures 1 and 2).

Cumulative production (to August 1, 1990), from three new Minton wells completed in Ordovician carbonates totals 5046 m^3, with an average of 37 m^3 (232 bbls.) per day (Table 1). One well (13-8-3-21W2) completed in the Winnipegosis Formation (Devonian) produced 65 m^3 (409 bbls.) per day in July, 1990.

The above average oil production from multiple zones in the Minton area has sparked renewed interest in the economic potential of Lower Paleozoic carbonates in southeastern Saskatchewan. This paper summarizes the stratigraphy, structure, reservoir characteristics and source rock potential of the primary target, the Herald and Yeoman Formations (Red River), in an area encompassing Townships 1 to 22 and Ranges 30W1 to 30W2 (Figure 1).

Published reports by Kendall (1976) and Osadetz *et al.* (1989) on this sequence in Saskatchewan, and by Kohm and Louden (1978, 1988) and Longman *et al.* (1983, 1987) on the Red River Formation in Montana and North Dakota provide the foundation for this summary.

1. Stratigraphy

Lower Paleozoic strata in the Williston Basin comprise a basal clastic unit and an upper sequence of carbonates and minor evaporites. A typical geophysical well log with the stratigraphic nomenclature used in southeastern Saskatchewan is illustrated in Figure 3. Strata of the Yeoman and Herald Formations were deposited in a great epeiric sea which, at maximum transgression during Yeoman time, covered much of the North American craton (Osadetz and Haidl, 1989). This succession has been correlated with the Red River Formation in the U.S. portion of the basin (Figure 4). Oil production in Saskatchewan is from the Lake Alma Member of the Herald Formation ("C" Laminated Member, Red River Formation) (Figure 5a) and from the upper portion of the Yeoman Formation ("C" Burrowed Member, Red River Formation) (Figure 5b,c).

a) Yeoman Formation

The Yeoman Formation consists of a thick sequence of burrow-mottled fossiliferous wackestones and mudstones which range in composition from dolomitic limestones to dolostones (Figure 5b,c). These sediments were deposited in a deep shelfal environment in aerobic to dysaerobic environments (Kendall, 1985).

Organic-rich laminites (kukersites) (Figure 5d) are also present in this sequence in the central portion of the study area. These beds are commonly associated with

Table 1 - Cumulative Production (to August 1, 1990)

Well Name	Location	Producing Horizon	DOP	Cumulative Production (m^3) Oil	Gas	Water
*Gulf Weir Hill	9-29-6-6W2	Yeoman	975	10 536.2	459.3	10 267.0
Esso Bromhead	6-28-3-12W2	Herald-Yeoman	1 588	7 539.7	667.5	25 569.7
Home *et al.* Oungre	4-22-3-15W2	Herald-Yeoman	296	1 482.8	48.4	4 849.5
CDR Mobil Beaubier	3-20-2-16W2	Herald	193	930.3	52.6	1 095.8
CDR S Lake Alma	1-14-1-17W2	Herald	5 282	39 130.5	989.5	41 151.2
Shell Lake Alma	7-23-1-17W2	Herald	696	3 002.2	0.0	2 374.6
Imperial Hummingbird	6-13-2-19W2	Herald-Yeoman	151	624.8	55.5	2 002.3
Mark *et al.* Minton	11-2-3-21W2	Yeoman	3 463	20 236.3	487.0	44 603.3
*Mark Saskoil Minton	13-8-3-21W2	Red River	13	282.1	1.0	152.8
*Mark Saskoil Minton	1-10-3-21W2	Red River	41	1 559.6	15.2	207.6
*Mark Saskoil Minton	3-17-3-21W2	Red River	85	3 204.1	0.0	822.3

*Currently producing from Herald/Yeoman. Note: DOP - days on production

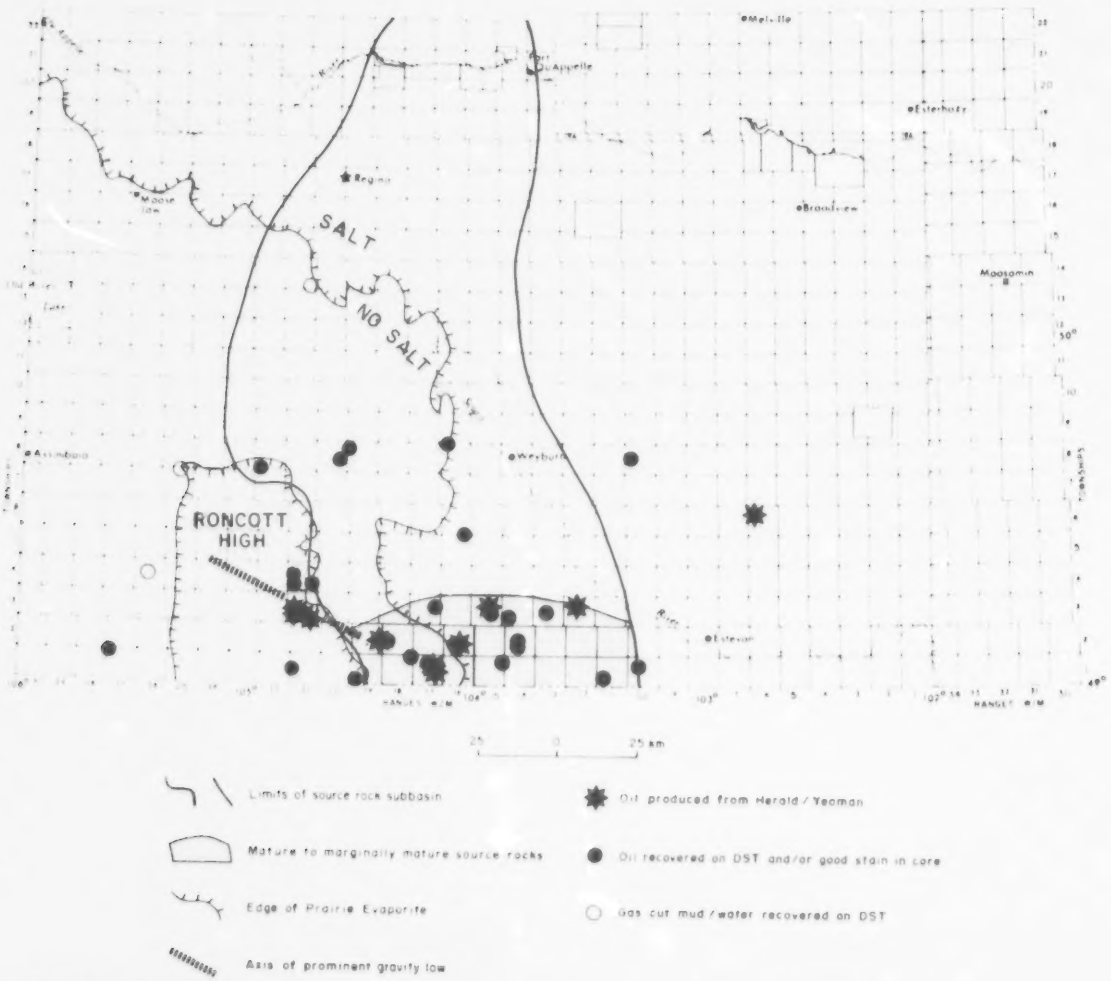
SALT
NO SALT
RONCOTT
HIGH
Limits of source rock subbasin
Mature to marginally mature source rocks
Edge of Prairie Evaporite
Axis of prominent gravity low
Oil produced from Herald / Yeoman
Oil recovered on DST and/or good stain in core
Gas cut mud / water recovered on DST

Figure 1 – Location map of the study area illustrating the distribution of oil shows and source rocks in the Herald and Yeoman Formations. Also shown are the distribution of the Prairie Evaporite (Fuzesy, 1982) and the axis of a pronounced gravity low. The source rock basin (Stasiuk and Osadetz, 1990) extends to the south through Montana and North Dakota and into South Dakota; it tapers to its northern limit in Tp. 24. The area of mature to marginally mature source rocks is delineated by the 2950 m depth contour (Osadetz et al., 1989).

hardground surfaces and the laminae may be disrupted by bioturbation and/or stylolitization (Stoakes *et al.*, 1987). These sediments record "episodes of basin stagnation, severe restriction and the development of euxinic bottom conditions" (Kendall, 1976, p48). The kukersitic layers are the source rocks of Ordovician oil in the Williston Basin (see below).

The Yeoman Formation increases in thickness toward the southeastern corner of the study area (Figure 8 in Kendall, 1976). Maximum thickness (136.2 m) of a normal Yeoman sequence is present in Socony Western Carievale 16-4-3-32W1. An anomalous thickness of 191.1 m in Imperial Lightning Creek 16-7-6-32W1 is attributed to reverse-faulting (Kendall, 1976).

The Yeoman Formation is conformably overlain by the Herald Formation and, in most of the study area, overlies the Winnipeg Formation with apparent disconformity (Paterson, 1971). In two wells in the southeast corner of the province, the Winnipeg Formation is absent and the Yeoman unconformably overlies the Deadwood Formation. These anomalies are attributed to non-deposition or erosion of the Winnipeg Formation due to uplift associated with basement tectonics (Paterson, 1971).

b) Herald Formation

The Herald Formation comprises a sequence of interbedded carbonates and anhydrites which can be subdivided into three units (in ascending order): Lake Alma, Coronach and Redvers (Figures 3 and 4). Each unit represents a depositional cycle or portions thereof. A complete cycle is composed of i) a basal argillaceous dolomite mudstone marker bed (commonly with lithoclasts), ii) a fossiliferous, commonly burrowed, wackestone or mudstone unit, iii) a slightly argillaceous

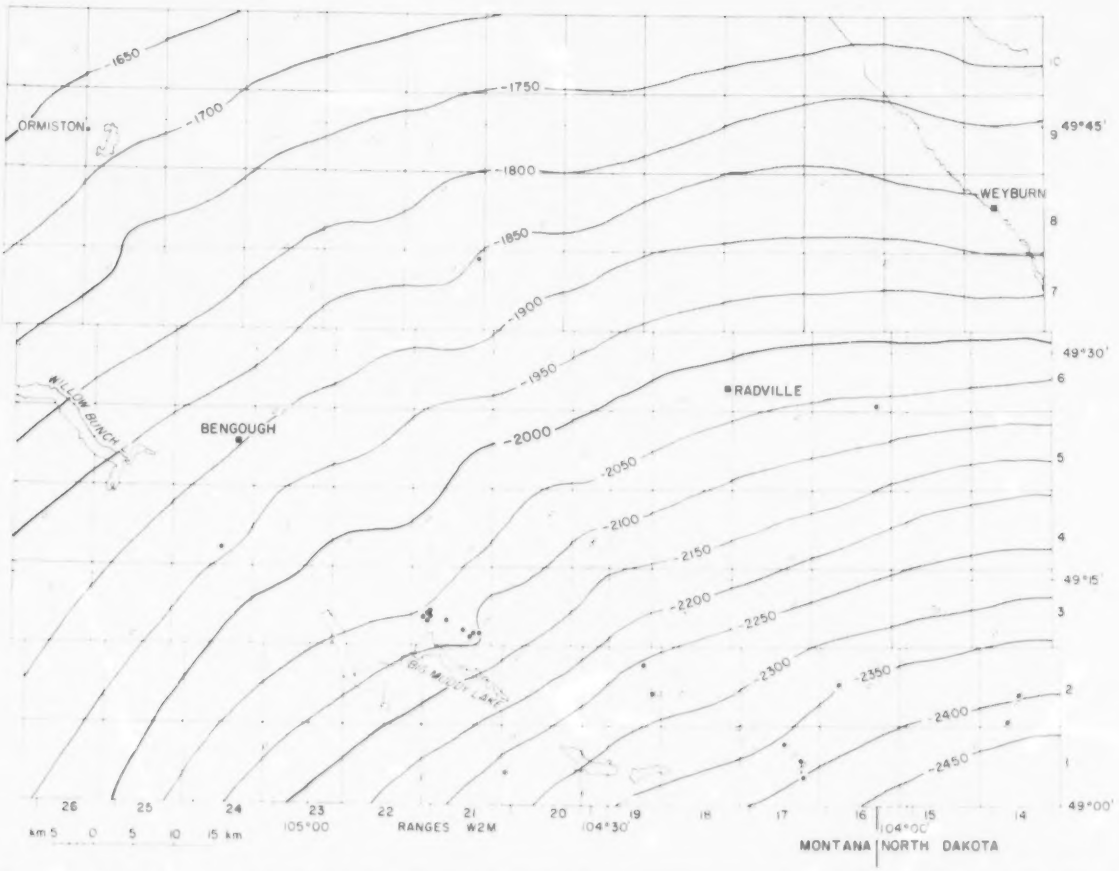

Figure 2 – Structure contours on the top of the Yeoman Formation in area encompassing the majority of producing Ordovician oil wells and hydrocarbon shows. All wells which penetrate the Herald/Yeoman Formations are shown. Note the density of wells in the Minton area (Tp.3, Rge.21W2). Contour interval is 50 m.

laminated mudstone unit (commonly dolomitized and unfossiliferous) and iv) an upper anhydrite unit (Kendall, 1976).

The Yeoman Formation constitutes the basal portion of the cycle capped by the Lake Alma anhydrite. The capping anhydrite is not present in the uppermost cycle (Redvers unit) in Saskatchewan but is present ("A" anhydrite) in the equivalent stratigraphic horizon in North Dakota (Figures 3 and 4). The bedded nature and basin-central location of the anhydrites, together with the thickness and widespread distribution of the cycle members and a paucity of evidence of subaerial exposure, support the interpretation that these "sedimentary cycles result from, and are a reflection of, cycles of increasing basin salinity" (Kendall, 1976, p54). A variation of this interpretation, proposed by Kendall (1984, 1988), suggests that a disconformity is present at the top of each fossiliferous wackestone/mudstone unit and that the laminated unit and the overlying anhydrite may have been deposited in a playa environment.

An isopach map of the Herald Formation defines an area of maximum thickness in the Lake Alma - Hummingbird area where this sequence reaches a thickness of 38.1 m in CDR Scurry S Lake Alma 1-14-1-17W2 (Figure 13 in Kendall, 1976). This pattern of distribution is largely attributable to an increased thickness of the Lake Alma Member (Kendall, 1976).

The Herald Formation is overlain by the Hartaven Member of the Stony Mountain Formation (Figure 3).

2. Structure

Structure contours on the top of the Yeoman and Herald Formations conform to the present-day configuration of the Williston Basin with strata dipping to the southeast towards the centre of the basin in North Dakota (Figure 2). In general, structure maps based on well data are characterized by smooth contours with very few well-defined anomalies. Two local structural highs are associated with oil production from Or-

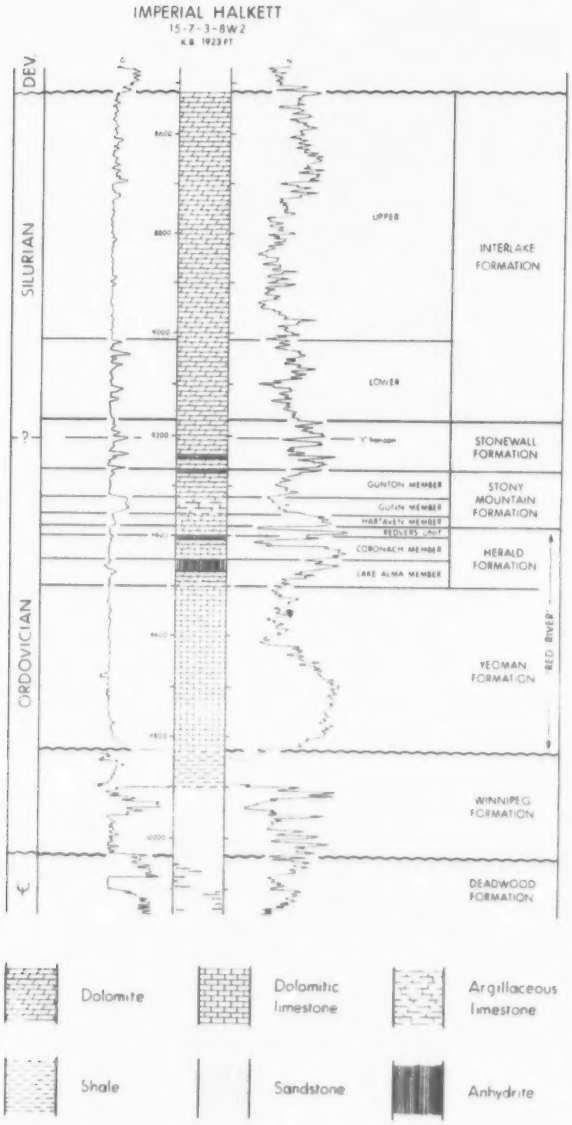

Figure 3 – A typical geophysical well log (gamma and neutron curves) and generalized lithologic column and nomenclature of Lower Paleozoic strata in southeastern Saskatchewan. Modified from Kendall (1976).

dovician reservoirs. In the Minton area, the top of the Yeoman is 40 m higher in 11-3-3-21W2 (-2086 m) than in 15-12-2-21W2 (-2126 m) (Figure 2) and in the Weir Hill area, the Yeoman top in 9-29-6-6W2 is 24 m higher than 15-29-6-6W2. Seismic data (Kent, 1973; Kendall, 1976) and an abundance of small structural highs (< 405 ha; < 1000 acres), defined by closely-spaced wells in areas of Red River production in North Dakota and Montana (Kohm and Louden, 1988), suggest that the paucity of structural anomalies defined on structure contour maps

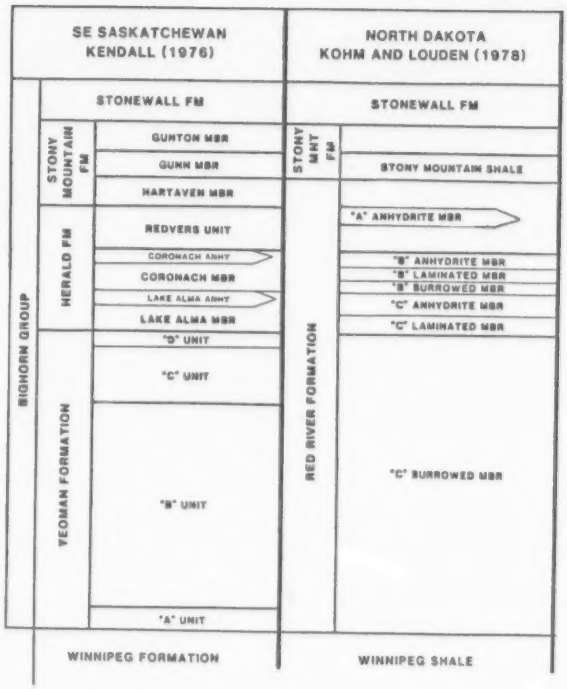

Figure 4 – Correlation chart of Ordovician strata in the Williston Basin.

in Saskatchewan can be attributed to a lack of data rather than an absence of local structural relief.

3. Reservoir Characteristics

Oil production occurs from laminated dolomites in the Lake Alma Member of the Herald Formation and from the upper portion of the Yeoman Formation.

a) Lake Alma Reservoirs

In the six wells that have produced from the Herald Formation (Table 1), the reservoir consists of laminated dolomites and calcareous dolomites in the basal 10 m of the Lake Alma Member (Figure 5a). Intercrystalline porosity is associated with microcrystalline to sucrosic textures. In CDR S Lake Alma 1-14-1-17W2, the most productive well (Table 1), porosity in the perforated zones ranges from 13 to 20 percent and permeability ranges from 5 to 86 md.

b) Yeoman Reservoirs

Production from the Yeoman Formation is from within the upper 10 m of this unit, with the exception of Home *et al.* Oungre 4-22-3-15W2, which is perforated in a number of intervals within the upper 30 m. The perforated intervals are cored in Mark *et al.* Minton 11-2-3-21W2 and Gulf Weir Hill 9-29-6-6W2.

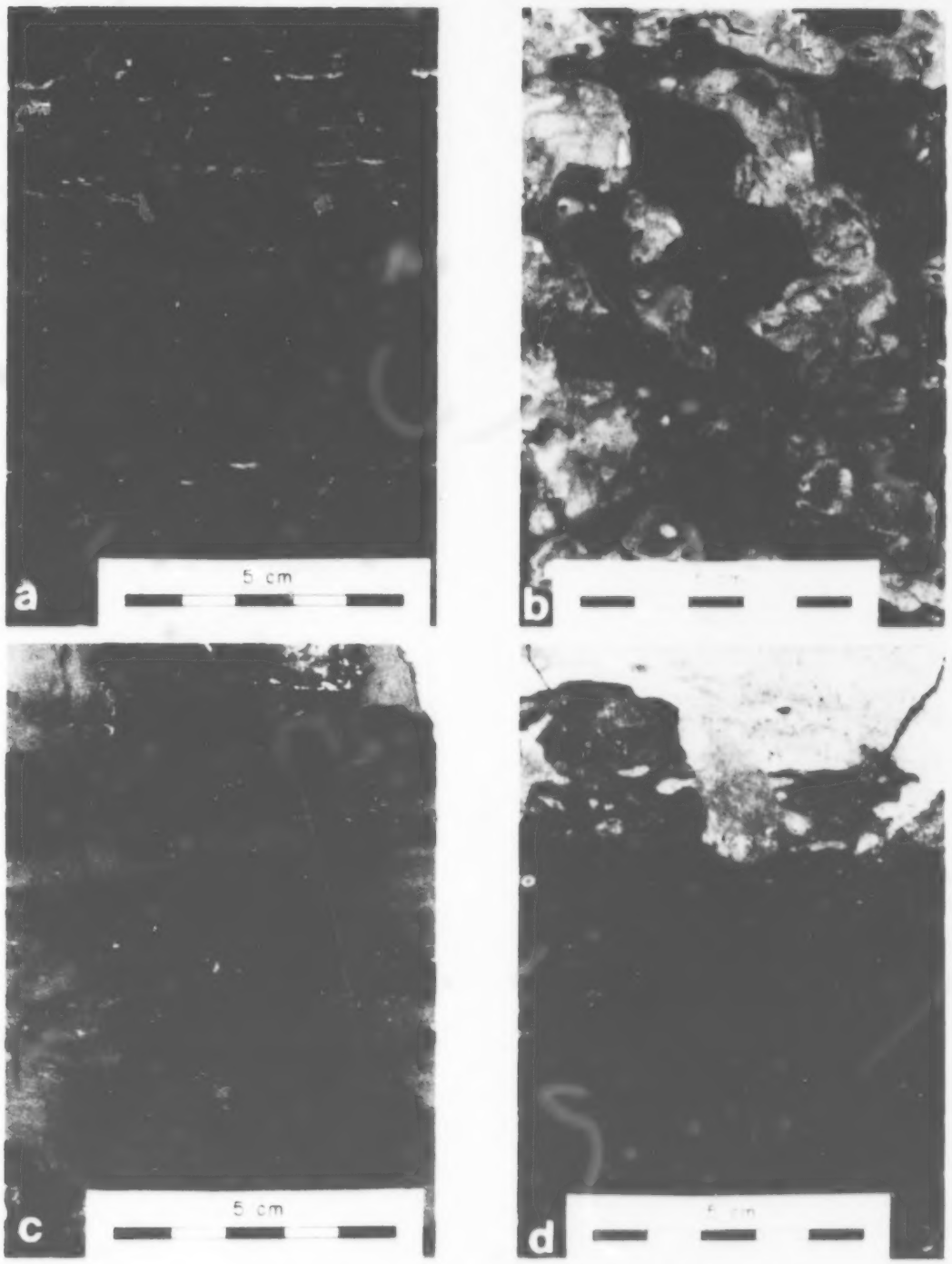

Figure 5 - a) Herald Formation, Lake Alma Member, CDR S Lake Alma 1-14-1-17W2, 3089.5 m; oil-stained microsucrosic laminated dolomite with load casts; this sample is located just below a perforated zone. b) Yeoman Formation, Mark et al. Minton 11-2-3-21W2, 2864.8 m; burrow-mottled skeletal packstone composed of calcareous dolomite; sample is near the base of the perforated zone; porosity is 9%, permeability is 48 md. c) Yeoman Formation, Gulf Weir Hill 9-29-6-6W2, 2480.9 m; dolomite mudstone with minor burrow-mottling; sample is in the middle of the perforated zone; porosity is 28%, permeability is 57 md. d) Yeoman Formation, Shell Lake Alma 16-36-1-18W2, 3061 m; lighter-coloured bioturbated dolopackstone overlying dark burrowed dolomudstone; the sharp contact between them is interpreted as a submarine hardground. The two very dark layers near the top of the dolomudstone unit are composed of kukersite laminae which are disrupted by small burrows.

Mark *et al.* Minton 11-2-3-21W2 has produced over 20,000 m^3 of oil from a dolomitic skeletal wackestone to packstone with abundant calcareous dolomite mottles (Figure 5b). The close packing of mottles, an abundance of tensional fractures in the mottles, and the brecciated appearance of some intervals suggest that these rocks have undergone significant chemical compaction (cf. Figures 8 to 10 in Kendall, 1985). This reservoir is characterized by interparticle, intercrystalline and fracture porosity ranging from 9 to 13 percent in the perforated interval. Permeability in this interval ranges from 27 to 48 md.

Of particular interest in several intervals of the Minton core is the presence of asphaltite bitumen in pores and fractures. Preliminary petrographic data suggest that kerogen and bitumen within these intervals have undergone anomalous thermal alteration, raising them to maturation levels above the local/regional values suggested by Osadetz *et al.* (1989) (L. Stasiuk, pers. comm.). Significant variation in the degree of alteration can be seen at both the microscopic and macroscopic scale.

The reservoir interval in Gulf Weir Hill 9-29-6-6W2 (Figure 5c) is primarily composed of dolomite mudstones with a much lower density of burrow mottles and a more bedded appearance than in 11-2-3-21W2. Porosity is primarily intercrystalline and ranges from 14 to 28 percent; permeability ranges from 4 to 65 md.

4. Source Rocks

Geochemical studies indicate that oil produced from the Herald and Yeoman Formations in Saskatchewan comes from organic-rich laminites in the Yeoman Formation (Brooks *et al.*, 1987). An alginite composed almost exclusively of *Gloeocapsomorpha prisca* is the primary component of these source rocks (kukersites) (Osadetz *et al.*, 1989). The kukersitic layers occur at four stratigraphic intervals, most commonly as relatively thin beds (< 15 cm) (Figure 5d). The thickest kukersite deposit (0.46 m) observed in core is from the BA Qu'-Appelle Hornung 2-4-22-15W2 well (Kendall, 1976). The axis of the source rock basin coincides roughly with the 104th Meridian but the basin limits are poorly delineated. Kendall (1976) suggests this basin covers an area south of Township 23, between Ranges 3W2 and 4W3. A more restricted distribution roughly encompassing Ranges 10W2 to 25W2, south of Township 25, is suggested by Osadetz *et al.* (1989) (Figure 1). A study of source rock distribution in the U.S. portion of the Williston Basin, currently underway at the Colorado School of Mines, tentatively outlines source rocks within an area which falls approximately between Ranges 6W2 and 24W2 and extends into northern South Dakota (R. Wilkinson, pers. comm.).

Geochemical analyses indicate that these kukersite layers contain up to 34.9 percent TOC, with an average of 8.44 percent TOC (Osadetz *et al.*, 1989). In Saskatchewan, it is estimated that these deposits have a potential of approximately 800 million m^3 (5 billion bbls.) of oil equivalent. Unfortunately, maturation studies indicate that thermal maturation of these source rocks occurred only in an area of anomalous heat flow, roughly centred around the 103rd Meridian at present-day depths of greater than 2950 m (Osadetz *et al.*, 1989) (Figure 1). This area of high heat flow is coincident with an area of recurring tectonic movement, which Majorowicz *et al.* (1988) suggest is in the vicinity of the North American Central Plains Conductivity Anomaly. The present-day Nesson anticline (and its earlier equivalents) is the dominant structure within this tectonically active area. An ancestral Nesson anticline was a positive feature during Yeoman deposition with kukersites only preserved on its western flank. Thus a large proportion of Ordovician source rocks in Saskatchewan lies outside the limits of thermal maturation (Figure 1). Despite this fact, it is estimated that the kukersitic sequences in the Yeoman Formation have generated approximately 32 million m^3 (200 million bbls.) of oil (Osadetz *et al.*, 1989).

The bulk of Ordovician source rocks in the U.S. portion of the Williston Basin have reached thermal maturity with significantly higher maturation levels attained in the deeper portions of the basin (K. Osadetz, pers. comm.). Long distance migration of this oil into Saskatchewan reservoirs from Montana and North Dakota may have occurred. Maturation profiles of high gravity oil (33°) produced from the Yeoman and Winnipegosis Formations in the Mark *et al.* Minton 11-2-3-21W2 well suggest that this oil was generated at higher temperatures than are estimated for this area (K. Osadetz, pers. comm.). This suggests that either a high heat anomaly existed in the Minton area at the time of oil generation (or later) or that oil migrated from deeper portions of the basin in Montana or North Dakota. Maturation profiles of the lower gravity oil (24°) produced from Gulf Weir Hill 9-29-6-6W2 well are consistent with generation from a source in Saskatchewan near the eastern edge of the thermally mature portion of kukersite deposits (K. Osadetz, pers. comm.).

5. Controls on Fluid Distribution

Two major factors control fluid distribution in Ordovician strata in Saskatchewan: structure and patterns of dolomitization.

a) Structure

The majority of Ordovician oil is trapped in reservoirs located on small structural highs (D. Potter, pers. comm.). An understanding of the origin of these structures is critical to the exploration and development of additional oil accumulations.

Several authors have suggested that episodic movement of blocks of the Precambrian basement have, at various times during the basin history, controlled the structure and patterns of sedimentation and diagenesis in the overlying sedimentary sequence (e.g. Mollard, 1959, 1987; Christopher 1961; Wilson *et al.*, 1963; Kent, 1973, 1974, 1987; Thomas, 1974; Kendall, 1976; Brown and Brown, 1987; Kohm and Louden, 1988; Osadetz *et al.*, 1989; Schurr *et al.*, 1989). The dominant trends of

such basement features or their manifestation in the overlying sequence are N45-55°W and N35-55°E (Table 1 in Penner *et al.*, 1987). Seismic data (e.g. Figure 6), the coincidence of the Lake Alma, Hummingbird and Minton producing areas with a pronounced basement gravity low (Figure 1), and isopach trends, suggest that local structural highs in the study area are related to basement tectonics.

Regional trends defined on isopach maps of the Herald and Yeoman Formations and the distribution of facies suggest that localized structural movement during deposition of these strata affected patterns of sedimentation (Ballard, 1969; Kent, 1973, 1987; Kendall, 1976; Osadetz *et al.*, 1989). In addition, the common coincidence of structural highs on the Herald and Yeoman Formations with thins on isopach maps of Silurian strata suggests that a significant portion of structural growth occurred during deposition of the Interlake (Kohm and Louden, 1988) or, more likely, resulted in erosion of Silurian strata during the period marked by the sub-Devonian unconformity. In the Minton area, the Upper Interlake unit (Figure 3) is 11 m thinner in 11-2-3-21W2 than in 15-12-3-21W2, just over 1 km away.

Faulting and fracturing induced by basement movement also play an important role in controlling fluid distribution. Faults can provide the trapping mechanism for oil in some places (Kohm and Louden, 1988). Faults and fractures also serve as fluid conduits and thus exercise a strong control over the migration paths of oil and water. Oil migration from Yeoman source rocks to Yeoman and Herald reservoirs is likely enhanced by the presence of fractures. Furthermore, production of Ordovician oil from the Winnipegosis Formation (Devonian) in 11-2-3-21W2 (K. Osadetz, pers. comm.) suggests that fractures provide the migration paths through otherwise impermeable anhydrite and carbonate units which separate the Winnipegosis reservoirs from Yeoman source rocks.

The relationship of fracture patterns, induced by basement movement, to water flow and dissolution of the salts in the Prairie Evaporite (Devonian) has been discussed by several authors (e.g. Christopher, 1961; Kent, 1973). A major area of salt dissolution coincides with the Lake Alma, Hummingbird, Minton producing areas (Figure 1) and localized salt dissolution occurs in the vicinity of the producing Gulf Weir Hill 9-29-6-6W2 well. Thus the distribution of the Prairie Evaporite serves as a useful indicator of basement tectonic movement (Kent, 1960).

It is also interesting to note that most lakes and rivers in the study area have a northwest or northeast trend (Figures 1 and 2), roughly coincident with trends of

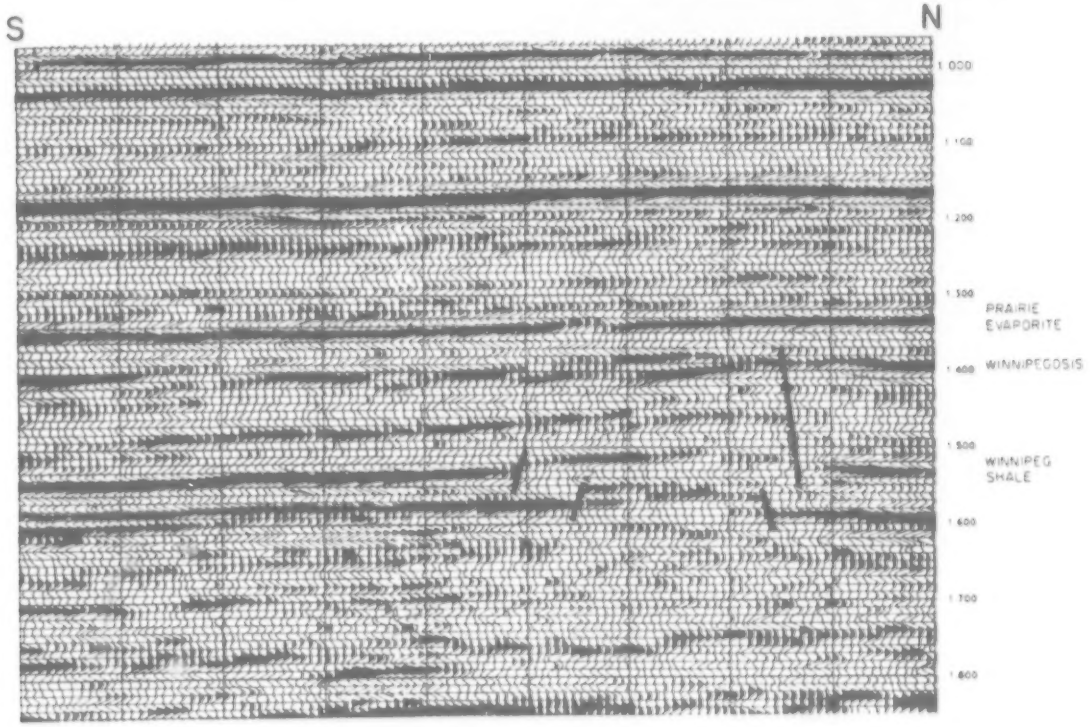

Figure 6 - Interpreted reflection seismic line in southeastern Saskatchewan; note the faults in the Precambrian basement and in overlying strata; seismic profile data courtesy of Suncor Inc., Resources Group; interpretation courtesy of Gulf Canada Resources Incorporated. From Osadetz and Haidl (1989).

major basement lineaments. In the immediate vicinity of the Mark Resources Minton wells, surface drainage has a well-defined northwest-southwest orthogonal pattern (J. Mollard, pers. comm.).

b) Dolomitization Patterns

The major control on porosity and permeability in Herald and Yeoman reservoirs is dolomitization. Several models have been proposed to explain the complex patterns of dolomitization which characterize this stratigraphic interval (e.g. Kendall, 1976, 1977, 1984, 1985; Kohm and Louden, 1978, 1982, 1988; Longman *et al.*, 1983, 1984). Evaluation of these models is beyond the scope of this study. However, the following observations are made based on a cursory examination of logs and cores in producing areas, on lithologic descriptions in Kendall (1976) and discussions of dolomitization by various authors.

1. The pervasive dolomitization of Lake Alma carbonates in the study area suggests that the flow of dense hypersaline brines associated with deposition of the Lake Alma anhydrite was a significant factor in the dolomitization of this interval.

2. The distribution in Lake Alma strata of a wide range of dolomite textures, from cryptocrystalline to sucrosic, and the complex distribution of dolomite in burrows and matrix in the Yeoman Formation, suggest that more than one phase of dolomitization occurred and that different factors may have controlled dolomitization at any given time and place. Some of the factors discussed by various authors include: i) localization of the flow of magnesium-rich brines during or immediately following deposition of the Lake Alma anhydrite by 'holes' in the anhydrite created by fractures, minor faults or expulsion of compaction waters (Longman *et al.*, 1983, 1987) or by distribution of mudcracks on the underlying playa surface (Kendall, 1984); ii) control on the downward movement of hypersaline Lake Alma pore fluids by fractures or faults initiated by basement movement following lithification of Herald and Yeoman sediments (Kohm and Louden, 1988); iii) models proposed in i) and ii) attribute a downward decrease in dolomitization to a decline in hydrostatic head and a decrease in magnesium-ion concentration as the hypersaline brines move through the sediments (Kohm and Louden, 1988; Longman *et al.*, 1983, 1987); iv) control on the path of dolomitizing fluids by the distribution of original porosity and permeability associated with different facies. This is of particular importance in the Yeoman Formation in which preferential dolomitization of the burrows is attributed to original higher porosity and permeability (e.g. Kendall, 1976; Carrol, 1978). There is also a relationship between depositional facies and dolomitization of matrix sediments (e.g. Parker and Powe, 1982; Kendall, 1985; Ballard, 1969; Derby and Kilpatrick, 1985); v) early diagenetic release of magnesium from magnesian calcites in Yeoman sediments, resulting in an increase in the Mg/Ca ratio in pore fluids, may have caused dolomitization of burrows in the Yeoman Formation (Kendall, 1976, 1977, 1985); and vi) the pattern of initial dolomitization affects subsequent diagenetic events, including chemical compaction and further dolomitization (Kendall, 1985).

3. Herald and Yeoman strata in the Lake Alma - Minton area are characterized by a downward decrease in dolomitization and a complex lateral distribution of dolomite similar to that documented in Richland County, Montana by Kohm and Louden (1978, 1988) and Longman *et al.* (1983, 1987) (D. Potter, pers. comm.).

4. Lateral changes in porosity and permeability in the Lake Alma dolomites commonly provide a stratigraphic component in the trapping of oil in these reservoirs. This is documented by Kohm and Louden (1978, 1988) in the Brush Lake Field in Montana and trapping of oil in the Lake Alma Member at CDR S Lake Alma 1-14-1-17W2 and Shell Lake Alma 7-23-1-17W2 is related, at least in part, to an updip decrease in porosity and permeability in these strata (Thomas, 1968).

6. Discussion

Given that present discoveries represent only a small proportion of the estimated 32 million m^3 of Ordovician oil generated in Saskatchewan and that additional oil may have migrated updip from the more thermally mature U.S. portion of the Williston Basin, the potential for new discoveries of hydrocarbons generated from Ordovician source rocks is high. The economic attractiveness of this play has been greatly enhanced by the recent discovery of Ordovician-sourced oil in multiple zones in several wells in the Minton area.

The key to successful hydrocarbon exploration in Ordovician rocks in Saskatchewan would appear to lie in an understanding of the tectonic framework of the Precambrian basement and of the controls exercised on the overlying sedimentary sequence by basement features. The small structural closures which trap most of the oil discovered in Ordovician strata of the Williston Basin are most likely associated with structural movement in the basement. Thus identification of zones of basement faulting is of prime importance in delineating prospective areas. Integrating regional seismic, aeromagnetic and gravity data with lineament trend analysis, surface drainage patterns, and thickness and facies distribution in Ordovician and Silurian strata may help define targets for more detailed seismic assessment. In addition, if fluid migration paths are also controlled in part by fracture patterns and faults related to basement tectonics, then prediction of porosity development and oil migration paths will also be enhanced by an understanding of the relationship between basement features and the sedimentary sequence.

Stratigraphic trapping mechanisms also must be considered in the exploration for oil in Ordovician strata. Such traps are important in Lake Alma strata (Kohm and Louden, 1988; Longman *et al.*, 1987; Thomas, 1968) and the complex distribution of dolomitization in

Table 2 - Locations of Oil Shows in Drill Stem Tests

Well Name	Location	DST Interval (m below K.B.)	Stratigraphic Unit	Recovery
Gulf Weir Hill	9-29-6-6W2	2465.0-2487.0	Herald-Yeoman	560 m gas cut oil, 28 m mud, 85 m oil-cut saltwater
Esso Bromhead	6-28-3-12W2	2845.0-2892.6	Herald-Yeoman	180.1 m oil, 1770.0 m water
Banff *et al.* Bromhead	16-16-3-13W2	2913.9-2932.5	Herald	219.5 m gas and saltwater cut mud, 1176.5 m oil cut saltwater
CDR Shell FPC Oungre	15-9-2-14W2	3053.5-3070.6	Herald-Yeoman	5.2 m gas cut oil, 166.1 m gas, oil and water cut mud, 406.3 m gas and oil cut water
Home TCPL W Oungre	14-15-3-15W2	2948.0-2959.0	Yeoman	720.0 m oil and mud cut water
CDR Mobil Beaubier	3-20-2-16W2	3051.7-3066.3	Herald-Yeoman	877.8 m gas cut oil
CDR Scurry S Lake Alma	1-14-1-17W2	3080.0-3091.9	Herald	301.8 m oil and saltwater cut mud, 499.9 m gas and oil cut water
		3093.7-3112.9	Yeoman	274.3 m clean mud, 658.4 m gas and oil cut water
Scurry *et al.* Lake Alma	1-23-1-17W2	3064.5-3077.0	Herald-Yeoman	51.8 m gas cut oil, 76.2 m gas and oil cut mud, 61 m gas cut saltwater
Shell Lake Alma	7-23-1-17W2	3052.0-3066.9	Herald-Yeoman	4.9 m oil, 85 m water
CDR *et al.* S Lake Alma	13-23-1-17W2	3063.2-3077.0	Yeoman	65.5 m gas and mud cut oil, 108.8 m mud cut saltwater
Shell Lake Alma	11-27-1-17W2	3053.0-3073.0	Herald-Yeoman	220.0 m oil, 558.0 m mud, 172.0 m water
Sun Imp Three Lakes	13-6-1-19W2	3017.5-3023.6	Herald-Yeoman	566.9 m oil and saltwater cut mud
Imp Hummingbird	6-13-2-19W2	2987.6-2999.2	Herald	137.2 m gas and oil cut mud
		3002.0-3010.0	Herald	68.6 m clean oil, 205.7 gas, oil and mud cut water
		3010.0-3016.0	Yeoman	235.9 m gas and saltwater cut oil, 175.6 saltwater
		3016.0-3022.1	Yeoman	9.1 m gas and saltwater cut mud
Sun Pangman	2-30-8-19W2	2470.4-2477.1	Yeoman	57.9 m mud cut oil, 27.4 m oil cut mud, 45.7 saltwater
Imperial Pangman	3-14-8-20W2	2518.9-2532.6	Yeoman	106.7 m gas and saltwater cut mud, 341.4 m gas, oil and mud cut water
Mark *et al* Minton	11-2-3-21W2	2855.1-2875.5	Herald-Yeoman	204.2 m oil, 368.8 saltwater
Tenn HB Bead Lake	6-8-4-21W2	2766.1-2773.7	Herald-Yeoman	378.0 m oil and gas cut saltwater
Dome Saskoil McKinnon	12-20-4-21W2	2746.9-2752.3	Herald-Yeoman	396.2 m oil cut saltwater

the Yeoman Formation suggests that stratigraphic traps should be more common in this interval. Successful exploration for Yeoman stratigraphic traps will require a creative exploration philosophy which integrates models of facies distribution, dolomitization and oil migration. Osadetz (pers. comm.) has proposed one such exploration model, the key elements of which are: 1) an oolitic shoal on a mud-dominated shelf in the upper Yeoman (Figure 4 in Stasiuk and Osadetz, 1990), 2) reflux dolomitization of facies similar to that described by Hartling *et al.* (1982) in Mississippian (Oungre) reservoirs in southeastern Saskatchewan and 3) long distance migration of oil from North Dakota at a time (approx. 75 million years ago) when the ancestral Nesson anticline was not active and, therefore, did not trap oil migrating updip from the centre of the basin.

7. Potential Exploration Targets

The scope for exploration and discovery of new oil reservoirs in the Herald and Yeoman Formations is immense. Only 165 wells penetrate these strata in the approximately 69,000 km^2 (27,000 miles^2) encompassed by the study area. Cores are available from only 73 of these wells and drillstem tests were run over this interval in 105 wells. The distribution of producing wells and hydrocarbon shows (Figure 1, Table 1) suggests that, on a regional basis, the most attractive area for exploration lies south of Township 15 and west of Range 5. However, given the sparse well control outside this area and the possibility of long distance oil migration, the potential of the remainder of the study area cannot be dismissed.

Two specific areas appear to have the greatest potential for new discoveries of oil in Ordovician reservoirs:

1) The area of the 'Roncott High', including the areas of salt dissolution (and their edges) to the east, west and north (Figure 1). There is abundant evidence of basement tectonism in this area and careful assessment of available data together with detailed seismic evaluation of selected targets should lead to the discovery of new pools of Ordovician oil trapped in Paleozoic strata.

2) The area along the Tatagwa - Weyburn - Steelman trend of Mississippian oilfields. The high heat flow anomaly linked to basement structures encompasses much of this area (Majorowicz *et al.*, 1988). Local salt dissolution in the Prairie Evaporite also occurs in this area, an indication of fracturing which is likely associated with basement tectonism. Evidence that oil was generated in or has migrated to this region is provided by production of Ordovician oil

from Gulf Weir Hill 9-29-6-6W2 and oil staining in three cores in the area (16-20-8-10W2, 8-2-6-16W2, 6-32-8-16W2; Figure 1).

It is of interest to note that Kendall's (1976) discussion of the economic potential of Ordovician strata also highlighted the two areas discussed here. It is hoped that current high oil prices and the high rates of production (30 to 65 m^3 per day) of Ordovician oil from Paleozoic strata in the Minton area will accelerate the exploration for hydrocarbons in the Herald and Yeoman Formations in southeastern Saskatchewan.

8. References

Ballard, W.W. (1969): Red River of northeast Montana and northwest North Dakota; Mont. Geol. Soc., Eastern Montana Symposium, p15-24.

Brooks, P.W., Snowdon, L.R. and Osadetz, K.G (1987): Families of oils in southeastern Saskatchewan; *in* Carlson, C.G. and Christopher, J.E. (eds.), Fifth International Williston Basin Symposium, Sask. Geol. Soc., Spec. Publ.9, p253-264.

Brown, D.L. and Brown, D.L. (1987): Wrench-style deformation and paleostructural influence on sedimentation in and around a cratonic basin; *in* Longman, M.W. (ed.), Williston Basin: Anatomy of a Cratonic Oil Province; Rocky Mtn. Assoc. Geol., p57-70.

Carroll, W.K. (1978): Depositional and paragenetic controls on porosity development, Upper Red River Formation, North Dakota; *in* 1978 Williston Basin Symposium, Mont. Geol. Soc., Guidebook, p79-94.

Christopher, J.E. (1961): Transitional Devonian-Mississippian Formations of southern Saskatchewan; Sask. Dep. Miner. Resour., Rep. 66, 103p.

Derby, J.R. and Kilpatrick, J.T. (1985): Red River dolomite reservoirs, Killdeer Field, North Dakota; *in* Roehl, P.O. and Choquette, P.W. (eds.), Carbonate Petroleum Reservoirs, Springer-Verlag, NY, p61-69.

Fuzesy, A. (1982): Potash in Saskatchewan; Sask. Energy and Mines, Rep. 181, 44p.

Hartling, A., Brewster, A. and Posehn, G. (1982): The geology and hydrocarbon trapping mechanisms of the Mississippian Oungre Zone (Ratcliffe Beds) of the Williston Basin; *in* Christopher, J.E. and Kaldi, J. (eds.), Fourth Williston Basin Symposium, Sask. Geol. Soc., Spec. Publ. 6, p217-223.

Kendall, A.C. (1976): The Ordovician carbonate succession (Bighorn Group) of southeastern Saskatchewan; Sask. Miner. Resour., Rep. 180, 185p.

_____ (1977): Origin of dolomite mottling in Ordovician limestones from Saskatchewan and Manitoba; Bull. Can. Petrol. Geol., v25, p480-504.

_____ (1984): Origin and geometry of Red River dolomite reservoirs, western Williston Basin: Discussion; Am. Assoc. Petrol. Geol., Bull., v68, p776-779.

_____ (1985): Depositional and diagenetic alterations of Yeoman (Lower Red River) carbonates from Harding Co., South Dakota; *in* Longman, M.W., Shanley, K.W., Lindsay, R.F. and Eby, D.E. (eds.), Rocky Mountain Carbonate Reservoirs - A Core Workshop; Soc. Econ. Paleon. Mineral., p95-124.

_____ (1988): Aspects of evaporite basin stratigraphy; *in* Schreiber, B.C. (ed.), Evaporites and Hydrocarbons, Columbia Univ. NY, p11-62.

Kent, D.M. (1960): The evaporites of the Upper Ordovician strata in the northern part of the Williston Basin; Sask. Dep. Min. Resour., Rep. 46, 46p.

_____ (1973): Paleozoic hydrocarbon reservoirs in Saskatchewan and their relationship to basement lineaments; J. Can. Petrol. Tech., v12, p20-24.

_____ (1974): Relationship between hydrocarbon accumulations and basement structural elements in the northern Williston Basin; *in* Parslow, G.R. (ed.), Fuels: a geological appraisal: Sask. Geol. Soc., Spec. Publ. 2, p63-80.

_____ (1987): Paleotectonic controls on sedimentation in the northern Williston Basin, Saskatchewan; *in* Longman, M.W. (ed.), Williston Basin: Anatomy of a Cratonic Oil Province; Rocky Mtn. Assoc. Geol., p45-56.

Kohm, J.A. and Louden, R.O. (1978): Ordovician Red River of eastern Montana - western North Dakota: relationships between lithofacies and production; *in* 1978 Williston Basin Symposium, Mont. Geol. Soc., Guidebook, p99-117.

_____ (1982): Ordovician Red River of eastern Montana and western North Dakota: relationships between lithofacies and production; *in* Fourth International Williston Basin Symposium, Christopher, J.E. and Kaldi, J. (eds.), Sask. Geol. Soc., Spec. Publ. 6, p27-28.

_____ (1988): Red River reservoirs of western North Dakota and eastern Montana; *in* Goolsby, S.M. and Longman, M.W. (eds.), Occurrence and physical properties of carbonate reservoirs in the Rocky Mountain region, 1988 Carbonate Symposium, Rocky Mtn. Assoc. Geol., p275-290 with plates p451-456.

Longman, M.W., Fertal, T.G. and Glennie, J.S. (1983): Origin and geometry of Red River dolomite reservoirs, western Williston Basin; Am. Assoc. Petrol. Geol., Bull., v67, p744-771.

_____ (1984): Origin and geometry of Red River dolomite reservoirs, western Williston Basin: Reply; Am. Assoc. Petrol. Geol., Bull., v68, p780-784.

_____ (1987): Origin and geometry of Red River dolomite reservoirs, western Williston Basin; *in* Longman, M.W.(ed.), Williston Basin: Anatomy of a Cratonic Oil Province; Rocky Mtn. Assoc. Geol., p83-104.

Majorowicz, J.A., Jones, F.W. and Osadetz, K.G. (1988): Heat flow environment of the electrical conductivity anomalies in the Williston Basin, and occurrence of hydrocarbons; Bull. Can. Petrol. Geol., v36, p86-90.

Mollard, J.D. (1959): Photogeophysics: its application in petroleum exploration over the glaciated plains of western Canada; *in* Second International Williston Basin Symposium, N. Dak. Geol. Soc./Sask. Geol. Soc., p109-117.

_____ (1987): Tableland photolineament pattern revisited; *in* Carlson, C.G. and Christopher, J.E. (eds.), Fifth International Williston Basin Symposium, Sask. Geol. Soc., Spec. Publ.9, p178-189.

Osadetz, K.G, and Haidl, F.M. (1989): Tippecanoe Sequence: Middle Ordovician to lowest Devonian: vestiges of a great epeiric sea; *in* Ricketts, B.D. (ed.), Western Canada Sedimentary Basin: A Case Study; Can. Soc. Petrol. Geol., p121-137.

Osadetz, K.G., Snowdon, L.R and Stasiuk, L.D. (1989): Association of enhanced hydrocarbon generation and crustal structure in the Canadian Williston Basin; *in* Current Research, Part D, Geol. Surv. Can., Pap. 89-1D, p35-47.

Parker, T.S. and Powe, W.H. (1982): Geology of the Raymond field area, Sheridan County, Montana; *in* Christopher, J.E. and Kaldi, J. (eds.), Fourth Williston Basin Symposium, Sask. Geol. Soc., Spec. Publ. 6, p225-234.

Paterson, D.F. (1971): The Winnipeg Formation (Ordovician) of Saskatchewan; Sask. Dep. Miner. Resour., Rep. 140, 57p.

Penner, L.A., Mollard, J.D. and Hodgson, R.A. (1987): Remote sensing for petroleum exploration in Saskatchewan; Saskatchewan Energy and Mines, Canada-Saskatchewan Heavy Oil/Fossil Fuels Research Program, Tech. Rep. 5, 199p.

Shurr, G.W., Larson, B.S. and Watkins, I.W. (1989): The basement block mosaic beneath the Montana plains; *in* French, O.E. and Grabb, R.F. (eds.), 1989 Field Conference Guidebook: Geologic Resources of Montana; Mont. Geol. Soc., p299-309.

Stasiuk, L.D. and Osadetz, K.G. (1990): The life cycle and phyletic affinity of *Gloeocapsomorpha prisca* Zalesky 1917 from Ordovician rocks in the Canadian Williston Basin; *in* Current Research, Part D, Geol. Surv. Can., Pap. 89-1D, p123-137.

Stoakes, F., Campbell, C. and Hassler, G. (1987): Sedimentology and hydrocarbon source potential of the Ordovician Bighorn Group southeast Saskatchewan; Stoakes Campbell Geoconsulting Ltd., Federal Contract #23294-6-0930/01-SG, 62p.

Thomas, G.E. (1968): Notes on textural and reservoir variations of Ordovician micro-dolomites, Lake Alma-Beaubier producing area, southern Saskatchewan; Sask. Dep. Miner. Resour. and Sask. Geol. Soc., Core Seminar on the Pre-Mississippian rocks of Saskatchewan.

Thomas, Gilbert E. (1974): Lineament-block tectonics: Williston-Blood Creek Basin; Am. Assoc. Petrol. Geol., Bull, v58, p1305-1322.

Wilson, W., Surjik, D.L. and Sawatzky, H.B. (1963): Hydrocarbon potential of the south Regina area Saskatchewan; Sask. Dep. Miner. Resour., Rep. 76, 15p.

Seismic Mapping of the Northern Williston Basin

Chengnan Zhu[1] *and Zoltan Hajnal*[1]

Zhu, C. and Hajnal, Z. (1990): Seismic mapping of the northern Williston Basin; *in* Summary of Investigations 1990, Saskatchewan Geological Survey; Saskatchewan Energy and Mines, Miscellaneous Report 90-4.

Since 1985, a seismic mapping project of the northern Williston Basin has been in progress with the aim to image stratigraphic features and structures within the basin and attempt to recognize and correlate similar aspects in the underlying basement. The information for the investigation consists of 1,300 km of seismic data (with over 20,000 shots) donated by 22 oil companies. The seismic lines cross the northern Williston basin from southwestern Manitoba through southern Saskatchewan to southeastern Alberta (Figure 1). Most of data is high quality and can be used for comprehensive stratigraphic interpretation.

Data processing in the basin is hampered by local near-surface velocity anomalies, shallow structures, glacial drift, buried valleys, weathered layers and young collapses. A special data processing method called 'correlation datuming' (Zhu and Hajnal, in press; Berryhill, 1979) has been developed to solve these problems. The regional section (Figure 2) uses a reflection horizon near the top of the Colorado Group (Cretaceous) as a datum to separate deformation of the basin into two portions. The use of the stratigraphic datum transfers the time delays of shallow structures to the surface. Use of the technique eliminates introduction of apparent structures to the seismic section.

We believe that the regional seismic profile describes time relationship (chronostratigraphy), which is difficult to establish by well logs or outcrop data (Badley, 1985). Comparing the seismic sections with well log information shows disagreement among many of the related formation picks previously made across the basin. We observe that confusion exists in regional correlation of the late Cretaceous formations, which we believe can be resolved using the compiled reflection section. Several stratigraphic contacts from the lower segment of the sedimentary column and the sediment-basement contact have been determined through regional correlation

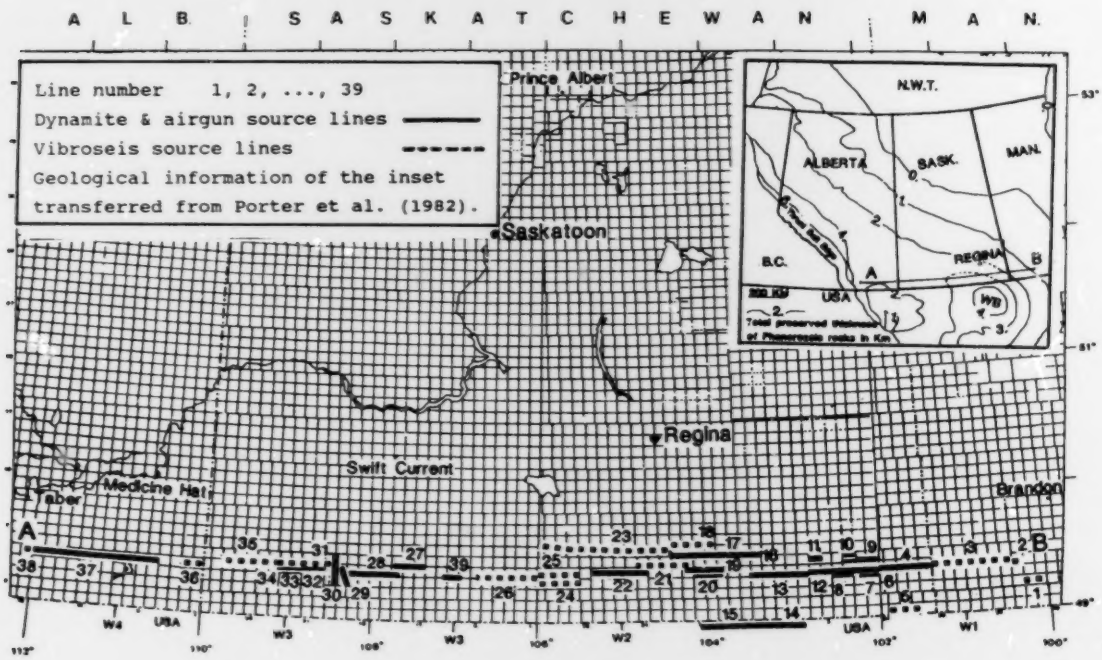

Figure 1 - Location map of seismic lines. The structure contour map (inset) shows the Western Interior Basins in Canada and U.S.A. (Porter et al., 1982). WB = the centre of the Williston Basin.

(1) Department of Geological Sciences, University of Saskatchewan, Saskatoon, Saskatchewan.

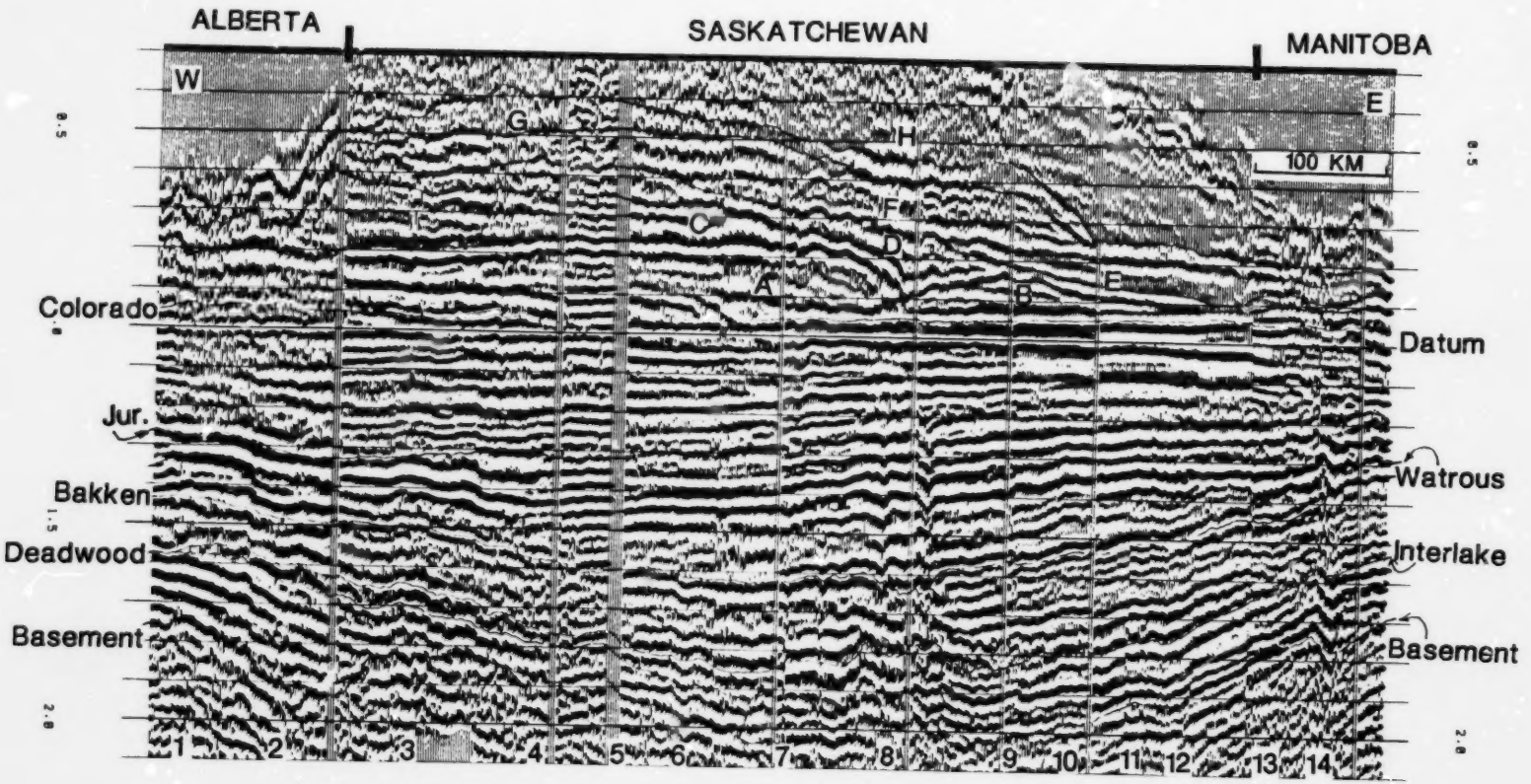

Figure 2 - Regional seismic section of the Williston Basin. Numbers 1 to 14 are locations of interpreted structures (Zhu and Hajnal, 1990). Letters A to H are Upper Cretaceous stratigraphic units from regional seismic section recognized by Zhu and Hajnal (1990).

of the seismic section. Many of these have not been defined by log picks.

The reflection profile displays several regional structures, some of which have not been correctly understood, some not even reported in geological literature. For example, the regional information reveals that the Regina trough was a relatively uplifted area during Pre-Mississippian and Post-Jurassic time. During Mississippian to Jurassic time, sediment thickness increased in the trough, relative to the basin, probably caused by salt dissolution. Renewed salt dissolution might still be induced by slight uplifts of the underlying basement.

1. Acknowledgments

The following companies are graciously thanked for donated seismic data for this project.

1. Amerada Mineral Corp. of Canada Ltd. (line 39)
2. Access Res. Ltd. (line 21)
3. Andex Oil Ltd. (line 32)
4. Bowrio Res. Ltd. (line 34)
5. Chevron Canada Res. (lines 1, 5, 10,11, 28, 30 and 31)
6. Coho Res. Ltd. (lines 4, 6 and 8)
7. Enron Oil Canada Ltd. (line 33)
8. Global-Taber Exp. (line 38)
9. Kary Data Cons. Ltd. (lines 14, 15 and 37)
10. Lunberg, Goodwin and Curts Geophy. Cons.
11. Noramex Ltd. (lines 20, 23, 24 and 25)
12. PanCanadian Petr. Ltd. (lines 16, 17 and 18)
13. Petro-Canada Inc. (line 27)
14. Petro-Venture (1979) (line 36)
15. Resources Ex. (1985) Ltd. (line 35)
16. Sefel Geophysical Ltd. (line 37)
17. L. Shapiro Man. Ltd. (lines 2, 3, 13, 22 and 38)
18. Shapco Tri Prospect Ltd. (lines 2, 3 and 9)
19. Shapco Universal Ltd. (lines 2, 3 and 9)
20. Sigma Ex. (1978) Ltd. (lines 7, 12 and 20)
21. Sourcex Geophysical ltd. (lines 19, 12 and 20)
22. Unocal Canada Ex. Ltd. (line 26)

2. References

Badley, M.E. (1985): Practical Seismic Interpretation; International Human Resources Development, Boston, P266.

Berryhill, J.R. (1979): Wave-equation datuming; Geophys., v44, p1329-1344.

Porter, J.W. Price, R.A. and McCrossan, R.G. (1982): The west Canada sedimentary basin; Phil. Trans. R. Soc. Lond., A305, p169-192.

Zhu, C. and Hajnal, Z. (1990): The regional seismic section of the Williston Basin: paper presented at the CSPG annual meeting, Calgary.

Zhu, C. and Hajnal, Z. (in press): Correlation datuming for improving seismic image, Geophys.

Progress of the Pore Geometry Reservoir Model Study for the Devonian Upper Winnipegosis Member in Southeast Saskatchewan

Melinda Yurkowski

Yurkowski, M. (1990): Progress of the pore geometry reservoir model study for the Devonian Upper Winnipegosis Member in southeast Saskatchewan; *in* Summary of Investigations 1990, Saskatchewan Geological Survey; Saskatchewan Energy and Mines, Miscellaneous Report 90-4.

A pore geometry model is being constructed for the Upper Winnipegosis Member of Middle Devonian age in southeast Saskatchewan. The study area (Figure 1) extends from the Manitoba - U.S. border to Township 10 Range 12W2M. Over sixty wells have been examined; of these 24 were selected for Mercury Injection Capillary Pressure (MICP), petrography and Scanning Electron Microscope (SEM) analyses. Eighty-four sample plugs were recovered from well core.

1. Geologic Setting

The Winnipegosis Formation of the Elk Point Group can be divided into two members: a lower, platform carbonate member consisting of bioturbated mudstones and wackestone and an upper member, which constitutes the reef buildup. The Ratner Member lies in the inter-reef areas between the buildups. It is a bituminous laminated mudstone interlayered with anhydrite. The Ratner lies conformably on the Lower Winnipegosis Member or on the flanks of the upper member reef buildup. Further details are available in Yurkowski (1989).

Figure 1 – Location map showing area of study (diagonal shading) and limits of Winnipegosis Formation.

The Upper Member can be divided into three gross petrographic facies: (1) a lower, peloid, codiacean algal facies comprised of foreslope mudstones, packstones and grainstones, as well as grainstones and bindstones of the reef interior; (2) a reef framework facies with either red digitate algae and stromatoporoids (tabular and massive as well as *Amphipora* and *Stachyodes*) or tabulate corals (for example Chaetitid and *Thamnopora*), and (3) a laminated dolostone capping the reef framework. Conformably overlying the buildups are the Whitkow anhydrites and halites.

These reefs have been extensively dolomitized and have had a complex diagenetic history (Martindale and MacDonald, 1989). The resultant lithology is a microcrystalline to cryptocrystalline dolomite with intercrystalline porosity throughout the buildups. Leaching of biotic constituents and dolomite have produced biomoldic and vuggy porosity. Fibrous anhydrite cements may partially or completely fill some of these vugs and some of the intercrystalline porosity found in the upper 1/3 of the reefs as well.

2. Capillary Pressure Analysis

Sample plugs approximately 3 cm long were taken from recovered well core. The analytical procedures followed were defined by Purcell (1949), Wardlaw and Taylor (1978) with modifications from Leibel (1980) and Akhurst (1984). Calculation of pore throat diameter is based on sheet pore geometry, typical of dolomites.

Kent (1987) identified six numerical parameters which can be obtained from MICP curves. These are: porosity, permeability, entry pressure (indicating the ability of a reservoir rock to accept non-wetting fluids), withdrawal efficiency (indicating the ability to release non-wetting fluids), unsaturated pore volume and standard deviation of pore throat sizes. To date, all parameters except the latter have been established for several of the samples.

Three basic curve types have been identified.

Type 1 curve: A type 1 curve is characterized by fairly low entry pressures, high ejection efficiencies (greater than 40 percent) and low unsaturated pore volume values (Figure 2).

These curves are indicative of a mixed intercrystal and vuggy porosity within the rock. The samples taken from the reservoir in 9-22-2-9W2M fall into this category. Plug W2 (Figure 2), for example, is a microcrystalline

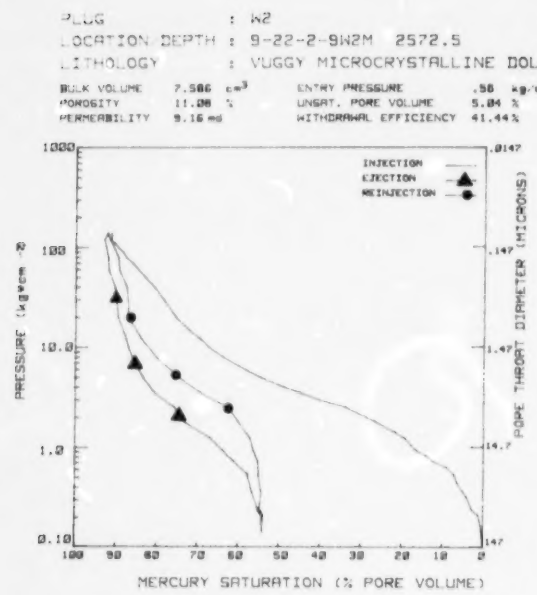

Figure 2 -Type 1 curve.

dolomite with patches of dark grey cryptocrystalline dolomite. Numerous solution enhanced mesovugs and microvugs, as well as biomoldic pores (coral?) occur in this specimen. Thus far, lithologies having this curve type have the best yield potential (average withdrawal efficiency of 41 percent).

Type 2 curve: The MICP curve for type 2 (Figure 3) shows a higher unsaturated pore volume than type 1.

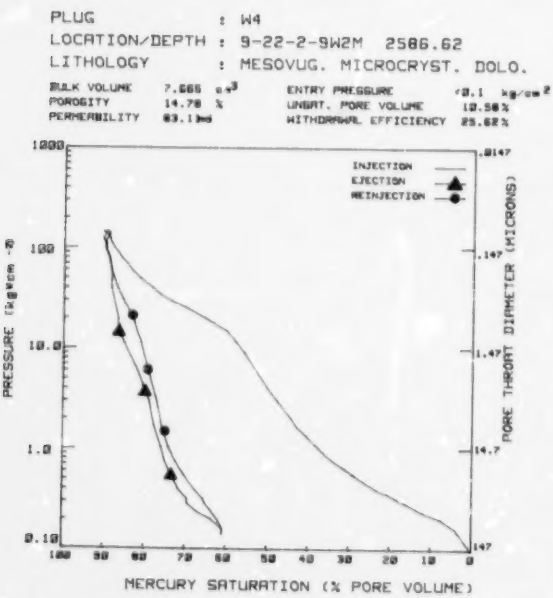

Figure 3 -Type 2 curve.

The pore throat diameters do not show the coarse skewness that type 1 does. Type 2 is considered to be influenced by predominantly vuggy porosity. The steepness of the injection curve slope suggests that the pore throat diameters were poorly sorted. Although permeability and porosity values are better than on the type 1 curve, the withdrawal efficiency is not as high. This is probably due to a snap-off phenomenon, whereby mercury snaps off when being ejected from larger opening through to smaller openings. Any oil production from this sample type would not be as high as from type 1. Also noted on this curve is the absence of an entry pressure, which suggests that the entry pressure was less than the minimum obtainable pressure. Work done by Akhurst (1984) identifies this problem and suggests that the initial invasion of the vugs occurred when the plugs were placed in the mercury. The hydrostatic head of the column of mercury was sufficient to cause entry of the outer pores. Plug W4 (Figure 3) is a light grey microcrystalline dolomite, densely populated with microvugs and mesovugs and resembles a dolomitized Chaetetid.

Type 3 curve: Type 3 curves are typical of non-reservoir rocks with high entry pressures, low withdrawal efficiencies, and no recorded permeability. The injection curve is somewhat flatter than curves 1 and 2, suggesting a better sorting of very fine pore throats. The low withdrawal efficiencies indicate a large amount of mercury trapped within the sample. SEM work, to be commenced in the near future, should help determine if the low withdrawal efficiency is due to the pore throat sorting, the fineness of the pore throats, or a combination of both. Plug W5 (Figure 4) is a light grey cryptocrystalline dolomite with less than 2 percent microvugs. Numerous faint bituminous partings occur in this sample.

3. Summary and conclusions

Curve type 1 shows the highest ejection efficiency, a low entry pressure and indicates coarse skewness of the pore throat diameters. Based on available data, lithologies giving type 1 curves have the best reservoir potential. As previously mentioned, plug W2 (Figure 2) was obtained from the reservoir in 9-22-2-9-W2M. As of December 1989, this has produced 19,856.6 m^3 oil, 2038.8 m^3 gas, and 10,429.9 m^3 water. Plug W4 (Figure 3), which yielded a type 2 curve and plug W5 (Figure 4), which gave a type 3 curve, were also from the 9-22 well (see Figure 5), but were down section from the reservoir.

Future work will include the completion of mercury injection analyses, SEM work, and thin section analyses.

4. Acknowledgements

The author is currently undertaking an M.Sc. thesis, University of Regina, under the direction of Dr. D.M. Kent. Saskatchewan Energy and Mines is gratefully acknowledged for their financial support of this research project.

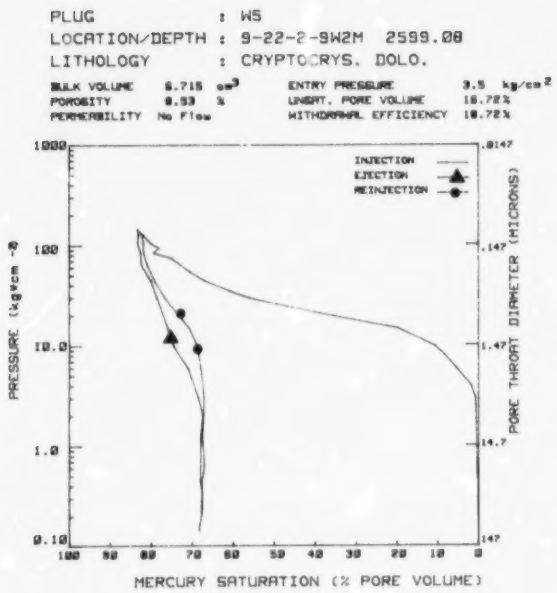

Figure 4 - Type 3 curve.

5. References

Akhurst, M.C. (1984): Pore geometry model of the Mississippian Madison Formation in southeastern Saskatchewan; unpubl. M.Sc. thesis, Univ. Regina.

Kent, D.M. (1987): Modelling carbonate reservoir porosity for enhanced recovery schemes; J. Can. Petrol. Tech., v26, no.4, p53-59.

Leibel, R.J. (1980): A pore geometry study of the Mississippian Midale carbonate of the Benson Field, southeastern Saskatchewan; unpubl. M.Sc. thesis, Univ. Regina.

Martindale, W. and MacDonald, R.W. (1989): Sedimentology and diagenesis of the Winnipegosis Formation, Tableland area, S.E. Saskatchewan; *in* Bloy, G., Hadley, M. and Curtis, B. (eds.), The Development of Porosity in Carbonate Rocks, CSPG Continuing Education Short Course Notes.

Purcel, W.R. (1949): Capillary pressures - their measurement using mercury and the calculation of permeability therefrom; J. Petrol. Tech., v1, p39-48.

Wardlaw, N.C. and Taylor, R.P. (1976): Mercury capillary pressure curves and the interpretation of pore structure and capillary behavior in reservoir rocks; Bull. Can. Petrol. Geol., v24, p225-262.

Yurkowski, M. (1989): Preliminary report on a pore geometry reservoir model for the carbonate buildups in the Winnipegosis Formation (Devonian) in southeast Saskatchewan; *in* Summary of Investigations 1989, Sask. Geol. Surv., Misc. Rep. 89-4, p137-140.

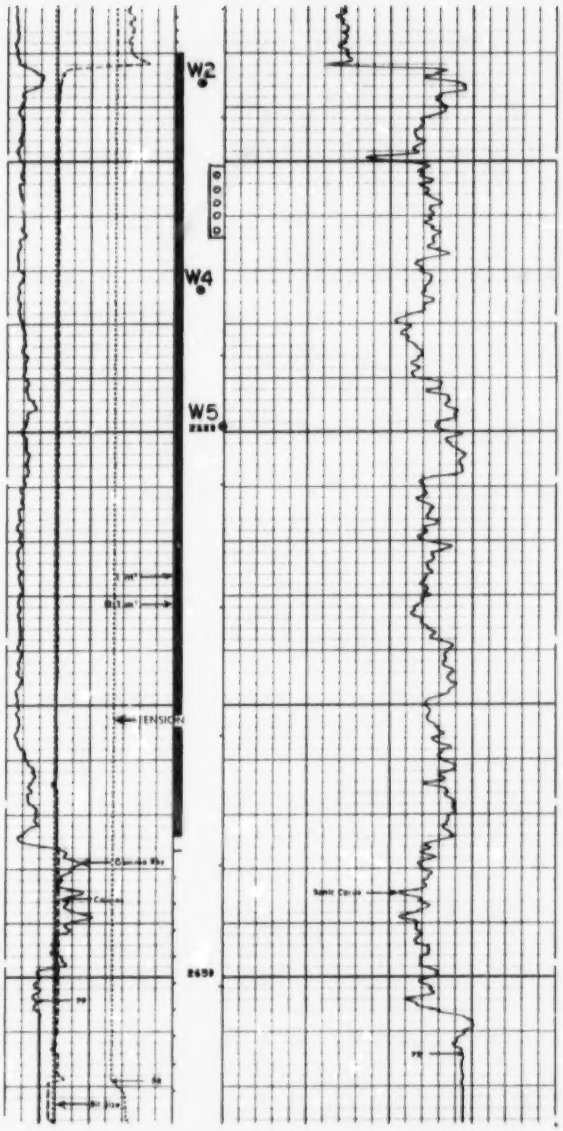

Figure 5 - Geophysical well log from Home SRD Tableland 9-22-2-9W2M, which indicates cored interval (heavy black line), completion zone (open circles) and sample locations for this study.

Lithogeochemical Study of the Cretaceous in Central Saskatchewan - Preliminary Report

Colin E. Dunn[1]

Dunn, D.E. (1990): Lithogeochemistry study of the Cretaceous in central Saskatchewan - Preliminary report; *in* Summary of Investigations 1990, Saskatchewan Geological Survey, Saskatchewan Energy and Mines, Miscellaneous Report 90-4.

'Environmental geochemistry' is a new program being developed at the Geological Survey of Canada. One component of this program is the compilation of comprehensive data bases of the Canadian landmass to provide baseline information on the natural distribution of chemical elements. The program is an extension of ongoing studies, such as the National Geochemical Reconnaissance (NGR), that have, over the past 20 years, been directed mostly toward mineral exploration (Friske and Hornbrook, in press).

Government agencies have had the foresight to carefully archive portions of samples collected during reconnaissance and exploration programs, and these materials are of immense value for further study in light of new knowledge and increasingly sophisticated analytical instrumentation. The sample set used for this report is the rock cuttings from hydrocarbon exploration drill holes, that have been archived (in vials) and catalogued by Saskatchewan Energy and Mines over the past 50 years.

The purpose of the current study is to document the chemistry of the Cretaceous strata that subcrop beneath glacial deposits of the Prairies and, through collaboration with health specialists, examine the patterns of element distribution with respect to the quality of human, animal and crop health. At Henribourg, 20 km northeast of Prince Albert, an unusually high incidence of multiple sclerosis has been reported by Irvine *et al.* (1988, 1989). The authors have examined the chemistry of soils and well waters and noted a multi-element association which may be related to the disease. Other studies suggesting a link between trace elements in the environment and the incidence of multiple sclerosis include reports from British Columbia (Gould and Warren, 1980) and Finland (Hasanen *et al.*, 1986).

The rationale for the present study is that the chemical composition of the subcropping sedimentary rocks is reflected in the overlying glacial deposits, and, therefore, in the ground waters and crops consumed by animals and the populace, particularly in rural areas. The provision of lithogeochemical maps will establish patterns of element enrichments, deficiencies or associations for investigation by health, veterinary, and agricultural specialists to seek links with various diseases. Once a link is identified, then mitigating measures may be taken to alleviate the problem. Rocks, in effect, form the bottom end of the food chain, and their chemistry can have a significant bearing on man's environment and health.

1. Scope of Study

The area examined is approximately 100 000 km^2 of central Saskatchewan within which 107 exploration holes have been drilled (Figure 1). Work was contracted to experts on the Cretaceous of the Central Plains to collect well-cuttings for analysis, and provide a) an updated 1:1,000,000 geology map of the Phanerozoic of the entire province beneath the Pleistocene cover, paying particular attention to the Cretaceous of the study area; b) a compilation at the same scale of a hydrogeological map of the province, with respect to vectors of water movement, and zones of recharge and discharge at the subcropping Cretaceous surface; c) stratigraphic cross sections of the study area; d) annotated geophysical logs and sample descriptions of the 96 wells sampled; and e) a report on the stratigraphy of Cretaceous, Tertiary and Pleistocene strata (Christopher and Koziol, 1990).

2. Sample Materials and Methods

In the 96 wells selected for study, each sample was a composite from two vials of well-cuttings over each 20 ft (6 m) interval throughout the top 200 ft (60 m) of the subcropping Cretaceous sedimentary rocks. This provided a maximum of 10 samples per well, although fewer were available from some wells such that a total of 720 (including standards and duplicates) were submitted for analysis. Samples were retrieved in accord with the following specifications:

a) A 2 to 3 g sample of well-cuttings was collected from each of the storage vials that were present over specified 6 m intervals. The rock chips were examined microscopically to select material representative of the stratigraphic interval (formation limits and lithologies were determined from geophysical well log signature).

b) A magnet was passed over each sample to remove any metallic contaminants derived from drilling and sample recovery operations. Plastic tweezers were used to make a composite sample, which was then split into two portions for different types of chemical analysis.

c) From the microscope examination of each composite sample a brief and systematic description was made of the lithology, grain size, colour, and any other noteworthy features. The well name, location,

(1) Geological Survey of Canada, 601 Booth St., Ottawa, Ont.

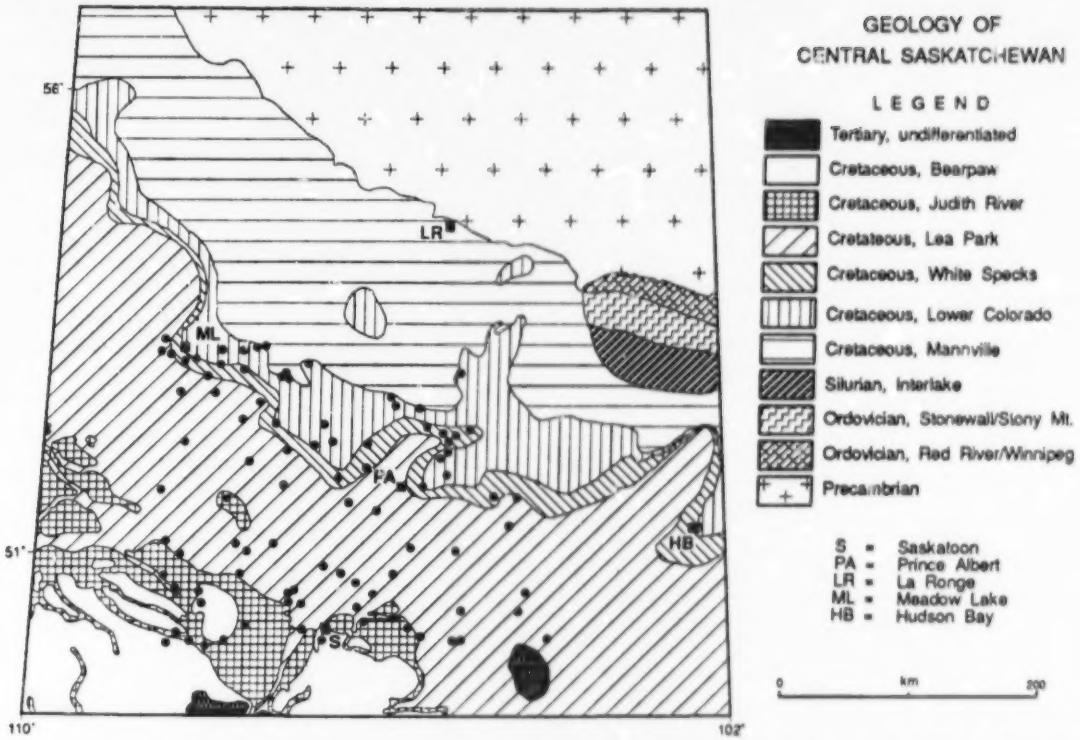

Figure 1 - Geology of central Saskatchewan showing locations of wells from which samples were collected. Map digitized from compilation by Christopher and Koziol (1990).

stratigraphic formation, and depth below kelly bushing were also recorded.

d) A 1 to 1.5 g split of each sample was accurately weighed into a numbered plastic vial and submitted for instrumental neutron activation analysis (INAA) at Activation Laboratories Ltd., Ancaster, Ontario. Analysis included Au, Ag, As, Ba, Br, Ca, Co, Cr, Cs, Fe, Hf, Hg, Ir, K, Mo, Na, Ni, Rb, Sb, Sc, Se, Sr, Ta, Th, U, W, Zn, and the rare-earth elements La, Ce, Nd, Sm, Eu, Tb, Yb, and Lu.

e) A second 0.5 to 1 g split of each sample was placed into a small envelope and submitted for inductively-coupled plasma emission spectroscopy (ICP) at Acme Analytical Laboratories, Vancouver. Prior to instrumental analysis each sample was hand-ground using an agate mortar and pestle, and a 0.5 g portion digested with 3 ml 3-1-2 HCl-HNO_3-H_2O at 95°C for one hour then diluted to 10 ml with distilled water. The multi-element ICP package included some of the same elements provided by INAA, providing a comparison of the analytical methods. The ICP package included determinations for Mo, Cu, Pb, Zn, Ag, Ni, Co, Mn, Fe, As, U, Au, Th, Sr, Cd, Sb, Bi, V, Ca, P, La, Cr, Mg, Ba, Ti, B, Al, Na, K, and W. For some rock types this acid leach may be partial for Mn, Fe, Na, K, Al, Sr, Ca, P, La, Cr, Mg, Ba, Ti, B, and W. However, for the shales comprising this study many elements are bound to clay minerals and are released by this acid digest. Comparison of ICP results with the INAA and standards results show that most analyses represent near total concentrations for elements other than those tightly bound in the crystal lattices of the aluminosilicate minerals, notably K, Al, and Ti, along with Ba, B, Sr, V and Cr.

f) The acid digest solutions obtained for ICP were analyzed separately for those elements that form hydrides, such as As, Sb, Se, Te, Bi, and Ge (partial). Detection limits are considerably lower than can be achieved from the direct ICP scan, and were required because of the environmental significance of these elements.

g) Within each batch of 20 samples a duplicate and a standard were inserted at random in the numerical sequence to provide control on the precision and accuracy of the analytical methods.

3. Geological Summary

Cretaceous strata dip gently southwestward and from the northern flank of the the Williston Basin (Figure 1). Except for a few rare Cretaceous outcrops, sandy glacial deposits blanket the entire area. The glacial deposits, locally more than 100 m thick, are mostly

sandy tills and stratified drift that contain variable amounts of clay and minor carbonate (rarely more than 5 percent).

The lowermost strata of the study area are predominantly sandy deposits of the Lower Cretaceous Mannville Group. Sandstones vary from coarse and kaolinitic to bedded fine sands and silts, interdigitated with mudstones. In broad terms the sequence fines upward. The overlying sediments of the Lower Colorado Group are shales, divided by a thin sandy sequence known as the Viking Formation. The Lower Colorado can not be subdivided with confidence in some of the older wells for which geophysical logs have poor sensitivity. Consequently, in some wells samples from this sequence were picked simply as 'Lower Colorado'. In others a lower sequence of dark grey shales comprising the Joli Fou Formation could be differentiated from an upper sequence of similar lithology known as the Big River Formation.

The White Speckled Shales (commonly known as the White Specks) form the basal sediments of the Montana Group. They constitute an important marker zone of kerogenous calcareous shale which, in the study area, can not be differentiated into the 'First' and 'Second' White Specks as it can farther to the south. The overlying sediments are open marine shales of the Lea Park Formation, overlain in turn by a cyclical sequence of glauconitic sandstones and shales comprising the Judith River Formation. Except for two isolated areas of Tertiary sediments east and south of Saskatoon, the youngest sedimentary rocks of the study area are the claystones and sandstones of the Upper Cretaceous Bearpaw Formation.

Figure 1 shows the near parallel outcrop pattern of the eroded up-dip ends of the formations, the shape of which is modified by structural flexures and preglacial erosion (Christopher and Koziol, 1990). More details of the Cretaceous in the area are given in Christopher (1980, 1984), and Caldwell (1982) for example.

4. Current Status

All the contracted work has been completed, providing more than 50,000 analytical determinations (71 elements for each of the 720 samples). These data have been transferred to a microcomputer database (R-base System V) and merged with the information provided for each sample (formation, lithology, colour etc.). The geological map and well locations have been digitized (Figure 1) and prepared for investigation using the SPANS (Tydac Corp., Ottawa) GIS system.

Summary statistics have been computed for the ICP and ICP-hydride data but not yet for the INAA determinations. Table 1 shows a compilation of the average element content of each stratigraphic interval. The most striking feature of this table is the relatively high level of many elements in the shales that comprise the White Specks. The main features of the table, in decreasing order of importance, are:

1) The White Specks are strongly enriched in Mo, V, Ca, Sb and Se. There is also enrichment in Cu, Zn, Sr, Cd, and As.

2) The Mannville shows enrichment in Mn and Fe, with depletion in P, Al, Na, K, and Ba. This composition reflects the dominance of sandstones in this basal sequence. The Mannville is the only stratigraphic Group to return W analyses above the detection level of 1 ppm.

3) The Bearpaw and Judith River Formations have relative enrichment of Cr, Mg, Ba, and Ti.

It is noteworthy that 20 km northeast of Prince Albert the Henribourg 'cluster focus' for multiple sclerosis (Irvine *et al.*, 1988, 1989) is located close to the subcrop of the metalliferous White Specks, at a site where there is a major structural flexure. Furthermore, this is an area of formation water discharge from the southwest (Christopher and Koziol, 1990). The coincidence of geological and geochemical conditions is, at present, merely an observation for which no causal association is suggested, but which may warrant investigation from the standpoint of an epidemiologist.

5. Lithogeochemical Maps

Sufficient data are available geographically and stratigraphically to be able to plot geochemical maps of a substantial part of central Saskatchewan, and the next phase of study will involve these compilations. The maps will provide a close prediction of the chemistry of the rocks at the Cretaceous/Pleistocene interface, and from first examination of the data it appears that the chemistry of each major stratigraphic interval is sufficiently uniform to extrapolate element contours from the Manitoba to the Alberta borders. Subsequently, input will be required from other professionals to seek associations with areas exhibiting unusual incidence of disease in crops, livestock and humans.

6. Acknowledgements

Some geochemical information on the Cretaceous supplied by Malcolm Gent (Sask. Geol. Survey) sparked the idea for this data collection and compilation. The study has been made possible by the meticulous work of Dr. Jim Christopher and Brenda Koziol in compiling the information required to provide the geological setting of the area, and in painstakingly collecting and recording representative samples of high quality for each stratigraphic interval. Thanks are extended to Kevin Beneteau for transferring the field and analytical data on to computer files, and to Rachael Cardinal for digitizing the maps. I thank, too, Wendy Spirito for advice and assistance on the computing aspects of this study.

7. References

Caldwell, W.G.E. (1982): The Cretaceous System in the Williston Basin - A modern appraisal; *in* Christopher, J.E. and Kaldi, J. (eds.), 4th International Williston Basin Symposium, Sask. Geol. Soc., Spec. Publ. No. 6, p295-312.

Table 1 - Average Concentrations of Elements in Cretaceous Sedimentary Rocks, Central Saskatchewan (ICP analysis of acid digest: determinations are partial for some elements - see text).

	Bearpaw	Judith River	Lea Park	White Specks	Viking	Joli Fou	Big River	Lower* Colorado	Mann-ville
No. of Samples	6	42	313	56	12	17	71	69	59
Fe %	2.8	2.1	3.5	2.5	2.0	2.1	2.1	2.0	5.3
Ca %	2.2	2.6	2.1	11.0	2.2	1.1	3.7	1.7	4.3
Al %	1.1	1.0	1.5	0.8	0.7	0.9	0.8	0.8	0.4
Na %	0.09	0.14	0.20	0.21	0.19	0.24	0.33	0.29	0.03
K %	0.20	0.16	0.22	0.22	0.16	0.20	0.23	0.18	0.08
Mg ppm	8600	7800	7700	3800	3500	3700	2900	4000	5900
P ppm	590	460	930	820	890	720	1020	910	360
Mn ppm	600	558	596	307	259	261	212	418	1368
Ti ppm	250	380	140	110	100	100	100	120	120
Cu ppm	24	29	31	50	16	20	23	18	14
Pb ppm	13	11	20	15	16	23	22	18	12
Zn ppm	78	90	117	189	68	82	90	77	78
Ni ppm	27	25	33	68	18	19	26	20	14
Co ppm	10	9	11	11	8	8	9	8	9
Cr ppm	20	22	25	18	11	11	9	10	10
Ba ppm	188	162	162	76	97	95	88	89	47
Sr ppm	78	76	97	170	76	88	113	77	80
V ppm	28	28	42	121	14	14	17	14	19
Cd ppm	<1	<1	<1	4	<1	<1	<1	<1	<1
Th ppm	5	6	6	5	10	9	8	8	4
B ppm	4	21	26	23	19	28	27	22	25
W ppm	<1	<1	<1	<1	<1	<1	<1	<1	2
Mo ppm	1	1	2	34	1	1	5	2	1
Ag ppm	0.4	0.2	0.2	0.4	0.1	0.1	0.2	0.1	0.2
As ppm	8	7	12	22	9	8	11	8	8
Sb ppm	0.6	0.5	0.7	3.5	0.4	0.3	0.6	0.3	0.3
Bi ppm	0.2	0.3	0.3	0.4	0.4	0.4	0.5	0.3	0.2
Se ppm	0.4	0.3	0.9	11.7	0.4	0.2	1.2	0.6	0.2
Te ppm	0.4	0.2	0.2	0.2	0.2	0.3	0.2	0.2	0.2
Ge ppm	0.3	0.3	0.2	0.1	0.1	0.1	0.1	0.2	0.1

*undifferentiated

Christopher, J.E. (1980): The Lower Cretaceous Mannville Group of Saskatchewan - A tectonic overview; *in* Beck, L.S., Christopher, J.C. and Kent, D.M. (eds.), Lloydminster and Beyond, Sask. Geol. Soc., Spec. Publ. No. 5, p3-32.

_____ (1984): Depositional patterns and oil field trends in the Lower Mesozoic of the northern Williston Basin, Canada; *in* Lorsong, J.A. and Wilson, M.A. (eds.), Oil and Gas in Saskatchewan, Sask. Geol. Soc., Spec. Publ. No. 7, p83-102.

Christopher, J.E., and Koziol, B. (1990): Geological setting of Cretaceous strata in context of a geochemical sampling program, central Saskatchewan; Unpubl. report prepared under Dep. Supply and Services Contract # 23226-9-1559/01-SZ entitled Collection and preparation of geological samples in support of the environmental geochemistry program, 18p plus maps and annexes.

Friske, P.W.B., and Hornbrook, E.H.W. (in press): Canada's National Geochemical Reconnaissance program; Trans. Inst. Min. and Metall.

Gould, C.E. and Warren, H.V. (1980): Trace elements in human biology and a preliminary report on a possible relationship to multiple sclerosis; Sci. Total Environ., v15, 262-268.

Hasanen, E., Kinnunen, E. and Alhonen, P. (1986): Relationship between the prevalence of multiple sclerosis and some physical and chemical properties of soil. Sci. Total Environ., v58, p263-272.

Irvine, D.G., Schiefer, H.B. and Hader, W.J. (1988): Geotoxicology of multiple sclerosis: the Henribourg, Saskatchewan, cluster focus II. The soil; Sci. Total Environ., v77, p175-188.

_____ (1989): Geotoxicology of multiple sclerosis: the Henribourg, Saskatchewan, cluster focus I. The water. Sci. Total Environ., v84, p45-59.

A Paleo-flow Model for a Devonian Winnipegosis Reef, Southeastern Saskatchewan

Ning Qiang[1,2] *and D.M. Kent*[1]

Qiang, N. and Kent, D.M. (1990): A paleo-flow model for a Devonian Winnipegosis reef, southeastern Saskatchewan; *in* Summary of Investigations 1990, Saskatchewan Geological Survey; Saskatchewan Energy and Mines, Miscellaneous Report 90-4.

Middle Devonian Winnipegosis reefs in southeastern Saskatchewan have become an important petroleum exploration target during the past four years. Major discoveries have been made at Tableland, Macoun and Oxbow. It has become evident from the exploratory and development drilling that most reefs have a flanking anhydrite interval of variable thickness from (1 to 25 m). The thicker accumulations of anhydrite can cause difficulties with seismic interpretations, since the distinction between the flanking anhydrite and the carbonate rock of the reef on a seismic trace is unclear. This identification problem has resulted in several boreholes being drilled off-target and encountering thick anhydrite intervals overlying thin reef carbonates.

This study is part of a more extensive investigation into the origin of the reef-flanking anhydrite. It is aimed at trying to determine paleo-fluid flow patterns in the reefs using trace element distribution trends. The approach taken is based on a proposal by Kendall (1978 and 1989) which suggests that the anhydrite formed on the flanks of the reefs and the fluids that dolomitized them were from the same system. He proposed that, following the development of the Middle Devonian Presqu'ile barrier in northwestern Alberta, the Elk Point seaway containing the Winnipegosis reefs underwent evaporative drawdown resulting in subaerial exposure of the seaway floor and the reefs. Topographically-driven brines from the Presqu'ile barrier entered strata underlying the basin and percolated upward through the reefs dolomitizing them. The brines emanated from the reefs as salt springs and deposited anhydrite on their flanks. Thus the proposal suggests that paleo-flow was from the bottoms to the tops of the reefs. By contrast, Stanford (1989) interprets that the paleo-fluids that dolomitized the reefs entered them from the top.

By establishing paleo-fluid flow trends it should be possible to focus on either hypothesis which will help determine the origin of and controls on reef-flanking anhydrite.

1. Method of Study

At the time this study commenced the most extensively cored Winnipegosis reef in southeastern Saskatchewan was at Tableland (Figure 1). Four borehole cores from the 9-22-2-9W2, 14-14-2-9W2, 6-27-2-9W2 and 11-30-2-9W2 wells were sampled extensively. Each specimen was thin sectioned and all sections were stained with a mixture of alizarin-red S and potassium ferricyanide to aid determination of the extent of dolomitization and recognition of variations in the types of dolomite. In addition, 36 thin sections, specifically from the 9-22 and the 14-14 wells, were prepared for microprobe analysis.

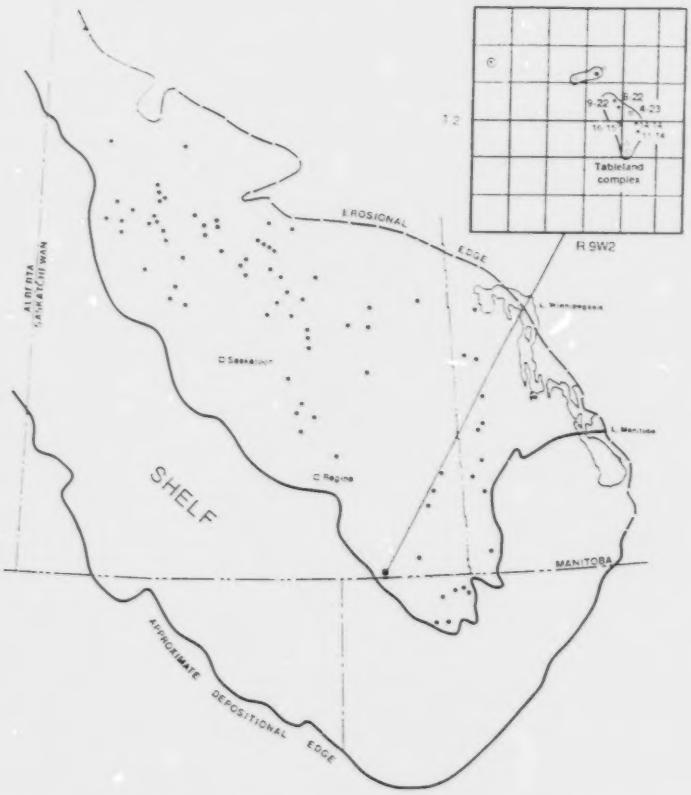

Figure 1 – Location of Tableland Reef in southeastern Saskatchewan. Inset - Outline of Tableland Reef and sampled well locations.

(1) Department of Geology, University of Regina, Regina, Saskatchewan, S4S 0A2.
(2) Present address: Department of Geology, University of Alberta, Edmonton, Alberta, T6G 2E3.

From these the concentrations of two major elements, (Ca and Mg), and seven trace elements (Mn, Sr, Fe, Ba, Pb, Zn and S) were determined for each of the different types of dolomite identified microscopically. The resulting data were computer processed to produce a series of regression line plots of Sr, Mn and Fe concentrations, as well as Sr/Ca ratios vs core depth, for each dolomite type.

2. Lithologies

a) The Reefs

The spatial dimensions of Winnipegosis reefs vary considerably. For example, a number of wells in southeastern Saskatchewan have penetrated more than 50 m of Winnipegosis reef carbonate (range from 51.5 to 69.8 m; the average is 57.05 m). These values are thought to be close to total reef thickness, but by contrast, another 42 wells have penetrated from 11 to 49.7 m of reef, all of which are thought to have been drilled in a reef flank position. With regard to areal dimensions, the Tableland Reef, one of the most extensively drilled, is about 3.2 km long by about 1.5 km wide and appears to be elongated in a north-south direction. By comparison, Winnipegosis reefs in the outcrop belt of western Manitoba range from about 30 to 100 m in height and from a small areal extent of 0.5 by 1.0 km to about 1.0 by 5.0 km. The authors believe that the dimensions of outcropping reefs are similar to those in the subsurface of southeastern Saskatchewan and that the Tableland Reef is one of the larger.

Each reef rests on an open marine, carbonate platform composed of burrow-mottled to wispy nodular, skeletal wackestone, averaging about 9 m thick. The biota present in these platform rocks include: brachiopods, rare solitary corals and crinoid remains. The base of each reef is commonly marked by a pronounced increase in crinoid remains, and also by the appearance of codiacean algae. The lower 40 to 50 m of the reef is composed of dolomitized peloidal wackestones to packstones. The wackestones also contain the codiacean algae *Litanaia* and *Lancicula*, thamnoporid corals and crinoid remains. In places, the wackestones and packstones of the buildups are brecciated and the breccia cavities are filled by a white dolomite cement, which later also fills stromatactis-like cavities in other parts of the reef. Near the margins of the reefs the wackestones and packstones have a layered appearance and dips of 20° to 30°.

The upper 10 to 20 m of the reefs contain colonial organisms such as stromatoporoids and corals, as well as encrusting red algae. In places, there are also what appear to be deposits of vadose origin. All of these uppermost lithologies are capped either by a breccia of angular to subangular carbonate clasts, generally cemented by anhydrite, or by an interval of anhydrite of variable thickness.

b) The Anhydrites

The existence of anhydrite between the Prairie Evaporite halite beds and the carbonates of the Winnipegosis is common but not necessarily ubiquitous. The main occurrence is in the inter-reef areas. The anhydrite proximal to the reefs is found on some flanks but not necessarily on all sides of individual reefs. The existence of anhydrite in two different settings has created a nomenclatural dilemma; many workers follow the approach of Fuzesy (1975) who considers the inter-reef and reef flanking anhydrites to be part of one stratigraphic unit. On the other hand, Kendall (1975) identified the two as different stratigraphic entities, calling the inter-reef anhydrites, the Ratner Member and the reef flank anhydrites, the Vonda Member, both included as parts of the Prairie Evaporite.

The inter-reef anhydrites range from 1 to about 40 m in thickness. They are generally composed of layered anhydrite and interlaminated anhydrite and dolomite, but in places any one bed may have a nodular appearance. Interlaminar interfaces are commonly emphasized by hairline accumulations of kerogenous material. In addition, there is generally a strong intermixing of black organic material in the anhydrite beds. By contrast, the reef flanking anhydrite has a variety of macroscopic features similar to those described by Kent (1968). Thus anhydrite, in part, has a chickenwire appearance, but it may also be layered. Proximal to the reef/anhydrite interface it contains pods and streaks of dolomite which impart the appearance of a mosaic or distorted mosaic anhydrite. In at least one core, the included carbonate in the anhydrite was clast-like. In places, the chickenwire and layered anhydrite appear to be sequential, with layered following chickenwire. Elsewhere, the layered anhydrite has a distorted appearance, as though it had flowed down the sloping flank of the reef in a semiplastic state.

The macroscopic appearance of the reef-flanking anhydrites presents conflicting evidence about their origin. Two hypotheses related to their origin are popular at this time. One suggests that the anhydrite was formed subaqueously, when the tops of the reefs were slightly above sea level. The hypothesis proposes that meteoric water percolating into the reef and outward to the flanks could reduce the salinity of the hypersaline water proximal to the reef, causing anhydrite to be precipitated on the reef flanks rather than halite. The second is the aforementioned hypothesis of Kendall (1978, 1989). Kendall's proposal requires that, following creation of the Presqu'ile barrier in northwestern Alberta and evaporative drawdown of the marine waters in the Elk Point Basin, seepage of marine water through the barrier caused the floor of the basin to be covered by shallow brine ponds, the waters of which enveloped the lower part of the reefs. The partially exposed reefs became discharge conduits for distant migrating saline groundwater which, upon coming in contact with the water of the brine ponds, released calcium sulfate minerals on the flanks of the reefs. Both hypotheses leave a number of questions unanswered, not the least of which comes from our observations of the Tableland Reef, where it appears as though anhydrite occurs only

on the south and east flank of the reef. Wardlaw and Reinson (1971) also found that anhydrite did not completely encompass the Winnipegosis reefs in south-central Saskatchewan.

3. The Paleo-Flow Model

a) Theoretical Considerations

Machel (1988) proposed a model for the recognition of the direction of diagenetic fluid movement in dolomitized rocks, based on the trends of specific trace elements. The model is qualitative and is based on a variant of the Heterogeneous Distribution Law which states that trace elements having distribution coefficients smaller than one are expected to show an increased concentration in the downflow direction. By contrast, those with distribution coefficients greater than one should decrease in concentration in the downflow direction. Strontium can be considered as being representative of trace elements with distribution coefficients <1 and Mn representative of trace elements with distribution coefficients >1. Machel identified a number of constraining variables to the model, not the least of which is the origin of the dolomite. For example, he points out that the aforementioned trace element distributions are specifically valid for dolomite cements. However, the principle may also be applied to replacement dolomite if, for example in the case of Sr, the replaced calcium carbonate has a higher Sr/Ca ratio than the diagenetic fluids. Alternatively Sr will decrease downflow if the opposite conditions prevail. Thus, for replacement dolomites, unless a reasonably accurate estimate of the trace element to calcium ratio can be established, the upflow and downflow directions cannot be readily determined and only the orientation of the flow direction is recognizable.

b) Dolomite Types and Trace Element Distribution

Identification of dolomite types is based primarily on microscopic characteristics, although both types 1 and 2 are also recognizable in hand specimen. The authors recognize three types of dolomite: 1) finely crystalline dolomite, 2) coarsely crystalline dolomite and 3) pore margin limpid dolomite.

Type 1 Dolomite

Finely crystalline dolomite is characterized by very fine to fine (0.005 to 0.03 mm), subhedral to anhedral, cloudy crystals that form an intergrown mosaic (Figure 2). The cloudy appearance is probably caused by micro-inclusions or entrapped terrigenous clay. In hand specimen, type 1 dolomite imparts the characteristic greyish colour observed in most Winnipegosis reef rocks. It makes up 75 percent or more of the total rock volume of the reef. In places type 1 dolomite was altered by later phases of dolomitization or replaced by anhydrite. In addition, there are places where it appears to have been recrystallized.

This type is the 'grey matrix dolomite' of Machel (1989) and the 'early pervasive dolomite' of Stanford (1989). We consider type 1 to represent the earliest phase of dolomitization.

Table 1 shows the average major and trace element concentration for type 1 dolomite from two cores that were analyzed, and Figures 3 to 6 show the regression plots of the trace element distribution for type 1 dolomite in both cores. It is clear from these two sets of plots that the concentrations of Sr and Mn decrease with depth and that of Fe increases. Figures 5 and 6 show that the Sr/Ca ratio for type 1 dolomite also decreases with depth in each core. Table 1 also shows that type 1 dolomite in the 9-22-2-9W2 well more closely approaches stoichiometric than does that of the 14-14-9-9W2 well. (Nearly stoichiometric is 50-51 mole% $CaCO_3$.)

Type 2 Dolomite

This dolomite type is widely distributed in Winnipegosis reefs. In cores and hand specimens it is white or light grey and appears to fill porosity ranging from mesopores to cavities. Although most of it may be cement, some appears to be due to replacement and recrystallization of older more finely crystalline dolomite.

Microscopically, type 2 dolomite is more coarsely crystalline than type 1 and lacks the cloudy appearance of that type. The crystals are 0.03 to 0.12 mm, averaging 0.05 mm. They are generally subhedral but may also be euhedral and anhedral and form an interlocking mosaic (Figures 2c and d).

Table 1 - Average concentration of major and trace elements for all dolomite types from the 9-22-2-9W2 and 14-14-2-9W2 wells.

Type of Dol.	Location (Well)	Ca (%)	Mg	Mn	Sr	Fe	$CaCO_3$: $MgCO_3$ (mol)	Range of $CaCO_3$ (mol)
Type 1	9-22-1	21.06	12.61	0.014	0.017	0.103	50.18 : 49.89	49.26 ~ 51.98
	14-14-2	21.54	12.67	0.001	0.011	0.185	52.19 : 47.81	50.16 ~ 59.98
Type 2	9-22-1	21.52	13.11	0.022	0.015	0.048	49.69 : 50.31	49.27 ~ 50.95
	14-14-2	21.97	13.08	0.026	0.012	0.099	50.19 : 49.81	49.11 ~ 50.19
Type 3	9-22-1	21.65	13.19	0.014	0.011	0.085	49.73 : 50.27	49.00 ~ 50.67
	14-14-2	22.00	12.95	0.033	0.003	0.157	50.68 : 49.32	50.38 ~ 51.32

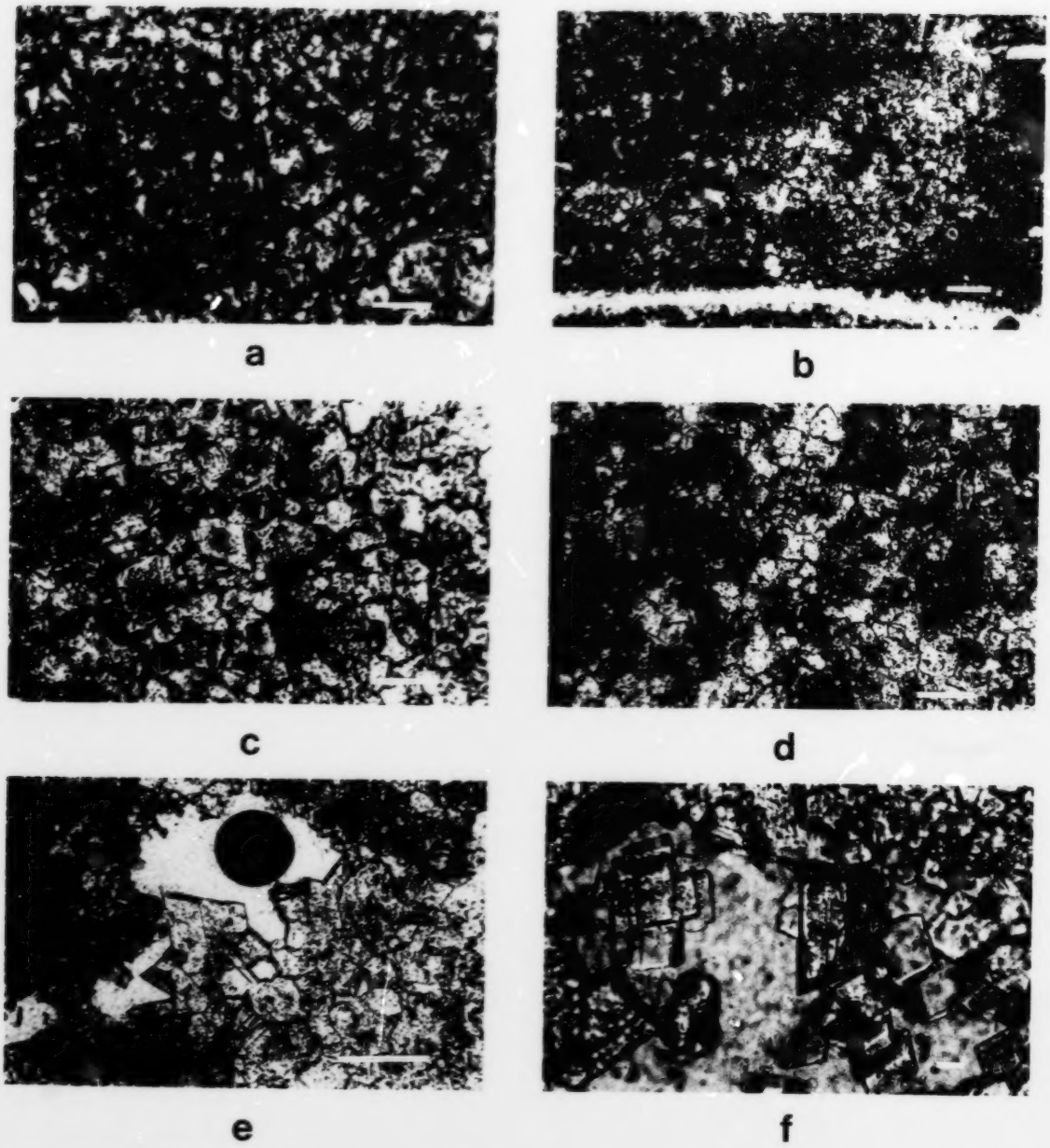

Figure 2 – The three types of dolomite a) finely crystalline dolomite (Type 1). Crystal boundaries are barely discernible. 9-22-2-9W2; 2578.8 m; crossed nicols; scale bar represents 0.05 mm. b) Skeletal debris in finely crystalline dolomite. Note dolomite invasion of fossil remains. 12-24-2-9W2; 2764.8 m; Plane polarized light; scale bar represents 0.05 mm. c) Typical of type 2 dolomite composed of euhedral, subhedral and anhedral crystals. 9-22-2-9W2; 2578.8 m; crossed nicols; scale bar represents 0.05 m. d) Patchy, type 2 dolomite possibly filling interparticle porosity between poorly preserved grains composed of finely crystalline dolomite. 9-22-2-9W2; 2574.5 m; crossed nicols; scale bar represents 0.1 mm. e and f) Typical crystals of type 3 dolomite developed at the margins of pores. Note their generally clear appearance. 9-22-2-9W2; 2583.3 m and 2617.7 m; both plane light; scale bars represent 0.2 and 0.01 mm, respectively.

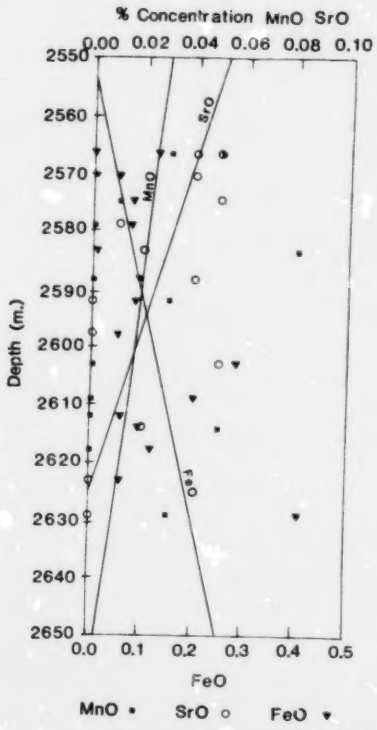

Figure 3 – Regression plots of Sr, Mn and Fe concentrations vs depth for type 1 dolomite in 9-22-2-9W2 well.

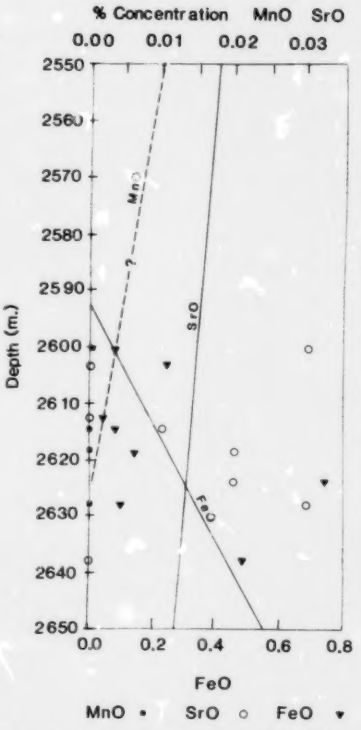

Figure 4 – Regression plots of Sr, Mn and Fe concentrations vs depth for type 1 dolomite in 14-14-2-9W2 well.

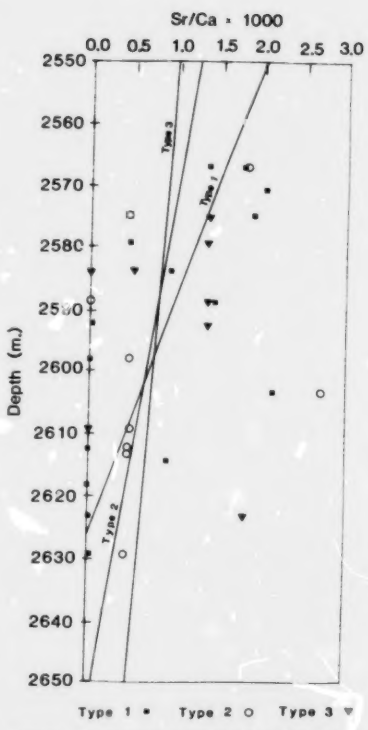

Figure 5 – Regression plots of Sr/Ca ratios of types 1, 2 and 3 dolomites in 9-22-2-9W2 well.

This type is interpreted as a later stage of dolomitization, related primarily to porosity infilling. However, it is possible that the finely crystalline dolomite of type 1 may have been enlarged by recrystallization in places, mimicking the porosity-filling dolomite of type 2. Recrystallization could be the reason for $CaCO_3$ depletion in some of the type 2 dolomites as shown in (Table 1). The Sr and Mn concentrations and the Sr/Ca ratio for type 2 dolomite decrease with depth and Fe increases.

Type 3 Dolomite

Type 3 is characterized by relatively clear, euhedral crystals that line the walls of megapores. They are much like limpid crystals but contain some inclusions that give them a zoned appearance (cloudy in the centre with clear rims). They are 0.03 to 1.0 mm in size, but are most commonly 0.05 to 0.08 mm.

Type 3 dolomite appears to have been the last to form. It is similar to the cathodoluminescent zoned dolomites of Stanford (1989).

Type 3 dolomite has trace element concentrations similar to type 1 but has major element concentrations similar to type 2 (Table 1). The regression plots for type 3 (Figures 5, 6, 9 and 10) have similar trends to the types 1 and 2. The reason for $CaCO_3$ depletion in type 3 dolomite of the 9-22-2-9W2 well by comparison with the nearly stoichiometric type 3 dolomite of the 14-14-2-9W2 well is not clear to us.

4. Discussion

Figures 3 to 10 all suggest that the direction of diagenetic fluid movement in the Tableland Reef was vertical. Since Sr has a distribution coefficient that is less than one, a decrease in Sr concentration with depth, in the coarsely crystalline and limpid dolomite, i.e. dolomite cements, implies from Machel's (1988) model that the flow direction was from the base of the reef to the top. However, Mn and Fe both have coefficients greater than one and, according to the model, should decrease in the downflow direction. If the direction of flow as indicated by Sr is valid then Fe follows the model's prediction and Mn does not.

Strontium concentration in the finely crystalline replacement dolomite also decreases with depth. According to the model, Sr increases in the downflow direction in replacement dolomite only if the initial Sr/Ca ratio of the dolomitizing fluid is less than that of the calcium carbonate being replaced. As in the dolomite cements, Mn departs from its predicted behaviour based on the flow direction interpreted from the Sr concentration.

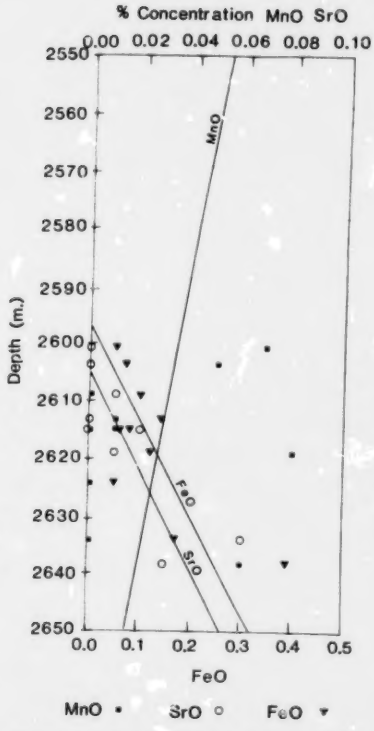

Figure 6 – Regression plots of Sr, Mn and Fe concentrations vs. depth for type 2 dolomite in 9-22-2-9W2 well.

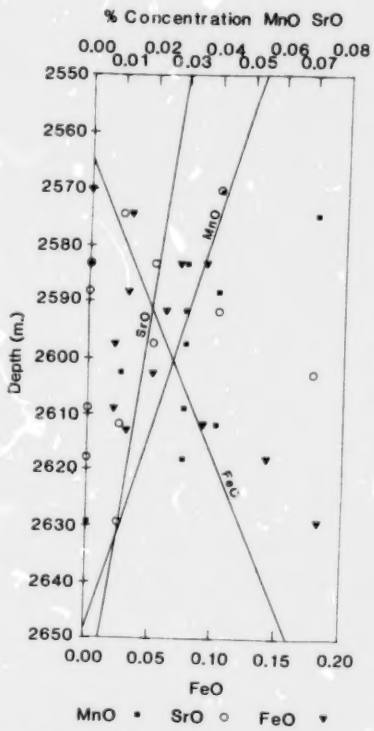

Figure 7 – Regression plots of Sr, Mn and Fe concentrations vs. depth for type 2 dolomite in 14-14-2-9W2 well.

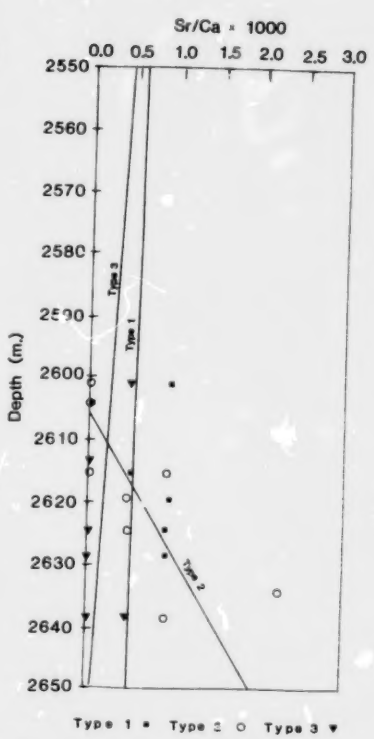

Figure 8 – Regression plots of Sr/Ca ratios of types 1, 2 and 3 dolomites in 14-14-2-9W2 well.

These results suggest two hypotheses:

1) The direction of dolomitizing fluid movement was from the bottom to the top of the reef, supporting Kendall's (1989) hypothesis. However, it requires that the Mn concentrations in these rocks are meaningless to any interpretation of fluid migration. In this interpretation they are disregarded and the Fe concentrations are accepted as indicating the trend for trace elements with distribution coefficients greater than one.

2) Taking into account that the finely crystalline dolomite may be the replacement for a calcium carbonate whose Sr/Ca ratio was less than that of the dolomitizing fluids, the Sr concentration would decrease in the downflow direction, suggesting a top to bottom migration of the initial dolomitizing fluids in the Tableland Reef. The Mn concentration concurs with this fluid migration direction but not the Fe. In the second phase of this model, the fluids carrying the dolomite cements entered the reef later from bottom to top. The distribution of Fe in the finely crystalline rocks may be an overprinting from the cementing fluids. The later origin of the Fe concurs with an observation by Land (1980) that large concentrations of Fe in dolomite are probably related to late phases of dolomitization concomittant with influxes of saline waters. This hypothesis still does not explain the contrary distribution of Mn in the cementing dolomites. However, it is possible that the Mn concentration could have been modified or reset during deep burial.

5. Conclusions

From this preliminary study, we conclude that a microprobe may not have detection limits sufficiently good to accurately detect the small concentrations of trace elements that are present in these dolomites. It is evident that samples from several other reefs need to be analyzed using techniques with lower detection limits to establish a better consensus of fluid migration pathways. The main advantage of the microprobe is that it permits analysis of specific dolomite types, which cannot be guaranteed when powdered samples are the analyzed medium (in most other analytical procedures).

6. References

Fuzesy, L. M. (1975): Geology and hydrocarbon potential of the Winnipegosis Formation in southeastern Saskatchewan: *in* Summary of Investigation 1975, Sask. Geol. Surv., Misc. Rep., p66-70.

Kendall, A.C. (1975): The Ashern, Winnipegosis and lower Prairie Evaporite Formations of the commercial potash areas; *in* Summary of Investigation 1975, Sask. Geol. Surv., Misc. Rep., p61-65.

_____ (1978): Carbonate-evaporite relations in Middle Devonian of Saskatchewan; Abstract, AAPG Bull. v62, p530.

_____ (1989): Possible brine mixing, and associated dolomitization, in the Middle Devonian of Western Canada and its possible significance to regional dolomitization; Sed. Geol., v64, p271-286.

Kent, D.M. (1968): The geology of the Upper Devonian Saskatchewan Group and equivalent rocks in western Saskatchewan and adjacent areas; Sask. Dep. Miner. Resour., Rep. 99, 221p.

Land, L.S. (1980): The isotopic and trace element geochemistry of dolomite: the state of the art; *in* Zenger, D.H., Dunham, J.B. and Ethington, R.L. (eds.), Concepts and Models of Dolomitization: SEPM, Spec. Publ. No. 28, p87-110.

Machel, H.G. (1988): Fluid flow direction during dolomite formation as deduced from trace element trends; *in* Shukla, V. and Baker, P. A. (eds.), Sedimentology and Geochemistry of Dolostones, SEPM, Spec. Publ. No. 43, p115-125.

Stanford, R.L. (1989): Sedimentology and diagenesis of the Winnipegosis Formation, Southeastern Saskatchewan: Unpubl. M.Sc. thesis, Univ. Alberta.

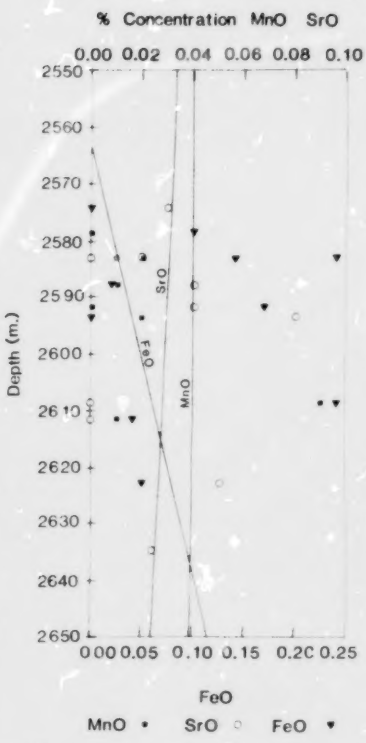

Figure 9 – Regression plots for Sr, Mn and Fe concentrations vs. depth for type 3 dolomite in 9-22-2-9W2 well.

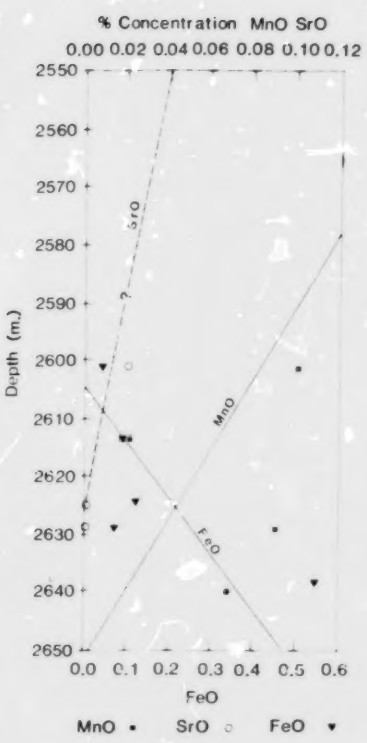

Figure 10 – Regression plots for Sr, Mn and Fe concentrations vs. depth for type 3 dolomite in 14-14-2-9W2 well.

Wardlaw, N.D. and Reinson, G.E. (1971): Carbonate and evaporite deposition and diagenesis, Middle Devonian Winnipegosis and Prairie Evaporite Formations of south-central Saskatchewan; AAPG Bull., v55, p1759-1786.

Industrial Minerals

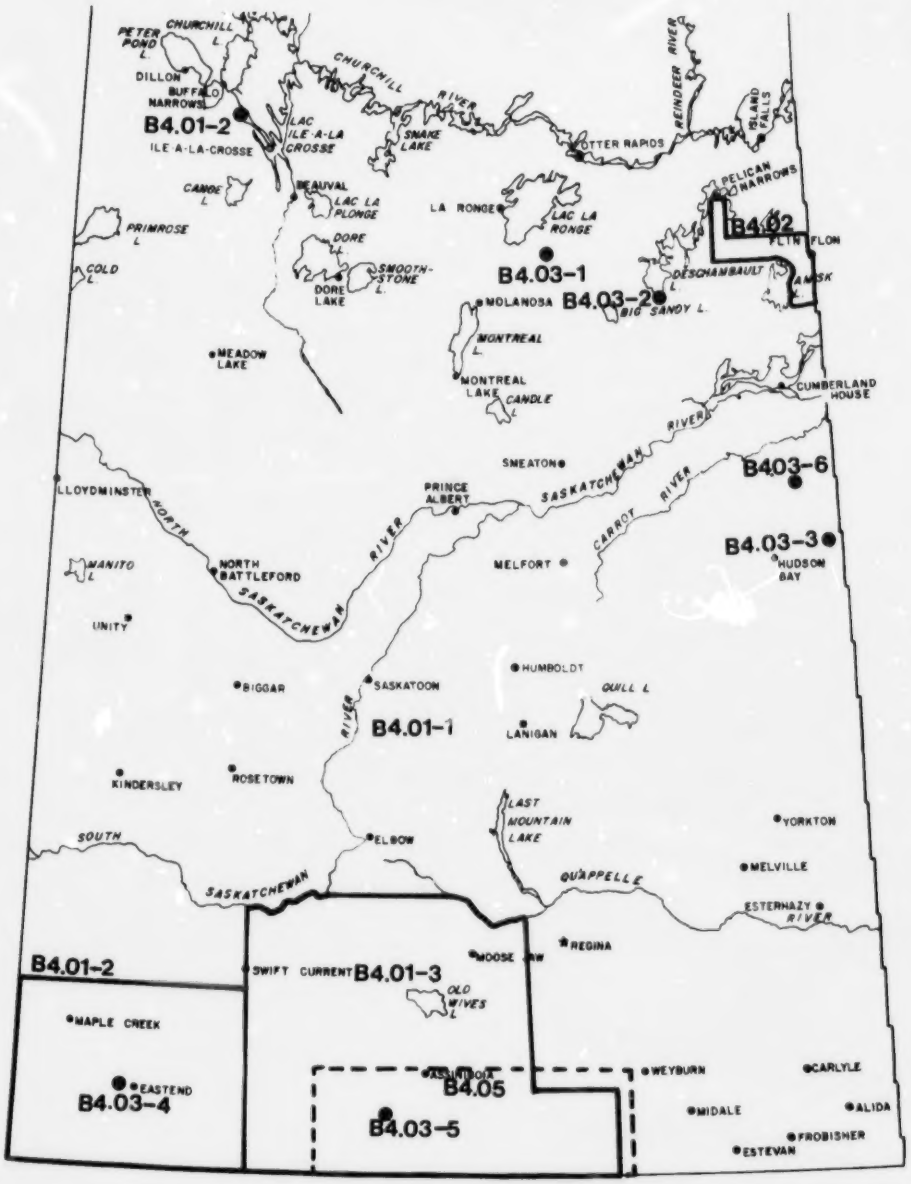

Figure 1 – Location of Industrial Minerals Projects.

B4.01: Regional Phanerozoic Anomalies (Diamond Studies): M. Gent

1. Gravity data compilation over a large part of the Phanerozoic basin
2. Site-specific ground magnetic surveys
3. Indicator mineral sampling

B4.02: Building Stone Investigations: G. Pearse (contract) Creighton-Hanson Lake Road - Pelican Narrows

Misc.: Brine Investigation: Basin-wide, M. Gent, K. Kreiss

B4.03: Industrial Minerals Sampling: M. Gent, P. Guliov

1. Silica sand, Nipekamew River
2. Dolomite, Deschambault Lake
3. Silica sand, Red Deer River
4. Calcium bentonite, Eastend (Knollys)
5. Kaolinized sand, Wood Mountain Area
6. Manganese nodules, Pasquia Hills

B4.04: Kimberlite Study: contract being negotiated

B4.05: Wood Mountain - Willow Bunch Coal Reserve Study: W. MacDougall Contract

Review of Industrial Minerals Investigations 1990-91

Paul Guliov and Malcolm Gent

Guliov, P. and Gent, M. (1990): Review of Industrial Minerals Investigations 1990-91; *in* Summary of Investigations 1990, Saskatchewan Geological Survey; Saskatchewan Energy and Mines, Miscellaneous Report 90-4.

The growing interest in Saskatchewan's industrial minerals in the past several years is attributed primarily to:

a) a need for new deposits to replace depleted or dwindling ones,
b) a need to diversify raw material sources and maintain security of supplies,
c) the desire of industry for economic diversification and
d) promotion by government agencies.

The direction of Sedimentary Geodata Branch projects is guided, in part, by the general trends in the industrial minerals industry and by the needs of specific sectors of the industry. Projects may also arise from a perceived mineral-related developmental opportunity for the province. As a result, several projects (Figure 1) were undertaken or continued, by the branch during the fiscal year:

1. Regional Phanerozoic anomalies studies relating to the diamond potential of the province
2. Building stone investigations
3. Industrial minerals sampling and testing
4. Kimberlite study
5. Coal reserves study
6. Subsurface brine resource investigations

1. Regional Phanerozoic Anomalies Project (B4.01)

The Regional Phanerozoic Anomalies Project (B4.01) continues from the previous fiscal year. Generally, the work is designed to provide regional data of relevance to diamond exploration and therefore serves to assist the industry as a whole. Where desirable, limited investigations are conducted in areas of anomalous geological and geophysical conditions. The project includes the following elements:

1. Gravity data compilation,
2. Ground magnetic surveys in southwestern and northwestern Saskatchewan, and
3. Indicator mineral sampling and analyses in south-central Saskatchewan.

a) Gravity Data compilation (B4.01-1)

The gravity data stored with Saskatchewan Energy and Mines is of substantial size and will require approximately two to three years to digitize, level and correct. Additional data of public or confidential status are also being solicited from industry for incorporation into this data base. The maps produced from this data will be published on an NTS basis as they are completed. The final product, whether in digital format or as finished maps will be of value for regional basement studies particularly for diamond and petroleum exploration.

b) Ground Magnetic Surveys (B4.01-2)

Ground magnetic surveys were conducted over two anomalous geophysical features. Fifty line kilometres conducted over a very favorable seismic structure in southwestern Saskatchewan detected a corresponding but weak (20 gamma) magnetic anomaly. Interpretation and investigation of this structure is ongoing.

A short proton magnetic ground survey test of an airborne magnetic anomaly 27.5 km southeast of Buffalo Narrows confirmed the presence of a magnetic anomaly (Figure 2) but time and field conditions did not permit sufficient surveying to confirm whether this magnetic anomaly is due to a basement feature or a kimberlitic intrusive.

c) Indicator Mineral Sampling and Analyses (B4.01-3)

Based upon apparent favourable structural geologic conditions and a generally thin overburden cover in south-central Saskatchewan, a sampling program was initiated to investigate this area's potential for diamond-bearing kimberlites. Results of the investigation should also resolve unsubstantiated reports of macrodiamond discoveries in this region.

Twenty eight samples averaging 35 kg of the < 1/4 inch fraction of gravels were collected and processed to extract heavy mineral indicators of diamond-bearing kimberlites. Results of this program are pending laboratory analyses.

2. Building Stone Investigations Project (B4.02)

Preliminary investigations of the building stone resource potential in east-central Saskatchewan continued from 1989-90. Field work of selected areas in proximity to roads was carried out in the region extending from Denare Beach to Creighton, westward along Highway 106, northwards along Highway 135 to Pelican Narrows and in the McNally Lake area. Rock types of principal interest are granodiorites, granites (Sahli Lake), volcanics, dolomite and metagabbro. Field evaluation includes the identification of potential quarry sites. A total of ten sample blocks of about 500 kg each were recovered from potential quarry sites. These blocks were slabbed

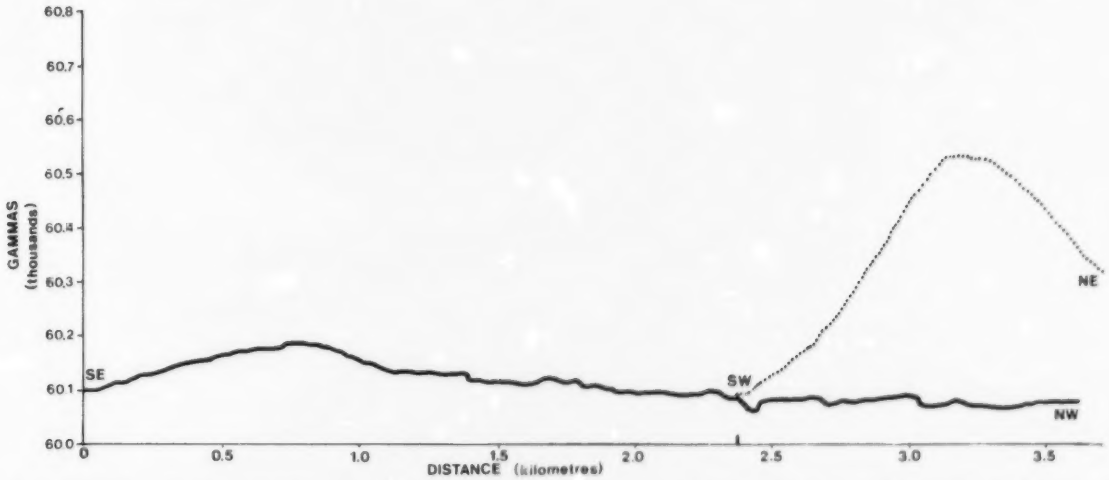

Figure 2 – Ground magnetic survey at Watchusk Bay, Buffalo Narrows area. — survey along highway 155; ..... survey line perpendicular to and northeast of highway 155.

and polished for evaluation and display. Additional specimens were prepared for ASTM engineering tests.

3. Industrial Mineral Sampling Project (B4.03)

Industrial mineral sampling under this project is directed toward key minerals of potential economic significance. Several hundred kilograms of mineral samples were taken from some sites (Figure 1), processed as necessary and subjected to physical and chemical analyses. The samples will be made available to various industrial users and producers of industrial minerals for technical evaluation.

Samples taken this fiscal year include:

1. Jurassic and/or Cretaceous silica sand along the Nipekamew River,
2. Dolomite from the Ordovician Red River Formation near Deschambault and Amisk Lakes,
3. Cretaceous silica sand along the Red Deer River,
4. Calcium bentonite from Late Cretaceous sediments near Eastend,
5. Late Cretaceous kaolinized sands of the Whitemud Formation near Wood Mountain and
6. Cretaceous manganese nodules from the Pasquia Hills.

a) Jurassic and/or Cretaceous Silica Sands Project (B4.03-1)

Jurassic or Cretaceous sands and gravels of fluvial origin with a high silica content from the Nipekamew River area are presently being investigated. These sands and gravels are similar to those of the Success Formation (Jurassic-Cretaceous) but also appear to correlate with the Mannville sands along the Red Deer River. Eleven samples are being tested for applications in silicon-based commodities in an identical manner to those from the Red Deer River exposures.

b) Dolomite Project (B4.03-2)

Samples of dolomite from the Ordovician Red River Formation are being evaluated for a variety of filler applications. At present two samples from the Deschambault Lake area and one from the Amisk Lake area are being tested.

c) Cretaceous Silica Sands Project (B4.03-3)

Fourteen samples of sands with a high silica content belonging to the marine-coastal deposits of the Cretaceous Mannville Formation are being tested for silica products and filler applications. Vertical channel samples at 1 and 2 m intervals were collected from exposures along the Red Deer River and from the Red Deer Silica Inc. pit face.

The chemical characteristics of these sands, for potential silicate-based products, are being analyzed to high precision for the <5, 5-10, 10-18, 18-35, 35-60, 60-100, 100-200, >200 sieve fractions. Chemical analyses will include: Al, Fe, Ca, Mg, Au, K, Mn, P, Ti, Ba, Cu, Cr, Ni, Zn, B, S and C. Silicon content will initially be determined by difference. Heavy mineral contents and filler application characteristics are also being evaluated.

d) Calcium Bentonite Project (B4.03-4)

Worcester (1937) reported the existence of an estimated two million tons of dry calcium bentonite about one kilometre south of Knollys (8 km southwest of Eastend). A brief field check was conducted to locate and sample the material. Two closely spaced occurrences outcrop along the base of the southern scarp of the Frenchman River Valley in the area reported by Worcester. The clay is thought to belong to the Battle Formation. At this location the calcium bentonite is topographically below the

older Whitemud Formation due to gravity slumping. The occurrence is probably too disturbed by faulting and slumping to be mineable but other, more favorable occurrences are thought to exist immediately to the south and southeast at higher elevations. Further investigations are planned.

e) Late Cretaceous Whitemud Formation Project (B4.03-5)

A sample of the lower part of the Whitemud Formation outcropping in the Wood Mountain area is being evaluated for its silica content. Analyses are designed to check the possibility of extracting silica from these sediments as a by-product of kaolin.

f) Manganese Nodules Project (B4.03-6)

Investigations of manganese nodules in the Pasquia Hills area by Beck (1974) indicated the nodules contain minor or trace amounts of several elements including base and precious metals and rare earths. Precision analysis of three grab samples of varying specific gravity (2.26 to 3.54) found maximum anomalous values of: Ag - 6.0 ppm, Ce - 92 ppm, Fe_2O_3 - 34.0%, Ge - 10 ppm, La - 46.9 ppm, MnO - 19.4%, Nd - 40 ppm, Sm - 7.5 ppm, Sn - 54 ppm, Pt - 10 ppb and U - 7.5 ppm.

Although these results are based on the analyses of a very limited set of samples, there appears to be a normal correlation between specific gravity and Ge, Sn and Pt values as well as an inverse correlation with Ag, Ce, La, Mn, Nd, Sm, and U values. Further investigation of these nodules and their host Cretaceous speckled shales for a potential polymetallic deposit appears warranted.

4. Kimberlite Study (B4.04)

A study of the Sturgeon Lake kimberlite is yet to be contracted.

5. Coal Reserve Project (B4.05)

The Coal Reserve Project is a continuation of work conducted in previous years under the Canada - Saskatchewan Fossil Fuels Technology Development Agreement and managed by Saskatchewan Energy and Mines. During fiscal 1990-91 the project was funded under MIDP and managed by the Geological Survey of Canada.

Work during the fiscal year concentrated on the Willow Bunch - Wood Mountain coal basin. Borehole and geophysical logs were interpreted, lithostratigraphic units were correlated throughout the basin, a coal reserve model was developed and various geographic and cultural parameters were digitized. The data are used to calculate mineable coal reserves based on various parameters including geological, qualitative, economic, geographic, cultural, environmental and others.

The project is more fully described in a separate paper in this volume.

6. Brine Investigation Project (B4.06)

Naturally occurring subsurface brines in a number of wells in Saskatchewan show high concentrations of a variety of elements, in particular; calcium, magnesium, sodium, and potassium. These brines compare favourably with, or in some instances exceed, brine concentrations found in wells produced on a commercial basis in the Michigan Basin, where subsurface brines provide the raw materials for a multi-billion dollar chemical industry. This suggests that subsurface brines in Saskatchewan may have the potential to compete in a very large and lucrative chemical industry, and therefore are worthy of investigation.

The Industrial Minerals section is currently investigating the occurrence and distribution of brines in all strata below the Upper Devonian Duperow Formation down to and including the Precambrian basement. Brines found in this stratigraphic interval generally have the greatest potential for economic accumulations. The immediate aim of the study is to produce an inventory of these brines. To accomplish this water analysis data from the well files of the Sedimentary Geodata Branch, and from published data on the geochemistry of brines in a number of potash mines in the province have been digitized. (i.e. 1,190 analyses) To date, this study has identified 14 locations with subsurface brines showing highly anomalous concentrations of calcium and\or magnesium ions (Table 1).

Table 1 - Occurrences of Anomalous Calcium and Magnesium Bearing Brines.

Anomaly Location	Ca mg\l	Mg mg\l	Formation	Age
2-29-02-02W2	34,000	—	Deadwood	Cambr.
13-24-02-03W2	33,759	—	Deadwood	Cambr.
01-06-02-04W2	32,112	—	Stony Mountain	Ordov.
09-34-03-04W2	940	—	Deadwood	Cambr.
07-24-04-05W2	37,290	—	Souris River	Devon.
03-16-06-06W2	32,040	—	Winnipegosis	Devon.
06-27-02-09W2	119,300	11,420	Dawson Bay	Devon.
02-04-04-11W2	36,650	—	Stonewall	Ordov.
			Stony Mountain	Ordov.
			Red River	Ordov.
06-13-02-19W2	33,802	—	Stony Mountain	Ordov.
08-20-17-20W2	36,161	51,303	Winnipegosis	Devon.
04-16-18-23W2	—	22,820	Dawson Bay	Devon.
04-18-35-08W3	64,500	11,900	Souris River	Devon.
03-21-35-08W3	44,400	—	Deadwood	Cambr.
08-18-21-20W3	93,053	11,470	Souris River	Devon.

Other elements of potential value that may occur in Saskatchewan brines include bromine, iodine, lithium, etc. Of these, the most anomalous occurrence found to date is that of bromine (335 mg/l) from a brine in the Souris River Formation found in well 16-10-21-25-W2.

This study will also attempt to identify areas of abnormally high formation pressure in an effort to locate connate brines. The next phase will be to further investigate

areas of anomalously high concentrations of Ca, Mg, Na, K, Br, and I, all elements of commercial interest. Estimates will be made of the approximate volumes of the most favourable brine reservoirs based on geological, geophysical log and drillstem test data. An extension of the investigation into brine qualities and distribution within overlying consolidated sedimentary strata of the province is also anticipated in the near future.

7. References

Beck, L.S. (1974): Geological investigations of the Pasquia Hills area; Sask. Dep. Miner. Resour., Rep. 158, 16p.

Worcester, W.G. (1937): Saskatchewan Bentonites; Can. Inst. Min. Metal., Vol. XL, p438-451.

Fluid Flow Events in the Elk Point Basin of Western Canada as Recorded in Evaporite Minerals[1]

D. Chipley[2], T.K. Kyser[2], and T. Danyluk[3]

Chipley, D., Kyser, T.K. and Danyluk, T. (1990): Fluid flow events in the Elk Point Basin of western Canada as recorded in evaporite minerals; *in* Summary of Investigations 1990, Saskatchewan Geological Survey; Saskatchewan Energy and Mines, Miscellaneous Report 90-4.

Halite in evaporite sequences provides an opportunity to study the fluids that initially precipitated and subsequently affected evaporite minerals during burial in sedimentary basins because halite is readily dissolved and precipitated by undersaturated fluids and often traps these fluids as inclusions. For example, different generations of halite sometimes are evident from petrographic relations (Knauth and Beeunas, 1986; Roedder, 1984a, 1984b) and from thermometry of the fluid inclusions (eg. Roedder, 1984a). In theory, each generation of halite could preserve in its fluid inclusions the fluid from a different episode of fluid-flow in the basin. Provided the inclusions are preserved as originally trapped, constraints can be placed on their chemical compositions using their thermometric characteristics (*ibid*). Extraction of the water from the fluid inclusions and analysis of the stable isotopic compositions of the hydrogen and oxygen should indicate the origin of the water as has been done for the Palo Duro Basin (Knauth and Beeunas, 1986) and the Delaware Basin (O'Neil *et al.*, 1986). Radiometric dating of different generations of halite and associated evaporite minerals may indicate the timing of fluid events that occurred in the basin (Wardlaw, 1968; Baadsgaard, 1987).

The Devonian Prairie Evaporite Formation, which extends over much of southern Saskatchewan, is a thick sequence of evaporite minerals within the Elk Point Basin of western Canada (Figures 1 and 2). Numerous potash mines in Saskatchewan offer easy access to sylvite- and carnallite-rich members near the top of the Prairie Evaporite Formation (Figure 2). Petrographic relations among halite and associated minerals and the chemical composition of the halite indicate that the evaporite minerals of the ore horizons have been recrystallized (Wardlaw, 1968). K-Ar, Rb-Sr, and K-Ca isotope systematics of halite, sylvite, and carnallite from the Prairie Evaporite Formation give Mississippian to Recent ages, indicating that recrystallization of the originally Devonian deposits has occurred (Wardlaw, 1968; Baadsgaard, 1987). Thus, fluid inclusions in halite of the Prairie Evaporite Formation of southern Saskatchewan should record evidence of discrete fluid flow events in their daughter mineral dissolution temperatures and their chemical and isotopic compositions that are significant to the interpretation of the evolution of the Elk Point Basin.

In this study, samples were collected from Saskatchewan potash mines situated within the Patience Lake Member of the Prairie Evaporite Formation in the Elk Point Basin. The samples contained halite with sylvite and carnallite. The petrographic and thermometric characteristics of fluid inclusions in the halite define different generations of halite and trapped fluids. The hydrogen and oxygen isotopic compositions of the

Figure 1 – Location and extent of the Elk Point Basin in western Canada and northern United States (modified from Burrows and Krause, 1987). The stippled pattern indicates the area of sylvite preserved in the Prairie Evaporite Formation. Insert shows the locations of the potash mines near Saskatoon from which samples were obtained: 1. Potash Corporation of Saskatchewan (PCS) Cory mine, 2. Central Canada Potash, 3. PCS Lanigan, 4. PCS Rocanville. The various arches and topographic anomalies integral in the formation of the basin are also indicated as is the eastern edge of the basin, which is erosional. The Elk Point Basin was active from Middle Devonian to Late Mississippian time and the Williston Basin, which comprises all of the sedimentary units in the circular southern portion of the Elk Point Basin, was actively subsiding from Middle Ordovician to Middle Jurassic time (Porter et al., 1982).

(1) Project funded by the Saskatchewan Potash Producers Association and NSERC Operating Grant
(2) Department of Geological Sciences, University of Saskatchewan, Saskatoon, Saskatchewan S7N 0W0
(3) Potash Corporation of Saskatchewan, Suite 500, 122 1st Ave. S. Saskatoon, Saskatchewan S7K 7G3

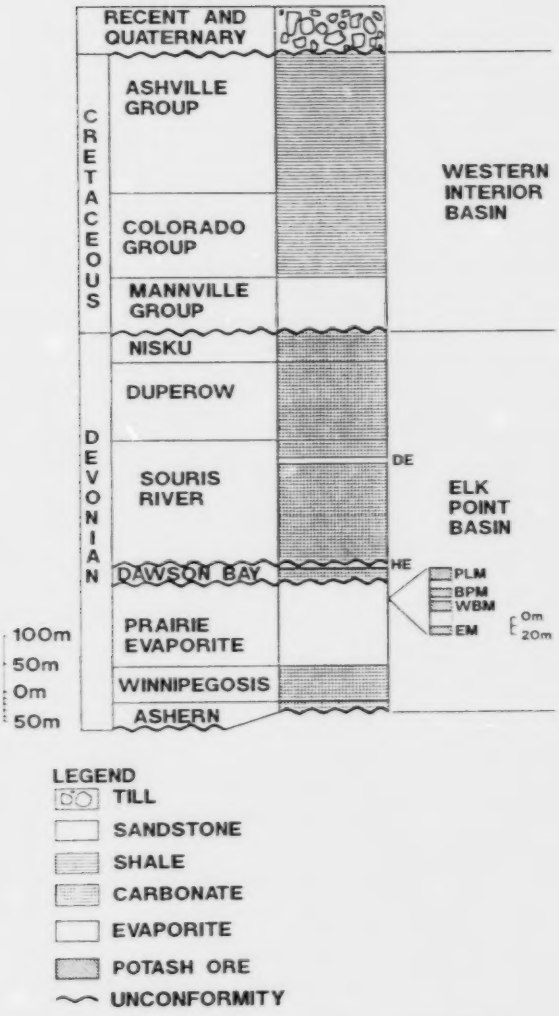

Figure 2 – Stratigraphic section near Saskatoon showing the preserved sedimentary sequences of the Elk Point Basin (Devonian) and the Western Interior Basin (Cretaceous) as modified from Holter, (1969) and Wittrup et al., (1987). The potash ore-bearing members, Esterhazy (EM), White Bear (WBM), Belle Plaine (BPM), and Patience Lake (PLM) in ascending stratigraphic position are near the top of the Prairie Evaporite Formation as shown. The Hubbard Evaporite (HE) and Davidson Evaporite (DE) represent the tops of the second and third sedimentary cycles and are composed of halite with no sylvite or carnallite.

water extracted from the fluid inclusions are used to indicate the possible source of the fluid that recrystallized the halite.

1. Fluid Inclusion Thermometry

Fluid inclusions in halite from the Prairie Evaporite Formation can be divided into two groups based on morphology and distribution. One group forms a chevron-texture in the halite and contains no daughter minerals. These inclusions are generally less than 12 μm in size and are closely spaced producing a cloudy appearance in the halite. The second group, up to 300 μm in size, are randomly distributed in clear halite. These inclusions may be single phase or may contain solid phases such as anhydrite, sylvite, or carnallite. Where the two types of inclusions occur in the same halite crystal, the chevron-textured halite is at the core of the crystal surrounded by clear halite, implying that the chevron-texture inclusions contain fluids from an earlier event. The inclusions containing anhydrite were not used for thermometry because inconsistent phase ratios suggest that the anhydrite was trapped as a solid at the time of formation of the inclusions.

The temperatures at which sylvite daughter minerals dissolve in the fluid inclusions in halite from the ore horizon at PCS Cory can be divided into two groups that correspond to the groups described petrographically as chevron-texture and randomly distributed fluid inclusions (Figure 3a). Sylvite daughter minerals which form during cooling and subsequently dissolve between 24°C and 44°C are mainly in chevron-textured halite. A few random inclusions have daughter mineral dissolution temperatures similar to those of the chevron-texture inclusions suggesting that some of the random inclusions may have formed from the same fluid that produced the chevron-texture. Daughter mineral dissolution temperatures of random inclusions in halite from PCS Cory range from 44°C to 70°C (Figure 3a), with a limited number of inclusions yielding dissolution temperatures greater than 70°C.

Daughter mineral dissolution temperatures, from the PCS Lanigan ore horizon samples, are similarly distributed as those from PCS Cory (Figure 3b). The ore zone at Lanigan contains carnallite as well as sylvite, but most of the daughter minerals in the fluid inclusions in halite are carnallite. Carnallite daughter mineral dissolution temperatures in chevron-textured halite range from 40°C to 58°C. Randomly distributed fluid inclusions in clear halite have higher carnallite daughter mineral dissolution temperatures, from 46°C to 113°C.

Identification of daughter minerals in fluid inclusions provide information about the chemical composition of the fluid (Roedder, 1984a). A fluid inclusion containing a daughter mineral is known to be saturated with respect to that mineral up to the temperature at which the daughter mineral dissolves. This allows determination of the concentrations of those components in the fluid. Inclusion fluids from the potash mines are at all times saturated in halite (NaCl). Inclusions with sylvite (KCl) or carnallite ($KMgCl_3.6H_2O$) daughter minerals are saturated with K^+ and/or Mg^{2+} for these minerals to form.

The temperature, when ice begins melting and when reactions between precipitated solid phases and the fluid occur, can also indicate the chemical constituents present in the fluid. Roedder (1984a) reported that fluid

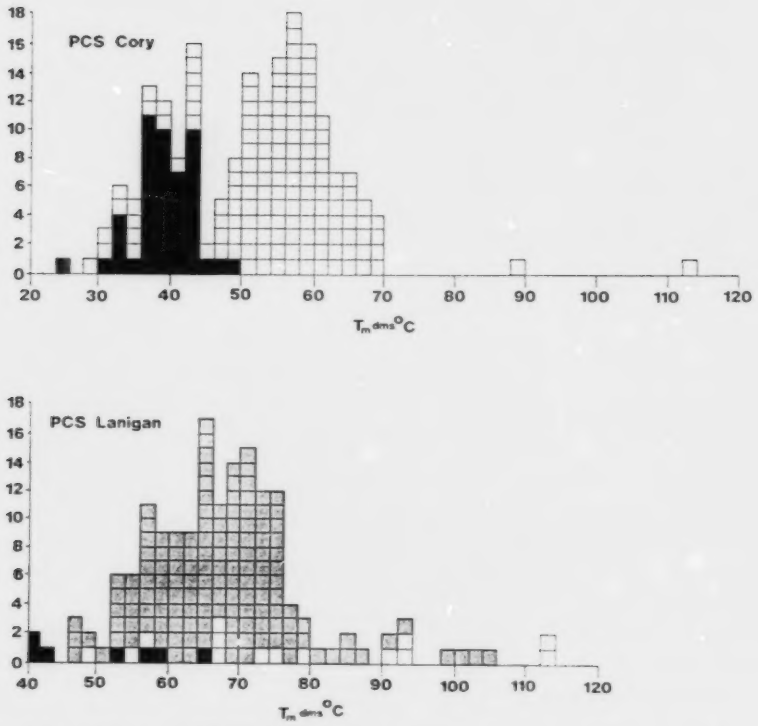

Figure 3 – Histograms of fluid inclusion daughter mineral dissolution temperatures (T_{m} dms) in halite samples from a) the sylvite-rich ore zone of the PCS Cory mine and b) the carnallite-rich ore zone of the PCS Lanigan mine. Dark squares represent fluid inclusions that produced sylvite in the chevron-textured halites, open squares represent larger, randomly distributed inclusions that contained sylvite daughter minerals, and stripes represent fluid inclusions that contained carnallite daughter minerals. Classes are 1.9°C wide (ie. from 40.0 to 41.9°C).

inclusions in halite from the Williston Basin of North Dakota have high concentrations of Ca^{2+} and Mg^{2+} as indicated by eutectic temperatures as low as -69.8°C. The temperatures of first melting of the random inclusions in this study are from -42 to as low as -65°C, indicating that the inclusions are filled with a complex brine containing Na^{+}/, K^{+}, Mg^{2+}, Ca^{2+}, Cl^{-},and SO_4^{2-} (Brodyla and Spencer, 1987).

Ions, such as Mg^{2+} and Ca^{2+} are contained in the inclusion fluid rather than in the crystal structure of halite (Moretto, 1988) and, thus, their ratio in the fluid will be reflected by analysis of the entire halite crystal without having to extract the inclusion fluid. Because concentrations of these ions are a function of the volume of fluid present in the fluid inclusions of the sample, only the ratio of Ca^{2+} to Mg^{2+} is meaningful. Ca^{2+} and Mg^{2+} are present in fluid inclusions from both PCS Cory and PCS Lanigan mines with Ca/Mg ratios ranging from 1 to 19 (Table 1). The Ca/Mg ratio of seawater is 0.3 and with evaporation, this decreases to 0.008 during halite facies deposition (McCaffrey *et al.*, 1987). Basinal brines presently in strata overlying the Prairie Evaporite Formation have Ca/Mg ratios ranging from 0.6 to 15.1 (Wittrup and Kyser, 1990). The Ca/Mg ratios of the inclusion fluids are similar to the ratios of formation fluids and significantly higher than the ratios for seawater and evaporated seawater.

The concentration of some ions in the fluid inclusions in halite from the Prairie Evaporite Formation can be estimated from the temperature at which the daughter minerals dissolve. Fluid inclusions in halite from the PCS Cory mine typically contain sylvite daughter minerals, which together with freezing tests and ICP-MS chemical analyses, indicate that Mg^{2+} is also present. Thus the fluid composition should lie along the sylvite-halite phase boundary in the K_2Cl_2-Na_2Cl_2-$MgCl_2$ system (Figure 4). In the pure halite-sylvite system, the concentration of NaCl ranges from 5.3 *m* to 4.8 *m* and KCl from 2.0 *m* to 4.0 *m* between 25°C and 80°C (Pabalan and Pitzer, 1987). Inclusions containing carnallite daughter minerals from PCS Lanigan, where both carnallite and sylvite are present in the ore zone, must have compositions along the carnallite-halite phase boundary but near the eutectic composition (Figure 4). The eutectic composition has KCl concentrations of

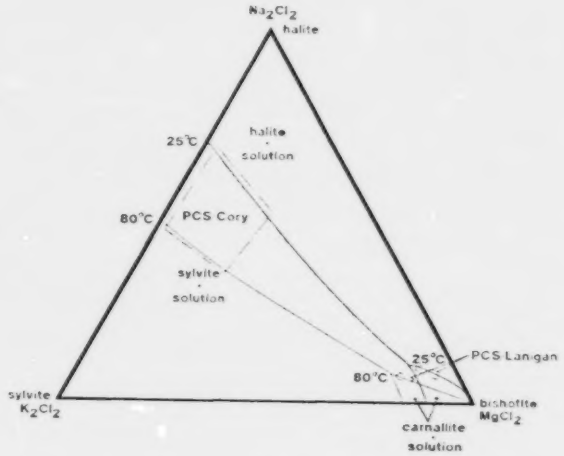

Figure 4 – The system K_2Cl_2-Na_2Cl_2-$MgCl_2$-solution at 25°C and 80°C. The 25°C diagram is from Wood (1975), and the 80°C data for pure NaCl-KCl and the eutectic composition is from Pabalan and Pitzer (1987), with all other 80°C phase boundaries assumed. Presumed compositions of the fluid inclusion brines are indicated.

0.59 *m* to 1.13 *m* and $MgCl_2$ concentrations of 3.77 *m* to 4.72 *m* over temperatures of 25°C to 80°C, whereas the NaCl concentration remains near 0.1 *m* through the same range of temperatures (Pabalan and Pitzer, 1987).

The similarity of halite textures, the distribution and homogenization temperatures of fluid inclusions, and the close proximity of the PCS Cory and PCS Lanigan mines (Figure 1) suggest that the ore horizons at both mines were probably affected by the same fluid events. If the ore horizons were affected by the same fluid flow event, then the chemical composition of the fluids, as indicated by the daughter minerals, is largely a function of the mineralogy of the ore horizon. The fluid that recrystallized the halite most likely was saturated with the components for sylvite or carnallite depending on which mineral was present in the environs of the halite. If the fluid was slightly undersaturated for the daughter mineral components at the time of trapping, the daughter mineral dissolution temperature would be lower than the trapping temperature. Because pressure has only a small effect on the solubility of evaporite minerals (Holser, 1979a), the temperatures at which the daughter minerals of sylvite and carnallite dissolve are minimum trapping temperatures. However, the presence of sylvite and carnallite in the ore zones, from which all samples were collected, in conjunction with their high solubilities would imply that the daughter mineral dissolution temperatures are likely to be similar to the temperatures at which the fluid inclusions were originally trapped.

2. Stable isotopes

During evaporation of seawater, the remaining brine initially becomes enriched in D and ^{18}O, but before halite precipitates, D and ^{18}O are preferentially lost to the vapour phase causing the residual brine to become progressively enriched in H and ^{16}O (Knauth and Beeunas, 1986). Factors influencing the rate of enrichment of the brine in D and ^{18}O during the initial stages of evaporation are the salinity of the water, the atmospheric humidity, and the difference in isotopic composition between the initial water and atmospheric vapour (Lloyd, 1966). The trajectories followed by the stable isotopic compositions of evaporating seawater on a δD versus $\delta^{18}O$ plot differ depending on humidity, but have been studied in natural evaporating systems up to halite facies deposition as shown in Figure 5a. The δD and $\delta^{18}O$ values of pre-gypsum, pre-halite, and post-halite-pre-sylvite waters from salt crystallizing ponds on Bonaire Island in the Caribbean as determined in this study are similar to the changes observed in the isotopic composition of evaporating brines in other studies (Figure 5a and b). The stable isotopic compositions of fluids extracted from fluid inclusions in Permian halite having chevron-textures (Knauth and Beeunas, 1986) are similar to those expected for seawater evaporated to halite facies deposition (Figure 5b).

Fluid inclusions from the chevron-textured halite in the Prairie Evaporite Formation represent the earliest fluid event preserved by halite because these textures are found in the centers of crystals and are surrounded by clear halite containing randomly distributed fluid inclusions. The chevron-texture is believed by some to reflect primary precipitation of halite at the sediment water interface (Deilwig, 1955; Wardlaw and Schwerdtner, 1966; Arthurton, 1973) and, thus, the fluid inclusions should contain evaporated seawater. The stable isotopic compositions of inclusion fluids from chevron-textured halite from the Prairie Evaporite Formation measured by Chipley and Kyser (1989) and in this study (Table 1) indicate the fluids cannot be evaporated seawater. Inclusion fluids, extracted from chevron-textured halite of the Patience Lake Member, have δD values near -92 and $\delta^{18}O$ values near -9 (Table 1), which differ greatly from those of evaporated seawater, water derived from the dehydration of gypsum (Figure 5b), and meteoric water from low latitudes that would be expected in this environment during the Devonian Period. If the stable isotopic composition of the fluids giving rise to the chevron-texture resulted from mixing of evaporated seawater with another fluid during initial precipitation of the evaporites, the extraneous fluid must have had very low δD values. Further, the constant δD and $\delta^{18}O$ values of the chevron-texture fluid inclusion waters throughout the Patience Lake Member requires that the mixing ratio of the fluids was constant over the time of deposition of the ore horizon (Table 1). Sonnenfeld (1984) reviewed estimates of the accumulation times for major evaporite deposits and concluded most require thousands to tens of thousands of years. Constant mixing ratios of fluids over this period of time is unlikely. In addition, the ratio of halite to sylvite varies substantially over the section sampled (Boys *et al.*, 1986), and requires changes in the degree of evaporation that are not reflected in the stable isotopic compositions of the chevron-texture fluids. The stable isotope results indicate that the chevron-texture does not require formation by surface processes as proposed by Deilwig (1955), Wardlaw and Schwerdtner (1966) and Arthurton (1973), but rather that it may form by recrystallization of the evaporite at depth after original deposition.

Since the chevron-texture halite represents the first recrystallization event, and the earliest event recorded by K-Ar systematics of sylvite is middle Mississippian (Wardlaw, 1968), the age of the fluid flow event that produced the chevron-texture is probably middle Mississippian. The minimum temperature, determined for this event from fluid inclusions, was between 24°C and 44°C, possibly indicating recrystallization and formation of the chevron-texture at a shallow depth in the near surface environment.

The stable isotopic compositions of water extracted from randomly distributed fluid inclusions are more variable than those of the chevron-texture inclusions and suggest that fluids from different sources have affected halite during evolution of the Elk Point Basin (Figure 5b; Table 1). No petrographic relations between the inclusions were found to define the relative timing of these recrystallization events except that they are later than the event that produced the chevron-textured halite. The most D- and ^{18}O-rich fluid inclusion waters have δD values of -72 and $\delta^{18}O$ values of -6 which resemble the evolved basinal brines resident in the overlying Dawson Bay Formation, and are isotopically distinct from the chevron-textured halite inclusion fluids. The most D- and

^{18}O-depleted fluid inclusion waters have δD values near -141 and $\delta^{18}O$ values near -15, similar to the values of water within the overlying Mannville Group aquifers of the Cretaceous Western Interior Basin (Figure 5b). The striking similarity between the isotopic compositions of waters in randomly distributed fluid inclusions and waters presently contained in formations above the Prairie Evaporite Formation suggests that the overlying formation waters were probably the sources of the recrystallizing fluids (Figure 5b).

The temperatures of brines presently in formations overlying the Prairie Evaporite Formation are lower than the daughter mineral dissolution temperatures of the fluid inclusions. If the fluids that affected the halite were from the overlying formations, as is suggested by stable isotopes, the temperatures of these fluids must have been higher in the past. Higher temperatures in the past, which would have facilitated exchange of oxygen isotopes between the water and minerals in the basin, could have resulted from greater depth of burial or higher geothermal gradients in the basin.

The daughter mineral dissolution temperatures of the randomly distributed fluid inclusions vary directly with the isotopic compositions of the inclusion fluid (Figure 6). A variable temperature during recrystallization may be due to a change in the temperature of the inflowing fluid possibly caused by mixing of different formation waters, changes in the depth of burial of the evaporite,

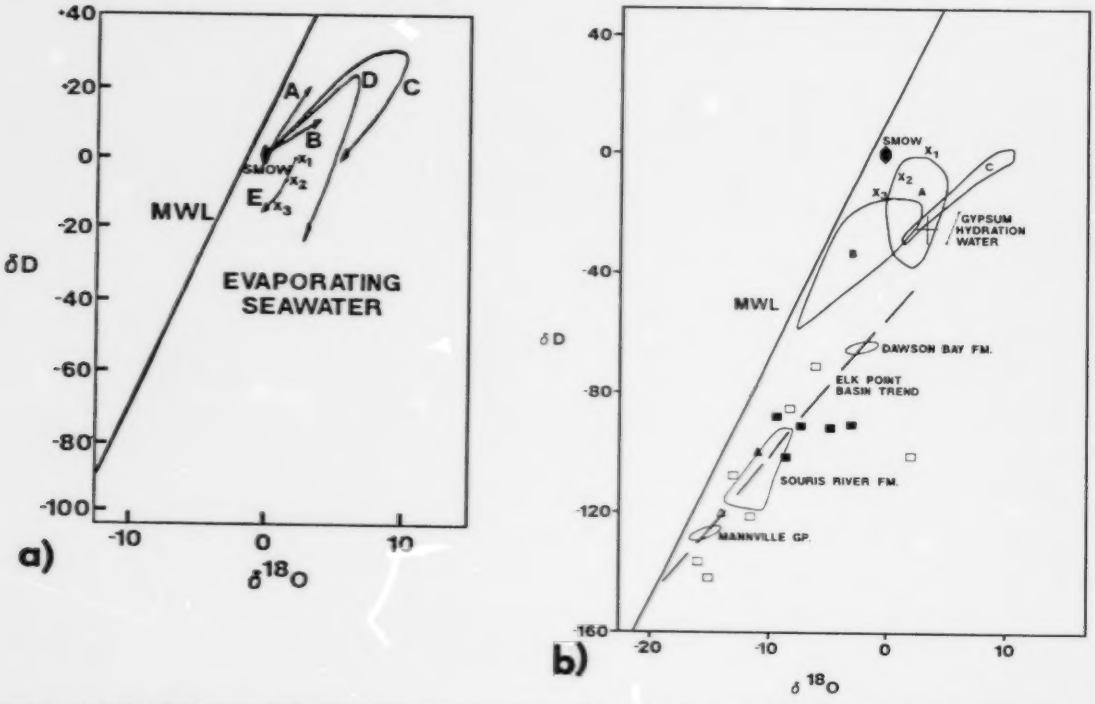

Figure 5 - a) Observed changes in the stable isotopic compositions of seawater during evaporation under different conditions (modified from Knauth and Beeunas, 1986). Curve A represents the initial stages of evaporation of seawater under humid conditions, and curve B 0under arid conditions. Curve C is based on experimental studies and natural systems (Holser, 1979b) of evaporation of seawater to near halite facies deposition. Curve D represents results from Ojo De Liebre lagoon, Mexico, evaporated to halite facies (Pierre et al., 1984). Curve E is the final stages of evaporation of salt crystallizing ponds on Bonaire Island. The stable isotopic composition of evaporating seawater from Bonaire Island salt crystallizers in the Caribbean (determined in this study) are indicated by X_1 (pre-gypsum), X_2 (pre-halite), and X_3 (post-halite, pre-sylvite).

b) Relation between δD and $\delta^{18}O$ values of water from fluid inclusions in halite of the Prairie Evaporite Formation and inclusions in halite from other studies. The stable isotopic compositions of waters extracted from fluid inclusions in halite from the Patience Lake Member of the Prairie Evaporite Formation in the Saskatoon area are represented by closed squares (PCS Cory) and triangles (PCS Lanigan) for chevron-textured halite and by open squares (PCS Cory) and triangles (PCS Lanigan) for clear halite. The range in stable isotopic composition of brines from the Dawson Bay and Souris River Formations and the Cretaceous Mannville Group, all stratigraphically above the Prairie Evaporite Formation in the Elk Point Basin and the overlying Western Interior Basin, form the present Elk Point Basin trend (Wittrup and Kyser, 1990) along which the fluid inclusion waters plot. Water extracted from fluid inclusions in halite of the Permian Salado Formation of the southern United States are represented by field A, which is compatible with evaporated Permian seawater, and field B, which represents the composition of inclusions formed from mixed evaporated seawater and meteoric water in Permian halite (Knauth and Beeunas, 1986). Field C is water extracted from Permian halite in the Delaware Basin, which was interpreted by O'Neil et al. (1986) to represent fluids from the dehydration of gypsum. The stable isotopic composition of evaporating seawater from Bonaire Island salt crystallizers in the Caribbean (determined in this study) are indicated by X_1 (pre-gypsum), X_2 (pre-halite), and X_3 (post-halite, pre-sylvite) and the values of the water that would result from dehydration of gypsum from Bonaire Island is indicated as 'gypsum hydration water'.

Table 1. Samples of halite from PCS Cory and PCS Lanigan (prefixed by "L") from which fluid inclusion results were obtained. Stratigraphic position is indicated, in cm, for those samples from PCS-Cory relative to the #1 clay seam near the top of the A-zone and samples from PCS-Lanigan are from the underlying B-zone. Range and average daughter mineral dissolution temperatures (T°C), the δD and $\delta^{18}O$ values of the inclusion fluids relative to SMOW, weight percent water as fluid inclusions and relative mole percent H_2O, CO_2, and SO_2 released from the fluid inclusions are also indicated. Ca/Mg ratios are assumed to be of the fluid inclusion brines, as explained in the text. "na" indicates not analyzed.

Sample Number	Sample Description	Strat. Pos.(cm)	δD	$\delta^{18}O$	T. rng.	T. ave.	Wt.% H_2O	Rel. SO_2	mole CO_2	% H_2O	Ca/Mg
14.12	chevron	+221	-92	-7.1	30-44	37	0.84	na	0.2	99.8	1.2
14.1	chevron	+42	-92	-9.8	30-38	34	0.17	na	7.4	92.6	9.5
15.17	chevron	-25	-103	-8.3	29-34	31	0.10	40.8	3.7	55.6	na
10.5	chevron	-254	-84	-11.2	35-45	40	0.27	10.6	3.8	85.6	8.1
15.3	chevron	-259	-92	-4.6	30-40	35	0.23	na	20.6	79.4	13.5
14.2	non-chevron	+65	-72	-5.6	52-56	54	0.04	5.1	21.4	73.5	na
15.14	non-chevron	-65	-86	-8.1	50-55	53	0.03	8.8	16.1	75.1	2.3
10.17	non-chevron	-107	-122	-11.8	50-67	58	0.02	9.4	48.8	41.8	9.2
10.6	non-chevron	-242	-141	-14.9	56-68	62	0.04	na	18.2	81.8	na
10.5	non-chevron	-254	-112	-13.6	56-64	60	0.13	na	16.9	83.1	na
15.3	non-chevron	-259	-136	-15.1	48-60	54	0.02	na	34.1	65.9	na
L-1	non-chevron	B-Zone	na	na	60-100	80	na	na	na	na	16.1
L-2	non-chevron	B-Zone	-104	+2.0	48-62	55	0.04	8.9	1.8	89.3	3.3

or changes in the geothermal gradient of the basin. The temperature and δD and $\delta^{18}O$ values of most basinal brines increase with depth (Clayton *et al.*, 1966; Hitchon and Friedman, 1969; Wittrup and Kyser, 1990). Mixing fluids that have low δD and $\delta^{18}O$ values from stratigraphically higher formations with fluids that have higher δD and $\delta^{18}O$ values from stratigraphically lower formations at some time in the evolution of the Elk Point Basin could have resulted in the variation of stable isotope values that are observed. However, the deeper fluid should have been warmer than the shallower fluid, so that the lower δD and $\delta^{18}O$ values should be accompanied by lower temperatures, the opposite of what is recorded in the inclusions (Figure 6). Instead, variations in the daughter mineral dissolution temperatures must be due either to changes in the depth of burial of the evaporites, or changes in the geothermal gradient of the basin. The relation between daughter mineral dissolution temperatures and the stable isotopic compositions of the fluids in the randomly distributed fluid inclusions (Figure 6) represent at least two distinct fluids and recrystallization events that occurred after formation of the chevron-textured halite. Because K-Ar, Rb-Sr, and K-Ca isotope systematics indicate that recrystallization has been occurring intermittently since deposition and may be continuing presently, the randomly distributed fluid inclusions represent recrystallization events corresponding to a wide range of ages from Mississippian to Present.

3. Conclusions

Fluid inclusions in halite of the Patience Lake Member of the Devonian Prairie Evaporite Formation represent at least three major fluid flow events that have affected a large portion of the evaporites in southern Saskatchewan. The chemical compositions of the fluids were acquired through recrystallization of the evaporites and, therefore, are neither representative nor indicative of the source of the recrystallizing fluid. The concentrations of Na^+, K^+, Mg^{2+}, and Cl^- in the inclusion fluids are largely a function of the temperature at the time of recrystallization of the evaporite minerals.

The first recrystallization event, possibly middle Mississippian in age, is represented by the chevron-textured halite. The recrystallizing fluid had a δD value near -92 and a $\delta^{18}O$ value near -9, typical of a mid-latitude inland fluid. The daughter mineral dissolution temperatures of 24°C to 44°C may indicate a near surface event.

At least two subsequent recrystallization events occurred at higher temperatures and are recorded in the randomly distributed fluid inclusions of the clear halite. The lower temperature event, with a minimum temperature of about 45°C, resulted from recrystallization by a fluid with a δD value of -72 and a $\delta^{18}O$ value of -6 similar to the isotopic compositions of the fluids presently in the Dawson Bay Formation. The highest temperature fluid inclusions, about 70°C, is determined from daughte

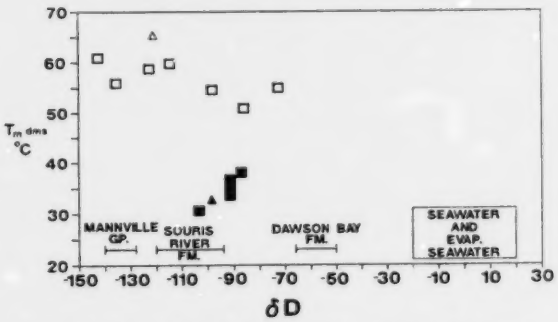

Figure 6 – Relation between D values and daughter mineral dissolution temperatures (T_m-dms) of fluid inclusions in halite from the Patience Lake Member of the Prairie Evaporite Formation. Closed squares (PCS Cory) and triangles (PCS Lanigan) represent fluid inclusions from chevron-textured halite and open squares(PCS Cory) and triangles (PCS Lanigan) are, randomly distributed fluid inclusion from the halite. The ranges in the δD values of the brines from formations overlying the Prairie Evaporite Formation, as well as seawater and evaporated seawater, are also indicated. Similarity between the δD values of the fluid inclusion waters and formation waters, but not evaporated seawater, are evident.

mineral dissolution temperatures, contain water with δD values near -141 and $\delta^{18}O$ values near -15, possibly derived from the Cretaceous aquifers of the Western Interior Basin at a time when the geothermal gradient was higher or the evaporite was buried much deeper. The chemical composition of the fluid is controlled by the mineralogy of the evaporites which are readily dissolved by undersaturated fluids.

Radiometric dating and structural analysis indicate times of dissolution of the Prairie Evaporite Formation from middle Mississippian to Present. The chevron-textured inclusions are probably representative of recrystallization during Mississippian time. The randomly distributed fluid inclusions are younger and therefore represent dissolution events that occurred from Post-Mississippian to Present.

4. REFERENCES

Arthurton, R.S. (1973): Experimentally produced halite compared to Triassic layered halite-rock from Cheshire, England; Sedimentology, v20, p145-160.

Baadsgaard, H. (1987): Rb - Sr and K - Ca isotope systematics in minerals from the Devonian potash salts in Saskatchewan, Canada; Chem. Geol. (Isotope Geosci. Sect.), v66, p1-15.

Boys, C., Langford, F.F., Renaut, R.W. and Danyluk, T. (1986): The clay rocks in the PCS Mining Limited, Cory Division Mine, Saskatchewan; *in* Summary of Investigations 1986, Sask. Geol. Surv., Misc. Rep. 86-4, p179-182.

Brodylo, L.A. and Spencer, R.J. (1987): Depositional environment of the Middle Devonian Telegraph salts, Alberta Canada; Bull. Can. Petrol. Geol., v35, p186-196.

Burrows, O.G. and Krause, F.F. (1987): Overview of the Devonian system: Subsurface of Western Canada Basin; *in* Krause, F.F. and Burrows, O.G. (eds.), Devonian Lithofacies and Reservoir Styles in Alberta, p1-20.

Chipley, D.B.L. and Kyser, T.K. (1989): Fluid inclusion evidence for the deposition and diagenesis of the Patience Lake Member of the Prairie Evaporite Formation, Saskatchewan, Canada; Sediment. Geol., v64, p287-295.

Clayton, R.N., Friedman, I., Graf, D.L., Mayeda, T.K., Meents, W.F. and Shimp, N.F. (1966): The origin of saline formation waters 1. Isotopic composition; J. Geophys. Res., v71, p3869-3882.

Dellwig, L.F. (1955): Origin of the salina salt of Michigan; J. Sediment. Petrol., v25, p83-110.

Hitchon, B. and Friedman, I. (1969): Geochemistry and origin of formation waters in the western Canada sedimentary basin I. Stable isotopes of hydrogen and oxygen; Geochim. Cosmochim. Acta, v33, p1321-1349.

Holser, W.T. (1979a): Mineralogy of Evaporites; *in* Burns, R.G. (ed.), Marine Minerals, Reviews in Mineralogy, Mineral. Soc. Amer., p211-294.

_____ (1979b): Trace elements and isotopes in evaporites; *in* Burns, R.G. (ed.), Marine Minerals, Reviews in Mineralogy, Mineral. Soc. Am., p295-346.

Holter, M.E. (1969): The Middle Devonian Prairie Evaporite of Saskatchewan; Sask. Dep. Miner. Resour., Rep.123, 134p.

Knauth, L.P. and Beeunas, M.A. (1986): Isotope geochemistry of fluid inclusions in Permian halite with implications for the isotopic history of ocean water and the origin of saline formation waters; Geochim. Cosmochim. Acta, v50, p419-433.

Lloyd, R.M. (1966): Oxygen isotope enrichment of seawater by evaporation; Geochim. Cosmochim. Acta, v30, p801-814.

McCaffrey, M.A., Lazar, B. and Holland, H.D. (1987): The evaporation path of seawater and the coprecipitation of Br^- and K^+ with halite; J. Sediment. Petrol., v57, p928-937.

Moretto, R. (1988): Observations on the incorporation of trace elements in halite of Oligocene salt beds, Bourg-en-Bresse Basin, France; Geochim. Cosmochim. Acta, v52, p2809-2814.

O'Neil, J.R., Johnson, C.M., White, L.D. and Roedder, E. (1986): The origin of fluids in the salt beds of the Delaware Basin, New Mexico and Texas; Applied Geochemistry 1, p265-271.

Pabalan, R.T. and Pitzer, K.S. (1987): Thermodynamics of concentrated electrolyte mixtures and the prediction of mineral solubilities to high temperatures for mixtures in the system Na-K-Mg-Cl-SO_4-OH-H_2O; Geochim. Cosmochim. Acta, v51, p2429-2443.

Pierre, C., Ortlieb, L. and Person, A. (1984): Supratidal evaporitic dolomite at Ojo De Liebre lagoon: Mineralogical and isotopic arguments for primary crystallization; J. Sediment. Petrol., v54, p1049-1061.

Porter, J.W., Price, R.A. and McCrossan, R.G. (1982): The Western Canada Sedimentary Basin; Roy. Soc. London, Phil. Trans. Ser. A305, p169-192.

Roedder, E. (1984a): Fluid Inclusions, Reviews in Mineralogy; Mineral. Soc. Am. 644p.

_____ (1984b): The fluids in salt; Am. Mineral., v69, p413-439.

Sonnenfeld, P. (1984): Brines and Evaporites; Academic Press, Inc., 366p.

Wardlaw, N.C. (1968): Carnallite-sylvite relationships in the Middle Devonian Prairie Evaporite Formation, Saskatchewan.; Geol. Soc. Am. Bull., v79, p1273-1294.

Wardlaw, N.C. and Schwerdtner, W.M. (1966): Halite-anhydrite seasonal layering in the Middle Devonian Evaporite Formation, Saskatchewan, Canada; Geol. Soc. Am. Bull., v77, p331-342.

Wittrup, M.B. and Kyser, T.K. (1990): The petrogenesis of brines in Devonian potash deposits of western Canada; Chem. Geol., v82, p103-128.

Wittrup, M.B., Kyser, T.K. and Danyluk, T. (1987): The use of stable isotopes to determine the source of brines in Saskatchewan potash mines; *in* Gilboy, C.F. and Vigrass, L.W. (eds.), Economic Minerals of Saskatchewan, Sask. Geol. Soc., Spec. Publ. No. 8, p159-165.

Wood, J.R. (1975): Thermodynamics of brine salt equilibria: I. The systems NaCl-KCl-$MgCl_2$-$CaCl_2$-H_2O and NaCl-$MgSO_4$-H2O at 25°C; Geochim. Cosmochim. Acta, v39, p1147-1163.

Stable Isotope Evidence for the Petrogenesis of Carnallite in the Middle Devonian Prairie Evaporite Formation, Saskatchewan[1]

G.D. Koehler[2], T.K. Kyser[2] and T. Danyluk[3]

Koehler, G.D., Kyser, T.K. and Danyluk, T. (1990): Stable isotope evidence for the petrogenesis of carnallite in the Middle Devonian Prairie Evaporite Formation, Saskatchewan; *in* Summary of Investigations 1990, Saskatchewan Geological Survey; Saskatchewan Energy and Mines, Miscellaneous Report 90-4.

The potash-bearing members of the Prairie Evaporite Formation in Saskatchewan are mainly composed of three chloride salts: halite (NaCl), sylvite (KCl), and carnallite ($KMgCl_3.6H_2O$). Other constituents, termed insolubles, typically make up less than 10 percent of the rock and consist of iron-oxides (haematite and goethite), dolomite, quartz, and clay. Sylvite is mined to produce potash whereas halite and carnallite are considered to be undesirable by-products.

The Prairie Evaporite Formation consists of a thick sequence of evaporites that extend from northern Alberta, through central and southeastern Saskatchewan, and into Manitoba and the northern USA (Figure 1). The formation reaches a thickness of 200 m near Saskatoon and thins toward a dissolution edge at the eastern margin. The Prairie Evaporite grades upward from basal layered halite and anhydrite into massive halite. This succession is capped by four potash-bearing members in the upper 80m. These are, in ascending stratigraphic order: the Esterhazy, White Bear, Belle Plaine, and Patience Lake Members (Holter, 1969). Carnallite occurs along the northern and northeastern rim of the Prairie Evaporite Formation (Figure 1), and is generally more abundant in the lower potash members (*ibid.*).

1. Thermodynamics of Carnallite-Sylvite Relationships

The occurrence of sylvite in evaporite sequences is problematic for the interpretation of ancient evaporite deposits because unlike carnallite, precipitation of sylvite directly from evaporating seawater is not predicted from chemical models (Holser, 1979; Harvie *et al.*, 1980). Carnallite, however, may undergo incongruent dissolution to sylvite by reaction with undersaturated fluids, a process which has been invoked to explain the occurrence of sylvite in several other evaporite deposits (see Lowenstein and Spencer 1990, for review). There is considerable petrographic evidence that sylvite and carnallite in the Prairie Evaporite Formation are genetically related, but commonly younger than coexisting halite (Wardlaw, 1968; Fuzesy, 1983; Baadsgaard, 1987) and may have been reversibly transformed from one to the other (Wardlaw, 1968). Further, stratigraphic relationships between carnallite- and sylvite-rich zones as described by Wardlaw (1968) indicate that sylvite generally overlies carnallite where both are present, the reverse of an expected sequence from simple evaporating seawater. This

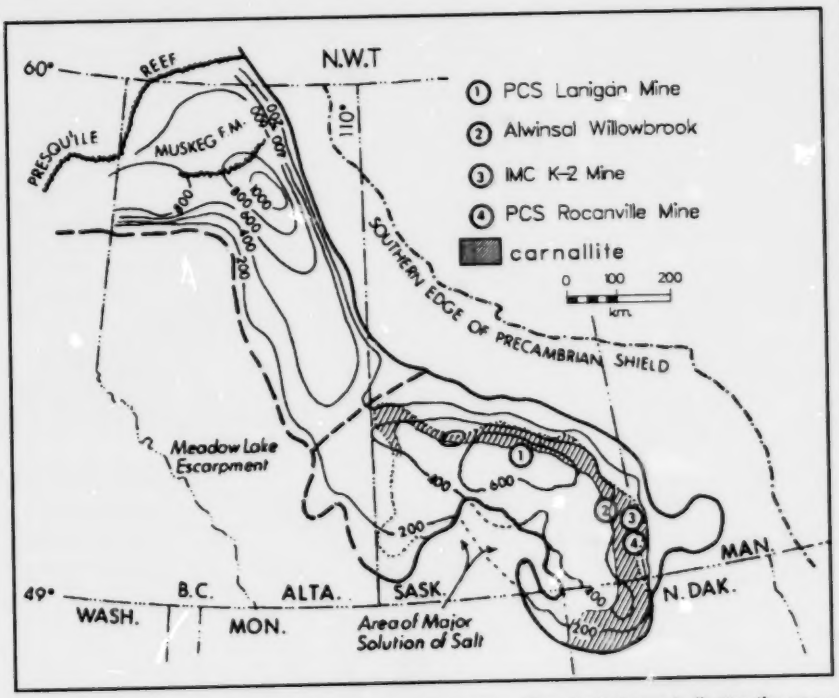

Figure 1 - Isopach map of the Prairie Evaporite Formation. The shaded area indicates the occurrence of carnallite (Holter, 1969) (modified from Baadsgaard, 1987).

(1) Project funded by the Saskatchewan Potash Producers Association and NSERC Operating Grant
(2) Department of Geological Sciences, University of Saskatchewan, Saskatoon, Saskatchewan, S7N 0W0
(3) Potash Corporation of Saskatchewan, Suite 500, 122 1st Ave. S., Saskatoon, Saskatchewan, S7K 7G3

evidence argues against a syndepositional origin for most of the sylvite and carnallite, and favours a sub-surface diagenetic process.

The behaviour of carnallite and sylvite in response to burial and diagenesis can be modelled with chemical thermodynamics. The reaction between carnallite and sylvite can be represented by:

$KMgCl_3.6H_2O = KCl + Mg^{2+} + 2Cl^- + 6H_2O$
carnallite = sylvite + solution

Carnallite precipitating from evaporating seawater forms from a solution that has an ion activity product (IAP) within the carnallite stability field at 1 bar pressure and approximately 30°C, shown as point A in Figure 2. Increasing the pressure as the carnallite is buried stabilizes the sylvite + solution field and moves the carnallite-sylvite boundary to higher values of K, so that at a pressure of 1 kilobar, which corresponds to a lithostatic load equivalent to 2-3 km depth, the IAP of the solution that precipitated the carnallite at 1 bar may now lie in the sylvite + solution field. If equilibrium is maintained, the carnallite will react to form further sylvite + solution. Thus, provided the temperature does not rise substantially, increasing pressure as a result of burial will favour the breakdown of carnallite to sylvite. As burial proceeds and the geotherm recovers, the temperature may become high enough to favour the formation of carnallite from sylvite + solution.

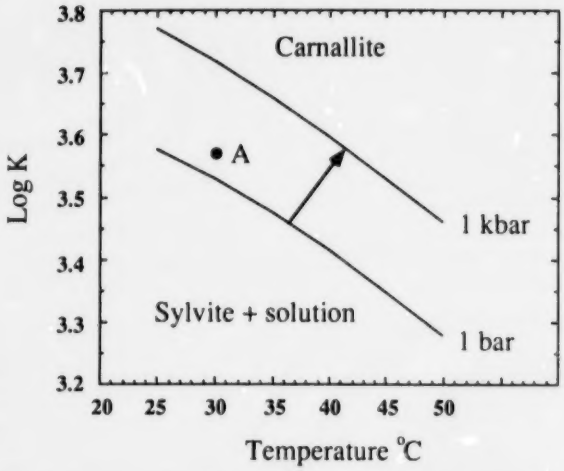

Figure 2 - Phase relationship between the equilibrium constant (K) and temperature for the reaction $KMgCl_3°6H_2O = KCl + Mg^{2+} + 2Cl^- + 6H_2O$, at various pressures. The ion activity product (IAP) is related to the product of the concentration of Cl^- and Mg^{2+} in the solution and is equal to K along the boundary between carnallite and sylvite. Thermodynamic data from Pabalan and Pitzer (1987).

2. Isotopic Properties of Carnallite

Carnallites may record, in their hydration waters, the stable isotopic compositions of fluids that were responsible for the diagenesis and recrystallization of the Prairie Evaporite Formation. To this end, measurement of the fractionation of hydrogen and oxygen isotopes between the hydration water of carnallite and the brine from which it formed is fundamental.

D and ^{18}O fractionations were measured between the hydration water of carnallite and brine for both carnallite grown in the laboratory, and for natural samples growing over a number of years in brine pools at PCS Lanigan and PCS Rocanville mines. At 25°C, laboratory experiments indicate that hydration water in carnallite is depleted in D by about 40 permil[4] and enriched in ^{18}O by about 2 permil relative to the brine from which it forms. Preliminary results from laboratory experiments, where carnallite was precipitated at higher temperature (41°C), suggest that the fractionation of hydrogen isotopes between the hydration water of carnallite and brine may be slightly temperature dependant. Natural carnallites from brine pools at PCS Lanigan show similar depletions in D, and enrichment in ^{18}O relative to the water in the brine pools. However, carnallite growing in brine pools at PCS Rocanville show depletions of D by about 20 permil and depletions rather than enrichments in ^{18}O by about 2 permil (Figure 3a, b, c). Both the brine pools are at similar temperatures, so the difference in the apparent carnallite-water D and ^{18}O fractionations must be due to differences in the chemical compositions of the brines, most notably, Ca^{2+}. The concentration of Ca^{2+} in brine at Rocanville is 4 times that at Lanigan. These fractionation factors are applicable for systems in which the amount of water in the fluid is substantially greater than the amount in the carnallite.

In addition to equilibrium fractionation of hydrogen and oxygen isotopes between fluid and carnallite, the isotopic composition of carnallite also can be affected by the rate of exchange of isotopes with any later post-depositional fluid. Fast isotopic exchange between carnallite and brine will result in measured stable isotopic compositions that are influenced by the last fluid in contact with the carnallite. On the other hand, if carnallite is resistant to isotope exchange with fluids, the stable isotopic compositions of the brine from which the carnallite was originally crystallized may be retained in its hydration water. Because the rate of isotope exchange is unknown, isotope exchange experiments were conducted in the laboratory under conditions of high fluid/carnallite ratios.

After 67 days of contact at 25°C, hydration water in carnallite was about 10 percent exchanged with brine saturated with respect to carnallite (Figure 4). This rate of isotope exchange is extremely rapid; carnallite in the potash deposits will be in isotopic equilibrium with any diagenetic fluid after contact for about one year. Therefore, carnallite will record the stable isotopic composition of the most recent diagenetic fluid with which it interacted and isotopic composition will be the most sensitive indicator of recent hydrologic activity affecting the potash deposit.

(4) Stable isotopic compositions are reported in the δ notation which is defined as: δ (‰) = [(Rsample/Rocean water) -1] x 1000 where R is the D/H or $^{18}O/^{16}O$ ratio. The units of difference are referenced to as permil (‰), equivalent to differences in the ratios of parts per thousand.

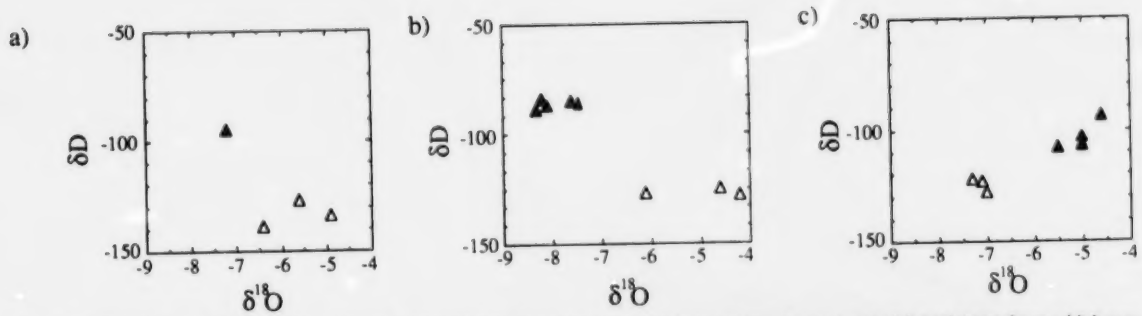

Figure 3 - Relationship between the isotopic compositions of hydration water in carnallite (open symbols) and brine from which carnallite precipitates (closed symbols). a) Carnallite grown in the laboratory at 25°C. b) Brine pool at PCS Lanigan. c) Brine pool at 408-00-07, PCS Rocanville. Errors for the δD measurements are ±5 and for $\delta^{18}O$ values are ±3 per mil.

3. Stable Isotopes in Natural Carnallite

Samples of carnallite were collected from the Esterhazy Member of the Prairie Evaporite Formation, from the Alwinsal Willowbrook well drill core (Baadsgaard, 1987), ore at PCS Rocanville, carnallite pods at PCS Rocanville, and from carnallite pods at IMC K-2. The hydration water in the carnallite was analyzed for hydrogen and oxygen isotopic compositions to constrain the origin of fluids responsible for the formation of carnallite in different locations within the basin. The Alwinsal Willowbrook samples and ore samples from Rocanville have stable isotopic compositions that, with a few exceptions, fall below the line formed by the stable isotopic compositions of waters from formations above the Prairie Evaporite Formation (Elk Point Basin Trend) (Wittrup *et al.*, 1987), but are roughly parallel to it (Figure 5a). The stable isotopic compositions of the parent brine from which these carnallites form can be estimated using the hydrogen and oxygen isotopic fractionations measured in the laboratory and in brine pools. The estimated stable isotopic compositions of the fluids in equilibrium with these carnallites tend to follow the Elk Point Basin Trend, suggesting that these carnallites formed from waters that have their origins in formations above the Prairie Evaporite and do not represent primary precipitation from ancient seawater.

Estimated fluid compositions that lie above the Elk Point Basin Trend, such as those which formed the carnallite pods at PCS Rocanville and IMC K-2 and some of the Alwinsal Willowbrook samples, most likely indicate that these carnallites formed by incorporating most of the water in the brine as the brine interacted with sylvite to form carnallite (Figure 5b). This mechanism is different from the direct precipitation of carnallite from a brine because most of the water responsible for carnallite precipitation is incorporated into the hydration water of the mineral. In this process, the fractionation of the stable isotopes of hydrogen and oxygen between the hydration water of carnallite and brine will be dependant on the amount of water incorporated into the mineral and, as a result, the δD and $\delta^{18}O$ values of the carnallite will more closely resemble those of the brine responsible for the formation of the carnallite.

4. Conclusions

The above thermodynamic and stable isotope constraints indicate that primary carnallite, formed from evaporated seawater during Late Devonian time, dehydrated much later to form sylvite under the influence of increasing lithostatic pressure during burial (Figure 6). Maximum burial of the Prairie Evaporite probably occurred during the Cretaceous, as reflected by the temperatures determined from fluid inclusions in halite (Chipley and Kyser, 1989) and by the preponderance of Rb-Sr ages on sylvite which correspond to the Cretaceous (Baadsgaard, 1987).

Reversion of sylvite to secondary carnallite may be a result of uplift during the Tertiary. From thermodynamic considerations, sylvite + solution may react to form carnallite as lithostatic pressure decreases, or as a result of interaction of sylvite with Mg-rich brines (Figure 6). Rb-Sr ages obtained from Alwinsal Willowbrook carnallites suggest that they

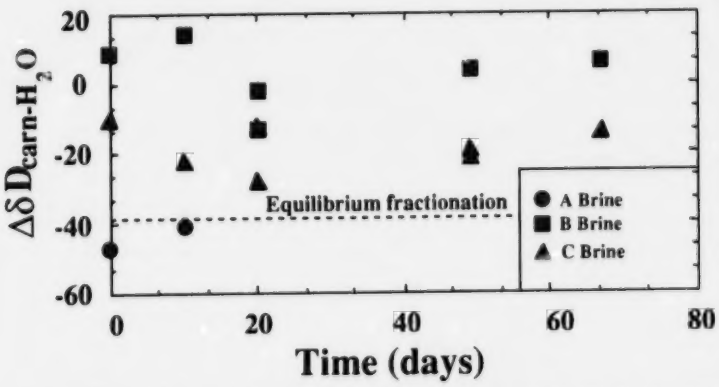

Figure 4 - Rate of hydrogen isotope exchange between hydration water in carnallite and brine at 25°C. Carnallite was allowed to exchange with 3 brines having different stable isotopic compositions. Exchange is evidenced by initial values approaching the equilibrium value of -37. $\Delta\delta D_{carn\text{-}H2O}$ is equal to the difference $\delta D_{carnallite} - \delta D_{water}$.

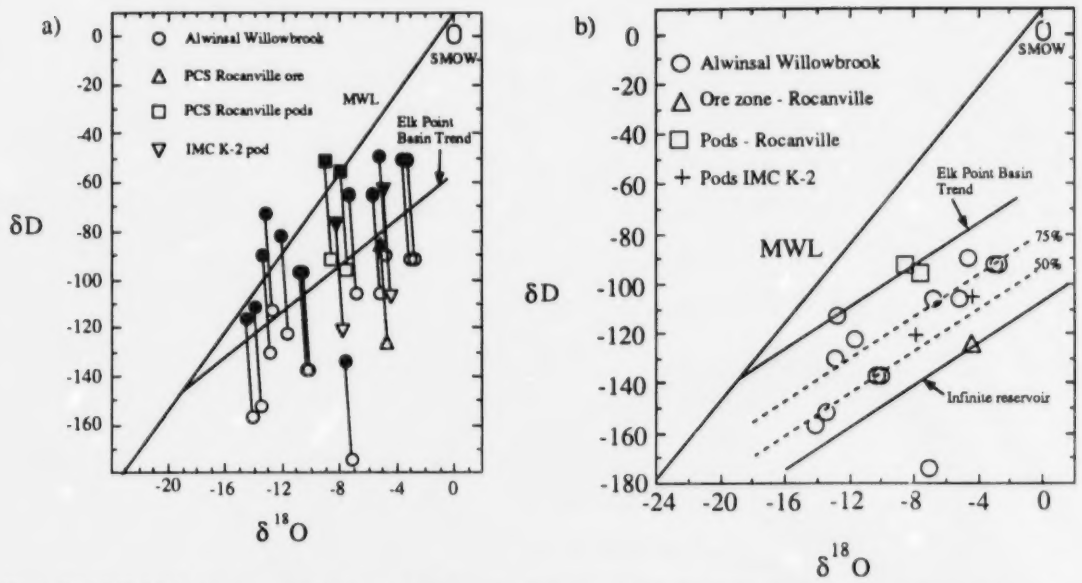

Figure 5 - (a) Stable isotope compositions of hydration water in carnallite from the Alwinsal Willowbrook well, ore at PCS Rocanville, pods at PCS Rocanville, and pods from IMC K-2 (open symbols), and the calculated isotopic composition of the water from which they formed (closed symbols) assuming the isotopic fractionations measured from laboratory experiments and an infinite reservoir of water. Natural variation in the isotopic composition of recent global precipitation produces the Meteoric Water Line (MWL). (b). Calculated isotopic compositions of brines that could have precipitated the carnallite from the Elk Point Basin under conditions where variable percentages of water in the brine enters the carnallite. Lines parallel to the Elk Point Basin Trend denote the possible percentage of the total water in the brine incorporated into the carnallite, assuming the water is from basinal brines that follow the Elk Point Basin Trend. Those samples of carnallite that have incorporated a high percentage of the available water in the brine into their structure (eg. >50%) most likely formed from the conversion of sylvite to carnallite.

were formed during the last 30 Ma (Baadsgaard, 1987). The hydrogen and oxygen isotopic composition of the carnallites indicate that they have been precipitated by waters that had their origin in formations above the Prairie Evaporite.

Carnallite contains an isotopic record of fluid events in its hydration water, the age of which can be determined using a variety of radiogenic methods. Thus, detailed study of carnallite will provide a history of fluid flow in the Prairie Evaporite Formation and afford a greater understanding of the fluid events and diagenesis related to the present structure and geology of the potash deposits.

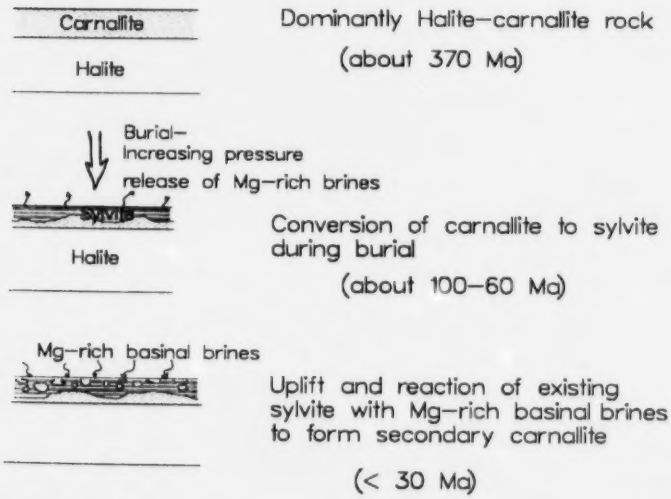

Figure 6 - Simple model of carnallite - sylvite relationships in the Prairie Evaporite Formation.

5. References

Baadsgaard, H. (1987): Rb-Sr and K-Ca isotope systematics from potassium horizons in the Prairie Evaporite Formation, Saskatchewan, Canada; Chem. Geol., v66, p1-15.

Chipley, D.L. and Kyser, T.K. (1989): Fluid inclusion evidence for the diagenesis of the Patience Lake Member of the Prairie Evaporite Formation; Sed. Geol., v64, p287-295.

Fuzesy, L.M. (1983): Petrology of the potash ore in the Middle Devonian Prairie Evaporite Formation of Saskatchewan; *in* McKercher, R.M. (ed.), Potash Technology, Pergamon Press, p47-57.

Harvie, C.E., Weare, J.H., Hardie, L.A. and Eugster, L.P. (1980): Evaporation of seawater: calculated mineral sequences; Sci., v208, p498-500.

Holser, W.T. (1979): Mineralogy of evaporites; *in* Burns, R.G. (ed.), Marine Minerals, Reviews in Mineralogy, Mineral. Soc. Am., Washington D.C., v6, p211-294.

Holter, M.E. (1969): The Middle Devonian Prairie Evaporite Formation of Saskatchewan; Sask. Dep. Miner. Resour., Rep. 123, 134p.

Lowenstein, T.K. and Spencer, R.J. (1990): Syndepositional origin of potash evaporites: petrographic and fluid inclusion evidence; Am. J. Sci., v290, p1-42.

Pabalan, R.T. and Pitzer, K.S. (1987): Thermodynamics of concentrated electrolyte mixtures and the prediction of mineral solubilities to high temperatures for mixtures in the system Na-K-Mg-Cl-SO_4-OH-H_2O; Geochim. Cosmochim. Acta, v51, p2429-2443.

Wardlaw, N.C. (1968): Carnallite-sylvite relationships in the Middle Devonian Prairie Evaporite Formation, Saskatchewan; Geol. Soc. Am. Bull., v79, p1273-1294.

Wittrup, M.B., Danyluk, T. and Kyser, T.K. (1987): The use of stable isotopes to determine the source of brines in Saskatchewan potash mines; *in* Gilboy, C.F. and Vigrass, L.W. (eds.), Economic Minerals of Saskatchewan, Sask. Geol. Soc., Spec. Publ. No. 8, p159-165.

Computer Modelling Saskatchewan's Coalfields using an Expert System

J.D. Hughes[1] *and W.J. McDougall*[1]

Hughes, J.D. and McDougall, W.J. (1990): Computer modelling Saskatchewan's coalfields using an Expert system; *in* Summary of Investigations 1990, Saskatchewan Geological Survey; Saskatchewan Energy and Mines, Miscellaneous Report 90-4.

In late 1988 a co-operative project between the Geological Survey of Canada and Saskatchewan Energy and Mines was initiated to assess the geological, economic and environmental characteristics of Saskatchewan's coal resources. This project involved the assessment of some 5,000 coal exploration boreholes contained in computer databases developed by the Geological Survey of Canada for its National Coal Inventory. Saskatchewan Energy and Mines provided financial resources to assist in the establishment of comprehensive geological correlation frameworks for these databases, and the Geological Survey of Canada provided its expertise in modelling coal deposits and access to the modelling system developed for the National Coal Inventory at the Institute of Sedimentary and Petroleum Geology in Calgary.

This report is intended to summarize the present status of this project, and to review the products and capabilities delivered by the expert geological modelling system used for geological and resource assessment. The figures presented here are examples of possible outputs, but the authors recognize that the quality of some are not up to publication standards (at page size) but they are included because their omission would be a detriment to the impact of the report.

1. Background

Coal resources in southern Saskatchewan are contained within the Ravenscrag Formation of early Tertiary age. This formation comprises non-marine strata deposited in a fluvial environment. Three main coalfields with commercially-extractable resources have been defined by extensive exploratory drilling and surface exploration over the past century. They are termed the Estevan, Wood Mountain/Willow Bunch and Shaunavon coalfields, located respectively in the southeast, south-central and southwest parts of the province. Surface mines operated by Manalta Coal Ltd. and Luscar Ltd. in the Estevan and Wood Mountain/Willow Bunch coalfields provide feedstock for thermal-electric generating plants that produce 70 percent of Saskatchewan's electricity, in addition to a small amount of coal exported from the province.

The first extensive review of Saskatchewan's coal resources was published in 1978 (Irvine *et al.*, 1978), and was based on some 2000 coal exploration boreholes available at that time. Exploration since the publication of this report has increased this total to more than 6000 boreholes, of which data from 5000 have been interpreted and stored in the Geological Survey of Canada's National Coal Inventory databases.

Computer techniques and software for coalfield geological modelling were in their infancy during the development of the 1978 coal resource report. A modelling system incorporating inhouse and commercially available software developed by one of the authors (Hughes) has automated much of the process of creating three-dimensional models from primary exploration data. This system delivers maps, cross-sections, reports and other analytical capabilities that have completely automated the manual cartographic methods used in the production of the 1978 report, and provides a much greater range of geological, economic and environmental products than was previously possible. The system also interfaces with commercially available three-dimensional Computer Aided Drafting (CAD), Geographic Information (GIS) and Image Analysis systems to extend the range of its capabilities. A brief overview of this system with some examples from the ongoing work in southern Saskatchewan is outlined below.

2. Geological Modelling System

Four major components are involved in the development of an integrated geological computer model. These can be termed data capture/verification, geological correlation, computer modelling and data integration. The flow of information and processes involved in these components are outlined in Figure 1, and discussed in more detail below.

a) Data Capture/Verification

Data capture/verification involves the conversion of a variety of hardcopy and electronic media into a consistently defined digital form. Hardcopy data includes: geophysical logs from exploration boreholes, drillers' and/or geologists' cuttings descriptions, and analytical reports for coal intersections which were sampled. The geophysical logs were interpreted, in conjunction with other available information, into lithological layers which were entered into the LITHOLOGY dataset (see Figure 1). A rigorous set of procedures helped maximize the consistency of lithological assignments between boreholes, followed by verification using graphical displays of each borehole compared to the hardcopy logs. Analytical information for sampled coal intervals was

(1) Institute of Sedimentary and Petroleum Geology, 3303 33rd St. N.W., Calgary, Alberta, T2L 2A7

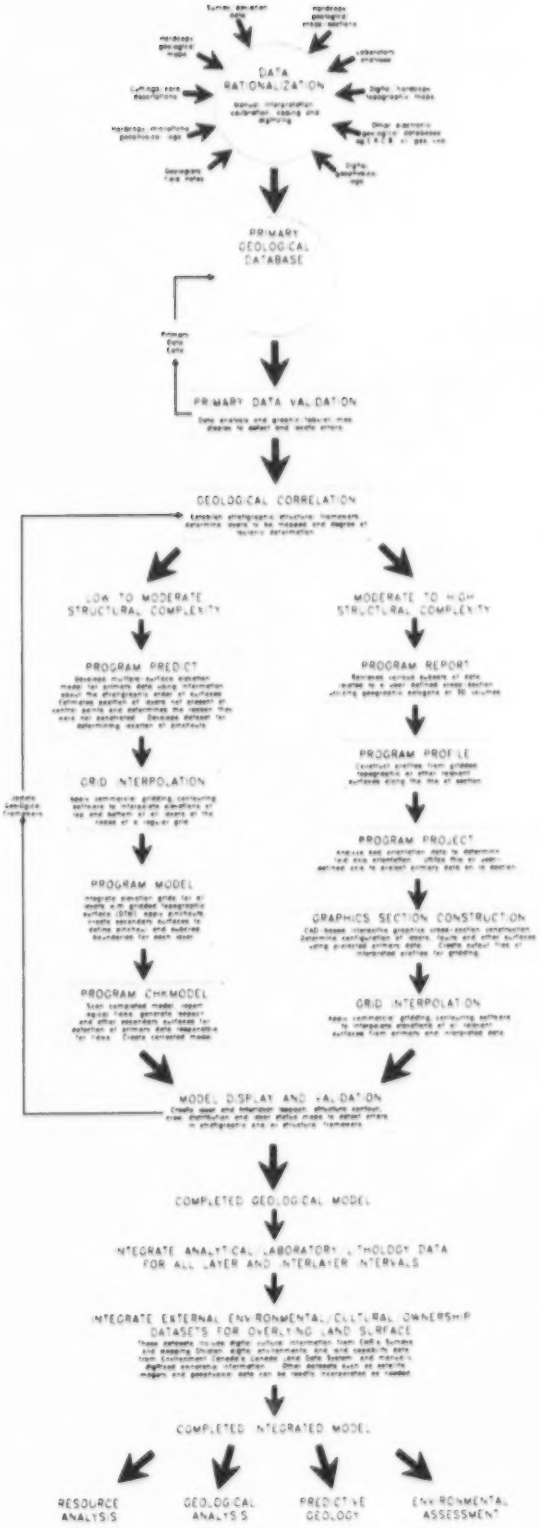

similarly incorporated into the ANALYTICAL dataset (Figure 1).

Other information requiring transformation to a digital format included digitizing contour information from 1:50,000 scale NTS topographic maps for each coalfield, along with spot heights and breaklines. From this a digital terrain model could be created for each area.

The database management system (DBMS) used in this study is Hewlett-Packards' IMAGE/TRANSACT software running on an HP3000/950 superminicomputer. This database system utilizes a full complement of data dictionaries and range checks to eliminate errors wherever possible on input. A microcomputer-based version of this database system has been written using the ORACLE DBMS software, and is currently undergoing testing.

The data capture/verification process is the single most labour-intensive part of developing a computer model, typically consuming 75-80 percent of the total personnel resources.

b) Geological Correlation

Geological correlation initially requires understanding the regional stratigraphy of all coal beds and markers that can be traced laterally between boreholes. The nomenclature scheme adopted in this study involved first defining groups of coal beds, termed ZONES, which occur at about the same stratigraphic position in the section, and then designating correlateable beds within each zone with a letter termed a ZONE-MODIFIER. Once the regional stratigraphic framework was established, correlations for each bed could be determined and entered into the database. In the Estevan Coalfield, five coal zones containing 24 beds were defined; in the Wood Mountain/Willow Bunch coalfield 28 beds occur within seven coal zones and in the Shaunavon Coalfield two coal zones contain nine beds.

c) Computer Modelling

Once correlations for all coal beds in all holes have been established, a computer model is generated and displayed as a series of maps, cross-sections and statistical tables that can be used to identify errors in the correlation framework. In most cases six or more iterations through the model building process are required before all errors are detected and eliminated.

Two different sets of computer-based processes can be used in the model building process depending on the structural complexity of the deposit. In this study, structural complexity was minimal, so that the processes on the left hand side of the diagram in Figure 1 could be utilized. These processes involve first retrieving elevation data on the top and base of each layer within the

Figure 1 - Flow diagram illustrating the principal processes and computer programs utilized in constructing an integrated geological computer model (see text).

database, together with elevations of the topography and the bedrock surface. The data are then processed by program PREDICT, which utilizes multiple-surface logic to identify the positions of missing layers and to determine the reason they are missing (ie. if they were eroded, pinched out, or if the hole was not drilled deep enough). Datasets created by PREDICT can be used to automatically define pinched out and eroded areas within each layer, as well as areas where several layers merge into a single seam. These datasets can be input into commercially available gridding and contouring software which create grids of the top and bottom elevations of each layer, and of the elevation of the bedrock surface. Program MODEL also incorporates multiple-surface logic and performs the assembly of the model. Elevation grids for the topographic and bedrock surfaces and for the top and bottom of each layer provide input to MODEL; output includes elevation grids which have been blanked in eroded and pinched out areas, along with a variety of other surfaces which are used to define pinch out and subcrop lines for each layer. Program CHKMODEL scans the completed model for logical flaws, such as crossing layers which may indicate errors in the primary database, reports a variety of statistics which can be used to assess the integrity of the model, and creates layer and interlayer isopach surfaces which can be displayed in map form to detect data points responsible for any errors.

d) Data Integration

Once an error-free model has been developed, a wide variety of other layers of information can be integrated into the model. Other datasets of interest include information on: the ash and sulphur content of each layer, the lithological composition of rock units between layers, the suitability of the overlying land surface for uses other than coal mining (eg. areas underlying towns or areas with high quality agricultural land) and information from Landsat-TM or airborne side-scanning radar (SAR). The geological models and all relevant datasets can be downloaded to a microcomputer-based GIS (Tydac SPANS), where a host of additional spatial analysis capabilities are available. Remotely sensed data, including Landsat-TM and SAR for the Estevan Coalfield, were processed with a microcomputer image analysis system (PCI EASI/PACE), and integrated into the GIS. A microcomputer-based three-dimensional CAD system (AUTOCAD) was also interfaced with the completed integrated model, and used to create several of the figures in the remainder of this report.

3. Analytical/Display/Reporting Capabilities

Once the model integrating all relevant datasets has been created, a wide selection of analytical, display and reporting capabilities grouped loosely into geological, resource analysis (economic and environmental characteristics of the contained coal resources) and interactive query categories. Some outputs from the system are illustrated below with examples from the assessment of the Estevan Coalfield.

a) Geological Analysis

As previously mentioned, 24 coal beds grouped into five coal zones were included in the computer model for the Estevan Coalfield. The nomenclature and mean thicknesses of intervals in the Estevan model are illustrated in Figure 2. The stratigraphic succession derived from the 368 boreholes available in this coalfield can be automatically summarized in a series of tables utilizing output from program PREDICT. The left hand side of Table 1, for example, lists the mean, range, standard deviation and number of penetrations for the till and for each layer and interlayer. It also lists a statistic (standard deviation divided by mean) which can be used to assess the variability of each layer (a high value for this statistic indicates lenticular units). The right hand side of Table 1 summarizes the depth statistics for the till and each layer and interlayer, and hence is a first look at the potential economic viability of the coal beds. The left hand side of Table 2 summarizes the mean, range and standard deviation of the spacing of borehole penetrations of each layer, and hence indicates the level of knowledge available for the layers. The level of knowledge is lower for the upper three coal zones (Short Creek, Roche Percee and Souris), where the mean borehole spacing ranges between 1.04 and 1.71 km, than for the Boundary and Estevan zones, where the mean spacing ranges between 0.88 and 1.17 km.

One of the products of program MODEL is a map showing the uppermost layer at each node in the model, which is analogous to a conventional geological map of the bedrock surface. Figure 3 illustrates the uppermost surface map for the Estevan Coalfield model. Each pattern on this map denotes a particular layer - stratigraphically higher layers occur in the south-central parts of the field, with Boundary and Estevan layers to the north and around the peripheries of the map. This reflects the structural dip of the coal measures to the south into the Williston Basin. The southern limit of the patterned area lies along the Canada-U.S.A. border.

The completed model can be sliced along cross-section lines at any orientation. Figure 4 is a cross-section constructed with a sea level datum in a west-east direction near the Canada-U.S.A. border. Figure 4 also shows borehole data located within 750 m of the section. The original plot of this section, which was created in AUTOCAD, was in full colour (hence the poor quality of the black and white reproduction). New models, created using a stratigraphic datum, can also be produced by program MODEL, as illustrated by the cross-section in Figure 5. All surfaces in this figure have been restored using the base of the Estevan G bed as a datum.

All of the layers of information in the integrated model can be imported into a three-dimensional CAD system and viewed from any orientation. Figure 6 illustrates the configuration of the top elevation of each coal zone in the Estevan Coalfield together with the elevation of the topographic surface. The interface to AUTOCAD allows a second dataset to be draped using colours on each 3D mesh (the original of this figure used colours to denote total coal thickness for each zone). Several

geological features of interest are noted on Figure 6, including the removal of the Boundary Coal Zone beneath the Estevan due to the presence of a southerly-flowing, fluvial channel during deposition of the Boundary coals in this area, and the removal of both Boundary and Estevan zones by a preglacial channel in the western part of the field.

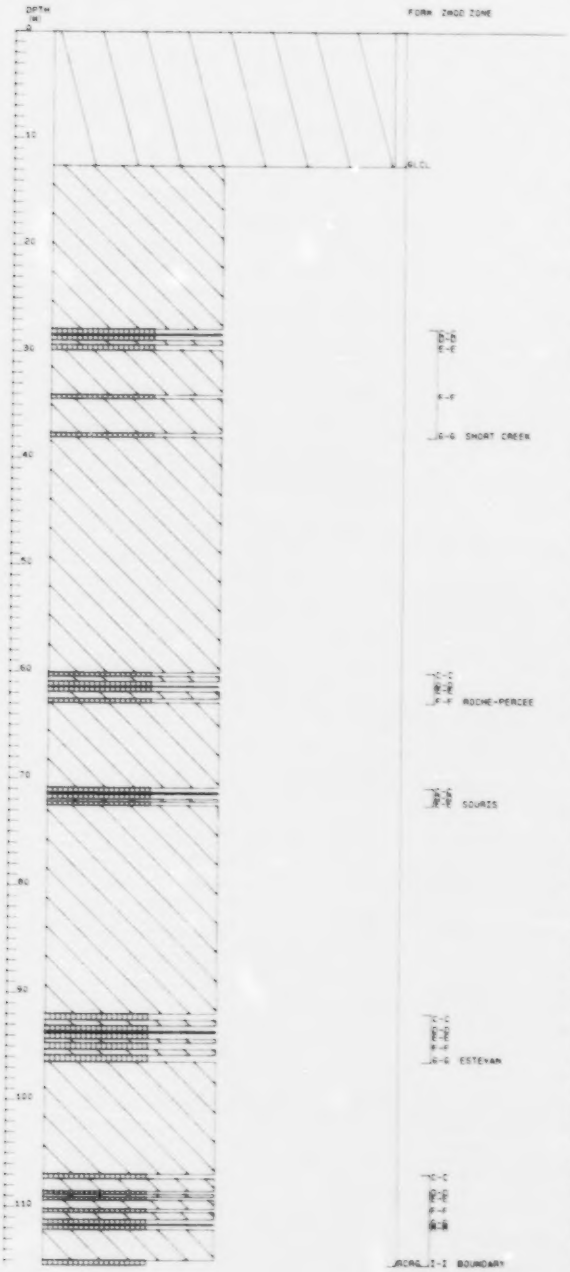

Figure 2 - Computer-generated composite stratigraphic section for the Estevan Coalfield constructed using the mean thickness of penetrations of glacial till and each layer and interlayer interval in 368 boreholes.

Other programs within the system allow the construction of lithological models which can be displayed in full colour cross-section or map form. These models can be developed, using any combination of lithologies denoted in the primary database, for the total thickness of each rock parting, or for slices of rock of user-defined thickness above and below a user-defined layer in the model. Lithology models may also be constructed relative to sea level or a stratigraphic datum. Figure 7 is a 3D display illustrating the coarse sand component of six, five metre thick slices taken in descending stratigraphic sequence below the Estevan Coal Zone. The net coal thickness of the Boundary Coal Zone is also shown where it occurs below the Estevan (ie. between 10 and 20 m below the Estevan). The position of the ancient river channel (also noted in Figure 6) is well defined by its coarse sand fill on the eastern edge of the field, and clearly indicates the reason the Boundary Coal Zone was not deposited in this area. Thick Boundary coal development occurs in interfluvial floodplain areas outside this channel.

b) Resource Analysis

National standards for the quantification of coal resources have been established by Hughes *et al.* (1989). Hughes developed a computer program (program RESOURCE) which accepts as input an elevation model of all layers and the ash and sulphur content. The user first determines the type of mine desired (ie. surface or underground), and then specifies parameters defining seam thickness and economic limits denoted in the National Standards. In the case of the Estevan Coalfield, a surface mine with three mining stages was specified. Two classes of resources defined according to feasibility of exploitation are determined by the program. Immediate interest resources were computed to a maximum stripping ratio of 13 bcm/tonne using a minimum coal bed thickness of 60 cm, and future interest resources were computed to a maximum stripping ratio of 20 bcm/tonne using a minimum coal bed thickness of 45 cm. A minimum extractable parting thickness of 15 cm was used for both immediate and future interest resources (Hughes *et al.*, *op. cit.*). Ash and sulphur data for each layer were expressed at a 30 percent bed moisture value. Resources were also subdivided into 'assurance of existence' categories based on the distance of each resource block from the nearest control point. In the Estevan example, measured resources were defined as those between 0 and 450 m from a borehole, indicated between 450 and 900 m, inferred between 900 and 2400 m, and speculative between 2400 and 3000 m. No resources were calculated for parts of the model more than 3000 m from a control point.

Program RESOURCE first determines which beds in each of the five defined mining horizons qualify for mining, based on the parameters specified. The program then compiles ash and sulphur data for qualifying layers to determine the values for the recoverable coal. Mining losses of 15 cm from the top and bottom of each mining horizon and 10 cm adjacent to internal partings

Table 1 - Summary of Thickness (left) and Depth Statistics (right) for Coalbeds in the Estevan Coalfield (based on 368 boreholes).

HORIZON NO.	ZONE NAME	ZONE MOD.	THICKNESS STATISTICS IN METRES MEAN	MIN.	MAX.	STD.DEV.	STD.DEV. /MEAN	HOLE COUNT
	TILL		12.58	.61	91.44	14.80	1.18	368
1	SHORT CREEK	C-C	15.30	.00	28.07	8.55	.56	21
			.50	.08	1.22	.30	.60	21
2	SHORT CREEK	D-D	.09	.00	.67	.18	2.08	21
			.48	.20	1.03	.20	.42	21
3	SHORT CREEK	E-E	.43	.00	1.83	.60	1.39	21
			.49	.12	1.61	.31	.64	21
4	SHORT CREEK	F-F	4.21	.88	10.94	2.50	.59	18
			.35	.11	.60	.13	.38	18
5	SHORT CREEK	G-G	3.24	.00	5.58	1.69	.52	14
			.40	.12	.64	.13	.33	17
6	ROCHE-PERCEE	C-C	22.03	16.17	27.52	3.81	.17	11
			.35	.13	.64	.13	.38	49
7	ROCHE-PERCEE	D-D	.49	.00	5.39	.94	1.90	49
			.44	.06	1.09	.22	.50	50
8	ROCHE-PERCEE	E-E	.05	.00	.83	.16	2.87	50
			.44	.06	1.40	.26	.58	51
9	ROCHE-PERCEE	F-F	.67	.00	5.49	1.15	1.72	45
			.39	.06	1.28	.23	.60	46
10	SOURIS	C-C	7.94	2.46	17.63	4.06	.51	44
			.45	.08	2.17	.28	.62	115
11	SOURIS	D-D	.15	.00	3.90	.48	3.19	115
			.47	.09	1.40	.26	.55	116
12	SOURIS	E-E	.24	.00	3.35	.49	2.07	116
			.36	.08	1.57	.20	.55	120
13	ESTEVAN	C-C	19.43	8.38	33.17	5.25	.27	90
			.59	.05	1.41	.29	.49	193
14	ESTEVAN	D-D	.53	.00	4.45	.89	1.69	192
			.51	.05	2.14	.32	.62	197
15	ESTEVAN	E-E	.16	.00	6.15	.58	3.61	195
			.56	.04	1.69	.32	.57	196
16	ESTEVAN	F-F	.36	.00	12.38	1.13	3.13	196
			.61	.05	1.83	.36	.59	200
17	ESTEVAN	G-G	.53	.00	3.73	.61	1.14	200
			.63	.05	2.56	.32	.51	214
18	BOUNDARY	C-C	10.47	3.23	23.26	4.46	.43	74
			.45	.09	1.52	.28	.64	117
19	BOUNDARY	D-D	1.15	.00	5.73	1.01	.87	112
			.30	.06	1.13	.17	.58	154
20	BOUNDARY	E-E	.26	.00	3.81	.57	2.17	153
			.29	.05	.83	.14	.50	156
21	BOUNDARY	F-F	.82	.00	6.28	1.09	1.33	151
			.31	.05	.92	.12	.39	156
22	BOUNDARY	G-G	.67	.00	3.74	.73	1.09	154
			.45	.05	1.34	.25	.55	159
23	BOUNDARY	H-H	.07	.00	1.95	.24	3.27	158
			.42	.05	.93	.21	.49	158
24	BOUNDARY	I-I	2.85	.24	7.23	1.96	.69	62
			.46	.07	1.47	.28	.61	68

HORIZON NO.	ZONE NAME	ZONE MOD.	DEPTH STATISTICS IN METRES MEAN	MIN.	MAX.	STD.DEV.	HOLE COUNT
	TILL		12.58	.61	91.44	14.80	368
1	SHORT CREEK	C-C TOP	20.28	3.26	30.51	7.99	21
1	SHORT CREEK	C-C BASE	20.78	3.46	30.82	8.07	21
2	SHORT CREEK	D-D TOP	20.86	3.46	31.12	8.06	21
2	SHORT CREEK	D-D BASE	21.34	3.66	31.70	8.16	21
3	SHORT CREEK	E-E TOP	21.78	3.87	32.98	8.42	21
3	SHORT CREEK	E-E BASE	22.27	4.33	33.38	8.45	21
4	SHORT CREEK	F-F TOP	28.60	13.49	39.55	6.80	18
4	SHORT CREEK	F-F BASE	28.95	13.72	39.66	6.81	18
5	SHORT CREEK	G-G TOP	29.17	3.32	41.70	11.18	17
5	SHORT CREEK	G-G BASE	29.56	3.75	42.00	11.16	17
6	ROCHE-PERCEE	C-C TOP	28.26	3.96	66.23	16.38	49
6	ROCHE-PERCEE	C-C BASE	28.61	4.19	66.75	16.41	49
7	ROCHE-PERCEE	D-D TOP	28.76	4.19	66.96	16.46	50
7	ROCHE-PERCEE	D-D BASE	29.20	4.42	67.72	16.48	50
8	ROCHE-PERCEE	E-E TOP	28.75	3.32	68.00	16.73	51
8	ROCHE-PERCEE	E-E BASE	29.19	4.39	68.49	16.65	51
9	ROCHE-PERCEE	F-F TOP	31.60	4.65	68.67	16.27	46
9	ROCHE-PERCEE	F-F BASE	31.99	4.88	69.16	16.34	46
10	SOURIS	C-C TOP	23.27	1.34	67.79	16.43	115
10	SOURIS	C-C BASE	23.72	2.07	68.07	16.35	115
11	SOURIS	D-D TOP	23.79	2.07	68.07	16.30	116
11	SOURIS	D-D BASE	24.26	2.34	68.36	16.21	116
12	SOURIS	E-E TOP	24.09	2.34	68.36	16.17	120
12	SOURIS	E-E BASE	24.45	2.59	68.64	16.13	120
13	ESTEVAN	C-C TOP	30.78	2.26	94.15	17.65	193
13	ESTEVAN	C-C BASE	31.37	2.47	94.87	17.65	193
14	ESTEVAN	D-D TOP	31.17	2.47	95.57	18.02	197
14	ESTEVAN	D-D BASE	31.69	2.65	95.83	17.95	197
15	ESTEVAN	E-E TOP	31.60	2.65	96.74	18.05	196
15	ESTEVAN	E-E BASE	32.16	2.84	96.87	18.00	196
16	ESTEVAN	F-F TOP	32.30	2.84	97.06	18.05	200
16	ESTEVAN	F-F BASE	32.91	3.02	97.54	18.09	200
17	ESTEVAN	G-G TOP	32.68	3.02	98.08	18.24	214
17	ESTEVAN	G-G BASE	33.31	3.20	98.51	18.19	214
18	BOUNDARY	C-C TOP	35.21	3.41	111.47	21.60	117
18	BOUNDARY	C-C BASE	35.65	3.87	112.35	21.67	117
19	BOUNDARY	D-D TOP	34.02	4.66	115.15	21.13	154
19	BOUNDARY	D-D BASE	34.32	4.95	115.28	21.11	154
20	BOUNDARY	E-E TOP	34.66	4.95	115.64	21.26	156
20	BOUNDARY	E-E BASE	34.95	5.24	116.43	21.27	156
21	BOUNDARY	F-F TOP	34.79	5.49	118.48	21.10	156
21	BOUNDARY	F-F BASE	35.10	5.94	118.67	21.06	156
22	BOUNDARY	G-G TOP	35.01	6.25	118.67	21.25	159
22	BOUNDARY	G-G BASE	35.46	6.64	118.87	21.12	159
23	BOUNDARY	H-H TOP	35.00	6.86	106.77	20.08	158
23	BOUNDARY	H-H BASE	35.42	7.56	107.14	19.96	158
24	BOUNDARY	I-I TOP	36.75	10.67	109.15	19.50	68
24	BOUNDARY	I-I BASE	37.21	11.03	109.70	19.57	68

Table 2 - Summary of Near-neighbour (left) and Borehole Status (right) Statistics for the Estevan Coalfield (based on 368 boreholes). Near-neighbour spacing is a measure of the level of knowledge on each layer (i.e. large near-neighbour spacings reflect less knowledge than small ones). Borehole status is determined by program PREDICT, which uses mutiple-layer logic to determine the reason layers were not penetrated.

HORIZON NO.	HORIZON ZONE NAME	HORIZON ZONE MOD.	NEAR-NEIGHBOR STATISTICS (KM) MEAN	MIN.	MAX.	STD.DEV.	HOLE COUNT
	TILL		.89	.02	8.75	.79	368
1	SHORT CREEK	C-C	1.71	1.53	2.46	.26	21
2	SHORT CREEK	D-D	1.71	1.53	2.46	.26	21
3	SHORT CREEK	E-E	1.71	1.53	2.46	.26	21
4	SHORT CREEK	F-F	1.72	1.53	2.46	.30	18
5	SHORT CREEK	G-G	1.76	1.53	2.46	.31	17
6	ROCHE-PERCEE	C-C	1.44	.55	4.64	.82	49
7	ROCHE-PERCEE	D-D	1.42	.55	4.64	.79	50
8	ROCHE-PERCEE	E-E	1.42	.55	4.64	.78	51
9	ROCHE-PERCEE	F-F	1.49	.66	4.13	.74	46
10	SOURIS	C-C	1.04	.02	2.88	.60	115
11	SOURIS	D-D	1.04	.02	2.88	.60	116
12	SOURIS	E-E	1.04	.02	2.88	.57	120
13	ESTEVAN	C-C	.94	.02	3.65	.66	193
14	ESTEVAN	D-D	.92	.02	3.65	.65	197
15	ESTEVAN	E-E	.90	.02	3.65	.62	196
16	ESTEVAN	F-F	.90	.02	3.65	.62	200
17	ESTEVAN	G-G	.88	.02	3.65	.62	214
18	BOUNDARY	C-C	1.08	.18	5.78	.85	117
19	BOUNDARY	D-D	.97	.18	5.78	.73	154
20	BOUNDARY	E-E	.98	.18	5.78	.73	156
21	BOUNDARY	F-F	.99	.18	5.78	.75	156
22	BOUNDARY	G-G	.98	.18	5.78	.74	159
23	BOUNDARY	H-H	.96	.18	5.78	.70	158
24	BOUNDARY	I-I	1.17	.37	4.91	.86	68

HORIZON NO.	HORIZON ZONE NAME	HORIZON ZONE MOD.	* HOLES WITH REAL OR ESTIMATED VALUES P	E	A	N	* HOLES WITHOUT REAL OR ESTIMATED VALUES NE	NA	NN	NC
1	SHORT CREEK	C-C TOP	21	28	2	0	277	0	0	39
1	SHORT CREEK	C-C BASE	21	28	2	0	277	0	0	39
2	SHORT CREEK	D-D TOP	21	28	2	0	277	0	0	39
2	SHORT CREEK	D-D BASE	21	28	2	0	277	0	0	39
3	SHORT CREEK	E-E TOP	21	28	2	0	277	0	0	39
3	SHORT CREEK	E-E BASE	21	28	2	0	277	0	0	39
4	SHORT CREEK	F-F TOP	18	23	10	0	277	0	0	39
4	SHORT CREEK	F-F BASE	18	23	10	0	277	0	0	39
5	SHORT CREEK	G-G TOP	17	34	12	2	263	0	0	39
5	SHORT CREEK	G-G BASE	17	34	12	2	263	0	0	39
6	ROCHE-PERCEE	C-C TOP	49	163	10	8	98	0	0	18
6	ROCHE-PERCEE	C-C BASE	49	163	10	8	98	0	0	18
7	ROCHE-PERCEE	D-D TOP	50	162	10	8	98	0	0	18
7	ROCHE-PERCEE	D-D BASE	50	162	10	8	98	0	0	18
8	ROCHE-PERCEE	E-E TOP	51	160	11	8	98	0	0	18
8	ROCHE-PERCEE	E-E BASE	51	160	11	8	98	0	0	18
9	ROCHE-PERCEE	F-F TOP	46	154	21	8	98	1	0	18
9	ROCHE-PERCEE	F-F BASE	46	154	21	8	98	1	0	18
10	SOURIS	C-C TOP	115	158	25	9	21	0	0	9
10	SOURIS	C-C BASE	115	158	25	9	21	0	0	9
11	SOURIS	D-D TOP	116	157	25	9	21	0	0	9
11	SOURIS	D-D BASE	116	157	25	9	21	0	0	9
12	SOURIS	E-E TOP	120	154	24	9	21	0	0	9
12	SOURIS	E-E BASE	120	154	24	9	21	0	0	9
13	ESTEVAN	C-C TOP	193	83	19	33	0	0	0	2
13	ESTEVAN	C-C BASE	193	83	19	33	0	0	0	2
14	ESTEVAN	D-D TOP	197	77	21	33	0	0	0	2
14	ESTEVAN	D-D BASE	197	77	21	33	0	0	0	2
15	ESTEVAN	E-E TOP	196	76	23	33	0	0	0	2
15	ESTEVAN	E-E BASE	196	76	23	33	0	0	0	2
16	ESTEVAN	F-F TOP	200	69	26	33	0	0	0	2
16	ESTEVAN	F-F BASE	200	69	26	33	0	0	0	2
17	ESTEVAN	G-G TOP	214	60	21	33	0	0	0	2
17	ESTEVAN	G-G BASE	214	60	21	33	0	0	0	2
18	BOUNDARY	C-C TOP	117	13	63	133	0	0	2	2
18	BOUNDARY	C-C BASE	117	13	63	133	0	0	2	2
19	BOUNDARY	D-D TOP	154	8	27	137	0	0	2	2
19	BOUNDARY	D-D BASE	154	8	27	137	0	0	2	2
20	BOUNDARY	E-E TOP	156	5	26	139	0	0	2	2
20	BOUNDARY	E-E BASE	156	5	26	139	0	0	2	2
21	BOUNDARY	F-F TOP	156	4	26	140	0	0	2	2
21	BOUNDARY	F-F BASE	156	4	26	140	0	0	2	2
22	BOUNDARY	G-G TOP	159	2	22	143	0	0	2	2
22	BOUNDARY	G-G BASE	159	2	22	143	0	0	2	2
23	BOUNDARY	H-H TOP	158	2	20	144	0	0	4	2
23	BOUNDARY	H-H BASE	158	2	20	144	0	0	4	2
24	BOUNDARY	I-I TOP	68	0	79	177	0	0	4	2
24	BOUNDARY	I-I BASE	68	0	79	177	0	0	4	2

* P = Penetrated
E = Eroded
A = Pinched out
N = Not deep enough

NE = eroded - no value calculated
NA = pinched out - no value calculated
NN = hole not deep enough - no value calculated
NC = no estimate - no value calculated

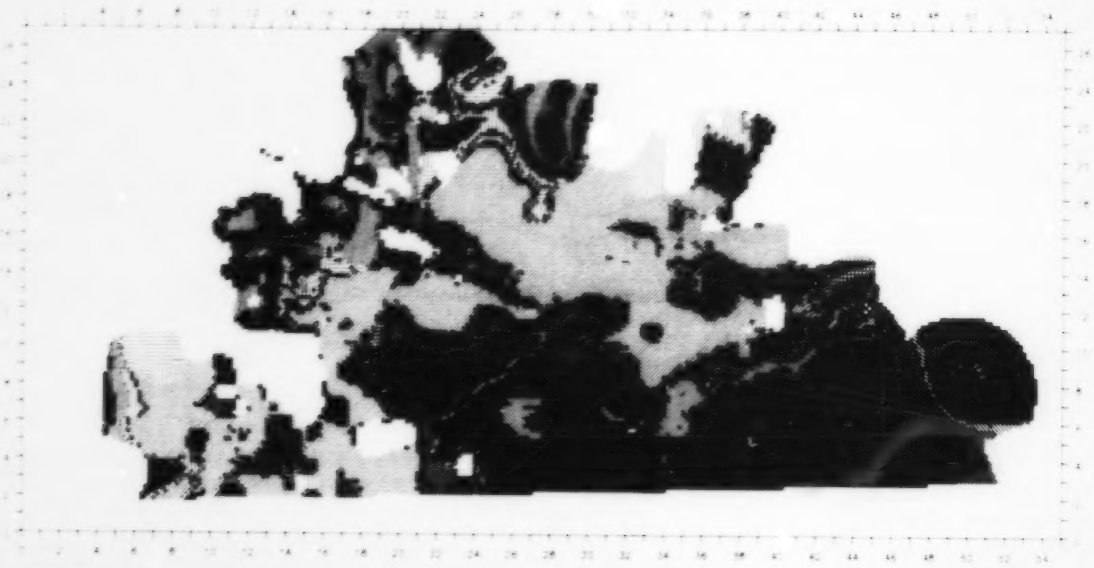

Figure 3 - Map showing which of the 24 coal beds in the Estevan Coalfield is uppermost at each node in the model. Coal beds dip southerly (i.e. towards bottom of the diagram), so that the stratigraphically lowest beds are at the north and around the peripheries; stratigraphically higher beds are in the south. The lower edge of the patterned area is the Canada-U.S.A. border. This map is analogous to a bedrock geology map and was generated by program MODEL. Distances are in kilometres.

were assumed. Non-extractable rock partings were included in the qualifying layers and assigned an ash content of 80 percent based on known mining practices. A specific gravity for volume to weight conversion for each cell in the model was computed using the compiled quality data.

The program then determines which of the mining horizons can be mined at each cell using the mining plan and economic limits specified by the user. Output from the program includes resource quantities subdivided by stripping ratio, depth, ash content, sulphur content, energy content and recoverable coal thickness for the overall mine plan and for each mining horizon and mining stage in the plan. Figure 8 illustrates some of the resource tables produced for the Estevan Coalfield by the program (108 tables were produced in all). The program also produces a new model showing only coal layers that are mineable. The mineable coal model can be overlaid on the geological model and displayed in cross-section form, as shown in Figure 9. Also produced are datasets which can be displayed in map form defining all aspects of the mine plan. These datasets include the number of qualifying stages throughout the field, the horizons which are mined on each stage, the depth, elevation, ash content, sulphur content, energy content, specific gravity etc. of each mining stage and each mining horizon (180 layers of information in all for the Estevan example).

c) Interactive Queries

All of the datasets in the integrated model can be downloaded into a microcomputer- based Geographic Information System, where many additional capabilities are available. The GIS is particularly well suited to interactive queries of any combination of datasets in the model, as well as developing ad hoc reports for any scenario that may be required by downstream users of the model. The availability of GIS's in many organizations means that information can be readily transferred between users. In the case of the Estevan example, more than one thousand layers of spatial data defining all aspects of the geological, economic and environmental characteristics of the coalfield have been incorporated into the GIS. The GIS thus becomes an extremely powerful management tool with which optimal development scenarios for these coal resources can be determined.

Other interactive applications include the ability to predict the outcome of boreholes before they are drilled, and to determine the optimal design of future exploration programs, based on knowledge of the distribution of geological features gained from the model.

4. Conclusions

Integrated geological computer models offer a degree of integrity and utility not possible with manual methods. The expert geological modelling system developed over the past decade by Hughes and others has automated the modelling process to the extent that a coalfield that previously required months of interactive work can now be modelled in a few hours. Geological aspects of coalfields, which previously would have required prohibitive amounts of time, can now be examined using large amounts of data to develop true predictive capabilities.

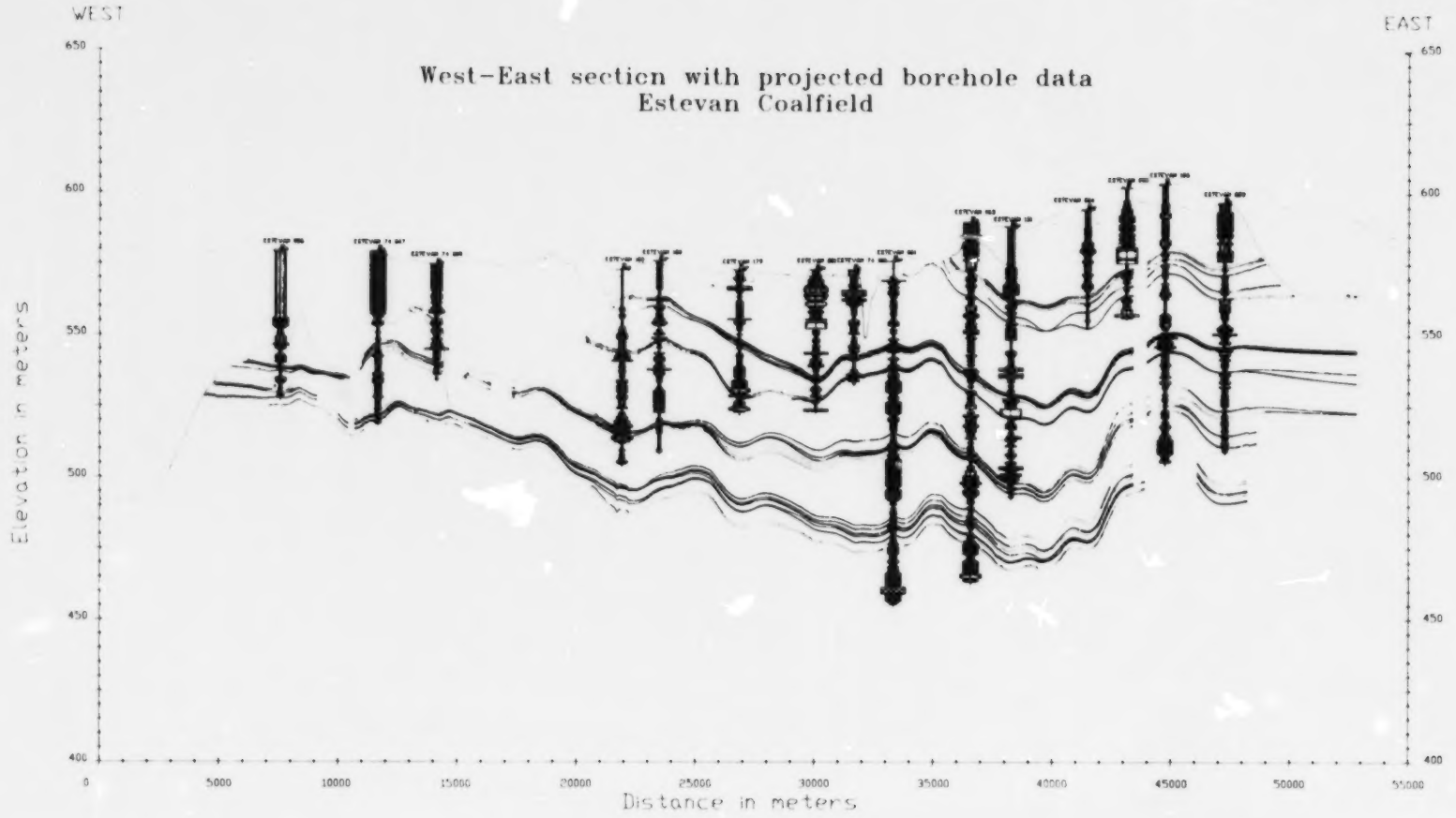

Figure 4 - Structural cross-section constructed in an west-east direction near the southern margin of the Estevan Coalfield. Profiles of all horizons are shown, along with borehole data projected from up to 750 m of the cross-section. This section was constructed directly from the primary geological database and from the profiled geological model using a GSC-developed interface to AUTOCAD. The rather poor reproduction quality of this figure is due to the fact that the original was in colour.

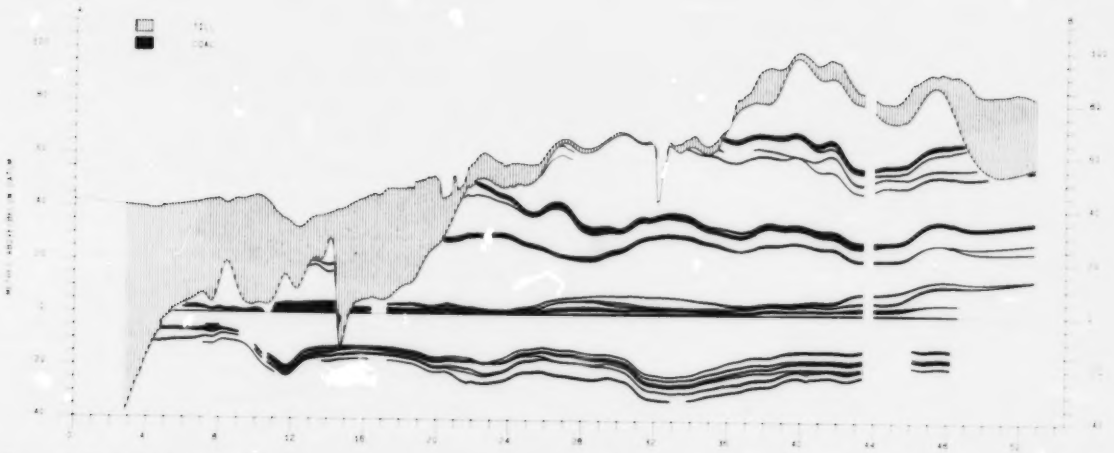

Figure 5 - Geological cross-section constructed along the same line as Figure 6 restored to a base Estevan G datum. The restored model used to create this section was created by program MODEL.

The need for manual cartography has also been completely eliminated by the system.

5. Acknowledgements

The authors wish to acknowledge the support of Saskatchewan Energy and Mines, who provided financial assistance for W.J. McDougall's work on the geological correlations of the Wood Mountain/Willow Bunch and Estevan coalfields. The Office of Energy Research and Development of the Federal Department of Energy, Mines and Resources provided funding to J.D. Hughes to complete the initial databases for these coalfields and to develop and apply the computer technologies used in their assessment. The authors are especially grateful to K.N. Nairn, of the Institute of Sedimentary and Petroleum Geology, for his continued support and advice in matters of computing.

6. References

Hughes, J.D., Klatzel-Mudry, L. and Nikols, D.J. (1989): A standardized coal resource/reserve reporting system for Canada; Geol. Surv. Can., Pap. 88-21, 17p.

Irvine, J.A., Whitaker, S.H. and Broughton, P.L. (1978): Coal resources of southern Saskatchewan: a model for evaluation methodology; Geol. Surv. Can., Econ. Geol. Rep. 30, text plus atlas.

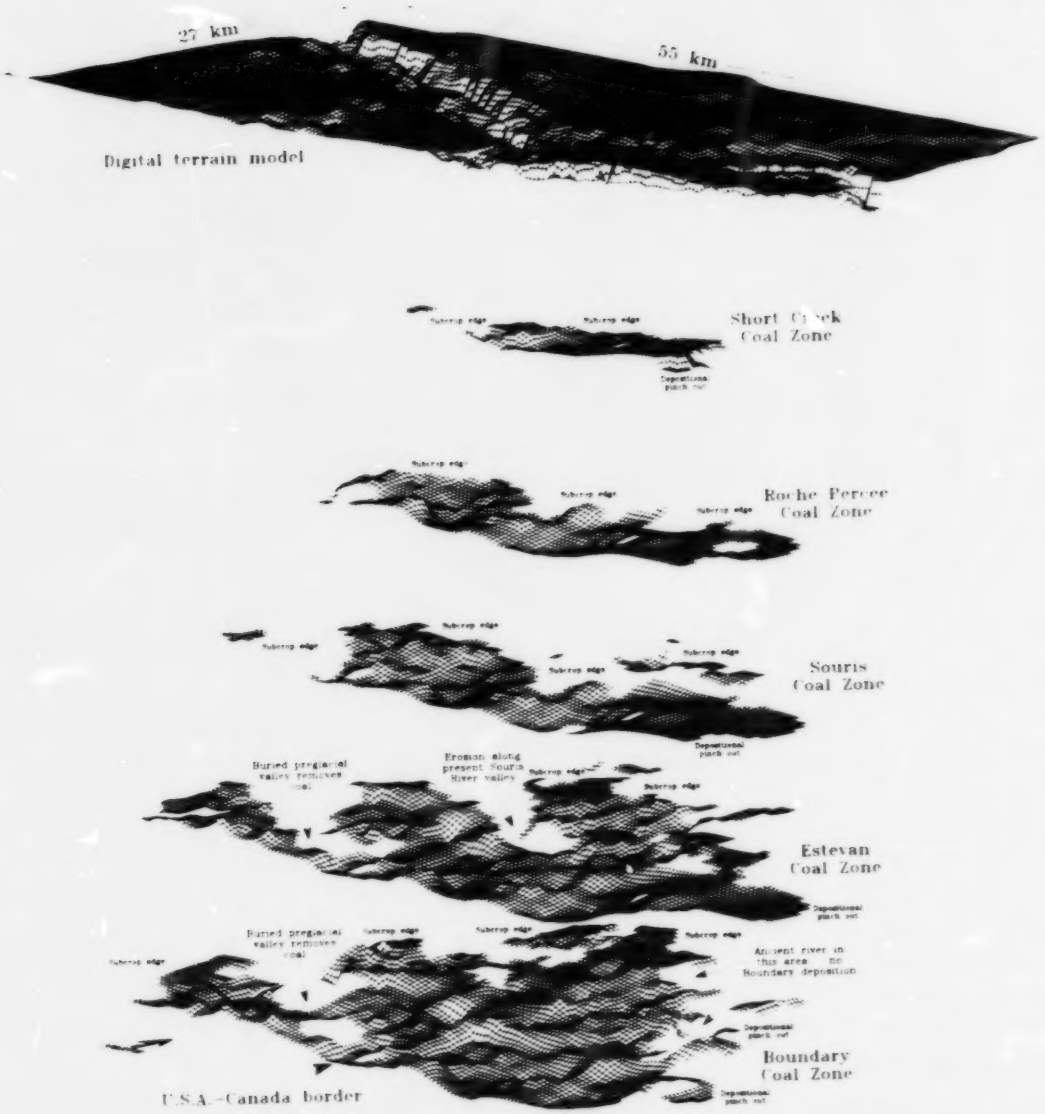

Figure 6 - Three-dimensional diagram of the Estevan Coalfield viewed from the southeast showing the structural configuration of the five coal zones in the Estevan Coalfield and the configuration of the topographic surface. This drawing was created using a GSC-developed interface to AUTOCAD (see text). Several prominent geological features are noted.

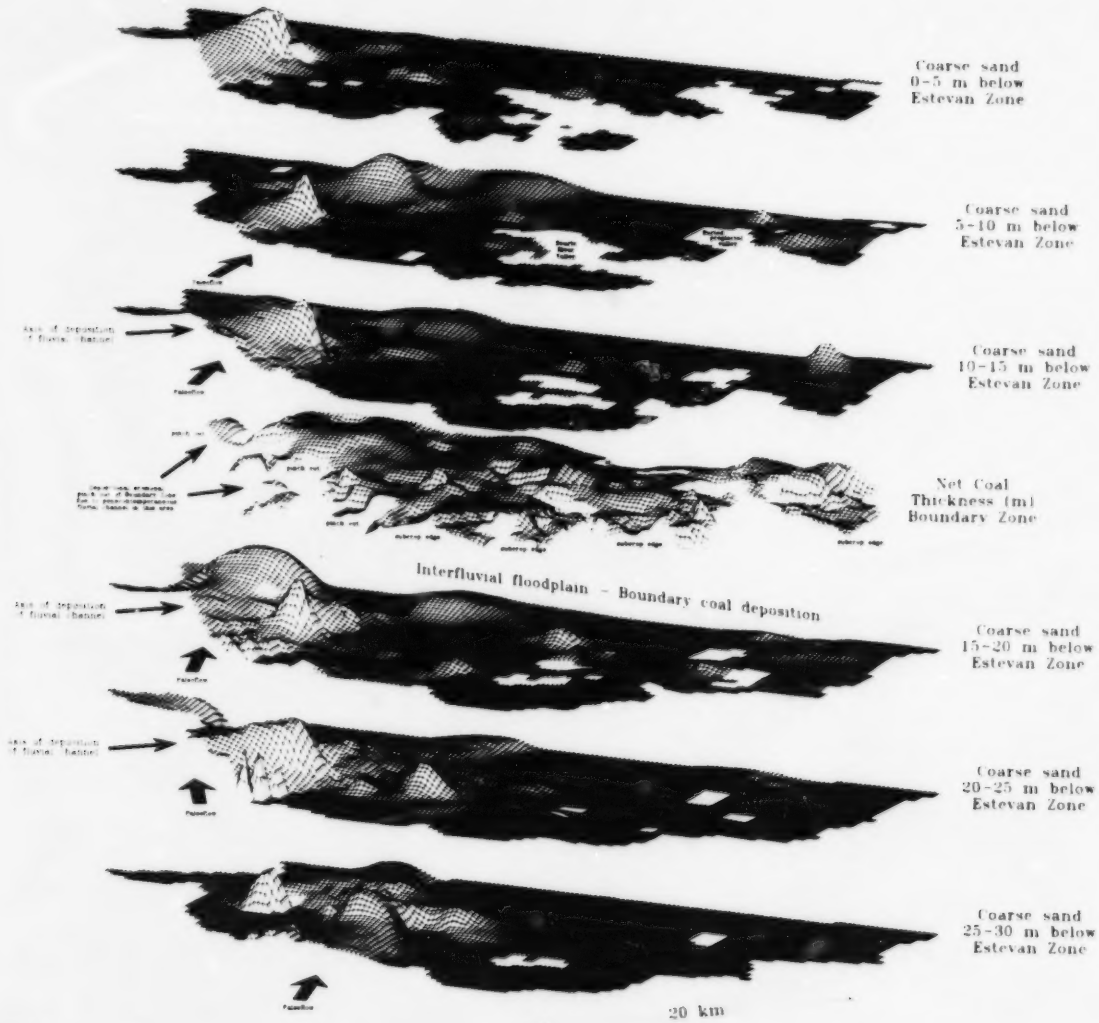

Figure 7 - Three-dimensional diagram of the Estevan Coalfield viewed from the northwest showing the distribution of coarse sand in five metre thick slices taken in descending sequence below the Estevan coal Zone. The net coal thickness of the Boundary Coal Zone is shown in its relative stratigraphic position in the center. A major fluvial channel contemporaneous with Boundary coal deposition can be seen on the coarse sand maps between 10 and 25 m, which has resulted in the lack of Boundary coal in that area (see also Figure 8). Boundary coals are well developed in the interfluvial area west of this channel.

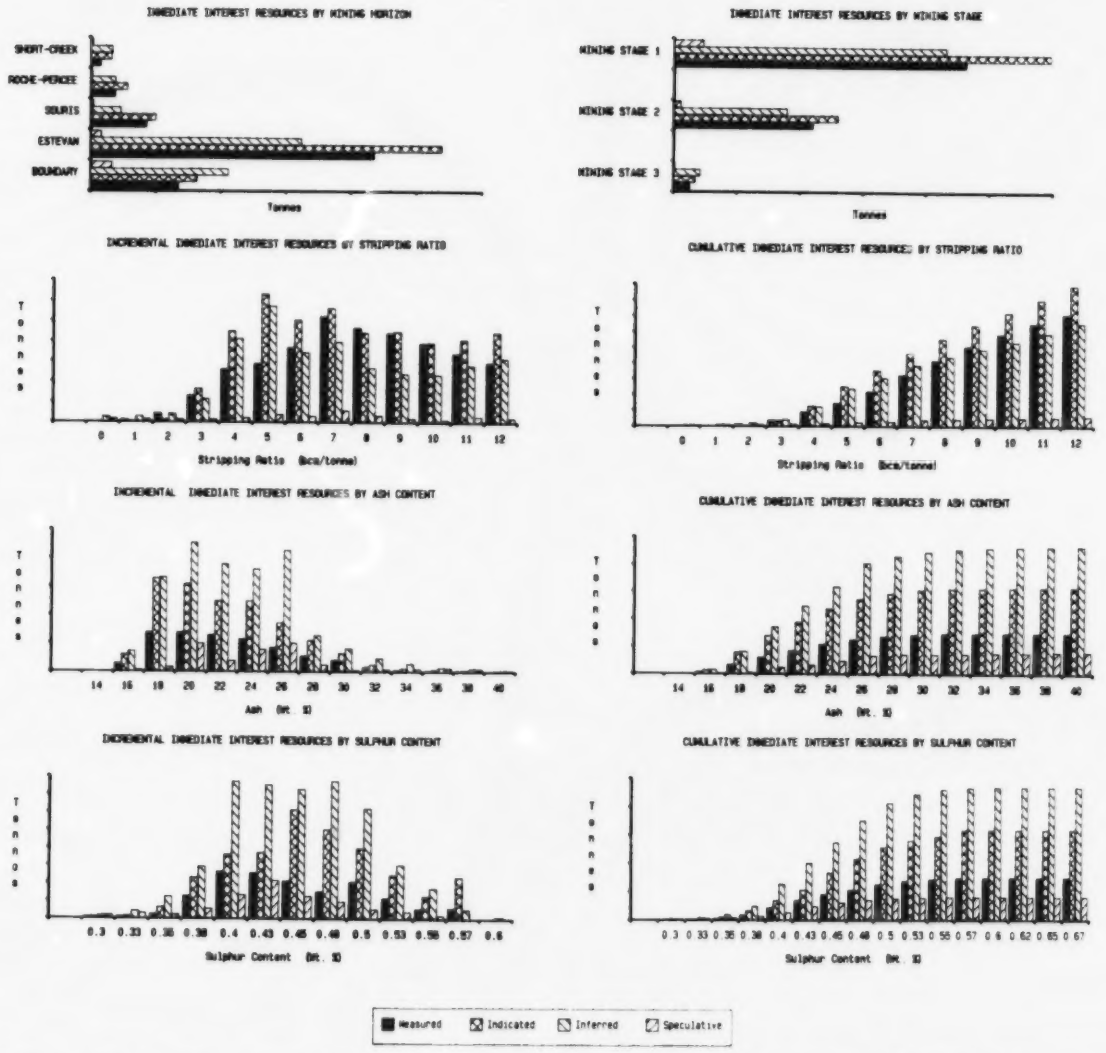

Figure 8 - Charts illustrating some of the categorizations of coal resources possible using program RESOURCE. These charts show only the proportional distribution of resource quantities, as values for the resource parameters are still being refined and the actual quantities are therefore not yet final.

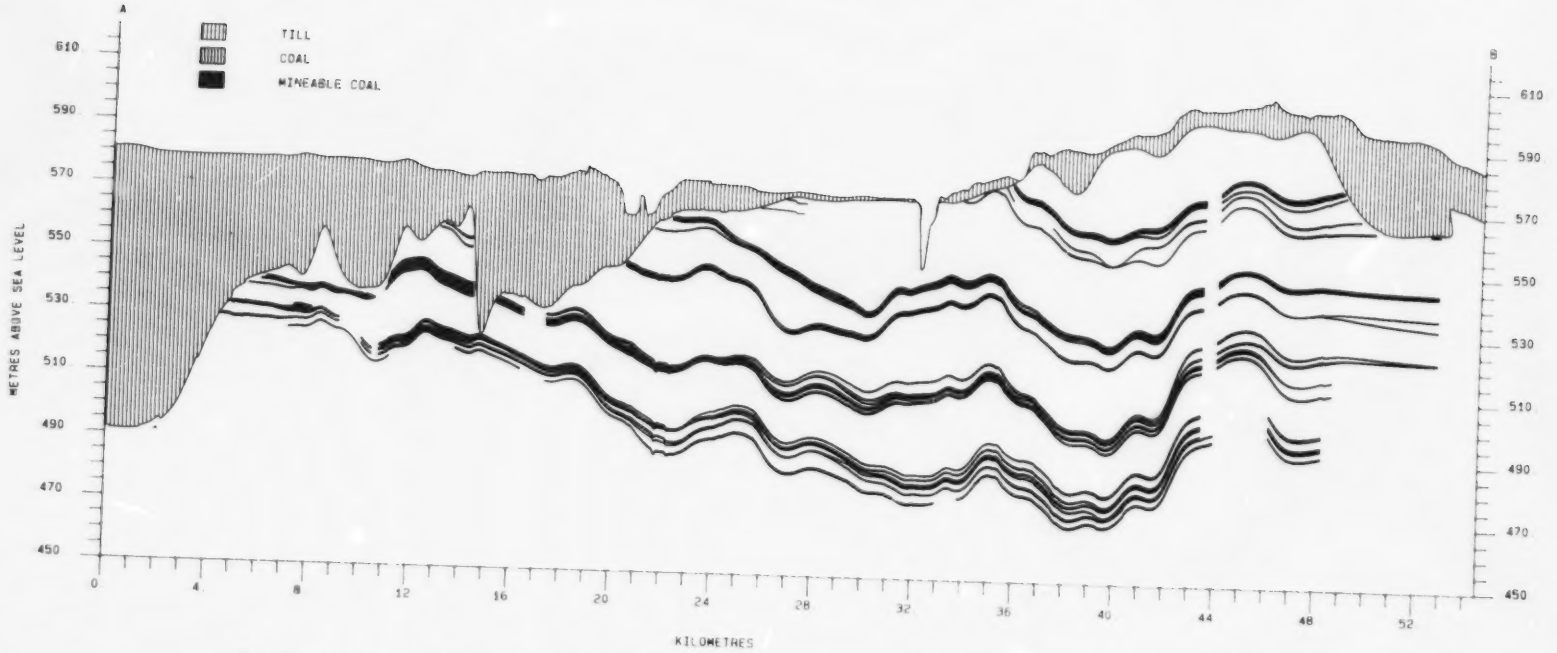

Figure 9 - Cross-section along the same line as the sections in Figures 4 and 5 profiling both the original geological model and the model defining mineable resource produced from program RESOURCE. Coals that are not mineable in this figure have an open hatch pattern, wheras those which are mineable have a solid black fill.

Appendices

Titles and Abstracts of Recent Saskatchewan Energy and Mines Publications and Papers by Staff of the Saskatchewan Geological Survey

1. Reports

Ramaekers, P. (1990): Geology of the Athabasca Group (Helikian) in northern Saskatchewan; Sask. Energy Mines, Rep. 195, 49p.

2. Reports Reprinted 1990

Byers, A.R. (1957): Geology and Mineral Deposits of the Hanson Lake area, Saskatchewan; Sask. Energy Mines, Rep. 30, 47p. (2nd reprinting).

Wilson, W., Surjik, D.L. and Sawatzky, H.B. (1963): Hydrocarbon potential of the South Reindeer area, Saskatchewan; Sask. Energy Mines, Rep. 76, 15p.

3. Miscellaneous Reports

Bennett, R.W. (1990a): Assessment Work Catalogue, Reindeer Area, Saskatchewan; Sask. Energy Mines, Misc. Rep. 90-5, 283p.

_____ (1990b): Assessment Work Catalogue, La Ronge Area, Saskatchewan; Sask. Energy Mines, Misc. Rep. 90-7, 380p.

_____ (1990c): Assessment Work Catalogue, Athabasca Area, Saskatchewan, Sask. Energy Mines, Misc. Rep. 90-8, 279p.

4. Open Files

Pearse, G.H.K. (1990): Building Stone potential in the Creighton-Denare Beach area of Saskatchewan; Sask. Energy Mines, Open File 90-1, 28p.

5. Data Files

Slimmon, W.L. (1990): Fond-du-Lac geological bibliography, NTS 740; Sask. Energy Mines, DF 14, 9p.

Gracie, A.J. and Scutt, A.G. (1990): Index to La Ronge core collection; Sask. Energy Mines, DF 15, 228p.

Slimmon, W.L. and Czornobay, B.M. (1990): Saskatchewan Precambrian Bibliography; Sask. Energy Mines, DF 16, 118p.

Slimmon, W.L., Czornobay, B.M. and Macdonald, R. (1990): Saskatchewan Geochronology Database; Sask. Energy Mines, DF 17 .

6. External Papers

Ashton, K.E. (1989a): The southern flank of the Kisseynew Gneiss Belt in Saskatchewan and its boundaries with the Flin Flon Volcanic Belt and Hanson Lake Block; in Investigations by the Geological Survey of Canada in Manitoba and Saskatchewan during the 1984-89 Mineral Development Agreements, Geol. Surv. Can., Open File 2133, p17-20.

Ashton, K.E. (1989b): Kisseynew Project: Kisseynew Lake - Florence Lake area; in Manitoba Energy and Mines, Minerals Division, Report of Field Activities, 1989, p65-71.

Ashton, K.E. (1990): The relationship between the Flin Flon Volcanic Belt and Kisseynew Gneiss Belt, Trans-Hudson Orogen, Saskatchewan; GAC-MAC Joint Annual Meeting, May 1990, Vancouver, Program with Abstracts, v15, pA5.

The boundary between the low-grade Flin Flon volcanic belt and high-grade Kisseynew gneiss belt has been traditionally viewed as an east-west metamorphic-deformational front across which stratigraphic relationships were unclear. Recent mapping has shown that all of the major units of the Flin Flon volcanic belt can be traced continuously into the Kisseynew gneisses, allowing broad stratigraphic correlation and northward extension of the two-fold Amisk-Missi stratigraphic subdivision. Medium- to high-grade Amisk volcanic rocks with associated Cu-Zn mineralization and Mg and carbonate alteration occur *in situ* within the Kisseynew terrain at Wildnest and Kisseynew Lakes and within structural outliers as at Sheridon, Manitoba. A gradual Amisk Group facies change from predominatly volcanic rocks in the south and west to a wacke-dominated succession in the northeast does not coincide everywhere with the steep metamorphic gradient historically used to mark the boundary between the two belts. Isograds marking the progressive appearance of biotite to sillimanite-garnet-biotite assemblages cut across the regional structure and are in turn displaced by a set of late sinistral shear zones north of Amisk Lake. Higher-pressure assemblages suggest deeper levels of crustal exposure adjacent to the Sturgeon-Weir shear zone, along which the composite Flin Flon-Kisseynew terrain has

been thrust southwestward over the Hanson Lake Block.

Ashton, K.E. and Leclair, A.D. (1990a): Gneiss, schist and foliate: A proposed revision of the terminology for foliated metamorphic rocks; GAC-MAC Joint Annual Meeting, May 1990, Vancouver, Program with Abstracts, v15, pA5.

The existing textural classification of metamorphic rocks fails to accommodate foliated rocks which lack compositional layering or an abundance of platy or prismatic minerals. Whereas most workers consider compositional layering an essential characteristic of gneisses, others apply the term to any foliated metamorphic rock. The term schist is commonly misused for rocks containing less than the required 50 percent platy or prismatic grains showing preferred parallel orientation. In order to clarify this confusion and better constrain the terminology it is suggested that the term foliate, introduced in the early 1900's, be reinstated for all foliated metamorphic rocks and used specifically as a name for rocks which lack compositional layering or at least 50 percent platy or prismatic grains exhibiting parallel orientation. As is the case for gneiss and schist, the term foliate is based on the main textural fabric of the rock and can accept compositional, mineralogical and/or genetic modifiers.

Percentage of minerals with lamellar or elongate prismatic habit showing preferred parallel alignment

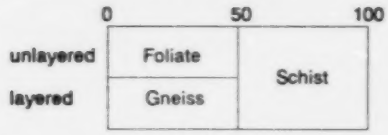

Ashton, K.E. and Leclair, A.D. (1990b): Foliate - A useful term to complement the textural classification of foliated metamorphic rocks; Can. J. Earth Sci., v27 .

The existing terminology for the textural classification of metamorphic rocks does not adequately take into account rocks which lack compositional layering or an abundance of platy or prismatic minerals. Whereas many workers consider compositional layering an essential characteristic of gneisses, others apply the name indiscriminately to almost any foliated metamorphic rock. The term schist is commonly misused for rocks containing less than the required 50 percent platy or prismatic grains displaying a preferred parallel orientation. In order to clarify this confusion and better constrain the existing terminology, it is suggested that the term foliate, introduced in the early 1900's, be reinstated to describe all foliated metamorphic rocks and used specifically as a name for rocks which lack compositional layering or at least 50 percent platy or prismatic grains exhibiting a parallel orientation. Mineralogical, compositional and/or genetic modifiers may be applied to foliate as they are to other textural rock names.

Beck, L.S. and Harper, C.T., eds. (1990): Modern Exploration Techniques; Sask. Geol. Soc., Spec. Publ. No. 10, 253p.

Delaney, G.D. (1990a): Structural hosted gold, Glennie Lake Domain, Lower Proterozoic Trans-Hudson Orogen; in Minerals Colloquium, January 1990, Ottawa, Geol. Surv. Can., Program with Abstracts, p18.

Structurally controlled gold mineralization in the Glennie Lake Domain is illustrated by two examples: the Seabee Deposit and the Brownell-Maynard Lakes showings.

The Seabee deposit has proven and probable ore reserves of 585,134 tonnes grading 12.5 g/t Au and possible reserves of 332,869 tonnes grading 12.5 g/t Au. Seabee ore is hosted in discontinuous quartz-tourmaline veins in northeasterly-trending shear zones, up to 200 m in length, in gabbroic and dioritic rocks of the Laonil Lake Intrusive Complex (ca. 1889 $\pm$ 8.7 Ma). The auriferous quartz veins are flanked by a potassic alteration halo and show a distinct spatial association with narrow, sulphide-bearing feldspar porphyry bodies. Shear zone formation is thought to be contemporaneous with development of the major Laonil Lake Shear Zone at the southern boundary of the basic intrusive complex with the tonalitic Eyahpaise Lake Pluton.

There are several gold showings in the east-west-trending Brownell Lake Greenstone Belt which comprises both supracrustal rocks and late stage composite intrusions. The belt is separated from the granitoid Oskikebuk Block to the south by the major Hartley Shear Zone. Many of the showings are in patchy irregular networks of quartz veins near the margins of a composite pluton. More economically significant gold concentrations are found, however, in two structural settings: 1) in narrow secondary shear zones, parallel or subparallel to the Hartley Shear Zone, that cut mafic to intermediate volcanics and 2) in heterogeneously sheared diorite of the Maynard Creek Pluton within a few hundred metres of the northern margin of the Hartley Shear Zone. The increasingly recognized association of gold mineralization and shear zones suggests that several recently identified structures in the southern Glennie Lake Domain warrant evaluation for gold potential.

Delaney, G.D. (1990b): Gold mineralization, Brownell-Wapawekka Lakes Greenstone Belt, Glennie Lake Domain, Trans-Hudson Orogen, Saskatchewan; GAC-MAC Joint Annual Meeting, May 1990, Vancouver, Program with Abstracts, v15, pA31.

The east-west-trending Lower Proterozoic Brownell-Wapawekka Lakes Greenstone Belt comprises amphibolite grade supracrustal rocks intruded by small plutons and bounded along much of the north and south sides by granitoid rocks. Two major episodes of deformation have affected these rocks. D1 formed a steeply dipping, east-west-trending foliation and moderate north-northeasterly-plunging stretching lineation. High strain zones occur along the contact with the bounding granitod rocks and within the greenstone belt. D2 formed north- to northwest-trending open folds.

Gold mineralization in the greenstone belt is found in quartz veins in two distinct settings: 1) at the margins of the Brownell Lake Pluton and 2) adjacent to the major Hartley Shear Zone at the southern margin of the greenstone belt. The composite calc-alkaline Brownell Lake Pluton forms the core of an open north-

east-plunging D2 anticline. At least seven gold showings have been defined in or adjacent to the margins of the northern granitic part of the intrusion. None of these showings appear to have significant grades or tonnages.

Gold-bearing quartz veins spatially associated with the Hartley Shear Zone are found in two settings: 1) in or adjacent to second and third order shear zones cutting mafic to intermediate flow and fragmental rocks; and 2) in heterogeneously sheared diorite of the Maynard Creek Pluton. In both of these settings vein geometry is varied and there is the potential for both significant grades and tonnage. The element association of the shear zone type gold showings is Au + Ag + As + Cu + Fe + Sb + W. The newly documented association of gold mineralization with major high strain zones suggests that several of these recently identified structures in the southern Glennie Lake Domain warrant evaluation for their gold potential.

Gracie, A.J. and Schwann, P.L. (1990): Uranium Exploration activity maintained; in Exploration and development highlights 1989, PDAC Annual Publication, Jan. 1990, v2, p37-39.

Kreis, K.K. (1990): Stratigraphy of the Jurassic System in the Wapella-Moosimin area, Southeastern Saskatchewan; unpubl. MSc. thesis, Univ. of Regina, 192p.

The Triassic/Jurassic section of southeastern Saskatchewan is an unconformity bound sequence between the Mississippian subcrop and the Cretaceous Mannville Formation. It is not readily correlatable with the Jurassic of the type area in the southwestern part of the province because one of the more readily recognizable units, the Lower Member of the Shaunavon Formation (which is critical to stratigraphic division), changes facies from west to east. For this reason, much of the Middle Jurassic section in the southeast has been considered "undifferentiated" prior to this study.

Five hundred geophysical well logs, 1500 metres of core and well cuttings from the Wapella-Moosomin area provide the database for a detailed study of the Jurassic stratigraphy, sedimentology and paleontology of this area. The combination of these make an interpretation of the paleo-environments and depositional history feasible.

There are four lithostratigraphic units in the Jurassic of southeastern Saskatchewan: Watrous, Gravelbourg, Red Jacket and Rierdon Formations. The Red Jacket, a new formation, is proposed as the lateral facies equivalent to strata lying between the lower member of the Gravelbourg and the Vanguard formations of the type area. The western limit of this unit has been arbitrarily established. A number of discontinuities within the Red Jacket Formation ranging from suspected diastems to an obvious disconformity with a distinct physical expression can be used to divide this formation into formally designated members and informal units. Thus, in ascending order, the Red Jacket Formation is divided into the Rocanville, Moosomin, and the Burrows members. The members are further divided into informal units including: Rocanville 'A', 'B' and 'C', Moosomin 'A' and 'B' and Burrows 'A' and 'B'. Locally, Moosomin 'A' includes subunits Moosomin 'A1' and 'A2'.

The Triassic/Jurassic (?) red beds of the lower member of the Watrous Formation represent the earliest post-Mississippian deposits in the study area. They appear to have been laid down in a restricted marine environment but the sediments were repeatedly exposed and oxidized, as well as reworked. This initial phase was followed by somewhat less restricted marine deposition in Bajocian time, as represented by the sedimentary sequence of the upper member of the Watrous Formation and unit A of the lower member of the Gravelbourg Formation. Unit B of the lower Gravelbourg is overlain by rocks which were deposited in a near-normal marine environment. In contrast, strata belonging to the succeeding Red Jacket Formation indicate a wide spectrum of depositional environments ranging from freshwater to brackish-water (estuarine) and near-normal to normal marine settings. This variation is considered to have been caused by minor yet frequent fluctuations in sea level causing broad geographic shifts in the depositional environments, and relatively progressive changes in the vertical rock column. In addition, there are abrupt changes represented by a number of discontinuities in the Red Jacket Formation which attest to some major disruptive events during Bajocian to Bathonian time. This unstable phase was followed by more quiet times during a strong and longer lasting marine transgression when normal marine conditions prevailed over vast areas, and the Rierdon shales were laid down in the study area in Late Bathonian to Callovian time.

Leckie, D.A., Gilboy., C.F., Bhattacharya, J., Campbell, R., Gilders, M., Lloyd, T., Norris, B., Safton, D., Sawicki, J. and Sawicki, O. (1990): Colorado/Alberta Group strata of the Western Canada Sedimentary Basin; in Basin Perspectives, 1990 CSPG Convention, May 1990, Calgary, Program & Abstracts, p89.

The Colorado/Alberta Group is a predominantly shale unit, which exceeds 1100 m in thickness in the northwestern portion of the Western Canada Sedimentary Basin and thins to less than 200 m in the east. The base of the group immediately overlies the top of the Mannville Formation. In the west, the top of the group is at the top of the Milk River Formation; in the east, it is at the top of the First White Speckled Shale. Coarse clastic units within the group are commonly major hydrocarbon producers. They include the Turonian Cardium, the Cenomanian Dunvegan and the Albian Viking formations. These formations are related to major fluctuations in relative sea level, and are described in detail elsewhere. Finer sandy units include the retrogradational shelf sandbodies of the Doe Creek Member, the shelf to coastal plain sandbodies of the Bad Heart Formation and Chinook Sandstone in northwestern Alberta, the shelf to shoreline sandbodies of the Medicine Hat Formation, the Milk River Formation (commonly placed in the Montana Group), the Chungo Member and the Barons Sand of southern Alberta, and the shelf deposits of the Medicine Hat and Newcastle formations in southern Saskatchewan. Several units are of particular economic importance as producers of nonassociated, sweet, dry biogenic shallow gas.

During deposition of Colorado Group sediments, warm marine waters extended north from the Gulf of Mexico and intermixed with boreal waters extending

south from the Arctic. The First White Speckled Shale, the Second White Speckled Shale and Fish Scale Zone occur as regional markers across most of the basin. They represent stratigraphically condensed marine sections related to maxima in marine transgressions. These condensed sections are characterized by high TOC contents and, where mature, form good potential hydrocarbon source rocks.

Norford, B.S., Cecile, M.P., Bezys, R.K., McCabe, H.R., Haidl, F.M. and Paterson, D.F. (1990): Middle Ordovician - Silurian strata of the Western Canada Sedimentary Basin; in Basin Perspectives, 1990 CSPG Convention, May 1990, Calgary, Program & Abstracts, p105.

This stratigraphic package corresponds to the Tippecanoe Sequence but includes older and younger rocks in the mountains. Its present distribution is severely constrained by erosion prior to the sub-Devonian Unconformity. The entire package is missing from virtually all of the basin north of the Meadow Lake Escarpment, and locally the Devonian rests directly on Precambrian. The base of the package is a regional unconformity (on Deadwood, Franklin Mountain and Precambrian units) except in the Rocky Mountains, where it is conformable with the McKay and Kechika groups. Unconformities are also present within the package, with significant downcutting in the extreme northwest.

The outcrop sequences of British Columbia, Mackenzie and Alberta disappear abruptly eastward in the subsurface below the sub-Devonian Unconformity. Nonda carbonates (up to 270 m) are the only rocks with any significant subsurface distribution. Preserved in the subsurface of southern Saskatchewan and Manitoba are a basal arenaceous unit (Winnipeg) and a sequence of platform carbonates that essentially was depositionally continuous with similar rocks in northeastern Manitoba and the Rocky Mountains. The eastern feather-edge (basal Red River; subsurface) is 150 km west of the Alberta-Saskatchewan border.

The stratigraphic package is thickest (about 500 m) in southeastern Saskatchewan adjacent to thicker developments in Montana and North Dakota. Above the Winnipeg (up to 75 m), the Red River, Stony Mountain, Stonewall and Interlake units represent subtidal to supratidal environments with deposition of shallow water carbonates. Thin evaporitic, argillaceous and sandy intervals provide stratigraphic marker horizons that can be traced for considerable distances in the subsurface.

Osadetz, K.G. and Haidl, F.M. (1989): Tippecanoe Sequence: Middle Ordovician to Lowest Devonian - Vestiges of a great epeiric sea; in Ricketts, B.O. (eds.), Western Canada Sedimentary Basin: A case history, ch. 8, p121-138.

Reilly, B.A. (1990): Hurwitz Group Metasediments: High-level allochthonous tectonic slices in northeastern Saskatchewan; GAC-MAC Joint Annual Meeting, May 1990, Vancouver, Program with Abstracts, v15, pA109.

The southerly extension of the Early Aphebian Hurwitz Group is found in the extreme northeastern corner of Saskatchewan. The Hurwitz Group comprises a metasedimentary sequence extending through Saskatchewan, Manitoba and the Northwest Territories. In Saskatchewan, a lower psammo-pelitic schist unit is conformably overlain by a dolomitic marble unit with subordinate calc-silicate rock layers. These units are correlative with the Watterson Formation. The Hurwitz Group has been effected by upper greenschist to lower amphibolite facies metamorphism.

The Hurwitz Group is in sheared contact with Mudjatik felsic gneisses (Archean/Proterozoic) and Ennadai Group metavolcanics (Archean). Kinematic indicators suggest that the predominant transport direction of the Hurwitz Group is toward the northwest. The Hurwitz Group is interpreted as a series of high-level allochthonous tectonic slices forming part of a northwest-directed fold-thrust belt. Correlation of the low-grade Hurwitz Group with the high-grade Wollaston Group to the south is complicated due to the abrupt change in lithology and metamorphic facies between these two groups of metasedimentary rocks.

Northwest-directed thrusting observed in the Hurwitz Group of Saskatchewan is consistent with current tectonic models proposed for the Trans-Hudson Orogen. Deposition of a shelf sequence (Hurwitz and Wollaston Groups) and subsequent deformation of this sequence, during a 1.87 Ga southeast collision, resulted in the development of a northwest vergent fold and thrust terrane.

Ruzicka, V., Sibbald, T.I.I., Kyser, K., Battey, G.C., Miezities, Y. and Eupene, G.S. (1990): Models for unconformity-type uranium deposits; International Conference on Mineral Deposit Modeling, Internat. Assoc. Genesis Ore Deposits, 8th Symposium, August 1990, Ottawa, poster paper Abstract.

Uranium and uranium-polymetallic deposits associated with Proterozoic unconformities in Canada and Australia exhibit common features that can be complied into a conceptual genetic model:

The deposits are part of uranium-enriched provinces. The uranium may originally have been introduced into the geochemical cycle through granitic magmatism, during the late Archean or Early Proterozoic. Uranium was afterwards concentrated in sedimentary rocks, particularly in pelites. The orogenic and post-orogenic events that took place during the Early Proterozoic locally caused remobilization and redeposition of uranium in veins. Subsequent peneplanation and lateritic weathering of the uranium-enriched terranes resulted in liberation of uranium and other metals, which became incorporated in oxidized fluids. These fluids percolated along fault and fracture zones in the basement rocks below the unconformities and consequently became reduced. They might also mix with water derived from deep-seated sources. These reduced fluids released uranium in structural and lithological traps in the basement rocks, thus forming deposits (e.g. Eagle Point, Canada; Ranger and Jabiluka, Australia). Tectonic and thermal events after deposition of the basinal sediments activated hydrothermal systems causing convective cycling of the fluids. Where the reduced fluids re-entered in ascending flows the sedimentary cover rocks and mingled with the downward and laterally moving

oxidized basinal waters, the uranium, associated metals and gangue minerals precipitated at this redox front (e.g. Key Lake and Cigar Lake deposits, Canada; and Kintyre deposit Australia). Uranium was commonly transported as uranyl carbonate complexes at temperatures between 130° and 270°C.

The mineralization was associated with alteration of the host rocks by chlorite, kaolinite and illite, superimposed on the preceding lateritic and regolithic alterations. The hydrothermal fluids introduced carbon dioxide, hydrogen sulphide and methane into the environment. Tourmalinization and magnesian alteration were common companions of these processes. The alteration was enhanced by ionization effects of radiation and by partial hydrolysis of the waters.

Geochemical processes (e.g. Eh and pH changes, adsorption and complexing) controlled not only the deposition of the ore-forming minerals, but also the specific mineral assemblages that formed and, apparently, their zonal arrangement. Polymetallic assemblages formed at the unconformities, i.e. at the interface between the basement and cover rocks, whereas monometallic assemblages formed within the basement rocks and farther above the unconformity.

In most deposits the mineralization was rejuvenated in one or more periods.

Sibbald, T.I.I. and Koziol, M. (1990): Base metal deposits in the Lower Proterozoic Hanson Lake metavolcanics, Saskatchewan; in Minerals Colloquium, Geol. Surv. Can., January 1990, Ottawa, Program with Abstracts, p32-33.

The Lower Proterozoic (ca. 1881 ± 6 Ma) Hanson Lake metavolcanics exposed 60 km west of Flin Flon host one historic lead-zinc producer, the Western Nuclear Mine, numerous subeconomic base metal showings and the recently discovered McIlvenna Bay volcanogenic massive sulphide deposit, containing in excess of 7 million tonnes of ore grading 1.1 percent Cu, 6.5 percent Zn, 34 g/t Ag and 0.7 g/t Au. The McIlvenna Bay deposit is located 5 km south of the Western Nuclear Mine, beneath a thin (ca. 15 m) cover of Ordovician dolomites and quartz-sandstones. Both deposits occur within felsic rocks, deformed and metamorphosed to upper greenschist-lower amphibolite facies during Hudsonian orogenesis. The exposed felsic edifice around the Western Nuclear Mine comprises predominant dacitic and rhyolitic lavas and pyroclastics overlain successively, by mixed felsic to mafic volcanics interlayered with oxide-silicate-sulphide faces iron formation and by greywackes. Subvolcanic, quartz-feldspar porphyry plutons intrude the felsic edifice and gabbroic sheets in the overlying sequence. In the McIlvenna Bay deposit, copper-zinc mineralization occurs within metres of the base of the overlying mixed volcanics, in three lenses of massive sulphides, typically underlain by copper-rich stringer 'ore' (reserves above are for lens 2 only). Host felsic rocks are finely laminated sericitic schists with chert (?) interlayers. Chloritic, silicic and argillic alteration is apparent below the massive sulphide lenses. The Western Nuclear deposit is hosted by a similar sericite schist-chert(?) sequence, but appears to occupy a different and possibly lower level of the felsic edifice.

Sibbald, T.I.I., Quirt, D.H. and Gracie, A.J. (1990): Uranium deposits of the Athabasca Basin, Saskatchewan (Field trip 11); 8th IAGOD Symposium field trip guidebook, Geol. Surv. Can., Open File 2166, 56p.

Slind, O.L., Tawadros, E.E., Andrews, G.D., Sallas, C.J., Murray, D.A., Norford, B.S. and Paterson, D.F. (1990): Middle Cambrian-Lower Ordovician strata of the Western Canada Sedimentary Basin; in Basin Perspectives, 1990 CSPG Convention, May 1990, Calgary, Program & Abstracts, p131.

The Cambrian succession is subdivided, correlated, and mapped in the subsurface from the Foothills of Alberta east through the Plains to its edge in Manitoba. An attempt is also made to correlate stratigraphic sections exposed in the Front and Main ranges with the subsurface.

The Cambrian and Lower Ordovician carbonate succession exposed in the Front and Main ranges forms a carbonate facies belt of cyclic peritidal dolomite and limestone. The succession extends eastward into the Foothills of Alberta and to some distance in the subsurface of the Plains before gradually changing facies, within Alberta, to shallow basin clastics. To the west, within the Main Ranges, the carbonate facies belt, with the exception of the Mural-Badshot and Ottertail Formations, abruptly changes along an ocean-facing submarine escarpment to dark, deepwater, fine-grained basinal clastics and carbonates.

In the subsurface of the Plains, the Cambrian rests unconformably on the Precambrian. It covers most of southern Alberta, as far north as Township 75, and southern Saskatchewan as far north as Township 65. North of these areas, the Sub-Devonian unconformity rests on the Precambrian. It is only present in Manitoba over a small area in the extreme southwest. A remnant of Cambrian strata is preserved in the Fort Nelson area of British Columbia.

In eastern Alberta and western Saskatchewan, the Cambrian and Lower Ordovician are represented by the Middle Cambrian Basal Sandstone unit, clastics of the Earlie Formation, and Upper Cambrian - Lower Ordovician clastics of the Deadwood Formation. The Cambrian section is overlain unconformably by Upper Ordovician carbonates in the east-central part of southern Alberta and western Saskatchewan. In eastern Saskatchewan and Manitoba, only the Deadwood persists and is overlain by the clastic Winnipeg Formation (Middle Ordovician). Where the Ordovician is eroded, the Cambrian is overlain by either Middle or Upper Devonian sediments.

In the western subsurface of the Plains and Foothills of Alberta, and in the front and eastern Main ranges, the succession composed of the Middle Cambrian Basal Sandstone unit (except for the Windsor Mountain, not observed in the Foothills, or mountains), Mount Whyte clastics, Cathedral carbonates, Stephen clastics, Eldon carbonates, Pika carbonates and clastics, and Arctomys clastics, and is overlain by the Upper Cambrian Waterfowl carbonates, Sullivan clastics, Upper Lynx carbonates and Lower Ordovician Survey Peak and Outram carbonates.

Thomas, D.J. and Harper, C.T. (1990): Regional- and deposit-scale characteristics of structurally-controlled lode gold mineralization in the La Ronge gold belt; in Beck, L.S. and Harper, C.T. (eds.), Modern Exploration Techniques, Sask. Geol. Soc., Spec. Publ. No. 10, p181-193.

During the 1980's, northern Saskatchewan received record levels of gold exploration and development expenditures (approximately $196 million) ranging from a low of $3 million in 1982 to an estimated $65 million in 1988. During this period several exciting new gold discoveries were made (eg. 21 zone, Rod zone, Jasper-James, North Lake, Bakos) while re-evaluation of many known prospects led to substantial increases over previous reserve estimates (eg. Seabee, Tower Lake, Jojay, Pap/Preview). This surge in gold exploration has delineated about 3 million ounces gold distributed between deposits presently in production and those undergoing advance stages of exploration. Over half of the estimated gold reserves in Saskatchewan occur in twelve main deposits (1.74 million ounces gold) in the La Ronge region.

Most gold discoveries in northern Saskatchewan have been in the greenstone belts of the La Ronge Domain and, to a lesser extent, the Glennie and Flin Flon Domains. This region is informally referred to as the La Ronge Gold Belt. In the La Ronge Domain gold deposits are concentrated in four principal areas; Waddy, Tower, Star and Sulphide Lakes. In the Glennie Domain the most significant gold deposit is in the Laonil Lake area. The majority of these gold deposits can be classified as structurally-controlled quartz vein- or lode-type, with a limited number interpreted as structurally modified stratiform-type. Regional- and deposit-scale characteristics are outlined and discussed for structurally-controlled lode gold mineralization.

Many features characterizing lode gold deposits in the more publicized Archean greenstone belts of eastern Canada are common to the Early Proterozoic La Ronge Gold Belt. There is excellent potential for gold discoveries in this area of northern Saskatchewan.

Wilcox, K.H. (1990): Geology of the Amisk - Welsh Lakes area, Saskatchewan; unpubl. MSc. thesis, Univ. of Calgary.

The Amisk-Welsh Lakes area in northeastern Saskatchewan contains Aphebian rocks of the Churchill Province. The area occupies the transition between the low-grade Flin Flon metavolcanic Domain and the high-grade Kisseynew sedimentary gneiss Domain of the Trans-Hudson Orogen.

The area is predominantly underlain by clastic rocks of the Missi Group. The Missi Group is interpreted to have been deposited in an alluvial fan to braided stream succession and to have been subsequently intruded by a porphyritic dacite to tonalite and a gabbroic to ultramafic suite of plugs and sills.

Three main phases of deformation are recognized. The first phase is inferred to have formed E-W trending folds. The second phase created an elongate N-S trending structural basin cored by the Missi Group in the Amisk Lake area. Sinistral E-W shearing during phase three deformation rotated the basin counterclockwise. Strain was concentrated in the Welsh Lake area. Ductile and brittle high strain zones were created by this phase.

Early sheet silicate growth occurred synkinematically with phase two deformation in an axial planar orientation (S2). Inclusion trails indicate that peak metamorphism postdated P2 but was synchronous with P3. The metamorphic grade increases northwestward. The area can be divided into three metamorphic zones; chlorite, biotite and garnet, separated by the biotite and garnet isograds. Bulk composition and deformation has controlled the location of the trace of these isograds. Geothermometric estimates indicate temperatures of 490° to 566°C near the garnet isograd.

Gold mineralization occurred during phase three deformation associated with high strain zones and greenschist facies overprint.

Structural elements in the western Flin Flon, Annabel Lake, Amisk-Welsh Lakes and Sturgeon-Weir River areas suggest that the histories of these areas can be integrated into a regional kinematic model. The Kisseynew Domain is interpreted to have been thrust to the SW over the Flin Flon Domain. The transition zone between the Flin Flon and Kisseynew Domain in these areas suggests that deformation response is strongly controlled by metamorphic grade and associated structural level. The high level, low metamorphic grade Flin Flon Domain primarily responded in a brittle manner, and the low level, high grade Kisseynew Domain responded in a viscous manner. The transition zone is unique because it predominantly responded in a ductile manner and preserved structural features such as folds.

Acknowledgments

The project leaders acknowledge the assistance in the field and office of Dwayne Sparks, Tracey Jungwirth, Danny Labelle, Kent Ellmers, Judy Adamson, Jennifer Stack, Kevin Spelly, Albert Scutt, Greg Gudmundson, Terri Uhrich, Myles Loydl, Joey Wright, Tim Mackay, Eric Strachan, Margaret Bertoldi, Mark Sombach, Lloyd Freeman, Darren Burrows, Adam Zasada and Jason Sturgeon.

The editors are grateful for assistance given in the editing and production process by Bill Slimmon, Laura Smith, Blaine Scott and Fran Haidl. This report was prepared with Ventura DeskTop Publisher and laser printer. Phil Weir handled preparation of some of the figures, and with assistance from Jim Bedo, Rick Pearce and Harry Buyze, assembled the manuscript maps.

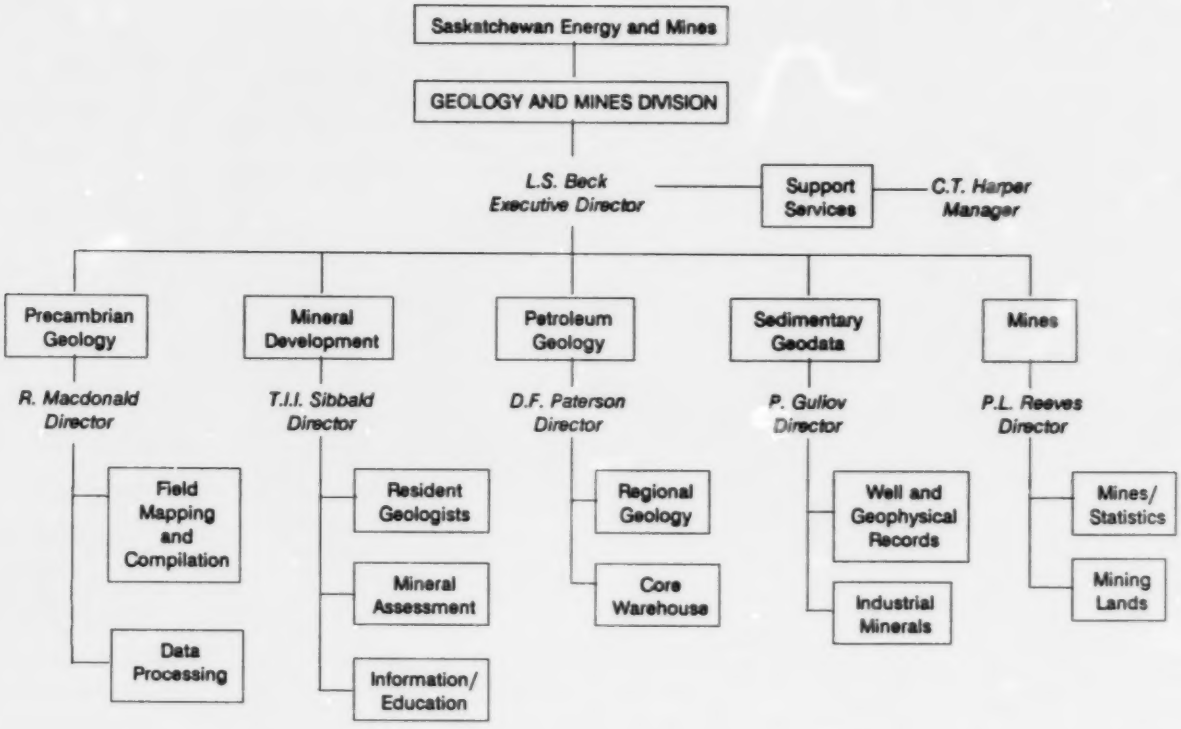

The Saskatchewan Geological Survey comprises the geoscience activities of the Precambrian Geology, Mineral Development, Petroleum Geology and Sedimentary Geodata Branches, and is represented by R. Macdonald, Chief Geologist.

Staff as of November 1, 1990

At 1914 Hamilton Street, Regina:

Geology and Mines Division Administration

Executive Director ..... L.S. Beck, *Ph.D, P.Eng.*

Secretaries ..... J. Adams
V. Ziegler

Saskatchewan Geological Survey

Chief Geologist ..... R. Macdonald, *Ph.D, P.Eng.*

At 1914 Hamilton Street, Regina:

Precambrian Geology Branch

Director ..... R. Macdonald, *Ph.D, P.Eng.*

Field Mapping and Compilation:

Project Geologists ..... G.D. Delaney, *Ph.D*
K.E. Ashton, *Ph.D*
B.A. Reilly, *M.Sc.*[1]
W.L. Slimmon, *B.Sc.*[1]
K. Wilcox, *M.Sc.*[1]

Office Geologist ..... B. Czornabay, *B.Sc.*[1]

Data Processing:
Geologist ..... N. Lee, *M.Sc.*[3]

Secretary ..... J. Bilkhu[2]

Mineral Development Branch

Director ..... T.I.I. Sibbald, *Ph.D, D.I.C.*

Mineral Deposit Studies/Compilation/Education:
Geologists ..... D.G. MacDougall, *B.Sc.(Hons.)*
B.P. Scott, *M.Sc., P.Eng.*
D.J. Thomas, *M.Sc.*

Mineral Assessment:
Geologists ..... H. Stolz, *B.Sc.*
R.W. Bennett, *B.Sc.(Hons.), P.Eng.*

Geological Assistant ..... L. Smith, *B.Sc.*

Resident Geologist Offices:

La Ronge:

Geologists ..... A.J. Gracie, *Ph.D, P.Eng.*
P.L. Schwann, *M.Sc.*

District Mineral Officer ..... vacant

At 1914 Hamilton Street, Regina:

Sedimentary Geodata Branch

Director ..... P. Gulilov, *M.Sc., P.Eng.*

Industrial Minerals:
Geologist ..... M.R. Gent, *M.Sc.*

Well and Geophysical Records:
Geologist ..... D.R. Troyer, *M.Sc., P.Eng.*
Coding Clerk ..... R. Kovacevic
Well File Clerk ..... J. Tanouye
Geophysical Clerk ..... K. Barrett

At 201 Dewdney Avenue East, Regina:

Petroleum Geology Branch

Director ..... D.F. Paterson, *Ph.D, P.Eng.*

Regional Geology:
Geologists ..... C.F. Gilboy, *Ph.D, P.Eng.*
F.M. Haidl, *M.Sc.*
L.K. Kreis, *B.Sc.*
M. Yurkowski, *B.Sc.*[1]

Warehouse:
Supervisor ..... D. Forsberg
Staff ..... R.L. McCall
R. Lavigne
D. Gallant

Secretaries ..... M. McNally
L. Sutyla

At 1914 Hamilton Street, Regina:

Support Services Section

Manager ..... C.T. Harper, *Ph.D, P.Eng.*

Review Geologist ..... N.M. Richmond-Johnson, *B.Sc.*[1]

Geological Survey Drafting Unit:
Supervisor ..... R.P. Kydd
Draftspersons ..... P.A. Weir
K.G. Jones

General Drafting Unit:
Supervisor ..... J.J. Bedo
Draftspersons ..... R.O. Pearce
A.H. Buyze

---

[1]Position contracted
[2]Also serving Mineral Development Branch
[3]Seconded to Mines Branch temporarily